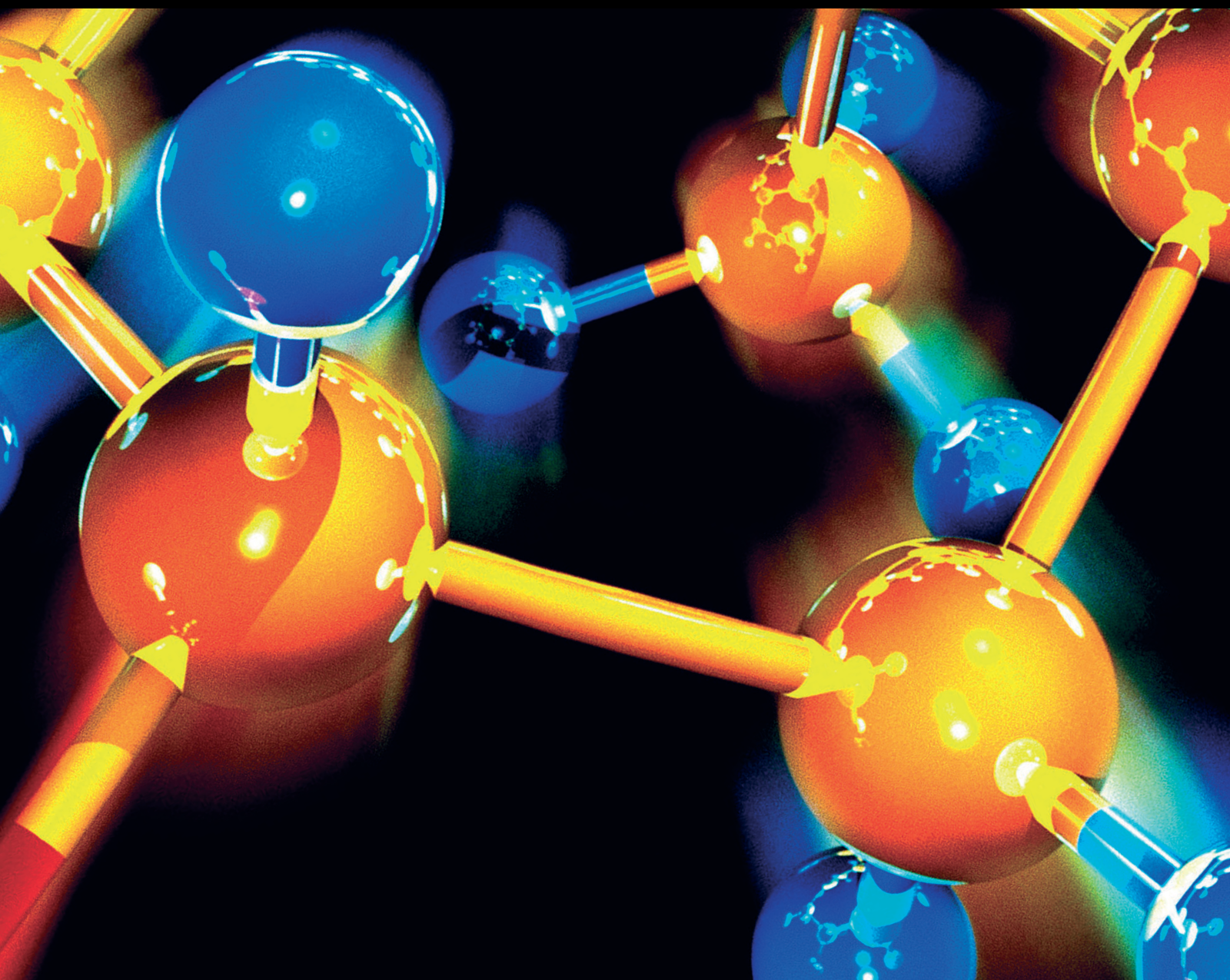


# Computational Invariant of Chemical Structures and their Applications

Lead Guest Editor: Kashif Ali

Guest Editors: Muhammad Faisal Nadeem and Muhammad Imran





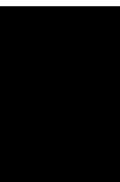
---

# **Computational Invariant of Chemical Structures and their Applications**

# **Computational Invariant of Chemical Structures and their Applications**

Lead Guest Editor: Kashif Ali

Guest Editors: Muhammad Faisal Nadeem and  
Muhammad Imran



---

Copyright © 2021 Hindawi Limited. All rights reserved.


This is a special issue published in "Journal of Chemistry." All articles are open access articles distributed under the Creative Commons Attribution License, which permits unrestricted use, distribution, and reproduction in any medium, provided the original work is properly cited.

# Chief Editor

Kaustubha Mohanty, India

## Associate Editors

Mohammad Al-Ghouti, Qatar


Tingyue Gu , USA

Teodorico C. Ramalho , Brazil

Artur M. S. Silva , Portugal


## Academic Editors

Jinwei Duan, China

Luqman C. Abdullah , Malaysia

Dr Abhilash , India

Amitava Adhikary, USA

Amitava Adhikary , USA

Mozhgan Afshari, Iran

Daryoush Afzali , Iran

Mahmood Ahmed, Pakistan


Islam Al-Akraa , Egypt


Juan D. Alché , Spain

Gomaa A. M. Ali , Egypt

Mohd Sajid Ali , Saudi Arabia

Shafaqat Ali , Pakistan


Patricia E. Allegretti , Argentina

Marco Anni , Italy

Alessandro Arcovito, Italy

Hassan Arida , Saudi Arabia


Umair Ashraf, Pakistan


Narcis Avarvari , France

Davut Avci , Turkey


Chandra Azad , USA

Mohamed Azaroual, France

Rasha Azzam , Egypt


Hassan Azzazy , Egypt

Renal Backov, France

Suresh Kannan Balasingam , Republic of Korea

Sukanta Bar , USA

Florent Barbault , France

Maurizio Barbieri , Italy

James Barker , United Kingdom

Salvatore Barreca , Italy

Jorge Barros-Velázquez , Spain

THANGAGIRI Baskaran , India

Haci Baykara, Ecuador

Michele Benedetti, Italy

Laurent Billon, France

Marek Biziuk, Poland

Jean-Luc Blin , France

Tomislav Bolanca , Croatia

Ankur Bordoloi , India

Cato Brede , Norway


Leonid Breydo , USA


Wybren J. Buma , The Netherlands

J. O. Caceres , Spain


Patrizia Calaminici , Mexico


Claudio Cameselle , Spain


Joaquin Campos , Spain

Dapeng Cao , China

Domenica Capasso , Italy

Stefano Caporali , Italy

Zenilda Cardeal , Brazil


Angela Cardinali , Italy

Stefano Carli , Italy

Maria F. Carvalho , Portugal


Susana Casal , Portugal


David E. Chavez, USA

Riccardo Chelli , Italy

Zhongfang Chen , Puerto Rico

Vladislav Chrastny , Czech Republic


Roberto Comparelli , Italy

Filomena Conforti , Italy

Luca Conti , Italy


Christophe Coquelet, France

Filomena Corbo , Italy


Jose Corchado , Spain

Maria N. D.S. Cordeiro , Portugal

Claudia Crestini, Italy

Gerald Culioli , France

Nguyen Duc Cuong , Vietnam

Stefano D'Errico , Italy


Matthias D'hooghe , Belgium

Samuel B. Dampare, Ghana

Umashankar Das, Canada

Victor David, Romania


Annalisa De Girolamo, Italy

Antonio De Lucas-Consuegra , Spain

Marccone A. L. De Oliveira , Brazil

Paula G. De Pinho , Portugal

Damião De Sousa , Brazil

Francisco Javier Deive , Spain

Tianlong Deng , China

Fatih Deniz , Turkey  
Claudio Di Iaconi, Italy  
Irene Dini , Italy  
Daniele Dondi, Italy  
Yingchao Dong , China  
Dennis Douroumis , United Kingdom  
John Drexler, USA  
Qizhen Du, China  
Yuanyuan Duan , China  
Philippe Dugourd, France  
Frederic Dumur , France  
Grégory Durand , France  
Mehmet E. Duru, Turkey  
Takayuki Ebata , Japan  
Arturo Espinosa Ferao , Spain  
Valdemar Esteves , Portugal  
Cristina Femoni , Italy  
Gang Feng, China  
Dieter Fenske, Germany  
Jorge F. Fernandez-Sanchez , Spain  
Alberto Figoli , Italy  
Elena Forte, Italy  
Sylvain Franger , France  
Emiliano Fratini , Italy  
Franco Frau , Italy  
Bartolo Gabriele , Italy  
Guillaume Galliero , France  
Andrea Gambaro , Italy  
Vijay Kumar Garlapati, India  
James W. Gauld , Canada  
Barbara Gawdzik , Poland  
Pier Luigi Gentili , Italy  
Beatrice Giannetta , Italy  
Dimosthenis L. Giokas , Greece  
Alejandro Giorgetti , Italy  
Alexandre Giuliani , France  
Elena Gomez , Spain  
Yves Grohens, France  
Katharina Grupp, Germany  
Luis F. Guido , Portugal  
Maolin Guo, USA  
Wenshan Guo , Australia  
Leena Gupta , India  
Muhammad J. Habib, USA  
Jae Ryang Hahn, Republic of Korea

Christopher G. Hamaker , USA  
Ashanul Haque , Saudi Arabia  
Yusuke Hara, Japan  
Naoki Haraguchi, Japan  
Serkos A. Haroutounian , Greece  
Rudi Hendra , Indonesia  
Javier Hernandez-Borges , Spain  
Miguel Herrero, Spain  
Mark Hoffmann , USA  
Hanmin Huang, China  
Doina Humelnicu , Romania  
Charlotte Hurel, France  
Nenad Ignjatović , Serbia  
Ales Imramovsky , Czech Republic  
Muhammad Jahangir, Pakistan  
Philippe Jeandet , France  
Sipak Joyasawal, USA  
Sławomir M. Kaczmarek, Poland  
Ewa Kaczorek, Poland  
Mostafa Khajeh, Iran  
Srećko I. Kirin , Croatia  
Anton Kokalj , Slovenia  
Sevgi Kolaylı , Turkey  
Takeshi Kondo , Japan  
Christos Kordulis, Greece  
Ioannis D. Kostas , Greece  
Yiannis Kourkoutas , Greece  
Henryk Kozłowski, Poland  
Yoshihiro Kudo , Japan  
Avvaru Praveen Kumar , Ethiopia  
Dhanaji Lade, USA  
Isabel Lara , Spain  
Jolanta N. Latosinska , Poland  
João Paulo Leal , Portugal  
Woojin Lee, Kazakhstan  
Yuan-Pern Lee , Taiwan  
Matthias Lein , New Zealand  
Huabing Li, China  
Jinan Li , USA  
Kokhwa Lim , Singapore  
Teik-Cheng Lim , Singapore  
Jianqiang Liu , China  
Xi Liu , China  
Xinyong Liu , China  
Zhong-Wen Liu , China

Eulogio J. Llorent-Martínez , Spain  
Pasquale Longo , Italy  
Pablo Lorenzo-Luis , Spain  
Zhang-Hui Lu, China  
Devanand Luthria, USA  
Konstantin V. Luzyanin , United Kingdom  
Basavarajaiah S M, India  
Mari Maeda-Yamamoto , Japan  
Isabel Mafra , Portugal  
Dimitris P. Makris , Greece  
Pedro M. Mancini, Argentina  
Marcelino Maneiro , Spain  
Giuseppe F. Mangiatordi , Italy  
Casimiro Mantell , Spain  
Carlos A Martínez-Huitle , Brazil  
José M. G. Martinho , Portugal  
Andrea Mastinu , Italy  
Cesar Mateo , Spain  
Georgios Matthaiolampakis, USA  
Mehrab Mehrvar, Canada  
Saurabh Mehta , India  
Oinam Romesh Meitei , USA  
Saima Q. Memon , Pakistan  
Morena Miciaccia, Italy  
Maurice Millet , France  
Angelo Minucci, Italy  
Liviu Mitu , Romania  
Hideto Miyabe , Japan  
Ahmad Mohammad Alakraa , Egypt  
Kaustubha Mohanty, India  
Subrata Mondal , India  
José Morillo, Spain  
Giovanni Morrone , Italy  
Ahmed Mourran, Germany  
Nagaraju Mupparapu , USA  
Markus Muschen, USA  
Benjamin Mwashote , USA  
Mallikarjuna N. Nadagouda , USA  
Lutfun Nahar , United Kingdom  
Kamala Kanta Nanda , Peru  
Senthilkumar Nangan, Thailand  
Mu. Naushad , Saudi Arabia  
Gabriel Navarrete-Vazquez , Mexico  
Jean-Marie Nedelec , France  
Sridhar Goud Nerella , USA  
Nagatoshi Nishiwaki , Japan  
Tzortzis Nomikos , Greece  
Beatriz P. P. Oliveira , Portugal  
Leonardo Palmisano , Italy  
Mohamed Afzal Pasha , India  
Dario Pasini , Italy  
Angela Patti , Italy  
Massimiliano F. Peana , Italy  
Andrea Penoni , Italy  
Franc Perdih , Slovenia  
Jose A. Pereira , Portugal  
Pedro Avila Pérez , Mexico  
Maria Grazia Perrone , Italy  
Silvia Persichilli , Italy  
Thijs A. Peters , Norway  
Christophe Petit , France  
Marinos Pitsikalis , Greece  
Rita Rosa Plá, Argentina  
Fabio Polticelli , Italy  
Josefina Pons, Spain  
V. Prakash Reddy , USA  
Thathan Premkumar, Republic of Korea  
Maciej Przybyłek , Poland  
María Quesada-Moreno , Germany  
Maurizio Quinto , Italy  
Franck Rabilloud , France  
C.R. Raj, India  
Sanchayita Rajkhowa , India  
Manzoor Rather , India  
Enrico Ravera , Italy  
Julia Revuelta , Spain  
Muhammad Rizwan , Pakistan  
Manfredi Rizzo , Italy  
Maria P. Robalo , Portugal  
Maria Roca , Spain  
Nicolas Roche , France  
Samuel Rokhum , India  
Roberto Romeo , Italy  
Antonio M. Romerosa-Nievas , Spain  
Arpita Roy , India  
Eloy S. Sanz P rez , Spain  
Nagaraju Sakkani , USA  
Diego Sampedro , Spain  
Shengmin Sang , USA

Vikram Sarpe , USA  
Adrian Saura-Sanmartin , Spain  
Stéphanie Sayen, France  
Ewa Schab-Balcerzak , Poland  
Hartwig Schulz, Germany  
Gulaim A. Seisenbaeva , Sweden  
Serkan Selli , Turkey  
Murat Senturk , Turkey  
Beatrice Severino , Italy  
Sunil Shah Shah , USA  
Ashutosh Sharma , USA  
Hideaki Shirota , Japan  
Cláudia G. Silva , Portugal  
Ajaya Kumar Singh , India  
Vijay Siripuram, USA  
Ponnurengam Malliappan Sivakumar ,  
Japan  
Tomás Sobrino , Spain  
Raquel G. Soengas , Spain  
Yujiang Song , China  
Olivier Soppera, France  
Radhey Srivastava , USA  
Vivek Srivastava, India  
Theocharis C. Stamatatos , Greece  
Athanasios Stavrakoudis , Greece  
Darren Sun, Singapore  
Arun Suneja , USA  
Kamal Swami , USA  
B.E. Kumara Swamy , India  
Elad Tako , USA  
Shoufeng Tang, China  
Zhenwei Tang , China  
Vijai Kumar Reddy Tangadanchu , USA  
Franco Tassi, Italy  
Alexander Tatarinov, Russia  
Lorena Tavano, Italy  
Tullia Tedeschi, Italy  
Vinod Kumar Tiwari , India  
Augusto C. Tome , Portugal  
Fernanda Tonelli , Brazil  
Naoki Toyooka , Japan  
Andrea Trabocchi , Italy  
Philippe Trens , France  
Ekaterina Tsipis, Russia  
Esteban P. Urriolabeitia , Spain

Toyonobu Usuki , Japan  
Giuseppe Valacchi , Italy  
Ganga Reddy Velma , USA  
Marco Viccaro , Italy  
Jaime Villaverde , Spain  
Marc Visseaux , France  
Balaga Viswanadham , India  
Alessandro Volonterio , Italy  
Zoran Vujcic , Serbia  
Chun-Hua Wang , China  
Leiming Wang , China  
Carmen Wängler , Germany  
Wieslaw Wiczowski , Poland  
Bryan M. Wong , USA  
Frank Wuest, Canada  
Yang Xu, USA  
Dharmendra Kumar Yadav , Republic of  
Korea  
Maria C. Yebra-Biurrún , Spain  
Dr Nagesh G Yernale, India  
Tomokazu Yoshimura , Japan  
Maryam Yousaf, China  
Sedat Yurdakal , Turkey  
Shin-ichi Yusa , Japan  
Claudio Zaccone , Italy  
Ronen Zangi, Spain  
John CG Zhao , USA  
Zhen Zhao, China  
Antonio Zizzi , Italy  
Mire Zloh , United Kingdom  
Grigoris Zoidis , Greece  
Deniz ŞAHİN , Turkey





# Contents

## **On the Hosoya Indices of Bicyclic Graphs with Small Diameter**

Tingzeng Wu  and Yong Yu




Research Article (14 pages), Article ID 5555700, Volume 2021 (2021)

## **Characterization of (Molecular) Graphs with Fractional Metric Dimension as Unity**

Muhammad Javaid , Muhammad Kamran Aslam, Abdulaziz Mohammed Alanazi , and Meshari M. Aljohani

Research Article (12 pages), Article ID 9910572, Volume 2021 (2021)

## **Topological Study of Zeolite Socony Mobil-5 via Degree-Based Topological Indices**

Nouman Saeed , Kai Long , Tanweer Ul Islam, Zeeshan Saleem Mufti , and Ayesha Abbas


Research Article (13 pages), Article ID 5522800, Volume 2021 (2021)

## **On the Computation of Some Topological Descriptors to Find Closed Formulas for Certain Chemical Graphs**

Muhammad Haroon Aftab , Muhammad Rafaqat , M. Hussain , and Tariq Zia 




Research Article (16 pages), Article ID 5533619, Volume 2021 (2021)

## **Analysis of Dendrimer Generation by Sombor Indices**

Shahid Amin, Abaid Ur Rehman Virk, M.A. Rehman, and Nehad Ali Shah 

Research Article (11 pages), Article ID 9930645, Volume 2021 (2021)

## **Forgotten Index of Generalized Operations on Graphs**

Muhammad Javaid , Saira Javed , Saima Q. Memon, and Abdulaziz Mohammed Alanazi 


Research Article (14 pages), Article ID 9971277, Volume 2021 (2021)

## **Application of Resolvability Technique to Investigate the Different Polyphenyl Structures for Polymer Industry**

Muhammad Faisal Nadeem , Mohsan Hassan, Muhammad Azeem , Salah Ud-Din Khan, Mohammed Rafi Shaik , Mohammed A. F. Sharaf, Abdelatty Abdelgawad, and Emad Mahrous Awwad





Research Article (8 pages), Article ID 6633227, Volume 2021 (2021)

## **Degree-Based Topological Indices of Polysaccharides: Amylose and Blue Starch-Iodine Complex**

Anam Rani and Usman Ali 


Research Article (10 pages), Article ID 6652014, Volume 2021 (2021)

## **Degree-Based Topological Indices of Boron B<sub>12</sub>**

Nouman Saeed , Kai Long , Zeeshan Saleem Mufti , Hafsa Sajid, and Abdul Rehman 


Research Article (6 pages), Article ID 5563218, Volume 2021 (2021)

## **COD Optimization Prediction Model Based on CAWOA-ELM in Water Ecological Environment**






Lili Jiang, Liu Yang , Yang Huang, Yi Wu, Huixian Li, XiYan Shen, Meng Bi, Lin Hong, Yiting Yang, Zuping Ding, and Wenjie Chen

Research Article (9 pages), Article ID 6611777, Volume 2021 (2021)





**Computing Bounds of Fractional Metric Dimension of Metal Organic Graphs**

Mohsin Raza, Dalal Awadh Alrowaili, Muhammad Javaid , and Khurram Shabbir  
Research Article (12 pages), Article ID 5539569, Volume 2021 (2021)



**An Approach to the Extremal Inverse Degree Index for Families of Graphs with Transformation Effect**

Muhammad Asif , Muhammad Hussain , Hamad Almohamedh , Khalid M. Alhamed , and Sultan Almotairi   
Research Article (8 pages), Article ID 6657039, Volume 2021 (2021)



**M-Polynomials and Degree-Based Topological Indices of the Molecule Copper(I) Oxide**

Faryal Chaudhry, Iqra Shoukat, Deeba Afzal , Choonkil Park , Murat Cancan , and Mohammad Reza Farahani   
Research Article (12 pages), Article ID 6679819, Volume 2021 (2021)

**Topological Indices of Derived Networks of Benzene Ring Embedded in  $P$ -Type Surface on  $2D$**

Feng Yin, Muhammad Numan, Saad Ihsan Butt , Adnan Aslam , and Andleeb Kausar  
Research Article (11 pages), Article ID 6614840, Volume 2021 (2021)

**Computing Analysis of Zagreb Indices for Generalized Sum Graphs under Strong Product**

Muhammad Javaid , Saira Javed , Abdulaziz Mohammed Alanazi, and Majdah R. Alotaibi  
Research Article (20 pages), Article ID 6663624, Volume 2021 (2021)

## Research Article

# On the Hosoya Indices of Bicyclic Graphs with Small Diameter

Tingzeng Wu  and Yong Yu

School of Mathematics and Statistics, Qinghai Nationalities University, Xining, Qinghai 810007, China

Correspondence should be addressed to Tingzeng Wu; [mathtzwu@163.com](mailto:mathtzwu@163.com)

Received 27 February 2021; Revised 7 June 2021; Accepted 17 August 2021; Published 3 September 2021

Academic Editor: Muhammad Faisal Nadeem

Copyright © 2021 Tingzeng Wu and Yong Yu. This is an open access article distributed under the Creative Commons Attribution License, which permits unrestricted use, distribution, and reproduction in any medium, provided the original work is properly cited.

Let  $G$  be a graph. The Hosoya index of  $G$ , denoted by  $z(G)$ , is defined as the total number of its matchings. The computation of  $z(G)$  is NP-Complete. Wagner and Gutman pointed out that it is difficult to obtain results of the maximum Hosoya index among tree-like graphs with given diameter. In this paper, we focus on the problem, and a sharp bound of Hosoya indices of all bicyclic graphs with diameter of 3 is determined.

## 1. Introduction

Hosoya index is an important topological index introduced by Hosoya [1]. It was found that Hosoya index is related to a variety of physicochemical properties of alkanes (= saturated hydrocarbons). In particular, the boiling points of alkanes are well correlated with Hosoya index. Another series of researches revealed the applicability of Hosoya index in the theory of conjugated  $\pi$ -electron systems [2, 3]. Jerrum [4] showed that the computing complexity of Hosoya index is NP-Complete. The Hosoya index got much attention by many researchers in the past decades. They have been interested in identifying the extremal value of Hosoya index for various classes of graphs, such as trees [5–7], unicyclic graphs [8–12], bicyclic graphs [13], and  $(n, m)$ -graphs [14, 15]. Wagner and Gutman [16] gave an exhaustive survey for Hosoya index, and they pointed out some open problems (also see [17]) as follows:

- It seems difficult to obtain results of the maximum Hosoya index among trees with a given number of leaves or given diameter. However, partial results are available, so the problem might not be totally intractable, and results in this direction would definitely be interesting.
- If the aforementioned questions can be answered for trees, then it is also natural to consider the analogous questions for tree-like graphs.

According to the open problems, Liu et al. [17] discussed the problem in which unicyclic graph with diameter of 3 or 4 has the maximum Hosoya index. In this paper, we focus on similar problems to the above. That is, which bicyclic graph with diameter of 3 has the maximum Hosoya index? We give an answer of the problem as follows.

**Theorem 1.**  $G \in \mathcal{B}_n^3$  and  $n \geq 10$ ; each of the following holds:

$$\begin{aligned}
 \text{(i) If } 10 \leq n \leq 15. \text{ Then } z(G) \leq & \begin{cases} \frac{3}{2}n^2 - 8n + 16, & \text{where } n \text{ is even, and the equality holds} \\ \text{iff } G \cong G_{14}\left(\frac{n-4}{2}, \frac{n-6}{2}\right); \\ \frac{3}{2}n^2 - 8n + 20, & \text{where } n \text{ is odd, and the equality holds} \\ \text{iff } G \cong G_{14}\left(\frac{n-5}{2}, \frac{n-5}{2}\right), \end{cases} \\
 \text{(ii) If } n \geq 16. \text{ Then } z(G) \leq & \begin{cases} \frac{2n^3 - 6n^2 + 63n - 54}{27}, & \text{where } n \equiv 0 \pmod{3}, \text{ and the equality holds} \\ \text{iff } G \cong G_{10}\left(\frac{n-3}{3}, \frac{n-3}{3}, \frac{n-3}{3}\right); \\ \frac{2n^3 - 6n^2 + 60n - 56}{27}, & \text{where } n \equiv 1 \pmod{3}, \text{ and the equality holds iff} \\ G \cong G_{10}\left(\frac{n-1}{3}, \frac{n-1}{3}, \frac{n-4}{3}\right) \cong G_{10}\left(\frac{n-4}{3}, \frac{n-1}{3}, \frac{n-1}{3}\right); \\ \frac{2n^3 - 6n^2 + 63n - 64}{27}, & \text{where } n \equiv 2 \pmod{3}, \text{ and the equality holds} \\ \text{iff } G \cong G_{10}\left(\frac{n-2}{3}, \frac{n-2}{3}, \frac{n-2}{3}\right). \end{cases} \tag{1}
 \end{aligned}$$

The rest of this paper is organized as follows. In Section 2, we shall present some definitions and lemmas. In Section 3, we will prove Theorem 1. Furthermore, some upper bounds for Hosoya index of some special classes of bicyclic graphs with diameter of 3 are also determined.

## 2. Preliminaries

In this paper, we only consider finite and simple graphs. Let  $G = (V(G), E(G))$  be a graph with  $n$  vertices and  $m$  edges. The neighborhood of vertex  $v \in V(G)$  in a graph  $G$ , denoted by  $N_G(v)$ , is the set of vertices adjacent to  $v$ . The degree of  $v$ , denoted by  $d(v)$ , is the number of neighbors of  $v$  in  $G$ . The distance of two vertices  $u, v \in V(G)$  is the length of a shortest path from  $u$  to  $v$ , denoted by  $d_G(u, v)$ . We will use  $G - v$  to represent the graph after  $G$  deleting the vertex  $v$ . The diameter of  $G$  is  $\max\{d_G(u, v) \mid u, v \in V(G)\}$ .

Let  $\mathcal{B}_n^3$  be the set of all bicyclic graphs with  $n$  vertices and diameter of 3. It is easy to verify that the structure of graph  $G \in \mathcal{B}_n^3$  must be isomorphic to  $G_i$ , where  $i = 1, 2, \dots, 14$ . The resulting graph  $G_i$  can be seen in Figure 1.

Let  $m(G, k)$  be the number of  $k$ -matchings of  $G$ . It is convenient to denote  $m(G, 0) = 1$  and  $m(G, k) = 0$  for  $k > \lfloor n/2 \rfloor$ . The Hosoya index of  $G$ , denoted by  $z(G)$ , is defined as the sum of all the numbers of its matchings; namely,

$$z(G) = \sum_{k=0}^{\lfloor n/2 \rfloor} m(G, k). \tag{2}$$

**Lemma 1** (see [16]). *Let  $G$  be a graph and let  $v$  be a vertex of graph  $G$ . Then*

- (i)  $z(G) = z(G - v) + \sum_{u \in N_G(v)} z(G - \{u, v\})$
- (ii)  $z(G) = \prod_{i=1}^t z(G_i)$ , where  $G_i$  is a component of  $G$

Let  $G$  be a graph obtained by joining the centers of two stars  $K_{1,p-1}$  and  $K_{1,q-1}$ , denoted by  $S(p, q)$ . By Lemma 1, we obtain the following result.

**Lemma 2**

- (i)  $z(K_{1,p}) = 1 + p$
- (ii)  $z(S_{p,q}) = pq + 1$

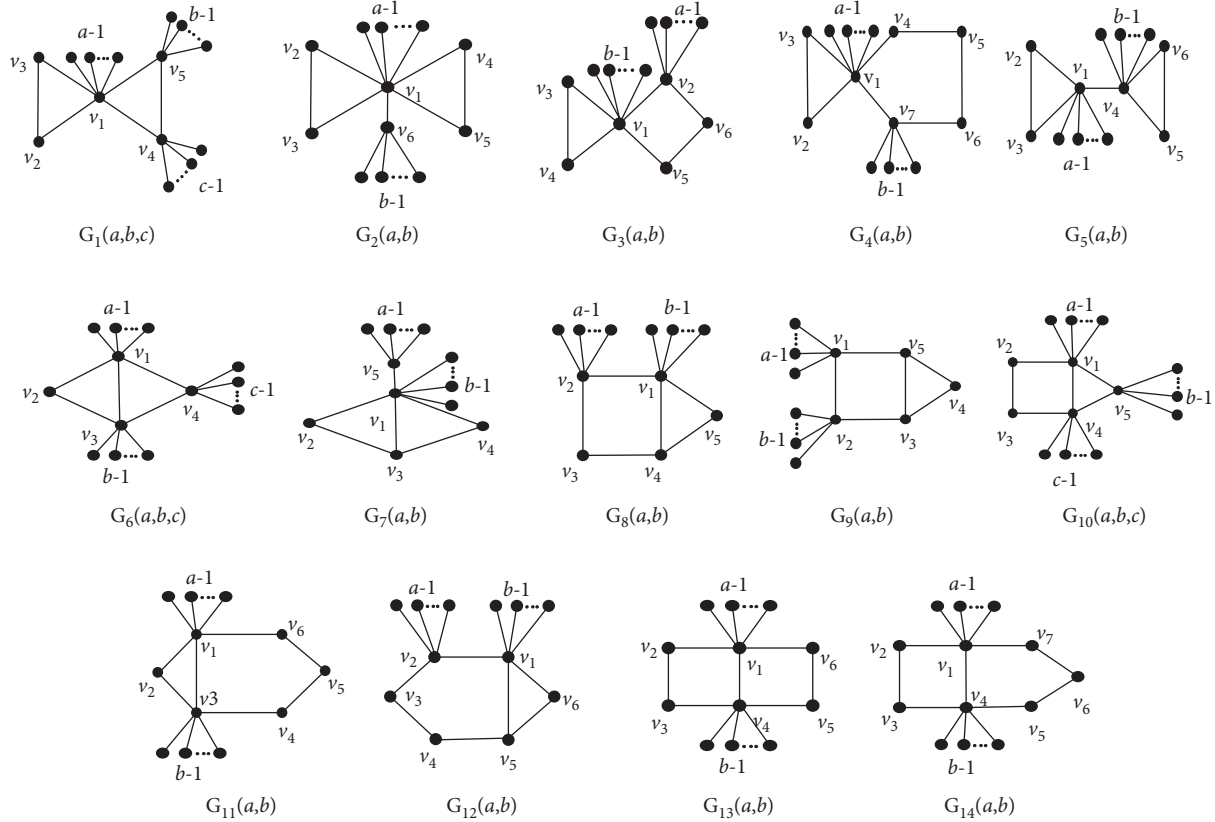


FIGURE 1: All bicyclic graphs  $G_i$ ,  $i = 1, 2, \dots, 14$ , with diameter of 3.

### 3. The Proof of Theorem 1

In order to prove Theorem 1, we first give some lemmas.

**Lemma 3.** Let  $G \in G_1(a, b, c)$  be a graph with  $n$  vertices. Then

$$z(G) \leq \begin{cases} \frac{2}{27}(n^3 - 3n^2 + 27n - 27), & \text{where } n \equiv 0 \pmod{3}, n \geq 9 \text{ and the equality holds iff} \\ & G \cong G_1\left(\frac{n-3}{3}, \frac{n-3}{3}, \frac{n}{3}\right) \cong G_1\left(\frac{n-3}{3}, \frac{n}{3}, \frac{n-3}{3}\right) \cong G_1\left(\frac{n-6}{3}, \frac{n}{3}, \frac{n}{3}\right); \\ \frac{2}{27}(n^3 - 3n^2 + 30n - 28), & \text{where } n \equiv 1 \pmod{3}, n \geq 10 \text{ and the equality holds} \\ & \text{iff } G \cong G_1\left(\frac{n-4}{3}, \frac{n-1}{3}, \frac{n-1}{3}\right); \\ \frac{2}{27}(n^3 - 3n^2 + 27n - 23), & \text{where } n \equiv 2 \pmod{3}, n \geq 11 \text{ and the equality holds} \\ & \text{iff } G \cong G_1\left(\frac{n-5}{3}, \frac{n-2}{3}, \frac{n+1}{3}\right) \cong G_1\left(\frac{n-5}{3}, \frac{n+1}{3}, \frac{n-2}{3}\right). \end{cases} \quad (3)$$

*Proof.* Consider that vertex  $v'$  of degree 1 is adjacent to  $v_1$  in  $G_1(a, b, c)$ . By Lemmas 1 and 2, we have  $z(G_1(a, b, c)) = 2abc + 2bc + 2a + 2b + 2c + 2$ . In the following, we use the method of Lagrange multipliers to find the sharp

bound of Hosoya index of  $G \in G_1(a, b, c)$ . First, we make auxiliary function as follows:  $L(a, b, c) = \lambda(a + b + c + 2 - n) + 2abc + 2a + 2b + 2c + 2bc + 2$ , where  $a + b + c + 2 = n$ ,  $a, b, c \geq 1$ , and at most one of them is 1. Taking the partial

derivatives of  $a, b, c$ , and  $\lambda$  in  $L(a, b, c, \lambda)$ , we can obtain the following equations:

$$\begin{cases} L_a = \lambda + 2bc + 2 = 0, \\ L_b = \lambda + 2ac + 2 + 2c = 0, \\ L_c = \lambda + 2ab + 2 + 2b = 0, \\ L_\lambda = a + b + c + 2 - n = 0, \\ a \geq 1, b \geq 1 \text{ and } c \geq 1. \end{cases} \quad (4)$$

Solving the equations as above, we obtain that  $a = (n-4)/3$ ,  $b = (n-1)/3$ , and  $c = (n-1)/3$ . Because  $((n-4)/3, t((n-1)/3)n, q((n-1)/3))$  is a unique stable point,  $((n-4)/3, t((n-1)/3)n, q((n-1)/3))$  must be a unique extreme point. Since  $a, b$ , and  $c$  are integers, we consider three cases.

Case 1: assume that  $n \equiv 0 \pmod{3}$ . We know that  $a = (n-3)/3$ ,  $b = (n-3)/3$ , and  $c = (n/3)$ ; or  $a = (n-3)/3$ ,  $b = (n/3)$ , and  $c = (n-3)/3$ ; or  $a = (n-6)/3$ ,  $b = (n/3)$ , and  $c = (n/3)$ . Thus,  $z(G_1((n-3)/3, (n/3), ((n-3)/3))) = z(G_1((n-3)/3, ((n-3)/3), (n/3))) = z(G_1((n-6)/3, (n/3), (n/3))) = (2/27)(n^3 - 3n^2 + 27n - 27)$ . It is easy to verify that  $z(G_1(a, b, c)) < (2/27)(n^3 - 3n^2 + 27n - 27)$  when  $a \neq ((n-6)/3)$ ,  $b \neq (n/3)$ , and  $c \neq (n/3)$ ; or  $a \neq ((n-3)/3)$ ,  $b \neq (n/3)$ , and  $c \neq ((n-3)/3)$ ; or  $a \neq ((n-3)/3)$ ,  $b \neq ((n-3)/3)$ , and  $c \neq (n/3)$ . This implies that  $z(G) \leq (2/27)(n^3 - 3n^2 + 27n - 27)$  and the equality

holds iff  $G \cong G_1((n-3)/3, ((n-3)/3, (n/3)) \cong G_1((n-3)/3, (n/3), ((n-3)/3)) \cong G_1((n-6)/3, t(n/3)n, q(n/3))$ .

Case 2: suppose that  $n \equiv 1 \pmod{3}$ . We have  $a = ((n-4)/3)$ ,  $b = ((n-1)/3)$ , and  $c = ((n-1)/3)$ . So  $z(G_1((n-4)/3, ((n-1)/3, ((n-1)/3))) = (2/27)(n^3 - 3n^2 + 30n - 28)$ . To simplify the calculation, we know that  $z(G_1(a, b, c)) < (2/27)(n^3 - 3n^2 + 30n - 28)$  when  $a \neq ((n-4)/3)$ ,  $b \neq ((n-1)/3)$ , and  $c \neq ((n-1)/3)$ . This means that  $z(G) \leq (2/27)(n^3 - 3n^2 + 30n - 28)$  and the equality holds iff  $G \cong G_1((n-4)/3, t((n-1)/3)n, q((n-1)/3))$ .

Case 3: assume that  $n \equiv 2 \pmod{3}$ . Then  $a = ((n-5)/3)$ ,  $b = ((n-2)/3)$ , and  $c = ((n+1)/3)$ ; or  $a = ((n-5)/3)$ ,  $b = ((n+1)/3)$ , and  $c = ((n-2)/3)$ . Thus,  $z(G_1((n-5)/3, ((n-2)/3, ((n+1)/3))) = z(G_1((n-5)/3, ((n+1)/3, ((n-2)/3))) = (2/27)(n^3 - 3n^2 + 27n - 23)$ . It is easy to check that  $z(G_1(a, b, c)) < (2/27)(n^3 - 3n^2 + 27n - 23)$  when  $a \neq ((n-5)/3)$ ,  $b \neq ((n-2)/3)$ , and  $c \neq ((n+1)/3)$ ; or  $a \neq ((n-5)/3)$ ,  $b \neq ((n+1)/3)$ , and  $c \neq ((n-2)/3)$ . This indicates that  $z(G) \leq (2/27)(n^3 - 3n^2 + 27n - 23)$  and the equality holds if and only if  $G \cong G_1((n-5)/3, ((n-2)/3, ((n+1)/3)) \cong G_1(((n-5)/3, t((n+1)/3)n, q((n-2)/3))$ .  $\square$

**Lemma 4.** Let  $G \in G_2(a, b)$  be a graph with  $n$  vertices. Then

$$z(G) \leq \begin{cases} n^2 - 4n + 8, & \text{where } n \geq 8 \text{ is even, and the equality holds iff } G \cong G_2\left(\frac{n-6}{2}, \frac{n-2}{2}\right); \\ n^2 - 4n + 7, & \text{where } n \geq 9 \text{ is odd, and the equality holds iff } G \cong G_2\left(\frac{n-7}{2}, \frac{n-1}{2}\right) \\ & \text{or } G \cong G_2\left(\frac{n-5}{2}, \frac{n-3}{2}\right). \end{cases} \quad (5)$$

*Proof.* Similar to the proof of Lemma 3, by Lemmas 1 and 2, we have  $z(G_2(a, b)) = 4ab + 8b + 4$ . By the method of Lagrange multipliers, we make an auxiliary function  $L(a, b) = \lambda(a + b + 4 - n) + 4ab + 8b + 4$ , where  $a + b + 4 = n$ ,  $a \geq 1$ , and  $b \geq 2$ . Taking the partial derivatives of  $a, b$ , and  $\lambda$  in  $L(a, b, \lambda)$ , we get the following equations:

$$\begin{cases} L_a = \lambda + 4b = 0, \\ L_b = \lambda + 4a + 8 = 0, \\ L_\lambda = a + b + 4 - n = 0, \\ a \geq 1 \text{ and } b \geq 2. \end{cases} \quad (6)$$

Solving the equations as above, we obtain that  $a = ((n-6)/2)$  and  $b = ((n-2)/2)$ . Because  $((n-6)/2, t((n-2)/2))$  is a unique stable point,  $((n-6)/2, t((n-2)/2))$  must be the unique extreme point. Since  $a$  and  $b$  are integers, in the following we consider two cases:

Case 1: suppose that  $n$  is even. Then  $a = ((n-6)/2)$  and  $b = ((n-2)/2)$ . Thus,  $z(G_2(((n-6)/2), ((n-2)/2))) = 4ab + 8b + 4 = n^2 - 4n + 8$ . To simplify calculation, we know that  $z(G_2(a, b)) < n^2 - 4n + 8$  when  $a \neq ((n-6)/2)$  and  $b \neq ((n-2)/2)$ . This implies that  $z(G) \leq n^2 - 4n + 8$  and the equality holds iff  $G \cong G_2(((n-6)/2), t((n-2)/2))$ .

Case 2: assume that  $n$  is odd. We obtain  $a = ((n-7)/2)$  and  $b = ((n-1)/2)$ , or  $a = ((n-5)/2)$  and  $b = ((n-3)/2)$ . So,  $z(G_2(((n-7)/2), ((n-1)/2))) = z(G_2(((n-5)/2), ((n-3)/2))) = n^2 - 4n + 7$ . It is easy to check that  $z(G_2(a, b)) < n^2 - 4n + 7$  when  $a \neq ((n-7)/2)$  and  $b \neq ((n-1)/2)$ , or  $a \neq ((n-5)/2)$  and  $b \neq ((n-3)/2)$ . This means that  $z(G) \leq n^2 - 4n + 7$  and

the equality holds iff  $G \cong G_2((n-7)/2, (n-1)/2) \cong G_2((n-5)/2, t((n-3)/2))$ .  $\square$

**Lemma 5.** Let  $G \in G_3(a, b)$  be a graph with  $n$  vertices. Then

$$z(G) \leq \begin{cases} n^2 - 4n + 8, & \text{where } n \geq 8 \text{ is even, and the equality holds iff} \\ & G \cong G_3\left(\frac{n-4}{2}, \frac{n-4}{2}\right) \cong G_3\left(\frac{n-2}{2}, \frac{n-6}{2}\right); \\ n^2 - 4n + 9, & \text{where } n \geq 7 \text{ is odd, and the equality holds iff } G \cong G_3\left(\frac{n-3}{2}, \frac{n-5}{2}\right). \end{cases} \quad (7)$$

*Proof.* Similar to the proof of Lemma 3, by Lemmas 1 and 2, we get that  $z(G_3(a, b)) = 4ab + 6a + 2b + 8$ . According to the method of Lagrange multipliers, we make an auxiliary function  $L(a, b) = \lambda(a + b + 4 - n) + 4ab + 6a + 2b + 8$ , where  $a + b + 4 = n$ ,  $a \geq 1$ , and  $b \geq 1$ . Taking the partial derivatives of  $a, b$ , and  $\lambda$  in  $L(a, b, \lambda)$ , we obtain the following equations:

$$\begin{cases} L_a = \lambda + 4b + 6 = 0, \\ L_b = \lambda + 4a + 2 = 0, \\ L_\lambda = a + b + 4 - n = 0, \\ a \geq 1 \text{ and } b \geq 1. \end{cases} \quad (8)$$

Solving the equations as above, we obtain that  $a = ((n-3)/2)$  and  $b = ((n-5)/2)$ . Because  $((n-3)/2, t((n-5)/2))$  is a unique stable point,  $((n-3)/2, t((n-5)/2))$  must be the unique extreme point. Since  $a$  and  $b$  are integers, we only consider two cases.

Case 1: assume that  $n$  is even. We obtain  $a = ((n-4)/2)$  and  $b = ((n-4)/2)$ , or  $a = ((n-2)/2)$  and  $b = ((n-6)/2)$ . Thus,  $z(G_3((n-4)/2, (n-4)/2)) = z(G_3((n-2)/2, (n-6)/2)) = n^2 - 4n + 8$ . It is easy to check that  $z(G_3(a, b)) < n^2 - 4n + 8$  when  $a \neq ((n-4)/2)$  and  $b \neq ((n-4)/2)$ , or  $a \neq ((n-2)/2)$  and  $b \neq ((n-6)/2)$ . This implies that  $z(G) \leq n^2 - 4n + 8$  and the equality holds if and only if  $G \cong G_3((n-4)/2, (n-4)/2) \cong G_3((n-2)/2, t((n-6)/2))$ .

Case 2: consider that  $n$  is odd. We have  $a = ((n-3)/2)$  and  $b = ((n-5)/2)$ . So,  $z(G_3((n-3)/2, (n-5)/2)) = n^2 - 4n + 9$ . It is easy to verify that  $z(G_3(a, b)) < n^2 - 4n + 9$  when  $a \neq ((n-3)/2)$  and  $b \neq ((n-5)/2)$ . This means that  $z(G) \leq n^2 - 4n + 9$  and the equality holds if and only if  $G \cong G_3((n-3)/2, t((n-5)/2))$ .  $\square$

**Lemma 6.** Let  $G \in G_4(a, b)$  be a graph with  $n$  vertices. Then

$$z(G) \leq \begin{cases} \frac{3}{2}n^2 - 8n + 16, & \text{where } n \geq 8 \text{ is even, and the equality holds iff } G \cong G_4\left(\frac{n-6}{2}, \frac{n-4}{2}\right); \\ \frac{3}{2}n^2 - 8n + \frac{29}{2}, & \text{where } n \geq 7 \text{ is odd, and the equality holds} \\ & \text{iff } G \cong G_4\left(\frac{n-5}{2}, \frac{n-5}{2}\right) \cong G_4\left(\frac{n-7}{2}, \frac{n-3}{2}\right). \end{cases} \quad (9)$$

*Proof.* Similar to the proof of Lemma 3, by Lemmas 1 and 2, we get  $z(G_4(a, b)) = 6ab + 4a + 10b + 12$ . According to the method of Lagrange multipliers, we make an auxiliary function  $L(a, b) = \lambda(a + b + 5 - n) + 6ab + 4a + 10b + 12$ , where  $a + b + 5 = n$ ,  $a \geq 1$ , and  $b \geq 1$ . Taking the partial derivatives of  $a, b$ , and  $\lambda$  in  $L(a, b, \lambda)$ , we can obtain the following equations:

$$\begin{cases} L_a = \lambda + 6b + 4 = 0, \\ L_b = \lambda + 6a + 10 = 0, \\ L_\lambda = a + b + 5 - n = 0, \\ a \geq 1 \text{ and } b \geq 1. \end{cases} \quad (10)$$

Solving the equations as above, we obtain that  $a = ((n-6)/2)$  and  $b = ((n-4)/2)$ . Because  $((n-6)/2, t((n-4)/2))$  is a unique stable point,  $((n-6)/2, t((n-4)/2))$  must be the unique extreme point. Since  $a$  and  $b$  are integers, we only consider two cases:

Case 1: consider that  $n$  is even. We have  $a = ((n-6)/2)$  and  $b = ((n-4)/2)$ . Thus  $z(G_4((n-6)/2, (n-4)/2)) = (3/2)n^2 - 8n + 16$ . To simplify calculation, we get  $z(G_4(a, b)) < (3/2)n^2 - 8n + 16$  when  $a \neq ((n-6)/2)$  and  $b \neq ((n-4)/2)$ . This implies that  $z(G) \leq (3/2)n^2 - 8n + 16$  and the equality holds iff  $G \cong G_4((n-6)/2, t((n-4)/2))$ .

Case 2: assume that  $n$  is odd. Then  $a = ((n-5)/2)$  and  $b = ((n-5)/2)$ , or  $a = ((n-7)/2)$  and  $b = ((n-3)/2)$ . So  $z(G_4(((n-5)/2), ((n-5)/2))) = z(G_4(((n-7)/2), ((n-3)/2))) = (3/2)n^2 - 8n + (29/2)$ . It is easy to check that  $z(G_4(a, b)) < (3/2)n^2 - 8n + (29/2)$  when  $a \neq ((n-5)/2)$  and  $b \neq ((n-5)/2)$ , or  $a \neq ((n-7)/2)$  and  $b \neq ((n-3)/2)$ . This implies that  $z(G) \leq (3/2)n^2 -$

$8n + (29/2)$  and the equality holds if and only if  $G \cong G_4(((n-5)/2), ((n-5)/2)) \cong G_4(((n-7)/2), t((n-3)/2))$ .  $\square$

**Lemma 7.** Let  $G \in G_5(a, b)$  be a graph with  $n$  vertices. Then

$$z(G) \leq \begin{cases} n^2 - 4n + 8, & \text{where } n \geq 6 \text{ is even, and the equality holds iff } G \cong G_5\left(\frac{n-4}{2}, \frac{n-4}{2}\right); \\ & \text{where } n \geq 7 \text{ is odd, and the equality holds} \\ n^2 - 4n + 7, & \text{iff } G \cong G_5\left(\frac{n-3}{2}, \frac{n-5}{2}\right) \cong G_5\left(\frac{n-5}{2}, \frac{n-3}{2}\right). \end{cases} \quad (11)$$

*Proof.* Similar to the proof of Lemma 3, by Lemmas 1 and 2, we get  $z(G_5(a, b)) = 4ab + 4a + 4b + 8$ . By the method of Lagrange multipliers, we make an auxiliary function  $L(a, b) = \lambda(a + b + 4 - n) + 4ab + 4a + 4b + 8$ , where  $a + b + 4 = n$ ,  $a \geq 1$ , and  $b \geq 1$ . Taking the partial derivatives of  $a, b$ , and  $\lambda$  in  $L(a, b, \lambda)$ , we can obtain the following equations:

$$\begin{cases} L_a = \lambda + 4b + 4 = 0, \\ L_b = \lambda + 4a + 4 = 0, \\ L_\lambda = a + b + 4 - n = 0, \\ a \geq 1 \text{ and } b \geq 1. \end{cases} \quad (12)$$

Solving the equations as above, we obtain that  $a = ((n-4)/2)$  and  $b = ((n-4)/2)$ . Because  $((n-4)/2, t((n-4)/2))$  is a unique stable point,  $((n-4)/2, t((n-4)/2))$  must be the unique extreme point. Since  $a$  and  $b$  are integers, in the following we only consider two cases.

Case 1: consider that  $n$  is even. We have  $a = ((n-4)/2)$  and  $b = ((n-4)/2)$ . Thus  $z(G_5(((n-4)/2), ((n-4)/2))) = n^2 - 4n + 8$ . To simplify calculation, we get  $z(G_5(a, b)) < n^2 - 4n + 8$  when  $a \neq ((n-4)/2)$  and  $b \neq ((n-4)/2)$ . This implies that  $z(G) \leq n^2 - 4n + 8$  and the equality holds iff  $G \cong G_5(((n-4)/2), t((n-4)/2))$ .

Case 2: assume that  $n$  is odd. Then  $a = ((n-3)/2)$  and  $b = ((n-5)/2)$ , or  $a = ((n-5)/2)$  and  $b = ((n-3)/2)$ . So  $z(G_5(((n-3)/2), ((n-5)/2))) = z(G_5(((n-5)/2), ((n-3)/2))) = n^2 - 4n + 7$ . It is easy to check that  $z(G_5(a, b)) < n^2 - 4n + 7$  when  $a \neq ((n-3)/2)$  and  $b \neq ((n-5)/2)$ , or  $a \neq ((n-5)/2)$  and  $b \neq ((n-3)/2)$ . This implies that  $z(G) \leq n^2 - 4n + 7$  and the equality holds if and only if  $G \cong G_5(((n-3)/2), ((n-5)/2)) \cong G_5(((n-5)/2), t((n-3)/2))$ .  $\square$

**Lemma 8.** Let  $G \in G_6(a, b, c)$  be a graph with  $n$  vertices. Then



$$z(G) \leq \begin{cases} \frac{n^3 + 3n^2 + 18n + 27}{27}, & \text{where } n \equiv 0 \pmod{3}, n \geq 9 \text{ and the equality holds} \\ & \text{if and only if } G \cong G_6\left(\frac{n-3}{3}, \frac{n}{3}, \frac{n}{3}\right) \cong G_6\left(\frac{n}{3}, \frac{n-3}{3}, \frac{n}{3}\right); \\ \frac{n^3 + 3n^2 + 18n + 32}{27}, & \text{where } n \equiv 1 \pmod{3}, n \geq 7 \text{ and the equality holds} \\ & \text{if and only if } G \cong G_6\left(\frac{n-1}{3}, \frac{n-1}{3}, \frac{n-1}{3}\right); \\ \frac{n^3 + 3n^2 + 21n + 19}{27}, & \text{where } n \equiv 2 \pmod{3}, n \geq 8 \text{ and the equality holds} \\ & \text{if and only if } G \cong G_6\left(\frac{n-2}{3}, \frac{n-2}{3}, \frac{n+1}{3}\right). \end{cases} \quad (13)$$

*Proof.* Similar to the proof of Lemma 3, by Lemmas 1 and 2, direct computing yields  $z(G_6(a, b, c)) = abc + bc + ac + a + b + c + 2$ . By the method of Lagrange multipliers, we make auxiliary function  $L(a, b, c) = \lambda(a + b + c + 1 - n) + abc + bc + ac + a + b + c + 2$ , where  $a + b + c + 1 = n$ ,  $a, b, c \geq 1$ , and at most one of them is 1. Taking the partial derivatives of  $a, b, c$ , and  $\lambda$  in  $L(a, b, c, \lambda)$ , we can obtain the following equations:

$$\begin{cases} L_a = \lambda + bc + c + 1 = 0, \\ L_b = \lambda + ac + c + 1 = 0, \\ L_c = \lambda + ab + b + a + 1 = 0, \\ L_\lambda = a + b + c + 1 - n = 0, \\ a \geq 1, b \geq 1 \text{ and } c \geq 1. \end{cases} \quad (14)$$

Solving the equations as above, we get  $c = a + 1 - (1/(a + 1))$ . Since  $c = a + 1 - (1/(a + 1))$  is an integer, we know that  $c = [a + 1 - (1/(a + 1))]$  or  $c = \lfloor a + 1 - (1/(a + 1)) \rfloor$ . By  $c = [a + 1 - (1/(a + 1))]$  and  $a + b + c + 1 = n$ , we can obtain that  $a = ((n - 2)/3)$ ,  $b = ((n - 2)/3)$ , and  $c = ((n + 1)/3)$ . Similarly, by  $c = \lfloor a + 1 - (1/(a + 1)) \rfloor$  and  $a + b + c + 1 = n$ , we also can obtain that  $a = ((n - 1)/3)$ ,  $b = ((n - 1)/3)$ , and  $c = ((n - 1)/3)$ . Thus, we discuss two cases as follows:

Case 1:  $a = ((n - 2)/3)$ ,  $b = ((n - 2)/3)$ , and  $c = ((n + 1)/3)$ .

Because  $a = ((n - 2)/3)$ ,  $b = ((n - 2)/3)$ , and  $c = ((n + 1)/3)$  is a unique root of (14),  $a = ((n - 2)/3)$ ,  $b = ((n - 2)/3)$ , and  $c = ((n + 1)/3)$  must be the unique extreme point. Since  $a, b$ , and  $c$  are integers, we consider three subcases:

Subcase 1: assume that  $n \equiv 0 \pmod{3}$ . Then  $a = ((n - 3)/3)$ ,  $b = (n/3)$ , and  $c = (n/3)$ , or  $a = (n/3)$ ,  $b = ((n - 3)/3)$ , and  $c = (n/3)$ . Thus  $z(G_6(((n - 3)/3), (n/3), (n/3))) = z(G_6((n/3), ((n - 3)/3), (n/3))) = (n^3 + 3n^2 + 18n + 27)/27$ . It is easy to verify that  $z(G_6(a, b, c)) < ((n^3 + 3n^2 + 18n + 27)/27)$

when  $a \neq ((n - 3)/3)$ ,  $b \neq ((n - 3)/3)$ , and  $c \neq ((n + 3)/3)$ , or  $a \neq ((n - 3)/3)$ ,  $b \neq ((n - 3)/3)$ , and  $c \neq ((n + 3)/3)$ . This implies that  $z(G) \leq ((n^3 + 3n^2 + 18n + 27)/27)$  and the equality holds if and only if  $G \cong G_6(((n - 3)/3), (n/3), (n/3)) \cong G_6((n/3), ((n - 3)/3), t(n/3))$ .

Subcase 2: suppose that  $n \equiv 1 \pmod{3}$ . Then  $a = ((n - 1)/3)$ ,  $b = ((n - 1)/3)$ , and  $c = ((n - 1)/3)$ . Thus  $z(G_6(((n - 1)/3), ((n - 1)/3), ((n - 1)/3))) = (n^3 + 3n^2 + 18n + 32)/27$ . It is easy to check that  $z(G_6(a, b, c)) < (n^3 + 3n^2 + 18n + 32)/27$  when  $a \neq ((n - 1)/3)$ ,  $b \neq ((n - 1)/3)$ , and  $c \neq ((n - 1)/3)$ . This implies that  $z(G) \leq ((n^3 + 3n^2 + 18n + 32)/27)$  and the equality holds iff  $G \cong G_6(((n - 1)/3), t((n - 1)/3)n, q((n - 1)/3))$ .

Subcase 3: consider that  $n \equiv 2 \pmod{3}$ . Then  $a = ((n - 2)/3)$ ,  $b = ((n - 2)/3)$ , and  $c = ((n + 1)/3)$ . Thus  $z(G_6(((n - 2)/3), ((n - 2)/3), ((n + 1)/3))) = ((n^3 + 3n^2 + 21n + 19)/27)$ . To simplify calculation, we know that  $z(G_6(a, b, c)) < ((n^3 + 3n^2 + 21n + 19)/27)$  when  $a \neq ((n - 2)/3)$ ,  $b \neq ((n - 2)/3)$ , and  $c \neq ((n + 1)/3)$ . This implies that  $z(G) \leq ((n^3 + 3n^2 + 21n + 19)/27)$  and the equality holds iff  $G \cong G_6(((n - 2)/3), t((n - 2)/3)n, q((n + 1)/3))$ .

Case 2:  $a = ((n - 1)/3)$ ,  $b = ((n - 1)/3)$ , and  $c = ((n - 1)/3)$ .

Similar to the proof of Case 1, because  $a = ((n - 1)/3)$ ,  $b = ((n - 1)/3)$ , and  $c = ((n - 1)/3)$  is a unique root of (14),  $a = ((n - 1)/3)$ ,  $b = ((n - 1)/3)$ , and  $c = ((n - 1)/3)$  must be the unique extreme point. Since  $a, b$ , and  $c$  are integers, we also consider the three following subcases:

Subcase 1: set  $n \equiv 0 \pmod{3}$ . Then  $a = ((n - 3)/3)$ ,  $b = (n/3)$ , and  $c = (n/3)$ , or  $a = (n/3)$ ,  $b = ((n - 3)/3)$ , and  $c = (n/3)$ . Thus  $z(G_6(((n - 3)/3), (n/3), (n/3))) = z(G_6((n/3), ((n - 3)/3), (n/3))) = (n^3 + 3n^2 + 18n + 27)/27$ . It is easy to verify that  $z(G_6(a, b, c)) < ((n^3 + 3n^2 + 18n + 27)/27)$  when

$a \neq ((n-3)/3)$ ,  $b \neq ((n-3)/3)$ , and  $c \neq ((n+3)/3)$ , or  $a \neq ((n-3)/3)$ ,  $b \neq ((n-3)/3)$ , and  $c \neq ((n+3)/3)$ . This implies that  $z(G) \leq ((n^3 + 3n^2 + 18n + 27)/27)$  and the equality holds if and only if  $G \cong G_6(((n-3)/3), (n/3), (n/3)) \cong G_6((n/3), ((n-3)/3), t(n/3))$ .  
 Subcase 2: suppose that  $n \equiv 1 \pmod{3}$ . Then  $a = ((n-1)/3)$ ,  $b = ((n-1)/3)$ , and  $c = ((n-1)/3)$ . Thus  $z(G_6(((n-1)/3), ((n-1)/3), ((n-1)/3))) = ((n^3 + 3n^2 + 18n + 32)/27)$ . It is easy to check that  $z(G_6(a, b, c)) < ((n^3 + 3n^2 + 18n + 32)/27)$  when  $a \neq ((n-1)/3)$ ,  $b \neq ((n-1)/3)$ , and  $c \neq ((n-1)/3)$ . This implies that  $z(G) \leq ((n^3 + 3n^2 + 18n + 32)/27)$  and the equality holds iff  $G \cong G_6(((n-1)/3), t((n-1)/3)n, q((n-1)/3))$ .

Subcase 3: consider that  $n \equiv 2 \pmod{3}$ . Then  $a = ((n-2)/3)$ ,  $b = ((n-2)/3)$ , and  $c = ((n+1)/3)$ . Thus  $z(G_6(((n-2)/3), ((n-2)/3), ((n+1)/3))) = ((n^3 + 3n^2 + 21n + 19)/27)$ . To simplify calculation, we know that  $z(G_6(a, b, c)) < ((n^3 + 3n^2 + 21n + 19)/27)$  when  $a \neq ((n-2)/3)$ ,  $b \neq ((n-2)/3)$ , and  $c \neq ((n+1)/3)$ . This implies that  $z(G) \leq ((n^3 + 3n^2 + 21n + 19)/27)$  and the equality holds iff  $G \cong G_6(((n-2)/3), t((n-2)/3)n, q((n+1)/3))$ .  $\square$

**Lemma 9.** Let  $G \in G_7(a, b)$  be a graph with  $n$  vertices. Then

$$z(G) \leq \begin{cases} \frac{3n^2 - 8n + 16}{4}, & \text{where } n \geq 6 \text{ is even, and the equality holds iff } G \cong G_7\left(\frac{n-2}{2}, \frac{n-4}{2}\right); \\ \frac{3n^2 - 8n + 17}{4}, & \text{where } n \geq 7 \text{ is odd, and the equality holds iff } G \cong G_7\left(\frac{n-1}{2}, \frac{n-5}{2}\right). \end{cases} \quad (15)$$

*Proof.* Similar to the proof of Lemma 3, by Lemmas 1 and 2, direct computing yields  $z(G_7(a, b)) = 3ab + 5a + 3$ . By the method of Lagrange multipliers, we make auxiliary function  $L(a, b) = \lambda(a + b + 3 - n) + 3ab + 5a + 3$ , where  $a + b + 3 = n$ ,  $a \geq 2$ , and  $b \geq 1$ . Taking the partial derivatives of  $a$ ,  $b$ , and  $\lambda$  in  $L(a, b, \lambda)$ , we can obtain the following equations:

$$\begin{cases} L_a = \lambda + 3b + 5 = 0, \\ L_b = \lambda + 3a = 0, \\ L_\lambda = a + b + 3 - n = 0, \\ a \geq 2 \text{ and } b \geq 1. \end{cases} \quad (16)$$

Solving the equations as above, we get  $a = b + (5/3)$ . Since  $a = b + (5/3)$  is an integer, we know that  $a = \lfloor b + (5/3) \rfloor$  or  $a = \lceil b + (5/3) \rceil$ . By  $a = \lfloor b + (5/3) \rfloor$  and  $a + b + 3 = n$ , we can obtain that  $a = ((n-2)/2)$  and  $b = ((n-4)/2)$ . Similarly, by  $a = \lceil b + (5/3) \rceil$  and  $a + b + 3 = n$ , we also can obtain that  $a = ((n-1)/2)$  and  $b = ((n-5)/2)$ . So, we discuss two cases as follows:

Case 1:  $a = ((n-2)/2)$  and  $b = ((n-4)/2)$ .

Because  $a = ((n-2)/2)$  and  $b = ((n-4)/2)$  is a unique root of (16),  $a = ((n-2)/2)$  and  $b = ((n-4)/2)$  must be the unique extreme point. Since  $a$  and  $b$  are integers, we consider two subcases:

Subcase 1: assume that  $n$  is even. Then  $a = ((n-2)/2)$  and  $b = ((n-4)/2)$ ; thus  $z(G_7(((n-2)/2), ((n-4)/2))) = (3n^2 - 8n + 16)/4$ . It is easy to verify that  $z(G_7(a, b)) < ((3n^2 - 8n + 16)/4)$  when  $a \neq ((n-2)/2)$  and  $b \neq ((n-4)/2)$ . This implies that

$z(G) \leq ((3n^2 - 8n + 16)/4)$  and the equality holds if and only if  $G \cong G_7(((n-2)/2), t((n-4)/2))$ .

Subcase 2: suppose that  $n$  is odd. We know that  $a = ((n-1)/2)$  and  $b = ((n-5)/2)$ . Thus  $z(G_7(((n-1)/2), ((n-5)/2))) = ((3n^2 - 8n + 17)/4)$ . It is easy to verify that  $z(G_7(a, b)) < ((3n^2 - 8n + 17)/4)$  when  $a \neq ((n-1)/2)$  and  $b \neq ((n-5)/2)$ . This implies that  $z(G) \leq ((3n^2 - 8n + 17)/4)$  and the equality holds iff  $G \cong G_7(((n-1)/2), t((n-5)/2))$ .

Case 2:  $a = ((n-1)/2)$  and  $b = ((n-5)/2)$ .

Similar to the proof of Case 1, because  $a = ((n-1)/2)$  and  $b = ((n-5)/2)$  is a unique root of (2),  $a = ((n-1)/2)$  and  $b = ((n-5)/2)$  must be the unique extreme point. Since  $a$  and  $b$  are integers, we also consider two subcases.

Subcase 1: consider that  $n$  is even. Then we get  $a = ((n-2)/2)$  and  $b = ((n-4)/2)$ ; thus  $z(G_7(((n-2)/2), ((n-4)/2))) = ((3n^2 - 8n + 16)/4)$ . It is easy to verify that  $z(G_7(a, b)) < ((3n^2 - 8n + 16)/4)$  when  $a \neq ((n-2)/2)$  and  $b \neq ((n-4)/2)$ . This implies that  $z(G) \leq ((3n^2 - 8n + 16)/4)$  and the equality holds if and only if  $G \cong G_7(((n-2)/2), t((n-4)/2))$ .

Subcase 2: assume that  $n$  is odd. We know that  $a = ((n-1)/2)$  and  $b = ((n-5)/2)$ . Thus  $z(G_7(((n-1)/2), ((n-5)/2))) = ((3n^2 - 8n + 17)/4)$ . It is easy to verify that  $z(G_7(a, b)) < ((3n^2 - 8n + 17)/4)$  when  $a \neq ((n-1)/2)$  and  $b \neq ((n-5)/2)$ . This implies that  $z(G) \leq ((3n^2 - 8n + 17)/4)$  and the equality holds iff  $G \cong G_7(((n-1)/2), t((n-5)/2))$ .  $\square$

**Lemma 10.** Let  $G \in G_8(a, b)$  be a graph with  $n$  vertices. Then

$$z(G) \leq \begin{cases} \frac{3n^2 - 8n + 16}{4}, & \text{where } n \geq 8 \text{ is even, and the equality holds iff } G \cong G_8\left(\frac{n-2}{2}, \frac{n-4}{2}\right); \\ \frac{3n^2 - 8n + 29}{4}, & \text{where } n \geq 7 \text{ is odd, and the equality holds iff } G \cong G_8\left(\frac{n-3}{2}, \frac{n-3}{2}\right). \end{cases} \quad (17)$$

*Proof.* Similar to the proof of Lemma 3, by Lemmas 1 and 2, we get  $z(G_8(a, b)) = 3ab + 3a + 2b + 5$ . By the method of Lagrange multipliers, we make an auxiliary function  $L(a, b) = \lambda(a + b + 3 - n) + 3ab + 3a + 2b + 5$ , where  $a + b + 3 = n$ ,  $a, b \geq 1$ , and at most one of them is 1. Taking the partial derivatives of  $a, b$ , and  $\lambda$  in  $L(a, b, \lambda)$ , we can obtain the following equations:

$$\begin{cases} L_a = \lambda + 3b + 3 = 0, \\ L_b = \lambda + 3a + 2 = 0, \\ L_\lambda = a + b + 3 - n = 0, \\ a \geq 1 \text{ and } b \geq 1. \end{cases} \quad (18)$$

Solving the equations as above, we get  $a = b + (1/3)$ . Since  $a = b + (1/3)$  is an integer, we know that  $a = \lfloor b + (1/3) \rfloor$  or  $a = \lceil b + (1/3) \rceil$ . By  $a = \lfloor b + (1/3) \rfloor$  and  $a + b + 3 = n$ , we can obtain that  $a = ((n-3)/2)$  and  $b = ((n-3)/2)$ . Similarly, by  $a = \lceil b + (1/3) \rceil$  and  $a + b + 3 = n$ , we also can obtain that  $a = ((n-2)/2)$  and  $b = ((n-4)/2)$ . So, we discuss two cases as follows:

Case 1:  $a = ((n-3)/2)$  and  $b = ((n-3)/2)$ .

Because  $a = ((n-3)/2)$  and  $b = ((n-3)/2)$  is a unique root of (18),  $a = ((n-3)/2)$  and  $b = ((n-3)/2)$  must be the unique extreme point. Since  $a$  and  $b$  are integers, we consider two subcases.

Subcase 1: consider that  $n$  is even. We have  $a = ((n-2)/2)$  and  $b = ((n-4)/2)$ . Thus  $z(G_8(((n-2)/2), ((n-4)/2))) = ((3n^2 - 8n + 16)/4)$ . To simplify calculation, we get  $z(G_8(a, b)) < ((3n^2 - 8n + 16)/4)$  when  $a \neq ((n-2)/2)$  and  $b \neq ((n-4)/2)$ . This implies that  $z(G) \leq ((3n^2 - 8n + 16)/4)$  and the equality holds iff  $G \cong G_8(((n-2)/2), t((n-4)/2))$ .

Subcase 2: assume that  $n$  is odd. Then  $a = ((n-3)/2)$  and  $b = ((n-3)/2)$ . So  $z(G_8(((n-3)/2), ((n-3)/2))) = ((3n^2 - 8n + 29)/4)$ . It is easy to check that  $z(G_8(a, b)) < ((3n^2 - 8n + 29)/4)$  when  $a \neq ((n-3)/2)$  and  $b \neq ((n-3)/2)$ . This implies that  $z(G) \leq ((3n^2 - 8n + 29)/4)$  and the equality holds if and only if  $G \cong G_8(((n-3)/2), t((n-3)/2))$ .

Case 2:  $a = ((n-2)/2)$  and  $b = ((n-4)/2)$ .

Similar to the proof of Case 1, because  $a = ((n-2)/2)$  and  $b = ((n-4)/2)$  is a unique root of (18),  $a = ((n-2)/2)$  and  $b = ((n-4)/2)$  must be the unique extreme point. Since  $a$  and  $b$  are integers, we consider two subcases.

Subcase 1: consider that  $n$  is even. We have  $a = ((n-2)/2)$  and  $b = ((n-4)/2)$ . Thus  $z(G_8(((n-2)/2), ((n-4)/2))) = ((3n^2 - 8n + 16)/4)$ . To simplify calculation, we get  $z(G_8(a, b)) < ((3n^2 - 8n + 16)/4)$  when  $a \neq ((n-2)/2)$  and  $b \neq ((n-4)/2)$ . This implies that  $z(G) \leq ((3n^2 - 8n + 16)/4)$  and the equality holds iff  $G \cong G_8(((n-2)/2), t((n-4)/2))$ .

Subcase 2: assume that  $n$  is odd. Then  $a = ((n-3)/2)$  and  $b = ((n-3)/2)$ . So  $z(G_8(((n-3)/2), ((n-3)/2))) = ((3n^2 - 8n + 29)/4)$ . It is easy to check that  $z(G_8(a, b)) < ((3n^2 - 8n + 29)/4)$  when  $a \neq ((n-3)/2)$  and  $b \neq ((n-3)/2)$ . This implies that  $z(G) \leq ((3n^2 - 8n + 29)/4)$  and the equality holds if and only if  $G \cong G_8(((n-3)/2), t((n-3)/2))$ .  $\square$

**Lemma 11.** Let  $G \in G_9(a, b)$  be a graph with  $n$  vertices. Then

$$z(G) \leq \begin{cases} n^2 - 4n + 8, & \text{where } n \geq 8 \text{ is even, and the equality holds iff } G \cong G_2\left(\frac{n-6}{2}, \frac{n-2}{2}\right); \\ n^2 - 4n + 7, & \text{where } n \geq 9 \text{ is odd, and the equality holds iff } G \cong G_2\left(\frac{n-7}{2}, \frac{n-1}{2}\right) \\ \text{Or} & G \cong G_2\left(\frac{n-5}{2}, \frac{n-3}{2}\right). \end{cases} \quad (19)$$

*Proof.* Similar to the proof of Lemma 3, by Lemmas 1 and 2, we get  $z(G_9(a, b)) = 4ab + 2a + 2b + 5$ . By the method of

Lagrange multipliers, we make an auxiliary function  $L(a, b) = \lambda(a + b + 3 - n) + 4ab + 2a + 2b + 5$ , where  $a + b +$

$3 = n, a, b \geq 1$ , and at most one of them is 1. Taking the partial derivatives of  $a, b$ , and  $\lambda$  in  $L(a, b, \lambda)$ , we can obtain the following equations:

$$\begin{cases} L_a = \lambda + 4b + 2 = 0, \\ L_b = \lambda + 4a + 2 = 0, \\ L_\lambda = a + b + 3 - n = 0, \\ a \geq 1 \text{ and } b \geq 1. \end{cases} \quad (20)$$

Solving the equations as above, we obtain that  $a = ((n - 3)/2)$  and  $b = ((n - 3)/2)$ . Because  $((n - 3)/2, t((n - 3)/2))$  is a unique stable point,  $((n - 3)/2, t((n - 3)/2))$  must be the unique extreme point. Since  $a$  and  $b$  are integers, we consider the two following cases.

Case 1: consider that  $n$  is even. We have  $a = ((n - 2)/2)$  and  $b = ((n - 4)/2)$ , or  $a = ((n - 4)/2)$  and  $b = ((n - 2)/2)$ . Thus  $z(G_9((n - 2)/2, (n - 4)/2)) =$

$z(G_9(((n - 4)/2), ((n - 2)/2))) = n^2 - 4n + 7$ . To simplify calculation, we get  $z(G_9(a, b)) < n^2 - 4n + 7$  when  $a \neq ((n - 2)/2)$  and  $b \neq ((n - 4)/2)$ , or  $a \neq ((n - 4)/2)$  and  $b \neq ((n - 2)/2)$ . This implies that  $z(G) \leq n^2 - 4n + 7$  and the equality holds iff  $G \cong G_9(((n - 2)/2), ((n - 4)/2)) \cong G_9(((n - 4)/2), t((n - 2)/2))$ .

Case 2: assume that  $n$  is odd. We know that  $a = ((n - 3)/2)$  and  $b = ((n - 3)/2)$ . Thus  $z(G_9(((n - 3)/2), ((n - 3)/2))) = n^2 - 4n + 8$ . It is easy to check that  $z(G_9(a, b)) < n^2 - 4n + 8$  when  $a \neq ((n - 3)/2)$  and  $b \neq ((n - 3)/2)$ . This implies that  $z(G) \leq n^2 - 4n + 8$  and the equality holds if and only if  $G \cong G_9(((n - 3)/2), t((n - 3)/2))$ .  $\square$

**Lemma 12.** Let  $G \in G_{10}(a, b, c)$  be a graph with  $n$  vertices. Then

$$z(G) \leq \begin{cases} \frac{2n^3 - 6n^2 + 63n - 54}{27}, & \text{where } n \equiv 0 \pmod{3}, n \geq 9 \text{ and the equality holds} \\ & \text{if and only if } G \cong G_{10}\left(\frac{n-3}{3}, \frac{n}{3}, \frac{n-3}{3}\right); \\ \frac{2n^3 - 6n^2 + 60n - 56}{27}, & \text{where } n \equiv 1 \pmod{3}, n \geq 10 \text{ and the equality holds} \\ & \text{if and only if } G \cong G_{10}\left(\frac{n-1}{3}, \frac{n-1}{3}, \frac{n-4}{3}\right) \cong G_{10}\left(\frac{n-4}{3}, \frac{n-1}{3}, \frac{n-1}{3}\right); \\ \frac{2n^3 - 6n^2 + 63n - 64}{27}, & \text{where } n \equiv 2 \pmod{3}, n \geq 8 \text{ and the equality holds} \\ & \text{if and only if } G \cong G_{10}\left(\frac{n-2}{3}, \frac{n-2}{3}, \frac{n-2}{3}\right). \end{cases} \quad (21)$$

*Proof.* Similar to the proof of Lemma 3, by Lemmas 1 and 2, direct computing yields  $z(G_{10}(a, b, c)) = 2abc + bc + ab + 2a + 3b + 2c + 2$ . By the method of Lagrange multipliers, we make auxiliary function  $L(a, b, c) = \lambda(a + b + c + 2 - n) + 2abc + bc + ab + 2a + 3b + 2c + 2$ , where  $a + b + c + 2 = n, a, b, c \geq 1$ , and at most one of them is 1. Taking the partial derivatives of  $a, b, c$ , and  $\lambda$  in  $L(a, b, c, \lambda)$ , we can obtain the following equations:

$$\begin{cases} L_a = \lambda + 2bc + b + 2 = 0, \\ L_b = \lambda + 2ac + c + a + 3 = 0, \\ L_c = \lambda + 2ab + b + 2 = 0, \\ L_\lambda = a + b + c + 2 - n = 0, \\ a \geq 1, b \geq 1 \text{ and } c \geq 1. \end{cases} \quad (22)$$

Solving the equations as above, we get  $b = a + 1 - (a/(a + 1))$ . Since  $b = a + 1 - (a/(a + 1))$  is an integer, we know that  $b = \lceil a + 1 - (a/(a + 1)) \rceil$  or  $b = \lfloor a + 1 - (a/(a + 1)) \rfloor$ . By  $b = \lceil a + 1 - (a/(a + 1)) \rceil$  and  $a + b + c + 2 = n$ , we can obtain that  $a = ((n - 3)/3), b = (n/3)$ , and  $c = ((n - 3)/3)$ . Similarly, by  $b = \lfloor a + 1 - (a/(a + 1)) \rfloor$  and  $a + b + c + 2 = n$ , we also can obtain that  $a = ((n - 2)/3), b = ((n - 2)/3)$ , and  $c = ((n - 2)/3)$ . Thus, we discuss two cases as follows:

Case 1:  $a = ((n - 3)/3), b = (n/3)$ , and  $c = ((n - 3)/3)$ . Because  $a = ((n - 3)/3), b = (n/3)$ , and  $c = ((n - 3)/3)$  is a unique root of (22),  $a = ((n - 3)/3), b = (n/3)$ , and  $c = ((n - 3)/3)$  must be the unique extreme point. Since  $a, b$ , and  $c$  are integers, we consider three subcases as follows:

Subcase 1: assume that  $n \equiv 0 \pmod{3}$ . Then  $a = ((n - 3)/3), b = (n/3)$ , and  $c = ((n - 3)/3)$ . Thus  $z(G_{10}(((n - 3)/3), (n/3), ((n - 3)/3))) = ((2n^3 - 6n^2 + 63n - 54)/27)$ . It is easy to verify that  $z(G_{10}(a, b, c)) < ((2n^3 - 6n^2 + 63n - 54)/27)$  when  $a \neq ((n - 3)/3), b \neq (n/3)$ , and  $c \neq ((n - 3)/3)$ . This implies that  $z(G) \leq ((2n^3 - 6n^2 + 63n - 54)/27)$  and the equality holds if and only if  $G \cong G_{10}(((n - 3)/3), t(n/3), q((n - 3)/3))$ .

Subcase 2: suppose that  $n \equiv 1 \pmod{3}$ . Then  $a = ((n - 1)/3), b = ((n - 1)/3)$ , and  $c = ((n - 4)/3)$ , or  $a = ((n - 4)/3), b = ((n - 1)/3)$ , and  $c = ((n - 1)/3)$ . Thus  $z(G_{10}(((n - 1)/3), ((n - 1)/3), ((n - 4)/3))) = z(G_{10}(((n - 4)/3), ((n - 1)/3), ((n - 1)/3))) = ((2n^3 - 6n^2 + 60n - 56)/27)$ . It is easy to check that  $z(G_{10}(a, b, c)) < ((2n^3 - 6n^2 + 60n - 56)/27)$  when  $a \neq ((n - 1)/3), b \neq ((n - 1)/3)$ , and

$c \neq ((n-4)/3)$ , or  $a \neq ((n-4)/3)$ ,  $b \neq ((n-1)/3)$ , and  $c \neq ((n-1)/3)$ . This implies that  $z(G) \leq ((2n^3 - 6n^2 + 60n - 56)/27)$  and the equality holds iff  $G \cong G_{10}(((n-1)/3), ((n-1)/3), ((n-4)/3)) \cong G_{10}(((n-4)/3), t((n-1)/3)n, q((n-1)/3))$ .

Subcase 3: consider that  $n \equiv 2 \pmod{3}$ . Then  $a = ((n-2)/3)$ ,  $b = ((n-2)/3)$ , and  $c = ((n-2)/3)$ . Thus  $z(G_{10}(((n-2)/3), ((n-2)/3), ((n-2)/3))) = ((2n^3 - 6n^2 + 63n - 64)/27)$ . To simplify calculation, we know that  $z(G_{10}(a, b, c)) < ((2n^3 - 6n^2 + 63n - 64)/27)$  when  $a \neq ((n-2)/3)$ ,  $b \neq ((n-2)/3)$ , and  $c \neq ((n-2)/3)$ . This implies that  $z(G) \leq ((2n^3 - 6n^2 + 63n - 64)/27)$  and the equality holds iff  $G \cong G_{10}(((n-2)/3), t((n-2)/3)n, q((n-2)/3))$ .

Case 2:  $a = ((n-2)/3)$ ,  $b = ((n-2)/3)$ , and  $c = ((n-2)/3)$ .

Similar to the proof of Case 1, because  $a = ((n-2)/3)$ ,  $b = ((n-2)/3)$ , and  $c = ((n-2)/3)$  is a unique root of (22),  $a = ((n-2)/3)$ ,  $b = ((n-2)/3)$ , and  $c = ((n-2)/3)$  must be the unique extreme point. Since  $a, b$ , and  $c$  are integers, after taking the integer, we also consider three subcases as follows:

Subcase 1: assume that  $n \equiv 0 \pmod{3}$ . Then  $a = ((n-3)/3)$ ,  $b = (n/3)$ , and  $c = ((n-3)/3)$ . Thus  $z(G_{10}(((n-3)/3), (n/3), ((n-3)/3))) = ((2n^3 - 6n^2 + 63n - 54)/27)$ . It is easy to verify that  $z(G_{10}(a, b, c)) < ((2n^3 - 6n^2 + 63n - 54)/27)$  when  $a \neq ((n-3)/3)$ ,  $b \neq (n/3)$ , and  $c \neq ((n-3)/3)$ . This implies that  $z(G) \leq ((2n^3 - 6n^2 + 63n - 54)/27)$  and

the equality holds if and only if  $G \cong G_{10}(((n-3)/3), t(n/3)n, q((n-3)/3))$ .

Subcase 2: suppose that  $n \equiv 1 \pmod{3}$ . Then  $a = ((n-1)/3)$ ,  $b = ((n-1)/3)$ , and  $c = ((n-4)/3)$ , or  $a = ((n-4)/3)$ ,  $b = ((n-1)/3)$ , and  $c = ((n-1)/3)$ . Thus  $z(G_{10}(((n-1)/3), ((n-1)/3), ((n-4)/3))) = z(G_{10}(((n-4)/3), ((n-1)/3), ((n-1)/3))) = ((2n^3 - 6n^2 + 60n - 56)/27)$ . It is easy to check that  $z(G_{10}(a, b, c)) < ((2n^3 - 6n^2 + 60n - 56)/27)$  when  $a \neq ((n-1)/3)$ ,  $b \neq ((n-1)/3)$ , and  $c \neq ((n-4)/3)$ , or  $a \neq ((n-4)/3)$ ,  $b \neq ((n-1)/3)$ , and  $c \neq ((n-1)/3)$ . This implies that  $z(G) \leq ((2n^3 - 6n^2 + 60n - 56)/27)$  and the equality holds iff  $G \cong G_{10}(((n-1)/3), ((n-1)/3), ((n-4)/3)) \cong G_{10}(((n-4)/3), t((n-1)/3)n, q((n-1)/3))$ .

Subcase 3: consider that  $n \equiv 2 \pmod{3}$ . Then  $a = ((n-2)/3)$ ,  $b = ((n-2)/3)$ , and  $c = ((n-2)/3)$ . Thus  $z(G_{10}(((n-2)/3), ((n-2)/3), ((n-2)/3))) = ((2n^3 - 6n^2 + 63n - 64)/27)$ . To simplify calculation, we know that  $z(G_{10}(a, b, c)) < ((2n^3 - 6n^2 + 63n - 64)/27)$  when  $a \neq ((n-2)/3)$ ,  $b \neq ((n-2)/3)$ , and  $c \neq ((n-2)/3)$ . This implies that  $z(G) \leq ((2n^3 - 6n^2 + 63n - 64)/27)$  and the equality holds iff  $G \cong G_{10}(((n-2)/3), t((n-2)/3)n, q((n-2)/3))$ .  $\square$

**Lemma 13.** Let  $G \in G_{11}(a, b)$  be a graph with  $n$  vertices. Then

$$z(G) \leq \begin{cases} \frac{3n^2 - 4n}{4}, & \text{where } n \geq 6 \text{ is even, and the equality holds iff } G \cong G_{11}\left(\frac{n-4}{2}, \frac{n-4}{2}\right); \\ \frac{3n^2 - 4n - 3}{4}, & \text{where } n \geq 8 \text{ is odd, and the equality holds} \\ & \text{iff } G \cong G_{11}\left(\frac{n-5}{2}, \frac{n-3}{2}\right) \cong G_{11}\left(\frac{n-3}{2}, \frac{n-5}{2}\right). \end{cases} \quad (23)$$

*Proof.* Similar to the proof of Lemma 3, by Lemmas 1 and 2, we get  $z(G_{11}(a, b)) = 3ab + 5a + 5b + 8$ . By the method of Lagrange multipliers, we make an auxiliary function  $L(a, b) = \lambda(a + b + 4 - n) + 3ab + 5a + 5b + 8$ , where  $a + b + 4 = n$ ,  $a \geq 1$ , and  $b \geq 1$ . Taking the partial derivatives of  $a, b$ , and  $\lambda$  in  $L(a, b, \lambda)$ , we can obtain the following equations:

$$\begin{cases} L_a = \lambda + 3b + 5 = 0, \\ L_b = \lambda + 3a + 5 = 0, \\ L_\lambda = a + b + 4 - n = 0, \\ a \geq 1 \text{ and } b \geq 1. \end{cases} \quad (24)$$

Solving the equations as above, we obtain that  $a = ((n-4)/2)$  and  $b = ((n-4)/2)$ . Because  $((n-4)/2, t((n-4)/2))$  is a unique stable point,  $((n-4)/2, t((n-4)/2))$  must be the unique extreme point. Since  $a$  and  $b$  are integers, in the following we consider two cases.

Case 1: consider that  $n$  is even. We have  $a = ((n-4)/2)$  and  $b = ((n-4)/2)$ . Thus  $z(G_{11}(((n-4)/2), ((n-4)/2))) = (3n^2 - 4n)/4$ . To simplify calculation, we get  $z(G_{11}(a, b)) < ((3n^2 - 4n)/4)$  when  $a \neq ((n-4)/2)$  and  $b \neq ((n-4)/2)$ . This implies that  $z(G) \leq ((3n^2 - 4n)/4)$  and the equality holds iff  $G \cong G_{11}(((n-4)/2), t((n-4)/2))$ .

Case 2: assume that  $n$  is odd. We know that  $a = ((n-5)/2)$  and  $b = ((n-3)/2)$ , or  $a = ((n-3)/2)$  and  $b = ((n-5)/2)$ . Thus  $z(G_{11}(((n-5)/2), ((n-3)/2))) = z(G_{11}(((n-3)/2), ((n-5)/2))) = (3n^2 - 4n - 3)/4$ . It is easy to check that  $z(G_{11}(a, b)) < ((3n^2 - 4n - 3)/4)$  when  $a \neq ((n-5)/2)$  and  $b \neq ((n-3)/2)$ , or

$a \neq ((n-3)/2)$  and  $b \neq ((n-5)/2)$ . This implies that  $z(G) \leq ((3n^2 - 4n - 3)/4)$  and the equality holds if and only if  $G \cong G_{11}(((n-5)/2), ((n-3)/2)) \cong G_{11}(((n-3)/2), t((n-5)/2))$ .  $\square$

**Lemma 14.** Let  $G \in G_{12}(a, b)$  be a graph with  $n$  vertices. Then

$$z(G) \leq \begin{cases} \frac{5n^2 - 24n + 48}{4}, & \text{where } n \geq 6 \text{ is even, and the equality holds iff } G \cong G_{12}\left(\frac{n-4}{2}, \frac{n-4}{2}\right); \\ \frac{5n^2 - 24n + 47}{4}, & \text{where } n \geq 7 \text{ is odd, and the equality holds iff } G \cong G_{12}\left(\frac{n-3}{2}, \frac{n-5}{2}\right). \end{cases} \quad (25)$$

*Proof.* Similar to the proof of Lemma 3, by Lemmas 1 and 2, direct computing yields  $z(G_{12}(a, b)) = 5ab + 5a + 3b + 8$ . Using the method of Lagrange multipliers, we make auxiliary function  $L(a, b) = \lambda(a + b + 4 - n) + 5ab + 5a + 3b + 8$ , where  $a + b + 4 - n, a \geq 1$ , and  $b \geq 1$ . Taking the partial derivatives of  $a, b$ , and  $\lambda$  in  $L(a, b, \lambda)$ , we can obtain the following equations:

$$\begin{cases} L_a = \lambda + 5b + 5 = 0, \\ L_b = \lambda + 5a + 3 = 0, \\ L_\lambda = a + b + 4 - n = 0, \\ a \geq 1 \text{ and } b \geq 1. \end{cases} \quad (26)$$

Solving the equations as above, we get  $a = b + (2/5)$ . Since  $a = b + (2/5)$  is an integer, we know that  $a = \lfloor b + (2/5) \rfloor$  or  $a = \lceil b + (2/5) \rceil$ . By  $a = \lfloor b + (2/5) \rfloor$  and  $a + b + 4 = n$ , we can obtain that  $a = ((n-4)/2)$  and  $b = ((n-4)/2)$ . Similarly, by  $a = \lceil b + (2/5) \rceil$  and  $a + b + 4 = n$ , we also can obtain that  $a = ((n-3)/2)$  and  $b = ((n-5)/2)$ . So, we discuss two cases as follows:

Case 1:  $a = ((n-4)/2)$  and  $b = ((n-4)/2)$ .

Because  $a = ((n-4)/2)$  and  $b = ((n-4)/2)$  is a unique root of (26),  $a = ((n-4)/2)$  and  $b = ((n-4)/2)$  must be the unique extreme point. Since  $a$  and  $b$  are integers, we consider two subcases.

Subcase 1: assume that  $n$  is even. Then  $a = ((n-4)/2)$  and  $b = ((n-4)/2)$ . Thus  $z(G_{12}(((n-4)/2), ((n-4)/2))) = (5n^2 - 24n + 48)/4$ . It is easy to verify that  $z(G_{12}(a, b)) < ((5n^2 - 24n + 48)/4)$  when  $a \neq ((n-4)/2)$  and  $b \neq ((n-4)/2)$ . This implies that  $z(G) \leq ((5n^2 - 24n + 48)/4)$  and the equality holds if and only if  $G \cong G_{12}(((n-4)/2), t((n-4)/2))$ .

Subcase 2: suppose that  $n$  is odd. We know that  $a = ((n-3)/2)$  and  $b = ((n-5)/2)$ . Thus  $z(G_{12}(((n-3)/2), ((n-5)/2))) = ((5n^2 - 24n + 47)/4)$ . It is easy to check that  $z(G_{12}(a, b)) < ((5n^2 - 24n + 47)/4)$  when  $a \neq ((n-3)/2)$  and  $b \neq ((n-5)/2)$ . This implies that  $z(G) \leq ((5n^2 - 24n + 47)/4)$  and the equality holds iff  $G \cong G_{12}(((n-3)/2), t((n-5)/2))$ .

Case 2:  $a = ((n-3)/2)$  and  $b = ((n-5)/2)$ .

Similar to the proof of Case 1, because  $a = ((n-4)/2)$  and  $b = ((n-4)/2)$  is a unique root of (26),  $a = ((n-4)/2)$  and  $b = ((n-4)/2)$  must be the unique extreme point. Since  $a$  and  $b$  are integers, we consider two subcases.

Subcase 1: assume that  $n$  is even. Then  $a = ((n-4)/2)$  and  $b = ((n-4)/2)$ . Thus  $z(G_{12}(((n-4)/2), ((n-4)/2))) = (5n^2 - 24n + 48)/4$ . It is easy to verify that  $z(G_{12}(a, b)) < ((5n^2 - 24n + 48)/4)$  when  $a \neq ((n-4)/2)$  and  $b \neq ((n-4)/2)$ . This implies that  $z(G) \leq ((5n^2 - 24n + 48)/4)$  and the equality holds if and only if  $G \cong G_{12}(((n-4)/2), t((n-4)/2))$ .

Subcase 2: suppose that  $n$  is odd. We know that  $a = ((n-3)/2)$  and  $b = ((n-5)/2)$ . Thus  $z(G_{12}(((n-3)/2), ((n-5)/2))) = (5n^2 - 24n + 47)/4$ . It is easy to check that  $z(G_{12}(a, b)) < ((5n^2 - 24n + 47)/4)$  when  $a \neq ((n-3)/2)$  and  $b \neq ((n-5)/2)$ . This implies that  $z(G) \leq ((5n^2 - 24n + 47)/4)$  and the equality holds iff  $G \cong G_{12}(((n-3)/2), t((n-5)/2))$ .  $\square$

**Lemma 15.** Let  $G \in G_{13}(a, b)$  be a graph with  $n$  vertices. Then

$$z(G) \leq \begin{cases} n^2 - 4n + 10, & \text{where } n \geq 6 \text{ is even, and the equality holds iff } G \cong G_{13}\left(\frac{n-4}{2}, \frac{n-4}{2}\right); \\ & \text{where } n \geq 7 \text{ is odd, and the equality holds} \\ n^2 - 4n + 9, & \text{iff } G \cong G_{13}\left(\frac{n-3}{2}, \frac{n-5}{2}\right) \cong G_{13}\left(\frac{n-5}{2}, \frac{n-3}{2}\right). \end{cases} \quad (27)$$

*Proof.* Similar to the proof of Lemma 3, by Lemmas 1 and 2, we get that  $z(G_{13}(a, b)) = 4ab + 4a + 4b + 10$ . According to the method of Lagrange multipliers, we make an auxiliary function  $L(a, b) = \lambda(a + b + 4 - n) + 4ab + 4a + 4b + 10$ , where  $a + b + 4 = n$ ,  $a \geq 1$ , and  $b \geq 1$ . Taking the partial derivatives of  $a, b$ , and  $\lambda$  in  $L(a, b, \lambda)$ , we obtain the following equations:

$$\begin{cases} L_a = \lambda + 4b + 4 = 0, \\ L_b = \lambda + 4a + 4 = 0, \\ L_\lambda = a + b + 4 - n = 0, \\ a \geq 1 \text{ and } b \geq 1. \end{cases} \quad (28)$$

Solving the equations as above, we obtain that  $a = ((n - 4)/2)$  and  $b = ((n - 4)/2)$ . Because  $((n - 4)/2, t((n - 4)/2))$  is a unique stable point,  $((n - 4)/2, t((n - 4)/2))$  must be the unique extreme point. Since  $a$  and  $b$  are integers, we only consider two cases.

Case 1: assume that  $n$  is even. We obtain  $a = ((n - 4)/2)$  and  $b = ((n - 4)/2)$ . Thus  $z(G_{13}((n -$

$4)/2, ((n - 4)/2)) = n^2 - 4n + 10$ . It is easy to check that  $z(G_{13}(a, b)) < n^2 - 4n + 10$  when  $a \neq ((n - 4)/2)$  and  $b \neq ((n - 4)/2)$ . This implies that  $z(G) \leq n^2 - 4n + 10$  and the equality holds if and only if  $G \cong G_{13}(((n - 4)/2), t((n - 4)/2))$ .

Case 2: consider that  $n$  is odd. We have  $a = ((n - 3)/2)$  and  $b = ((n - 5)/2)$ , or  $a = ((n - 5)/2)$  and  $b = ((n - 3)/2)$ . So,  $z(G_{13}(((n - 3)/2), ((n - 5)/2))) = z(G_{13}(((n - 5)/2), ((n - 3)/2))) = n^2 - 4n + 9$ . It is easy to verify that  $z(G_{13}(a, b)) < n^2 - 4n + 9$  when  $a \neq ((n - 3)/2)$  and  $b \neq ((n - 5)/2)$ , or  $a \neq ((n - 5)/2)$  and  $b \neq ((n - 3)/2)$ . This means that  $z(G) \leq n^2 - 4n + 9$  and the equality holds if and only if  $G \cong G_3(((n - 3)/2), ((n - 5)/2)) \cong G_3(((n - 5)/2), t((n - 3)/2))$ .  $\square$

**Lemma 16.** Let  $G \in G_{14}(a, b)$  be a graph with  $n$  vertices. Then

$$z(G) \leq \begin{cases} \frac{3}{2}n^2 - 8n + 16, & \text{where } n \text{ is even, } n \geq 8 \text{ and the equality holds iff} \\ & G \cong G_{14}\left(\frac{n-4}{2}, \frac{n-6}{2}\right) \cong G_{14}\left(\frac{n-6}{2}, \frac{n-4}{2}\right); \\ \frac{3}{2}n^2 - 8n + \frac{35}{2}, & \text{where } n \text{ is odd, } n \geq 7 \text{ and the equality holds iff } G \cong G_{14}\left(\frac{n-5}{2}, \frac{n-5}{2}\right). \end{cases} \quad (29)$$

*Proof.* Similar to the proof of Lemma 3, by Lemmas 1 and 2, we obtain that  $z(G_{14}(a, b)) = 6ab + 7a + 7b + 15$ . According to the method of Lagrange multipliers, we make an auxiliary function  $L(a, b) = \lambda(a + b + 5 - n) + 6ab + 7a + 7b + 15$ , where  $a + b + 5 = n$ ,  $a \geq 1$ , and  $b \geq 1$ . Taking the partial derivatives of  $a, b$ , and  $\lambda$  in  $L(a, b, \lambda)$ , we can obtain the following equations:

$$\begin{cases} L_a = \lambda + 6b + 7 = 0, \\ L_b = \lambda + 6a + 7 = 0, \\ L_\lambda = a + b + 5 - n = 0, \\ a \geq 1 \text{ and } b \geq 1. \end{cases} \quad (30)$$

Solving the equations as above, we obtain that  $a = ((n - 5)/2)$  and  $b = ((n - 5)/2)$ . Because  $((n - 5)/2, t((n - 5)/2))$  is a unique stable point,  $((n - 5)/2, t((n - 5)/2))$  must be the unique extreme point. Since  $a$  and  $b$  are integers, we only consider two cases.

Case 1: consider that  $n$  is even. We have  $a = ((n - 4)/2)$  and  $b = ((n - 6)/2)$ , or  $a = ((n - 6)/2)$  and  $b = ((n - 4)/2)$ . Thus  $z(G_{14}(((n - 4)/2), ((n - 6)/2))) = z(G_{14}(((n - 6)/2), ((n - 4)/2))) = (3/2)n^2 - 8n + 16$ . To simplify calculation, we get  $z(G_{14}(a, b)) < (3/2)n^2 - 8n + 16$  when  $a \neq ((n - 4)/2)$

and  $b \neq ((n - 6)/2)$ , or  $a \neq ((n - 6)/2)$  and  $b \neq ((n - 4)/2)$ . This implies that  $z(G) \leq (3/2)n^2 - 8n + 16$  and the equality holds iff  $G \cong G_{14}(((n - 4)/2), ((n - 6)/2)) \cong G_{14}(((n - 6)/2), t((n - 4)/2))$ .

Case 2: assume that  $n$  is odd. Then  $a = ((n - 5)/2)$  and  $b = ((n - 5)/2)$ . So  $z(G_{14}(((n - 5)/2), ((n - 5)/2))) = (3/2)n^2 - 8n + (35/2)$ . It is easy to check that  $z(G_{14}(a, b)) < (3/2)n^2 - 8n + (35/2)$  when  $a \neq ((n - 5)/2)$  and  $b \neq ((n - 5)/2)$ . This implies that  $z(G) \leq (3/2)n^2 - 8n + (35/2)$  and the equality holds if and only if  $G \cong G_{14}(((n - 5)/2), t((n - 5)/2))$ .  $\square$

*Proof of Theorem 1.* By Lemmas 3–16, we know the maximum Hosoya index in  $G_i$  ( $i = 1, 2, \dots, 14$ ). Employing Mathematica 12.0 to compute the difference of the maximum Hosoya indices of  $G_i$  and  $G_j$ , it yields directly the result in Theorem 1.  $\square$

#### 4. Concluding Remark

In this paper, we characterize the sharp upper bound of Hosoya indices of all graphs in  $\mathcal{B}_n^3$ . Furthermore, we also determine the upper bound of every type of bicyclic graphs. There exists an interesting problem:

**Problem 1.** Which graph  $G \in \mathcal{B}_n^3$  has the minimum Hosoya index?

We attempted to find a solution to the problem; however, the problem is very difficult for us.

### Data Availability

No data were used to support this study.

### Conflicts of Interest

The authors declare that they have no known competing financial interests or personal relationships that could have appeared to influence the work reported in this study.

### Acknowledgments

This work was supported by the National Natural Science Foundation of China (no. 11761056), Natural Science Foundation of Qinghai Province (no. 2020-ZJ-920), and the Scientific Research Innovation Team in Qinghai Nationalities University.

### References

- [1] H. Hosoya, "Topological index. A newly proposed quantity characterizing the topological nature of structural isomers of saturated hydrocarbons," *Bulletin of the Chemical Society of Japan*, vol. 44, no. 9, pp. 2332–2339, 1971.
- [2] H. Hosoya and K. Hosoi, "Topological index as applied to  $\pi$ -electron systems, III. Mathematical relations among various bond orders," *The Journal of Chemical Physics*, vol. 64, no. 3, pp. 1065–1073, 1976.
- [3] H. Hosoya, K. Hosoi, and I. Gutman, "A topological index for the total  $\pi$ -electron energy  $\pi$ -electron energy, Proof of a generalised Hckel rule for an arbitrary network," *Theoretica Chimica Acta*, vol. 38, no. 1, pp. 37–47, 1975.
- [4] M. Jerrum, "Two-dimensional monomer-dimer systems are computationally intractable," *Journal of Statistical Physics*, vol. 48, no. 1-2, pp. 121–134, 1987.
- [5] Y. Hou, "On acyclic systems with minimal Hosoya index," *Discrete Applied Mathematics*, vol. 119, no. 3, pp. 251–257, 2002.
- [6] H. Liu, "The proof of a conjecture concerning acyclic molecular graphs with maximal Hosoya index and diameter 4," *Journal of Mathematical Chemistry*, vol. 43, no. 3, pp. 1199–1206, 2008.
- [7] S. Wagner, "Extremal trees with respect to Hosoya index and Merrifield-Simmons index," *MATCH Communications in Mathematical and in Computer Chemistry*, vol. 57, pp. 221–233, 2007.
- [8] H. Deng and S. Chen, "The extremal unicyclic graphs with respect to Hosoya index and Merrifield-Simmors index," *MATCH Communications in Mathematical and in Computer Chemistry*, vol. 59, pp. 171–190, 2008.
- [9] H. Hua, "Hosoya index of unicyclic graphs with prescribed pendent vertices," *Journal of Mathematical Chemistry*, vol. 43, no. 2, pp. 831–844, 2008.
- [10] J. Ou, "On extremal unicyclic molecular graphs with prescribed girth and minimal Hosoya index," *Journal of Mathematical Chemistry*, vol. 42, no. 3, pp. 423–432, 2007.
- [11] K. Xu and B. Xu, "Some extremal unicyclic graphs with respect to Hosoya index and Merrifield-Simmons index," *MATCH Communications in Mathematical and in Computer Chemistry*, vol. 62, pp. 629–648, 2009.
- [12] G. Yu, L. Feng, and A. Ilic, "The largest  $n - 1$  Hosoya indices of unicyclic graphs," *Filomat*, vol. 30, no. 9, pp. 2573–2581, 2016.
- [13] H. Deng, "The largest Hosoya index of  $(n, n + 1)$ -graphs," *Applied Mathematics and Computation*, vol. 56, pp. 2499–2506, 2006.
- [14] X. Pan and Z. Sun, "The  $(n, m)$ -graphs of minimum Hosoya index," *MATCH Communications in Mathematical and in Computer Chemistry*, vol. 64, pp. 811–820, 2010.
- [15] W. So and W. Wang, "Finding the least element of the ordering of graphs with respect to their matching numbers," *MATCH Communications in Mathematical and in Computer Chemistry*, vol. 73, pp. 225–238, 2015.
- [16] S. Wagner and I. Gutman, "Maxima and minima of the hosoya index and the merrifield-simmons index," *Acta Applicandae Mathematica*, vol. 112, no. 3, pp. 323–346, 2010.
- [17] W. Liu, J. Ban, L. Feng, T. Cheng, F. Emmert-Streib, and M. Dehmer, "The maximum Hosoya Index of unicyclic graphs with diameter at most four," *Symmetry*, vol. 11, no. 8, p. 1034, 2019.



## Research Article

# Characterization of (Molecular) Graphs with Fractional Metric Dimension as Unity

Muhammad Javaid <sup>1</sup>, Muhammad Kamran Aslam,<sup>1</sup> Abdulaziz Mohammed Alanazi <sup>2</sup>,  
and Meshari M. Aljohani<sup>3</sup>

<sup>1</sup>Department of Mathematics, School of Science, University of Management and Technology, Lahore, Pakistan

<sup>2</sup>Department of Mathematics, University of Tabuk, Tabuk, Saudi Arabia

<sup>3</sup>Department of Chemistry, University of Tabuk, Tabuk, Saudi Arabia

Correspondence should be addressed to Muhammad Javaid; [javidmath@gmail.com](mailto:javidmath@gmail.com)

Received 5 March 2021; Accepted 11 June 2021; Published 28 June 2021

Academic Editor: Kashif Ali

Copyright © 2021 Muhammad Javaid et al. This is an open access article distributed under the Creative Commons Attribution License, which permits unrestricted use, distribution, and reproduction in any medium, provided the original work is properly cited.

Distance-based dimensions provide the foreground for the identification of chemical compounds that are chemically and structurally different but show similarity in different reactions. The reason behind this similarity is the occurrence of a set  $\mathbb{S}$  of atoms and their same relative distances to some ordered set  $\mathbb{T}$  of atoms in both compounds. In this article, the aforementioned problem is considered as a test case for characterising the (molecular) graphs bearing the fractional metric dimension (FMD) as 1. For the illustration of the theoretical development, it is shown that the FMD of path graph is unity. Moreover, we evaluated the extremal values of fractional metric dimension of a tetrahedral diamond lattice.

## 1. Introduction

Day by day, the nexus of chemistry is progressing by the advancements in drug discovery, formation of chemical compounds, and development of testing kits for the diagnosis of different diseases and medical anomalies. Besides different concepts that arose as a result of the emergence of cheminformatics, distance-based dimensions also have their stake in this concern. Assume that, in a graph  $\mathbb{C}$ , the shortest path between the 2 vertices  $s, t$  is given by  $d(s, t)$ . Let  $\mathbb{S} = \{s_1, s_2, s_3, \dots, s_k\} \subseteq V(\mathbb{C})$  and  $u \in V(\mathbb{C})$ ; then, the  $k$ -tuple metric form of  $\mathbb{S}$  in terms of  $u$  is given by  $r(u|\mathbb{S}) = (d(u, s_1), d(u, s_2), d(u, s_3), \dots, d(u, s_k))$ . The set  $\mathbb{S}$  becomes a resolving set having  $k$  elements for a graph  $\mathbb{C}$  if each pairs of vertices in  $\mathbb{C}$  bears distinct  $k$ -tuple metric forms. The resolving set with minimum cardinality in  $\mathbb{C}$  forms its metric basis, and its cardinality represents its metric dimension.

The terminology of resolving sets was introduced by Slater [1, 2] by naming them as locating sets. Harary and Melter [3] personally discovered these terminologies and

called them as the metric dimension of  $\mathbb{C}$ . Afterward, many researchers have studied different graph structures for the calculation of metric dimensions. The results for the metric dimensions of path, cycle, Peterson, and generalized Peterson graphs can be found in [4–6]. For various results on metric dimensions of graphs, we refer to [7–9] and [10]. Chartrand et al. [11] employed metric dimension to find the solution of an integer programming problem (IPP). Subsequently, Currie and Oellermann introduced the concept of fractional metric dimension (FMD) and obtained the solution of IPP with higher accuracy [12]. Arumugam and Mathew [13] after discovering the hidden properties of FMD formally defined it. Since then, many researchers have tried their luck in this area by attacking different graph structures. The results for the FMD of graph structures as obtained from Cartesian, hierarchial, corona, lexicographic, and comb product of connected graph structures can be seen in [14–16] and [17, 18]. Recently, Liu et al. [19] calculated the fractional metric dimension of the generalized Jahangir graph  $J_{5,k}$  and Raza et al. calculated the FMD of a metal organic network [20, 21]. Alisyah et al. presented the concept of local

fractional metric dimension (LFMD) and found the LFMD of the corona product of two connected networks [22]. Liu et al. calculated the LFMD of rotationally symmetric and planar networks [23]. Recently, Javaid et al. calculated the bounds for the LFMD of connected and cycle-related networks in [24, 25].

Johnson [26, 27] employed the concept of metric dimension for creating proficiency of large datasets of chemical graph structures. The mathematical study of chemical structures concerns the development of mathematical classification of chemical compounds. The graph-theoretic version of chemical compounds naturally exists. Despite having different chemical and structural aspects, two chemical compounds show similar behaviour during the reactions. The reason behind this peculiarity is the existence of certain common substructures within these compounds. If in two compounds, the elements of the set  $\mathbb{S}$  of atoms and the elements of the ordered set  $\mathbb{T}$  are relatively equidistant, then we call these compounds to be similar or equivalent [28]. Finding a  $\mathbb{T}$  with minimum cardinality such that the ordered lists associated with every two distinct vertices of  $\mathbb{S}$  are distinct has applications to classification problems in chemistry, as described in [11].

In this article, we are going to characterise the (molecular) graphs with FMDs as unity. As a test case, we have considered the allotropic form of carbon called by tetrahedral diamond developed by Ali et al. This article propels in the following manner: Section 1 is for introduction, Section 2 is devoted for the applications of FMD in chemistry, Section 3 is for preliminaries, Section 4 concerns with the development of a tool for the characterization of graphs with FMD as 1, and Section 5 deals with the resolving neighbourhood sets of  $\mathbb{T}\mathbb{D}(n)$ . In Section 6, we have calculated the FMD of  $\mathbb{T}\mathbb{D}(n)$ . Section 7 gives the conclusion.

## 2. Applications in Chemistry

In a molecular graph, atoms are denoted by nodes and bond between them by edges. The fraternity of chemists and pharmacists is always in search of finding out chemical compounds in some collection bearing physiochemical properties in common at some particular places. This objective is achieved by the identification of the substructure having the smallest number of atoms. In graph theory, this problem is the same as finding the FMD of the graph under consideration. In this way, druggists and chemists will be able to capture the aforementioned features of these compounds and comprehend whether they are responsible for some pharmacological activity for a newly developed drug. For more on the applications like these, see [11].

## 3. Preliminaries

For  $c \in V(\mathbb{C})$  and  $\{a, b\} \subseteq V(\mathbb{C})$ ,  $\{a, b\}$  is said to be resolved by  $c$  if  $d(a, c) \neq d(b, c)$ . The set formed by the pair of nodes comprising nodes such as  $c$  is called resolving neighbourhood. The resolving neighbourhood (RN) of  $\{a, b\}$  is mathematically given by  $R\{a, b\} = \{c \in V(\mathbb{C}) | d(a, c) \neq d(b, c)\}$ .

Suppose a connected network  $\mathbb{C}(V(\mathbb{C}), E(\mathbb{C}))$  having order  $p$ . A function  $\tau: V(\mathbb{C}) \rightarrow [0, 1]$  is known as the resolving function (RF) of  $\mathbb{C}$  if  $\tau(R\{a, b\}) \geq 1 \forall a, b \in V(\mathbb{C})$ , where  $\tau(R\{x, y\}) = \sum_{z \in R\{x, y\}} \tau(z)$ . An RF  $\eta$  of  $\mathbb{C}$  is known as a minimal resolving function (MRF) if any function  $\phi: V(\mathbb{C}) \rightarrow [0, 1]$  such that  $\phi \leq \eta$  and  $\phi(z) \neq \eta(z)$  for at least one  $z \in V(\mathbb{C})$  that is not an RF of  $\mathbb{C}$ . Then, the FMD of the network  $\mathbb{C}$  is given by  $\dim_f(\mathbb{C}) = \min\{|\eta|: \eta \text{ is the MRF of } \mathbb{C}\}$ , where  $|\eta| = \sum_{z \in V(\mathbb{C})} \eta(z)$  [13].

**3.1. Construction of Tetrahedral Diamond.** The tetrahedral diamond graph is an  $n$ -dimensional lattice, comprising  $n_i$  layers where  $1 \leq i \leq n$ . Figures 1 and 2 show  $\mathbb{T}\mathbb{D}(n)$  for  $3 \leq n \leq 5$ .

Each  $n_i$  layer is having  $n_i^2$  vertices,  $((n_i - 2)(n_i - 1)/2)$  hexagons, and three pendent edges. The vertices of each layer are denoted by  $v_j^{n_i}$  where  $1 \leq j \leq n_i$ . The first layer is isomorphic to  $K_1$ , and layer two is isomorphic to  $K_{1,3}$ , whereas for  $1 \leq i \leq n$ , each  $n_{i-1}$  layer is the subgraph of the  $n_i$ -th layer. Hence, the graph formed by each layer is denoted by  $S_{n_i}^{n_i}$ . Similarly, following are the subgraphs found to be in all the layers:  $S_{n_i}^{n_i, p}$ ,  $P_{n_i - n_{i-1}}^{n_i, p}$ ,  $P_s^{n_i, p}$ , and  $K_1^{n_i, p}$ , where  $1 \leq j, s \leq n_i - 1$  and  $p$  describes their position that can be top, top right, top left, bottom, bottom right, bottom left, middle, middle right, middle left, and bottom denoted by  $t, tr, tl, b, br, bl, m, mr$ , and  $ml$ , respectively. Figure 3 shows all the subsets of  $\mathbb{T}\mathbb{D}(n)$ .

It can be seen from the figure that, in each layer,  $v_1^{n_i}$  is adjacent to  $v_2^{n_i+1}$ ,  $v_{n_i}^{n_i}$  is adjacent to  $v_{n_i-1}^{n_i+1}$ , and  $v_{n_i}^{n_i}$  is adjacent to  $v_{n_i-1}^{n_i+1}$ . Apart from them, every vertex with an odd label in the  $n_i - 1$  layer is adjacent to the vertex with an even label in the  $n_i$  layer and vice versa.

## 4. Characterization of Graphs with FMD as Unity

In this section of the article, we are giving generic criteria for identifying graphs with FMD as 1. These criteria have been shaped up as a theorem given below.

**Theorem 1.** Let  $\mathbb{C}$  be a connected graph and  $R\{a, b\}$  be a resolving neighbourhood set of the pair of vertices  $a, b$  in  $\mathbb{C}$ . If  $\cap R\{a, b\} \neq \Phi$ , then

$$\dim_{\text{frac}}(\mathbb{C}) = 1, \quad (1)$$

where  $|V(\mathbb{C})| \geq 3$ .

*Proof.* Assume that  $R = R\{a, b\}$  is an arbitrary resolving neighbourhood set for  $\{a, b\} \subset V(\mathbb{C})$  and  $Y = \cap R$ . Now, we define the function  $\psi: V(\mathbb{C}) \rightarrow [0, 1]$  as  $c = \sum_{x \in Y} \psi(x)$  and  $1 - c = \sum_{x \in (R-Y) \cap X} \psi(x)$ , where  $c$  is a real number that approaches to 1 and  $X = V(\mathbb{C})$ . For  $a, b \in V(\mathbb{C})$  and  $c \rightarrow 1$ ,

$$\begin{aligned} \psi(R) &= \sum_{x \in R} \psi(x) = \sum_{x \in Y} \psi(x) + \sum_{x \in (R-Y) \cap X} \psi(x), \\ &= c + w(1 - c) \\ &\geq 1, \end{aligned} \quad (2)$$

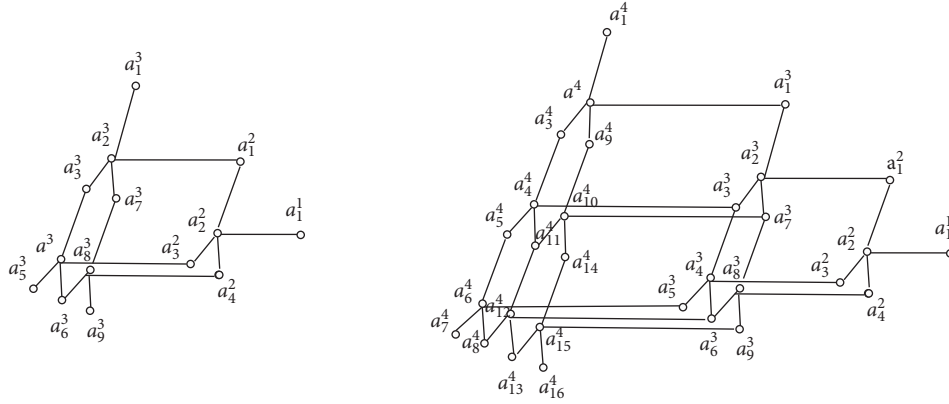


FIGURE 1: Tetrahedral diamond lattice with 3 (a) and 4 (b) layers.

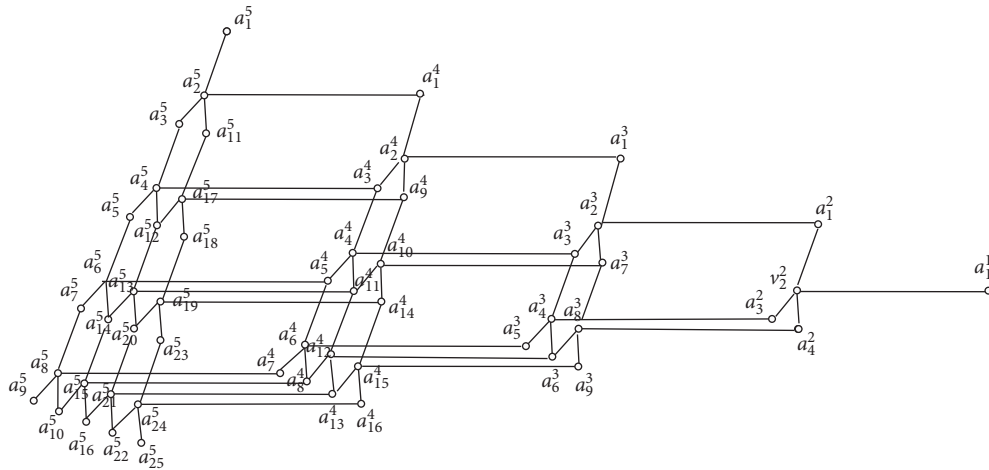


FIGURE 2: Tetrahedral diamond lattice with 5 layers.

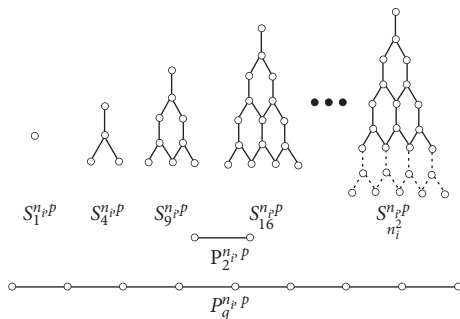


FIGURE 3: Subsets of the tetrahedral diamond lattice.

where  $w = (|V(\mathbb{C})||V(\mathbb{C}) - 1|/2)$ . It implies that  $\psi$  is a resolving function. To check that  $\psi$  is a minimal resolving function, assume that there is another minimal resolving function  $\tau$  such that  $\tau \leq \psi$ . By definition,  $\tau(x) < \psi(x)$  for some  $x \in X$ . Now, for some resolving neighbourhood set  $R$ , we have

$$\begin{aligned} \tau(R) &= \sum_{x \in Y} \tau(x) + \sum_{x \in (R-Y) \cap X} \tau(x) \\ &< \sum_{x \in Y} \psi(x) + \sum_{x \in (R-Y) \cap X} \psi(x), \quad (3) \\ &= c + (1 - c) = 1. \end{aligned}$$

Consequently,  $\tau(R) < 1$  which implies that  $\tau$  is not a resolving function. Thus,  $\psi$  is a minimal resolving function. Let  $\bar{\psi}$  be another minimal resolving function of  $\mathbb{C}$ . Now, we have the following possibilities:

- (i)  $\bar{\psi}(x) < \psi(x) \forall x \in X$
- (ii)  $\bar{\psi}(x) \geq \psi(x) \forall x \in X$
- (iii)  $\bar{\psi}(x) < \psi(x)$  for some  $x \in X$  □

Case 1. If  $\bar{\psi}(x) < \psi(x)$  for all  $x \in X$ , then for each resolving neighbourhood set  $R$ ,  $\bar{\psi}(R) < 1 \Rightarrow \bar{\psi}$  is not a resolving function; therefore, this case does not hold.

Case 2. If  $\bar{\psi}(x) \geq \psi(x)$  for all  $x \in X$ , then we have the following subcases:

Subcase A: for  $1 \leq r, s \leq w$  and  $R_r - Y \cap R_s - Y = \Phi$ , we have

$$\begin{aligned} |\bar{\psi}| &= \sum_{x \in Y} \bar{\psi}(x) + \sum_{x \in (R-Y) \cap X} \bar{\psi}(x) \\ &> \sum_{x \in Y} \psi(x) + \sum_{x \in (R-Y) \cap X} \psi(x), \quad (4) \\ &= c + w(1 - c) = |\psi|. \end{aligned}$$

As  $c \rightarrow 1$ ,  $\dim_{\text{frac}}(\mathbb{C}) = |\psi| = c + w(1 - c) = 1$ .

Subcase B: for  $1 \leq r, s \leq w$  and  $R_r - Y \cap R_s - Y \neq \Phi$ , we have

$$|\bar{\psi}| = \sum_{x \in Y} \bar{\psi}(x) + \sum_{x \in \bar{R}_t} \bar{\psi}(x), \quad (5)$$

where  $\bar{R}_t = R_t \cap [X - \cap_{j=1}^{t-1} R_j - Y]$ . Then,

$$\begin{aligned} |\bar{\psi}| &= \sum_{x \in Y} \bar{\psi}(x) + \sum_{x \in \bar{R}_t} \bar{\psi}(x) \\ &\geq \sum_{x \in Y} \psi(x) + \sum_{x \in \bar{R}_t} \psi(x), \quad (6) \\ &= c + \sum_{x \in \bar{R}_t} \psi(x). \end{aligned}$$

So,

$$\begin{aligned} \dim_{\text{frac}}(\mathbb{C}) &= c + \sum_{x \in \bar{R}_t} \psi(x) \\ &\leq c + \sum_{x \in (R-Y) \cap X} \psi(x), \quad (7) \\ &= c + w(1 - c), \\ &= 1. \end{aligned}$$

Thus,  $\dim_{\text{frac}}(\mathbb{C}) \leq 1$ . But, by definition,  $\dim_{\text{frac}}(\mathbb{C}) \geq 1$ . Therefore,

$$\dim_{\text{frac}}(\mathbb{C}) = 1. \quad (8)$$

Case 3. If  $\bar{\psi}(x) < \psi(x)$  for some  $x \in X$ , this case is a consequent of the abovementioned two cases (Case I and II); therefore, we have  $\dim_{\text{frac}}(\mathbb{C}) = 1$ .

Consequently, from Case 1-3, we arrive at the following conclusion:

$$\dim_{\text{frac}}(\mathbb{C}) = 1. \quad (9)$$

Using the result presented above, we are now going to prove the following fact:

**Proposition 1.** Suppose that, for any  $n \geq 3$ ,  $\mathbb{G} \cong P_n$ ; then,  $\dim_{\text{frac}}(\mathbb{G}) = 1$ .

*Proof*

Case 1: for  $n = 3$ : the resolving neighbourhood sets for the current case are  $R_1 = R\{a_1, a_2\} = \{a_1, a_2, a_3\}$ ,  $R_2 = R\{a_2, a_3\} = \{a_1, a_2, a_3\}$ , and  $R_3 = R\{a_1, a_3\} = \{a_1, a_3\}$ . It can be seen that  $\cap_{t=1}^3 R_t = \{a_1, a_3\} \neq \Phi$ . Therefore, from Theorem 1, we arrive at the conclusion that  $\dim_{\text{frac}}(P_3) = 1$ .

Case 2: for  $n \geq 4$ : the resolving neighbourhood sets of  $P_n$  are  $R\{a_i, a_{i+p}\} = V(P_n) - \{a_{(2i+p/2)}\}$  and  $R\{a_i, a_{i+s}\} = V(\mathbb{P}_n)$ , where  $p, s \geq 1$ ,  $1 \leq i \leq n$ ,  $p \equiv 0 \pmod{2}$ , and  $s \equiv 1 \pmod{2}$ .

It can be seen that  $\cap_{t=1}^n R_t = \{a_1, a_n\} \neq \Phi$ . Therefore, from Theorem 1, it implies that

$$\dim_{\text{frac}}(P_n) = 1. \quad (10) \quad \square$$

*Remark 1.* The abovementioned proposition strengthens the result proved in [13].

## 5. Resolving Neighbourhood Sets of $\mathbb{T}\mathbb{D}(n)$

In this section, we present some the results regarding the resolving neighbourhood sets of  $\mathbb{T}\mathbb{D}(n)$ . Lemma 1 deals with the resolving neighbourhoods of  $\mathbb{T}\mathbb{D}(n)$  having minimum cardinality followed by Lemma 2 and Lemma 3 that are concerned with resolving neighbourhood sets of maximum cardinalities.

**Lemma 1.** Suppose that  $\mathbb{C} \cong \mathbb{T}\mathbb{D}(n)$  is an  $n$ -dimensional tetrahedral diamond lattice. Then, the minimum resolving neighbourhood sets are as follows:

- (a) For  $n \geq 4$ ,  $n \equiv 0 \pmod{2}$ ,  $\alpha = (n/2)$ ,  $\beta = \alpha + 1$ ,  $\gamma = 2\alpha - 1$ , and  $\eta = 2\beta - 1$ ,  $|R_t| = |R\{a_1^\alpha, a_1^\beta\}| = |R\{a_\gamma^\alpha, a_\eta^\beta\}| = |R\{a_{\alpha^2}^\alpha, a_{\beta^2}^\beta\}| = (n(n^2 + 3n + 2)/12)$  and  $|\cup_{t=1}^3 R_t| = (n(n^2 + 3n + 2)/6)$ .
- (b) For  $n \geq 3$ ,  $n \equiv 1 \pmod{2}$ ,  $\alpha = (n - 1/2)$ ,  $\beta = (n + 1/2)$ ,  $\gamma = (n + 3/2)$ ,  $\eta = 2\alpha - 1$ ,  $\lambda = 2\beta - 1$ , and  $\mu = 2\gamma - 1$ ,  $|R_t| = |R\{a_1^\alpha, a_1^\beta\}| = |R\{a_\gamma^\alpha, a_\eta^\beta\}| = |R\{a_\lambda^\alpha, a_\mu^\beta\}| = |R\{a_{\alpha^2}^\alpha, a_{\beta^2}^\beta\}| = |R\{a_{\beta^2}^\beta, a_{\gamma^2}^\gamma\}| = (n^3 + 3n^2 + 5n + 3/12)$  and  $|\cup_{t=1}^6 R_t| = (n^3 + 6n^2 + 11n - 30/6)$ .

*Proof*

- (a) The resolving neighbourhood sets of  $R\{a_1^\alpha, a_1^\beta\}$ ,  $R\{a_\gamma^\alpha, a_\eta^\beta\}$ , and  $R\{a_{\alpha^2}^\alpha, a_{\beta^2}^\beta\}$  are  $R\{a_1^\alpha, a_1^\beta\} = V(\mathbb{C}) - \cup_{j=\beta}^n (S_{j^2}^j - S_{(j-2)^2}^{j,t})$ ,  $R\{a_\gamma^\alpha, a_\eta^\beta\} = V(\mathbb{C}) - \cup_{j=\beta}^n (S_{j^2}^j - S_{(j-2)^2}^{j,bl})$ , and  $R\{a_{\alpha^2}^\alpha, a_{\beta^2}^\beta\} = V(\mathbb{C}) - \cup_{j=\beta}^n (S_{j^2}^j - S_{(j-2)^2}^{j,br})$ . We note that  $|R_t| = |R\{a_1^\alpha, a_1^\beta\}| = |R\{a_\gamma^\alpha, a_\eta^\beta\}| = |R\{a_{\alpha^2}^\alpha, a_{\beta^2}^\beta\}| = (n(n^2 + 3n + 2)/12)$ ,  $\cup_{t=1}^3 R_t = \cup_{j=1}^\alpha S_{j^2}^j \cup \cup_{j=\alpha+1}^n (S_{(j-\alpha)^2}^{j,t} \cup S_{(j-\alpha)^2}^{j,br} \cup S_{(j-\alpha)^2}^{j,bl})$ , and  $|\cup_{t=1}^3 R_t| = (n(n^2 + 3n + 2)/6)$ .

- (b) The resolving neighbourhood sets of  $R\{a_1^\alpha, a_1^\beta\}$ ,  $R\{a_1^\beta, a_1^\gamma\}$ ,  $R\{a_\eta^\alpha, a_\lambda^\beta\}$ ,  $R\{a_\lambda^\beta, a_\mu^\gamma\}$ ,  $R\{a_{\alpha_2}^\alpha, a_{\beta_2}^\beta\}$ ,  $R\{a_{\beta_2}^\beta, a_{\gamma_2}^\gamma\}$  are  $R\{a_1^\alpha, a_1^\beta\} = V(\mathbb{C}) - \cup_{j=\beta}^n (S_j^j - S_{(j-2)^2}^{j,t})$ ,  $R\{a_\eta^\alpha, a_\lambda^\beta\} = V(\mathbb{C}) - \cup_{j=\beta}^n (S_j^j - S_{(j-2)^2}^{j,bl})$ , and  $R\{a_{\alpha_2}^\alpha, a_{\beta_2}^\beta\} = V(\mathbb{C}) - \cup_{j=\beta}^n (S_j^j - S_{(j-2)^2}^{j,br})$  and  $R\{a_1^\beta, a_1^\gamma\} = V(\mathbb{C}) - \cup_{j=\gamma}^n (S_j^j - S_{(j-2)^2}^{j,t})$ ,  $R\{a_\lambda^\beta, a_\mu^\gamma\} = V(\mathbb{C}) - \cup_{j=\gamma}^n (S_j^j - S_{(j-2)^2}^{j,bl})$ , and  $R\{a_{\beta_2}^\beta, a_{\gamma_2}^\gamma\} = V(\mathbb{C}) - \cup_{j=\gamma}^n (S_j^j - S_{(j-2)^2}^{j,br})$ . We note that  $|R_t| = |R\{a_1^\alpha, a_1^\beta\}| = |R\{a_1^\beta, a_1^\gamma\}| = |R\{a_\eta^\alpha, a_\lambda^\beta\}| = |R\{a_\lambda^\beta, a_\mu^\gamma\}| = |R\{a_{\alpha_2}^\alpha, a_{\beta_2}^\beta\}| = |R\{a_{\beta_2}^\beta, a_{\gamma_2}^\gamma\}| = (n^3 + 3n^2 + 5n + 3/12)$ ,  $\cup_{t=1}^6 R_t = \cup_{j=1}^n S_j^j \cup \cup_{j=\gamma+1}^n (S_{(j-\gamma)^2}^{j,t} \cup S_{(j-\gamma)^2}^{j,br} \cup S_{(j-\gamma)^2}^{j,bl})$ , and  $|\cup_{t=1}^6 R_t| = (n^3 + 6n^2 + 11n - 30/6)$ .  $\square$

**Lemma 2.** Suppose that  $\mathbb{C} \cong \mathbb{T}\mathbb{D}(n)$  is an  $n$ -dimensional tetrahedral diamond lattice with  $n \geq 3$  and  $n \equiv 1 \pmod{n}$ . Then,

- (a) For  $1 \leq \alpha \leq n$ ,  $\beta = \alpha + 1$ ,  $\gamma = 2\alpha - 1$ , and  $\eta = 2\beta - 1$ ,  $|R_t| < |R\{a_1^\alpha, a_1^\beta\}| = |R\{a_\gamma^\alpha, a_\eta^\beta\}| = |R\{a_{\alpha_2}^\alpha, a_{\beta_2}^\beta\}|$  and  $|R\{a_1^\alpha, a_1^\beta\} \cap \cup_{t=1}^6 R_t| = |R\{a_\gamma^\alpha, a_\eta^\beta\} \cap \cup_{t=1}^6 R_t| = |R\{a_{\alpha_2}^\alpha, a_{\beta_2}^\beta\} \cap \cup_{t=1}^6 R_t| \geq |R_t|$
- (b) For  $1 \leq \alpha \leq n$ ,  $\beta = \alpha + 1$  and  $2 \leq \gamma \leq 2\alpha - 1$ ,  $|R_t| < |R\{a_\gamma^\alpha, a_\gamma^\beta\}|$  and  $|R\{a_\gamma^\alpha, a_\gamma^\beta\} \cup \cup_{t=1}^6 R_t| \leq |R_t|$
- (c) For  $2 \leq \alpha \leq n$ ,  $\beta = 2\alpha - 1$ ,  $\gamma = 2\alpha + 2$ ,  $\eta = \alpha^2 - 3$ , and  $\mu = \alpha^2$ ,  $|R_t| < |R\{a_\beta^\alpha, a_\gamma^\alpha\}| = |R\{a_\eta^\alpha, a_\mu^\alpha\}|$  and  $|R\{a_\beta^\alpha, a_\gamma^\alpha\} \cup \cup_{t=1}^6 R_t| = |R\{a_\eta^\alpha, a_\mu^\alpha\} \cup \cup_{t=1}^6 R_t| = |R\{a_\eta^\alpha, a_\mu^\alpha\} \cup \cup_{t=1}^6 R_t| \geq |R_t|$
- (d) For any  $\{a_\alpha^\alpha, a_\beta^\beta\} \in E(\mathbb{C})$ ,  $\gamma \geq 1$ ,  $\eta \geq 2$ ,  $\gamma \equiv 1 \pmod{2}$ , and  $\eta \equiv 0 \pmod{2}$ ,  $|R_t| < |R\{a_\alpha^\alpha, a_\beta^\beta\}| = |R\{a_\alpha^\alpha, a_{\alpha+\gamma}^{\alpha+\eta}\}| = |V(\mathbb{C})| = (n(2n^2 + 3n + 1)/6)$  and  $|R\{a_\alpha^\alpha, a_\beta^\beta\} \cap \cup_{t=1}^6 R_t| \geq |R_t|$

*Proof*

- (a) The resolving neighbourhood sets of  $R\{a_1^\alpha, a_1^\beta\}$ ,  $\{a_1^\alpha, a_3^\alpha\}$ ,  $\{a_1^\alpha, a_4^\alpha\}$ ,  $\{a_\eta^\alpha, a_1^\beta\}$ , and  $R\{a_\gamma^\alpha, a_\eta^\beta\}$  are  $R\{a_1^\alpha, a_1^\beta\} = V(\mathbb{C}) - \cup_{j=\beta}^n (S_j^j - S_{(j-1)^2}^{j,t})$ ,  $R\{a_\gamma^\alpha, a_\eta^\beta\} = V(\mathbb{C}) - \cup_{j=2}^\beta (S_j^j - S_{(j-1)^2}^{j,bl})$ , and  $R\{a_{\alpha_2}^\alpha, a_{\beta_2}^\beta\} = V(\mathbb{C}) - \cup_{j=\beta}^n (S_j^j - S_{(j-1)^2}^{j,br})$ , respectively. Since  $|R\{a_1^\alpha, a_1^\beta\}| = |R\{a_\gamma^\alpha, a_\eta^\beta\}| = |R\{a_{\alpha_2}^\alpha, a_{\beta_2}^\beta\}| = (2n^3 + 3n^2 + n + 6\alpha(n+1)(\alpha-n) - 6\alpha\beta(\alpha-\beta-1)/6)$ , thus  $|R_t| = (2n^3 + 3n^2 + n + 6\alpha(n+1)(\alpha-n) - 6\alpha\beta(\alpha-\beta-1)/6)$ . Therefore,  $|R\{a_1^\alpha, a_1^\beta\} \cap \cup_{t=1}^6 R_t| = |R\{a_\gamma^\alpha, a_\eta^\beta\} \cap \cup_{t=1}^6 R_t| = |R\{a_{\alpha_2}^\alpha, a_{\beta_2}^\beta\} \cap \cup_{t=1}^6 R_t| \geq |R_t|$ .

- (b) First of all, we introduce a notation for simplification.

$$\mu = \begin{cases} \frac{\gamma}{2}, & \text{for } n \equiv 0 \pmod{n}, \\ \frac{\gamma-1}{2}, & \text{for } n \equiv 1 \pmod{n}. \end{cases} \quad (11)$$

The resolving neighbourhood for  $R\{a_\gamma^\alpha, a_\gamma^\beta\}$  is  $R\{a_\gamma^\alpha, a_\gamma^\beta\} = V(\mathbb{C}) - \cup_{j=\alpha-\mu+1}^\alpha S_j^j \cup \cup_{j=\beta}^\beta S_j^j \cup \cup_{j=\mu+1}^{\mu+n-\alpha} S_j^j$ . It can be seen that  $|R\{a_\gamma^\alpha, a_\gamma^\beta\}| = (n-1-4(\mu+1)^3 + 6(\mu+1)^2 - \mu + 2b^3 - 3b^2 + b + 2(\mu+n-\alpha+1)^3 - (\mu+n-\alpha+1)^2 - \alpha/6) > |R_t|$ . Therefore,  $|R\{a_3^\alpha, a_4^\alpha\} \cup \cup_{t=1}^6 R_t| \geq |R_t|$ . Also, by the symmetry of the network,  $|R_t| < |R\{a_\gamma^\alpha, a_\gamma^\beta\}|$  and  $|R\{a_\gamma^\alpha, a_\gamma^\beta\} \cup \cup_{t=1}^6 R_t| \geq |R_t|$ .

- (c) The resolving neighbourhood for  $R\{a_\beta^\alpha, a_\gamma^\alpha\}$  and  $R\{a_\eta^\alpha, a_\mu^\alpha\}$  are  $R\{a_\beta^\alpha, a_\gamma^\alpha\} = V(\mathbb{C}) - S_1^1 \cup \cup_{j=3}^\alpha P_j^{j,l} \cup \cup_{j=\alpha+1}^n (P_j^{j,l} - S_{(j-\alpha)^2}^{j,l})$  and  $R\{a_\eta^\alpha, a_\mu^\alpha\} = V(\mathbb{C}) - S_1^1 \cup \cup_{j=3}^{\alpha^2} P_j^{j,r} \cup \cup_{j=\alpha+1}^n (P_j^{j,r} - S_{(j-\alpha)^2}^{j,r})$ . It can be seen that  $|R\{a_\beta^\alpha, a_\gamma^\alpha\}| = |R\{a_\eta^\alpha, a_\mu^\alpha\}| = (2(n+1)^3 - 3(n+1)^2 + 2n + 8 - 7\alpha + 6(2\alpha-2)(n-\alpha+1) + 2(n-\alpha+1)^3 - 3(n-\alpha+1)^2/6)$ . Hence,  $|R_t| < (2(n+1)^3 - 3(n+1)^2 + 2n + 8 - 7\alpha + 6(2\alpha-2)(n-\alpha+1) + 2(n-\alpha+1)^3 - 3(n-\alpha+1)^2/6)$  and  $|R\{a_\beta^\alpha, a_\gamma^\alpha\} \cup \cup_{t=1}^6 R_t| = |R\{a_\eta^\alpha, a_\mu^\alpha\} \cup \cup_{t=1}^6 R_t| \geq |R_t|$ .
- (d) The resolving neighbourhood sets  $R\{a_\alpha^\alpha, a_\beta^\beta\}$  and  $R\{a_\alpha^\alpha, a_{\alpha+\gamma}^{\alpha+\eta}\}$  are  $R\{a_\alpha^\alpha, a_\beta^\beta\} = V(\mathbb{C}) = R\{a_\alpha^\alpha, a_{\alpha+\gamma}^{\alpha+\eta}\}$ . Clearly,  $|R\{a_\alpha^\alpha, a_\beta^\beta\}| = |R\{a_\alpha^\alpha, a_{\alpha+\gamma}^{\alpha+\eta}\}| = (n(n+1)(2n+1)/6) > |R_t|$ . Also,  $|R\{a_\alpha^\alpha, a_\beta^\beta\} \cup \cup_{t=1}^6 R_t| = |R\{a_\alpha^\alpha, a_{\alpha+\gamma}^{\alpha+\eta}\} \cup \cup_{t=1}^6 R_t| \geq |R_t|$ .  $\square$

**Lemma 3.** Suppose that  $\mathbb{C} \cong \mathbb{T}\mathbb{D}(n)$  is an  $n$ -dimensional tetrahedral diamond lattice with  $n \geq 4$  and  $n \equiv 0 \pmod{n}$ . Then,

- (a) For  $1 \leq \alpha \leq n$ ,  $\beta = \alpha + 1$ ,  $\gamma = 2\alpha - 1$ , and  $\eta = 2\beta - 1$ ,  $|R_t| < |R\{a_1^\alpha, a_1^\beta\}| = |R\{a_\gamma^\alpha, a_\eta^\beta\}| = |R\{a_{\alpha_2}^\alpha, a_{\beta_2}^\beta\}|$  and  $|R\{a_1^\alpha, a_1^\beta\} \cap \cup_{t=1}^3 R_t| = |R\{a_\gamma^\alpha, a_\eta^\beta\} \cap \cup_{t=1}^3 R_t| = |R\{a_{\alpha_2}^\alpha, a_{\beta_2}^\beta\} \cap \cup_{t=1}^3 R_t| \geq |R_t|$
- (b) For  $1 \leq \alpha \leq n$ ,  $\beta = \alpha + 1$ , and  $2 \leq \gamma \leq 2\alpha - 1$ ,  $|R_t| < |R\{a_\gamma^\alpha, a_\gamma^\beta\}|$  and  $|R\{a_\gamma^\alpha, a_\gamma^\beta\} \cup \cup_{t=1}^3 R_t| \leq |R_t|$
- (c) For  $2 \leq \alpha \leq n$ ,  $\beta = 2\alpha - 1$ ,  $\gamma = 2\alpha + 2$ ,  $\eta = \alpha^2 - 3$ , and  $\mu = \alpha^2$ ,  $|R_t| < |R\{a_\beta^\alpha, a_\gamma^\alpha\}| = |R\{a_\eta^\alpha, a_\mu^\alpha\}|$  and  $|R\{a_\beta^\alpha, a_\gamma^\alpha\} \cup \cup_{t=1}^3 R_t| = |R\{a_\eta^\alpha, a_\mu^\alpha\} \cup \cup_{t=1}^3 R_t| = |R\{a_\eta^\alpha, a_\mu^\alpha\} \cup \cup_{t=1}^3 R_t| \geq |R_t|$
- (d) For any  $\{a_\alpha^\alpha, a_\beta^\beta\} \in E(\mathbb{C})$ ,  $\gamma \geq 1$ ,  $\eta \geq 2$ ,  $\gamma \equiv 1 \pmod{2}$ , and  $\eta \equiv 0 \pmod{2}$ ,  $|R_t| < |R\{a_\alpha^\alpha, a_\beta^\beta\}| =$

$$|R\{a_\alpha^\alpha, a_{\alpha+\gamma}^{\alpha+\eta}\}| = |V(\mathbb{C})| = (n(2n^2 + 3n + 1)/6) \quad \text{and} \\ |R\{a_\alpha^\alpha, a_\beta^\beta\} \cap \cup_{t=1}^3 R_t| \geq |R_t|$$

*Proof.* The proof is the same as that of Lemma 2.  $\square$

## 6. Fractional Metric Dimension of $\mathbb{T}\mathbb{D}(n)$

In this section, the FMD of  $\mathbb{T}\mathbb{D}(n)$  is calculated and the criterion of their evaluation is devised by the following result.

**Theorem 2.** *If  $\mathbb{C} \cong \mathbb{T}\mathbb{D}(n)$  is an  $n$ -dimensional tetrahedral diamond lattice with  $n \geq 3$  and  $n \equiv 1 \pmod{2}$ , then*

$$1 < \dim_{\text{frac}}(\mathbb{C}) \leq 2 \left( \frac{n^3 + 6n^2 + 11n - 30}{n^3 + 3n^2 + 5n + 3} \right). \quad (12)$$

*Proof*

Case 1: when  $n = 3$ .

The resolving neighbourhood sets are as shown in Tables 1–4.

The resolving neighbourhood sets that are equal due to symmetry are given by the following:

Now, for  $uv \in E(\mathbb{C})$  and  $47 \leq L \leq 62$ , we have

$$R\{uv\} = V(\mathbb{C}). \quad (13)$$

In the same manner, the pairwise resolving neighbourhood sets that equals  $V(\mathbb{C})$  are as follows:

As we can see, Table 3 shows the resolving neighbourhood sets of  $\mathbb{T}\mathbb{D}(3)$  having the maximum cardinality of 13 and  $\cup_{L=63}^{84} R_L = V(\mathbb{T}\mathbb{D}(3))$ . Table 4, on the other hand, shows the resolving neighbourhood sets with minimum cardinality of 6 and  $\cup_{t=1}^6 R_t = V(\mathbb{T}\mathbb{D}(3))$ . Suppose that, for  $63 \leq L \leq 84$ ,  $|R_L| = \gamma$ , for  $1 \leq t \leq 6$ ,  $|R_t| = \lambda$ ,  $\eta = |\cup_{L=63}^{84} R_L| = |V(\mathbb{T}\mathbb{D}(3))| = 13$ , and  $\delta = |\cup_{t=1}^6 R_t| = |V(\mathbb{T}\mathbb{D}(3))| = 13$ . Now, we define a mapping  $\kappa: V(\mathbb{T}\mathbb{D}(3)) \rightarrow [0, 1]$  such that  $\kappa(a) = (1/13)$  for all  $a \in \cup_{L=63}^{84} R_L$ ; assigning the value of  $(1/13)$  to all the elements of  $\cup_{L=63}^{84} R_L$  and summing up all the labels, we get  $|\kappa| = \sum_{a \in \cup_{L=63}^{84} R_L} \kappa(a) = (13/13) = 1$ ; thus,  $\dim_{\text{frac}}(\mathbb{T}\mathbb{D}(3)) = |\kappa| = 1$ , as all the  $R_L$  for  $63 \leq L \leq 84$  are all having  $V(\mathbb{T}\mathbb{D}(3))$  in common. Similarly, we define another mapping  $\tau: V(\mathbb{T}\mathbb{D}(3)) \rightarrow [0, 1]$  such that  $\tau = (1/\lambda) = (1/6)$  for all  $a \in \cup_{t=1}^6 R_t$ , and giving labels to the elements of  $\cup_{t=1}^6 R_t$  and later on summing them up, we get  $|\tau| = \sum_{a \in \cup_{t=1}^6 R_t} \tau(a) = (13/6) = 2.33$ ; hence,  $\dim_{\text{frac}}(\mathbb{C}) < 2.33$  as all the  $R_t$  for  $1 \leq t \leq 6$  are pairwise overlapping. Therefore, we arrive at the following conclusion:

$$1 < \dim_{\text{frac}}(\mathbb{T}\mathbb{D}(3)) \leq 2.33. \quad (14)$$

Case 2: when  $n \geq 5$ .

The required minimum resolving neighbourhood sets are

$$R\{a_1^\alpha, a_1^\beta\}, R\{a_1^\beta, a_1^\gamma\}, R\{a_\eta^\alpha, a_\lambda^\beta\}, R\{a_\lambda^\beta, a_\mu^\gamma\},$$

TABLE 1: Resolving neighbourhood sets of  $\mathbb{T}\mathbb{D}(3)$ .

Resolving neighbourhood sets	Elements
$R_1 = R\{a_1^1, a_1^1\}$	$V(\mathbb{C}) - \{a_2^2, a_2^2, a_2^2\} \cup \{a_3^3, a_3^3, a_3^3, a_3^3, a_3^3\}$
$R_2 = R\{a_1^1, a_2^3\}$	$V(\mathbb{C}) - \{a_1^1, a_2^2, a_2^2\} \cup \{a_3^3, a_3^3, a_3^3, a_3^3, a_3^3\}$
$R_3 = R\{a_1^1, a_2^2\}$	$V(\mathbb{C}) - \{a_1^1, a_2^2, a_2^2\} \cup \{a_3^3, a_3^3, a_3^3, a_3^3, a_3^3\}$
$R_4 = R\{a_2^2, a_3^3\}$	$V(\mathbb{C}) - \{a_2^2, a_2^2, a_2^2, a_2^2, a_2^2, a_2^2, a_2^2, a_2^2, a_2^2\}$
$R_5 = R\{a_2^2, a_3^3\}$	$V(\mathbb{C}) - \{a_1^1, a_2^2, a_2^2, a_2^2, a_2^2, a_2^2, a_2^2, a_2^2, a_2^2\}$
$R_6 = R\{a_2^2, a_3^3\}$	$V(\mathbb{C}) - \{a_1^1, a_2^2, a_2^2, a_2^2, a_2^2, a_2^2, a_2^2, a_2^2, a_2^2\}$
$R_7 = R\{a_2^2, a_3^3\}$	$V(\mathbb{C}) - \{a_1^1, a_2^2, a_2^2, a_2^2, a_2^2, a_2^2, a_2^2, a_2^2, a_2^2\}$
$R_8 = R\{a_2^2, a_3^3\}$	$V(\mathbb{C}) - \{a_1^1, a_2^2, a_2^2, a_2^2, a_2^2, a_2^2, a_2^2, a_2^2, a_2^2\}$
$R_9 = R\{a_2^2, a_3^3\}$	$V(\mathbb{C}) - \{a_1^1, a_2^2, a_2^2, a_2^2, a_2^2, a_2^2, a_2^2, a_2^2, a_2^2\}$
$R_{10} = R\{a_2^2, a_3^3\}$	$V(\mathbb{C}) - \{a_1^1, a_2^2, a_2^2, a_2^2, a_2^2, a_2^2, a_2^2, a_2^2, a_2^2\}$
$R_{11} = R\{a_2^2, a_3^3\}$	$V(\mathbb{C}) - \{a_1^1, a_2^2, a_2^2, a_2^2, a_2^2, a_2^2, a_2^2, a_2^2, a_2^2\}$
$R_{12} = R\{a_2^2, a_3^3\}$	$V(\mathbb{C}) - \{a_1^1, a_2^2, a_2^2, a_2^2, a_2^2, a_2^2, a_2^2, a_2^2, a_2^2\}$
$R_{13} = R\{a_2^2, a_3^3\}$	$V(\mathbb{C}) - \{a_1^1, a_2^2, a_2^2, a_2^2, a_2^2, a_2^2, a_2^2, a_2^2, a_2^2\}$
$R_{14} = R\{a_2^2, a_3^3\}$	$V(\mathbb{C}) - \{a_1^1, a_2^2, a_2^2, a_2^2, a_2^2, a_2^2, a_2^2, a_2^2, a_2^2\}$
$R_{15} = R\{a_2^2, a_3^3\}$	$V(\mathbb{C}) - \{a_1^1, a_2^2, a_2^2, a_2^2, a_2^2, a_2^2, a_2^2, a_2^2, a_2^2\}$
$R_{16} = R\{a_2^2, a_3^3\}$	$V(\mathbb{C}) - \{a_1^1, a_2^2, a_2^2, a_2^2, a_2^2, a_2^2, a_2^2, a_2^2, a_2^2\}$
$R_{17} = R\{a_2^2, a_3^3\}$	$V(\mathbb{C}) - \{a_1^1, a_2^2, a_2^2, a_2^2, a_2^2, a_2^2, a_2^2, a_2^2, a_2^2\}$
$R_{18} = R\{a_2^2, a_3^3\}$	$V(\mathbb{C}) - \{a_1^1, a_2^2, a_2^2, a_2^2, a_2^2, a_2^2, a_2^2, a_2^2, a_2^2\}$
$R_{19} = R\{a_2^2, a_3^3\}$	$V(\mathbb{C}) - \{a_1^1, a_2^2, a_2^2, a_2^2, a_2^2, a_2^2, a_2^2, a_2^2, a_2^2\}$
$R_{20} = R\{a_2^2, a_3^3\}$	$V(\mathbb{C}) - \{a_1^1, a_2^2, a_2^2, a_2^2, a_2^2, a_2^2, a_2^2, a_2^2, a_2^2\}$
$R_{21} = R\{a_2^2, a_3^3\}$	$V(\mathbb{C}) - \{a_1^1, a_2^2, a_2^2, a_2^2, a_2^2, a_2^2, a_2^2, a_2^2, a_2^2\}$
$R_{22} = R\{a_2^2, a_3^3\}$	$V(\mathbb{C}) - \{a_1^1, a_2^2, a_2^2, a_2^2, a_2^2, a_2^2, a_2^2, a_2^2, a_2^2\}$
$R_{23} = R\{a_2^2, a_3^3\}$	$V(\mathbb{C}) - \{a_1^1, a_2^2, a_2^2, a_2^2, a_2^2, a_2^2, a_2^2, a_2^2, a_2^2\}$
$R_{24} = R\{a_2^2, a_3^3\}$	$V(\mathbb{C}) - \{a_1^1, a_2^2, a_2^2, a_2^2, a_2^2, a_2^2, a_2^2, a_2^2, a_2^2\}$
$R_{25} = R\{a_2^2, a_3^3\}$	$V(\mathbb{C}) - \{a_1^1, a_2^2, a_2^2, a_2^2, a_2^2, a_2^2, a_2^2, a_2^2, a_2^2\}$
$R_{26} = R\{a_2^2, a_3^3\}$	$V(\mathbb{C}) - \{a_1^1, a_2^2, a_2^2, a_2^2, a_2^2, a_2^2, a_2^2, a_2^2, a_2^2\}$
$R_{27} = R\{a_2^2, a_3^3\}$	$V(\mathbb{C}) - \{a_1^1, a_2^2, a_2^2, a_2^2, a_2^2, a_2^2, a_2^2, a_2^2, a_2^2\}$
$R_{28} = R\{a_2^2, a_3^3\}$	$V(\mathbb{C}) - \{a_1^1, a_2^2, a_2^2, a_2^2, a_2^2, a_2^2, a_2^2, a_2^2, a_2^2\}$
$R_{29} = R\{a_2^2, a_3^3\}$	$V(\mathbb{C}) - \{a_1^1, a_2^2, a_2^2, a_2^2, a_2^2, a_2^2, a_2^2, a_2^2, a_2^2\}$
$R_{30} = R\{a_2^2, a_3^3\}$	$V(\mathbb{C}) - \{a_1^1, a_2^2, a_2^2, a_2^2, a_2^2, a_2^2, a_2^2, a_2^2, a_2^2\}$
$R_{31} = R\{a_2^2, a_3^3\}$	$V(\mathbb{C}) - \{a_1^1, a_2^2, a_2^2, a_2^2, a_2^2, a_2^2, a_2^2, a_2^2, a_2^2\}$
$R_{32} = R\{a_2^2, a_3^3\}$	$V(\mathbb{C}) - \{a_1^1, a_2^2, a_2^2, a_2^2, a_2^2, a_2^2, a_2^2, a_2^2, a_2^2\}$
$R_{33} = R\{a_2^2, a_3^3\}$	$V(\mathbb{C}) - \{a_1^1, a_2^2, a_2^2, a_2^2, a_2^2, a_2^2, a_2^2, a_2^2, a_2^2\}$
$R_{34} = R\{a_2^2, a_3^3\}$	$V(\mathbb{C}) - \{a_1^1, a_2^2, a_2^2, a_2^2, a_2^2, a_2^2, a_2^2, a_2^2, a_2^2\}$
$R_{35} = R\{a_2^2, a_3^3\}$	$V(\mathbb{C}) - \{a_1^1, a_2^2, a_2^2, a_2^2, a_2^2, a_2^2, a_2^2, a_2^2, a_2^2\}$

$R\{a_\alpha^\alpha, a_\beta^\beta\}$ , and  $R\{a_\beta^\beta, a_\gamma^\gamma\}$ , where  $\alpha = (n - 1/2)$ ,  $\beta = (n + 1/2)$ ,  $\gamma = (n + 3/2)$ ,  $\eta = 2\alpha - 1$ ,  $\lambda = 2\beta - 1$ , and  $\mu = 2\gamma - 1$ . Lemma 1 clarifies that

$$|R_t| = |R\{a_1^\alpha, a_1^\beta\}| = \\ |R\{a_1^\beta, a_1^\gamma\}| = |R\{a_\eta^\alpha, a_\lambda^\beta\}| = |R\{a_\lambda^\beta, a_\mu^\gamma\}| = \\ |R\{a_\alpha^\alpha, a_\beta^\beta\}| = |R\{a_\beta^\beta, a_\gamma^\gamma\}| = (n^3 + 3n^2 + 5n + 3/12) \leq |R\{a, b\}| \quad \text{for all } a, b \in V(\mathbb{C}) \quad \text{and} \\ \cup_{t=1}^6 R_t = \cup_{j=1}^{\gamma} S_j^j \cup \cup_{j=\gamma+1}^n (S_{(j-\gamma)^2}^{j,t} \cup S_{(j-\gamma)^2}^{j,br} \cup S_{(j-\gamma)^2}^{j,bl}).$$

Also, the resolving neighbourhood sets with maximum cardinality of  $|V(\mathbb{C})|$ , as clarified by Lemma 2, are  $R_1 = R\{a_\alpha^\alpha, a_{\alpha+\gamma}^{\alpha+\eta}\}$  and  $R_1 = R\{a_\alpha^\alpha, a_\beta^\beta\}$  and  $R_1 = R\{a_\alpha^\alpha, a_{\alpha+\eta}^{\alpha+\eta}\}$ , respectively. Moreover,  $\cup_{L=1}^2 R_L = V(\mathbb{C})$ . Let

$|R\{a_\alpha^\alpha, a_{\alpha+\eta}^{\alpha+\eta}\}| = |R\{a_\alpha^\alpha, a_\beta^\beta\}| = \gamma$ ,  $|R_t| = \lambda$ ,  $|\cup_{L=1}^2 R_L| = \eta$ , and  $|\cup_{t=1}^6 R_t| = \delta$ . To find the minimum value for the  $\dim_{\text{frac}}(\mathbb{C})$ , we define a mapping  $\kappa: V(\mathbb{C}) \rightarrow [0, 1]$  such that

$$\kappa(a) = \begin{cases} \frac{1}{\kappa} & \text{for } a \in \bigcup_{L=1}^2 R_L, \\ 0 & \text{for } a \in V(\mathbb{C}) - \bigcup_{L=1}^2 R_L, \end{cases} \quad (15)$$

where  $\gamma = \eta = (n(2n^2 + 3n + 1)/6)$ . Assigning the labels to the elements of  $\bigcup_{L=1}^2 R_L$  and summing them up, we get  $|\kappa| = \sum_{a \in \bigcup_{L=1}^2 R_L} (1/\gamma) = 1$ .

Similarly, for the maximum value of  $\dim_{\text{frac}}(\mathbb{C})$ , we define another mapping  $\tau: V(\mathbb{C}) \rightarrow [0, 1]$  such that

$$\tau(a) = \begin{cases} \frac{1}{\lambda} & \text{for } a \in \bigcup_{t=1}^6 R_t, \\ 0 & \text{for } a \in V(\mathbb{C}) - \bigcup_{t=1}^6 R_t. \end{cases} \quad (16)$$

It can be seen that  $\tau$  is a resolving function for  $\mathbb{C}$  with  $n \geq 3$  because  $\tau(R\{u, v\}) \geq 1 \forall u, v \in V(\mathbb{C})$ . On the contrary, assume that there is another resolving function  $\rho$  such that  $\rho(u) \leq \tau(u)$ , for at least one  $u \in V(\mathbb{C}) \rho(u) \neq \tau(u)$ . As a consequence,  $\rho(R\{u, v\}) < 1$ , where  $R\{u, v\}$  is a resolving neighbourhood of  $\mathbb{C}$  with minimum cardinality  $\lambda$ . It shows that  $\rho$  is not a resolving function which is a contradiction. Therefore,  $\tau$  is a minimal resolving function that attains minimum  $|\tau|$  for  $\mathbb{C}$ . Since all the  $R_t$  have nonempty intersection, there is another minimal resolving function of  $\bar{\tau}$  of  $\mathbb{C}$  such that  $|\bar{\tau}| \leq |\tau|$ . Hence, assigning  $(1/\lambda)$  to the vertices of  $\mathbb{C}$  in  $\bigcup_{t=1}^3 R_t$  and calculating the summation of all the weights, we get

$$\dim_{\text{frac}}(\mathbb{C}) = \sum_{t=1}^{\delta} \frac{1}{\lambda} \leq 2 \frac{n^3 + 6n^2 + 11n - 30}{n^3 + 3n^2 + 5n + 3}. \quad (17)$$

In the end, we arrive at the following finding:

$$1 < \dim_{\text{frac}}(\mathbb{C}) \leq 2 \left( \frac{n^3 + 6n^2 + 11n - 30}{n^3 + 3n^2 + 5n + 3} \right). \quad (18)$$

□

**Theorem 3.** If  $\mathbb{C} \cong \mathbb{T}\mathbb{D}(n)$  is an  $n$ -dimensional tetrahedral diamond lattice with  $n \geq 4$  and  $n \equiv 0 \pmod{2}$ , then

$$1 < \dim_{\text{frac}}(\mathbb{C}) \leq 2. \quad (19)$$

*Proof*

Case 1: when  $n = 4$ .

The resolving neighbourhood sets are as shown in Tables 4–6.

The resolving neighbourhood sets that are equal due to symmetry are given by the following:

For  $109 \leq L \leq 149$  and  $\{uv\} \in V(\mathbb{C})$ , we have

$$R_L = R\{uv\} = V(\mathbb{C}). \quad (20)$$

Similarly, the pairwise resolving neighbourhood sets that equals  $V(\mathbb{C})$  are as follows:

As we can see, Table 7 shows the resolving neighbourhood sets of  $\mathbb{C}$  having the maximum cardinality of

TABLE 2: Resolving neighbourhood sets of  $\mathbb{T}\mathbb{D}(3)$  equal due to symmetry.

Resolving neighbourhood sets	Elements
$R_{36} = R\{a_1^1, a_1^3\}$	$R\{a_2^2, a_3^3\}$
$R_{38} = R\{a_1^1, a_5^3\}$	$R\{a_2^2, a_4^3\}$
$R_{40} = R\{a_3^3, a_7^3\}$	$R\{a_2^2, a_2^1\}$
$R_{42} = R\{a_6^3, a_7^3\}$	$R\{a_1^1, a_3^3\}$
$R_{44} = R\{a_3^3, a_6^3\}$	$R\{a_1^1, a_4^1\}$
$R_{46} = R\{a_1^1, a_9^3\}$	$R\{a_1^1, a_4^1\}$
$R_{37} = R\{a_1^1, a_3^3\}$	$R\{a_1^1, a_4^1\}$
$R_{39} = R\{a_1^1, a_9^3\}$	$R\{a_2^2, a_3^3\}$
$R_{41} = R\{a_4^3, a_8^3\}$	$R\{a_2^2, a_4^1\}$
$R_{43} = R\{a_7^3, a_9^3\}$	$R\{a_2^2, a_2^1\}$
$R_{45} = R\{a_1^1, a_5^3\}$	$R\{a_2^2, a_3^3\}$

TABLE 3: Resolving neighbourhood sets of  $\mathbb{T}\mathbb{D}(3)$  equal to  $V(\mathbb{T}\mathbb{D}(3))$ .

Resolving neighbourhood sets	Elements
$R_{63} = R\{a_1^1, a_2^3\}$	$V(\mathbb{C})$
$R_{65} = R\{a_1^1, a_8^3\}$	$V(\mathbb{C})$
$R_{67} = R\{a_7^3, a_3^3\}$	$V(\mathbb{C})$
$R_{69} = R\{a_2^2, a_3^3\}$	$V(\mathbb{C})$
$R_{71} = R\{a_2^2, a_6^3\}$	$V(\mathbb{C})$
$R_{73} = R\{a_2^2, a_9^3\}$	$V(\mathbb{C})$
$R_{75} = R\{a_3^3, a_4^1\}$	$V(\mathbb{C})$
$R_{77} = R\{a_4^1, a_2^3\}$	$V(\mathbb{C})$
$R_{79} = R\{a_4^1, a_8^3\}$	$V(\mathbb{C})$
$R_{81} = R\{a_1^1, a_3^3\}$	$V(\mathbb{C})$
$R_{83} = R\{a_2^2, a_6^3\}$	$V(\mathbb{C})$
$R_{64} = R\{a_1^1, a_4^1\}$	$V(\mathbb{C})$
$R_{66} = R\{a_1^1, a_4^1\}$	$V(\mathbb{C})$
$R_{68} = R\{a_7^3, a_3^3\}$	$V(\mathbb{C})$
$R_{70} = R\{a_2^2, a_5^3\}$	$V(\mathbb{C})$
$R_{72} = R\{a_2^2, a_7^3\}$	$V(\mathbb{C})$
$R_{74} = R\{a_2^2, a_3^3\}$	$V(\mathbb{C})$
$R_{76} = R\{a_3^3, a_8^3\}$	$V(\mathbb{C})$
$R_{78} = R\{a_4^1, a_4^1\}$	$V(\mathbb{C})$
$R_{80} = R\{a_1^1, a_4^1\}$	$V(\mathbb{C})$
$R_{82} = R\{a_7^3, a_2^3\}$	$V(\mathbb{C})$
$R_{84} = R\{a_2^2, a_9^3\}$	$V(\mathbb{C})$

TABLE 4: Resolving neighbourhood sets of  $\mathbb{T}\mathbb{D}(3)$  with minimum cardinality.

Resolving neighbourhood sets	Elements
$R_1 = R\{a_1^1, a_2^1\}$	$V(\mathbb{C}) - \{a_2^2, a_3^2, a_4^2\} \cup \{a_4^3, a_5^3, a_6^3, a_8^3, a_9^3\}$
$R_2 = R\{a_1^1, a_2^3\}$	$V(\mathbb{C}) - \{a_2^2, a_2^2, a_4^2\} \cup \{a_1^3, a_2^3, a_7^3, a_8^3, a_9^3\}$
$R_3 = R\{a_1^1, a_4^1\}$	$V(\mathbb{C}) - \{a_1^1, a_2^2, a_3^2\} \cup \{a_1^3, a_2^3, a_3^3, a_4^3, a_5^3\}$
$R_4 = R\{a_2^1, a_3^1\}$	$V(\mathbb{C}) - \{a_2^2, a_3^2, a_4^2, a_5^2, a_6^2, a_7^2, a_8^2, a_9^2\}$
$R_5 = R\{a_3^1, a_5^1\}$	$V(\mathbb{C}) - \{a_1^3, a_2^3, a_3^3, a_4^3, a_6^3, a_7^3, a_8^3, a_9^3\}$
$R_6 = R\{a_4^1, a_9^1\}$	$V(\mathbb{C}) - \{a_1^1, a_2^1, a_3^1, a_4^1, a_5^1, a_6^1, a_7^1, a_8^1\}$

30 and  $\bigcup_{L=150}^{240} R_L = V(\mathbb{C})$ . Table 8, on the other hand, shows the resolving neighbourhood sets with a minimum cardinality of 10 and  $\bigcup_{t=1}^3 R_t = V(\mathbb{C}) - \{a_2^3, a_3^3, a_4^3, a_6^3, a_7^3, a_8^3\} \cup \{a_4^4, a_{10}^4, a_{11}^4, a_{12}^4\}$ . Suppose that, for  $150 \leq L \leq 240$ ,  $|R_L| = \gamma$ , for  $1 \leq t \leq 3$ ,  $|R_t| = \lambda$ ,  $\eta = |\bigcup_{L=63}^{84} R_L| = |V(\mathbb{T}\mathbb{D}(3))| = 30$ , and  $\delta = |\bigcup_{t=1}^6 R_t| = |V(\mathbb{T}\mathbb{D}(3))| = 20$ . Now, we define a

TABLE 5: Resolving neighbourhood sets of  $\mathbb{T}\mathbb{D}(4)$  that are not equal to each other.

Resolving neighbourhood sets	Elements
$R_1 = R\{a_1^2, a_3^1\}$	$V(C) - \{a_2^3, a_3^3, a_4^3, a_5^3, a_6^3, a_7^3, a_8^3, a_9^3\} \cup \{a_1^4, a_2^4, a_3^4, a_4^4, a_5^4, a_6^4, a_7^4, a_8^4, a_9^4, a_{10}^4, a_{11}^4, a_{12}^4, a_{13}^4, a_{14}^4, a_{15}^4, a_{16}^4\}$
$R_2 = R\{a_3^2, a_5^3\}$	$V(C) - \{a_1^3, a_2^3, a_3^3, a_4^3, a_6^3, a_7^3, a_8^3, a_9^3\} \cup \{a_1^4, a_2^4, a_3^4, a_4^4, a_5^4, a_6^4, a_7^4, a_8^4, a_9^4, a_{10}^4, a_{11}^4, a_{12}^4, a_{13}^4, a_{14}^4, a_{15}^4, a_{16}^4\}$
$R_3 = R\{a_4^2, a_9^3\}$	$V(C) - \{a_1^3, a_2^3, a_3^3, a_4^3, a_5^3, a_6^3, a_7^3, a_8^3\} \cup \{a_1^4, a_2^4, a_3^4, a_4^4, a_5^4, a_6^4, a_7^4, a_8^4, a_9^4, a_{10}^4, a_{11}^4, a_{12}^4, a_{13}^4\}$
$R_1 = R\{a_1^2, a_2^1\}$	$V(C) - \{a_2^2, a_3^2, a_4^2\} \cup \{a_3^3, a_5^3, a_6^3, a_8^3, a_9^3\} \cup \{a_6^4, a_7^4, a_8^4, a_{12}^4, a_{13}^4, a_{15}^4, a_{16}^4\}$
$R_2 = R\{a_1^2, a_2^1\}$	$V(C) - \{a_1^2, a_2^2, a_2^1\} \cup \{a_1^3, a_2^3, a_7^3, a_8^3, a_9^3\} \cup \{a_1^4, a_2^4, a_4^4, a_9^4, a_{10}^4, a_{11}^4, a_{15}^4, a_{16}^4\}$
$R_3 = R\{a_1^2, a_2^1\}$	$V(C) - \{a_2^2, a_2^1\} \cup \{a_1^3, a_2^3, a_3^3, a_4^3, a_5^3\} \cup \{a_1^4, a_2^4, a_3^4, a_4^4, a_5^4, a_6^4, a_7^4\}$
$R_4 = R\{a_1^2, a_2^1\}$	$V(C) - \{a_1^1\} \cup \{a_2^2, a_2^1\} \cup \{a_3^3, a_8^3, a_9^3\} \cup \{a_3^4, a_4^4, a_5^4, a_{11}^4, a_{15}^4, a_{16}^4\}$
$R_5 = R\{a_1^2, a_2^1\}$	$V(C) - \{a_1^1\} \cup \{a_2^2, a_2^1\} \cup \{a_3^3, a_3^2, a_3^1\} \cup \{a_6^4, a_7^4, a_8^4, a_{10}^4, a_{11}^4, a_{14}^4\}$
$R_6 = R\{a_1^2, a_2^1\}$	$V(C) - \{a_3^2\} \cup \{a_1^3, a_2^3, a_7^3, a_8^3, a_9^3\} \cup \{a_1^4, a_2^4, a_9^4, a_{10}^4, a_{14}^4, a_{15}^4, a_{16}^4\}$
$R_{12} = R\{a_1^2, a_5^3\}$	$V(C) - \{a_2^2\} \cup \{a_3^3, a_8^3, a_9^3\} \cup \{a_3^4, a_4^4, a_5^4, a_{11}^4, a_{15}^4, a_{16}^4\}$
$R_{13} = R\{a_1^2, a_6^3\}$	$V(C) - \{a_2^2, a_2^1\} \cup \{a_3^3, a_7^3\} \cup \{a_4^4, a_4^3, a_4^2, a_4^1, a_{10}^4, a_{14}^4\}$
$R_{14} = R\{a_1^2, a_7^3\}$	$V(C) - \{a_2^2\} \cup \{a_3^3, a_3^2, a_3^1\} \cup \{a_1^4, a_2^4, a_3^4, a_4^4, a_5^4, a_6^4, a_7^4\}$
$R_{15} = R\{a_1^2, a_9^3\}$	$V(C) - \{a_4^2\} \cup \{a_3^3, a_3^2, a_3^1, a_2^3\} \cup \{a_1^4, a_2^4, a_3^4, a_4^4, a_5^4, a_6^4, a_7^4\}$
$R_{16} = R\{a_2^2, a_2^1\}$	$V(C) - \{a_4^2\} \cup \{a_4^3, a_5^3, a_7^3\} \cup \{a_6^4, a_7^4, a_8^4, a_{10}^4, a_{11}^4, a_{14}^4\}$
$R_{17} = R\{a_1^2, a_4^1\}$	$V(C) - \{a_1^2\} \cup \{a_4^3, a_5^3, a_6^3, a_8^3, a_9^3\} \cup \{a_6^4, a_7^4, a_8^4, a_{12}^4, a_{13}^4, a_{15}^4, a_{16}^4\}$
$R_{18} = R\{a_1^2, a_4^1\}$	$V(C) - \{a_2^2, a_3^2, \dots, a_4^2\}$
$R_{19} = R\{a_1^2, a_5^1\}$	$V(C) - \{a_3^2, a_3^1, a_3^0\} \cup \{a_1^4, a_2^4, \dots, a_4^4\}$
$R_{20} = R\{a_1^2, a_7^1\}$	$V(C) - \{a_3^2, a_3^1, a_3^0\} \cup \{a_{10}^4, a_{14}^4, a_{15}^4, a_{16}^4\}$
$R_{21} = R\{a_1^2, a_8^1\}$	$V(C) - \{a_4^2, a_6^2\} \cup \{a_4^3, a_6^3\} \cup \{a_4^4, a_{11}^4, a_{15}^4, a_{16}^4\}$
$R_{22} = R\{a_1^2, a_9^1\}$	$V(C) - \{a_4^2, a_8^2\} \cup \{a_4^3, a_8^3\} \cup \{a_4^4, a_{10}^4, a_{14}^4\}$
$R_{23} = R\{a_1^2, a_{11}^1\}$	$V(C) - \{a_6^2, a_7^2, a_8^2, a_9^2\} \cup \{a_1^4, a_2^4, \dots, a_4^4\}$
$R_{24} = R\{a_1^2, a_{14}^1\}$	$V(C) - \{a_3^2, a_4^2, a_5^2, a_7^2, a_8^2, a_9^2\} \cup \{a_3^4, a_9^4\}$
$R_{25} = R\{a_1^2, a_{16}^1\}$	$V(C) - \{a_6^2, a_7^2, a_8^2, a_9^2\} \cup \{a_4^4, a_5^4, a_6^4, a_7^4\}$
$R_{26} = R\{a_2^2, a_2^1\}$	$V(C) - \{a_6^2, a_8^2\} \cup \{a_6^4, a_7^4, a_{10}^4, a_{11}^4\}$
$R_{27} = R\{a_2^2, a_4^1\}$	$V(C) - \{a_1^2\} \cup \{a_4^2, a_5^2, \dots, a_8^2, a_{10}^2, \dots, a_{10}^4\}$
$R_{28} = R\{a_2^2, a_6^1\}$	$V(C) - \{a_3^2, a_4^2, a_5^2, a_6^2\} \cup \{a_1^4, a_2^4, a_9^4, a_{10}^4, a_{14}^4, a_{15}^4, a_{16}^4\}$
$R_{29} = R\{a_2^2, a_{10}^1\}$	$V(C) - \{a_4^2, a_6^2\} \cup \{a_4^3, a_6^3\} \cup \{a_4^4, a_{11}^4, a_{15}^4, a_{16}^4\}$
$R_{30} = R\{a_2^2, a_{12}^1\}$	$V(C) - \{a_6^2, a_7^2, a_8^2, a_9^2\} \cup \{a_1^4, a_2^4, a_3^4, a_4^4, a_5^4, a_6^4, a_7^4\}$
$R_{31} = R\{a_2^2, a_{15}^1\}$	$V(C) - \{a_4^2, a_5^2, a_8^2, a_9^2\} \cup \{a_4^4, a_{10}^4, a_{14}^4\}$
$R_{32} = R\{a_3^2, a_1^1\}$	$V(C) - \{a_6^2, a_8^2\} \cup \{a_5^4, a_6^4, a_{10}^4, a_{11}^4\}$
$R_{33} = R\{a_3^2, a_4^1\}$	$V(C) - \{a_1^2\} \cup \{a_3^2, a_4^2, a_5^2, \dots, a_9^2, \dots, a_{16}^2\}$
$R_{34} = R\{a_3^2, a_5^1\}$	$V(C) - \{a_5^2\} \cup \{a_4^4, a_{15}^4, a_{16}^4\}$
$R_{35} = R\{a_3^2, a_8^1\}$	$V(C) - \{a_4^2, a_5^2, a_6^2, a_8^2, a_9^2\} \cup \{a_4^4, a_5^4, a_{10}^4, a_{11}^4, a_{13}^4\}$
$R_{36} = R\{a_3^2, a_9^1\}$	$V(C) - \{a_1^2, a_2^2, a_3^2, a_3^1\} \cup \{a_8^4, a_{11}^4, a_{12}^4, a_{13}^4\}$
$R_{37} = R\{a_3^2, a_{11}^1\}$	$V(C) - \{a_6^2, a_7^2, a_8^2, a_9^2\} \cup \{a_1^4, a_2^4, \dots, a_7^4\}$
$R_{38} = R\{a_3^2, a_{13}^1\}$	$V(C) - \{a_6^2, a_8^2\} \cup \{a_6^4, a_7^4, a_{10}^4, a_{11}^4\}$
$R_{39} = R\{a_3^2, a_{14}^1\}$	$V(C) - \{a_8^2\} \cup \{a_8^4, a_{11}^4, a_{12}^4, a_{13}^4\}$
$R_{40} = R\{a_3^2, a_{16}^1\}$	$V(C) - \{a_8^2\} \cup \{a_8^4, a_{12}^4\}$
$R_{41} = R\{a_4^2, a_2^1\}$	$V(C) - \{a_2^2, a_7^2\} \cup \{a_4^4, a_5^4, a_{15}^4, a_{16}^4\}$
$R_{42} = R\{a_4^2, a_4^1\}$	$V(C) - \{a_1^2, a_2^2, a_3^2, a_7^2\} \cup \{a_6^4, a_7^4, a_8^4, a_{12}^4, a_{13}^4, a_{15}^4, a_{16}^4\}$
$R_{43} = R\{a_4^2, a_6^1\}$	$V(C) - \{a_5^2\} \cup \{a_1^4, a_2^4, a_3^4, a_4^4, \dots, a_9^4, \dots, a_{16}^4\}$
$R_{44} = R\{a_4^2, a_{10}^1\}$	$V(C) - \{a_8^2, a_9^2\} \cup \{a_4^4, a_5^4\}$
$R_{45} = R\{a_4^2, a_{15}^1\}$	$V(C) - \{a_7^2, a_8^2\} \cup \{a_{11}^4, a_{12}^4\}$
$R_{46} = R\{a_5^2, a_1^1\}$	$V(C) - \{a_2^2, a_3^2\} \cup \{a_4^4, a_{11}^4, a_{15}^4, a_{16}^4\}$
$R_{47} = R\{a_5^2, a_3^1\}$	$V(C) - \{a_2^2, a_7^2\} \cup \{a_5^4, a_{12}^4, a_{13}^4\}$
$R_{48} = R\{a_5^2, a_5^1\}$	$V(C) - \{a_2^2\} \cup \{a_1^3, a_2^3, a_3^3, a_7^3\} \cup \{a_1^4, a_2^4, \dots, a_4^4, a_9^4, a_{10}^4, a_{11}^4, a_{14}^4\}$
$R_{49} = R\{a_5^2, a_7^1\}$	$V(C) - \{a_1^2, a_2^2, \dots, a_6^2, a_8^2, \dots, a_{16}^2\}$
$R_{50} = R\{a_5^2, a_8^1\}$	$V(C) - \{a_6^2, a_7^2, a_8^2, a_9^2\} \cup \{a_1^4, a_2^4, a_3^4, a_4^4, a_5^4, a_6^4, a_7^4\}$
$R_{51} = R\{a_5^2, a_9^1\}$	$V(C) - \{a_8^2, a_9^2\} \cup \{a_4^4, a_{12}^4, a_{13}^4\}$
$R_{52} = R\{a_5^2, a_{11}^1\}$	$V(C) - \{a_8^2, a_9^2\} \cup \{a_4^4, a_{12}^4, a_{13}^4\}$
$R_{53} = R\{a_5^2, a_{13}^1\}$	$V(C) - \{a_7^2, a_8^2\} \cup \{a_1^4, a_2^4, a_3^4, a_4^4, a_8^4\}$
$R_{54} = R\{a_5^2, a_{14}^1\}$	$V(C) - \{a_1^2, a_3^2, a_8^2\} \cup \{a_3^4, a_4^4, a_8^4\}$
$R_{55} = R\{a_5^2, a_{16}^1\}$	$V(C) - \{a_7^2, a_8^2\} \cup \{a_1^4, a_2^4, a_{11}^4, a_{12}^4\}$
$R_{56} = R\{a_6^2, a_1^1\}$	$V(C) - \{a_1^2\} \cup \{a_2^2\} \cup \{a_4^4, a_5^4, a_{10}^4, a_{15}^4\}$
$R_{57} = R\{a_6^2, a_{16}^1\}$	$V(C) - \{a_1^2, a_2^2, \dots, a_{15}^2\}$
$R_{58} = R\{a_7^2, a_2^1\}$	$V(C) - \{a_1^1\} \cup \{a_2^2, a_2^1\} \cup \{a_1^3, a_2^3, a_3^3, a_7^3\} \cup \{a_1^4, a_2^4, a_3^4, a_4^4, a_8^4\}$
$R_{59} = R\{a_5^2, a_6^1\}$	$V(C) - \{a_1^1\} \cup \{a_1^2, a_2^2, a_3^2\} \cup \{a_1^3, a_2^3, a_3^3, a_4^3\} \cup \{a_1^4, a_2^4, a_3^4, a_4^4, a_8^4\}$
$R_{60} = R\{a_2^2, a_{12}^1\}$	$V(C) - \{a_1^1\} \cup \{a_2^2\} \cup \{a_1^3, a_7^3\} \cup \{a_4^4, a_{10}^4\}$
$R_{61} = R\{a_3^2, a_3^1\}$	$V(C) - \{a_1^1\} \cup \{a_2^2, a_2^1\} \cup \{a_3^3, a_8^3, a_9^3, a_3^3\} \cup \{a_3^4, a_4^4, a_5^4, a_{11}^4, a_{15}^4, a_{16}^4\}$
$R_{62} = R\{a_2^2, a_8^1\}$	$V(C) - \{a_1^1\} \cup \{a_2^2, a_3^2\} \cup \{a_4^3, a_5^3, a_3^3, a_2^3\} \cup \{a_6^4, a_7^4, a_9^4, a_{10}^4, a_{11}^4, a_{14}^4\}$



TABLE 5: Continued.

Resolving neighbourhood sets	Elements
$R_{63} = R\{a_2^3, a_7^3\}$	$V(\mathbb{C}) - \{a_1^1\} \cup \{a_2^2\} \cup \{a_3^3, a_6^3\} \cup \{a_3^4, a_4^4, a_{15}^4, a_{16}^4\}$
$R_{64} = R\{a_3^3, a_9^3\}$	$V(\mathbb{C}) - \{a_1^1\} \cup \{a_2^2\} \cup \{a_6^3, a_7^3\} \cup \{a_6^4, a_7^4, a_9^4, a_{10}^4\}$
$R_{65} = R\{a_1^3, a_3^3\}$	$V(\mathbb{C}) - \{a_1^1\} \cup \{a_2^2, a_2^3, a_4^2\} \cup \{a_3^3, a_7^3, a_8^3\} \cup \{a_3^4, a_{10}^4, a_{14}^4, a_{15}^4, a_{16}^4\}$
$R_{66} = R\{a_1^3, a_7^3\}$	$V(\mathbb{C}) - \{a_1^1\} \cup \{a_2^2, a_2^3, a_4^2\} \cup \{a_3^3, a_3^4, a_5^3\} \cup \{a_4^4, a_5^4, a_6^4, a_7^4, a_9^4\}$
$R_{67} = R\{a_1^4, a_3^4\}$	$V(\mathbb{C}) - \{a_1^1\} \cup \{a_2^2, a_2^3, a_4^2\} \cup \{a_3^3, a_3^4, a_5^3\} \cup \{a_2^4, a_9^4, a_{10}^4, a_{14}^4, a_{15}^4, a_{16}^4\}$
$R_{68} = R\{a_1^4, a_7^4\}$	$V(\mathbb{C}) - \{a_1^1\} \cup \{a_2^2, a_2^3, a_4^2\} \cup \{a_3^3, a_3^4, a_5^3\} \cup \{a_2^4, a_3^4, a_4^4, a_5^4, a_6^4, a_7^4\}$
$R_{69} = R\{a_6^3, a_9^3\}$	$V(\mathbb{C}) - \{a_1^1\} \cup \{a_2^2, a_2^3, a_4^2\} \cup \{a_3^3, a_2^3, a_7^3, a_8^3\} \cup \{a_4^4, a_2^4, a_9^4, a_{10}^4, a_{13}^4\}$
$R_{70} = R\{a_5^3, a_9^3\}$	$V(\mathbb{C}) - \{a_1^1\} \cup \{a_2^2, a_2^3\} \cup \{a_3^3, a_3^4, a_6^3\} \cup \{a_4^4, a_4^5, a_{11}^4, a_{12}^4\}$
$R_{71} = R\{a_5^4, a_{14}^4\}$	$V(\mathbb{C}) - \{a_1^1\} \cup \{a_2^2, a_2^3\} \cup \{a_3^3, a_2^3, a_6^3\} \cup \{a_4^4, a_2^4, a_{11}^4, a_{12}^4\}$
$R_{72} = R\{a_7^4, a_{16}^4\}$	$V(\mathbb{C}) - \{a_1^1\} \cup \{a_2^2, a_2^3\} \cup \{a_3^3, a_2^3, a_6^3\} \cup \{a_4^4, a_2^4, a_{11}^4, a_{12}^4\}$
$R_{73} = R\{a_1^4, a_1^4\}$	$V(\mathbb{C}) - \{a_2^3, a_3^3, a_7^3\} \cup \{a_6^4, a_7^4, a_8^4, a_{12}^4, a_{13}^4, a_{15}^4, a_{16}^4\}$
$R_{74} = R\{a_1^4, a_7^4\}$	$V(\mathbb{C}) - \{a_3^3, a_3^4, a_6^3\} \cup \{a_1^4, a_2^4, a_9^4, a_{10}^4, a_{14}^4, a_{15}^4, a_{16}^4\}$
$R_{75} = R\{a_1^4, a_9^4\}$	$V(\mathbb{C}) - \{a_3^3, a_3^4, a_6^3\} \cup \{a_1^4, a_2^4, a_4^4, a_5^4, a_6^4, a_7^4\}$
$R_{76} = R\{a_2^3, a_9^3\}$	$V(\mathbb{C}) - \{a_6^3, a_7^3, a_8^3\} \cup \{a_1^4, a_2^4, a_3^4, a_4^4, a_5^4, a_6^4, a_7^4\}$
$R_{77} = R\{a_9^3, a_{14}^3\}$	$V(\mathbb{C}) - \{a_2^2\} \cup \{a_1^3, a_2^3, a_3^3, a_7^3\} \cup \{a_1^4, a_2^4, \dots, a_4^4, a_4^5, a_{10}^4, a_{11}^4, a_{14}^4\}$
$R_{78} = R\{a_2^3, a_2^3\}$	$V(\mathbb{C}) - \{a_3^3\} \cup \{a_4^4, a_5^4, \dots, a_8^4, a_{10}^4, \dots, a_{16}^4\}$

mapping  $\kappa: V(\mathbb{T}(3)) \rightarrow [0, 1]$  such that  $\kappa(a) = (1/30)$  for all  $a \in \cup_{L=63}^{84} R_L$ , and assigning the value of  $(1/30)$  to all the elements of  $\cup_{L=63}^{84} R_L$  and summing up all the labels, we get  $|\kappa| = \sum_{a \in \cup_{L=63}^{84} R_L} \kappa(a) = (30/30) = 1$ ; thus,  $\dim_{\text{frac}}(\mathbb{C}) = |\kappa| = 1$ , as all the  $R_L$  for  $150 \leq L \leq 240$  are all having  $V(\mathbb{T}(3))$  in common. Similarly, we define another mapping  $\tau: V(\mathbb{T}(3)) \rightarrow [0, 1]$  such that  $\tau = (1/\lambda) = (1/10)$  for all  $a \in \cup_{t=1}^3 R_t$ , and giving labels to the elements of  $\cup_{t=1}^3 R_t$  and latter on summing them up, we get  $|\tau| = \sum_{a \in \cup_{t=1}^3 R_t} \tau(a) = (20/10) \leq 2$ ; hence,  $\dim_{\text{frac}}(\mathbb{C}) < 2$  as all the  $R_t$  for  $1 \leq t \leq 6$  are pairwise overlapping. Therefore, we arrive at the following conclusion:

$$1 < \dim_{\text{frac}}(\mathbb{T}(3)) \leq 2. \quad (21)$$

Case 2: when  $n \geq 6$ .

The required minimum resolving neighbourhood sets are  $R\{a_1^\alpha, a_1^\beta\}$ ,  $R\{a_\gamma^\alpha, a_\eta^\beta\}$ , and  $R\{a_{\alpha^2}^\alpha, a_{\beta^2}^\beta\}$ , where  $\alpha = (n/2)$ ,  $\beta + 1$ ,  $\gamma = 2\alpha - 1$ , and  $\eta = 2\beta - 1$ . As it is evident from Lemma 1,  $|R_t| = |R\{a_1^\alpha, a_1^\beta\}| = |R\{a_\gamma^\alpha, a_\eta^\beta\}| = |R\{a_{\alpha^2}^\alpha, a_{\beta^2}^\beta\}| = (n(n^2 + 3n + 1)/12) \leq |\text{acute}R\{a, b\}|$  for all  $a, b \in V(\mathbb{C})$  and  $\cup_{t=1}^3 R_t = \cup_{j=1}^\alpha S_j^2 \cup \cup_{j=\alpha+1}^n (S_{(j-\alpha)^2}^{j,t} \cup S_{(j-\alpha)^2}^{j,br} \cup S_{(j-\alpha)^2}^{j,bl})$ . Moreover,  $|R\{u, v\} \cap \cup_{t=1}^3 R_t| \geq |R_t|$  for all  $u, v \in V(\mathbb{C})$ . Also, by Lemma 3 (d), the resolving neighbourhood sets with maximum cardinality of  $|V(\mathbb{C})| = (n(2n^2 + 3n + 1)/6)$  are  $R_1 = R\{a_\alpha^\alpha, a_\beta^\beta\}$  and  $R_2 = R\{a_\alpha^\alpha, a_{\alpha+\gamma}^{\alpha+\eta}\}$  with  $\cup_{L=1}^2 R_L = V(\mathbb{C})$ . Let  $|R_t| = \lambda$ ,  $|R_L| = \gamma$ ,  $|\cup_{L=1}^2 R_L| = \eta$ , and  $|\cup_{t=1}^3 R_t| = \delta$ ; to find the minimum value of  $\dim_{\text{frac}}(\mathbb{C})$ , we define a mapping  $\kappa: V(\mathbb{C}) \rightarrow [0, 1]$  such that

$$k(a) = \begin{cases} \frac{1}{k} & \text{for } a \in \bigcup_{L=1}^3 R_L, \\ 0, & \text{for } a \in V(\mathbb{C}) - \bigcup_{t=1}^3 R_L. \end{cases} \quad (22)$$

TABLE 6: Resolving neighbourhood sets of  $\mathbb{T}(4)$  that are equal due to symmetry.

Resolving neighbourhood sets	Equality	Resolving neighbourhood sets	Equality
$R_{79} = R\{a_3^3, a_{13}^4\}$	$R\{a_3^3, a_8^4\}$	$R_{80} = R\{a_3^3, a_6^3\}$	$R\{a_2^2, a_2^2\}$
$R_{81} = R\{a_5^4, a_8^4\}$	$R\{a_7^2, a_8^3\}$	$R_{82} = R\{a_5^5, a_{10}^5\}$	$R\{a_2^2, a_2^2\}$
$R_{83} = R\{a_6^3, a_7^3\}$	$R\{a_7^2, a_2^3\}$	$R_{84} = R\{a_{13}^4, a_{14}^4\}$	$R\{a_2^2, a_2^2\}$
$R_{85} = R\{a_7^2, a_4^3\}$	$R\{a_7^2, a_3^3\}$	$R_{86} = R\{a_2^3, a_3^3\}$	$R\{a_2^2, a_2^2\}$
$R_{87} = R\{a_2^3, a_3^3\}$	$R\{a_2^2, a_2^3\}$	$R_{88} = R\{a_2^3, a_3^3\}$	$R\{a_2^2, a_2^2\}$
$R_{89} = R\{a_2^3, a_6^3\}$	$R\{a_7^2, a_2^3\}$	$R_{90} = R\{a_2^3, a_3^3\}$	$R\{a_2^2, a_2^2\}$
$R_{91} = R\{a_5^4, a_{11}^4\}$	$R\{a_5^3, a_6^3\}$	$R_{92} = R\{a_5^4, a_{11}^4\}$	$R\{a_3^3, a_6^3\}$
$R_{93} = R\{a_7^4, a_{13}^4\}$	$R\{a_2^3, a_6^3\}$	$R_{94} = R\{a_{13}^4, a_{14}^4\}$	$R\{a_6^3, a_3^3\}$
$R_{95} = R\{a_{12}^4, a_{15}^4\}$	$R\{a_6^3, a_6^3\}$	$R_{96} = R\{a_8^4, a_{16}^4\}$	$R\{a_6^3, a_3^3\}$
$R_{97} = R\{a_5^4, a_{14}^4\}$	$R\{a_5^3, a_3^3\}$	$R_{98} = R\{a_8^4, a_{14}^4\}$	$R\{a_3^3, a_3^3\}$
$R_{99} = R\{a_7^4, a_{13}^4\}$	$R\{a_2^3, a_2^3\}$	$R_{100} = R\{a_8^4, a_{16}^4\}$	$R\{a_3^3, a_3^3\}$
$R_{101} = R\{a_2^4, a_{10}^4\}$	$R\{a_7^2, a_2^3\}$	$R_{102} = R\{a_2^4, a_4^4\}$	$R\{a_3^3, a_3^3\}$
$R_{103} = R\{a_3^3, a_4^3\}$	$R\{a_2^3, a_4^4\}$	$R_{104} = R\{a_2^4, a_{11}^4\}$	$R\{a_3^3, a_3^3\}$
$R_{105} = R\{a_9^4, a_{11}^4\}$	$R\{a_1^3, a_3^3\}$	$R_{106} = R\{a_3^3, a_{11}^4\}$	$R\{a_9^4, a_{14}^4\}$
$R_{107} = R\{a_5^3, a_5^3\}$	$R\{a_9^4, a_{14}^4\}$	$R_{108} = R\{a_3^3, a_3^3\}$	$R\{a_2^2, a_2^2\}$

where  $\gamma = \eta = (n(2n^2 + 3n + 1)/6)$ . Assigning the labels to the elements of  $\bigcup_{L=1}^2 R_L$  and summing them up, we get  $|\kappa| = \sum_{a \in \cup_{L=1}^2 R_L} (1/\gamma) = 1$ .

Similarly, for the maximum value of  $\dim_{\text{frac}}(\mathbb{C})$ , we define another mapping  $\tau: V(\mathbb{C}) \rightarrow [0, 1]$  such that

$$\tau(a) = \begin{cases} \frac{1}{\lambda} & \text{for } a \in \bigcup_{t=1}^3 R_t, \\ 0, & \text{for } a \in V(\mathbb{C}) - \bigcup_{t=1}^3 R_t. \end{cases} \quad (23)$$

It can be seen that  $\tau$  is a resolving function for  $\mathbb{C}$  with  $n \geq 3$  because  $\tau(R\{u, v\}) \geq 1 \forall u, v \in V(\mathbb{N})$ . On the contrary, we assume that there is another resolving function  $\rho$  such that  $\rho(u) \leq \tau(u)$ , for at least one  $u \in V(\mathbb{C}) \rho(u) \neq \tau(u)$ . As a consequence,  $\rho(R\{u, v\}) < 1$ , where  $R\{u, v\}$  is a resolving neighbourhood of  $\mathbb{C}$  with minimum cardinality  $\kappa$ . It shows

TABLE 7: Resolving neighbourhood sets of  $\mathbb{T}\mathbb{D}(4)$  that are equal to  $V(\mathbb{T}\mathbb{D}(4))$ .

Resolving neighbourhood sets	Elements	Resolving neighbourhood sets	Elements
$R_{150} = R\{a_1^1, a_2^2\}$	$V(C)$	$R_{151} = R\{a_1^1, a_4^4\}$	$V(C)$
$R_{152} = R\{a_1^1, a_8^8\}$	$V(C)$	$R_{153} = R\{a_1^1, a_2^2\}$	$V(C)$
$R_{154} = R\{a_1^1, a_4^4\}$	$V(C)$	$R_{155} = R\{a_1^1, a_6^6\}$	$V(C)$
$R_{156} = R\{a_1^1, a_{10}^{10}\}$	$V(C)$	$R_{157} = R\{a_1^1, a_{12}^{12}\}$	$V(C)$
$R_{158} = R\{a_1^1, a_{15}^{15}\}$	$V(C)$	$R_{159} = R\{a_1^2, a_3^3\}$	$V(C)$
$R_{160} = R\{a_1^2, a_4^4\}$	$V(C)$	$R_{161} = R\{a_1^2, a_8^8\}$	$V(C)$
$R_{162} = R\{a_2^2, a_3^3\}$	$V(C)$	$R_{163} = R\{a_2^2, a_6^6\}$	$V(C)$
$R_{164} = R\{a_2^2, a_8^8\}$	$V(C)$	$R_{165} = R\{a_2^2, a_{10}^{10}\}$	$V(C)$
$R_{166} = R\{a_2^2, a_{12}^{12}\}$	$V(C)$	$R_{167} = R\{a_2^2, a_{15}^{15}\}$	$V(C)$
$R_{168} = R\{a_3^3, a_4^4\}$	$V(C)$	$R_{169} = R\{a_3^3, a_6^6\}$	$V(C)$
$R_{170} = R\{a_3^3, a_8^8\}$	$V(C)$	$R_{171} = R\{a_3^3, a_{10}^{10}\}$	$V(C)$
$R_{172} = R\{a_3^3, a_{12}^{12}\}$	$V(C)$	$R_{173} = R\{a_3^3, a_{15}^{15}\}$	$V(C)$
$R_{174} = R\{a_3^3, a_4^4\}$	$V(C)$	$R_{175} = R\{a_3^3, a_6^6\}$	$V(C)$
$R_{176} = R\{a_3^3, a_8^8\}$	$V(C)$	$R_{177} = R\{a_3^3, a_{10}^{10}\}$	$V(C)$
$R_{178} = R\{a_3^3, a_{12}^{12}\}$	$V(C)$	$R_{179} = R\{a_3^3, a_{15}^{15}\}$	$V(C)$
$R_{180} = R\{a_4^4, a_{10}^{10}\}$	$V(C)$	$R_{181} = R\{a_4^4, a_{12}^{12}\}$	$V(C)$
$R_{182} = R\{a_4^4, a_{12}^{12}\}$	$V(C)$	$R_{183} = R\{a_4^4, a_{15}^{15}\}$	$V(C)$
$R_{184} = R\{a_4^4, a_5^5\}$	$V(C)$	$R_{185} = R\{a_4^4, a_{11}^{11}\}$	$V(C)$
$R_{186} = R\{a_4^4, a_{14}^{14}\}$	$V(C)$	$R_{187} = R\{a_4^4, a_{13}^{13}\}$	$V(C)$
$R_{188} = R\{a_4^4, a_8^8\}$	$V(C)$	$R_{189} = R\{a_4^4, a_6^6\}$	$V(C)$
$R_{190} = R\{a_4^4, a_{16}^{16}\}$	$V(C)$	$R_{191} = R\{a_4^4, a_{15}^{15}\}$	$V(C)$
$R_{192} = R\{a_4^4, a_{12}^{12}\}$	$V(C)$	$R_{193} = R\{a_4^4, a_{13}^{13}\}$	$V(C)$
$R_{194} = R\{a_4^4, a_2^2\}$	$V(C)$	$R_{195} = R\{a_4^4, a_8^8\}$	$V(C)$
$R_{196} = R\{a_4^4, a_{13}^{13}\}$	$V(C)$	$R_{197} = R\{a_4^4, a_{16}^{16}\}$	$V(C)$
$R_{198} = R\{a_1^1, a_2^2\}$	$V(C)$	$R_{199} = R\{a_1^1, a_4^4\}$	$V(C)$
$R_{200} = R\{a_1^1, a_6^6\}$	$V(C)$	$R_{201} = R\{a_1^1, a_{12}^{12}\}$	$V(C)$
$R_{202} = R\{a_1^1, a_{15}^{15}\}$	$V(C)$	$R_{203} = R\{a_1^2, a_3^3\}$	$V(C)$
$R_{204} = R\{a_1^2, a_4^4\}$	$V(C)$	$R_{205} = R\{a_1^2, a_8^8\}$	$V(C)$
$R_{206} = R\{a_1^2, a_{12}^{12}\}$	$V(C)$	$R_{207} = R\{a_1^2, a_{15}^{15}\}$	$V(C)$
$R_{208} = R\{a_1^2, a_6^6\}$	$V(C)$	$R_{209} = R\{a_1^2, a_{10}^{10}\}$	$V(C)$
$R_{210} = R\{a_2^2, a_3^3\}$	$V(C)$	$R_{211} = R\{a_2^2, a_4^4\}$	$V(C)$
$R_{212} = R\{a_2^2, a_8^8\}$	$V(C)$	$R_{213} = R\{a_2^2, a_{10}^{10}\}$	$V(C)$
$R_{214} = R\{a_2^2, a_{12}^{12}\}$	$V(C)$	$R_{215} = R\{a_2^2, a_{15}^{15}\}$	$V(C)$
$R_{216} = R\{a_2^2, a_{13}^{13}\}$	$V(C)$	$R_{217} = R\{a_2^2, a_{16}^{16}\}$	$V(C)$
$R_{218} = R\{a_2^2, a_6^6\}$	$V(C)$	$R_{219} = R\{a_2^2, a_{11}^{11}\}$	$V(C)$
$R_{220} = R\{a_2^2, a_{10}^{10}\}$	$V(C)$	$R_{221} = R\{a_2^2, a_{14}^{14}\}$	$V(C)$
$R_{222} = R\{a_2^2, a_{12}^{12}\}$	$V(C)$	$R_{223} = R\{a_2^2, a_{15}^{15}\}$	$V(C)$
$R_{224} = R\{a_3^3, a_4^4\}$	$V(C)$	$R_{225} = R\{a_3^3, a_6^6\}$	$V(C)$
$R_{226} = R\{a_3^3, a_{10}^{10}\}$	$V(C)$	$R_{227} = R\{a_3^3, a_{12}^{12}\}$	$V(C)$
$R_{228} = R\{a_3^3, a_{15}^{15}\}$	$V(C)$	$R_{229} = R\{a_3^3, a_{13}^{13}\}$	$V(C)$
$R_{230} = R\{a_3^3, a_8^8\}$	$V(C)$	$R_{231} = R\{a_3^3, a_{16}^{16}\}$	$V(C)$
$R_{232} = R\{a_3^3, a_6^6\}$	$V(C)$	$R_{233} = R\{a_3^3, a_{11}^{11}\}$	$V(C)$
$R_{234} = R\{a_3^3, a_{15}^{15}\}$	$V(C)$	$R_{235} = R\{a_3^3, a_4^4\}$	$V(C)$
$R_{236} = R\{a_3^3, a_{12}^{12}\}$	$V(C)$	$R_{237} = R\{a_3^3, a_8^8\}$	$V(C)$
$R_{238} = R\{a_3^3, a_2^2\}$	$V(C)$	$R_{239} = R\{a_3^3, a_{10}^{10}\}$	$V(C)$
$R_{240} = R\{a_3^3, a_{11}^{11}\}$	$V(C)$		

TABLE 8: Resolving neighbourhood sets of  $\mathbb{T}\mathbb{D}(4)$  that are not equal to each other.

Resolving neighbourhood sets	Elements
$R_1 = R\{a_2^1, a_3^1\}$	$V(C) - \{a_2^3, a_3^3, a_4^3, a_5^3, a_6^3, a_7^3, a_8^3, a_9^3\} \cup \{a_4^4, a_5^4, a_6^4, a_7^4, a_8^4, a_9^4, a_{10}^4, a_{11}^4, a_{12}^4, a_{13}^4, a_{14}^4, a_{15}^4, a_{16}^4\}$
$R_2 = R\{a_3^2, a_5^2\}$	$V(C) - \{a_1^3, a_2^3, a_3^3, a_4^3, a_6^3, a_7^3, a_8^3, a_9^3\} \cup \{a_1^4, a_2^4, a_3^4, a_4^4, a_5^4, a_6^4, a_{10}^4, a_{11}^4, a_{12}^4, a_{13}^4, a_{14}^4, a_{15}^4, a_{16}^4\}$
$R_3 = R\{a_4^2, a_9^2\}$	$V(C) - \{a_1^3, a_2^3, a_3^3, a_4^3, a_5^3, a_6^3, a_7^3, a_8^3\} \cup \{a_1^4, a_2^4, a_3^4, a_4^4, a_5^4, a_6^4, a_7^4, a_8^4, a_9^4, a_{10}^4, a_{11}^4, a_{12}^4, a_{13}^4\}$

that  $\rho$  is not a resolving function which is a contradiction. Therefore,  $\tau$  is a minimal resolving function that attains minimum  $|\tau|$  for  $C$ . Since  $1 \leq t \leq 3$   $R_t$  has a nonempty intersection, thus there exists another minimal resolving function  $\bar{\tau}$  of  $C$  such that  $|\bar{\tau}| \leq |\tau|$ . Thus, assigning  $(1/\lambda)$  to the vertices of  $C$  in  $\cup_{t=1}^3 R_t$  and calculating the summation of all the weights, we get  $\dim_{\text{frac}}(C) = \sum_{t=1}^{\delta} (1/\lambda) \leq (12n(n^2 + 3n + 2)/6n(n^2 + 3n + 2)) = 2$ . Therefore, we arrive at the following result:

$$1 < \dim_{\text{frac}}(C) \leq 2. \quad (24) \quad \square$$

## 7. Conclusions

We conclude our discussion by the following remarks:

- (i) In this article, we have made a characterization of graphs having the FMD as unity
- (ii) It is computed that the FMD of the path is 1 that strengthens the result proved in [13]
- (iii) We have calculated the extremal values of FMD of  $\mathbb{T}\mathbb{D}(n)$  as (i) for  $n \equiv 0 \pmod{2}$ ,  $1 < \dim_{\text{frac}}(C) \leq 2$  and (ii) for  $n \equiv 1 \pmod{2}$ ,  $1 < \dim_{\text{frac}}(C) \leq 2(n^3 + 6n^2 + 11n - 30/n^3 + 3n^2 + 5n + 3)$
- (iv) Now, we close our discussion with the open problem that investigates the families of graphs other than  $P_n$  having FMD as unity

## Data Availability

All the data are included within this article. However, the reader may contact the corresponding author for more details of the data.

## Conflicts of Interest

The authors have no conflicts of interest.

## References

- [1] P. J. Slater, "Leaves of trees," *Congruent number*, vol. 14, no. 1, pp. 549–559, 1975.
- [2] P. J. Slater, "Domination and location in acyclic graphs," *Networks*, vol. 17, no. 1, pp. 55–64, 1987.
- [3] F. Harary and R. A. Melter, "On the metric dimension of a graph," *Ars Combinatoria*, vol. 2, no. 1, pp. 191–195, 1976.
- [4] I. Javaid, M. T. Rahim, and K. Ali, "Families of regular graphs with constant metric dimension," *Utilitas Mathematica*, vol. 75, no. 1, pp. 21–33, 2008.
- [5] I. Tomescu and I. Javaid, "On the metric dimension of the Jahangir graph," *Bulletin mathématique de la Société des Sciences*, vol. 50, no. 98, pp. 371–376, 2007.
- [6] M. Imran, A. Q. Baig, M. K. Shafiq, and I. Tomescu, "On metric dimension of generalized Petersen graphs  $P(n, 3)$ ," *ARS Combinatoria*, vol. 117, no. 1, pp. 113–130, 2014.
- [7] M. Fehr, S. Gosselin, and O. R. Oellermann, "The metric dimension of Cayley digraphs," *Discrete Mathematics*, vol. 306, no. 1, pp. 31–41, 2006.
- [8] R. A. Melter and I. Tomescu, "Metric bases in digital geometry," *Computer Vision, Graphics, and Image Processing*, vol. 25, no. 1, pp. 113–121, 2014.
- [9] S. Khuller, B. Raghavachari, and A. Rosenfield, "Landmarks in graphs," *Discrete Applied Mathematics*, vol. 70, no. 1, pp. 217–229, 1996.
- [10] P. S. Buczowski, G. Chartrand, C. Poisson, and P. Zhang, "On k- dimensional graphs and their bases," *Periodica Mathematica Hungarica*, vol. 46, no. 1, pp. 9–15, 2003.
- [11] G. Chartrand, L. Eroh, M. A. Johnson, and O. R. Oellermann, "Resolvability in graphs and the metric dimension of a graph," *Discrete Applied Mathematics*, vol. 105, no. 1-3, pp. 99–113, 2000.
- [12] J. Currie and O. R. Oellermann, "The metric dimension and metric independence of a graph," *Journal of Combinatorial Mathematics and Combinatorial*, vol. 39, no. 1, pp. 157–167, 2001.
- [13] S. Arumugam and V. Mathew, "The fractional metric dimension of graphs," *Discrete Mathematics*, vol. 312, no. 9, pp. 1584–1590, 2012.
- [14] S. Arumugam, V. Mathew, and J. Shen, "On fractional metric dimension of graphs Discrete Mathematics," *Algorithms and Applications*, vol. 5, no. 4, pp. 1–8, 2013.
- [15] M. Feng, B. Lv, and K. Wang, "On the fractional metric dimension of graphs," *Discrete Applied Mathematics*, vol. 170, no. 19, pp. 55–63, 2014.
- [16] M. Feng and K. Wang, "On the metric dimension and fractional metric dimension of the hierarchical product of graphs," *Applicable Analysis and Discrete Mathematics*, vol. 7, no. 1, pp. 302–313, 2013.
- [17] S. W. Saputro, A. Semanicova Fenovcikova, M. Baca, and M. Lascsakova, "On fractional metric dimension of comb product graphs," *Statistics, Optimization & Information Computing*, vol. 6, no. 1, pp. 150–158, 2018.
- [18] M. Feng and K. Wang, "On the fractional metric dimension of corona product graphs and lexicographic product graph  $\sigma$ ," <https://arxiv.org/abs/1206.1906>.
- [19] B. Jia, A. Kashif, T. Rasheed, and M. Javaid, "Fractional metric dimension of generalized Jahangir graph," *Mathematics*, vol. 4, no. 1, pp. 371–376, 2019.
- [20] M. Raza, M. Javaid, and N. Saleem, "Fractional metric dimension of metal-organic frameworks," *Main Group Metal Chemistry*, vol. 44, no. 1, pp. 92–102, 2021.
- [21] M. Raza, D. A. Alrowaili, M. Javaid, and K. Shabbir, "Computing bounds of fractional metric dimension of metal organic graphs," *Journal of Chemistry*, vol. 2021, Article ID 5539569, 12 pages, 2021.
- [22] S. Aisyah, M. I. Utoyo, and L. Susilowati, "On the local fractional metric dimension of corona product graphs," *IOP Conference Series: Earth and Environmental Science, Hungarica*, vol. 243, 2019.
- [23] J.-B. Liu, M. K. Aslam, and M. Javaid, "Local fractional metric dimensions of rotationally symmetric and planar networks," *IEEE Access*, vol. 8, no. 1, pp. 82404–82420, 2020.
- [24] M. Javaid, M. Raza, P. Kumam, and J.-B. Liu, "Sharp bounds of local fractional metric dimensions of connected networks," *IEEE Access*, vol. 8, no. 2, pp. 172329–172342, 2020.
- [25] M. Javaid, M. S. Behzad, U. Farooq, and M. K. Aslam, "Computing sharp bounds for local fractional metric dimensions of cycle related graphs," *Computational Journal of Combinatorial Mathematics*, vol. 1, pp. 31–75, 2020.
- [26] M. A. Johnson, "Browseable structure-activity datasets," in *Advances in Molecular Similarity*, R. Carbó-Dorca and P. Mezey, Eds., pp. 153–170, JAI Press, Connecticut, 1998.

- [27] M. Johnson, "Structure-activity maps for visualizing the graph variables arising in drug design," *Journal of Biopharmaceutical Statistics*, vol. 3, pp. 203–236, 1993.
- [28] G. Chartrand and P. Zhang, "The theory and applicaitons of resolvability in graphs," *Congruent number*, vol. 160, no. 1, pp. 47–68, 2003.

## Research Article

# Topological Study of Zeolite Socony Mobil-5 via Degree-Based Topological Indices

Nouman Saeed <sup>1</sup>, Kai Long <sup>1</sup>, Tanweer Ul Islam,<sup>2</sup> Zeeshan Saleem Mufti <sup>3</sup>,  
and Ayesha Abbas<sup>3</sup>

<sup>1</sup>State Key Laboratory for Alternate Electrical Power System with Renewable Energy Sources,  
North China Electric Power University, Beijing 102206, China

<sup>2</sup>National University of Sciences and Technology, Islamabad, Pakistan

<sup>3</sup>The University of Lahore, Lahore Campus, Lahore, Pakistan

Correspondence should be addressed to Nouman Saeed; noumansaeed7846@gmail.com

Received 2 March 2021; Accepted 26 May 2021; Published 24 June 2021

Academic Editor: Teodorico C. Ramalho

Copyright © 2021 Nouman Saeed et al. This is an open access article distributed under the Creative Commons Attribution License, which permits unrestricted use, distribution, and reproduction in any medium, provided the original work is properly cited.

Graph theory is a subdivision of discrete mathematics. In graph theory, a graph is made up of vertices connected through edges. Topological indices are numerical parameters or descriptors of graph. Topological index tells the symmetry of compound and helps us to compare those mathematical values, with boiling point, melting point, density, viscosity, hydrophobic surface area, polarity, etc., of that compound. In the present research paper, degree-based topological indices of Zeolite Socony Mobil-5 are calculated. Names of those topological indices are Randić index, first Zagreb index, general sum connectivity index, hyper-Zagreb index, geometric index, ABC index, etc.

## 1. Introduction

In graph theory, the term graph was suggested in eighteenth century by Leonhard Euler (1702–1782). He was a Swiss mathematician. He manipulated graphs to solve Konigsberg bridge problem [1–3]. Chemical graph theory is a topological division of mathematical chemistry that practices graph theory to model chemical structures mathematically. It studies chemistry and graph theory to view the detailed physical and chemical properties of compounds. A graph  $G = (V, E)$  is comprised through a set of vertices  $V$  and an edges set  $E$  [4].

Topological indices study the properties of graphs that remain constant/unchanged after continuous change in structure. Topological indices explain formation and symmetry of chemical compounds numerically and then help in advancement of QSAR (qualitative structure activity relationship) and QSPR (quantitative structure property relationship). Both QSAR and QSPR are used to build a relation among molecular structure and mathematical tools. These descriptors are helpful to correlate physio-chemical

properties of compounds (enthalpy, boiling and melting point, strain energy, etc.) that is why these descriptors have a large number of applications in chemistry, biotechnology, nanotechnology, etc.

Topological indices are invariants of graph that is why topological indices are independent of pictorial representation of graph. In other words, it is a numerical value that describes the structure of chemical graph [5, 6]. Among the three types of topological indices, degree-based indices have great importance. The need to define these indices is to explain physical properties of every chemical structure with a number. Continuous change in shape does not affect the value of topological index. Topological indices are useful in the study of QSAR and QSPR because topological indices show the physical properties and convert the chemical structure into a numerical value.

Distance-based topological indices deal with distances of graph, degree-based topological indices use the concept of degree, and counting-based topological index depends upon counting the edges. Randić explained some characteristics of a topological index. Some of them are explained here.

A topological index should

- (i) have architectural interpretation
- (ii) be well-defined
- (iii) be related with at least one physio-chemical property of compound
- (iv) be uncomplicated
- (v) display an appropriate size dependence
- (vi) modify with modification in structure
- (vii) locally defined
- (viii) have related with other indices

Topological indices show translations of chemical compounds into distinctive structural descriptors as a numerical value that can be used by QSAR [7, 8]. Topological indices are awfully beneficial in describing the properties of given compound. Chemists can use these indices to correlate considerable range of characteristics. Medicine industry is developing new drug designs that are useful for humans, plants, and animals. Many graph theoretical techniques have been established for forecasting of medicinal, environmental, and physio-chemical properties of compounds. It is not astonishing to see such a great victory of graph theory and topological indices in analyzing biological and physical characteristics of chemical compounds.

**1.1. ZSM.** Zeolites (alumino silicate) are tetrahedrally-linked structures based on silicate and aluminate tetrahedral. Structural chemistry deals with the framework of zeolites; it also works out on the arrangement of cations and other molecules in pore spaces. It belongs to a pentasil class of zeolite. It consists of silica (Si) and alumina (Al). It is named as ZSM-5 due to pore diameter of five angstrom; also, it has Si/Al ratio of five [9]. Size of the molecule depends on the type of structure. It is a crystalline powder. Geometry of pores can be connected in channels in one, two, or three dimensions.

**1.1.1. Motivations.** The structure of ZSM-5 has great importance in the field of chemistry, petroleum, and medicine industry. ZSM-5 is useful because of its stability, favorable selectivity, metal tolerance, and flexibility. It is also useful for the treatment of fertilizers. It helps to separate oxygen and nitrogen in the air. This unique structure is useful in petroleum industry as a catalyst. It is generally used in the conversion of methanol to gasoline as well as refining of oil. Through dehydration, it changes alcohol into petrol. Efficiency of LPG can also be increased through ZSM-5 catalyst. It keeps unusual hydrophobicity that is useful to separate hydrocarbons from polar compounds. Basic reason of calculation of topological indices is the industrial uses of ZSM-5 structure.

- (1) *First General Zagreb Index.* This index was first presented by Li and Zhao. Its mathematical form is defined in [10–12] as follows:

$$M_{\alpha}(G) = \sum_{p \in V(G)} (d_p)^{\alpha}. \quad (1)$$

*First and Second Zagreb Index.* There are two Zagreb groups of indices, denoted by  $M_1$  and  $M_2$  [13–15]. Both of these indices are explained in 1970s by Gutman and Tranjistic.

- (2) *First Zagreb Index.* It is defined in [16, 17]:

$$M_1(G) = \sum_{pq \in E(G)} (d_p + d_q). \quad (2)$$

- (3) *Second Zagreb Index.* It is defined in [11, 16]:

$$M_2(G) = \sum_{pq \in E(G)} (d_p \times d_q). \quad (3)$$

Multiple and polynomial Zagreb indices:

In 2012, new kinds of Zagreb indices were introduced by Ghorbani and Azimi, named as first and second multiple Zagreb indices represented as  $PM_1(G)$  and  $PM_2(G)$  [11, 15, 18]. The polynomials are used to find the Zagreb index. First and second Zagreb polynomial indices are written as  $M_1(G, j)$  and  $M_2(G, j)$ .

- (4) First and second multiple Zagreb indices:

$$PM_1(G) = \prod_{pq \in E(G)} (d_p + d_q), \quad (4)$$

$$PM_2(G) = \prod_{pq \in E(G)} (d_p \times d_q). \quad (5)$$

- (5) First and second polynomial Zagreb indices:

$$M_1(G, j) = \sum_{pq \in E(G)} j^{(d_p + d_q)}, \quad (6)$$

$$M_2(G, j) = \sum_{pq \in E(G)} j^{(d_p \times d_q)}. \quad (7)$$

- (6) *Hyper-Zagreb Index.* Modified Zagreb index is called hyper-Zagreb and that was introduced in 2013 by Shirdil, Rezapour, and Sayadi [19–21], mathematically written as

$$HM(G) = \sum_{pq \in E(G)} (d_p + d_q)^2. \quad (8)$$

- (7) Second modified Zagreb index:

$$M_2(G) = \sum_{pq \in E(G)} \frac{1}{(d_p \times d_q)}. \quad (9)$$

- (8) *Reduced second Zagreb index.* This index was proposed by Furtula and it is defined as

$$RM_2(G) = \sum_{pq \in E(G)} (d_p - 1 \times d_q - 1). \quad (10)$$

(9) *Atom Bond Connectivity Index*. It was written in 1998 by Ernesto Estrada and Torres [15, 22–24]. It is used to model thermodynamic characteristics of organic compounds (especially alkanes). Mathematically,

$$ABC(G) = \sum_{pq \in E(G)} \sqrt{\frac{d_p + d_q - 2}{d_p d_q}}. \quad (11)$$

(10) *Fourth Atom Bond Connectivity Index*. In 2010, Ghorbani et al. introduced this index [13, 14]. It is written as  $ABC_4$  index:

$$ABC_4(G) = \sum_{pq \in E(G)} \sqrt{\frac{S_p + S_q - 2}{S_p S_q}}. \quad (12)$$

(11) *General Randić Connectivity Index*. First degree-based TI was proposed in 1975 by Millan Randić. At that time, it was called as branching index [8, 17, 18] and used to measure the branching of hydrocarbons. In 1998, Eddrös and Bollobás wrote the general term of this index by changing the factor  $(-1/2)$  with  $\alpha \in \mathbb{R}$  [25]. It is defined as the total sum of weights  $(d(p)d(q))^\alpha$  of all the edges  $pq$ ,  $d(p)$  is the degree of  $p$ ,  $d(q)$  is the degree of  $q$ , and  $\alpha \in \mathbb{R}$ .

$$R_\alpha(G) = \sum_{pq \in E(G)} (d_p d_q)^\alpha. \quad (13)$$

(12) *Randić index*:

This index can also be called as first genuine degree-based topological index [15, 23]. Randić index is defined as

$$R(G) = \sum_{pq \in E(G)} \frac{1}{\sqrt{d_p d_q}}. \quad (14)$$

(13) *Reciprocal Randić Index*. This index was first studied by Favaron, Mahéo, and Saclé [26]. The index is helpful in modeling of boiling points of hydrocarbons. It is defined as

$$RR(G) = \sum_{pq \in E(G)} \sqrt{d_p d_q}. \quad (15)$$

(14) *Reduced Reciprocal Randić Index*. It is the analogue of reciprocal Randić index [26, 27]. It is defined as follows:

$$RRR(G) = \sum_{pq \in E(G)} \sqrt{(d_p - 1)(d_q - 1)}. \quad (16)$$

(15) *Geometric Arithmetic Index*. GA index was proposed by Vukicević and Furtula [6, 14, 15]; it is stated as

$$GA(G) = \sum_{pq \in E(G)} \frac{2\sqrt{d_p d_q}}{d_p + d_q}. \quad (17)$$

(16) *Fifth Geometric Arithmetic Index*. In 2011, Grovac et al. introduced this index [7]. Mathematically, it is written as

$$GA_5(G) = \sum_{pq \in E(G)} \frac{2\sqrt{S_p S_q}}{S_p + S_q}. \quad (18)$$

(17) *Forgotten Index*. This index was given by Gutman and Furtula in 2015 [16, 28, 29]. It is denoted by  $F(G)$  or  $F$  index:

$$F(G) = \sum_{pq \in E(G)} (d_p^2 + d_q^2). \quad (19)$$

(18) *General Sum Connectivity Index*. The index was proposed by Zhou and Trinajstić [15, 23, 30]. Mathematically,

$$\chi_\alpha(G) = \sum_{pq \in E(G)} (d_p + d_q)^\alpha, \quad (20)$$

where  $\alpha \in \mathbb{R}$ .

(19) *Symmetric Division Index*. In 2010, Vukicević and Furtula proposed this useful index denoted by  $SD(G)$  [28, 31, 32]:

$$SD(G) = \sum_{pq \in E(G)} \frac{d_p^2 + d_q^2}{(d_p \times d_q)}. \quad (21)$$

(20) *Harmonic Index*. Siemion Fajtlowicz wrote a computer program that works for the automatic generation of conjectures in graph theory [11, 15]. He also examined the relationship between graph invariants; while doing this work, he found a vertex degree-based quantity. Later on, (in 2012) Zhang rediscovered that unknown quantity and named it as harmonic index. It is written as

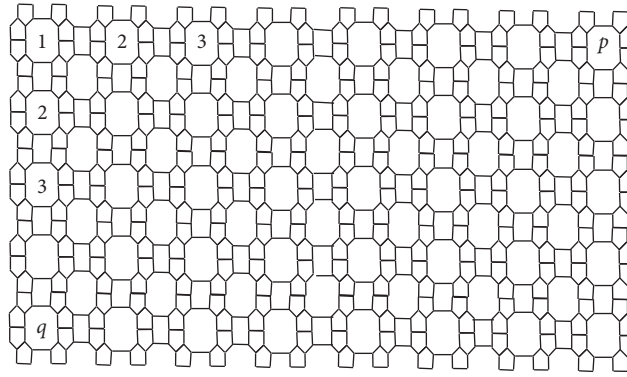
$$H(G) = \sum_{pq \in E(G)} \frac{2}{(d_p + d_q)}. \quad (22)$$

## 2. Topological Indices of ZSM-5 Graphs

Topological indices remain constant for a given compound; they do not depend on the direction or position of graph. We can predict many physical properties of compounds such as solubility, soil sorption, boiling and melting properties, biodegradability, toxicity, vaporization, and thermodynamic properties.

*2.1. Description of ZSM-5 Graph*. The graph of ZSM-5 is given in Figure 1 and it is represented by  $G^*$ . There are  $24pq + 4p$  vertices and  $36pq + 2p - 2q$  edges in  $G^*$ .

**Theorem 1.** Let  $G^*$  be a graph of ZSM-5. Then, first general Zagreb index is

FIGURE 1:  $(p, q)$  form of graph of ZSM-5.

$$M_\alpha(G^*) = 4p2^\alpha + (8p + 8q)2^\alpha + (36pq - 10p - 10q)3^\alpha. \quad (23)$$

$$M_1(G) = -4p - 20q + 216pq. \quad (26)$$

*Proof.*  $G^*$  is given in Figure 1. There are  $24pq + 4p$  vertices,  $8p + 4q$  of degree 2 vertices, and  $24pq - 4p - 4q$  of degree 3 vertices.

Also,  $M_\alpha(G^*)$  is defined as (1):

$$M_\alpha(G) = \sum_{p \in V(G)} (d_p)^\alpha. \quad (24)$$

We get  $M_\alpha(G^*)$  by using the following formula:

$$M_\alpha(G^*) = 4p2^\alpha + (8p + 8q)2^\alpha + (36pq - 10n - 10p)3^\alpha. \quad (25)$$

□

**Theorem 2.**  $G^*$  is the graph of ZSM-5. First Zagreb index is as follows:

*Proof.* Assume  $G^*$  is a graph of ZSM-5. Then,  $\mathbb{E}(G^*)$  is cleaved into 3 classes.

The 1<sup>st</sup> edges group  $\mathbb{E}_1(G^*)$  contains  $4p$  edges  $pq$ , and  $d_p = d_q = 2$ .

The 2<sup>nd</sup> class  $\mathbb{E}_2(G^*)$  has  $8p + 8q$  edges  $pq$ ; here,  $d_p = 2$ ,  $d_q = 3$ .

The 3<sup>rd</sup> arc division  $\mathbb{E}_3(G^*)$  has  $36pq - 10p - 10q$  arcs  $pq$ ; here,  $d_p = 3$ ,  $d_q = 3$ .

It is easily understood that

$$\begin{aligned} |\mathbb{E}_1(G^*)| &= e_{2,2}, \\ |\mathbb{E}_2(G^*)| &= e_{2,3}, \\ |\mathbb{E}_3(G^*)| &= e_{3,3}. \end{aligned} \quad (27)$$

We define  $M_1(G)$  in equation (29) as

$$\begin{aligned} M_1(G) &= \sum_{pq \in E(G)} (d_p + d_q), \\ M_1(G) &= \sum_{pq \in E_1(G)} (d_p + d_q) + \sum_{pq \in E_2(G)} (d_p + d_q) + \sum_{pq \in E_3(G)} (d_p + d_q) \\ &= |E_1(G)|4 + |E_2(G)|5 + |E_3(G)|6 \\ &= (4p)4 + (8p + 8q)5 + (36pq - 10p - 10q)6 \\ &= 4p(4) + 8p(5) + 8q(5) + 36pq(6) - 10p(6) - 10q(6). \end{aligned} \quad (28)$$

□

**Theorem 3.**  $G^*$  is a graph of ZSM-5 and its 1st and 2nd polynomial Zagreb index is

- (1)  $M_1(G^*, j) = (4p)j^4 + (8p + 8q)j^5 + (36pq - 10p - 10q)j^6$ ;
- (2)  $M_2(G^*, j) = (4p)j^4 + (8p + 8q)j^6 + (36pq - 10p - 10q)j^9$ .

*Proof.*  $G^*$  is a graph of ZSM-5.  $\mathbb{E}(G^*)$  is divided into three parts.

$\mathbb{E}_1(G^*)$  has  $4n$  edges  $pq$  ( $d_p = d_q = 2$ ),  $\mathbb{E}_2(G^*)$  has  $8n + 8m$  arcs  $pq$  ( $d_p = 2, d_q = 3$ ), and  $\mathbb{E}_3(G^*)$  keeps  $36pq - 10p - 10q$  arcs  $pq$  and ( $d_p = 3, d_q = 3$ ).

By using the definition of  $M_1(G^*, j)$  in equation (6):



$$M_1(G, j) = \sum_{pq \in E(G)} j^{(d_p + d_q)}, \quad (29)$$

$$\begin{aligned} M_1(G^*, j) &= \sum_{pq \in E_1(G)} j^{(d_p + d_q)} + \sum_{pq \in E_2(G)} j^{(d_p + d_q)} + \sum_{pq \in E_3(G)} j^{(d_p + d_q)} \\ &= \sum_{pq \in E_1(G)} j^4 + \sum_{pq \in E_2(G)} j^5 + \sum_{pq \in E_3(G)} j^6 \\ &= |E_1(G)|j^4 + |E_2(G)|j^5 + |E_3(G)|j^6 \\ &= (4p)j^4 + (8p + 8q)j^5 + (36pq - 10p - 10q)j^6. \end{aligned} \quad (30)$$

From (3), we have

$$\begin{aligned} M_2(G, j) &= \sum_{pq \in E(G)} j^{(d_p \times d_q)} \\ M_2(G^*, j) &= \sum_{pq \in E_1(G^*)} j^{(d_p \times d_q)} + \sum_{pq \in E_2(G^*)} j^{(d_p \times d_q)} + \sum_{pq \in E_3(G^*)} j^{(d_p \times d_q)} \\ &= \sum_{pq \in E_1(G^*)} j^4 + \sum_{pq \in E_2(G^*)} j^6 + \sum_{pq \in E_3(G^*)} j^9 \\ &= |E_1(G^*)|j^4 + |E_2(G^*)|j^6 + |E_3(G^*)|j^9 \\ &= (4p)j^4 + (8p + 8q)j^6 + (36pq - 10p - 10q)j^9, \end{aligned} \quad (31)$$

which completes the proof.  $\square$

**Theorem 4.** First and second multiple Zagreb index of  $G^*$  of ZSM-5 is given as

- (1)  $PM_1(G^*) = 4^4p \times 5^{8p+8q} \times 6^{36pq-10p-10q}$ ,
- (2)  $PM_2(G^*) = 4^4p \times 6^{8p+8q} \times 9^{36pq-10p-10q}$ .

*Proof.*  $E(G^*)$  is classified into 3 edge classes based on the degree of end vertices.  $E_1(G^*)$  has  $4p$  edges  $pq$ , where  $d_p = d_q = 2$ .  $E_2(G^*)$  contains  $8p + 8q$  edges  $pq$ , where  $d_p = 2, d_q = 3$ .  $E_3(G^*)$  contains  $36pq - 10p - 10q$  edges  $pq$ , where  $d_p = 3, d_q = 3$ . Also consider  $|E_1(G^*)| = e_{2,2}$ ,  $|E_2(G^*)| = e_{2,3}$ , and  $|E_3(G^*)| = e_{3,3}$ . We define  $PM_1(G^*)$  as (4):

$$\begin{aligned} PM_1(G^*) &= \prod_{pq \in E(G^*)} (d_p + d_q), \\ PM_1(G^*) &= \prod_{pq \in E_1(G^*)} (d_p + d_q) \times \prod_{pq \in E_2(G^*)} (d_p + d_q) \times \prod_{pq \in E_3(G^*)} (d_p + d_q) \\ &= 4^{|E_1(G^*)|} \times 5^{|E_2(G^*)|} \times 6^{|E_3(G^*)|} = 4^4p \times 5^{8p+8q} \times 6^{36pq-10p-10q}. \end{aligned} \quad (32)$$

Now, we define  $PM_2(G^*)$  as (5):

$$\begin{aligned} PM_2(G) &= \prod_{pq \in E(G)} (d_p \times d_q), \\ PM_2(G^*) &= \prod_{pq \in E_1(G^*)} (d_p \times d_q) \times \prod_{pq \in E_2(G^*)} (d_p \times d_q) \times \prod_{pq \in E_3(G^*)} (d_p \times d_q) \\ &= 4^{|E_1(G^*)|} \times 6^{|E_2(G^*)|} \times 9^{|E_3(G^*)|} \\ &= 4^4p \times 6^{8p+8q} \times 9^{36pq-10p-10q}, \end{aligned} \quad (33)$$

which completes the proof.  $\square$

**Theorem 5.** Then, hyper-Zagreb of  $G^*$  is written as follows:

$$\text{HM}(G^*) = 4p(16) + 8p(25) + 8q(25) + 36pq(36) - 10p(36) - 10q(36). \quad (34)$$

*Proof.*  $\mathbb{E}(G^*)$  is divided into 3 edge divisions based on the degree of end vertices.  $\mathbb{E}_1(G)$  holds  $4p$  edges  $pq$ , where  $d_p = d_q = 2$ .  $\mathbb{E}_2(G)$  holds  $8p + 8q$  edges  $pq$ , where  $d_p = 2$ ,  $d_q = 3$ .  $\mathbb{E}_3(G)$  holds  $36pq - 10p - 10q$  edges  $pq$ , where  $d_p = 3$ ,  $d_q = 3$ .  $|\mathbb{E}_1(G^*)| = e_{2,2}$ ,

$$|\mathbb{E}_2(G^*)| = e_{2,3}, \quad (35)$$

$$|\mathbb{E}_3(G^*)| = e_{3,3}.$$

Since, we have (8),

$$\begin{aligned} \text{HM}(G) &= \sum_{pq \in E(G)} (d_p + d_q)^2, \\ \text{HM}(G^*) &= \sum_{pq \in E_1(G^*)} [d_p + d_q]^2 + \sum_{pq \in E_2(G^*)} [d_p + d_q]^2 + \sum_{pq \in E_3(G^*)} [d_p + d_q]^2 \\ &= 16|E_1(G^*)| + 25|E_2(G^*)| + 36|E_3(G^*)| \\ &= 16(4p) + 25(8p + 8q) + 36(36pq - 10p - 10q) \\ &= -96p - 160q + 1296pq, \end{aligned} \quad (36)$$

which completes our proof.  $\square$

**Theorem 6.**  $G^*$  is the graph of ZSM-5. The second modified Zagreb index is given as

$$M_2(G^*)(G) = \frac{11}{9}p + \frac{2}{9}q + 4pq. \quad (37)$$

*Proof.* Consider  $G^*$  to be a graph of ZSM-5.  $E(G^*)$  is divided into 3 sets based on the degree of end vertices.  $E_1(G^*)$  contains  $4n$  edges  $pq$ , where  $d_p = d_q = 2$ .  $E_2(G^*)$  holds  $8p + 8q$  edges  $pq$ , where  $d_p = 2$ ,  $d_q = 3$ .  $E_3(G^*)$  holds  $36pq - 10p - 10q$  edges  $pq$ , where  $d_p = 3$ ,  $d_q = 3$ .  $|\mathbb{E}_1(G^*)| = e_{2,2}$ ,  $|\mathbb{E}_2(G^*)| = e_{2,3}$ , and  $|\mathbb{E}_3(G^*)| = e_{3,3}$ .

We know the definition of  $M_2(G^*)$  as (9):

$$M_2(G) = \sum_{pq \in E(G)} \frac{1}{(d_p \times d_q)},$$

$$\begin{aligned} M_2(G^*) &= |E_1(G^*)| \left( \frac{1}{4} \right) + |E_2(G^*)| \left( \frac{1}{6} \right) + |E_3(G^*)| \left( \frac{1}{9} \right) \\ &= \frac{(4p)}{4} + \frac{(8p + 8q)}{6} + \frac{(36pq - 10p - 10q)}{9} \\ &= \frac{11}{9}p + \frac{2}{9}q + 4pq. \end{aligned} \quad (38)$$

$\square$

**Theorem 7.** Let  $G^*$  be the graph of ZSM-5. Then, reduced second Zagreb index is

$$RM_2(G^*) = 156pq - 8p - 8q. \quad (39)$$

$$\begin{aligned} |E_1(G^*)| &= e_{(2,2)}, \\ |E_2(G^*)| &= e_{(2,3)}, \\ |E_3(G^*)| &= e_{(3,3)}. \end{aligned} \quad (40)$$

*Proof.* Assume  $G^*$  to be a graph of ZSM-5.  $E(G^*)$  is divided into parts.

$E_1(G^*)$  holds  $4p$  edges  $pq$ , where  $d_p = d_q = 2$ .  
 $E_2(G)$  has  $8p + 8q$  lines  $pq$ , where  $d_p = 2, d_q = 3$ .  
 $E_3(G^*)$  holds  $36pq - 10p - 10q$  lines  $pq$ , where  $d_p = 3, d_q = 3$ . Also consider

From equation (10), we have the definition of reduced second Zagreb index:

$$\begin{aligned} RM_2(G) &= \sum_{pq \in E(G)} (d_p - 1 \times d_q - 1), \\ RM_2(G^*) &= |E_1(G^*)|(2-1)(2-1) + |E_2(G^*)|(2-1)(3-1) + |E_3(G^*)|(3-1)(3-1) \\ &= (4p) + (8p + 8q)(2) + (36pq - 10p - 10q)(4) \\ &= 4p + 8q(2) + 8p(2) + 36pq(4) - 10p(4) - 10q(4). \end{aligned} \quad (41)$$

□

**Theorem 8.** Atom bond connectivity index of  $G^*$  of ZSM-5 is as follows:

$$\begin{aligned} ABC(G^*) &= 12p\left(\frac{1}{2\sqrt{2}}\right) + 8q\left(\frac{1}{2\sqrt{2}}\right) + 36pq\left(\frac{2}{3}\right) \\ &\quad - 10p\left(\frac{2}{3}\right) - 10q\left(\frac{2}{3}\right). \end{aligned} \quad (42)$$

*Proof.*  $G^*$  is our graph of ZSM-5.  $E(G^*)$  is divided into three edge groups.

$E_1(G^*)$  holds  $4n$  edges  $pq$ , ( $d_p = d_q = 2$ ).  
 $E_2(G^*)$  keeps  $8n + 8m$  number of lines  $pq$ , and ( $d_p = 2, d_q = 3$ ).  
 $E_3(G^*)$  has  $36mn - 10m - 10n$  lines  $pq$ , where ( $d_p = 3, d_q = 3$ ). We define  $ABC(G)$  in (11):

$$\begin{aligned} ABC(G) &= \sum_{pq \in E(G)} \sqrt{\frac{d_p + d_q - 2}{d_p d_q}}, \\ ABC(G^*) &= |E_1(G^*)|\frac{1}{2\sqrt{2}} + |E_2(G^*)|\frac{1}{2\sqrt{2}} + |E_3(G^*)|\frac{2}{3} \\ &= (4p)\frac{1}{2\sqrt{2}} + (8p + 8q)\frac{1}{2\sqrt{2}} + (36pq - 10p - 10q)\frac{2}{3} \\ &= 4p\left(\frac{1}{2}\right)\sqrt{2} + \left(8p\left(\frac{1}{2}\right) + 8q\left(\frac{1}{2}\right)\right)\sqrt{2} + 36pq\left(\frac{2}{3}\right) \\ &\quad - 10p\left(\frac{2}{3}\right) - 10q\left(\frac{2}{3}\right). \end{aligned} \quad (43)$$

□

**Theorem 9.** ABC-4 index of ZSM-5 is as follows:

$$\begin{aligned} ABC_4(G^*) &= 4p\left(\frac{2}{5\sqrt{2}}\right) + \frac{4}{7\sqrt{14}} + 8p\left(\frac{1}{20\sqrt{110}}\right) - 4 + 4q\left(\frac{1}{42\sqrt{462}}\right) \\ &\quad + 4p\left(\frac{1}{2}\right) + 2q\left(\frac{1}{3\sqrt{2}}\right) + 2p\left(\frac{1}{8\sqrt{14}}\right) + 12q\left(\frac{1}{12\sqrt{30}}\right) \\ &\quad + 8p\left(\frac{1}{12\sqrt{30}}\right) + 36pq\left(\frac{4}{9}\right) - 24p\left(\frac{4}{9}\right) - 20q\left(\frac{4}{9}\right). \end{aligned} \quad (44)$$

*Proof.* ZSM-5 has  $36pq + 2p - 2q$  number of edges.

Consider an arc set relies on degree summation of neighbors of end vertices and  $E(G^*)$  is divided into nine disjoint groups of edges, such as

$$\begin{aligned} E_i(G^*), \quad i = 5, 6, \dots, 13; \\ \text{here,} \\ E(G^*) = \bigcup_{i=5}^{13} E_i(G^*). \end{aligned} \quad (45)$$

$E_5(G^*)$  holds  $4p$  number of edges  $pq$ , where  $S_p = S_q = 5$ ,  $E_6(G^*)$  has 4 lines  $pq$ , where  $S_p = 5$  and  $S_q = 7$ ,  $E_7(G^*)$  has  $8p - 4$  edges  $pq$ , where  $S_p = 5$  and  $S_q = 8$ ,  $E_8(G^*)$  has  $4q + 4$  edges  $pq$ , where  $S_p = 6$  and  $S_q = 7$ ,  $E_9(G^*)$  contains  $4p - 4$  edges  $pq$ , where  $S_p = 6$  and  $S_q = 8$ ,  $E_{10}(G^*)$  holds  $2q + 4$  lines  $pq$ , where  $S_p = 7$  and  $S_q = 9$ ,  $E_{11}(G^*)$  consists of  $2p$  number of arcs  $pq$ , where  $S_p = S_q = 8$ ,  $E_{12}(G^*)$  has  $12p + 8q - 16$  lines  $pq$ , where  $S_p = 8$  and  $S_q = 9$ , and  $E_{13}(G^*)$  contains  $36pq - 24p - 20q + 12$  number of edges  $pq$ , where  $S_p = S_q = 9$ . The index is defined in equation (12):

$$\begin{aligned} ABC_4(G) &= \sum_{pq \in E(G)} \sqrt{\frac{S_p + S_q - 2}{S_p S_q}}, \\ ABC_4(G^*) &= \sqrt{\frac{5+5-2}{5 \times 5}} |E_5(G^*)| + \sqrt{\frac{5+7-2}{5 \times 7}} |E_6(G^*)| + \sqrt{\frac{5+8-2}{5 \times 8}} |E_7(G^*)| \\ &\quad + \sqrt{\frac{6+7-2}{6 \times 7}} |E_8(G^*)| + \sqrt{\frac{6+8-2}{6 \times 8}} |E_9(G^*)| + \sqrt{\frac{7+9-2}{7 \times 9}} |E_{10}(G^*)| \\ &\quad + \sqrt{\frac{8+8-2}{8 \times 8}} |E_{11}(G^*)| + \sqrt{\frac{8+9-2}{8 \times 9}} |E_{12}(G^*)| + \sqrt{\frac{9+9-2}{9 \times 9}} |E_{13}(G^*)| \\ &= \sqrt{\frac{8}{25}} |E_5(G^*)| + \sqrt{\frac{10}{35}} |E_6(G^*)| + \sqrt{\frac{11}{40}} |E_7(G^*)| + \sqrt{\frac{11}{42}} |E_8(G^*)| \\ &\quad + \sqrt{\frac{12}{48}} |E_9(G^*)| + \sqrt{\frac{14}{63}} |E_{10}(G^*)| + \sqrt{\frac{14}{64}} |E_{11}(G^*)| + \sqrt{\frac{15}{72}} |E_{12}(G^*)| \\ &\quad + \sqrt{\frac{17}{81}} |E_{13}(G^*)|. \end{aligned} \quad (46)$$

After putting the values of  $E(G^*) = \cup_{i=5}^{13} E_i(G^*)$ , we get

$$\begin{aligned} &= \sqrt{\frac{8}{25}} (4p) + \sqrt{\frac{10}{35}} (4) + \sqrt{\frac{11}{40}} (8p - 4) + \sqrt{\frac{11}{42}} (4q + 4) + \sqrt{\frac{12}{48}} (4q - 4) \\ &\quad + \sqrt{\frac{14}{63}} (2q + 4) + \sqrt{\frac{14}{64}} (2p) + \sqrt{\frac{15}{72}} (12p + 8q - 16) + \sqrt{\frac{16}{81}} (36pq - 24p - 20q + 12), \end{aligned} \quad (47)$$

and after simplification,

$$\begin{aligned} &= \frac{8}{5\sqrt{2}} p + \frac{4}{7\sqrt{14}} + \frac{1}{20\sqrt{110}} (8p - 4) + \frac{1}{42\sqrt{462}} (4q + 4) - \frac{62}{9} q + \frac{10}{3} \\ &\quad + \frac{1}{3\sqrt{2}} (2q + 4) + \frac{1}{4\sqrt{14}} p + \frac{1}{12\sqrt{30}} (12p + 8q - 16) + 16pq - \frac{32}{3} q, \end{aligned} \quad (48)$$

**Theorem 10.** Let  $G^*$  be the graph of ZSM-5. Fifth generation geometric arithmetic index is as follows:

□

$$\begin{aligned}
 GA_5(G) &= 6p + \frac{2}{3\sqrt{35}} + \frac{4}{13}(8p-4)\sqrt{10} + \frac{4}{13}q(2\sqrt{42}) + \frac{2297}{9282} + \frac{2}{7}q(8\sqrt{3}) \\
 &+ \frac{1}{4}q(3\sqrt{7}) + \frac{12}{17}p(12\sqrt{2}) + \frac{8}{17}p(12\sqrt{2}) + 2pq(18) - \frac{4}{3}p(18) \\
 &- \frac{10}{9}q(18).
 \end{aligned} \tag{49}$$

*Proof.* ZSM-5 has  $36pq + 2p - 2q$  number of edges.

Consider an arc set relies on degree summation of neighbors of end vertices and  $E(G^*)$  is divided into nine disjoint groups of edges, such as

$$\begin{aligned}
 E_i(G^*), \quad i = 5, 6, \dots, 13; \\
 \text{here,} \\
 E(G^*) = \bigcup_{i=5}^{13} E_i(G^*).
 \end{aligned} \tag{50}$$

$E_5(G^*)$  holds  $4p$  number of edges  $pq$ , where  $S_p = S_q = 5$ ,  $E_6(G^*)$  has 4 lines  $pq$ , where  $S_p = 5$  and  $S_q = 7$ ,  $E_7(G^*)$  has  $8p - 4$  edges  $pq$ , where  $S_p = 5$  and  $S_q = 8$ ,  $E_8(G^*)$  has  $4q + 4$  edges  $pq$ , where  $S_p = 6$  and  $S_q = 7$ ,  $E_9(G^*)$  contains  $4p - 4$  edges  $pq$ , where  $S_p = 6$  and  $S_q = 8$ ,  $E_{10}(G^*)$  holds  $2q + 4$  lines  $pq$ , where  $S_p = 7$  and  $S_q = 9$ ,  $E_{11}(G^*)$  consists of  $2p$  number of arcs  $pq$ , where  $S_p = S_q = 8$ ,  $E_{12}(G^*)$  has  $12p + 8q - 16$  lines  $pq$ , where  $S_p = 8$  and  $S_q = 9$ , and  $E_{13}(G^*)$  contains  $36pq - 24p - 20q + 12$  number of edges  $pq$ , where  $S_p = S_q = 9$ . The index is defined in equation (18):

$$\begin{aligned}
 GA_5(G) &= \sum_{pq \in E(G)} \frac{2\sqrt{S_p \times S_q}}{S_p + S_q}, \\
 GA_5(G^*) &= \frac{2\sqrt{5 \times 5}}{5+5} |E_5(G^*)| + \frac{2\sqrt{5 \times 7}}{5+7} |E_6(G^*)| + \frac{2\sqrt{5 \times 8}}{5+8} |E_7(G^*)| \\
 &+ \frac{2\sqrt{6 \times 7}}{6+7} |E_8(G^*)| + \frac{2\sqrt{6 \times 8}}{6+8} |E_9(G^*)| + \frac{2\sqrt{7 \times 9}}{7+9} |E_{10}(G^*)| \\
 &+ \frac{2\sqrt{8 \times 8}}{8+8} |E_{11}(G^*)| + \frac{2\sqrt{8 \times 9}}{8+9} |E_{12}(G^*)| + \frac{2\sqrt{9 \times 9}}{9+9} |E_{13}(G^*)|.
 \end{aligned} \tag{51}$$

After putting the values  $E(G^*) = \cup_{i=5}^{13} E_i(G^*)$ , we get

$$\begin{aligned}
 &= \frac{2\sqrt{25}}{10} (4p) + \frac{2\sqrt{35}}{12} (4) + \frac{2\sqrt{40}}{13} (8p-4) + \frac{2\sqrt{42}}{13} (4q+4) + \frac{2\sqrt{48}}{14} (4q-4) \\
 &+ \frac{2\sqrt{63}}{16} (2q+4) + \frac{2\sqrt{64}}{16} (2p) + \frac{2\sqrt{72}}{17} (12p+8q-16) + \frac{2\sqrt{81}}{18} (36pq-24p-20q+12).
 \end{aligned} \tag{52}$$

After simplification,

$$\begin{aligned}
 &= -18p + \frac{2}{3\sqrt{35}} + \frac{4}{13}\sqrt{10}(8p-4) + \frac{2}{13\sqrt{42}}(4q+4) + \frac{4}{7\sqrt{3}}(4q-4) \\
 &+ \frac{3}{8\sqrt{7}}(2q+4) + \frac{12}{17}\sqrt{2}(12p+8q-16) + 36pq - 20q + 12.
 \end{aligned} \tag{53}$$

□

**Theorem 11.** Let  $G^*$  be the graph of ZSM-5. Then, general Randic connectivity index is as follows:

$$R_\alpha(G^*) = 4p(4^\alpha) + 8p(6^\alpha) + 8q(6^\alpha) + 36pq(9^\alpha) - 10p(9^\alpha) - 10q(9^\alpha). \quad (54)$$

*Proof.* The graph  $G^*$  of zeolite encounters  $36pq + 2p - 2q$  edges and  $24pq + 4p$  vertices.

The numeral of vertices of degree 2 are  $8p + 4q$  and of degree 3 are  $24pq - 4p - 4q$ .  $\mathbb{E}$  of  $G^*$  are  $36pq + 2p - 2q$ .  $\mathbb{E}(G^*)$  is divided into three edge groups.  $\mathbb{E}_1(G^*)$  has  $4p$

edges  $pq$ , where  $d_p = d_q = 2$ ,  $\mathbb{E}_2(G^*)$  contains  $8p + 8q$  edges  $pq$ , where  $d_p = 2$  and  $d_q = 3$ , and  $\mathbb{E}_3(G^*)$  supports  $36pq - 10p - 10q$  arcs  $pq$ , where  $d_p = d_q = 3$ .

By using definition of Randić index (13),

$$R_\alpha(G) = \sum_{pq \in E(G)} (d_p d_q)^\alpha. \quad (55)$$

Now, we have

$$\begin{aligned} R_\alpha(G^*) &= \sum_{pq \in E_1(G^*)} (d_p d_q)^\alpha + \sum_{pq \in E_2(G^*)} (d_p d_q)^\alpha + \sum_{xy \in E_3(G^*)} (d_p d_q)^\alpha \\ &= 4|E_1(G^*)| + 6|E_2(G^*)| + 9|E_3(G^*)| \\ &= 4(4p) + 6(8p + 8q) + 9(36pq - 10p - 10q). \end{aligned} \quad (56)$$

After simplification, we get

$$= -26p - 42q + 324pq. \quad (57) \quad \square$$

**Theorem 12.** Let  $G^*$  be the graph of ZSM-5. Then, the reciprocal Randić index is as follows:

$$RRR(G^*) = -\frac{4}{3}p + \frac{1}{6\sqrt{6}}(8p + 8q) + 12pq - \frac{10}{3}q. \quad (58)$$

*Proof.* The graph  $G^*$  of zeolite encounters  $36mn + 2n - 2m$  edges and  $24pq + 4p$  vertices.

The numeral of vertices of degree 2 are  $8p + 4q$  and of degree 3 are  $24pq - 4p - 4q$ .  $\mathbb{E}$  of  $G^*$  are  $36pq + 2p - 2q$ .  $\mathbb{E}(G^*)$  cleaves into three disunite edge groups:

$$\mathbb{E}(G^*) = \mathbb{E}_1(G^*) \cup \mathbb{E}_2(G^*) \cup \mathbb{E}_3(G^*). \quad (59)$$

$\mathbb{E}_1(G^*)$  has  $4p$  arcs  $pq$ , where  $d_p = d_q = 2$ ,  $\mathbb{E}_2(G^*)$  contains  $8p + 8q$  edges  $pq$ , where  $d_p = 2$  and  $d_q = 3$ , and  $\mathbb{E}_3(G^*)$  supports  $36pq - 10p - 10q$  arcs  $pq$ , where  $d_p = d_q = 3$ .

We define this index in equation (16):

$$\begin{aligned} RRR(G) &= \sum_{pq \in E(G)} \sqrt{(d_p - 1)(d_q - 1)}, \\ RRR(G^*) &= \sum_{pq \in E_1(G^*)} \sqrt{(d_p - 1)(d_q - 1)} + \sum_{pq \in E_2(G^*)} \sqrt{(d_p - 1)(d_q - 1)} \\ &\quad + \sum_{pq \in E_3(G^*)} \sqrt{(d_p - 1)(d_q - 1)} \\ &= 1|E_1(G^*)| + \sqrt{2}|E_2(G^*)| + 2|E_3(G^*)| \\ &= (4p) + \sqrt{2}(8p + 8q) + 2(36pq - 10p - 10q) \\ &= -16p + \sqrt{2}(8p + 8q) + 72pq - 20m. \end{aligned} \quad (60) \quad \square$$

**Theorem 13.** Consider  $G^*$  to be the graph of ZSM-5. Geometric arithmetic index is described as follows:

$$GA(G^*) = \frac{2}{5\sqrt{6}}(8p + 8q) + 36pq - 10p - 10q. \quad (61)$$

*Proof.* The graph  $G^*$  of zeolite encounters  $36pq + 2p - 2q$  edges and  $24pq + 4p$  vertices. The grouping of the vertices is given as follows:

The vertices of degree two are  $8p + 4q$  and of degree three are  $24pq - 4p - 4q$ . Cardinality of  $\mathbb{E}$  of  $G^*$  is  $36pq + 2p - 2q$ . The arc group  $\mathbb{E}(G^*)$  cleaves in 3 disjoint arc groups that rely on the degrees of the end vertices, such as

$$\mathbb{E}(G^*) = \mathbb{E}_1(G^*) \cup \mathbb{E}_2(G^*) \cup \mathbb{E}_3(G^*). \quad (62)$$

$\mathbb{E}_1(G^*)$  has  $4p$  lines  $pq$ , where  $d_p = d_q = 2$ .

$\mathbb{E}_2(G^*)$  has  $8p + 8q$  lines  $pq$ , where  $d_p = 2$  and  $d_q = 3$ .

$\mathbb{E}_3(G^*)$  supports  $36pq - 10p - 10q$  lines  $pq$ , where  $d_p = d_q = 3$ .

We define this index in equation (17) as

$$\begin{aligned}
 \text{GA}(G) &= \sum_{pq \in E(G)} \frac{2\sqrt{d_p d_q}}{d_p + d_q}, \\
 \text{GA}(G^*) &= \sum_{pq \in E_1(G^*)} \frac{2\sqrt{d_p d_q}}{d_p + d_q} + \sum_{pq \in E_2(G^*)} \frac{2\sqrt{d_p d_q}}{d_p + d_q} + \sum_{xy \in E_3(G^*)} \frac{2\sqrt{d_p d_q}}{d_p + d_q} \\
 &= 1|E_1(G^*)| + \left(\frac{2}{5\sqrt{6}}\right)|E_2(G^*)| + 1|E_3(G^*)| \quad (63) \\
 &= (4p) + \left(\frac{2}{5\sqrt{6}}\right)(8p + 8q) + (36pq - 10p - 10q) \\
 &= -6p + \left(\frac{2}{5\sqrt{6}}\right) + 36pq - 10q. \quad \square
 \end{aligned}$$

**Theorem 14.** *Forgotten index of graph  $G^*$  of ZSM-5 is as follows:*

$$\begin{aligned}
 F(G^*) &= 4p(4) + 8p(13) + 8q(13) + 36pq(18) - 10p(18) \\
 &\quad - 10q(18). \quad (64)
 \end{aligned}$$

*Proof.* The graph  $G^*$  encounters  $36pq + 2p - 2q$  edges and  $24pq + 4p$  vertices.

The points of degree 2 are  $8p + 4q$  and the points of degree 3 are  $24pq - 4p - 4q$ . The cardinality edge group  $\mathbb{E}$  of  $G^*$  is  $36pq + 2p - 2q$ .  $E(G^*)$  cleaves into three disjoint line groups that are as follows:  $\mathbb{E}_1(G^*)$  holds  $4n$  arcs and  $d_p = d_q = 2$ .  $\mathbb{E}_2(G^*)$  supports  $8n + 8m$  arcs  $pq$ , where  $d_p = 2$  and  $d_q = 3$ , and  $\mathbb{E}_3(G^*)$  has  $36mn - 10n - 10m$  arcs  $pq$ , where  $d_p = d_q = 3$ .

By using the definition of forgotten index (19),

$$\begin{aligned}
 F(G) &= \sum_{pq \in E(G)} (d_p^2 + d_q^2), \\
 F(G^*) &= \sum_{pq \in E_1(G^*)} (d_p^2 + d_q^2) + \sum_{pq \in E_2(G^*)} (d_p^2 + d_q^2) + \sum_{xy \in E_3(G^*)} (d_p^2 + d_q^2) \\
 &= 8|E_1(G^*)| + 13|E_2(G^*)| + 18|E_3(G^*)| \quad (65) \\
 &= 8(4p) + 13(8p + 8q) + 18(36pq - 10p - 10q) \\
 &= -44p - 76q + 648pq. \quad \square
 \end{aligned}$$

**Theorem 15.** *Let  $G^*$  be the graph of ZSM-5, then the general sum connectivity index is as follows:*

$$\begin{aligned}
 X_\alpha(G^*) &= 4p(4^\alpha) + 8p(5^\alpha) + 8q(5^\alpha) + 36pq(6^\alpha) \\
 &\quad - 10p(6^\alpha) - 10q(6^\alpha). \quad (66)
 \end{aligned}$$

*Proof.* The graph  $G^*$  of zeolite encounters  $36pq + 2p - 2q$  edges and  $24pq + 4p$  vertices.

Vertices of degree two are  $8n + 4m$  and of degree three are  $24pq - 4p - 4q$ .  $E$  of  $G^*$  are  $36pq + 2p - 2q$ .  $E(G^*)$  cleaves into 3 disjoint edge groups.  $\mathbb{E}_1(G^*)$  holds  $4p$  edges

$pq$ , where  $d_p = d_q = 2$ ,  $\mathbb{E}_2(G^*)$  holds  $8p + 8q$  edges  $pq$ , where  $d_p = 2$  and  $d_q = 3$ ,  $\mathbb{E}_3(G^*)$  holds  $36pq - 10p - 10q$

edges  $pq$ , where  $d_p = d_q = 3$ . From (20), we get the definition of general sum connectivity index:

$$\begin{aligned}\chi_\alpha(G) &= \sum_{pq \in E(G)} (d_p + d_q)^\alpha, \\ \chi_\alpha(G^*) &= \sum_{pq \in E_1(G^*)} (d_p + d_q)^\alpha + \sum_{pq \in E_2(G^*)} (d_p + d_q)^\alpha + \sum_{xy \in E_3(G^*)} (d_p + d_q)^\alpha \\ &= (4)^\alpha |E_1(G^*)| + (5)^\alpha |E_2(G^*)| + (6)^\alpha |E_3(G^*)| \\ &= (4)^\alpha (4p) + (5)^\alpha (8p + 8q) + (6)^\alpha (36pq - 10q - 10p).\end{aligned}\quad (67)$$

**Theorem 16.**  $G^*$  is the graph of ZSM-5 and its symmetric division index is as follows:

$$SD(G^*) = \frac{16}{3}p - \frac{8}{3}q + 72pq. \quad (68)$$

*Proof.*  $G^*$  of zeolite encounters  $36pq + 2p - 2q$  edges and  $24pq + 4p$  vertices.

The number of vertices of degree two are  $8n + 4m$  and the number of vertices of degree 3 are  $24pq - 4p - 4q$ .  $\mathbb{E}$  of  $G^*$  are  $36pq + 2p - 2q$ .  $\mathbb{E}(G^*)$  cleaves into three disjoint edge groups.  $\mathbb{E}_1(G^*)$  holds  $4p$  edges  $pq$ , where  $d_p = d_q = 2$ ,  $\mathbb{E}_2(G^*)$  holds  $8p + 8q$  edges  $pq$ , where  $d_p = 2$  and  $d_q = 3$ , and  $\mathbb{E}_3(G^*)$  holds  $36pq - 10p - 10q$  edges  $pq$ , where  $d_p = d_q = 3$ .

From (21), we get

$$\begin{aligned}SD(G) &= \sum_{pq \in E(G)} \frac{d_p^2 + d_q^2}{(d_p \times d_q)}, \\ SD(G^*) &= \sum_{pq \in E_1(G^*)} \frac{d_p^2 + d_q^2}{(d_p \times d_q)} + \sum_{pq \in E_2(G^*)} \frac{d_p^2 + d_q^2}{(d_p \times d_q)} \\ &\quad + \sum_{pq \in E_3(G^*)} \frac{d_p^2 + d_q^2}{(d_p \times d_q)} \\ &= (2)|E_1(G^*)| + \left(\frac{13}{5}\right)|E_2(G^*)| + (2)|E_3(G^*)| \\ &= 2(4p) + \left(\frac{13}{5}\right)(8p + 8q) + 2(36pq - 10q - 10p).\end{aligned}\quad (69)$$

After simple calculations,

$$= -12p + \frac{13}{5} + 72pq - 20q. \quad (70)$$

**Theorem 17.**  $G^*$  is the graph of ZSM-5 and its harmonic index is as follows:

$$H(G) = -\frac{4}{3}p + 8p\left(\frac{2}{5}\right) + 8q\left(\frac{2}{5}\right) + 12pq - \frac{10}{3}q. \quad (71)$$

*Proof.* The graph  $G^*$  of zeolite encounters  $36pq + 2p - 2q$  edges and  $24pq + 4p$  vertices.

The number of vertices of degree 2 are  $8p + 4q$  and of degree 3 are  $24pq - 4p - 4q$ .  $E$  of  $G^*$  are  $36pq + 2p - 2q$ .  $E(G^*)$  cleaves into three disjoint edge groups.

$\mathbb{E}(G^*) = E_1(G^*) \cup \mathbb{E}_2(G^*) \cup \mathbb{E}_3(G^*)$ .  $\mathbb{E}_1(G^*)$  holds  $4p$  edges  $pq$ , where  $d_p = d_q = 2$ ,  $\mathbb{E}_2(G^*)$  holds  $8p + 8q$  edges  $pq$ , where  $d_p = 2$  and  $d_q = 3$ , and  $\mathbb{E}_3(G^*)$  holds  $36pq - 10p - 10q$  edges  $pq$ , where  $d_p = d_q = 3$ . Harmonic index is defined in equation (22) as

$$\begin{aligned}H(G) &= \sum_{pq \in E(G)} \frac{2}{(d_p + d_q)}, \\ H(G^*) &= \sum_{pq \in E_1(G^*)} \frac{2}{(d_p + d_q)} + \sum_{pq \in E_2(G^*)} \frac{2}{(d_p + d_q)} \\ &\quad + \sum_{pq \in E_3(G^*)} \frac{2}{(d_p + d_q)} \\ &= \left(\frac{2}{4}\right)|E_1(G^*)| + \left(\frac{2}{5}\right)|E_2(G^*)| + \left(\frac{2}{6}\right)|E_3(G^*)| \\ &= \left(\frac{1}{2}\right)(4p) + \left(\frac{2}{5}\right)(8p + 8q) + \left(\frac{1}{3}\right)(36pq - 10q - 10p) \\ &= 2p + \left(\frac{16}{5}\right)(16p + 16q) + \left(\frac{2}{3}\right)(18pq - 5q - 5p) \\ &= \frac{37}{30}.\end{aligned}\quad (72)$$

### 3. Conclusion

We correlate the uses of topological indices with chemical structure of ZSM-5. The main interest of the research is to present a concise introduction to some basic concepts about topological indices and their uses to find physicochemical properties of chemical structures. We conclude that physical properties of ZSM-5 can easily be calculated through topological indices. The consequences lay out noteworthy contribution in the field of graph theory and chemistry. This



research contains the results theoretically not experimentally.

## Data Availability

No data were used in this study.

## Conflicts of Interest

The authors declare that they have no conflicts of interest.

## References

- [1] D. Chassapis and M. Kotsakosta, "Crossing the bridges of Königsberg in a primary mathematics classroom mathematics in school," vol. 32, no. 1, pp. 11–13, 2003.
- [2] F. Harary, *A Seminar on Graph Theory*, Courier Dover Publications, Mineola, NY, USA, 2015.
- [3] B. Mondal and K. De, "An overview applications of graph theory in real field," *International Journal of Scientific Research in Computer Science, Engineering and Information Technology*, vol. 2, no. 5, pp. 751–759, 2017.
- [4] J. A. Bondy and U. S. R. Murty, *Graph Theory with Applications*, Macmillan, London, UK, 1976.
- [5] K. C. Das, I. Gutman, and B. Furtula, "Survey on geometric-arithmetic indices of graphs," *MATCH Communications in Mathematical and in Computer Chemistry*, vol. 65, no. 3, pp. 595–644, 2011.
- [6] J. M. Rodriguez and J. M. Sigarreta, "On the geometric-arithmetic index," *MATCH Communications in Mathematical and in Computer Chemistry*, vol. 74, pp. 103–120, 2015.
- [7] K. C. Das, "On geometric-arithmetic index of graph," *MATCH Communications in Mathematical and in Computer Chemistry*, vol. 64, no. 3, pp. 619–630, 2010.
- [8] R. Gozalbes, J. Doucet, and F. Derouin, "Application of topological descriptors in QSAR and drug design: history and new trends," *Current Drug Target-Infectious Disorders*, vol. 2, no. 1, pp. 93–102, 2002.
- [9] G. Gottardi and E. Galli, *Natural Zeolites*, Springer Science & Business Media, Berlin, Germany, 2012.
- [10] G. H. Fath-Tabar, "Old and new Zagreb indices of graphs," *MATCH Communications in Mathematical and in Computer Chemistry*, vol. 65, pp. 79–84, 2011.
- [11] Y. Huo, H. Ali, M. A. Binyamin, S. S. Asghar, U. Babar, and J.-B. Liu, "On topological indices of  $m$ th chain hex-derived network of third type," *Frontiers in Physics*, vol. 8, Article ID 593275, 2020.
- [12] S. Zhang and H. Zhang, "Unicyclic graphs with the first three smallest and largest first general Zagreb index," *MATCH Communications in Mathematical and in Computer Chemistry*, vol. 55, no. 20, p. 6, 2006.
- [13] U. Babar, H. Ali, H. Ali, S. Hussain Arshad, and U. Sheikh, "Multiplicative topological properties of graphs derived from honeycomb structure," *AIMS Mathematics*, vol. 5, no. 2, pp. 1562–1587, 2020.
- [14] M. Ghorbani and M. Ghazi, "Computing some topological indices of Triangular Benzenoid," *Digest Journal of Nanomaterials and Biostructures*, vol. 5, no. 4, pp. 1107–1111, 2010.
- [15] I. Gutman, "Degree-based topological indices," *Croatica Chemica Acta*, vol. 86, no. 4, pp. 351–361, 2013.
- [16] K. C. Das and I. Gutman, "Some properties of the second Zagreb index," *MATCH Communications in Mathematical and in Computer Chemistry*, vol. 52, no. 1, pp. 3–1, 2004.
- [17] E. Deutsch and S. Klavžar, "M-polynomial and degree-based topological indices," 2014, <https://arxiv.org/abs/1407.1592>.
- [18] S. C. Basak, A. T. Balaban, G. D. Grunwald, and B. D. Gute, "Topological indices: their nature and mutual relatedness," *Journal of Chemical Information and Computer Sciences*, vol. 40, no. 4, pp. 891–898, 2000.
- [19] M. Imran, S. Hayat, and M. Y. H. Maillk, "On topological indices of certain interconnection networks," *Applied Mathematics and Computation*, vol. 244, pp. 936–951, 2014.
- [20] V. R. Kulli, "Reduced second hyper-Zagreb index and its polynomial of certain silicate networks," *Journal of Mathematics and Informatics*, vol. 14, pp. 11–16, 2018.
- [21] <https://pisrt.org/psr-press/journals/oms-vol-4-2020/on-the-entire-zagreb-indices-of-the-line-graph-and-line-cut-vertex-graph-of-the-subdivision-graph>.
- [22] K. C. Das, I. Gutman, and B. Furtula, "On atom-bond connectivity index," *Chemical Physical Letters*, vol. 511, no. 4–6, pp. 452–454, 2011.
- [23] M. Munir, W. Nazeer, S. Rafique, and S. Kang, "M-polynomial and related topological indices of nanostar dendrimers," *Symmetry*, vol. 8, no. 9, p. 97, 2016.
- [24] <https://pisrt.org/psr-press/journals/oms-vol-5-2021/super-cyclic-antimagic-covering-for-some-families-of-graphs>.
- [25] X. Li and Y. Shi, "A survey on the Randic index," *MATCH Communications in Mathematical and in Computer Chemistry*, vol. 59, no. 1, pp. 127–156, 2008.
- [26] I. Gutman, B. Furtula, and C. Elphick, "Three new/old vertex-degree-based topological indices," *MATCH Communications in Mathematical and in Computer Chemistry*, vol. 72, no. 3, pp. 617–632, 2014.
- [27] M. Munir, W. Nazeer, S. Rafique, and S. Kang, "M-polynomial and degree-based topological indices of polyhex nanotubes," *Symmetry*, vol. 8, no. 12, p. 149, 2016.
- [28] G. Dustigeer, H. Ali, M. Imran Khan, and Y.-M. Chu, "On multiplicative degree based topological indices for planar octahedron networks," *Main Group Metal Chemistry*, vol. 43, no. 1, pp. 219–228, 2020.
- [29] H. Siddiqui and M. R. Farahani, "Forgotten polynomial and forgotten index of certain interconnection networks," *Open Journal of Mathematical Analysis*, vol. 1, no. 1, pp. 45–60, 2017.
- [30] B. Zhou and N. Trinajstić, "On general sum-connectivity index," *Journal of Mathematical Chemistry*, vol. 47, no. 1, pp. 210–218, 2010.
- [31] A. Ali, S. Elumalai, and T. Mansour, "On the symmetric division deg index of molecular graphs," *MATCH Communications in Mathematical and in Computer Chemistry*, vol. 83, pp. 205–220, 2020.
- [32] S. Nikolić, G. Kovačević, A. Miličević, and N. Trinajstić, "The Zagreb indices 30 years after," *Croatica Chemica Acta*, vol. 76, no. 2, pp. 113–124, 2003.

## Research Article

# On the Computation of Some Topological Descriptors to Find Closed Formulas for Certain Chemical Graphs

Muhammad Haroon Aftab <sup>1</sup>, Muhammad Rafaqat <sup>1</sup>, M. Hussain <sup>2</sup> and Tariq Zia <sup>2</sup>

<sup>1</sup>Department of Mathematics, The University of Lahore, Lahore, Pakistan

<sup>2</sup>Department of Mathematics, COMSATS University Islamabad, Lahore Campus, Islamabad, Pakistan

Correspondence should be addressed to Muhammad Haroon Aftab; haroon.aftab@math.uol.edu.pk

Received 20 February 2021; Accepted 2 May 2021; Published 21 May 2021

Academic Editor: Muhammad Imran

Copyright © 2021 Muhammad Haroon Aftab et al. This is an open access article distributed under the Creative Commons Attribution License, which permits unrestricted use, distribution, and reproduction in any medium, provided the original work is properly cited.

In this research paper, we will compute the topological indices (degree based) such as the ordinary generalized geometric-arithmetic (OGA) index, first and second Gourava indices, first and second hyper-Gourava indices, general Randić' index  $R_\gamma(G)$ , for  $c = \{\pm 1, \pm 1/2\}$ , harmonic index, general version of the harmonic index, atom-bond connectivity (ABC) index, SK, SK<sub>1</sub>, and SK<sub>2</sub> indices, sum-connectivity index, general sum-connectivity index, and first general Zagreb and forgotten topological indices for various types of chemical networks such as the subdivided polythiophene network, subdivided hexagonal network, subdivided backbone DNA network, and subdivided honeycomb network. The discussion on the aforementioned networks will give us very remarkable results by using the aforementioned topological indices.

## 1. Introduction

The branch of mathematics that is related to the study of implementation of chemistry and graph theory together is called chemical graph theory. This theory is used to model the molecules of a chemical compound mathematically. This theory helps us to understand the physical properties of that chemical/molecular compound. In this theory, we construct the structure of a chemical compound in the form of a graph. In chemical graph theory, atoms are used as nodes, and bonds between the atoms are utilized as edges. A topological index is a numerical parameter of a graph that explains its topology. The topological index is also called a molecular descriptor and a connectivity index. It is obtained by transforming the chemical information into a numerical quantity. Topological indices are used as molecular descriptors in the construction of quantitative structure-activity relationships and quantitative structure-property relationships as well. The theoretical models such as quantitative structure-activity relationships (QSARs) relate the quantitative measure of a chemical structure to a biological property or a physical property, and quantitative

structure-property relationships (QSPRs) relate mathematically physical/chemical properties to the structure of a molecule. Topological indices such as ordinary generalized geometric-arithmetic (OGA) index, first and second Gourava indices, first and second hyper-Gourava indices, general Randić index  $R_\gamma(G)$ , for  $\gamma = \{\pm 1, \pm 1/2\}$ , harmonic index, general version of harmonic index [1, 2], atom-bond connectivity (ABC) index [3, 4], SK, SK<sub>1</sub>, and SK<sub>2</sub> indices, sum-connectivity index, general sum-connectivity index, and first general Zagreb [5] and forgotten topological indices have very significant roles in QSAR and QSPR studies and are used to discuss the bioactivity of molecular structures.

In 2009, D. Vukičević and B. Furtula established the first GA index in [6–11]. The first geometric-arithmetic (GA) index of a graph  $\xi$  was calculated by

$$GA(\xi) = \sum_{gh \in E(\xi)} \frac{2\sqrt{d_g d_h}}{d_g + d_h} \quad (1)$$

An ordinary geometric-arithmetic index of  $\xi$  was produced in 2011 in [12] and formulated by, for each positive real number  $k$ ,

$$\text{OGA}_k(\xi) = \sum_{gh \in E(\xi)} \left[ \frac{\sqrt{4d_g d_h}}{d_g + d_h} \right]^k. \quad (2)$$

In 2017, V. R. Kulli proposed the first and second Gourava and hyper-Gourava indices in [13, 14]. The first and second Gourava and hyper-Gourava indices of a graph  $\xi$  were formulated by

$$\begin{aligned} \text{GO}_1(\xi) &= \sum_{gh \in E(\xi)} [(d_g + d_h) + (d_g d_h)], \\ \text{GO}_2(\xi) &= \sum_{gh \in E(\xi)} [(d_g + d_h) + (d_g d_h)], \\ \text{HGO}_1(\xi) &= \sum_{gh \in E(\xi)} [(d_g + d_h) + (d_g d_h)]^2, \\ \text{HGO}_2(\xi) &= \sum_{gh \in E(\xi)} [(d_g + d_h) + (d_g d_h)]^2. \end{aligned} \quad (3)$$

In 1975, Randić' index [15–17] was introduced by Milan Randić'. It is often used in chemoinformatics to investigate the compounds of chemicals. The Randić' index is also called "the connectivity index of the graph" and formulated by

$$R_{(1/2)}(\xi) = \sum_{uv \in E(\xi)} \frac{1}{\sqrt{(d_u \cdot d_v)}}, \quad (4)$$

where  $d_u$  and  $d_v$  are the degrees of the nodes.

Later, Bollobás and Erdos furnished its generalized version for  $\gamma$ , where  $\gamma \in R$ , known as the general Randić' index [18–21] defined as

$$R_\gamma(G) = \sum_{gh \in E(G)} (d_g \cdot d_h)^\gamma, \quad \text{for } \gamma = \left\{ -1, 1, -\frac{1}{2}, \frac{1}{2} \right\}. \quad (5)$$

In 2012, L. Zhong described the harmonic index in [22, 23], and it is given by

$$\text{HI}(G) = \sum_{gh \in E(G)} \frac{2}{d_g + d_h}. \quad (6)$$

In 2015, L. Yan introduced the general version of the harmonic index in [24] and defined by

$$H_k I(G) = \sum_{gh \in E(G)} \left[ \frac{2}{d_g + d_h} \right]^k. \quad (7)$$

In 2008, Ernesto Estrada et al. [25, 26] introduced a new topological index, named atom-bond connectivity (ABC) index, calculated by

$$\text{ABC}(G) = \sum_{gh \in E(G)} \sqrt{\frac{d_g + d_h - 2}{d_g d_h}}. \quad (8)$$

The ABC index is an excellent valuable index in the formation of heat in alkanes [25, 26].

*Definition 1.* For a graph  $\xi$ , the SK index [27] can be computed by

$$\text{SK}(\xi) = \sum_{gh \in E(\xi)} \frac{d_g + d_h}{2}. \quad (9)$$

Let  $d_g$  and  $d_h$  be the degrees of nodes  $g$  and  $h$  in  $\xi$ , respectively.

*Definition 2.* For a graph  $\xi$ , the  $\text{SK}_1$  index can be computed by

$$\text{SK}_1(\xi) = \sum_{gh \in E(\xi)} \frac{d_g d_h}{2}. \quad (10)$$

Let  $d_g$  and  $d_h$  be the degrees of nodes  $g$  and  $h$  in  $\xi$ , respectively.

*Definition 3.* For a graph  $\xi$ , the  $\text{SK}_2$  index can be computed by

$$\text{SK}_2(\xi) = \sum_{gh \in E(\xi)} \left[ \frac{d_g + d_h}{2} \right]^2. \quad (11)$$

Let  $d_g$  and  $d_h$  be the degrees of nodes  $g$  and  $h$  in  $\xi$ , respectively.

In 2009, B. Lučić proposed the sum-connectivity index ( $\chi$ ) in [28] calculated by

$$\chi_{-(1/2)}(G) = \sum_{gh \in E(G)} [d_g + d_h]^{-1/2}. \quad (12)$$

In 2010, B. Zhou and Trinajstić furnished an index named general sum-connectivity index in [24, 29] and formulated as follows:

$$\chi_k(\xi) = \sum_{gh \in E(\xi)} [d_g + d_h]^k. \quad (13)$$

In 2005, X. Li and J. Zheng produced the generalized form of the first Zagreb index by calling it the "first general Zagreb index." The first general Zagreb index [30–35] of a graph  $\xi$  was computed by  ${}^k M_1(\xi) = \sum_{gh \in E(\xi)} [d_g^{k-1} + d_h^{k-1}]$ ;  $k$  belongs to  $R$ , and  $k \neq 0$  and  $k \neq 1$ .

In 2015, Boris Furtula and Ivan Gutman discovered an index named as "forgotten topological index" [36–38] and computed as

$$F(G) = \sum_{gh \in E(G)} [d_g^2 + d_h^2]. \quad (14)$$

## 2. Topological Indices on Certain Chemical Graphs

In this part of the research paper, we will compute the topological indices (degree based) such as ordinary generalized geometric-arithmetic (OGA) index, first and second Gourava indices, first and second hyper-Gourava indices, general Randić index  $R_\gamma(\xi)$ , for  $\gamma = \{ \pm 1, \pm 1/2 \}$ , harmonic index, general version of harmonic index, atom-bond connectivity (ABC) index, SK,  $\text{SK}_1$ , and  $\text{SK}_2$  indices, sum-connectivity index, general sum-connectivity index, first general Zagreb index, and forgotten topological indices for various types of chemical networks such as subdivided

polythiophene network, subdivided hexagonal network, subdivided backbone DNA network, and subdivided honeycomb network.

**2.1. Results for the Subdivided Polythiophene Network.** Polythiophenes are rings with five elements having one heteroatom together with their benzo and other carbocyclic. Polythiophene is used in electronic devices such as water purification devices, biosensors, and light-emitting diodes and in hydrogen storage [39]. In a subdivided polythiophene network, shown in Figure 1, we insert another vertex (degree 2) in every edge of  $\xi$ . In this way, we get a subdivided polythiophene network. In this section, we compute the subdivided polythiophene network using the above-defined topological indices. In the subdivided polythiophene network  $SPLY_n$  we have the number of nodes  $11n-1$  and edges  $12n-2$ . A subdivided polythiophene network for  $n=5$  is shown in Figure 1. We get two kinds of edges (degree based) that are (2, 2) and (2, 3). Table 1 gives us two types of edges. A subdivided polythiophene network  $SPLY_5$  is displayed in Figure 1.

**Theorem 1.** For the subdivided polythiophene network,  $SPLY_n$ , the ordinary generalized geometric-arithmetic index is calculated by

$$OGA_k(\xi) = 6n \left\{ 1 + \left[ \frac{\sqrt{24}}{5} \right]^k \right\} + \left\{ 4 - 6 \left[ \frac{\sqrt{24}}{5} \right]^k \right\}. \quad (15)$$

*Proof.* By letting  $\xi$  as a subdivided polythiophene network  $SPLY_n$ , from Table 1, we know

$$OGA_k(\xi) = \sum_{gh \in E(\xi)} \left[ \frac{\sqrt{4d_g d_h}}{d_g + d_h} \right]^k, \quad (16)$$

$$OGA_k(\xi) = (6n+4) \left[ \frac{\sqrt{16}}{2+2} \right]^k + (6n-6) \left[ \frac{\sqrt{24}}{5} \right]^k,$$

and by doing some calculations, we get

$$OGA_k(\xi) = 6n \left[ 1 + \left( \frac{\sqrt{24}}{5} \right)^k \right] + \left[ 4 - 6 \left( \frac{\sqrt{24}}{5} \right)^k \right]. \quad (17)$$

**Theorem 2.** For the subdivided polythiophene network,  $SPLY_n$ , the first and second Gourava indices are calculated by  $GO_1(\xi) = 114n - 34$  and  $GO_2(\xi) = 276n - 116$ .

*Proof.* By letting  $\xi$  as a subdivided polythiophene network  $SPLY_n$ , from Table 1, we know

$$\begin{aligned} GO_1(\xi) &= \sum_{gh \in E(\xi)} [(d_g + d_h) + (d_g d_h)], \\ GO_2(\xi) &= \sum_{gh \in E(\xi)} [(d_g + d_h) + (d_g d_h)], \end{aligned} \quad (18)$$

and by doing some calculations, we get

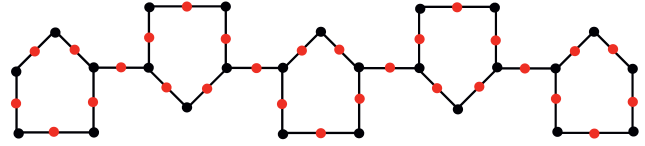


FIGURE 1:  $SPLY_5$ .

TABLE 1: Division of edges of a graph  $\xi$  found on the degree of terminating nodes of each of the edges.

$(d_g, d_h)$ for $gh \in E(\xi)$	Number of $E(\xi)$
(2, 2)	$6n + 4$
(2, 3)	$6(n - 1)$

$$GO_1(\xi) = (6n+4)[(4) + (4)] + (6n-6)[(5) + (6)] = 114n - 34,$$

$$GO_2(\xi) = (6n+4)[16] + (6n-6)[30] = 276n - 116. \quad (19)$$

**Theorem 3.** For the subdivided polythiophene network,  $SPLY_n$ , the first and second hyper-Gourava indices are calculated by  $HGO_1(\xi) = 1110n - 470$  and  $HGO_2(\xi) = 6936n - 4376$ .

*Proof.* By letting  $\xi$  as a subdivided polythiophene network,  $SPLY_n$ , from Table 1, we know

$$\begin{aligned} HGO_1(\xi) &= \sum_{gh \in E(\xi)} [(d_g + d_h) + (d_g d_h)]^2, \\ HGO_2(\xi) &= \sum_{gh \in E(\xi)} [(d_g + d_h) + (d_g d_h)]^2, \end{aligned} \quad (20)$$

and by doing some calculations, we get  $HGO_1(\xi) = (6n+4)[64] + (6n-6)[121] = 1110n - 470$ , and

$$HGO_2(\xi) = (6n+4)[256] + (6n-6)[900] = 6936n - 4376. \quad (21)$$

**Theorem 4.** For the subdivided polythiophene network,  $SPLY_n$ , the general Randić' index is calculated by

$$R_\gamma(SPLY_n) = \begin{cases} \frac{5}{2}n, & \text{for } \gamma = -1, \\ n \left( \frac{109}{20} \right) + \left( \frac{8}{5} \right), & \text{for } \gamma = -\frac{1}{2}, \\ n \left( \frac{267}{10} \right) - \left( \frac{67}{10} \right), & \text{for } \gamma = \frac{1}{2}, \\ 60n - 20, & \text{for } \gamma = 1. \end{cases} \quad (22)$$

*Proof.* By letting  $\xi$  as a subdivided polythiophene network  $SPLY_n$  of  $n$  dimensions, we have the number of nodes and

edges in  $SPLY_n$  as  $|V(SPLY_n)| = 11n - 1$  and  $|E(SPLY_n)| = 12n - 2$ , respectively.

We know that

$$R_\gamma(\xi) = \sum_{gh \in E(\xi)} (d_g \cdot d_h)^\gamma, \quad (23)$$

for  $\gamma = \{-1, 1, -1/2, 1/2\}$ .

Case 1: if  $\gamma = -1$ , the application of Randić' index  $R_\gamma(\xi)$

$$R_{-1}(\xi) = \sum_{gh \in E(\xi)} \frac{1}{d_g d_h}, \quad (24)$$

using (23). From Table 1, we know  $R_{-1}(\xi) = (6n + 4)(4)^{-1} + (6n - 6)(6)^{-1}$ . By doing some calculations, we get  $R_{-1}(\xi) = (5/2)n$ .

Case 2: if  $\gamma = -1/2$ , the application of Randić' index  $R_\gamma(\xi)$

$$R_{-(1/2)}(\xi) = \sum_{gh \in E(\xi)} \frac{1}{\sqrt{(d_g \cdot d_h)}}, \quad (25)$$

using (23),

$$R_{-(1/2)}(\xi) = (6n + 4)\frac{1}{\sqrt{4}} + (6n - 6)\frac{1}{\sqrt{6}}, \quad (26)$$

and by doing some calculations, we get  $R_{-(1/2)}(\xi) = n(109/20) + (8/5)$ .

Case 3: if  $\gamma = 1/2$ , the application of Randić' index  $R_\gamma(\xi)$

$$R_{(1/2)}(\xi) = \sum_{gh \in E(\xi)} \sqrt{d_g \cdot d_h}, \quad (27)$$

using (23),

$$R_{(1/2)}(\xi) = (6n + 4)\sqrt{4} + (6n - 6)\sqrt{6}, \quad (28)$$

and by doing some calculations, we get  $R_{(1/2)}(\xi) = n(267/10) - (67/10)$ .

Case 4: if  $\gamma = 1$ , the application of Randić' index  $R_\gamma(\xi)$

$$R_1(\xi) = \sum_{gh \in E(\xi)} (d_g \cdot d_h)^1, \quad (29)$$

using (23),

$$R_1(\xi) = (6n + 4)(4) + (6n - 6)(6), \quad (30)$$

and by doing some calculations, we get  $R_1(\xi) = 60n - 20$ .

**Theorem 5.** For the subdivided polythiophene network,  $SPLY_n$ , the harmonic index is calculated by

$$HI(\xi) = \frac{2n - 2}{5}. \quad (31)$$

*Proof.* By letting  $\xi$  as a subdivided polythiophene network  $SPLY_n$ , from Table 1, we know

$$HI(\xi) = \sum_{gh \in E(\xi)} \frac{2}{d_g + d_h}, \quad (32)$$

and by doing some calculations, we get

$$HI(\xi) = (6n + 4)\left[\frac{1}{2}\right] + (6n - 6)\left[\frac{2}{5}\right] = \frac{2}{5}(n - 1). \quad (33)$$

**Theorem 6.** For the subdivided polythiophene network,  $SPLY_n$ , the general version of the harmonic index is calculated by

$$H_k I(\xi) = \frac{6n\{5^k + 4^k\} + 4\{5^k\} - 6\{4^k\}}{\{10^k\}}. \quad (34)$$

*Proof.* By letting  $\xi$  as a subdivided polythiophene network  $SPLY_n$ , from Table 1, we know

$$H_k I(\xi) = \sum_{gh \in E(\xi)} \left[\frac{2}{d_g + d_h}\right]^k, \quad (35)$$

and by doing some calculations, we get

$$\begin{aligned} H_k I(\xi) &= (6n + 4)\left[\frac{2}{2 + 2}\right]^k + (6n - 6)\left[\frac{2}{2 + 3}\right]^k, \\ &= \frac{6n(5^k + 4^k) + 4(5^k) - 6(4^k)}{(10)^k}. \end{aligned} \quad (36)$$

**Theorem 7.** For the subdivided polythiophene network,  $SPLY_n$ , the atom-bond connectivity index is calculated by

$$ABC(\xi) = 6\sqrt{2}n - \sqrt{2}. \quad (37)$$

*Proof.* By letting  $\xi$  as a subdivided polythiophene network  $SPLY_n$ , from Table 1, we know

$$ABC(\xi) = \sum_{gh \in E(\xi)} \sqrt{\frac{d_g + d_h - 2}{d_g d_h}}, \quad (38)$$

and by doing some calculations, we get

$$\begin{aligned} ABC(\xi) &= (6n + 4)\sqrt{\frac{2 + 2 - 2}{4}} + (6n - 6)\sqrt{\frac{2 + 3 - 2}{6}} \\ &= \sqrt{2}(6n - 1). \end{aligned} \quad (39)$$

**Theorem 8.** For the subdivided polythiophene network,  $SPLY_n$ ,  $SK$ ,  $SK_1$ , and  $SK_2$  indices are calculated by  $SK(\xi) = 27n - 7$ ,  $SK_1(\xi) = 30n - 10$ , and  $SK_2(\xi) = (1/2)(123n - 43)$ , respectively.

*Proof.* By letting  $\xi$  as a subdivided polythiophene network  $SPLY_n$ , from Table 1, we know

$$\begin{aligned}
 SK(\xi) &= \sum_{gh \in E(\xi)} \left[ \frac{d_g + d_h}{2} \right], \\
 SK_1(\xi) &= \sum_{gh \in E(\xi)} \left[ \frac{d_g d_h}{2} \right], \\
 SK_2(\xi) &= \sum_{gh \in E(\xi)} \left[ \frac{d_g + d_h}{2} \right]^2,
 \end{aligned} \tag{40}$$

and by doing some calculations, we get

$$\begin{aligned}
 SK(\xi) &= (6n + 4)(2) + (6n - 6)\left(\frac{5}{2}\right) = 27n - 7, \\
 SK_1(\xi) &= (6n + 4)(2) + (6n - 6)(3) = 30n - 10, \\
 SK_2(\xi) &= (6n + 4)(4) + (6n - 6)\left(\frac{25}{4}\right) = \frac{1}{2}(123n - 43).
 \end{aligned} \tag{41}$$

**Theorem 9.** For the subdivided polythiophene network,  $SPLY_n$ , the sum-connectivity index is calculated by

$$\chi_{-(1/2)}(\xi) = n \left\{ 3 + \frac{6}{\sqrt{5}} \right\} + \left\{ 2 - \frac{6}{\sqrt{5}} \right\}. \tag{42}$$

*Proof.* By letting  $\xi$  as a subdivided polythiophene network  $SPLY_n$ , from Table 1, we know

$$\chi_{-(1/2)}(\xi) = \sum_{gh \in E(\xi)} [d_g + d_h]^{-(1/2)}, \tag{43}$$

$$\chi_{-(1/2)}(\xi) = (6n + 4)\left(\frac{1}{2}\right) + (6n - 6)\left(\frac{1}{\sqrt{5}}\right),$$

and by doing some calculations, we get

$$\chi_{-(1/2)}(\xi) = n \left\{ 3 + \frac{6}{\sqrt{5}} \right\} + \left\{ 2 - \frac{6}{\sqrt{5}} \right\}. \tag{44}$$

**Theorem 10.** For the subdivided polythiophene network,  $SPLY_n$ , the general sum-connectivity index is calculated by

$$\chi_k(\xi) = 6n\{5^k + 4^k\} + 4\{4^k\} - 6\{5^k\}. \tag{45}$$

*Proof.* By letting  $\xi$  as a subdivided polythiophene network  $SPLY_n$ , from Table 1, we know

$$\chi_k(\xi) = \sum_{gh \in E(\xi)} [d_g + d_h]^k, \tag{46}$$

$$\chi_k(\xi) = (6n + 4)(4^k) + (6n - 6)(5^k),$$

and by doing some calculations, we get

$$\chi_k(\xi) = 6n(5^k + 4^k) + 4(4^k) - 6(5^k). \tag{47}$$

**Theorem 11.** For the subdivided polythiophene network,  $SPLY_n$ , the first general Zagreb index is calculated by

$${}^k M_1(\xi) = 9n\{2^k\} + 2n\{3^k\} + 2\left\{\frac{2^k}{2} - 3^k\right\}. \tag{48}$$

*Proof.* By letting  $\xi$  as a subdivided polythiophene network  $SPLY_n$ , from Table 1, we know

$${}^k M_1(\xi) = \sum_{gh \in E(\xi)} [d_g^{k-1} + d_h^{k-1}], \quad k > 1, \tag{49}$$

$${}^k M_1(\xi) = (6n + 4)(2^k) + (6n - 6)(2^{k-1} + 3^{k-1}),$$

and by doing some calculations, we get

$${}^k M_1(\xi) = 9n\{2^k\} + 2n\{3^k\} + 2\left\{\frac{2^k}{2} - 3^k\right\}. \tag{50}$$

**Theorem 12.** For the subdivided polythiophene network,  $SPLY_n$ , the forgotten index is calculated by

$$F(\xi) = 2\{63n - 23\}. \tag{51}$$

*Proof.* By letting  $\xi$  as a subdivided polythiophene network  $SPLY_n$ , from Table 1, we know

$$F(\xi) = \sum_{gh \in E(\xi)} [d_g^2 + d_h^2], \tag{52}$$

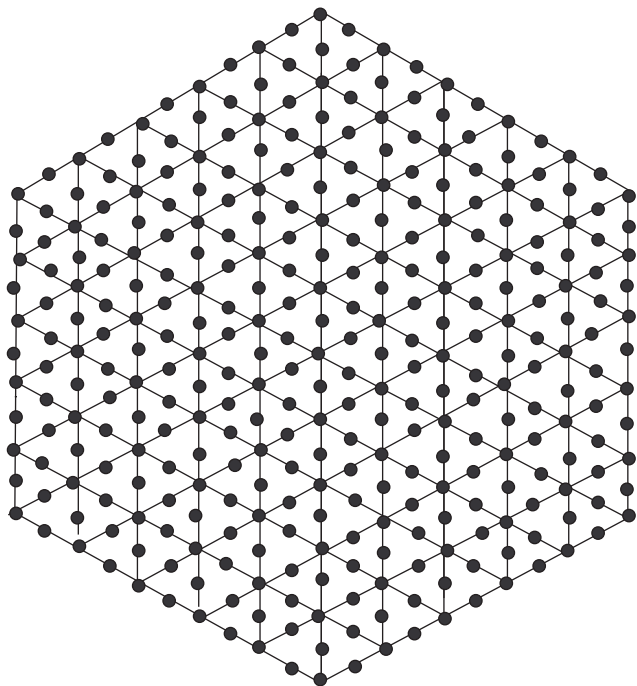
$$F(\xi) = (6n + 4)(8) + (6n - 6)(13),$$

and by doing some calculations, we get

$$F(\xi) = 126n - 46. \tag{53}$$

**2.2. Results for the Subdivided Hexagonal Network.** We construct a subdivided hexagonal network shown in Figure 2 by adding a new vertex in each edge. For this process, a triangular tiling is used. In this way, an  $n$ -dimensional subdivided hexagonal network is obtained and denoted by  $SHX_n$ . A subdivided hexagonal network for  $n = 6$  is shown in Figure 2, whereas  $n$  shows the number of nodes. The order of  $SHX_n$  is  $12n^2 - 18n + 7$  for  $n > 1$ , and the size is  $18n^2 - 30n + 12$  for  $n > 1$ . After the subdivision of this network, we have three types of edges that are (2, 3), (2, 4), and (2, 6). The division of edges is shown in Table 2. A subdivided hexagonal network  $SHX_6$  is displayed in Figure 2.

**Theorem 13.** For the subdivided hexagonal network,  $SHX_n$ , the ordinary generalized geometric-arithmetic index is calculated by

FIGURE 2: SHX<sub>6</sub>.TABLE 2: Division of edges of a graph  $\xi$  found on the degree of terminating nodes of each of the edges.

$(d_g, d_h)$ for $gh \in E(\xi)$	Number of $E(\xi)$
(2, 3)	18
(2, 4)	$24(n-2)$
(2, 6)	$6(3n^2 - 9n + 7)$

$$\begin{aligned} \text{OGA}_k(\xi) &= 18n^2 \left\{ \frac{\sqrt{48}}{8} \right\}^k + n \left[ 24 \left\{ \frac{\sqrt{32}}{6} \right\}^k - 54 \left\{ \frac{\sqrt{48}}{8} \right\}^k \right] \\ &+ \left[ 42 \left\{ \frac{\sqrt{48}}{8} \right\}^k - 48 \left\{ \frac{\sqrt{32}}{6} \right\}^k \right]. \end{aligned} \quad (54)$$

*Proof.* By letting 1 as a subdivided hexagonal network SHX<sub>n</sub>, from Table 2, we know

$$\begin{aligned} \text{OGA}_k(\xi) &= \sum_{gh \in E(\xi)} \left[ \frac{\sqrt{4d_g d_h}}{d_g + d_h} \right]^k, \\ \text{OGA}_k(\xi) &= (18) \left[ \frac{\sqrt{24}}{5} \right]^k + 24(n-2) \left[ \frac{\sqrt{32}}{6} \right]^k \\ &+ 6(3n^2 - 9n + 7) \left[ \frac{\sqrt{48}}{8} \right]^k, \end{aligned} \quad (55)$$

and by doing some calculations, we get

$$\begin{aligned} \text{OGA}_k(\xi) &= 18n^2 \left\{ \frac{\sqrt{48}}{8} \right\}^k + n \left[ 24 \left\{ \frac{\sqrt{32}}{6} \right\}^k - 54 \left\{ \frac{\sqrt{48}}{8} \right\}^k \right] \\ &+ \left[ 42 \left\{ \frac{\sqrt{48}}{8} \right\}^k - 48 \left\{ \frac{\sqrt{32}}{6} \right\}^k \right]. \end{aligned} \quad (56)$$

**Theorem 14.** For the subdivided hexagonal network, SHX<sub>n</sub>, the first and second Gourava indices are calculated by

$$\begin{aligned} \text{GO}_1(\xi) &= 360n^2 - 744n + 366, \\ \text{GO}_2(\xi) &= 1728n^2 - 4032n + 2268. \end{aligned} \quad (57)$$

*Proof.* By letting  $\xi$  as a subdivided hexagonal network SHX<sub>n</sub>, from Table 2, we know

$$\begin{aligned} \text{GO}_1(\xi) &= \sum_{gh \in E(\xi)} [(d_g + d_h) + (d_g d_h)], \\ \text{GO}_2(\xi) &= \sum_{gh \in E(\xi)} [(d_g + d_h) + (d_g d_h)], \end{aligned} \quad (58)$$

and by doing some calculations, we get

$$\begin{aligned} \text{GO}_1(\xi) &= (18)[(5) + (6)] + 24(n-2)[(6) + (8)] \\ &+ 6(3n^2 - 9n + 7)[(8) + (12)] \\ &= 360n^2 - 744n + 366, \\ \text{GO}_2(\xi) &= (18)[30] + 24(n-2)[48] \\ &+ 6(3n^2 - 9n + 7)[96], \\ &= 1728n^2 - 4032n + 2268. \end{aligned} \quad (59)$$

**Theorem 15.** For the subdivided hexagonal network, SHX<sub>n</sub>, the first and second hyper-Gourava indices are calculated by  $\text{HGO}_1(\xi) = 7200n^2 - 16896n + 9570$  and  $\text{HGO}_2(\xi) = 165888n^2 - 442368n + 292680$ .

*Proof.* By letting  $\xi$  as a subdivided hexagonal network SHX<sub>n</sub>, from Table 2, we know

$$\begin{aligned} \text{HGO}_1(\xi) &= \sum_{gh \in E(\xi)} [(d_g + d_h) + (d_g d_h)]^2, \\ \text{HGO}_2(\xi) &= \sum_{gh \in E(\xi)} [(d_g + d_h) + (d_g d_h)]^2, \end{aligned} \quad (60)$$

and by doing some calculations, we get

$$\begin{aligned} \text{HGO}_1(\xi) &= (18)[121] + 24(n-2)[196] \\ &+ 6(3n^2 - 9n + 7)[400] \\ &= 7200n^2 - 16896n + 9570, \\ \text{HGO}_2(\xi) &= (18)[900] + 24(n-2)[2304] \\ &+ 6(3n^2 - 9n + 7)[9216], \\ &= 165888n^2 - 442368n + 292680. \end{aligned} \quad (61)$$

**Theorem 16.** For the subdivided hexagonal network,  $SHX_n$ ,  $n > 1$ , the general Randić' index is calculated by

$$R_\gamma(SHX_n) = \begin{cases} \frac{3n^2 - 3n + 1}{2}, & \text{for } \gamma = -1, \\ 3n^2\sqrt{3} + n\{\sqrt{72} - 9\sqrt{3}\} + 2.501, & \text{for } \gamma = \frac{1}{2}, \\ 62.35n^2 - 119.17n + 53.82, & \text{for } \gamma = \frac{1}{2}, \\ 216n^2 - 456n + 228, & \text{for } \gamma = 1. \end{cases} \quad (62)$$

*Proof.* By letting  $\xi$  as a subdivided hexagonal network  $SHX_n$  of  $n$  dimensions, we have the number of nodes and edges in  $SHX_n$  as  $|V(SHX_n)| = 12n^2 - 18n + 7$  for  $n > 1$  and  $|E(SHX_n)| = 18n^2 - 30n + 12$  for  $n > 1$ , respectively. We know that

$$R_\gamma(\xi) = \sum_{gh \in E(\xi)} (d_g \cdot d_h)^\gamma, \quad (63)$$

for  $\gamma = \{-1, 1, -1/2, 1/2\}$ .

Case 1: if  $\gamma = -1$ , the application of Randić' index  $R_\gamma(\xi)$

$$R_{-1}(\xi) = \sum_{gh \in E(\xi)} \frac{1}{d_g d_h}, \quad (64)$$

using (63). From Table 2, we know

$$R_{-1}(\xi) = (18)(6)^{-1} + 24(n-2)(8)^{-1} + 6(3n^2 - 9n + 7)(12)^{-1}. \quad (65)$$

By doing some calculations, we get  $R_{-1}(\xi) = (3n^2 - 3n + 1/2)$ .

Case 2: if  $\gamma = -1/2$ , the application of Randić' index  $R_\gamma(\xi)$

$$R_{-1/2}(\xi) = \sum_{gh \in E(\xi)} \frac{1}{\sqrt{(d_g \cdot d_h)}}, \quad (66)$$

using (63),

$$R_{-1/2}(\xi) = (18)\frac{1}{\sqrt{6}} + 24(n-2)\frac{1}{\sqrt{8}} + 6(3n^2 - 9n + 7)\frac{1}{\sqrt{12}}. \quad (67)$$

By doing some calculations, we get

$$R_{-1/2}(\xi) = 3n^2\sqrt{3} + n\{\sqrt{72} - 9\sqrt{3}\} + 2.501. \quad (68)$$

Case 3: if  $\gamma = 1/2$ , the application of Randić' index  $R_\gamma(\xi)$

$$R_{1/2}(\xi) = \sum_{gh \in E(\xi)} \sqrt{d_g \cdot d_h}, \quad (69)$$

using (63),

$$R_{1/2}(\xi) = (18)\sqrt{6} + 24(n-2)\sqrt{8} + 6(3n^2 - 9n + 7)\sqrt{12}. \quad (70)$$

By doing some calculations, we get

$$R_{1/2}(\xi) = 62.35n^2 - 119.17n + 53.82. \quad (71)$$

Case 4: if  $\gamma = 1$ , the application of Randić' index  $R_\gamma(\xi)$

$$R_1(\xi) = \sum_{gh \in E(\xi)} (d_g \cdot d_h)^1, \quad (72)$$

using (63),

$$R_1(\xi) = (18)(6) + 24(n-2)(8) + 6(3n^2 - 9n + 7)(12). \quad (73)$$

By doing some calculations, we get

$$R_1(\xi) = 216n^2 - 456n + 228. \quad (74)$$

**Theorem 17.** For the subdivided hexagonal network,  $SHX_n$ , the harmonic index is calculated by

$$HI(\xi) = 4.5n^2 - 5.5n + 1.7. \quad (75)$$

*Proof.* By letting  $\xi$  as a subdivided hexagonal network  $SHX_n$ , from Table 2, we know

$$HI(\xi) = \sum_{gh \in E(\xi)} \frac{2}{d_g + d_h}. \quad (76)$$

By doing some calculations, we get

$$HI(\xi) = (18)\left[\frac{2}{5}\right] + 24(n-2)\left[\frac{2}{6}\right] + 6(3n^2 - 9n + 7)\left[\frac{2}{8}\right], \\ = \frac{1}{10}(45n^2 - 55n + 17) = 4.5n^2 - 5.5n + 1.7. \quad (77)$$

**Theorem 18.** For the subdivided hexagonal network,  $SHX_n$ , the general version of the harmonic index is calculated by

$$H_k I(\xi) = 18n^2\{4^{-k}\} + 2n\{12\{3^{-k}\} - 27\{4^{-k}\}\} \\ + [18\{2^k\{5^{-k}\}\} - 48\{3^{-k}\} + 42\{4^{-k}\}]. \quad (78)$$

*Proof.* By letting  $\xi$  as a subdivided hexagonal network  $SHX_n$ , from Table 2, we know

$$H_k I(\xi) = \sum_{gh \in E(\xi)} \left[\frac{2}{d_g + d_h}\right]^k. \quad (79)$$

By doing some calculations, we get



$$\begin{aligned}
H_k I(\xi) &= (18) \left[ \frac{2}{2+3} \right]^k + 24(n-2) \left[ \frac{2}{2+4} \right]^k \\
&\quad + 6(3n^2 - 9n + 7) \left[ \frac{2}{2+6} \right]^k \\
&= n^2 \left( \frac{18}{4^k} \right) + n \left( \frac{24}{3^k} - \frac{54}{4^k} \right) + \left( 18 \left( \frac{2^k}{5^k} \right) - \frac{48}{3^k} + \frac{42}{4^k} \right) \\
&= 18n^2 \{4^{-k}\} + 2n \{12\{3^{-k}\} - 27\{4^{-k}\}\} \\
&\quad + [18\{2^k\{5^{-k}\}\} - 48\{3^{-k}\} + 42\{4^{-k}\}].
\end{aligned} \tag{80}$$

**Theorem 19.** For the subdivided hexagonal network,  $SHX_m$ , the atom-bond connectivity index is calculated by

$$ABC(\xi) = 9\sqrt{2}n^2 - 15\sqrt{2}n + 6\sqrt{2}. \tag{81}$$

*Proof.* By letting  $\xi$  as a subdivided hexagonal network  $SHX_m$ , from Table 2, we know

$$ABC(\xi) = \sum_{gh \in E(\xi)} \sqrt{\frac{d_g + d_h - 2}{d_g d_h}}, \tag{82}$$

and by doing some calculations, we get

$$\begin{aligned}
ABC(\xi) &= (18) \sqrt{\frac{2+3-2}{6}} + 24(n-2) \sqrt{\frac{2+4-2}{8}} \\
&\quad + 6(3n^2 - 9n + 7) \sqrt{\frac{2+6-2}{12}} \\
&= 9\sqrt{2}n^2 - 15\sqrt{2}n + 6\sqrt{2}.
\end{aligned} \tag{83}$$

**Theorem 20.** For the subdivided hexagonal network,  $SHX_m$ ,  $SK$ ,  $SK_1$ , and  $SK_2$  indices are calculated by  $SK(\xi) = 72n^2 - 144n + 69$ ,  $SK_1(\xi) = 108n^2 - 228n + 498$ , and  $SK_2(\xi) = 288n^2 - 648n + 7052$ , respectively.

*Proof.* By letting  $\xi$  as a subdivided hexagonal network  $SHX_m$ , from Table 2, we know

$$\begin{aligned}
SK(\xi) &= \sum_{gh \in E(\xi)} \left[ \frac{d_g + d_h}{2} \right], \\
SK_1(\xi) &= \sum_{gh \in E(\xi)} \left[ \frac{d_g d_h}{2} \right], \\
SK_2(\xi) &= \sum_{gh \in E(\xi)} \left[ \frac{d_g + d_h}{2} \right]^2,
\end{aligned} \tag{84}$$

and by doing some calculations, we get

$$\begin{aligned}
SK(\xi) &= (18) \left( \frac{5}{2} \right) + 24(n-2) \left( \frac{6}{2} \right) + 6(3n^2 - 9n + 7) \left( \frac{8}{2} \right) \\
&= 72n^2 - 144n + 69.
\end{aligned}$$

$$\begin{aligned}
SK_1(\xi) &= 18(3) + 24(n-2)(4) + 36(3n^2 - 9n + 7) \\
&= 108n^2 - 228n + 498.
\end{aligned}$$

$$\begin{aligned}
SK_2(\xi) &= (18) \left( \frac{25}{4} \right) + 24(n-2)(9) + 6(3n^2 - 9n + 7)(16) \\
&= 288n^2 - 648n + \frac{705}{2}.
\end{aligned}$$

(85)

**Theorem 21.** For the subdivided hexagonal network,  $SHX_m$ , the sum-connectivity index is calculated by

$$\chi_{-(1/2)}(\xi) = 18n^2 \left\{ \frac{1}{\sqrt{8}} \right\} + n \left\{ \frac{24}{\sqrt{6}} - \frac{54}{\sqrt{8}} \right\} + \left\{ \frac{18}{\sqrt{5}} - \frac{48}{\sqrt{6}} + \frac{42}{\sqrt{8}} \right\}. \tag{86}$$

*Proof.* By letting  $\xi$  as a subdivided hexagonal network  $SHX_m$ , from Table 2, we know

$$\begin{aligned}
\chi_{-(1/2)}(\xi) &= \sum_{gh \in E(\xi)} [d_g + d_h]^{-1/2}, \\
\chi_{-(1/2)}(\xi) &= (18) \left( \frac{1}{\sqrt{6}} \right) + 24(n-2) \left( \frac{1}{\sqrt{8}} \right) \\
&\quad + 6(3n^2 - 9n + 7) \left( \frac{1}{\sqrt{12}} \right),
\end{aligned} \tag{87}$$

and by doing some calculations, we get

$$\begin{aligned}
\chi_{-(1/2)}(\xi) &= n^2 \left( \frac{18}{\sqrt{8}} \right) + n \left( \frac{24}{\sqrt{6}} - \frac{54}{\sqrt{8}} \right) + \left( \frac{18}{\sqrt{5}} - \frac{48}{\sqrt{6}} + \frac{42}{\sqrt{8}} \right) \\
&= 18n^2 \left( \frac{1}{\sqrt{8}} \right) + n \left( \frac{24}{\sqrt{6}} - \frac{54}{\sqrt{8}} \right) + \left( \frac{18}{\sqrt{5}} - \frac{48}{\sqrt{6}} + \frac{42}{\sqrt{8}} \right).
\end{aligned} \tag{88}$$

**Theorem 22.** For the subdivided hexagonal network,  $SHX_m$ , the general sum-connectivity index is calculated by

$$\begin{aligned}
\chi_k(\xi) &= 18n^2 \{8^k\} + n \{24(6^k) - 54(8^k)\} \\
&\quad + \{18(5^k) - 48(6^k) + 42(8^k)\}.
\end{aligned} \tag{89}$$

*Proof.* By letting  $\xi$  as a subdivided hexagonal network  $SHX_m$ , from Table 2, we know

$$\begin{aligned}\chi_k(\xi) &= \sum_{gh \in E(\xi)} [d_g + d_h]^k, \\ \chi_k(\xi) &= (18)(5^k) + 24(n-2)(6^k) + 6(3n^2 - 9n + 7)(8^k),\end{aligned}\quad (90)$$

and by doing some calculations, we get

$$\begin{aligned}\chi_k(\xi) &= 18n^2\{8^k\} + n\{24(6^k) - 54(8^k)\} \\ &+ \{18(5^k) - 48(6^k) + 42(8^k)\}.\end{aligned}\quad (91)$$

**Theorem 23.** For the subdivided hexagonal network,  $SHX_n$ , the first general Zagreb index is calculated by

$$\begin{aligned}{}^k M_1(\xi) &= n^2\{\{3\{6^k\}\} + 9\{2^k\}\} + n\{6\{4^k\} - 15\{2^k\} \\ &- 9\{6^k\}\} + \{6\{2^k\} + 6\{3^k\} - 12\{4^k\} + 7\{6^k\}\}.\end{aligned}\quad (92)$$

*Proof.* By letting  $\xi$  as a subdivided hexagonal network  $SHX_n$ , from Table 2, we know

$$\begin{aligned}{}^k M_1(\xi) &= \sum_{gh \in E(\xi)} [d_g^{k-1} + d_h^{k-1}], \quad k > 1, \\ {}^k M_1(\xi) &= \{18\}\left(\frac{2^k}{2} + \frac{3^k}{3}\right) + \{24n - 48\}\left(\frac{2^k}{2} + \frac{4^k}{4}\right) \\ &+ 6(3n^2 - 9n + 7)(2^{k-1} + 6^{k-1}),\end{aligned}\quad (93)$$

and by doing some calculations, we get

$$\begin{aligned}{}^k M_1(\xi) &= n^2\{36^k + 92^k\} + n64^k - 152^k - 96^k \\ &+ \{62^k + 63^k - 124^k + 76^k\}.\end{aligned}\quad (94)$$

**Theorem 24.** For the subdivided hexagonal network,  $SHX_n$ , the forgotten index is calculated by

$$F(\xi) = 2\{360n^2 - 840n + 477\}.\quad (95)$$

*Proof.* By letting  $\xi$  as a subdivided hexagonal network  $SHX_n$ , from Table 2, we know

$$\begin{aligned}F(\xi) &= \sum_{gh \in E(\xi)} [d_g^2 + d_h^2], \\ F(\xi) &= (18)(13) + 24(n-2)(20) + 6(3n^2 - 9n + 7)(40),\end{aligned}\quad (96)$$

and by doing some calculations, we get

$$F(\xi) = 2\{360n^2 - 840n + 477\}.\quad (97)$$

**2.3. Results for the Subdivided Backbone DNA Network.** The structure of DNA is called a double helix as it is made of two strands that wind around each other that looks like a

staircase [40]. Each strand has a backbone made of deoxyribose, sugar, and a phosphate group. These sugar and phosphates make up the backbone, while the nitrogen bases are found in the centre and hold the two strands together. There are 4 bases attached to each sugar which are adenine, cytosine, guanine, and thymine. Both ends of DNA have a number, i.e., one end is '5 and the other is '3. In a subdivided backbone DNA network, shown in Figure 3, we insert another node (degree 2) in each edge of  $\xi$ . In this way, we get a subdivided backbone DNA network of  $n$  dimensions. A subdivided backbone DNA network for  $n = 4$  is displayed in Figure 3. A subdivided backbone DNA network is symbolized as  $SBB_{DNA}(n)$ . The order and size of  $SBB_{DNA}(n)$  are  $15n - 5$  and  $16n - 6$ , respectively. We obtain two types of edges (degree based) that are (2, 2) and (2, 3). Table 3 gives us two kinds of edges. A subdivided backbone DNA network  $SBB_{DNA}(4)$  is shown in Figure 3.

**Theorem 25.** For the subdivided backbone DNA network,  $SBB_{DNA}(n)$ , the ordinary generalized geometric-arithmetic index is calculated by

$$OGA_k(\xi) = 2 \left\{ n \left[ 5 + 3 \left\{ \frac{\sqrt{24}}{5} \right\}^k \right] - 3 \left\{ \frac{\sqrt{24}}{5} \right\}^k \right\}.\quad (98)$$

*Proof.* By letting  $\xi$  as a subdivided backbone DNA network  $SBB_{DNA}(n)$ , from Table 3, we know

$$OGA_k(\xi) = \sum_{gh \in E(\xi)} \left[ \frac{\sqrt{4d_g d_h}}{d_g + d_h} \right]^k,\quad (99)$$

$$OGA_k(\xi) = 10n \left[ \frac{\sqrt{16}}{2+2} \right]^k + (6n-6) \left[ \frac{\sqrt{24}}{5} \right]^k,$$

and by doing some calculations, we get

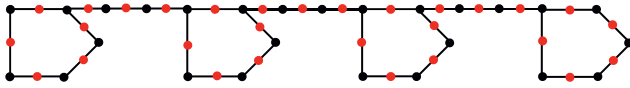
$$OGA_k(\xi) = 2 \left\{ n \left[ 5 + 3 \left\{ \frac{\sqrt{24}}{5} \right\}^k \right] - 3 \left\{ \frac{\sqrt{24}}{5} \right\}^k \right\}.\quad (100)$$

**Theorem 26.** For the subdivided backbone DNA network,  $SBB_{DNA}(n)$ , the first and second Gourava indices are calculated by  $GO_1(\xi) = 146n - 66$  and  $GO_2(\xi) = 340n - 180$ .

*Proof.* By letting  $\xi$  as a subdivided backbone DNA network  $SBB_{DNA}(n)$ , from Table 3, we know

$$\begin{aligned}GO_1(\xi) &= \sum_{gh \in E(\xi)} [(d_g + d_h) + (d_g d_h)], \\ GO_2(\xi) &= \sum_{gh \in E(\xi)} [(d_g + d_h) + (d_g d_h)],\end{aligned}\quad (101)$$

and by doing some calculations, we get

FIGURE 3:  $SBB_{DNA}(4)$ .TABLE 3: Division of edges of a graph  $\xi$  found on the degree of terminating nodes of each of the edges.

$(d_g, d_h)$ for $gh \in E(\xi)$	Number of $E(\xi)$
(2, 2)	10n
(2, 3)	6(n-1)

$$GO_1(\xi) = 10n[(4) + (4)] + (6n - 6)[(5) + (6)] = 146n - 66,$$

$$GO_2(\xi) = 10n[16] + (6n - 6)[30] = 340n - 180.$$

(102)

**Theorem 27.** For the subdivided backbone DNA network,  $SBB_{DNA}(n)$ , the first and second hyper-Gourava indices are calculated by

$$\begin{aligned} HGO_1(\xi) &= 1366n - 726, \\ HGO_2(\xi) &= 7960n - 5400. \end{aligned} \quad (103)$$

*Proof.* By letting  $\xi$  as a subdivided backbone DNA network  $SBB_{DNA}(n)$ , from Table 3, we know

$$\begin{aligned} HGO_1(\xi) &= \sum_{gh \in E(\xi)} [(d_g + d_h) + (d_g d_h)]^2, \\ HGO_2(\xi) &= \sum_{gh \in E(\xi)} [(d_g + d_h) + (d_g d_h)]^2, \end{aligned} \quad (104)$$

and by doing some calculations, we get

$$\begin{aligned} HGO_1(\xi) &= 10n[64] + (6n - 6)[121] = 1366n - 726, \\ HGO_2(\xi) &= 10n[256] + (6n - 6)[900] = 7960n - 5400. \end{aligned} \quad (105)$$

**Theorem 28.** For the subdivided backbone DNA network,  $SBB_{DNA}(n)$ , the general Randić' index is calculated by

$$R_\gamma(SBB_{DNA}(n)) = \begin{cases} \frac{7}{2}n - 1, & \text{for } \gamma = -1, \\ n\left\{\frac{149}{20}\right\} - \left\{\frac{49}{20}\right\}, & \text{for } \gamma = -\frac{1}{2}, \\ n\left\{\frac{347}{10}\right\} - \left\{\frac{147}{10}\right\}, & \text{for } \gamma = \frac{1}{2}, \\ 76n - 36, & \text{for } \gamma = 1. \end{cases} \quad (106)$$

*Proof.* By letting  $\xi$  as a subdivided backbone DNA network  $SBB_{DNA}(n)$  of  $n$  dimensions, we have the order and size of  $\xi$  in  $SBB_{DNA}(n)$  as  $|V(SBB_{DNA}(n))| = 15n - 5$  and  $|E(SBB_{DNA}(n))| = 16n - 6$ , respectively.

We know that

$$R_\gamma(\xi) = \sum_{gh \in E(\xi)} (d_g \cdot d_h)^\gamma, \quad (107)$$

for  $\gamma = \{-1, 1, -1/2, 1/2\}$ .

Case 1: if  $\gamma = -1$ , the application of Randić' index  $R_\gamma(\xi)$

$$R_{-1}(\xi) = \sum_{gh \in E(\xi)} \frac{1}{d_g d_h}, \quad (108)$$

using (107). From Table 3, we know  $R_{-1}(\xi) = 10n(4)^{-1} + (6n - 6)(6)^{-1}$ . By doing some calculations, we get  $R_{-1}(\xi) = (7/2)n - 1$ .

Case 2: if  $\gamma = -(1/2)$ , the application of Randić' index  $R_\gamma(\xi)$

$$R_{-(1/2)}(\xi) = \sum_{gh \in E(\xi)} \frac{1}{\sqrt{(d_g \cdot d_h)}}, \quad (109)$$

using (107),

$$R_{-(1/2)}(\xi) = 10n \frac{1}{\sqrt{4}} + (6n - 6) \frac{1}{\sqrt{6}}, \quad (110)$$

and by doing some calculations, we get  $R_{-(1/2)}(\xi) = n(149/20) - (49/20)$ .

Case 3: if  $\gamma = (1/2)$ , the application of Randić' index  $R_\gamma(\xi)$

$$R_{(1/2)}(\xi) = \sum_{gh \in E(\xi)} \sqrt{d_g \cdot d_h}, \quad (111)$$

using (107),

$$R_{(1/2)}(\xi) = 10n\sqrt{4} + (6n - 6)\sqrt{6}, \quad (112)$$

and by doing some calculations, we get  $R_{(1/2)}(\xi) = n(347/10) - (147/10)$ .

Case 4: if  $\gamma = 1$ , the application of Randić' index  $R_\gamma(\xi)$

$$R_1(\xi) = \sum_{gh \in E(\xi)} (d_g \cdot d_h)^1, \quad (113)$$

using (107),

$$R_1(\xi) = 10n(4) + (6n - 6)(6), \quad (114)$$

and by doing some calculations, we get  $R_1(\xi) = 76n - 36$ .

**Theorem 29.** For the subdivided backbone DNA network,  $SBB_{DNA}(n)$ , the harmonic index is calculated by

$$HI(\xi) = \frac{37n - 12}{5}. \quad (115)$$

*Proof.* By letting  $\xi$  as a subdivided backbone DNA network  $SBB_{DNA}(n)$ , from Table 3, we know

$$HI(\xi) = \sum_{gh \in E(\xi)} \frac{2}{d_g + d_h}, \quad (116)$$

and by doing some calculations, we get

$$HI(\xi) = 10n \left[ \frac{1}{2} \right] + (6n - 6) \left[ \frac{2}{5} \right] = \frac{37n - 12}{5}. \quad (117)$$

**Theorem 30.** For the subdivided backbone DNA network,  $SBB_{DNA}(n)$ , the general version of the harmonic index is calculated by

$$H_k I(\xi) = 2n \left\{ \frac{5}{2^k} + \frac{3}{5^k} 2^k \right\} - \frac{6}{5^k} 2^k. \quad (118)$$

*Proof.* By letting  $\xi$  as a subdivided backbone DNA network  $SBB_{DNA}(n)$ , from Table 3, we know

$$H_k I(\xi) = \sum_{gh \in E(\xi)} \left[ \frac{2}{d_g + d_h} \right]^k, \quad (119)$$

and by doing some calculations, we get

$$\begin{aligned} H_k I(\xi) &= 10n \left[ \frac{2}{2+2} \right]^k + (6n - 6) \left[ \frac{2}{2+3} \right]^k \\ &= 2n \left\{ \frac{5}{2^k} + \frac{3}{5^k} 2^k \right\} - \frac{6}{5^k} 2^k. \end{aligned} \quad (120)$$

**Theorem 31.** For the subdivided backbone DNA network,  $SBB_{DNA}(n)$ , the atom-bond connectivity index is calculated by

$$ABC(\xi) = \frac{2\{8n - 3\}}{\sqrt{2}}. \quad (121)$$

*Proof.* By letting  $\xi$  as a subdivided backbone DNA network  $SBB_{DNA}(n)$ , from Table 3, we know

$$ABC(\xi) = \sum_{gh \in E(\xi)} \sqrt{\frac{d_g + d_h - 2}{d_g d_h}}. \quad (122)$$

By doing some calculations, we get

$$ABC(\xi) = 10n \sqrt{\frac{2+2-2}{4}} + (6n - 6) \sqrt{\frac{2+3-2}{6}} = \frac{2\{8n - 3\}}{\sqrt{2}}. \quad (123)$$

**Theorem 32.** For the subdivided backbone DNA network,  $SBB_{DNA}(n)$ ,  $SK$ ,  $SK_1$ , and  $SK_2$  indices are calculated by  $SK(\xi) = 35n - 15$ ,  $SK_1(\xi) = 38n - 18$ , and  $SK_2(\xi) = (1/2)(155n - 75)$ , respectively.

*Proof.* By letting  $\xi$  as a subdivided backbone DNA network  $SBB_{DNA}(n)$ , from Table 3, we know

$$SK(\xi) = \sum_{gh \in E(\xi)} \left[ \frac{d_g + d_h}{2} \right],$$

$$SK_1(\xi) = \sum_{gh \in E(\xi)} \left[ \frac{d_g d_h}{2} \right], \quad (124)$$

$$SK_2(\xi) = \sum_{gh \in E(\xi)} \left[ \frac{d_g + d_h}{2} \right]^2.$$

By doing some calculations, we get

$$SK(\xi) = 10n(2) + (6n - 6) \left( \frac{5}{2} \right) = 35n - 15,$$

$$SK_1(\xi) = 10n(2) + (6n - 6)(3) = 38n - 18, \quad (125)$$

$$SK_2(\xi) = 10n(4) + (6n - 6) \left( \frac{25}{4} \right) = \frac{1}{2}(155n - 75).$$

**Theorem 33.** For the subdivided backbone DNA network,  $SBB_{DNA}(n)$ , the sum-connectivity index is calculated by

$$\chi_{-(1/2)}(\xi) = n \left\{ 5 + \frac{6}{\sqrt{5}} \right\} - \frac{6}{\sqrt{5}}. \quad (126)$$

*Proof.* By letting  $\xi$  as a subdivided backbone DNA network  $SBB_{DNA}(n)$ , from Table 3, we know

$$\chi_{-(1/2)}(\xi) = \sum_{gh \in E(\xi)} [d_g + d_h]^{-(1/2)}, \quad (127)$$

$$\chi_{-(1/2)}(\xi) = 10n \left( \frac{1}{2} \right) + (6n - 6) \left( \frac{1}{\sqrt{5}} \right).$$

By doing some calculations, we get

$$\chi_{-(1/2)}(\xi) = n \left\{ 5 + \frac{6}{\sqrt{5}} \right\} - \frac{6}{\sqrt{5}}. \quad (128)$$

**Theorem 34.** For the subdivided backbone DNA network,  $SBB_{DNA}(n)$ , the general sum-connectivity index is calculated by

$$\chi_k(\xi) = n \{ 10 \{ 4^k \} + 6 \{ 5^k \} \} - 6 \{ 5^k \}. \quad (129)$$

*Proof.* By letting  $\xi$  as a subdivided backbone DNA network  $SBB_{DNA}(n)$ , from Table 3, we know

$$\chi_k(\xi) = \sum_{gh \in E(\xi)} [d_g + d_h]^k, \quad (130)$$

$$\chi_k(\xi) = 10n(4^k) + (6n - 6)(5^k).$$

By doing some calculations, we get

$$\chi_k(\xi) = n \{ 10 \{ 4^k \} + 6 \{ 5^k \} \} - 6 \{ 5^k \}. \quad (131)$$

**Theorem 35.** For the subdivided backbone DNA network,  $SBB_{DNA}(n)$ , the first general Zagreb index is calculated by

$${}^k M_1(\xi) = n\{10\{2^k\} + 3\{2^k\} + 2\{3^k\}\} - \{3\{2^k\} + 2\{3^k\}\}. \quad (132)$$

*Proof.* By letting  $\xi$  as a subdivided backbone DNA network  $SBB_{DNA}(n)$ , from Table 3, we know

$${}^k M_1(\xi) = \sum_{gh \in E(\xi)} [d_g^{k-1} + d_h^{k-1}], \quad k > 1, \quad (133)$$

$${}^k M_1(\xi) = 10n(2^k) + (6n - 6)(2^{k-1} + 3^{k-1}),$$

and by doing some calculations, we get

$${}^k M_1(\xi) = n\{10\{2^k\} + 3\{2^k\} + 2\{3^k\}\} - \{3\{2^k\} + 2\{3^k\}\}. \quad (134)$$

**Theorem 36.** For the subdivided backbone DNA network,  $SBB_{DNA}(n)$ , the forgotten index is calculated by

$$F(\xi) = 2\{79n - 39\}. \quad (135)$$

*Proof.* By letting  $\xi$  as a subdivided backbone DNA network  $SBB_{DNA}(n)$ , from Table 3, we know

$$F(\xi) = \sum_{gh \in E(\xi)} [d_g^2 + d_h^2], \quad (136)$$

$$F(\xi) = 10n(8) + (6n - 6)(13),$$

and by doing some calculations, we get

$$F(\xi) = 2\{79n - 39\}. \quad (137)$$

**2.4. Results for the Subdivided Honeycomb Network.** The honeycomb network is a hexagon. It can be made in different methods. The first honeycomb network is symbolized by  $HC_{(1)}$ . The next honeycomb network is produced by attaching more hexagons to each of its edges. This newly formed honeycomb network is symbolized by  $HC_{(2)}$ ; similarly, the next honeycomb network is produced by attaching more hexagons to each of its edges. In this way, the newly formed honeycomb network is denoted by  $HC_{(3)}$ . By repeating this process, we finally obtain a honeycomb network of  $n$  dimensions and denote by  $HC_{(n)}$ . The honeycomb network is being used in computer graphics, image processing, and cellular phone base stations; moreover, it is used in chemistry for the representation of benzenoid hydrocarbons. To get the subdivided honeycomb network shown in Figure 4, we insert a new node on each of its edges. The  $n$ -dimensional subdivided honeycomb network is symbolized by  $SHC_n$ . A subdivided honeycomb network for  $n=4$  is displayed in Figure 4. The number of nodes and edges in the subdivided honeycomb networks are  $15n^2 - 3n$  and  $18n^2 - 6n$ , respectively. We have obtained two different types of edges in  $SHC_4$  shown in Table 4, whereas Figure 4 shows  $SHC_4$ .

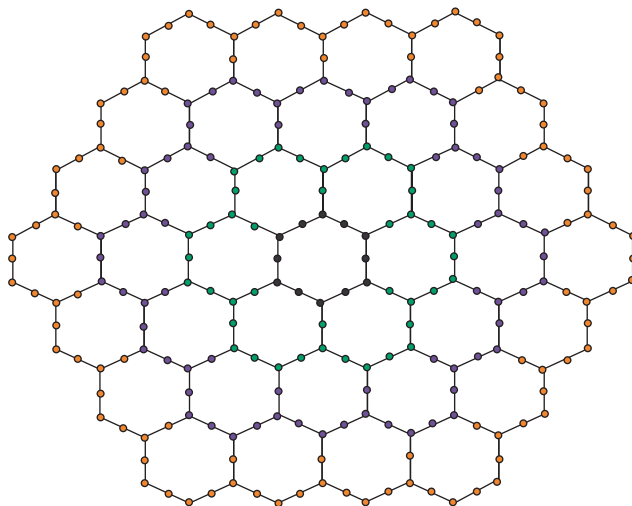


FIGURE 4: 4-dimensional  $SHC_4$ .

TABLE 4: Division of edges of a graph  $\xi$  found on the degree of terminating nodes of each of the edges.

$(d_g, d_h)$ for $gh \in E(\xi)$	Number of $E(\xi)$
(2, 2)	$12n$
(2, 3)	$18n(n - 1)$

**Theorem 37.** For the subdivided honeycomb network,  $SHC_n$ , the ordinary generalized geometric-arithmetic index is calculated by

$$OGA_k(\xi) = 6 \left[ 3n^2 \left\{ \frac{\sqrt{24}}{5} \right\}^k + n \left\{ 2 - 3 \left\{ \frac{\sqrt{24}}{5} \right\}^k \right\} \right]. \quad (138)$$

*Proof.* By letting  $\xi$  as a subdivided honeycomb network  $SHC_n$ , from Table 4, we know

$$OGA_k(\xi) = \sum_{gh \in E(\xi)} \left[ \frac{\sqrt{4d_g d_h}}{d_g + d_h} \right]^k, \quad (139)$$

$$OGA_k(\xi) = (12n) \left[ \frac{\sqrt{16}}{2+2} \right]^k + 18n(n-1) \left[ \frac{\sqrt{24}}{5} \right]^k,$$

and by doing some calculations, we get

$$OGA_k(\xi) = 6 \left[ 3n^2 \left\{ \frac{\sqrt{24}}{5} \right\}^k + n \left\{ 2 - 3 \left\{ \frac{\sqrt{24}}{5} \right\}^k \right\} \right]. \quad (140)$$

**Theorem 38.** For the subdivided honeycomb network,  $SHC_n$ , the first and second Gourava indices are calculated by  $GO_1(\xi) = 198n^2 - 102n$  and  $GO_2(\xi) = 540n^2 - 492n$ .

*Proof.* By letting  $\xi$  as a subdivided honeycomb network  $SHC_n$ , from Table 4, we know

$$\begin{aligned} GO_1(\xi) &= \sum_{gh \in E(\xi)} [(d_g + d_h) + (d_g d_h)], \\ GO_2(\xi) &= \sum_{gh \in E(\xi)} [(d_g + d_h) + (d_g d_h)], \end{aligned} \quad (141)$$

and by doing some calculations, we get

$$\begin{aligned} GO_1(\xi) &= (12n)[(4) + (4)] + 18n(n-1)[(5) + (6)] \\ &= 198n^2 - 102n, \\ GO_2(\xi) &= (12n)[16] + 18n(n-1)[30] = 540n^2 - 492n. \end{aligned} \quad (142)$$

**Theorem 39.** For the subdivided honeycomb network,  $SHC_n$ , the first and second hyper-Gourava indices are calculated by  $HGO_1(\xi) = 2178n^2 - 1410n$  and  $HGO_2(\xi) = 16200n^2 - 13128n$ .

*Proof.* By letting  $\xi$  as the subdivided honeycomb network  $SHC_n$ , from Table 4, we know

$$\begin{aligned} HGO_1(\xi) &= \sum_{gh \in E(\xi)} [(d_g + d_h) + (d_g d_h)]^2, \\ HGO_2(\xi) &= \sum_{gh \in E(\xi)} [(d_g + d_h) + (d_g d_h)]^2, \end{aligned} \quad (143)$$

and by doing some calculations, we get

$$\begin{aligned} HGO_1(\xi) &= (12n)[64] + 18n(n-1)[121] \\ &= 2178n^2 - 1410n, \\ HGO_2(\xi) &= (12n)[256] + 18n(n-1)[900] \\ &= 16200n^2 - 13128n. \end{aligned} \quad (144)$$

**Theorem 40.** For the subdivided honeycomb network,  $SHC_n$ , the general Randić' index is calculated by

$$R_\gamma(SHC_n) = \begin{cases} 3n^2, & \text{for } \gamma = -1, \\ 3\{n^2\sqrt{6} + n\{2 - \sqrt{6}\}\}, & \text{for } \gamma = \frac{1}{2}, \\ 6\{3n^2\sqrt{6} + n\{4 - 3\sqrt{6}\}\}, & \text{for } \gamma = \frac{1}{2}, \\ 108n^2 - 60n, & \text{for } \gamma = 1. \end{cases} \quad (145)$$

*Proof.* By letting  $\xi$  as a subdivided honeycomb network  $SHC_n$  of  $n$  dimensions, we have the order and size of  $\xi$  in  $SHC_n$  as  $|V(SHC_n)| = 15n^2 - 3n$  and  $|E(SHC_n)| = 18n^2 - 6n$ , respectively. We know that

$$R_\gamma(\xi) = \sum_{gh \in E(\xi)} (d_g \cdot d_h)^\gamma, \quad (146)$$

for  $\gamma = \{-1, 1, -1/2, 1/2\}$ .

Case 1: if  $\gamma = -1$ , the application of Randić' index  $R_\gamma(\xi)$

$$R_{-1}(\xi) = \sum_{gh \in E(\xi)} \frac{1}{d_g d_h}, \quad (147)$$

using (146). From Table 4, we obtain  $R_{-1}(\xi) = 12n(4)^{-1} + 18n(n-1)(6)^{-1}$ .

By doing some calculations, we obtain  $R_{-1}(\xi) = 3n^2$ .

Case 2: if  $\gamma = -(1/2)$ , the application of Randić' index  $R_\gamma(\xi)$

$$R_{-(1/2)}(\xi) = \sum_{gh \in E(\xi)} \frac{1}{\sqrt{(d_g \cdot d_h)}}, \quad (148)$$

using (146). From Table 4, we obtain  $R_{-(1/2)}(\xi) = 12n(1/\sqrt{4}) + 18n(n-1)(1/\sqrt{6})$ .

By doing some calculations, we obtain  $R_{-(1/2)}(\xi) = 3\{n^2\sqrt{6} + n\{2 - \sqrt{6}\}\}$ .

Case 3: if  $\gamma = (1/2)$ , the application of Randić index  $R_\gamma(\xi)$

$$R_{(1/2)}(\xi) = \sum_{gh \in E(\xi)} \sqrt{d_g \cdot d_h}, \quad (149)$$

using (146). From Table 4, we obtain  $R_{(1/2)}(\xi) = 12n\sqrt{4} + 18n(n-1)\sqrt{6}$ .

By doing some calculations, we obtain  $R_{(1/2)}(\xi) = 6\{3n^2\sqrt{6} + n\{4 - 3\sqrt{6}\}\}$ .

Case 4: if  $\gamma = 1$ , the application of Randić' index  $R_\gamma(\xi)$

$$R_1(\xi) = \sum_{gh \in E(\xi)} (d_g \cdot d_h)^1, \quad (150)$$

using (146). From Table 4, we obtain  $R_1(\xi) = 12n(4) + 18n(n-1)(6)$ .

By doing some calculations, we obtain  $R_1(\xi) = 108n^2 - 60n$ .

**Theorem 41.** For the subdivided honeycomb network,  $SHC_n$ , the harmonic index is calculated by

$$HI(\xi) = \frac{36n^2 - 6n}{5}. \quad (151)$$

*Proof.* By letting  $\xi$  as a subdivided honeycomb network  $SHC_n$ , from Table 4, we know

$$HI(\xi) = \sum_{gh \in E(\xi)} \frac{2}{d_g + d_h}, \quad (152)$$

and by doing some calculations, we get

$$HI(\xi) = (12n) \left[ \frac{1}{2} \right] + 18n(n-1) \left[ \frac{2}{5} \right] = \frac{36n^2 - 6n}{5}. \quad (153)$$

**Theorem 42.** For the subdivided honeycomb network,  $SHC_m$ , the general version of the harmonic index is calculated by

$$H_k I(\xi) = 6 \left[ 3n^2 \left\{ \frac{2}{5} \right\}^k + n \left\{ \frac{2}{2^k} - 3 \left\{ \frac{2}{5} \right\}^k \right\} \right]. \quad (154)$$

*Proof.* By letting  $\xi$  as a subdivided honeycomb network  $SHC_m$ , from Table 4, we know

$$H_k I(\xi) = \sum_{gh \in E(\xi)} \left[ \frac{2}{d_g + d_h} \right]^k, \quad (155)$$

and by doing some calculations, we get

$$\begin{aligned} H_k I(\xi) &= (12n) \left[ \frac{2}{2+2} \right]^k + 18n(n-1) \left[ \frac{2}{2+3} \right]^k, \\ &= 6 \left[ 3n^2 \left\{ \frac{2}{5} \right\}^k + n \left\{ \frac{2}{2^k} - 3 \left\{ \frac{2}{5} \right\}^k \right\} \right]. \end{aligned} \quad (156)$$

**Theorem 43.** For the subdivided honeycomb network,  $SHC_m$ , the atom-bond connectivity index is calculated by

$$ABC(\xi) = n\sqrt{2}[9n-3]. \quad (157)$$

*Proof.* By letting  $\xi$  as a subdivided honeycomb network  $SHC_m$ , from Table 4, we know

$$ABC(\xi) = \sum_{gh \in E(\xi)} \sqrt{\frac{d_g + d_h - 2}{d_g d_h}}, \quad (158)$$

and by doing some calculations, we get

$$\begin{aligned} ABC(\xi) &= 12n \sqrt{\frac{2+2-2}{4}} + 18n(n-1) \sqrt{\frac{2+3-2}{6}}, \\ &= n\sqrt{2}[9n-3]. \end{aligned} \quad (159)$$

**Theorem 44.** For the subdivided honeycomb network,  $SHC_m$ ,  $SK$ ,  $SK_1$ , and  $SK_2$  indices are calculated by  $SK(\xi) = 45n^2 - 21n$ ,  $SK_1(\xi) = 54n^2 - 30n$ , and  $SK_2(\xi) = (1/2)(225n^2 - 129n)$ , respectively.

*Proof.* By letting  $\xi$  as a subdivided honeycomb network  $SHC_m$ , from Table 4, we know

$$SK(\xi) = \sum_{gh \in E(\xi)} \left[ \frac{d_g + d_h}{2} \right],$$

$$SK_1(\xi) = \sum_{gh \in E(\xi)} \left[ \frac{d_g d_h}{2} \right], \quad (160)$$

$$SK_2(\xi) = \sum_{gh \in E(\xi)} \left[ \frac{d_g + d_h}{2} \right]^2,$$

and by doing some calculations, we get

$$SK(\xi) = (12n)(2) + 18n(n-1) \left( \frac{5}{2} \right) = 45n^2 - 21n,$$

$$SK_1(\xi) = (12n)(2) + 18n(n-1)(3) = 54n^2 - 30n,$$

$$SK_2(\xi) = (12n)(4) + 18n(n-1) \left( \frac{25}{4} \right) = \frac{1}{2}(225n^2 - 129n). \quad (161)$$

**Theorem 45.** For the subdivided honeycomb network,  $SHC_m$ , the sum-connectivity index is calculated by

$$\chi_{-(1/2)}(\xi) = \frac{1}{\sqrt{5}} [18n^2 + n\{6\sqrt{5} - 18\}]. \quad (162)$$

*Proof.* By letting  $\xi$  as a subdivided honeycomb network  $SHC_m$ , from Table 4, we know

$$\chi_{-(1/2)}(\xi) = \sum_{gh \in E(\xi)} [d_g + d_h]^{-(1/2)}, \quad (163)$$

$$\chi_{-(1/2)}(\xi) = (12n) \left( \frac{1}{2} \right) + 18n(n-1) \left( \frac{1}{\sqrt{5}} \right),$$

and by doing some calculations, we get

$$\chi_{-(1/2)}(\xi) = \frac{1}{\sqrt{5}} [18n^2 + n\{6\sqrt{5} - 18\}]. \quad (164)$$

**Theorem 46.** For the subdivided honeycomb network,  $SHC_m$ , the general sum-connectivity index is calculated by

$$\chi_k(\xi) = 18\{5^k\}n^2 + 6n\{2\{4^k\} - 3\{5^k\}\}. \quad (165)$$

*Proof.* By letting  $\xi$  as a subdivided honeycomb network  $SHC_m$ , from Table 4, we know

$$\chi_k(\xi) = \sum_{gh \in E(\xi)} [d_g + d_h]^k, \quad (166)$$

$$\chi_k(\xi) = (12n)(4^k) + 18n(n-1)(5^k),$$

and by doing some calculations, we get

$$\chi_k(\xi) = 18\{5^k\}n^2 + 6n\{2\{4^k\} - 3\{5^k\}\}. \quad (167)$$

**Theorem 47.** For the subdivided honeycomb network,  $SHC_m$ , the first general Zagreb index is calculated by

$${}^k M_1(\xi) = 18n^2\{2^{k-1} + 3^{k-1}\} + 6n\{2\{2^k\} - 3n\{2^{k-1} + 3^{k-1}\}\}. \quad (168)$$

*Proof.* By letting  $\xi$  as a subdivided honeycomb network  $SHC_m$ , from Table 4, we know

$${}^k M_1(\xi) = \sum_{gh \in E(\xi)} [d_g^{k-1} + d_h^{k-1}], \quad k > 1, \quad (169)$$

$${}^k M_1(\xi) = (12n)(2^k) + 18n(n-1)(2^{k-1} + 3^{k-1}),$$

and by doing some calculations, we get

$${}^k M_1(\xi) = 18n^2\{2^{k-1} + 3^{k-1}\} + 6n\{2\{2^k\} - 3n\{2^{k-1} + 3^{k-1}\}\}. \quad (170)$$

**Theorem 48.** For the subdivided honeycomb network,  $SHC_m$ , the forgotten index is calculated by

$$F(\xi) = 2n\{117n - 69\}. \quad (171)$$

*Proof.* By letting  $\xi$  as a subdivided honeycomb network  $SHC_m$ , from Table 4, we know

$$F(\xi) = \sum_{gh \in E(\xi)} [d_g^2 + d_h^2], \quad (172)$$

$$F(\xi) = (12n)(8) + 18n(n-1)(13),$$

and by doing some calculations, we get  $F(\xi) = 2n\{117n - 69\}$ .

### 3. Conclusions

In this paper, we have computed the topological indices (degree based) such as ordinary generalized geometric-arithmetic (OGA) index, first and second Gourava indices, first and second hyper-Gourava indices, general Randić' index  $R_\gamma(\xi)$ , for  $\gamma = \{\pm 1, \pm(1/2)\}$ , harmonic index, general version of the harmonic index, atom-bond connectivity (ABC) index, SK, SK<sub>1</sub>, and SK<sub>2</sub> indices, sum-connectivity index, general sum-connectivity index, and first general Zagreb and forgotten topological indices for different kinds of chemical networks such as the subdivided polythiophene network, subdivided hexagonal network, subdivided backbone DNA network, and subdivided honeycomb network. The above computed topological indices are used as molecular descriptors in the construction of "quantitative structure-activity relationships and quantitative structure-property relationships." These indices give us results that can

be correlated with the molecular structures to understand their chemical and physical properties.

For the next research papers, our goal is to compute more topological indices for some new graphs to know their topologies.

### Data Availability

No data were used to support this study.

### Disclosure

This paper has not been published elsewhere, and it will not be submitted anywhere else for publication.

### Conflicts of Interest

The authors declare that they have no conflicts of interest.

### Authors' Contributions

All authors contributed equally to this work.

### Acknowledgments

The authors like to show their gratitude to the concerned people for sharing their pearls of wisdom with them during this research work.

### References


- [1] A. Ali, L. Zhong, and I. Gutman, "Harmonic index and its generalizations: extremal results and bounds," *MATCH Communications in Mathematical and in Computer*, vol. 81, pp. 249–311, 2019.
- [2] A. Ali, I. Gutman, E. Milovanovic, and I. Milovanovic, "Sum of powers of the degrees of graphs: extremal results and bounds," *MATCH Communications in Mathematical and in Computer*, vol. 80, pp. 5–84, 2018.
- [3] A. Ali, K. C. Das, D. Dimitrov, and B. Furtula, "Atom-bond connectivity index of graphs: a review over extremal results and bounds," *Discrete Mathematics Letters*, vol. 5, pp. 68–93, 2021.
- [4] Z. S. Mufti, M. F. Nadeem, W. Gao, and Z. Ahmad, "Topological study of the para-line graphs of certain pentacene via topological indices," *Open Chemistry*, vol. 16, no. 1, pp. 1200–1206, 2018.
- [5] B. Borovicanin, K. C. Das, B. Furtula, and I. Gutman, "Bounds for zagreb indices," *MATCH Communications in Mathematical and in Computer*, vol. 78, pp. 17–100, 2017.
- [6] A. Portilla, J. M. Rodriguez, and J. M. Sgarreta, "Recent lower bounds for geometric-arithmetic index," *Discrete Mathematics Letters*, vol. 1, pp. 59–82, 2019.
- [7] B. Zhou, I. Gutman, B. Furtula, and Z. Du, "On two types of geometric-arithmetic index," *Chemical Physics Letters*, vol. 482, no. 1–3, pp. 153–155, 2009.
- [8] D. Vukičević and B. Furtula, "Topological index based on the ratios of geometrical and arithmetical means of end-vertex degrees of edges," *Journal of Mathematical Chemistry*, vol. 46, no. 4, pp. 1369–1376, 2007.



- [9] G. Fath-Tabar, B. Furtula, and I. Gutman, "A new geometric-arithmetic index," *Journal of Mathematical Chemistry*, vol. 47, no. 1, pp. 477–486, 2010.
- [10] K. C. Das, I. Gutman, and B. Furtula, "Survey on geometric–arithmetic indices of graphs," *MATCH Communications in Mathematical and in Computer Chemistry*, vol. 65, pp. 595–644, 2011.
- [11] Y. Yuan, B. Zhou, and N. Trinajstić, "On geometric-arithmetic index," *Journal of Mathematical Chemistry*, vol. 47, no. 2, pp. 833–841, 2010.
- [12] M. Eliasi and I. Ali, "On ordinary generalized geometric–arithmetic index," *Applied Mathematics Letters*, vol. 24, no. 4, pp. 582–587, 2011.
- [13] V. R. Kulli, "The Gourava indices and coindices of Graphs," *Annals of Pure and Applied Mathematics*, vol. 14, no. 1, pp. 33–38, 2017.
- [14] V. R. Kulli, "On hyper-Gourava indices and coindices," *International Journal of Mathematical Archive*, vol. 8, no. 12, pp. 116–120, 2017.
- [15] M. Randić, "On characterization of molecular branching," *Journal of the American Chemical Society*, vol. 97, pp. 6609–6615, 1975.
- [16] M. R. Farahani, "On the randic and sum-connectivity index of nanotubes," *Annals of West University of Timisoara Mathematics*, vol. 51, no. 2, pp. 29–37, 2013.
- [17] X. Li and Y. Shi, "A survey on the randic index," *MATCH Communications in Mathematical and in Computer Chemistry*, vol. 59, pp. 127–156, 2008.
- [18] B. Bollobás and P. Erdos, "Graphs of extremal weights," *Ars Combinatoria*, vol. 50, pp. 225–233, 1998.
- [19] B. Wu and L. Zhang, "Unicyclic graphs with minimum general Randić index," *MATCH Communications in Mathematical and in Computer Chemistry*, vol. 54, pp. 455–464, 2005.
- [20] X. Li and I. Gutman, *Mathematical Aspects of Randić-type Molecular Structure Descriptors*, University of Kragujevac, Kragujevac, Serbia, 2006.
- [21] Y. Hu, X. Li, and Y. Yuan, "Trees with minimum general Randić index," *MATCH Communications in Mathematical and in Computer Chemistry*, vol. 52, pp. 119–128, 2004.
- [22] L. Zhong, "The harmonic index for graphs," *Applied Mathematics Letters*, vol. 25, no. 3, pp. 561–566, 2012.
- [23] S. Fajtlowicz, "On conjectures of Graffiti – II," *Congressus Numerantium*, vol. 60, pp. 187–197, 1987.
- [24] L. Yan, W. Gao, and J. Li, "General harmonic index and general sum connectivity index of polyomino chains and nanotubes," *Journal of Computational and Theoretical Nanoscience*, vol. 12, no. 10, pp. 3940–3944, 2015.
- [25] E. Estrada, L. Torres, L. Rodriguez, and I. Gutman, "An atom-bond connectivity index: modelling the enthalpy of formation of alkanes," *Indian Journal of Chemistry*, vol. 37, pp. 849–855, 1998.
- [26] E. Estrada, "Atom-bond connectivity and the energetic of branched alkanes," *Chemical Physics Letters*, vol. 463, no. 4–6, pp. 422–425, 2008.
- [27] V. S. Shegehalli and R. Kanabur, "Computation of new degree-based topological indices of graphene," *Journal of Mathematics*, vol. 5, p. 6, Article ID 4341919, 2016.
- [28] B. Lučić, N. Trinajstić, and B. Zhou, "Comparison between the sum-connectivity index and product-connectivity index for benzenoid hydrocarbons," *Chemical Physics Letters*, vol. 475, no. 1–3, pp. 146–148, 2009.
- [29] B. Zhou and N. Trinajstić, "On general sum-connectivity index," *Journal of Mathematical Chemistry*, vol. 47, no. 1, pp. 210–218, 2010.
- [30] H. M. Awais, M. Javaid, and A. Ali, "Frist general zagreb index of generalized f-sum graphs," *Discrete Dynamics in Nature and Society*, vol. 2020, Article ID 2954975, 16 pages, 2020.
- [31] J.-B. Liu, S. Javed, M. Javaid, and K. Shabbir, "Computing first general Zagreb index of operations on graphs," *IEEE Access*, vol. 7, pp. 47494–47502, 2019.
- [32] S. M. Hosamani and I. Gutman, "Zagreb indices of transformation graphs and total transformation graphs," *Applied Mathematics and Computation*, vol. 247, pp. 1156–1160, 2014.
- [33] S. Zhang and H. Zhang, "Unicyclic graphs with the first three smallest and largest first general zagreb index," *MATCH Communications in Mathematical and in Computer Chemistry*, vol. 55, pp. 427–438, 2006.
- [34] X. Li and J. Zheng, "A unified approach to the extremal trees for different indices," *MATCH Communications in Mathematical and in Computer Chemistry*, vol. 54, pp. 195–208, 2005.
- [35] X. Li and H. Zhao, "Trees with the first three smallest and largest generalized topological indices," *MATCH Communications in Mathematical and in Computer Chemistry*, vol. 50, pp. 57–62, 2004.
- [36] B. Furtula and I. Gutman, "A forgotten topological index," *Journal of Mathematical Chemistry*, vol. 53, no. 4, pp. 1184–1190, 2012.
- [37] H. Abdo, D. Dimitrov, and I. Gutman, "On extremal trees with respect to the F-index," 2013, <https://arxiv.org/abs/1509.03574>.
- [38] N. De, A. Nayeem, and A. Pal, "F-index of some graph operations," 2015, <https://arxiv.org/abs/1511.06661>.
- [39] Y. Kongyang, C. Xiaosong, J. Zhepeng, Z. Cong, W. Dacheng, and L. Yunqi, "Two-dimensional cross-linked polythiophene network," *Journal of Materials Chemistry C*, vol. 7, 2019.
- [40] A. Ghosh and M. Bansal, "A glossary of DNA structures from A to Z," *Acta Crystallographica Section D*, vol. 59, no. 4, pp. 620–626, 2003.

## Research Article

# Analysis of Dendrimer Generation by Sombor Indices

Shahid Amin,<sup>1</sup> Abaid Ur Rehman Virk,<sup>2</sup> M.A. Rehman,<sup>1</sup> and Nehad Ali Shah <sup>3,4</sup>

<sup>1</sup>Department of Mathematics, University of Management and Technology, Lahore, Pakistan

<sup>2</sup>Department of Mathematics, University of Sialkot, Sialkot, Pakistan

<sup>3</sup>Informetrics Research Group, Ton Duc Thang University, Ho Chi Minh, Vietnam

<sup>4</sup>Faculty of Mathematics and Statistics, Ton Duc Thang University, Ho Chi Minh, Vietnam

Correspondence should be addressed to Nehad Ali Shah; [nehadali199@yahoo.com](mailto:nehadali199@yahoo.com)

Received 6 March 2021; Revised 17 March 2021; Accepted 26 April 2021; Published 7 May 2021

Academic Editor: Kashif Ali

Copyright © 2021 Shahid Amin et al. This is an open access article distributed under the Creative Commons Attribution License, which permits unrestricted use, distribution, and reproduction in any medium, provided the original work is properly cited.

Dendrimers are highly branched, star-shaped macromolecules with nanometer-scale dimensions. Dendrimers are defined by three components: a central core, an interior dendritic structure (the branches), and an exterior surface with functional surface groups. Topological indices are numerical numbers that help us to understand the topology of different dendrimers and can be used to predict the properties without performing experiments in the wet lab. In the present paper, we computed the Sombor index and the reduced version of the Sombor index for the molecular graphs of phosphorus-containing dendrimers, porphyrin-cored dendrimers, PDI-cored dendrimers, triazine-based dendrimers, and aliphatic polyamide dendrimers. We also plotted our results by using Maple 2015 which help us to see the dependence of the Sombor index and reduced Sombor index on the involved parameters. Our results may help to develop better understanding about phosphorus-containing dendrimers, porphyrin-cored dendrimers, PDI-cored dendrimers, triazine-based dendrimers, and aliphatic polyamide dendrimers. Our results are also useful in the pharmaceutical industry and drug delivery.

## 1. Introduction

Dendrimers are highly branched star-molded macromolecules with nanometer-scale measurements [1]. A dendrimer consists of three modules: a central core, an interior surface (branches), and the outer surface. A functional surface group is attached with the outer core. Various blends of these parts yield results of various shapes and sizes with protected inside centers that are an ideal contender for applications in both organic and materials sciences [2]. The characteristics of a dendrimer depend on the external group attached with the outer surface. Dendrimers have acquired a wide scope of uses in supramolecular science, especially in drug delivery, gene transfection, catalysis, energy harvesting, photo activity, molecular weight and size determination, rheology modification, and nanoscale science and technology. A dendrimer acts as a solubilizing agent in different reactions. Dendrimers have a wide range of applications in different fields of sciences [3]. The construction of dendrimers is presented in Figure 1.

Mathematical chemistry is the branch of mathematics in which mathematical tools are used to solve the problems arising in chemistry [4]. One of these tools is graphical representation of chemical compounds, and this representation is known as the molecular graph of the concerned chemical compound [5]. In the molecular graph of a chemical compound, atoms are represented as vertices, and bonds are represented as edges [6]. Topological invariants of molecular graphs are numerical numbers that enable us to collect information about concerned chemical structure and give us its hidden properties without performing experiments [7–11]. The first topological index was put forward by Wiener in 1947 [12] when he was trying to find the boiling points of alkane. This discovery led to the beginning of the theory of topological indices. The first degree-based topological index was put forward by Randić in 1975 [13]. After the success of the Randić index, Gutman introduced the Zagreb indices. There are hundreds of topological indices present in the literature [14–18]. Recently, Gutman, in 2021 [19], defined the idea of Sombor indices. Sombor

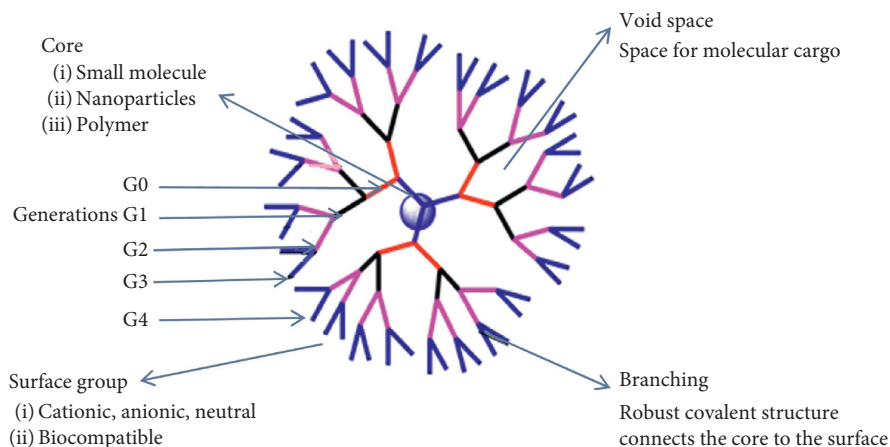


FIGURE 1: Modules of the dendrimer.

indices have two variants, Sombor index and reduced Sombor index, as follows:

$$\begin{aligned} \text{SO}(G) &= \sum_{ij \in (E(G))} \sqrt{d_i^2 + d_j^2}, \\ \text{SO}_{\text{red}}(G) &= \sum_{ij \in (E(G))} \sqrt{(d_i - 1)^2 + (d_j - 1)^2}. \end{aligned} \quad (1)$$

The aim of this paper is to study the phosphorus-containing dendrimers, porphyrin-cored dendrimers, PDI-cored dendrimers, triazine-based dendrimers, and aliphatic polyamide dendrimers. We computed the Sombor index and the reduced version of the Sombor index for the aforementioned dendrimers. We also present graphical representations of our results to see the dependence of computed indices on the involved parameters.

Throughout this paper, we consider all graphs to be simple and connected, and  $d_u$  denotes the degree of vertex  $u$  which is equal to the number of vertices at distance one to it. For the notation used in this paper but not defined, we refer to in [20, 21] and references therein.

## 2. Methodology

Firstly, we obtain the molecular graphs of phosphorus-containing dendrimers, porphyrin-cored dendrimers, PDI-cored dendrimers, triazine-based dendrimers, and aliphatic polyamide dendrimers. Secondly, we compute the order and size of these molecular graphs and classify their edge sets and vertex sets into different classes with respect to the degrees of vertices. Thirdly, we compute the Sombor and reduced Sombor indices for the molecular

graphs of phosphorus-containing dendrimers, porphyrin-cored dendrimers, PDI-cored dendrimers, triazine-based dendrimers, and aliphatic polyamide dendrimers. Lastly, we plot our obtained results by using Maple 2015 software.

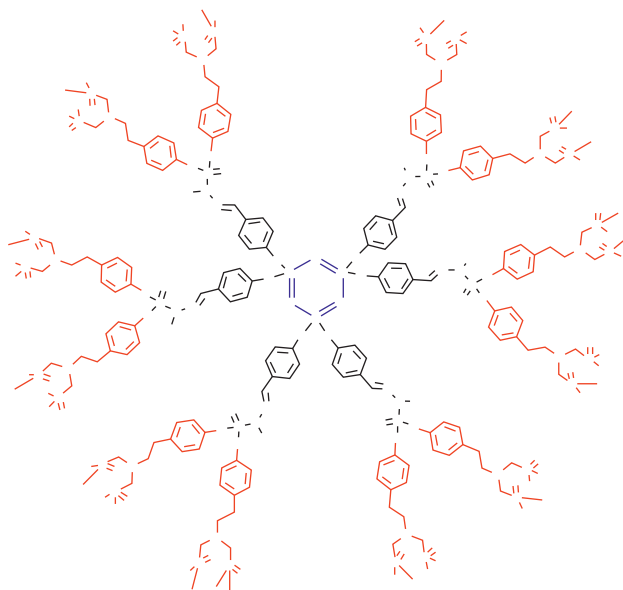
## 3. Main Results

In this section, we present Sombor and reduced Sombor indices for phosphorus-containing dendrimers, porphyrin-cored dendrimers, PDI-cored dendrimers, triazine-based dendrimers, and aliphatic polyamide dendrimers.

**3.1. Phosphorus-Containing Dendrimers.** Phosphorus-containing dendrimers have functionalities with pendant nitroxyl radicals, and these radicals show a solid attractive trade interaction. Let us consider  $D_1(m)$  to be the molecular graph of phosphorus-containing dendrimers, where  $m$  shows the generation stage of  $D_1(m)$ . Figure 2 shows the molecular graph  $D_1(m)$  of phosphorus-containing dendrimers.

From Figure 2, we can observe that the order and size of  $D_1(m)$  are  $9(11 \times 2^{m+1} - 8)$  and  $6(9 \times 2^{m+2} - 13)$ , respectively. If  $\mathcal{V}(D_1(m))$  is the vertex set, then from Figure 2, we can classify  $\mathcal{V}(D_1(m))$  into four subsets  $\mathcal{V}_1$ ,  $\mathcal{V}_2$ ,  $\mathcal{V}_3$ , and  $\mathcal{V}_4$  of vertices of degrees 1, 2, 3, and 4 such that  $|\mathcal{V}(D_1(m))| = |\mathcal{V}_1(D_1(m))| + |\mathcal{V}_2(D_1(m))| + |\mathcal{V}_3(D_1(m))| + |\mathcal{V}_4(D_1(m))|$ . The cardinalities of  $\mathcal{V}_1(D_1(m))$ ,  $\mathcal{V}_2(D_1(m))$ ,  $\mathcal{V}_3(D_1(m))$ , and  $\mathcal{V}_4(D_1(m))$  are  $42 \times 2^m - 12$ ,  $96 \times 2^m - 39$ ,  $42 \times 2^m - 18$ , and  $18 \times 2^m - 3$ , respectively.

If  $\mathcal{E}(D_1(m))$  represents the edge set, then Figure 2 shows that there are the following six different types of edges with respect to the degrees of end vertices present in the molecular graph of  $D_1(m)$ :

FIGURE 2:  $D_1(m)$  for  $m = 3$ .TABLE 1: Degree-based edge partition of  $D_1(m)$ .

$\varepsilon$	$\varepsilon_{(d_u, d_v)}$	Frequency
$\varepsilon_1$	$\varepsilon_{(1,3)}$	$6(2^m - 1)$
$\varepsilon_2$	$\varepsilon_{(1,4)}$	$6(5 \times 2^m - 1)$
$\varepsilon_3$	$\varepsilon_{(2,2)}$	$18(2^{m+1} - 1)$
$\varepsilon_4$	$\varepsilon_{(2,3)}$	$6(2^{m+4} - 7)$
$\varepsilon_5$	$\varepsilon_{(2,4)}$	$(3 \times 2^{m+3})$
$\varepsilon_6$	$\varepsilon_{(3,4)}$	$6(3 \times 2^m - 1)$

$$\begin{aligned}
 \varepsilon_1(D_1(m)) &= \varepsilon_{(1,3)}(D_1(m)) = \{e = uv \in \varepsilon(D_1(m)): d_u = 1, d_v = 3\}, \\
 \varepsilon_2(D_1(m)) &= \varepsilon_{(1,4)}(D_1(m)) = \{e = uv \in \varepsilon(D_1(m)): d_u = 1, d_v = 4\}, \\
 \varepsilon_3(D_1(m)) &= \varepsilon_{(2,2)}(D_1(m)) = \{e = uv \in \varepsilon(D_1(m)): d_u = 2, d_v = 2\}, \\
 \varepsilon_4(D_1(m)) &= \varepsilon_{(2,3)}(D_1(m)) = \{e = uv \in \varepsilon(D_1(m)): d_u = 2, d_v = 3\}, \\
 \varepsilon_5(D_1(m)) &= \varepsilon_{(2,4)}(D_1(m)) = \{e = uv \in \varepsilon(D_1(m)): d_u = 2, d_v = 4\}, \\
 \varepsilon_6(D_1(m)) &= \varepsilon_{(3,4)}(D_1(m)) = \{e = uv \in \varepsilon(D_1(m)): d_u = 3, d_v = 4\}.
 \end{aligned} \tag{2}$$

Table 1 explains the edge partition of the edge set of  $D_1(m)$  in detail.

Frequency means the total number of edges in the particular class.

**Theorem 1.** The  $SO$  and  $SO_{red}$  indices for  $D_1(m)$  are as follows:

$$(i) SO(G) = 2^{((1/2)+m)} \sqrt{5} - 6\sqrt{2} \sqrt{5} + 72 \times 2^{((1/2)+m)} + 48\sqrt{5}2^m + 96\sqrt{13}2^m + 30\sqrt{17}2^m - 36\sqrt{2} - 42\sqrt{13} - 6\sqrt{17} + 90 \times 2^m - 30$$

$$(ii) SO_{red}(G) = 24 \times 2^{((1/2)+m)} \sqrt{5} + 18\sqrt{13}2^m + 362^{((1/2)+m)} + 96\sqrt{5}2^m + 282 \times 2^m - 18\sqrt{2} - 6\sqrt{13} - 42\sqrt{5} - 66$$

*Proof.* For the edge partition of the vertex set of  $D_1(m)$ , we have the following computations for SO and  $SO_{red}$  indices:

$$\begin{aligned}
 SO(D_1) &= \sum_{ij} \sqrt{d_i^2 + d_j^2} = \sqrt{1^2 + 3^2}(6(2^m - 1)) + \sqrt{1^2 + 4^2}(6(5 \times 2^m - 1)) + \sqrt{2^2 + 2^2}(18(2^{m+1} - 1)) + \sqrt{2^2 + 3^2}(6(2^{m+4} - 7)) \\
 &\quad + \sqrt{2^2 + 4^2}(3 \times 2^{m+3}) + \sqrt{3^2 + 4^2}(6(3 \times 2^m - 1)) = 2^{(1/2)+m} \sqrt{5} - 6\sqrt{10} + 72 \times 2^{(1/2)+m} + 48\sqrt{5}2^m + 96\sqrt{13}2^m \\
 &\quad + 30\sqrt{17}2^m - 36\sqrt{2} - 42\sqrt{13} - 6\sqrt{17} + 902^m - 30, \\
 SO_{red}(D_1) &= \sum_{ij} \sqrt{(d_i - 1)^2 + (d_j - 1)^2} = \sqrt{(1 - 1)^2 + (3 - 1)^2}(6(2^m - 1)) + \sqrt{(1 - 1)^2 + (4 - 1)^2}(6(5 \times 2^m - 1)) \\
 &\quad + \sqrt{(2 - 1)^2 + (2 - 1)^2}(18(2^{m+1} - 1)) + \sqrt{(2 - 1)^2 + (3 - 1)^2}(6(2^{m+4} - 7)) + \sqrt{(2 - 1)^2 + (4 - 1)^2}(3 \times 2^{m+3}) \\
 &\quad + \sqrt{(3 - 1)^2 + (4 - 1)^2}(6(3 \times 2^m - 1))24 \times 2^{((1/2)+m)} \sqrt{5} + 18\sqrt{13}2^m + 36 \times 2^{((1/2)+m)} + 96\sqrt{5}2^m + 282 \times 2^m \\
 &\quad - 18\sqrt{2} - 6\sqrt{13} - 42\sqrt{5} - 66.
 \end{aligned} \tag{3}$$

**3.2. Porphyrin-Cored Dendrimers.** Figure 3 shows the molecular graph  $D_2(m)$  of porphyrin-cored dendrimers, where  $m$  represents different generations of  $D_2(m)$ .

From Figure 3, we can observe that the order and size of  $D_2(m)$  are  $4(2^{m+3} + 9)$  and  $4(2^{m+3} + 11)$ , respectively. If  $\mathcal{V}(D_2(m))$  is the vertex set, then from Figure 3, we can classify this vertex set into four subsets  $\mathcal{V}_1(D_2(m))$ ,  $\mathcal{V}_2(D_2(m))$ ,  $\mathcal{V}_3(D_2(m))$ , and  $\mathcal{V}_4(D_2(m))$  with respect to

degrees such that  $|\mathcal{V}(D_2(m))| = |\mathcal{V}_1(D_2(m))| + |\mathcal{V}_2(D_2(m))| + |\mathcal{V}_3(D_2(m))| + |\mathcal{V}_4(D_2(m))|$ . The cardinalities of  $\mathcal{V}_1(D_2(m))$ ,  $\mathcal{V}_2(D_2(m))$ ,  $\mathcal{V}_3(D_2(m))$ , and  $\mathcal{V}_4(D_2(m))$  are  $12 \times 2^m - 8$ ,  $12 \times 2^m + 32$ ,  $4 \times 2^m + 16$ , and  $4 \times 2^m - 4$  vertices, respectively.

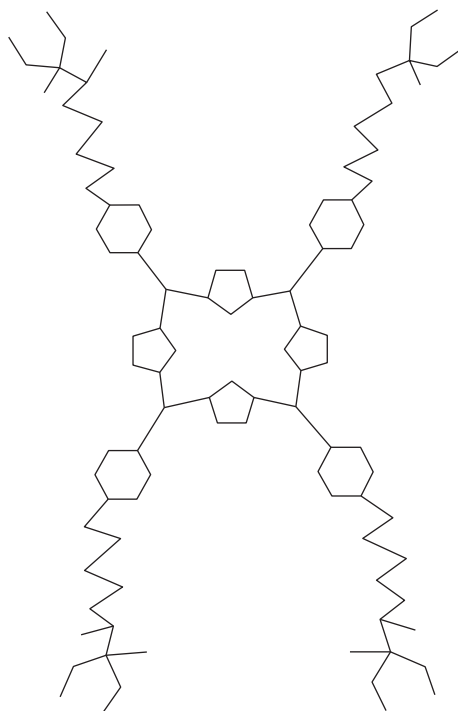
If  $\mathcal{E}(D_2(m))$  represents the edge set, then Figure 3 shows that there are the following eight different types of edges present in the molecular graph of  $D_2(m)$ :

$$\begin{aligned}
 \mathcal{E}_1(D_2(m)) &= \mathcal{E}_{(1,2)}(D_2(m)) = \{e = uv \in \mathcal{E}(D_2(m)): d_u = 1, d_v = 2\}, \\
 \mathcal{E}_2(D_2(m)) &= \mathcal{E}_{(1,3)}(D_2(m)) = \{e = uv \in \mathcal{E}(D_2(m)): d_u = 1, d_v = 3\}, \\
 \mathcal{E}_3(D_2(m)) &= \mathcal{E}_{(1,4)}(D_2(m)) = \{e = uv \in \mathcal{E}(D_2(m)): d_u = 1, d_v = 4\}, \\
 \mathcal{E}_4(D_2(m)) &= \mathcal{E}_{(2,2)}(D_2(m)) = \{e = uv \in \mathcal{E}(D_2(m)): d_u = 2, d_v = 2\}, \\
 \mathcal{E}_5(D_2(m)) &= \mathcal{E}_{(2,3)}(D_2(m)) = \{e = uv \in \mathcal{E}(D_2(m)): d_u = 2, d_v = 3\}, \\
 \mathcal{E}_6(D_2(m)) &= \mathcal{E}_{(2,4)}(D_2(m)) = \{e = uv \in \mathcal{E}(D_2(m)): d_u = 2, d_v = 4\}, \\
 \mathcal{E}_7(D_2(m)) &= \mathcal{E}_{(3,3)}(D_2(m)) = \{e = uv \in \mathcal{E}(D_2(m)): d_u = 3, d_v = 3\}, \\
 \mathcal{E}_8(D_2(m)) &= \mathcal{E}_{(3,4)}(D_2(m)) = \{e = uv \in \mathcal{E}(D_2(m)): d_u = 3, d_v = 4\}.
 \end{aligned} \tag{4}$$

Table 2 gives the detailed explanation about the edge partition of the edge set of  $D_1(m)$ .

**Theorem 2.** The SO and  $SO_{red}$  indices for  $D_2(m)$  are as follows:

$$\begin{aligned}
 (i) \quad SO(G) &= 4 \times 2^{((1/2)+m)} \sqrt{5} + 20\sqrt{5}2^m - 4\sqrt{2}\sqrt{5} + 82^{((1/2)+m)} + 4\sqrt{17}2^m + 4\sqrt{13}2^m - 16\sqrt{5} + 202^m + 76\sqrt{2} - 4\sqrt{17} + 32\sqrt{13} - 20 \\
 (ii) \quad SO_{red}(G) &= 8 \times 2^{((1/2)+m)} \sqrt{5} + 4\sqrt{5}2^m - 8\sqrt{2}\sqrt{5} + 4 \times 2^{((1/2)+m)} + 4\sqrt{13}2^m + 32\sqrt{5} + 242^m + 44\sqrt{2} - 4\sqrt{13} - 20
 \end{aligned}$$

FIGURE 3:  $D_2(m)$  for  $m = 1$ .TABLE 2: Degree-based edge partition of  $D_2(m)$ .

$\mathcal{E}$	$\mathcal{E}_{(d_u, d_v)}$	Frequency
$\mathcal{E}_1$	$\mathcal{E}_{(1,2)}$	$4 \times 2^m$
$\mathcal{E}_2$	$\mathcal{E}_{(1,3)}$	$4 \times 2^m - 4$
$\mathcal{E}_3$	$\mathcal{E}_{(1,4)}$	$4 \times 2^m - 4$
$\mathcal{E}_4$	$\mathcal{E}_{(2,2)}$	$4 \times 2^m + 20$
$\mathcal{E}_5$	$\mathcal{E}_{(2,3)}$	$4 \times 2^m + 32$
$\mathcal{E}_6$	$\mathcal{E}_{(2,4)}$	$8 \times 2^m - 8$
$\mathcal{E}_7$	$\mathcal{E}_{(3,3)}$	12
$\mathcal{E}_8$	$\mathcal{E}_{(3,4)}$	$4 \times 2^m - 4$

*Proof.* From the edge partition of  $D_2(m)$  given in Table 2, we have the following computations of SO and  $SO_{\text{red}}$  indices:

$$\begin{aligned}
 SO(D_2) &= \sum_{ij} \sqrt{d_i^2 + d_j^2} = \sqrt{1^2 + 2^2}(4 \times 2^m) + \sqrt{1^2 + 3^2}(4 \times 2^m - 4) + \sqrt{1^2 + 4^2}(4 \times 2^m - 4) + \sqrt{2^2 + 2^2}(4 \times 2^m + 20) \\
 &\quad + \sqrt{2^2 + 3^2}(4 \times 2^m + 32) + \sqrt{2^2 + 4^2}(8 \times 2^m - 8) + \sqrt{3^2 + 3^2}(12) + \sqrt{3^2 + 4^2}(4 \times 2^m - 4) \\
 &= 4 \times 2^{((1/2)+m)}\sqrt{5} + 20\sqrt{5}2^m - 4\sqrt{2}\sqrt{5} + 82^{((1/2)+m)} + 4\sqrt{17}2^m + 4\sqrt{13}2^m - 16\sqrt{5} + 202^m + 76\sqrt{2} - 4\sqrt{17} + 32\sqrt{13} - 20, \\
 SO_{\text{red}}(D_2) &= \sum_{ij} \sqrt{(d_i - 1)^2 + (d_j - 1)^2} = \sqrt{(1-1)^2 + (2-1)^2}(4 \times 2^m) + \sqrt{(1-1)^2 + (3-1)^2}(4 \times 2^m - 4) + \sqrt{(1-1)^2 + 4^2}(4 \times 2^m - 4) \\
 &\quad + \sqrt{(2-1)^2 + (2-1)^2}(4 \times 2^m + 20) + \sqrt{(2-1)^2 + (3-1)^2}(4 \times 2^m + 32) + \sqrt{(2-1)^2 + (4-1)^2}(8 \times 2^m - 8) \\
 &\quad + \sqrt{(3-1)^2 + (3-1)^2}(12) + \sqrt{(3-1)^2 + (4-1)^2}(4 \times 2^m - 4) = 8 \times 2^{((1/2)+m)}\sqrt{5} + 4\sqrt{5}2^m - 8\sqrt{2}\sqrt{5} + 4 \times 2^{((1/2)+m)} + 4\sqrt{13}2^m 32\sqrt{5} \\
 &\quad + 242^m + 44\sqrt{2} - 4\sqrt{13} - 20.
 \end{aligned}$$

(5)  
□

**3.3. PDI-Cored Dendrimers.** The water-dissolvable PDI-cored dendrimers have various accommodations, containing low cytotoxicity, solid red fluorescence, high quantum yield, amazing photostability, and flexible surface alteration. These dendrimers have numerous applications in different fields such as fluorescence live-cell imaging and labeling. Let  $D_3(m)$  be the molecular graph of PDI-cored dendrimers; then, Figure 4 shows the 2D graph of  $D_3(m)$ .

From Figure 4, we can observe that the order and size of  $D_3(m)$  are  $20 \times 2^m + 20$  and  $20 \times 2^{2m} + 20$ , respectively. If

$\mathcal{V}(D_3(m))$  is the vertex set, then by observing Figure 4, we can classify this vertex set into three subsets  $\mathcal{V}_1(D_3(m))$ ,  $\mathcal{V}_2(D_3(m))$ , and  $\mathcal{V}_3(D_3(m))$  such that  $|\mathcal{V}(D_3(m))| = |\mathcal{V}_1(D_3(m))| + |\mathcal{V}_2(D_3(m))| + |\mathcal{V}_3(D_3(m))|$ . The cardinalities of  $\mathcal{V}_1(D_3(m))$ ,  $\mathcal{V}_2(D_3(m))$ , and  $\mathcal{V}_3(D_3(m))$  are  $2 \times 2^{m+1} + 4$ ,  $6 \times 2^{m+1}$ , and  $2 \times 2^{m+1} + 16$ , respectively.

If  $\mathcal{E}(D_3(m))$  represents the edge set, then Figure 4 shows that there are the following five different types of edges present in the molecular graph of  $D_3(m)$ :

$$\begin{aligned}\mathcal{E}_1(D_3(m)) &= \mathcal{E}_{(1,2)}(D_3(m)) = \{e = uv \in \mathcal{E}(D_3(m)): d_u = 1, d_v = 2\}, \\ \mathcal{E}_2(D_3(m)) &= \mathcal{E}_{(1,3)}(D_3(m)) = \{e = uv \in \mathcal{E}(D_3(m)): d_u = 1, d_v = 3\}, \\ \mathcal{E}_3(D_3(m)) &= \mathcal{E}_{(2,2)}(D_3(m)) = \{e = uv \in \mathcal{E}(D_3(m)): d_u = 2, d_v = 2\}, \\ \mathcal{E}_4(D_3(m)) &= \mathcal{E}_{(2,3)}(D_3(m)) = \{e = uv \in \mathcal{E}(D_3(m)): d_u = 2, d_v = 3\}, \\ \mathcal{E}_5(D_3(m)) &= \mathcal{E}_{(3,3)}(D_3(m)) = \{e = uv \in \mathcal{E}(D_3(m)): d_u = 3, d_v = 3\}.\end{aligned}\tag{6}$$

Table 3 gives the detailed explanation about the edge partition of the edge set of  $D_3(m)$ .

**Theorem 3.** The SO and  $SO_{red}$  indices for  $D_3(m)$  are as follows:

$$(i) \text{SO}(D_3) = 2^{((3/2)+m)}\sqrt{5} + \sqrt{5} \times 2^{(m+1)} + 12 \times 2^{((1/2)+m)} + 10\sqrt{132^m} + 4\sqrt{10} + 68\sqrt{2}$$

$$(ii) \text{SO}_{red}(D_3) = 6 \times 2^{((1/2)+m)} + 10\sqrt{52^m} + 6 \times 2^m + 45\sqrt{2} + 8$$

*Proof.* From the edge partition of  $D_3(m)$  given in Table 3, we have the following computations of SO and  $SO_{red}$  indices:

$$\begin{aligned}\text{SO}(D_3) &= \sum_{ij} \sqrt{d_i^2 + d_j^2} + \sqrt{2^2 + 2^2}(3 \times 2^{m+1} + 1) = \sqrt{1^2 + 2^2}(2^{m+1}) + \sqrt{1^2 + 3^2}(4(2^{m-1} + 1)) \\ &\quad + \sqrt{2^2 + 3^2}(20 \times 2^{m-1}) + \sqrt{3^2 + 3^2}(22) = 2^{((3/2)+m)}\sqrt{5} + \sqrt{5} \times 2^{(m+1)} + 12 \times 2^{((1/2)+m)} + 10\sqrt{132^m} + 4\sqrt{10} + 68\sqrt{2}, \\ \text{SO}_{red}(D_3) &= \sum_{ij} \sqrt{(d_i - 1)^2 + (d_j - 1)^2} = \sqrt{(1 - 1)^2 + (2 - 1)^2}(2^{m+1}) + \sqrt{(1 - 1)^2 + (3 - 1)^2}(4(2^{m-1} + 1)) \\ &\quad + \sqrt{(2 - 1)^2 + (2 - 1)^2}(3 \times 2^{m+1} + 1) + \sqrt{(2 - 1)^2 + (3 - 1)^2}(20 \times 2^{m-1}) + \sqrt{(3 - 1)^2 + (3 - 1)^2}(22) \\ &= 6 \times 2^{((1/2)+m)} + 10\sqrt{52^m} + 6 \times 2^m + 45\sqrt{2} + 8.\end{aligned}\tag{7}$$

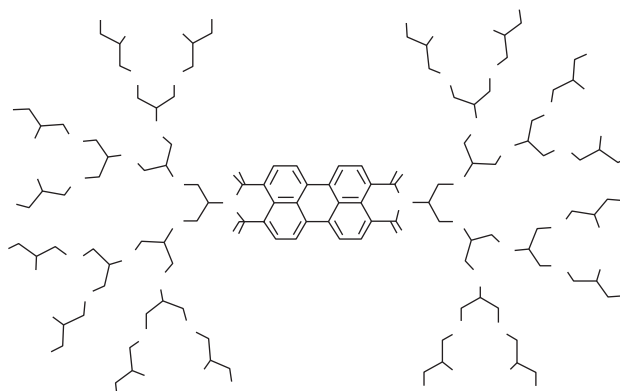
**3.4. Triazine-Based Dendrimers.** The divergent method is used for the synthesis of triazine-based dendrimers. Triazine-based dendrimers are less toxic and can be further studied as drug carriers. Let  $D_4(m)$  represent the molecular graph of triazine-based dendrimer drug carriers in the future. Figure 5 shows the molecular graph of  $D_4(m)$ .

From Figure 5, we can observe that the order and size of  $D_3(m)$  are  $(2(5 \times 2^{2m+2} + 1)/3)$  and  $7 \times 2^{2m+1} + 1$ , respectively. If  $\mathcal{V}(D_4(m))$  is the vertex set, then by observing

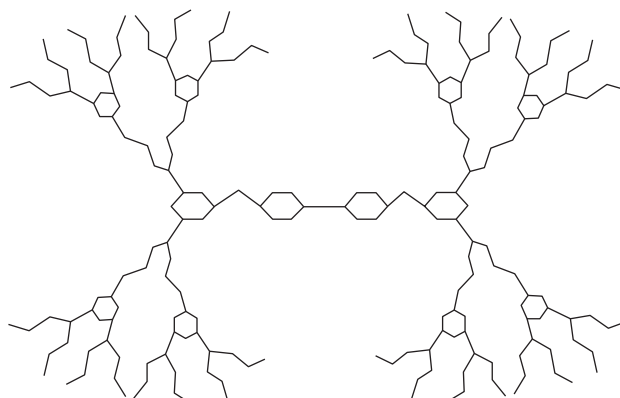
Figure 5, we can classify this vertex set into four subsets  $\mathcal{V}_1(D_4(m))$ ,  $\mathcal{V}_2(D_4(m))$ , and  $\mathcal{V}_3(D_4(m))$  such that  $|\mathcal{V}(D_4(m))| = |\mathcal{V}_1(D_4(m))| + |\mathcal{V}_2(D_4(m))| + |\mathcal{V}_3(D_4(m))|$ . The cardinalities of  $\mathcal{V}_1(D_4(m))$ ,  $\mathcal{V}_2(D_4(m))$ , and  $\mathcal{V}_3(D_4(m))$  are  $2^{2m+1}$ ,  $2^{2m+1} + (7 \times 4^{m+1}/6) + (4^{m+1}/3)$ , and  $4 + (5 \times 4^{m+1}/6) - (10/3)$ , respectively.

If  $\mathcal{E}(D_4(m))$  represents the edge set, then Figure 5 shows that there are the following four different types of edges present in the molecular graph of  $D_4(m)$ :

□

FIGURE 4:  $D_3(m)$  for  $m = 1$ .TABLE 3: Degree-based edge partition of  $D_3(m)$ .

$\mathcal{E}$	$\mathcal{E}_{(d_u, d_v)}$	Frequency
$\mathcal{E}_1$	$\mathcal{E}_{(1,2)}$	$2^{m+1}$
$\mathcal{E}_2$	$\mathcal{E}_{(1,3)}$	$4(2^{m-1} + 1)$
$\mathcal{E}_3$	$\mathcal{E}_{(2,2)}$	$3 \times 2^{m+1} + 1$
$\mathcal{E}_4$	$\mathcal{E}_{(2,3)}$	$20 \times 2^{m-1}$
$\mathcal{E}_5$	$\mathcal{E}_{(3,3)}$	22

FIGURE 5:  $D_4(m)$  for  $m = 2$ .

$$\begin{aligned}
 \mathcal{E}_1(D_4(m)) &= \mathcal{E}_{(1,2)}(D_4(m)) = \{e = uv \in \mathcal{E}(D_4(m)): d_u = 1, d_v = 2\}, \\
 \mathcal{E}_2(D_4(m)) &= \mathcal{E}_{(2,2)}(D_4(m)) = \{e = uv \in \mathcal{E}(D_4(m)): d_u = 2, d_v = 2\}, \\
 \mathcal{E}_3(D_4(m)) &= \mathcal{E}_{(2,3)}(D_4(m)) = \{e = uv \in \mathcal{E}(D_4(m)): d_u = 2, d_v = 3\}, \\
 \mathcal{E}_4(D_4(m)) &= \mathcal{E}_{(3,3)}(D_4(m)) = \{e = uv \in \mathcal{E}(D_4(m)): d_u = 3, d_v = 3\}.
 \end{aligned} \tag{8}$$

Table 4 gives the detailed explanation about the edge set of  $D_4(m)$ .

**Theorem 4.** The  $SO$  and  $SO_{red}$  indices for  $D_4(m)$  are as follows:

$$(i) \quad SO(D_4) = \sqrt{52}^{(m+1)} + (32/3)\sqrt{24}^m - (14/3)\sqrt{2} + (22/3)\sqrt{132}^m + (8/3)\sqrt{13}$$

$$(ii) \quad SO_{red}(D_4) = 4 \times 2^m + 6\sqrt{24}^m - (8/3)\sqrt{2} + (22/3)\sqrt{52}^m + (8/3)\sqrt{5}$$

*Proof.* From the edge partition of the edge set of  $D_4(m)$  given in Table 4, we have the following computations for  $SO$  and  $SO_{red}$  indices:



TABLE 4: Degree-based edge partition of  $D_4(m)$ .

$\mathcal{E}$	$\mathcal{E}_{(d_u, d_v)}$	Frequency
$\mathcal{E}_1$	$\mathcal{E}_{(1,2)}$	$2^{m+1}$
$\mathcal{E}_2$	$\mathcal{E}_{(2,2)}$	$(2(5 \times 2^{2m} - 2)/3)$
$\mathcal{E}_3$	$\mathcal{E}_{(2,3)}$	$(2(11 \times 2^{2m} + 4)/3)$
$\mathcal{E}_4$	$\mathcal{E}_{(3,3)}$	$(2 \times 2^{2m+1} - 1/3)$

$$\begin{aligned}
\text{SO}(D_4) \sum_{ij} \sqrt{d_i^2 + d_j^2} + \sqrt{2^2 + 2^2} (3 \times 2^{m+1} + 1) &= \sqrt{1^2 + 2^2} (2^{m+1}) + \sqrt{2^2 + 2^2} \left( \frac{2(5 \times 2^{2m} - 2)}{3} \right) \\
&+ \sqrt{2^2 + 3^2} \left( \frac{2(11 \times 2^{2m} + 4)}{3} \right) + \sqrt{3^2 + 3^2} \left( \frac{2 \times 2^{2m+1} - 1}{3} \right) \\
&\sqrt{5} 2^{(m+1)} + \frac{32}{3} \sqrt{2} 4^m - \frac{14}{3} \sqrt{2} + \frac{22}{3} \sqrt{13} 2^m + \frac{8}{3} \sqrt{13}, \\
\text{SO}_{\text{red}}(D_4) &= \sum_{ij} \sqrt{(d_i - 1)^2 + (d_j - 1)^2} = \sqrt{(1 - 1)^2 + (2 - 1)^2} (2^{m+1}) \\
&+ \sqrt{(2 - 1)^2 + (2 - 1)^2} \left( \frac{2(5 \times 2^{2m} - 2)}{3} \right) \\
&+ \sqrt{(2 - 1)^2 + (3 - 1)^2} \left( \frac{2(11 \times 2^{2m} + 4)}{3} \right) \\
&+ \sqrt{(3 - 1)^2 + (3 - 1)^2} \left( \frac{2 \times 2^{2m+1} - 1}{3} \right) \\
&4 \times 2^m + 6 \sqrt{2} 4^m - \frac{8}{3} \sqrt{2} + \frac{22}{3} \sqrt{5} 2^m + \frac{8}{3} \sqrt{5}.
\end{aligned} \tag{9}$$

3.5. *Aliphatic Polyamide Dendrimers.* Recently, Jishkariani, for the first time, studied aliphatic polyamide dendrimers containing ethylenediamine and piperazine. These dendrimers are enzymatically and hydrolytically stable. Let  $D_5(m)$  represent the molecular graph of the aliphatic polyamide-based dendrimer. Figure 6 shows the molecular graph of  $D_5(m)$ .

From Figure 6, we can observe that the order and size of  $D_5(m)$  are  $2(2^{m+3} - 5)$ . If  $\mathcal{V}(D_5(m))$  is the vertex set, then

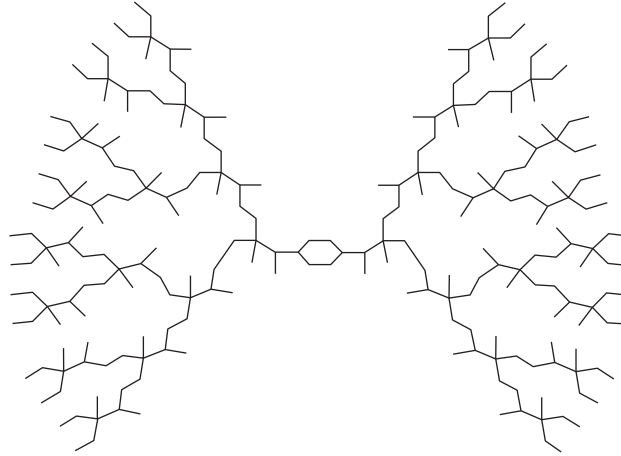
by observing Figure 6, we can classify this vertex set into three subsets  $\mathcal{V}_1(D_5(m))$ ,  $\mathcal{V}_2(D_5(m))$ , and  $\mathcal{V}_3(D_5(m))$  such that  $|\mathcal{V}(D_5(m))| = |\mathcal{V}_1(D_5(m))| + |\mathcal{V}_2(D_5(m))| + |\mathcal{V}_3(D_5(m))| + |\mathcal{V}_4(D_5(m))|$ . The cardinalities of  $\mathcal{V}_1(D_5(m))$ ,  $\mathcal{V}_2(D_5(m))$ , and  $\mathcal{V}_3(D_5(m))$  are  $4(3 \times 2^{m-1} - 1)$ ,  $4(3 \times 2^{m-1} - 1)$ , and  $2^{m+1} 2(2^m - 1)$ , respectively.

If  $\mathcal{E}(D_5(m))$  represents the edge set, then Figure 6 shows that there are the following four different types of edges present in the molecular graph of  $D_5(m)$ :

$$\begin{aligned}
\mathcal{E}_1(D_5(m)) &= \mathcal{E}_{(1,2)}(D_5(m)) = \{e = uv \in \mathcal{E}(D_5(m)): d_u = 1, d_v = 2\}, \\
\mathcal{E}_2(D_5(m)) &= \mathcal{E}_{(2,3)}(D_5(m)) = \{e = uv \in \mathcal{E}(D_5(m)): d_u = 2, d_v = 3\}, \\
\mathcal{E}_3(D_5(m)) &= \mathcal{E}_{(1,3)}(D_5(m)) = \{e = uv \in \mathcal{E}(D_5(m)): d_u = 1, d_v = 3\}, \\
\mathcal{E}_4(D_5(m)) &= \mathcal{E}_{(1,4)}(D_5(m)) = \{e = uv \in \mathcal{E}(D_5(m)): d_u = 1, d_v = 4\}.
\end{aligned} \tag{10}$$

Table 5 gives the detailed explanation about the edge set of  $D_5(m)$ .

**Theorem 5.** *The SO and SO<sub>red</sub> indices for  $D_5(m)$  are as follows:*

FIGURE 6:  $D_5(m)$  for  $m = 4$ .TABLE 5: Degree-based edge partition of  $D_5(m)$ .

$\mathcal{E}$	$\mathcal{E}_{(d_u, d_v)}$	Frequency
$\mathcal{E}_1$	$\mathcal{E}_{(1,2)}$	$2^{m+1}$
$\mathcal{E}_2$	$\mathcal{E}_{(2,3)}$	$2^{m+1}$
$\mathcal{E}_3$	$\mathcal{E}_{(1,3)}$	$2(2^m - 1)$
$\mathcal{E}_4$	$\mathcal{E}_{(1,4)}$	$2(2^m - 1)$
$\mathcal{E}_5$	$\mathcal{E}_{(2,2)}$	$2(2^m - 1)$
$\mathcal{E}_6$	$\mathcal{E}_{(3,4)}$	$2(2^m - 1)$
$\mathcal{E}_7$	$\mathcal{E}_{(3,3)}$	2
$\mathcal{E}_8$	$\mathcal{E}_{(2,4)}$	$2^{m+2} - 4$

$$(ii) SO_{red}(D_5) = 6\sqrt{132}^m + \sqrt{52}^{m+1} + 2^{((3/2)+m)} + 18 \times 2^m + 2\sqrt{2} - 6\sqrt{13} - 14$$

*Proof.* From the edge partition of the edge set of  $D_5(m)$  given in Table 5, we have the following computations of SO and  $SO_{red}$  indices:

$$(i) SO(D_5) = 2^{((3/2)+m)}\sqrt{5} + 10\sqrt{52}^m + 2^{(m+1)}\sqrt{17} - 2\sqrt{10} + \sqrt{132}^{(m+1)} + 4 \times 2^{((1/2)+m)} - 2\sqrt{17} - 8\sqrt{5} + 2\sqrt{2} + 10 \times 2^m - 10$$

$$SO(D_5) = \sum_{ij} \sqrt{d_i^2 + d_j^2} + \sqrt{2^2 + 2^2}(3 \times 2^{m+1} + 1) = \sqrt{1^2 + 2^2}(2^{m+1}) + \sqrt{2^2 + 3^2}(2^{m+1}) + \sqrt{1^2 + 3^2}(2(2^m - 1)) + \sqrt{1^2 + 4^2}(2(2^m - 1)) + \sqrt{2^2 + 2^2}(2(2^m - 1)) + \sqrt{3^2 + 4^2}(2(2^m - 1))$$

$$\sqrt{3^2 + 3^2}(2) + \sqrt{2^2 + 4^2}(2^{m+2} - 4) = 2^{((3/2)+m)}\sqrt{5} + 10\sqrt{52}^m + 2^{(m+1)}\sqrt{17} - 2\sqrt{10} + \sqrt{132}^{(m+1)} + 4 \times 2^{((1/2)+m)} - 2\sqrt{17} - 8\sqrt{5} + 2\sqrt{2} + 10 \times 2^m - 10,$$

$$SO_{red}(D_5) = \sum_{ij} \sqrt{(d_i - 1)^2 + (d_j - 1)^2} = \sqrt{(1-1)^2 + (2-1)^2}(2^{m+1}) + \sqrt{(2-1)^2 + (3-1)^2}(2^{m+1}) + \sqrt{(1-1)^2 + (3-1)^2}(2(2^m - 1)) + \sqrt{(1-1)^2 + (4-1)^2}(2(2^m - 1)) + \sqrt{(2-1)^2 + (2-1)^2}(2(2^m - 1)) + \sqrt{(3-1)^2 + (4-1)^2}(2(2^m - 1)) + \sqrt{(3-1)^2 + (3-1)^2}(2) + \sqrt{(2-1)^2 + (4-1)^2}(2^{m+2} - 4) = 6\sqrt{132}^m + \sqrt{52}^{m+1} + 2^{((3/2)+m)} + 18 \times 2^m + 2\sqrt{2} - 6\sqrt{13} - 14.$$

(11)

□

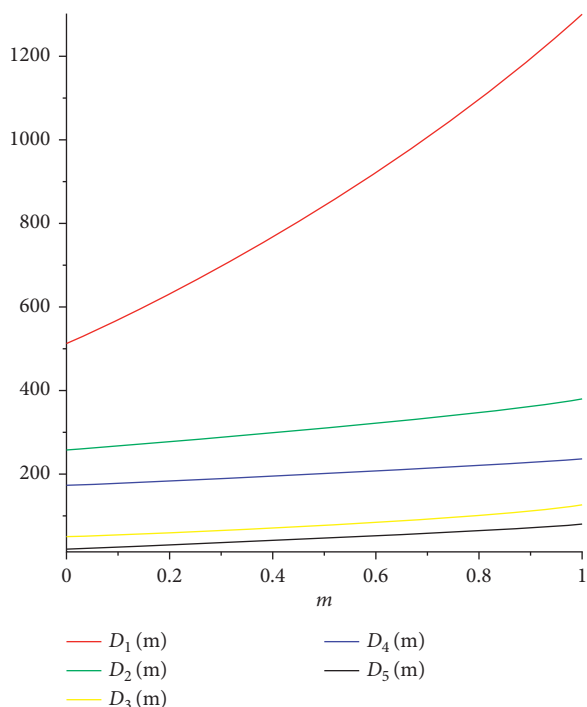


FIGURE 7: Comparison of SO for  $D_1(m)$ ,  $D_2(m)$ ,  $D_3(m)$ ,  $D_4(m)$ , and  $D_5(m)$ .

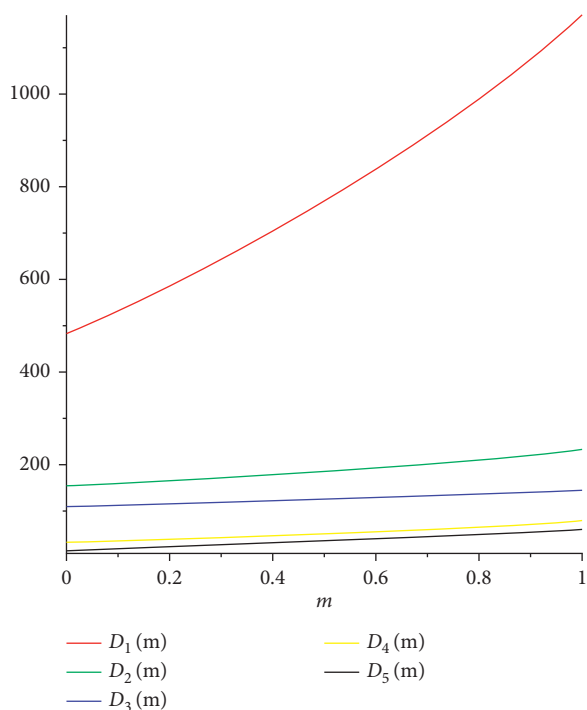


FIGURE 8: Comparison of  $SO_{red}$  for  $D_1(m)$ ,  $D_2(m)$ ,  $D_3(m)$ ,  $D_4(m)$ , and  $D_5(m)$ .

#### 4. Conclusion

Topological indices found numerous applications in many regions of material science, arithmetic, informatics, biology, and so on. However, their most important use is in the

nonexact quantitative structure-property relationships (QSPR) and quantitative structure-activity relationships (QSAR). Topological indices have an interconnection with the structure of the chemical structure. In this paper, we computed the newly introduced Sombor indices for phosphorus-containing dendrimers, porphyrin-cored dendrimers, PDI-cored dendrimers, triazine-based dendrimers, and aliphatic polyamide dendrimers. Figures 7 and 8 give the graphical comparison of computed results for the aforementioned dendrimers.

#### Data Availability

All the data required for this research are included within this paper.

#### Conflicts of Interest

The authors declare no conflicts of interest.

#### Authors' Contributions

Shahid Amin proved the main results, Abaid Ur Rehman Virk designed the problem, M.A. Rehman verified the results, and Nehad Ali Shah wrote the whole paper.

#### References

- [1] B. K. Nanjwade, H. M. Bechra, G. K. Derkar, F. V. Manvi, and V. K. Nanjwade, "Dendrimers: emerging polymers for drug-delivery systems," *European Journal of Pharmaceutical Sciences*, vol. 38, no. 3, pp. 185–196, 2009.
- [2] D. Astruc, E. Boisselier, and C. Ornelas, "Dendrimers designed for functions: from physical photophysical and supramolecular properties to applications in sensing catalysis molecular electronics photonics and nanomedicine," *Chemical Reviews*, vol. 110, no. 4, pp. 1857–1959, 2010.
- [3] R. K. Tekade, T. Dutta, V. Gajbhiye, and N. K. Jain, "Exploring dendrimer towards dual drug delivery: pH responsive simultaneous drug-release kinetics," *Journal of Microencapsulation*, vol. 26, no. 4, pp. 287–296, 2009.
- [4] A. Shabbir, M. F. Nadeem, S. Mukhtar, and A. Raza, "On edge version of some degree-based topological indices of HAC5C7  $[p, q]$  and VC5C7  $[p, q]$  nanotubes," *Polycyclic Aromatic Compounds*, pp. 1–17, 2020.
- [5] A. Ahmad, K. Elahi, R. Hasni, and M. F. Nadeem, "Computing the degree based topological indices of line graph of benzene ring embedded in P-type-surface in 2D network," *Journal of Information and Optimization Sciences*, vol. 40, no. 7, pp. 1511–1528, 2019.
- [6] M. F. Nadeem, M. Azeem, and H. M. A. Siddiqui, "Comparative study of Zagreb indices for capped semi-capped and uncapped carbon nanotubes," *Polycyclic Aromatic Compounds*, pp. 1–18, 2021.
- [7] F. M. Brückler, T. Dožalic, A. Graovac, and I. Gutman, "On a class of distance-based molecular structure descriptors," *Chemical Physics Letters*, vol. 503, no. 4–6, pp. 336–338, 2011.
- [8] H. Gonzalez-Diaz, S. Vilar, L. Santana, and E. Uriarte, "Medicinal chemistry and bioinformatics - current trends in drugs discovery with networks topological indices," *Current Topics in Medicinal Chemistry*, vol. 7, no. 10, pp. 1015–1029, 2007.

- [9] H. Hosoya, K. Hosoi, and I. Gutman, "A topological index for the total  $\pi$ -electron energy," *Theoretica Chimica Acta*, vol. 38, no. 1, 1975.
- [10] M. Munir, W. Nazeer, S. Rafique, and S. Kang, "M-polynomial and degree-based topological indices of polyhex nanotubes," *Symmetry*, vol. 8, no. 12, p. 149, 2016.
- [11] M. Munir, W. Nazeer, Z. Shahzadi, and S. Kang, "Some invariants of circulant graphs," *Symmetry*, vol. 8, no. 11, p. 134, 2016.
- [12] H. Wiener, "Structural determination of paraffin boiling points," *Journal of the American Chemical Society*, vol. 69, no. 1, pp. 17–20, 1947.
- [13] M. Randić, "Characterization of molecular branching," *Journal of the American Chemical Society*, vol. 97, no. 23, pp. 6609–6615, 1975.
- [14] M. Munir, W. Nazeer, S. Rafique, and S. Kang, "M-polynomial and related topological indices of Nanostar dendrimers," *Symmetry*, vol. 8, no. 9, p. 97, 2016.
- [15] A. R. Virk, "Multiplicative shingali and kanabour indices for bismuth tri-iodide," *Journal of Prime Research in Mathematics*, vol. 16, no. 2, pp. 80–88, 2020.
- [16] Y. Kwun, A. Virk, W. Nazeer, M. Rehman, and S. Kang, "On the multiplicative degree-based topological indices of silicon-carbon  $\text{Si}_2\text{C}_3\text{-I}$   $[p, q]$  and  $\text{Si}_2\text{C}_3\text{-II}$   $[p, q]$ ," *Symmetry*, vol. 10, no. 8, p. 320, 2018.
- [17] A. u. R. Virk, M. N. Jhangeer, M. N. Jhangeer, and M. A. Rehman, "Reverse Zagreb and reverse hyper-zagreb indices for silicon carbide  $\text{Si}_2\text{C}_3\text{I}$   $[r, s]$  and  $\text{Si}_2\text{C}_3\text{II}$   $[r, s]$ ," *Engineering and Applied Science Letters*, vol. 1(2018), no. 2, pp. 37–50, 2018.
- [18] Z. Shao, A. R. Virk, M. S. Javed, M. A. Rehman, and M. R. Farahani, "Degree based graph invariants for the molecular graph of bismuth tri-iodide," *Engineering and Applied Science Letters*, vol. 2, no. 1, pp. 01–11, 2019.
- [19] I. Gutman, "Some basic properties of Sombor indices," *Open Journal of Discrete Applied Mathematics*, vol. 4, no. 1, pp. 1–3, 2021.
- [20] M. Numan, S. I. Butt, S. I. Butt, and A. Taimur, "Super cyclic antimagic covering for some families of graphs," *Open Journal of Mathematical Sciences*, vol. 5, no. 1, pp. 27–33, 2021.
- [21] H. M. Nagesh and V. R. Girish, "On the entire Zagreb indices of the line graph and line cut-vertex graph of the subdivision graph," *Open Journal of Mathematical Sciences*, vol. 4, no. 1, pp. 470–475, 2020.

## Research Article

# Forgotten Index of Generalized Operations on Graphs

Muhammad Javaid <sup>1</sup>, Saira Javed <sup>1</sup>, Saima Q. Memon,<sup>2</sup>  
and Abdulaziz Mohammed Alanazi <sup>3</sup>

<sup>1</sup>Department of Mathematics, School of Science, University of Management and Technology, Lahore 54770, Pakistan

<sup>2</sup>M. A. Kazi Institute of Chemistry, University of Sindh, Jamshoro, Pakistan

<sup>3</sup>Department of Mathematics, University of Tabuk, Tabuk 71491, Saudi Arabia

Correspondence should be addressed to Muhammad Javaid; javaidmath@gmail.com

Received 4 March 2021; Revised 21 March 2021; Accepted 27 March 2021; Published 3 May 2021

Academic Editor: Kashif Ali

Copyright © 2021 Muhammad Javaid et al. This is an open access article distributed under the Creative Commons Attribution License, which permits unrestricted use, distribution, and reproduction in any medium, provided the original work is properly cited.

In theoretical chemistry, several distance-based, degree-based, and counting polynomial-related topological indices (TIs) are used to investigate the different chemical and structural properties of the molecular graphs. Furtula and Gutman redefined the  $F$ -index as the sum of cubes of degrees of the vertices of the molecular graphs to study the different properties of their structure-dependency. In this paper, we compute  $F$ -index of generalized sum graphs in terms of various TIs of their factor graphs, where generalized sum graphs are obtained by using four generalized subdivision-related operations and the strong product of graphs. We have analyzed our results through the numerical tables and the graphical presentations for the particular generalized sum graphs constructed with the help of path (alkane) graphs.

## 1. Introduction

Throughout the paper, we consider a simple and undirected graph  $H = (V(H), E(H))$  with vertex-set  $V(H) = \{v_1, v_2, v_3, \dots, v_n\}$  and edge-set  $E = \{e_1, e_2, \dots, e_m\} \subseteq V(H) \times V(H)$ , where  $n = |V(H)|$  and  $m = |E(H)|$ . A molecular graph is a connected and undirected graph in which atoms are presented by vertices, and chemical bonds between these atoms are shown by edges (see Figure 1). For a finite set of graphs  $\mathcal{G}$  and set of real numbers  $\mathbb{R}$ , the function  $I: \mathcal{G} \rightarrow \mathbb{R}$  defined by  $I(H) = \sum_{u \in V(H)} f(u)$  is called a degree-based topological index (TI), where the graph  $H$  belongs to  $\mathcal{G}$  and  $f(u)$  is a degree-function from the vertex-set of  $H$  to the degree-set of its vertices. It is important to know that  $I(H) = I(K)$  if and only if  $H$  is isomorphic to  $K$ . For more details, see [1, 2].

Graph-theoretic modeling of the molecular graphs plays a fundamental part in the analysis of the quantitative structures activity/property relationships (QSAR/QSPR). In chemistry, the study of structural relationships is used to characterize the various physicochemical properties of

organic molecules such as surface tension, density, melting, freezing point, solubility, heat of evaporation, and heat of formation [3]. In last two decades, many TIs are introduced, but degree-based TIs got much more attention of the researchers, see the latest survey [4]. In 1947, Winer introduced the first distance-based TI to compute the boiling point of paraffin [5]. Also, we refer [6].

In molecular graph theory, the different operations on a graph perform a fundamental role in the formation of different new classes of graphs. Yan et al. [7] introduced the four operations  $S_1$ ,  $R_1$ ,  $Q_1$ , and  $T_1$  on a graph  $H$  and computed the Wiener indices for the graphs  $F_1(H)$ , where  $F_1 \in \{S_1, R_1, Q_1, T_1\}$ . Eliazi and Taeri [8] defined the  $F_1$ -sum graphs  $(H_{1+F_1}H_2)$  using the Cartesian product on graphs  $F_1(H_1)$  and  $H_2$ , where  $H_1$  and  $H_2$  are any two simple and connected graphs. They also computed the Wiener indices for these  $F_1$ -sum graphs. Furthermore, Deng et al. [9] calculated the  $M_1$  and  $M_2$  Zagreb indices, Imran and Shehbaz [10] computed the  $F$ -index, Liu et al. [11] computed the first general Zagreb, Chu et al. [12] calculated the bounds of first general Zagreb index and general Randic index, and

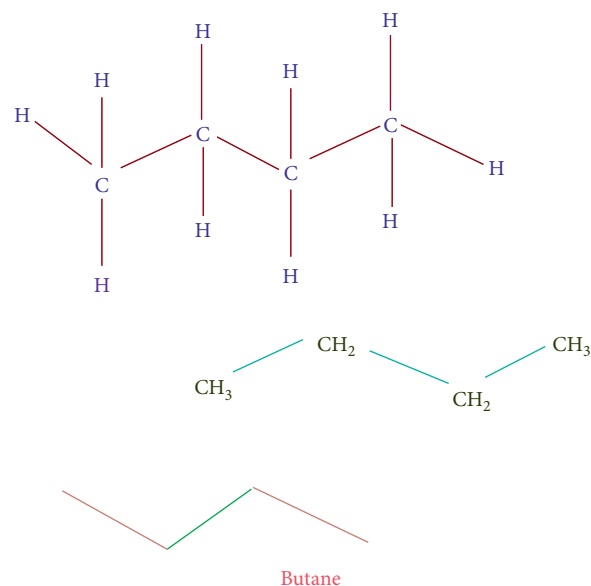


FIGURE 1: Clearly, structural formula of butane is isomorphic to  $P_4$ .

Sarala et al. [13] computed the  $F$ -index for these  $F_1$ -sum graphs under the Cartesian and strong products. We also refer [14–20].

Recently, for  $k \geq 1$ , Liu et al. [21] defined the generalized  $F$ -sum ( $F_k$ -sum) graphs using Cartesian product and computed their Zagreb indices. Moreover, Awais et al. computed the  $F$ -index [22], hyper-Zagreb [23], and FGZ index [24] for these generalized  $F$ -sum graphs. Recently, Javaid et al. [25] computed first and second Zagreb indices for the generalized  $F$ -sum graphs under the strong product.

In this paper, we compute  $F$ -index of generalized sum graphs in terms of various TIs of their factor graphs, where generalized sum graphs are obtained by using four generalized subdivision-related operations and the strong product of graphs. We have analyzed our results through the numerical tables and the graphical presentations for the particular generalized sum graphs constructed with the help of path (alkane) graphs. The remaining paper is managed as follows: Section 2 consists of elementary definitions, Section 3 includes main results, and Section 4 covers the application and conclusion.

## 2. Preliminaries

**2.1. Degree-Based Topological Indices.** In 1972, Trainajsi and Gutman defined first and second Zagreb indices that are utilized to find the  $\pi$ -electron energy of molecular graphs [26]. Let  $H$  be any graph (molecular structure), then the first and second Zagreb indices are defined as  $M_1(H) = \sum_{v \in V(H)} d^2(v)$  and  $M_2(H) = \sum_{uv \in E(H)} d(u)d(v)$ .

In 2015, Furtula and Gutman [22] redefined a TI called by forgotten TI [27]. The forgotten TI of a (molecular) graph  $H$  is defined as

$$F(H) = \sum_{v \in V(H)} d^3(v). \quad (1)$$

They also verified that the different predictive abilities of  $F$ -index and first Zagreb index are same. In particular, both the indices yield the values of correlation coefficients for entropy and acentric factor more than 0.95. For more results on its mathematical properties and chemical applications, see [23].

**2.2. Four Generalized Operations.** Let  $H_1$  be a (molecular) graph, then for the integral value  $k \geq 1$ , the graphs  $(F_k(H_1))$  under the four generalized operations ( $F_k \in \{S_k, R_k, Q_k, T_k\}$ ) on  $H_1$  are defined as follows [21]:

- (i)  $k$ -subdivision graph: we add  $k$  new vertices in every edge of  $H_1$  and obtain the new  $k$ -subdivision graph  $S_k(H_1)$
- (ii)  $k$ -semitotal point graph: the graph  $k$ -semitotal point ( $R_k(H_1)$ ) is defined from the graph  $S_k(H_1)$  by joining the vertices of  $S_k(H_1)$  which were adjacent in  $H_1$
- (iii)  $k$ -semitotal line graph: the  $k$ -semitotal line graph  $Q_k(H_1)$  is defined from the graph  $S_k(H_1)$  by joining the newly added  $k$  vertices for each incident pair of edges of  $H_1$
- (iv)  $k$ -total point graph: the  $k$ -total point graph is defined from the graph  $S_k(H_1)$  by applying both the operations  $R_k$  and  $Q_k$ , respectively. For more details, see Figures 2–4.

**2.3. Generalized Sum Operation for Strong Product.** Let  $H_1$  and  $H_2$  be two graphs,  $F_k \in \{S_k, R_k, Q_k, T_k\}$  presents generalized operations and  $F_k(H_1)$  is obtained after applying  $F_k$  on  $H_1$  having edge-set  $E(F_k(H_1))$  and node-set  $V(F_k(H_1))$ . The generalized  $F$ -sum graphs  $(H_{1F_k} \boxtimes H_2)$  under the operation of strong product is a graph having a vertex-set:

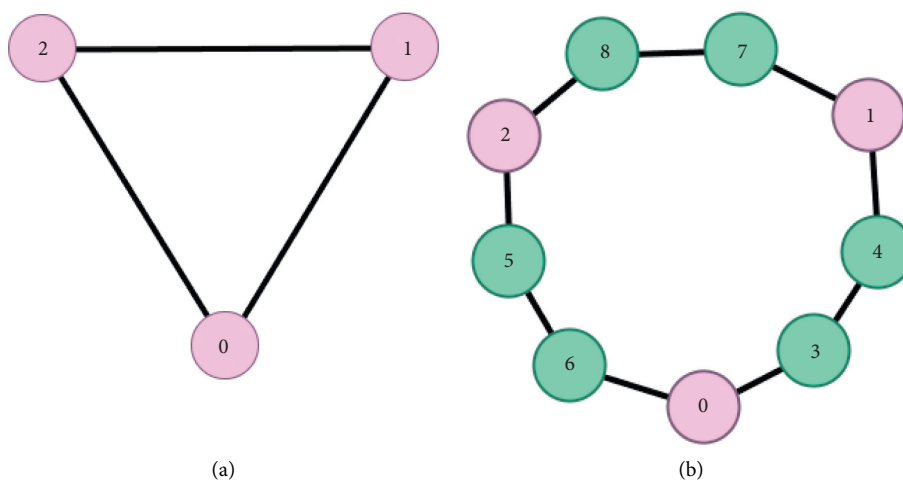


FIGURE 2: (a)  $H_1 \cong C_3$ . (b)  $S_3(H_1)$ .

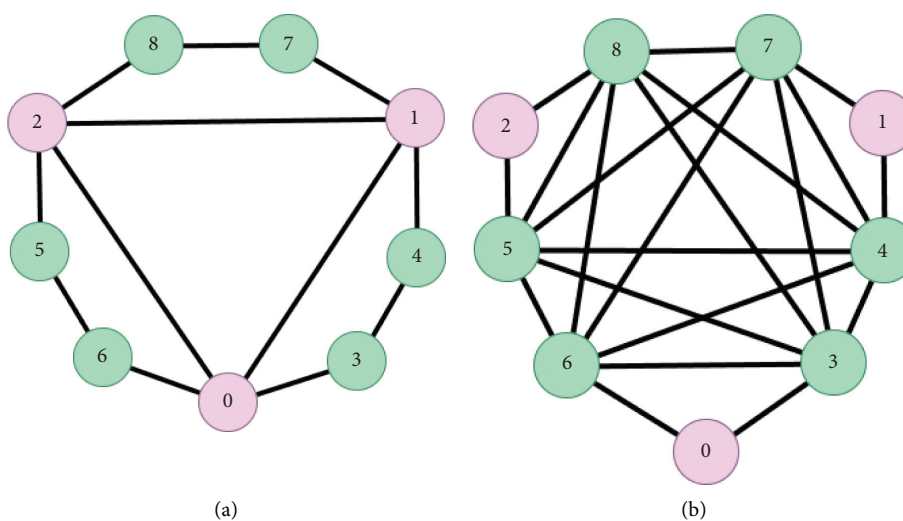


FIGURE 3: (a)  $R_3(H_1)$ . (b)  $Q_3(H_1)$ .

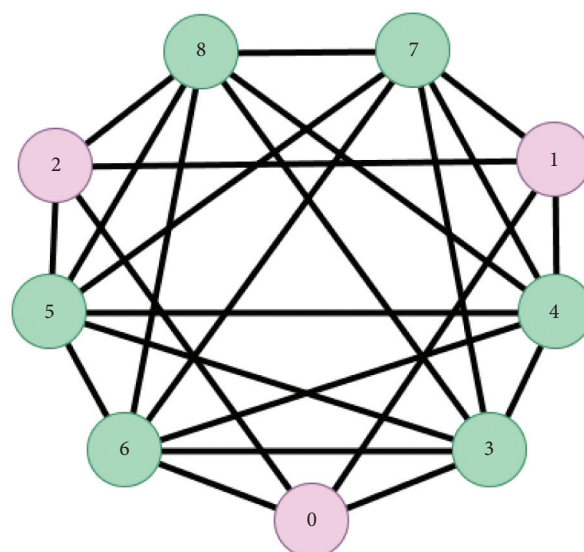


FIGURE 4:  $T_3(H_1)$ .

$$\begin{aligned} V(H_{1F_k} \boxtimes H_2) &= V(F_k(H_1)) \times V(H_2) \\ &= (V(H_1) \cup kE(H_1)) \times V(H_2), \end{aligned} \quad (2)$$

such that two vertices  $(s_1, t_1)$  and  $(s_2, t_2)$  of  $V(H_{1F_k} \boxtimes H_2)$  are adjacent iff  $s_1 = s_2 \in V(H_1)$  and  $(t_1, t_2) \in E(H_2)$  or  $t_1 = t_2 \in V(H_2)$  and  $(s_1, s_2) \in E(F_k(H_1))$  or  $(t_1, t_2) \in E(H_2)$  and  $(s_1, s_2) \in E(F_k(H_1))$ , where  $k \geq 1$  is natural number. Furthermore, the generalized  $F$ -sum graphs  $(H_{1F_k} \boxtimes H_2)$  contain  $|V(H_2)|$  copies of graphs  $F_k(H_1)$  that are labeled

with the vertices of  $H_2$ . For more explanation, see Figures 5–7.

### 3. Methodology

This section presents the main results.

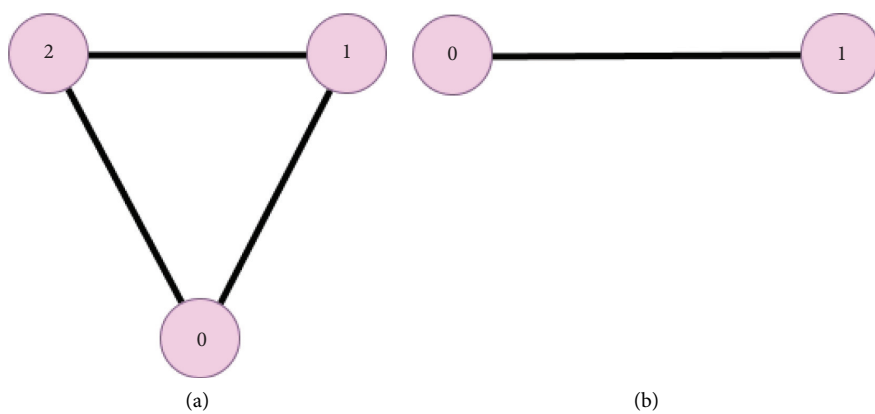
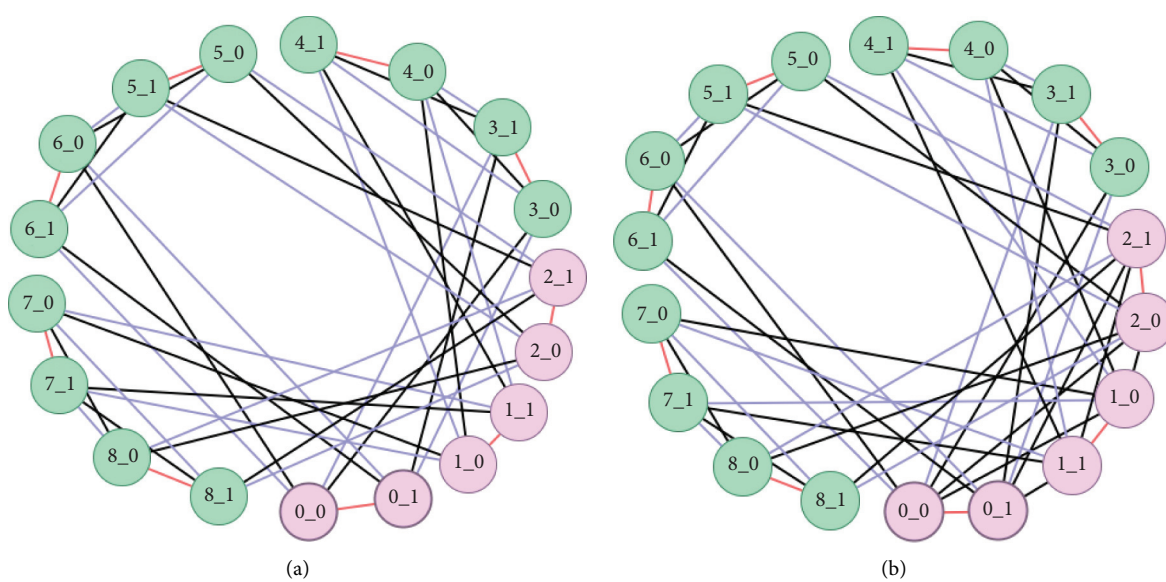
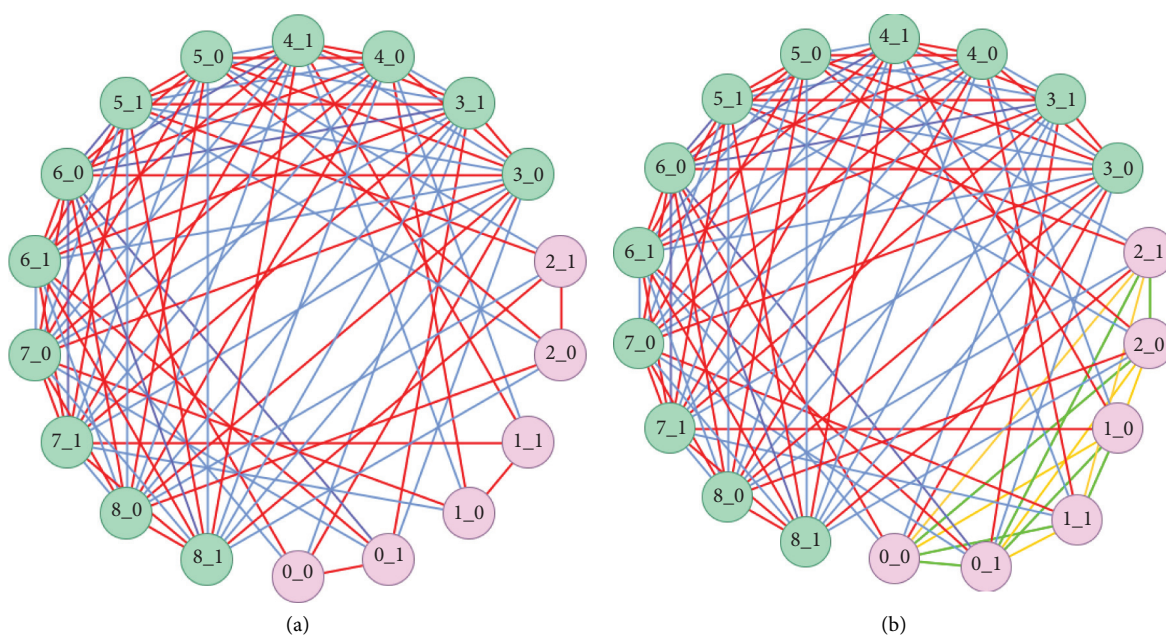
**Theorem 1.** Let  $H_1$  and  $H_2$  be two connected graphs, then

$$\begin{aligned} F(H_{1S_k} \boxtimes H_2) &= [|V(H_2)| + 3M_1(H_2) + 6|E(H_2)|]F(H_1) + [|V(H_1)| + 3M_1(H_1) + 14|E(H_1)|]F(H_2) \\ &\quad + 6|E(H_2)|M_1(H_1) + 30|E(H_1)|M_1(H_2) + 6M_1(H_1)M_1(H_2) + 48|E(H_1)||E(H_2)|| \\ &\quad + 8(k-1)|E(H_1)|[6|E(H_2)| + |V(H_2)| + F(H_2) + 3M_1(H_2)] + F(H_1)F(H_2) \\ &\quad + 8|V(H_2)||E(H_1) \end{aligned} \quad (3)$$

*Proof.* Let  $d(s, t) = d_{H_{1S_k} \boxtimes H_2}(s, t)$  is the degree of the vertex  $(s, t)$  in  $H_{1S_k} \boxtimes H_2$ , then

$$\begin{aligned} F(H_{1S_k} \boxtimes H_2) &= \sum_{(s,t) \in V(H_{1S_k} \boxtimes H_2)} d(s,t)^3 = \sum_{(s_1,t_1)(s_2,t_2) \in E(H_{1S_k} \boxtimes H_2)} [d(s_1,t_1)^2 + d(s_2,t_2)^2] \\ &= \sum_{s \in V(H_1)} \sum_{t_1, t_2 \in E(H_2)} [d(s,t_1)^2 + d(s,t_2)^2] + \sum_{t \in V(H_2)} \sum_{s_1, s_2 \in E(S_k(H_1))} [d(s_1,t)^2 + d(s_2,t)^2] \\ &\quad + \sum_{t_1, t_2 \in E(H_2)} \sum_{s_1, s_2 \in E(S_k(H_1))} [d(s_1,t_1)^2 + d(s_2,t_2)^2] = \sum_A + \sum_B + \sum_C. \\ \sum_A &= \sum_{s \in V(H_1)} \sum_{t_1, t_2 \in E(H_2)} [(d(s) + d(t_1) + d(s)d(t_1))^2 + (d(s) + d(t_2) + d(s)d(t_2))^2] \\ &= \sum_{s \in V(H_1)} \sum_{t_1, t_2 \in E(H_2)} [2d(s)^2 + (d(t_1)^2 + d(t_2)^2) + d^2(s)(d^2(t_1) + d^2(t_2))] \\ &\quad + 2d(s)(d(t_1) + d(t_2)) + 2d^2(s)(d(t_1) + d(t_2)) + 2d(s)(d^2(t_1) + d^2(t_2))] \\ &= 2|E(H_2)|M_1(H_1) + |V(H_1)|F(H_2) + 4|E(H_1)|M_1(H_2) + M_1(H_1)F(H_2) \\ &\quad + 2M_1(H_1)M_1(H_2) + 4|E(H_1)|F(H_2), \\ \sum_B &= \sum_{t \in V(H_2)} \sum_{s_1, s_2 \in E(S_k(H_1))} [d^2(s_1, t) + d^2(s_2, t)] = \sum_{t \in V(H_2)} \sum_{\substack{s_1 \in V(H_1), \\ s_2 \in V(S_k(H_1)-H_1)}} [d^2(s_1, t) + d^2(s_2, t)] \\ &\quad + \sum_{t \in V(H_2)} \sum_{s_1, s_2 \in V(S_k(H_1)-H_1)} [d^2(s_1, t) + d^2(s_2, t)] = \sum_{B_1} + \sum_{B_2}. \\ \sum_{B_1} &= \sum_{t \in V(H_2)} \sum_{\substack{s_1, s_2 \in E(S_k(H_1)), \\ s_2 \in V(S_k(H_1)-H_1)}} [(d(s_1) + d(t) + d(s_1)d(t))^2 + (d(s_2) + d(s_2)d(t))^2] \\ &= \sum_{t \in V(H_2)} \sum_{\substack{s_1, s_2 \in E(S_k(H_1)), \\ s_2 \in V(S_k(H_1)-H_1)}} [d(s_1)^2 + d(s_2)^2 + d(t)^2(d(s_1)^2 + d(s_2)^2)] \\ &\quad + 2d(t)(d(s_1)^2 + d(s_2)^2) + 2d(t)(d(s_1) + 2d^2(t))(d(s_1) + d^2(t))]. \end{aligned} \quad (4)$$



FIGURE 5: (a)  $H_1 = C_3$ . (b)  $H_2 = P_2$ .FIGURE 6: (a)  $H_{1s_2} \boxtimes H_2$ . (b)  $H_{1r_2} \boxtimes H_2$ .FIGURE 7: (a)  $H_{1o_2} \boxtimes H_2$ . (b)  $H_{1r_2} \boxtimes H_2$ .

Since  $s_1 \in V(H_1)$  and  $s_2 \in V(S_k(H_1) - H_1)$ , therefore

$$= |V(H_2)|F(S_1(H_1)) + 2|E(H_1)|M_1(H_2) + 4|E(H_2)M_1(H_1) + 4|E(H_2)F(S_1(H_1)) + M_1(H_2)F(S_1(H_1)) + 2M_1(H_1)M_1(H_2). \quad (5)$$

We know that  $F(S_1(H_1)) = F(H_1) + 8|E(H_1)|$ .

$$\begin{aligned} &= [|V(H_2)| + 4|E(H_2) + M_1(H_2)] [F(H_1) + 8|E(H_1)|] + 2|E(H_1)|M_1(H_2) + 4|E(H_2)M_1(H_1) \\ &+ 4|E(H_2) + 2M_1(H_1)M_1(H_2), \\ \sum_{B_2} &= \sum_{t \in V(H_2)} \sum_{\substack{s_1, s_2 \in E(S_k(H_1))_{s_1}, \\ s_2 \in V(S_k(H_1) - H_1)}} [(d(s_1) + d(s_1)d(t))^2 + (d(s_2) + d(s_2)d(t))^2] \\ &= \sum_{t \in V(H_2)} \sum_{\substack{s_1, s_2 \in E(S_k(H_1))_{s_1}, \\ s_2 \in V(S_k(H_1) - H_1)}} [d(s_1)^2 + d(s_2)^2 + d(t)^2(d(s_1)^2 + d(s_2)^2) + 2d(t)(d(s_1)^2 + d(s_2)^2)] \\ &= \sum_{t \in V(H_2)} \sum_{\substack{s_1, s_2 \in E(S_k(H_1))_{s_1}, \\ s_2 \in V(S_k(H_1) - H_1)}} [(2)^2 + (2)^2 + 8d_{H_2}(t)^2 + 16d_{H_2}(t)]. \end{aligned} \quad (6)$$

Since in this case  $|E(S_k(H_1))| = |E(H_1)|(k - 1)$ , so

$$\begin{aligned} &= 8(k - 1)|V(H_2)||E(H_1)| + 8(k - 1)M_1(H_2)|E(H_1)| + 32(k - 1)|E(H_2)||E(H_1)|, \\ \sum_C &= \sum_{t_1, t_2 \in E(H_2)} \sum_{s_1, s_2 \in E(S_k(H_1))} [d^2(s_1, t_1) + d^2(s_2, t_2)] = \sum_{t_1, t_2 \in E(H_2)} \sum_{\substack{s_1 \in V(H_1), \\ s_2 \in V(S_k(H_1) - H_1)}} [d^2(s_1, t_1) + d^2(s_2, t_2)] \\ &+ \sum_{t_1, t_2 \in E(H_2)} \sum_{s_1, s_2 \in V(S_k(H_1) - H_1)} [d^2(s_1, t_1) + d^2(s_2, t_2)] = \sum_{C_1} + \sum_{C_1} \\ \sum_{C_1} &= \sum_{t_1, t_2 \in V(H_2)} \sum_{\substack{s_1, s_2 \in E(S_k(H_1))_{s_1} \in V(H_1), \\ s_2 \in V(S_k(H_1) - H_1)}} [(d(s_1) + d(t_1) + d(s_1)d(t_1))^2 + (d(s_2) + d(s_2)d(t_2))^2] \\ &= \sum_{t \in V(H_2)} \sum_{\substack{s_1, s_2 \in E(S_k(H_1))_{s_1} \in V(H_1), \\ s_2 \in V(S_k(H_1) - H_1)}} [d(s_1)^2 + d(s_2)^2 + d(t_1)^2d(s_1)^2 + d(t_2)^2d(s_2)^2] \\ &+ 2d(t_1)d(s_1)^2 + 2d(t_2)d(s_2)^2 + 2d(t_1)(d(s_1) + 2d^2(t_1))(d(s_1) + d_{H_2}^2(t_1))] \\ &= 2|E(H_2)||F(G_1) + 16|E(H_1)||E(H_2)| + 2|E(H_1)|F(G_2) + F(G_1)F(G_2) + 2M_1(H_1)M_1(H_2) \\ &+ 2F(G_1)M_1(H_2) + 2M_1(H_1)F(G_2) + 8|E(H_1)|F(G_2) + 16|E(H_1)|M_1(H_2), \\ \sum_{C_2} &= \sum_{t_1, t_2 \in E(H_2)} \sum_{\substack{s_1, s_2 \in E(S_k(H_1))_{s_1}, \\ s_2 \in V(S_k(H_1) - H_1)}} [(d(s_1) + d(s_1)d(t_1))^2 + (d(s_2) + d(s_2)d(t_2))^2] \\ &= \sum_{t_1, t_2 \in E(H_2)} \sum_{\substack{s_1, s_2 \in E(S_k(H_1))_{s_1}, \\ s_2 \in V(S_k(H_1) - H_1)}} [8 + 4(d^2(t_1) + d^2(t_2)) + 8(d(t_1) + d(t_2))] \\ &= 16(k - 1)|E(H_2)||E(H_1)| + 8(k - 1)F(H_2)|E(H_1)| + 16(k - 1)|E(H_1)|M_1(H_2). \end{aligned} \quad (7)$$

We arrive at our desired result.

□ **Theorem 2.** Let  $H_1$  and  $H_2$  be two connected graphs, then

$$\begin{aligned}
F(H_{1R_k} \boxtimes H_2) &= 8[|V(H_2)| + 6|E(H_2)|]F(H_1) + [ |V(H_1)| + 20|E(H_1)| ]F(H_2) + 8F(H_1)F(H_2) \\
&+ 24|E(H_2)|M_1(H_1) + 36|E(H_1)|M_1(H_2) + 24M_1(H_1)M_1(H_2) + 24F(H_1)M_1(H_2) \\
&+ 8|V(H_2)||E(H_1)| + 8(k-1)|E(H_1)|[ |V(H_2)| + F(H_2) + 4|E(H_2)| + 3M_1(H_2) ] \\
&+ 48|E(H_1)||E(H_2)| + 12F(H_2)M_1(H_1).
\end{aligned} \tag{8}$$

*Proof.* Let  $d(s, t) = d_{H_{1R_k} \boxtimes H_2}(s, t)$  is the degree of the vertex  $(s, t)$  in  $H_{1R_k} \boxtimes H_2$ , then

$$\begin{aligned}
F(H_{1R_k} \boxtimes H_2) &= \sum_{(s,t) \in V(H_{1R_k} \boxtimes H_2)} d(s, t)^3 = \sum_{(s_1, t_1), (s_2, t_2) \in E(H_{1R_k} \boxtimes H_2)} [d(s_1, t_1)^2 + d(s_2, t_2)^2] \\
&= \sum_{s \in V(H_1)} \sum_{t_1, t_2 \in E(H_2)} [d(s, t_1)^2 + d(s, t_2)^2] + \sum_{t \in V(H_2)} \sum_{s_1, s_2 \in E(R_k(H_1))} [d(s_1, t)^2 + d(s_2, t)^2] \\
&+ \sum_{t_1, t_2 \in E(H_2)} \sum_{s_1, s_2 \in E(R_k(H_1))} [d(s_1, t_1)^2 + d(s_2, t_2)^2] = \sum_A + \sum_B + \sum_C. \\
\sum_A &= \sum_{s \in V(H_1)} \sum_{t_1, t_2 \in E(H_2)} [d(s, t_1)^2 + d(s, t_2)^2] = 8|E(H_2)|M_1(H_1) + |V(H_1)|F(H_2) \\
&+ 4M_1(H_1)F(H_2) + 8|E(H_1)|M_1(H_2) + 8M_1(H_1)M_1(H_2) + 8|E(H_1)|F(H_2), \\
\sum_B &= \sum_{t \in V(H_2)} \sum_{\substack{s_1, s_2 \in V(H_1), \\ s_1, s_2 \in V(H_1)}} [d^2(s_1, t) + d^2(s_2, t)] + \sum_{t \in V(H_2)} \sum_{\substack{s_1 \in V(H_1), \\ s_2 \in V(R_k(H_1) - H_1)}} [d^2(s_1, t) + d^2(s_2, t)] \\
&+ \sum_{t \in V(H_2)} \sum_{s_1, s_2 \in V(R_k(H_1) - H_1)} [d^2(s_1, t) + d^2(s_2, t)] = \sum_{B_1} + \sum_{B_2} + \sum_{B_3}. \\
\sum_{B_1} &= \sum_{t \in V(H_2)} \sum_{\substack{s_1, s_2 \in E(R_k(H_1)), \\ s_2 \in V(H_1)}} [(d(s_1) + d(t) + d(s_1)d(t))^2 + (d(s_2) + d(t) + d(s_2)d(t))^2] \\
&= \sum_{t \in V(H_2)} \sum_{\substack{s_1, s_2 \in E(R_k(H_1)), \\ s_2 \in V(H_1)}} [4(d^2(s_1) + d^2(s_2)) + 2d^2(t) + 4d^2(t)(d^2(s_1) + d^2(s_2))] \\
&+ 4d(t)(d(s_1) + d(s_2)) + 4d^2(t)d(s_1) + d(s_2) + 8d(t)(d^2(s_1) + d^2(s_2))] \\
&= 4|V(H_2)|F(H_1) + 2|E(H_1)|M_1(H_2) + 4M_1(H_2)F(H_1) + 8|E(H_2)|M_1(H_1) \\
&+ 4M_1(H_1)M_1(H_2) + 16|E(H_2)|F(H_1), \\
\sum_{B_2} &= \sum_{t \in V(H_2)} \sum_{\substack{s_1, s_2 \in E(R_k(H_1)), \\ s_2 \in V(R_k(H_1) - H_1)}} [(d(s_1) + d(t) + d(s_1)d(t))^2 + (d(s_2) + d(s_2)d(t))^2] \\
&= \sum_{t \in V(H_2)} \sum_{\substack{s_1, s_2 \in E(R_k(H_1)), \\ s_2 \in V(R_k(H_1) - H_1)}} [4d(s_1)^2 + d(s_2)^2 + d(t)^2(4d(s_1)^2 + d(s_2)^2)] \\
&+ 8d(t)(d(s_1)^2 + 4d(t)d(s_1) + 4d^2(t)(d(s_1) + d^2(t) + 2d(s_2)^2d(t))] \\
&= 4|V(H_2)|F(H_1) + 10|E(H_1)|M_1(H_2) + 4M_1(H_2)F(H_1) + 8|E(H_2)|M_1(H_1)a \\
&+ 4M_1(H_1)M_1(H_2) + 16|E(H_2)|F(H_1) + 8|V(H_2)||E(H_1)| + 32|E(H_1)||E(H_2)|, \\
\sum_{B_3} &= \sum_{t \in V(H_2)} \sum_{\substack{s_1, s_2 \in E(R_k(H_1)), \\ s_2 \in V(R_k(H_1) - H_1)}} [(d(s_1) + d(s_1)d(t))^2 + (d(s_2) + d(s_2)d(t))^2] \\
&= \sum_{t \in V(H_2)} \sum_{\substack{s_1, s_2 \in E(R_k(H_1)), \\ s_2 \in V(R_k(H_1) - H_1)}} [(d(s_1)^2 + d(s_2)^2) + d(t)^2(d(s_1)^2 + d(s_2)^2) + 2d(t)(d^2(s_1) + d^2(s_2))]
\end{aligned}$$

$$\begin{aligned}
&= 8(k-1)|V(H_2)||E(H_1)| + 8(k-1)M_1(H_2)|E(H_1)| + 32(k-1)|E(H_2)||E(H_1)|, \\
\sum_C &= \sum_{t_1 t_2 \in E(H_2)} \sum_{s_1 s_2 \in V(H_1)} [d^2(s_1, t_1) + d^2(s_2, t_2)] + \sum_{t_1 t_2 \in E(H_2)} \sum_{\substack{s_1 \in V(H_1), \\ s_2 \in V(R_k(H_1)-H_1)}} [d^2(s_1, t_1) + d^2(s_2, t_2)] \\
&+ \sum_{t_1 t_2 \in E(H_2)} \sum_{s_1, s_2 \in V(R_k(H_1)-H_1)} [d^2(s_1, t_1) + d^2(s_2, t_2)] = \sum_{C_1} + \sum_{C_2} + \sum_{C_3}. \\
\sum_{C_1} &= \sum_{t_1 t_2 \in V(H_2)} \sum_{\substack{s_1 s_2 \in E(R_k(H_1)), s_1, \\ s_2 \in V(H_1)}} [(d(s_1) + d(t_1) + d(s_1)d(t_1))^2 + (d(s_2) + d(t_2) + d(s_2)d(t_2))^2] \\
&= \sum_{t_1 t_2 \in V(H_2)} \sum_{\substack{s_1 s_2 \in E(R_k(H_1)), s_1, \\ s_2 \in V(H_1)}} [d(s_1)^2 + d(s_2)^2 + d^2(t_1) + d^2(t_2) + d(t_1)^2 d(s_1)^2 + d^2(t_2) d(s_2)^2 + 2 d(t_1) d(s_1)] \\
&+ 2 d(t_2) d(s_2) + 2 d^2(t_1) d(s_1) + 2 d^2(t_2) d(s_2) + 2 d(t_1) d^2(s_1) + 2 d^2(t_2) d(s_2)] \\
&= 8|E(H_2)|F(H_1) + 2|E(H_1)|F(H_2) + 4F(H_1)F(H_2) + 4M_1(H_1)M_1(H_2) \\
&+ 4M_1(H_1)F(H_2) + 8M_1(H_2)F(H_1), \\
\sum_{C_2} &= \sum_{t_1 t_2 \in V(H_2)} \sum_{\substack{s_1 s_2 \in E(R_k(H_1)), s_1 \in V(H_1), \\ s_2 \in V(R_k(H_1)-H_1)}} [(d(s_1) + d(t_1) + d(s_1)d(t_1))^2 + (d(s_2) + d(s_2)d(t_2))^2] \tag{9} \\
&= \sum_{t_1 t_2 \in V(H_2)} \sum_{\substack{s_1 s_2 \in E(R_k(H_1)), s_1 \in V(H_1), \\ s_2 \in V(R_k(H_1)-H_1)}} [d(s_1)^2 + d(s_2)^2 + d^2(t_1) + d(t_1)^2 d(s_1)^2 + 2 d(t_1) d(s_1) + 2 d(t_1) d(s_1)^2] \\
&+ 2 d^2(t_1) d(s_1) + d(t_2)^2 d(s_2)^2 + 2 d(t_2) d(s_2)^2] \\
&= 8|E(H_2)|F(G_1) + 16|E(H_1)||E(H_2)| + 4F(G_1)F(G_2) + 4M_1(H_1)M_1(H_2) + 8F(G_1)M_1(H_2) \\
&+ 2|E(H_1)|F(G_2) + 4M_1(H_1)F(G_2) + 8|E(H_1)|F(G_2) + 16|E(H_1)||M_1(H_2), \\
\sum_{C_3} &= \sum_{t_1 t_2 \in E(H_2)} \sum_{\substack{s_1 s_2 \in E(R_k(H_1)), s_1, \\ s_2 \in V(R_k(H_1)-H_1)}} [(d(s_1) + d(s_1)d(t_1))^2 + (d(s_2) + d(s_2)d(t_2))^2] \\
&= \sum_{t_1 t_2 \in E(H_2)} \sum_{\substack{s_1 s_2 \in E(R_k(H_1)), s_1, \\ s_2 \in V(R_k(H_1)-H_1)}} [(2 + 2 d(t_1))^2 + (2 + 2 d(t_2))^2] \\
&= 16(k-1)|E(H_2)||E(H_1)| + 8(k-1)F(H_2)|E(H_1)| + 16(k-1)|E(H_1)||M_1(H_2).
\end{aligned}$$

We arrive at our desired result.

□ **Theorem 3.** Let  $H_1$  and  $H_2$  be two connected graphs, then

$$\begin{aligned}
F(H_{1_{Q_k}} \boxtimes H_2) &= 2(k-1)[F(H_1) + 2M_2(H_1)][3n(H_2) + 5M_1(H_2) + 14|E(H_2)| + F(H_2)] + k[|V(H_2)| \\
&+ 6|E(H_2)| + 3M_1(H_2) + F(H_2)][M_4(H_1) - 2F(H_1) + 2M_2(H_1) - 4M_2(H_1) \\
&+ \sum_{u \in V(H_1)} d^2(u) \sum_{v \in N(u)} d(v)] + 6|E(H_2)||M_1(H_1) + 10|E(H_2)|F(H_2) + 3F(H_1)F(H_2) \\
&+ 6M_1(H_1)M_1(H_2) + F(H_2)[|V(H_1)| + 3M_1(H_1) + 6|E(H_2)| + 4M_2(H_1)] \\
&+ F(H_1)[|V(H_2)| + 7M_1(H_2)] + 6|E(H_2)||M_2(H_1) + 8M_2(H_1)[|E(H_2)| + M_1(H_2)]. \tag{10}
\end{aligned}$$

*Proof.* Let  $d(s, t) = d_{H_{1_{Q_k}} \boxtimes H_2}(s, t)$  is the degree of the vertex  $(s, t)$  in  $H_{1_{Q_k}} \boxtimes H_2$ , then

$$\begin{aligned}
F(H_{1Q_k} \boxtimes H_2) &= \sum_{(s,t) \in V(H_{1Q_k} \boxtimes H_2)} d(s,t)^3 = \sum_{(s_1,t_1)(s_2,t_2) \in E(H_{1Q_k} \boxtimes H_2)} [d(s_1,t_1)^2 + d(s_2,t_2)^2] \\
&= \sum_{s \in V(H_1)} \sum_{t_1,t_2 \in E(H_2)} [d(s,t_1)^2 + d(s,t_2)^2] + \sum_{t \in V(H_2)} \sum_{s_1,s_2 \in E(Q_k(H_1))} [d(s_1,t)^2 + d(s_2,t)^2] \\
&\quad + \sum_{t_1,t_2 \in E(H_2)} \sum_{s_1,s_2 \in E(Q_k(H_1))} [d(s_1,t_1)^2 + d(s_2,t_2)^2] = \sum_A + \sum_B + \sum_C. \\
\sum_A &= \sum_{s \in V(H_1)} \sum_{t_1,t_2 \in E(H_2)} [d(s,t_1)^2 + d(s,t_2)^2] = 2|E(H_2)|M_1(H_1) + |V(H_1)|F(H_2) \\
&\quad + M_1(H_1)F(H_2) + 4|E(H_1)|M_1(H_2) + 2M_1(H_1)M_1(H_2) + 4|E(H_1)|F(H_2). \\
\sum_B &= \sum_{t \in V(H_2)} \sum_{s_1,s_2 \in E(Q_k(H_1))} [d^2(s_1,t) + d^2(s_2,t)] = \sum_{t \in V(H_2)} \sum_{\substack{s_1 \in V(H_1), \\ s_2 \in V(Q_k(H_1)-H_1)}} [d^2(s_1,t) + d^2(s_2,t)] \\
&\quad + \sum_{t \in V(H_2)} \sum_{s_1,s_2 \in V(Q_k(H_1)-H_1)} [d^2(s_1,t) + d^2(s_2,t)] = \sum_{B_1} + \sum_{B_2}. \\
\sum_{B_1} &= \sum_{t \in V(H_2)} \sum_{\substack{s_1,s_2 \in E(Q_k(H_1)), \\ s_1 \in V(H_1), \\ s_2 \in V(Q_k(H_1)-H_1)}} [(d(s_1) + d(t) + d(s_1)d(t))^2 + (d(s_2) + d(s_2)d(t))^2] \\
&= \sum_{t \in V(H_2)} \sum_{\substack{s_1,s_2 \in E(Q_k(H_1)), \\ s_1 \in V(H_1), \\ s_2 \in V(Q_k(H_1)-H_1)}} [d(s_1)^2 + d(s_2)^2 + d(t)^2(d(s_1)^2 + d(s_2)^2) + 2d(t)d(s_1)^2 + 2d(t)d^2(s_2)^2] \\
&\quad + 2d(t)d^2(s_2)^2 + 2d(t)d(s_1) + d^2(t)].
\end{aligned} \tag{11}$$

Consider  $s_1 \in V(H_1)$  and  $d^2(s_1)$  occurs  $d(s_1)$  times. Thus,

$$D_1 = \sum_{\substack{s_1,s_2 \in E(Q(H_1)), \\ s_1 \in V(H_1), s_2 \in V(Q(H_1)-V(H_1))}} d^3(s_1) = F(H_1). \tag{12}$$

Let

$$D_2 = \sum_{\substack{s_1,s_2 \in E(Q(H_1)), \\ s_1 \in V(H_1), s_2 \in V(Q(H_1)-V(H_1))}} d^2(s_2). \tag{13}$$

as  $s_2 = uv \in E(H_1)$  and  $d^2(s_2)$  occurs two times. Therefore,

$$\begin{aligned}
D_2 &= 2 \sum_{s_2 = uv \in V(Q(H_1)-V(H_1))} [d(u) + d(v)]^2 = 2 \sum_{uv \in E(H_1)} [d^2(u) + d^2(v) + 2d(u)d(v)] = 2[F(H_1) + 2M_2(H_1)] \\
&= |V(H_2)|F(H_1) + 2|E(H_1)|M_1(H_2) + M_1(H_2)F(H_1) + 4|E(H_2)|[M_1(H_1) + F(H_1)] + 2M_1(H_1)M_1(H_2) \\
&\quad + 2|V(H_2)|[F(H_1) + 2M_2(H_1)] + 2M_1(H_2)[F(H_1) + 2M_2(H_1)] + 8|E(H_2)|[F(H_1) + 2M_2(H_1)]. \\
\sum_{B_2} &= \sum_{t \in V(H_2)} \sum_{s_1,s_2 \in E(Q_k(H_1)), s_1,s_2 \in V(Q_k(H_1)-H_1)} [(d(s_1) + d(s_1)d(t))^2 + (d(s_2) + d(s_2)d(t))^2].
\end{aligned} \tag{14}$$

Now, we split sum in two parts,  $s_1$  and  $s_2$ , where  $s_1, s_2 \in V(Q_k(H_1)) - V(H_1)$ . Suppose that  $\sum_{B_2} = \sum_{B_{21}} + \sum_{B_{22}}$ , where  $\sum_{B_{21}}$  covers the edges of  $Q_k(H_1)$  which are in the

same edges of  $H_1$  and  $\sum_{B_{22}}$  of  $Q_k(H_1)$  in two different adjacent edges of  $H_1$ .

$$\begin{aligned}
\sum_{B_{21}} &= \sum_{t \in V(H_1)} \sum_{s_1, s_2 \in E(Q(H_1))} [\{d(s_1) + d(s_1)d(t)\}^2 + \{d(s_2) + d(s_2)d(t)\}^2] \\
&= \sum_{t \in V(H_2)} \sum_{s_1, s_2 \in E(Q(H_1))} [[d^2(s_1) + d^2(s_2)] + d^2(t)[d^2(s_1) + d^2(s_2)] + 2d(t)[d^2(s_1) + d^2(s_2)]] \\
&= \sum_{t \in V(H_2)} 2(k-1)[F(H_1) + 2M_2(H_1)] + d^2(t)[F(H_1) + 2M_2(H_1)] + 2d(t)[F(H_1) + 2M_2(H_1)] \\
&= 2(k-1)[F(H_1) + 2M_2(H_1)][|V(H_2)| + M_1(H_2) + 4|E(H_2)|], \tag{15} \\
\sum_{B_{22}} &= \sum_{t \in V(H_2)} \sum_{\substack{s_1, s_2 \in E(Q_k(H_1)), \\ s_2 \in V(Q_k(H_1)-H_1)}} [d(s_1)^2 + d(s_2)^2 + d(t)^2(d(s_1)^2 + d(s_2)^2) + 2d(t)(d(s_1)^2 + d(s_2)^2)] \\
D_3 &= \sum_{\substack{s_1, s_2 \in E(Q(H_1)), \\ s_2 \in V(Q(H_1)-V(H_1))}} [d^2(s_1) + d^2(s_2)].
\end{aligned}$$

In  $D_3$ , the coefficient of

$$\begin{aligned}
d^2(u) &= 2 \binom{2}{d(H_1)(u)} + \sum_{v \in N(u)} d(v) - d(u) \\
&= d^2(u) - 2d(u) + \sum_{v \in N(u)} d(v). \tag{16}
\end{aligned}$$

Therefore,

$$\begin{aligned}
\sum_{u \in V(H_1)} d^2(u) &= M_4(H_1) - 2F(H_1) + \sum_{u \in V(H_1)} d^2(u) \\
&\cdot \sum_{v \in N(u)} d(v). \tag{17}
\end{aligned}$$

For the coefficient of  $dudv$ , let  $s_1s_2 \in E(Q(H_1))$  with  $s_1 = uv$  and  $s_2 = wz$ . As  $s_1s_2 \in E(Q(H_1))$ , we have either  $v = w$  or  $z$  or  $u = w$  or  $z$ . So,  $uv$  is adjacent to all those vertices in  $H_1$  which are adjacent to  $u$  and  $v$ . So, the number of such  $dudv$  is  $(du + dv - 2)$ . Therefore,

$$\begin{aligned}
2 \sum_{uv \in E(H_1)} dudv &= 2 \sum_{uv \in E(H_1)} (du + dv - 2)dudv \\
&= 2 \sum_{uv \in E(H_1)} (du + dv)dudv - 4 \sum_{uv \in E(H_1)} dudv \tag{18} \\
&= 2M_2^1(H_1) - 4M_2(H_1).
\end{aligned}$$

So,

$$\begin{aligned}
D_3 &= M_4(H_1) - 2F(H_1) + \sum_{u \in V(H_1)} d^2(u) \sum_{v \in N(u)} d(v) + 2M_2^1(H_1) - 4M_2(H_1) \\
\sum_{B_{22}} &= (k)[|V(H_2)| + 4|E(H_2)| + M_1(H_2)][M_4(H_1) - 2F(H_1) + 2M_2^1(H_1) - 4M_2(H_1) \\
&\quad + \sum_{u \in V(H_1)} d^2(u) \sum_{v \in N(u)} d(v)], \\
\sum_C &= \sum_{t_1, t_2 \in E(H_2)} \sum_{s_1, s_2 \in E(Q_k(H_1))} [d^2(s_1, t_1) + d^2(s_2, t_2)] = \sum_{t_1, t_2 \in E(H_2)} \sum_{\substack{s_1 \in V(H_1), \\ s_2 \in V(Q_k(H_1)-H_1)}} [d^2(s_1, t_1) + d^2(s_2, t_2)] \\
&\quad + \sum_{t_1, t_2 \in E(H_2)} \sum_{s_1, s_2 \in V(Q_k(H_1)-H_1)} [d^2(s_1, t_1) + d^2(s_2, t_2)] = \sum_{C_1} + \sum_{C_2}. \\
\sum_{C_1} &= \sum_{t_1, t_2 \in V(H_2)} \sum_{\substack{s_1, s_2 \in E(Q_k(H_1)), \\ s_2 \in V(Q_k(H_1)-H_1)}} [(d(s_1) + d(t_1) + d(s_1)d(t_1))^2 + (d(s_2) + d(s_2)d(t_2))^2] \\
&= \sum_{t \in V(H_2)} \sum_{\substack{s_1, s_2 \in E(Q_k(H_1)), \\ s_2 \in V(Q_k(H_1)-H_1)}} [d(s_1)^2 + d(t_1)^2d(s_1)^2 + 2d(t_1)d(s_1) + 2d^2(t_1)d(s_1) + 2d(t_1)d(s_1)^2] \\
&\quad + d^2(t_1) + d(s_2)^2 + d(t_2)^2d(s_2)^2 + 2d(t_2)d(s_2)^2] \\
&= 6[|E(H_2)| + M_1(H_2)]F(H_1) + 3F(H_1)F(H_2) + 2M_1(H_1)M_1(H_2) + 2[|E(H_1)| + M_1(H_1) \\
&\quad + 2M_2(H_1)]F(H_2) + 8M_2(H_1)[|E(H_2)| + M_1(H_2)]. \\
\sum_{C_2} &= \sum_{t_1, t_2 \in E(H_2)} \sum_{\substack{s_1, s_2 \in E(Q_k(H_1)), \\ s_2 \in V(Q_k(H_1)-H_1)}} [(d(s_1) + d(s_1)d(t_1))^2 + (d(s_2) + d(s_2)d(t_2))^2]. \tag{19}
\end{aligned}$$

TABLE 1:  $F$ -index of  $F_1$ -sum path graphs.

$[n_1, n_2]$	$F(P_{n_1 s_1} \boxtimes P_{n_2})$	$F(P_{n_1 R_1} \boxtimes P_{n_2})$	$F(P_{n_1 Q_1} \boxtimes P_{n_2})$	$F(P_{n_1 T_1} \boxtimes P_{n_2})$
(3, 3)	1808	6414	3442	8048
(4, 4)	4836	18120	8826	22,110
(5, 5)	9320	35,746	16,692	43,118
(6, 6)	15,260	59,292	27,040	71,072
(7, 7)	22,656	88,758	39,870	105,972

TABLE 2:  $F$ -index of  $F_2$ -sum path graphs.

$[n_1, n_2]$	$F(P_{n_1 s_2} \boxtimes P_{n_2})$	$F(P_{n_1 R_2} \boxtimes P_{n_2})$	$F(P_{n_1 Q_2} \boxtimes P_{n_2})$	$F(P_{n_1 T_2} \boxtimes P_{n_2})$
(3, 3)	2496	7102	5764	10,370
(4, 4)	6516	19,800	14,496	27,780
(5, 5)	12,424	38,850	27,168	53,594
(6, 6)	20,220	64,252	43,780	87,812
(7, 7)	29,904	96,006	64,332	130,434

Now, we split this sum into two parts for the vertices,  $t_1$  and  $t_2$ , where  $s_1 s_2 \in V(Q_k(G) - V(G))$ . Assume that (Tex translation failed), where (Tex translation failed) cover

the edges of  $Q_k(H_1)$  which are in the same edges of  $H_1$  and (Tex translation failed) of  $Q_k(H_1)$  in two different adjacent edges of  $H_1$ .

$$\begin{aligned}
\sum_{C_{21}} &= \sum_{t_1 t_2 \in E(H_2)} \sum_{\substack{s_1 s_2 \in E(Q_k(H_1))_{s_1}, \\ s_2 \in V(Q_k(H_1) - H_1)}} [(d(s_1) + d(s_1)d(t_1))^2 + (d(s_2) + d(s_2)d(t_2))^2] \\
&= \sum_{t_1 t_2 \in E(H_2)} \sum_{\substack{s_1 s_2 \in E(Q_k(H_1))_{s_1}, \\ s_2 \in V(Q_k(H_1) - H_1)}} [d^2(s_1) + d^2(s_2) + d^2(s_1)d^2(t_1) + d^2(s_2)d^2(t_2) + 2[d^2(s_1)d(t_1) + d^2(s_2)d(t_2)]] \\
&= 2(k-1)[F(H_1) + 2M_2(H_1)][2|E(H_2)| + F(H_2) + 2M_1(H_2)], \tag{20} \\
\sum_{C_{22}} &= \sum_{t_1 t_2 \in E(H_2)} \sum_{\substack{s_1 s_2 \in E(Q_k(H_1))_{s_1}, \\ s_2 \in V(Q_k(H_1) - H_1)}} [(d(s_1) + d(s_1)d(t_1))^2 + (d(s_2) + d(s_2)d(t_2))^2] \\
&= (k)[2|E(H_2)| + F(H_2) + 2M_1(H_2)]([M_4(H_1) - 2F(H_1) + 2M_2(H_1) - 4M_2(H_1)] \\
&\quad + \sum_{u \in V(H_1)} d^2(u) \sum_{v \in N(u)} d(v)).
\end{aligned}$$

We arrive at our desired result.  $\square$

**Theorem 4.** Let  $H_1$  and  $H_2$  be two connected graphs, then

$$\begin{aligned}
F(H_{1T_k} \boxtimes H_2) &= 2(k-1)[F(H_1) + 2M_2(H_1)][n(H_2) + 3M_1(H_2) + 6|E(H_2)| + F(H_2)] + k[|V(H_2)| \\
&\quad + 6|E(H_2)| + 3M_1(H_2) + F(H_2)][M_4(H_1) - 2F(H_1) + 2M_2(H_1) - 4M_2(H_1)] \\
&\quad + \sum_{u \in V(H_1)} d^2(u) \sum_{v \in N(u)} d(v) + [F(H_1) + 2M_2(H_1)][2n(H_2) + 6M_1(H_2) + 12|E(H_2)| + 2F(H_2)] \tag{21} \\
&\quad + 4F(H_1)[2n(H_2) + 6M_1(H_2) + 12|E(H_2)| + 2F(H_2)] + F(H_2)[n(H_1) + 12M_1(H_1) \\
&\quad + 12|E(H_2)|] + 12|E(H_1)|M_1(H_2) + 16|E(H_2)|M_1(H_1) + 20M_1(H_1)M_1(H_2).
\end{aligned}$$

*Proof.* It follows from Theorems 2 and 3.  $\square$

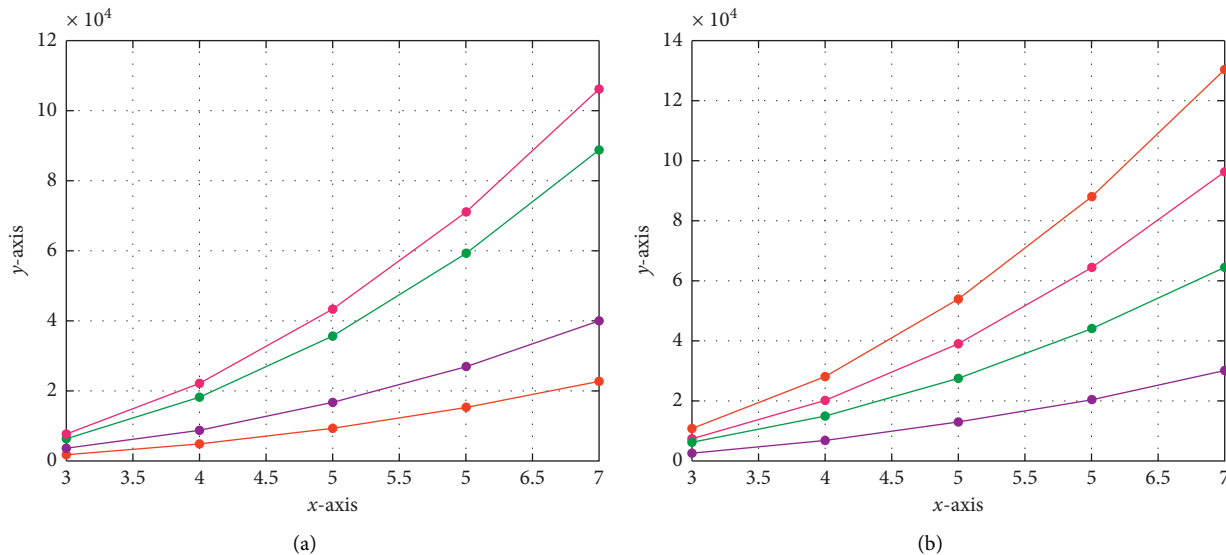


FIGURE 8: (a)  $F(P_{n_{1S_1}} \boxtimes P_{n_2})$ ,  $F(P_{n_{1Q_1}} \boxtimes P_{n_2})$ ,  $F(P_{n_{1R_1}} \boxtimes P_{n_2})$ , and  $F(P_{n_{1T_1}} \boxtimes P_{n_2})$  denoted by red, purple, green, and pink colours, respectively. (b)  $F(P_{n_{1S_2}} \boxtimes P_{n_2})$ ,  $F(P_{n_{1Q_2}} \boxtimes P_{n_2})$ ,  $F(P_{n_{1R_2}} \boxtimes P_{n_2})$ , and  $F(P_{n_{1T_2}} \boxtimes P_{n_2})$  denoted by purple, green, pink, and red colours, respectively.

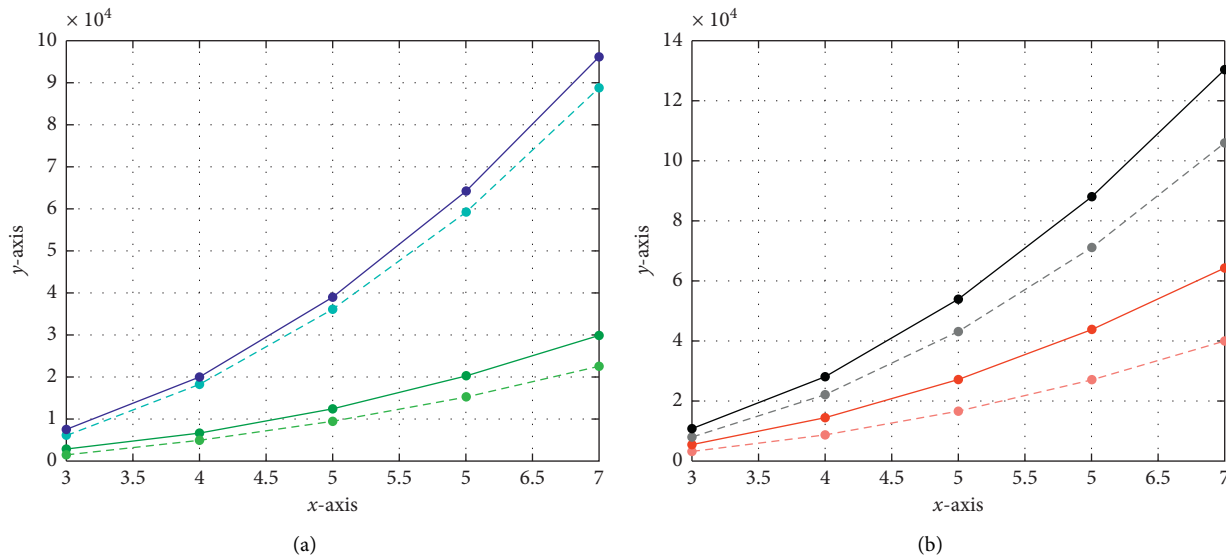


FIGURE 9: Compression between  $F$ -index of  $F_1$ -sum and  $F_2$ -sum graphs. (a)  $F(P_{n_{1S_1}} \boxtimes P_{n_2})$  and  $F(P_{n_{1S_2}} \boxtimes P_{n_2})$  are denoted by light green dotted line and dark green solid line, and  $F(P_{n_{1R_1}} \boxtimes P_{n_2})$  and  $F(P_{n_{1R_2}} \boxtimes P_{n_2})$  are denoted by sky blue dotted line and blue solid line, respectively. (b)  $F(P_{n_{1Q_1}} \boxtimes P_{n_2})$  and  $F(P_{n_{1Q_2}} \boxtimes P_{n_2})$  are denoted by pink dotted line and red solid line, and  $F(P_{n_{1T_1}} \boxtimes P_{n_2})$  and  $F(P_{n_{1T_2}} \boxtimes P_{n_2})$  by grey dotted line and black solid line, respectively.

### 4. Applications and Discussion

In this paper, we computed the  $F$ -index of the generalized sum graphs. Assume that  $H_1 = P_{n_1}$  and  $H_2 = P_{n_2}$  are particular alkane called as paths of orders  $n_1, n_2 \geq 3$ , and  $k \geq 1$ , respectively. Then, the following outcomes are the direct consequences of the achieved results:

$$(i) F(P_{n_{1S_k}} \boxtimes P_{n_2}) = 128k(n_1 - 1) + 250(n_2 + n_1) + 512(n_2 - 2)(n_1 - 2) + 216k(n_1 - 1)(n_2 - 2) - 892$$

$$(ii) F(P_{n_{1R_k}} \boxtimes P_{n_2}) = 128k(n_1 - 1) + 216k(n_1 - 1)(n_2 - 2) + 2744(\tilde{n}_2 - 2)(n_1 - 2) + 1458n_1 + 1024n_2 - 4464$$

$$(iii) F(P_{n_{1Q_k}} \boxtimes P_{n_2}) = 432k(n_1 - 1) + 729k(n_1 - 1)(n_2 - 2) + 512(\tilde{n}_2 - 2)(n_1 - 2) + 250(n_1 + n_2) - 892$$

$$(iv) F(P_{n_{1T_k}} \boxtimes P_{n_2}) = 432k(n_1 - 1) + 729k(n_1 - 1)(n_2 - 2) + 2744(\tilde{n}_2 - 2)(n_1 - 2) + 1458n_1 + 1024n_2 - 4464$$

(1) Four subdivision operations  $(S_1(G), R_1(G), Q_1(G), T_1(G))$  are restricted in case of newly



- addition of vertices upto  $k = 1$ , while four subdivision operations  $(S_k(G), R_k(G), Q_k(G), T_k(G))$  are not restricted in case of newly addition of vertices as  $k$  can be any natural number.
- (2) For a certain graph  $G$ , newly constructed graphs  $(S_1(G), R_1(G), Q_1(G), T_1(G))$  will have specific number of edges. While, in  $(S_k(G), R_k(G), Q_k(G), T_k(G))$ , the number of edges will be varying according to  $k$ .
  - (3) Molecular structure of  $(S_k(G), R_k(G), Q_k(G), T_k(G))$  is more general as compared to the  $(S_1(G), R_1(G), Q_1(G), T_1(G))$ .
  - (4) Molecular structure of  $F_k$ -sum is more complex and general as compared to the molecular structure of  $F_1$ -sum.
  - (5) In this paper, main results  $F(H_{1_{S_k}} \boxtimes H_2)$ ,  $F(H_{1_{Q_k}} \boxtimes H_2)$ ,  $F(H_{1_{R_k}} \boxtimes H_2)$ , and  $F(H_{1_{T_k}} \boxtimes H_2)$  based on strong product are generalization of  $F(H_{1_{S_1}} \boxtimes H_2)$ ,  $F(H_{1_{Q_1}} \boxtimes H_2)$ ,  $F(H_{1_{R_1}} \boxtimes H_2)$ , and  $F(H_{1_{T_1}} \boxtimes H_2)$  based on strong product.

Now, we present its tabular form, Table 1 and Table 2 and graphical representations in Figures 8 and 9 for  $k = 1$  and  $k = 2$ .

In this paper, we computed the  $F$ -index of the subdivision-related generalized  $F$ -sum graphs based on strong product. However, the problem is still open for other topological indices on the generalized  $F$ -sum graphs.

## Data Availability

The data used to support the findings of this study are included within the article. However, additional data may be provided by the corresponding author upon request.

## Conflicts of Interest

The authors declare that they have no conflicts of interest.

## References

- [1] N. Trinajstić, *Chemical Graph Theory*, 2nd edition, 1992.
- [2] I. Gutman, B. Rušćić, N. Trinajstić, and C. F. Wilcox, "Graph theory and molecular orbitals. XII. Acyclic polyenes," *The Journal of Chemical Physics*, vol. 62, no. 9, pp. 3399–3405, 1975.
- [3] R. Todeschini and V. Consonni, *Molecular Descriptors for Chemoinformatics*, Wiley-VCH Verlag GmbH, Weinheim, Germany, 2nd edition, 2009.
- [4] I. Gutman, "Degree-based topological indices," *Croatica Chemica Acta*, vol. 86, no. 4, pp. 351–361, 2013.
- [5] H. Wiener, "Structural determination of paraffin boiling points," *Journal of the American Chemical Society*, vol. 69, no. 1, 1947.
- [6] I. Gutman and N. Trinajstić, "Graph theory and molecular orbitals," *New Concepts*, vol. 2, pp. 49–93, 1973.
- [7] W. Yan, B.-Y. Yang, and Y.-N. Yeh, "The behavior of Wiener indices and polynomials of graphs under five graph decorations," *Applied Mathematics Letters*, vol. 20, no. 3, pp. 290–295, 2007.
- [8] M. Eliasi and B. Taeri, "Four new sums of graphs and their Wiener indices," *Discrete Applied Mathematics*, vol. 157, no. 4, pp. 794–803, 2009.
- [9] H. Deng, D. Sarala, S. K. Ayyaswamy, and S. Balachandran, "The Zagreb indices of four operations on graphs," *Applied Mathematics and Computation*, vol. 275, pp. 422–431, 2016.
- [10] S. Akhter and M. Imran, "Computing the forgotten topological index of four operations on graphs," *AKCE International Journal of Graphs and Combinatorics*, vol. 14, no. 1, pp. 70–79, 2017.
- [11] J.-B. Liu, S. Javed, M. Javaid, and K. Shabbir, "Computing first general Zagreb index of operations on graphs," *IEEE Access*, vol. 7, pp. 47494–47502, 2019.
- [12] Y.-M. Chu, S. Javed, M. Javaid, and M. Kamran Siddiqui, "On bounds for topological descriptors of  $\varphi$ -sum graphs," *Journal of Taibah University for Science*, vol. 14, no. 1, pp. 1288–1301, 2020.
- [13] D. Sarala, H. Deng, C. Natarajan, and S. K. Ayyaswamy, " $F$  index of graphs based on four new operations related to the strong product," *AKCE International Journal of Graphs and Combinatorics*, vol. 17, no. 1, pp. 25–37, 2020.
- [14] M. Munir, W. Nazeer, S. Rafique, and S. Kang, " $M$ -polynomial and degree-based topological indices of polyhex nanotubes," *Symmetry*, vol. 8, no. 12, p. 149, 2016.
- [15] YC. Kwun, M. Munir, W. Nazeer, S. Rafique, and S. M. Kang, " $M$ -Polynomials and topological indices of V-phenylenic nanotubes and nanotori," *Scientific Reports*, vol. 7, no. 1, pp. 1–9, 2017.
- [16] H. M. Awais, M. Javaid, and A. Akbar, "First general Zagreb index of generalized  $F$ -sum graphs," *Discrete Dynamics in Nature and Society*, vol. 2020, Article ID 2954975, 16 pages, 2020.
- [17] J. H. Tang, U. Ali, M. Javaid, and K. Shabbir, "Zagreb connection indices of subdivision and semi-total point operations on graphs," *Journal of Chemistry*, vol. 2019, Article ID 9846913, 14 pages, 2019.
- [18] M. F. Nadeem, S. Zafar, and Z. Zahid, "On the edge version of geometric-arithmetic index of nanocones," *Studia Universitatis Babeş-Bolyai, Chimia*, vol. 61, no. 1, pp. 273–282, 2016.
- [19] J. B. Liu, S. Akram, M. Javaid, A. Raheem, and R. Hasni, "Bounds of degree-based molecular descriptors for generalized-sum graphs," *Discrete Dynamics in Nature and Society*, vol. 2021, Article ID 8821020, 17 pages, 2021.
- [20] A. Ahmad, K. Elahi, R. Hasni, and M. F. Nadeem, "Computing the degree based topological indices of line graph of benzene ring embedded in  $P$ -type-surface in 2D network," *Journal of Information and Optimization Sciences*, vol. 40, no. 7, pp. 1511–1528, 2019.
- [21] J. B. Liu, M. Javaid, and H. M. Awais, "Computing Zagreb indices of the subdivision-related generalized operations of graphs," *IEEE Access*, vol. 7, pp. 105479–105488, 2019.
- [22] H. M. Awais, M. Javaid, and M. Jamal, "Forgotten index of generalized  $F$ -sum graphs," *Journal of Prime Research in Mathematics*, vol. 15, pp. 115–128, 2019.
- [23] H. M. Awais, M. Javaid, and A. Raheem, "Hyper-Zagreb index of graphs based on generalized subdivision related operations," *Punjab University Journal of Mathematics*, vol. 52, no. 5, pp. 89–103, 2019.
- [24] X. Zhang, H. M. Awais, M. Javaid, and M. K. Siddiqui, "Multiplicative Zagreb indices of molecular graphs," *Journal of Chemistry*, vol. 2019, Article ID 5294198, 19 pages, 2019.
- [25] M. Javaid, S. Javed, A. M. Alanazi, and M. R. Alotaibi, "Computing analysis of Zagreb indices for generalized sum

- graphs under strong product," *Journal of Chemistry*, vol. 2021, Article ID 6663624, 20 pages, 2021.
- [26] I. Gutman and N. Trinajstić, "Graph theory and molecular orbitals. Total  $\varphi$ -electron energy of alternant hydrocarbons," *Chemical Physics Letters*, vol. 17, no. 4, pp. 535–538, 1972.
- [27] B. Furtula and I. Gutman, "A forgotten topological index," *Journal of Mathematical Chemistry*, vol. 53, no. 4, pp. 1184–1190, 2015.

## Research Article

# Application of Resolvability Technique to Investigate the Different Polyphenyl Structures for Polymer Industry

Muhammad Faisal Nadeem <sup>1</sup>, Mohsan Hassan,<sup>1</sup> Muhammad Azeem <sup>2</sup>,  
Salah Ud-Din Khan,<sup>3</sup> Mohammed Rafi Shaik <sup>4</sup>, Mohammed A. F. Sharaf,<sup>5</sup>  
Abdelatty Abdelgawad,<sup>5</sup> and Emad Mahrous Awwad<sup>6</sup>

<sup>1</sup>Department of Mathematics, COMSATS University Islamabad, Lahore Campus, Lahore, Pakistan

<sup>2</sup>Department of Aerospace Engineering, Faculty of Engineering, University Putra Malaysia, Seri Kembangan, Malaysia

<sup>3</sup>Sustainable Energy Technologies (SET) Center, College of Engineering, King Saud University, P. O. Box 800, Riyadh 11421, Saudi Arabia

<sup>4</sup>Department of Chemistry, College of Science, King Saud University, P. O. Box 2455, Riyadh 11451, Saudi Arabia

<sup>5</sup>Department of Industrial Engineering, College of Engineering, King Saud University, P. O. Box 800, Riyadh-11421, Saudi Arabia

<sup>6</sup>Department of Electrical Engineering, College of Engineering, King Saud University, P. O. Box 800, Riyadh, Saudi Arabia

Correspondence should be addressed to Mohammed Rafi Shaik; mrshaik@ksu.edu.sa

Received 29 November 2020; Revised 13 December 2020; Accepted 31 March 2021; Published 20 April 2021

Academic Editor: Leena Gupta

Copyright © 2021 Muhammad Faisal Nadeem et al. This is an open access article distributed under the Creative Commons Attribution License, which permits unrestricted use, distribution, and reproduction in any medium, provided the original work is properly cited.

Polyphenyl is used in a variety of applications including high-vacuum devices, optics, and electronics, and in high-temperature and radiation-resistant fluids and greases, it has low volatility, ionizing radiation stability, and high thermal-oxidative properties. The structure of polyphenyls can be represented using a molecular graph, where atoms represent vertices and bonds between atom edges. In a chemical structure, an item/vertex  $v$  resolves two items  $v_1$  and  $v_2$  if  $d(v_1, v) \neq d(v_2, v)$ ; similarly, the ordered subset  $\phi$  of vertices resolves each pair of distinct vertices named as the resolving set, and its minimum cardinality is described as metric dimension. In the pharmaceutical industry, the competition to find new chemical entities for treating a disease dictates larger project teams that encompass more extensive and diverse synthetic efforts directed at increasingly complicated activity spectra. In this paper, we determine the metric dimension of para-, meta-, and ortho-polyphenyl structures, which are used for structure-activity analysis of these polyphenyl structures.

## 1. Introduction

Chemists require the mathematical representation of a chemical compound to work with the chemical structure. In a chemical structure, a set of selected atoms gave mathematical representations so that it gave distinct representations to distinct atoms of the structure. The chemical structure can be defined in the form of vertices, which mentions the atom and edges indicate the bonds types, respectively. Thus, a graph-theoretic analysis of this idea yields the representations of all vertices in a structure in such a way that different vertices have distinct representations with respect to some specific atoms of that structure. The

following are some mathematical definitions to indicate these concepts.

In 1975, the concept of locating set was proposed by Slater [1] and called the minimum cardinality of a locating set of a graph locating number. On the same pattern, in 1976, the idea of metric dimension of a graph was individually introduced by Harary and Melter in [2], and these time metric generators were named as resolving sets. Members of metric basis set were assigned as a sonar or loran station [1].

A connected, simple graph  $G(V, E)$  with  $V$  is the set of vertices (also can say atoms), and  $E$  is the set of edges (bond types); the distance between two vertices/bonds  $a_1, a_2 \in V$  is

the length of geodesic between them and denoted by  $d(a_1, a_2)$ . Let  $\phi = \{\phi_1, \phi_2, \dots, \phi_l\}$  be an order subset of vertices belonging to a graph  $G$  and  $a$  be a vertex. The representation  $r(a|\phi)$  of  $a$  corresponding to  $\phi$  is the  $l$ -tuple  $(d(a, \phi_1), d(a, \phi_2), d(a, \phi_3), \dots, d(a, \phi_l))$ , where  $\phi$  is called a resolving set [2] or locating set [1], if every vertex of  $G$  is uniquely determined by its distances from the vertices of  $\phi$  or, on the contrary, if different vertices of  $G$  have unique representations with respect to  $\phi$ . The minimum cardinality of the resolving set  $\phi$  is called the metric dimension of  $G$ , and it is denoted by  $\dim(G)$  [1]. For a given ordered set of vertices  $\phi = \{\phi_1, \phi_2, \dots, \phi_l\} \subset V$ , the  $c$ th location of  $r(a|\phi) = 0$  if and only if  $a = \phi_c$ . Thus, to verify that  $\phi$  is a resolving set, it is enough to show that  $r(a_1|\phi) \neq r(a_2|\phi)$  for every possible distinct pair of vertices  $a_1, a_2 \in V(G) \setminus \phi$ .

Metric dimension of a graph or a structure is a resolvability parameter that has been applied in numerous applications of graph theory, for the drug discovery in pharmaceutical chemistry [3, 4], robot navigation [5], combinatorial optimization concept studied in [6], various coin weighing problems [7, 8], and utilization of the idea in pattern recognition and processing of images, few of which also associate with the use in hierarchical data structures [1].

Due to numerous uses of resolvability parameters in the chemical field, many works have been done with graph perspectives, and metric dimension is also considered important to study different structures with it, such as the structure of H-naphthalenic and  $VC_5C_7$  nanotubes discussed with metric concept [9], some upper bounds of cellulose network considering metric dimension as a point of discussion [10], resolving sets of silicate star determined in [11], metric basis of 2D lattice of alpha-boron nanotubes discussed with specific applications [12], and sharp bound on the metric dimension of honeycomb and its related network [13]; for more interesting literature work on metric dimension, metric basis, resolving set, and other resolvability parameters, refer to [13–28].

## 2. Results of Polyphenyl Chemical Networks

In the results of this article, we discuss the metric dimension of para-, meta-, and ortho-polyphenyl chemical networks constructed by different polygons. Usually, the networks are made up with the chain of hexagons using chemical operations ortho, para, and meta; in this work, we extend this to any order of polygons. Moreover, using  $\eta = 6$  with arbitrary  $h$  in Theorems 1–5, we can produce the para-, meta-, and ortho-polyphenyl chain of hexagons and retrieve its corresponding metric dimension as well.

**2.1. Metric Dimension of  $O(\eta, h)$ .** Let  $O(\eta, h)$  be a connected graph of ortho-polyphenyl network of cycle graph  $C_\eta$ , and  $h$  are the copies of cycle graph with order  $\lambda = \eta h$  and size  $h(\eta + 1) - 1$ . For the following theorems, Figure 1 shows the resolving set in dark black vertices.

**Theorem 1.** *If  $\eta \geq 3$  and  $h = 2$ , then  $\dim(O(\eta, 2))$  is 2.*

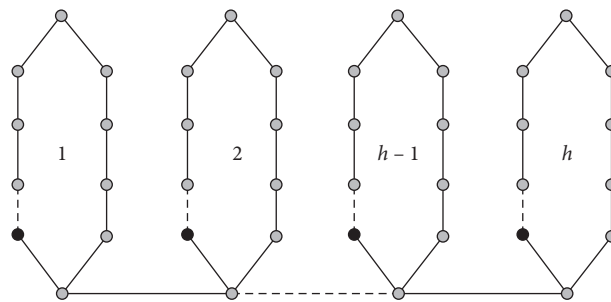


FIGURE 1:  $O(\eta, h)$ .

*Proof.* To prove that  $\dim(O(\eta, 2)) \leq 2$ , for this assume, a resolving set  $\phi = \{v_1, v_{\eta+1}\}$ . We construct the following cases on vertex set of  $O(\eta, 2)$ :

$$r_1(v_\zeta | \phi) = \begin{cases} \zeta - 1; & \text{if } \zeta = 1, 2, 3, \dots, \frac{\eta}{2} + 1; \\ \eta - \zeta + 1; & \text{if } \zeta = \frac{\eta}{2} + 2, \dots, \eta; \\ \zeta - \eta + 2; & \text{if } \zeta = \eta + 1, \eta + 2, \dots, \eta + \frac{\eta}{2}; \\ 2\eta - \zeta + 2; & \text{if } \zeta = \eta + \frac{\eta}{2} + 1, \dots, 2\eta. \end{cases} \quad (1)$$

Second vector representations are as follows:

$$r_2(v_\zeta | \phi) = \begin{cases} \zeta + 2; & \text{if } \zeta = 1, 2, 3, \dots, \frac{\eta - 1}{2}, \\ \eta - \zeta + 2; & \text{if } \zeta = \frac{\eta - 1}{2} + 1, \dots, \eta, \\ \zeta - \eta; & \text{if } \zeta = \eta + 1, \eta + 2, \dots, \eta + \frac{\eta + 2}{2}, \\ 2\eta - \zeta + 1; & \text{if } \zeta = \eta + 1 + \frac{\eta + 2}{2}, \eta + 2 + \frac{\eta + 2}{2}, \dots, 2\eta. \end{cases} \quad (2)$$

Hence, it follows from the above arguments in the form of representation that  $\dim(O(\eta, 2)) \leq 2$  because all the vertices of  $O(\eta, 2)$  have unique representations with respect to resolving set  $\phi$ .

For reverse inequality that  $\dim(O(\eta, 2)) \geq 2$ , by contradiction, our assertion becomes  $\dim(O(\eta, 2)) < 2$ , implying that  $\dim(O(\eta, 2)) = 1$ , and it is not possible because only the path graph exists having the metric dimension 1. All discussion concludes that when  $\eta \geq 3$  and  $h = 2$ ,

$$\dim(O(\eta, 2)) = 2. \quad (3) \quad \square$$

**Theorem 2.** *If  $\eta, h \geq 3$ , then  $\dim(O(\eta, h))$  is  $h$ .*

*Proof.* To show that  $\dim(O(\eta, h)) = h$ , we will apply the induction method on  $h$  the number of copies of base graph.

The base case for  $h = 2$  is proved in Theorem 1; now, assume that the assertion is true for  $h = m$ :

$$\dim(O(\eta, m)) = m. \quad (4)$$

We will show that it is true for  $h = m + 1$ . Suppose

$$\dim(O(\eta, m + 1)) = \dim(O(\eta, m)) + \dim(O(\eta, 2)) - 1. \quad (5)$$

Using equations (3) and (4) in equation (5), we will get

$$\dim(O(\eta, m + 1)) = m + 2 - 1 = m + 1. \quad (6)$$

Hence, the result is true for all positive integers  $h \geq 3$ .  $\square$

**2.2. Metric Dimension of  $M(\eta, h)$ .** Let  $M(\eta, h)$  be a connected graph of meta-polyphenyl network of cycle graph  $C_\eta$ , and  $h$  are the copies of cycle graph with order  $\lambda = \eta h$  and size  $h(\eta + 1) - 1$ . For the following theorems, Figure 2 shows the resolving set in dark black vertices.

**Theorem 3.** *If  $\eta \geq 4$  (even) and  $h = 2$ , then  $\dim(M(\eta, 2))$  is 2.*

*Proof.* To prove that  $\dim(M(\eta, 2)) \leq 2$ , we construct a resolving set  $\phi = \{v_1, v_{\eta+2}\}$  from the vertex set of  $M(\eta, 2)$ . We assume the following cases on vertex set of  $M(\eta, 2)$ :

$$r(v_\zeta | \phi) = \left( \frac{\zeta + 1}{2}, \frac{\eta + 4}{2} - \frac{\zeta}{2} \right), \quad \zeta = 1, 3, 5, \dots, \eta - 1,$$

$$r(v_\zeta | \phi) = \left( \frac{\zeta - 1}{2}, \frac{\eta + 2}{2} - \frac{\zeta - 1}{2} \right), \quad \zeta = 2, 4, 6, \dots, \eta,$$

$$r(v_\zeta | \phi) = \left( \frac{\zeta - 1}{2}, \frac{\zeta - \eta + 1}{2} \right), \quad \zeta = \eta + 1, \eta + 3, \eta + 5, \dots, 2\eta - 1,$$

$$r(v_\zeta | \phi) = \left( \frac{\zeta}{2}, \frac{\zeta - \eta - 2}{2} \right), \quad \zeta = \eta + 2, \eta + 4, \eta + 6, \dots, 2\eta.$$

(7)

Hence, it follows from the above discussion that  $\dim(M(\eta, 2)) \leq 2$  because all the vertices of  $M(\eta, 2)$  have unique representations with respect to resolving set  $\phi$ .

For converse  $\dim(M(\eta, 2)) \geq 2$ , we use contradiction, and  $\dim(M(\eta, 2)) = 1$  is not possible because only the path

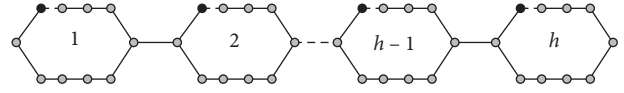


FIGURE 2:  $M(\eta, h)$ .

graph exists having the metric dimension 1. All discussion concludes that when  $\eta \geq 4$  (even) and  $h = 2$ ,

$$\dim(M(\eta, 2)) = 2. \quad (8) \quad \square$$

**Theorem 4.** *If  $\eta \geq 4$  (even) and  $h \geq 3$ , then  $\dim(M(\eta, h))$  is  $h$ .*

*Proof.* To show that  $\dim(M(\eta, h)) = h$ , we will apply the induction method on  $h$  showing the copies of base graph. The base case for  $h = 2$  is proved in Theorem 3; now, assume that the assertion is true for  $h = m$ :

$$\dim(M(\eta, m)) = m. \quad (9)$$

We will show that it is true for  $h = m + 1$ . Suppose

$$\dim(M(\eta, m + 1)) = \dim(M(\eta, m)) + \dim(M(\eta, 2)) - 1. \quad (10)$$

Using equations (8) and (9) in equation (10), we have

$$\dim(M(\eta, m + 1)) = m + 2 - 1 = m + 1. \quad (11)$$

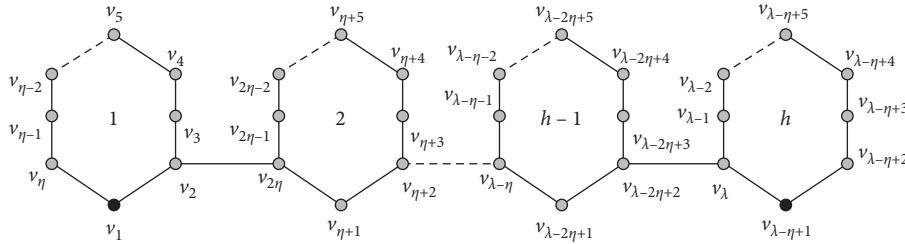
Hence, the result is true for all positive integers  $h \geq 3$ .  $\square$

**2.3. Metric Dimension of  $L(\eta, h)$ .** Let  $L(\eta, h)$  be a connected graph of para-polyphenyl network of cycle graph  $C_\eta$ , and  $h$  are the copies of cycle graph with order  $\lambda = \eta h$  and size  $h(\eta + 1) - 1$ . For the following theorems, vertices are labeled, as shown in Figure 3; moreover, it also shows the resolving set in dark black vertices.

**Theorem 5.** *If  $\eta \geq 5$  and  $h \geq 2$ , then  $\dim(L(\eta, h))$  is 2.*

*Proof.* Firstly, we prove that  $\dim(L(\eta, h)) \leq 2$ ; for this construction, a resolving set  $\phi = \{v_1, v_{\lambda-\eta+1}\}$  from the vertex set of  $L(\eta, h)$ . We assume the following cases on vertex set of  $G$  and on the copies of cycle graph, i.e.,  $h$ :

$$r_1(v_\zeta | \phi) = \begin{cases} \zeta - 1, & \text{if } \zeta = 1, 2, 3, \dots, \frac{\eta + 1}{2}, \\ \eta - \zeta + 1, & \text{if } \zeta = \frac{\eta + 1}{2} + 1, \frac{\eta + 1}{2} + 2, \dots, \eta, \\ 3\frac{\zeta}{\eta} + \zeta - 1 - \eta\frac{\zeta}{\eta}, & \text{if } \zeta \equiv 1, 2, 3, \dots, \frac{\eta - 1}{2} \pmod{\eta}, \\ \eta\frac{\zeta}{\eta} + 2 - \zeta, & \text{if } \zeta \equiv 0, \frac{\eta - 1}{2} + 1, \frac{\eta - 1}{2} + 2, \dots, \eta - 1 \pmod{\eta}. \end{cases} \quad (12)$$

FIGURE 3:  $L(\eta, h)$ .

If  $\zeta \equiv 0, ((\eta - 1)/2) + 1, ((\eta - 1)/2) + 2, \dots, \eta - 1 \pmod{\eta}$  and  $\zeta > 2\eta$ ,

$$r_1(v_\zeta|\phi) = \eta \frac{\zeta + ((\eta - 1)/2) + 1}{\eta} - \zeta + 2 + 3 \left( \frac{\zeta + ((\eta - 1)/2) + 1}{\eta} - 2 \right). \quad (13)$$

$$r_2(v_\zeta|\phi) = \begin{cases} 3, & \text{if } \zeta = 1; \\ \zeta, & \text{if } \zeta = 2, 3, \dots, \frac{\eta + 2}{2}; \\ \eta - \zeta + 4, & \text{if } \zeta = \frac{\eta + 2}{2} + 1, \dots, \eta. \end{cases} \quad (14)$$

Second vector representations are as follows:

Case 1.  $h = 2$ :

Case 2.  $h \geq 3$ :

$$r_2(v_\zeta|\phi) = \begin{cases} 3 \left( \frac{\eta(h-1) + 1}{\eta} - 1 \right) + \zeta, & \text{if } \zeta = 1, \\ 3 \left( \frac{\zeta}{\eta} - 1 \right) + \zeta, & \text{if } \zeta = 2, 3, \dots, \frac{\eta + 2}{2}, \\ \eta - \zeta + 4 + 3 \left( \frac{\eta(h-1) + 1}{\eta} - 1 \right), & \text{if } \zeta = \frac{\eta + 2}{2} + 1, \dots, \eta. \end{cases} \quad (15)$$

Subcase 2.1. If  $\zeta = \eta(h-1) + 1, \eta(h-1) + 2, \dots, \eta(h-1) + (\eta/2)$ ,

$$r_2(v_\zeta|\phi) = \zeta - \eta(h-1) - 1. \quad (16)$$

Subcase 2.2. If  $\zeta = \eta(h-1) + (\eta/2) + 1, \eta(h-1) + (\eta/2) + 2, \dots, \eta h$ ,

$$r_2(v_\zeta|\phi) = \eta h - \zeta + 1. \quad (17)$$

Subcase 2.3. If  $\zeta \equiv 2, 3, \dots, ((\eta + 2)/2) \pmod{\eta}$ , and  $\zeta \geq \eta + 1$ ,

$$r_2(v_\zeta|\phi) = 3 \left( h - \frac{\zeta - 1}{\eta} - 2 \right) + 2 + \zeta - \left( 2 + \eta \frac{\zeta}{\eta} \right). \quad (18)$$

Subcase 2.4. If  $\zeta \equiv 0, ((\eta + 2)/2) + 1, \dots, \eta - 1 \pmod{\eta}$ , and  $\zeta \geq \eta + 1$ ,

$$r_2(v_\zeta|\phi) = 3 \left( h - \frac{\zeta - 1}{\eta} - 2 \right) + 4 - \zeta + \eta \frac{\zeta + ((\eta + 2)/2)}{\eta}. \quad (19)$$

Subcase 2.5. If  $\zeta \equiv 1 \pmod{\eta}$ , and  $\zeta \geq \eta + 1$ ,

$$r_2(v_\zeta|\phi) = 3 \left( h - \frac{\zeta}{\eta} - 1 \right). \quad (20)$$

Hence, it follows from the above discussion that  $\dim(L(\eta, h)) \leq 2$  because all the vertices of  $L(\eta, h)$  have unique representations with respect to resolving set  $\phi$ .

For reverse inequality that  $\dim(L(\eta, h)) \geq 2$ , by contradiction, our assertion becomes  $\dim(L(\eta, h)) < 2$ , implying that  $\dim(L(\eta, h)) = 1$ , and it is not possible because only the path graph exists having the metric dimension 1. All discussion concluding that when  $\eta \geq 5$  and  $h \geq 2$ ,

$$\dim(L(\eta, h)) = 2. \quad (21)$$

□

2.4. *Metric Dimension of  $L_S(\eta, h)$ .* Let  $L_S(\eta, h)$  be a connected graph of para-polyphenyl network of sun graph  $S_\eta$ , where  $h$  are the copies of sun graph and  $\eta$  is the order of interior cycle of sun graph. The order and size of network are

$|V(L_S(\eta, h))| = \lambda = 2\eta h$  and  $|E(L_S(\eta, h))| = h(2\eta + 1) - 1$ , respectively. The vertices are labeled, as shown in Figure 4.

**Theorem 6.** *If  $\eta \geq 5$  (odd) and  $h \geq 2$ , then  $\dim(L_S(\eta, h))$  is 2.*

*Proof.* To prove that  $\dim(L_S(\eta, h)) \leq 2$ , for this construct, a resolving set  $\phi = \{v_{((\eta+3)/2)}, v_\xi\}$ , where  $\xi = ((\eta(4h-3)-1)/2)$  from the vertex set of  $L_S(\eta, h)$ . We assume the following cases on vertex set of  $L_S(\eta, h)$ :

Case 1.  $1 \leq \zeta \leq 2\eta$ :

$$r_1(v_\zeta|\phi) = \begin{cases} \frac{\eta+3}{2} - \zeta, & \text{if } \zeta = 1, 2, \dots, \frac{\eta+3}{2}, \\ \zeta - \frac{\eta+3}{2}, & \text{if } \zeta = \frac{\eta+5}{2}, \frac{\eta+5}{2}, \dots, \eta, \\ \frac{\eta+1}{2}, & \text{if } \zeta = \eta+1, \\ \frac{3\eta+5}{2} - \zeta, & \text{if } \zeta = \eta+2, \eta+3, \dots, \frac{3\eta+3}{2}, \\ \zeta - \frac{3\eta+1}{2}, & \text{if } \zeta = \frac{3\eta+5}{2}, \frac{3\eta+7}{2}, \dots, 2\eta. \end{cases} \quad (22)$$

Case 2. If  $\zeta \equiv ((\eta+1)/2), ((\eta+3)/2), \dots, \eta \pmod{2\eta}$ ,  $\zeta \geq ((5\eta+1)/2)$ ,

$$r_1(v_\zeta|\phi) = \left( \frac{\eta-1}{2} + 3\eta + 2 \left( \frac{\zeta-1}{3\eta} \right) \eta - \zeta + 3 \frac{\zeta}{2\eta} + 2 \left( \frac{\zeta}{2\eta} \right) - 1 \right). \quad (23)$$

Case 3. If  $\zeta \equiv 1, 2, \dots, ((\eta-1)/2) \pmod{2\eta}$ ,  $\zeta \geq 2\eta+1$ ,

$$r_1(v_\zeta|\phi) = \left( \frac{\eta-1}{2} + \zeta + 5 \frac{\zeta}{2\eta} - \frac{\eta(4h-3)-1}{2} + \frac{\eta-5}{2} \right). \quad (24)$$

Case 4. If  $\zeta \equiv \eta+1, \eta+2, \dots, (3\eta-1/2) \pmod{2\eta}$ ,  $\zeta \geq 3\eta+1$ ,

$$r_1(v_\zeta|\phi) = \left( \zeta - \frac{\eta(4((\zeta/2\eta)+1)-3)-1}{2} + 3 \frac{\zeta}{2\eta} + 2 \left( \frac{\zeta}{2\eta} - 1 \right) \right). \quad (25)$$

Case 5. If  $\zeta \equiv 0, ((3\eta+1)/2), ((3\eta+3)/2), \dots, 2\eta-1 \pmod{2\eta}$ ,  $\zeta \geq ((7\eta+1)/2)$ ,

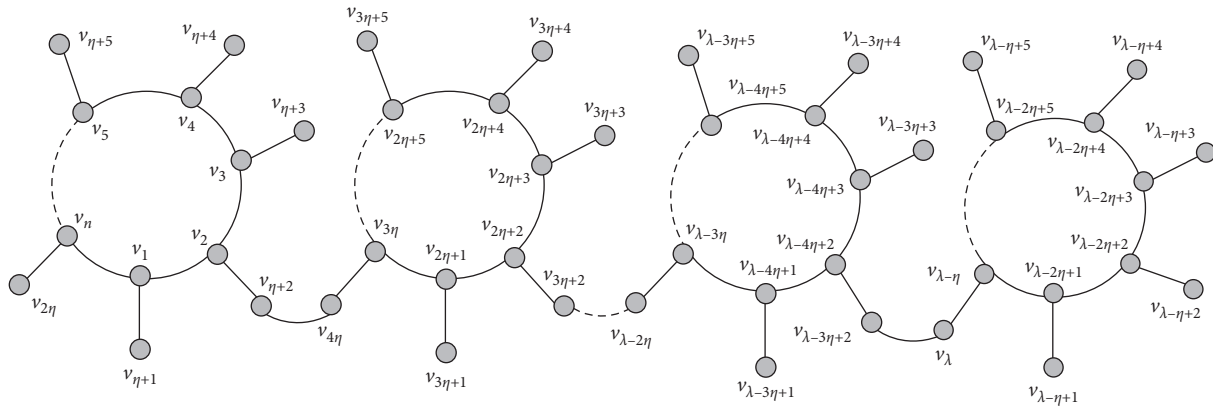
$$r_1(v_\zeta|\phi) = \left( \frac{\eta-1}{2} + 4 \frac{\zeta-1}{2\eta} + 2 \left( \frac{\zeta}{2\eta} - 1 \right) - \zeta + \eta \left( 2 \frac{\zeta-1}{2\eta} \right) - \frac{\zeta-\eta-1}{3\eta} + z \right), \quad (26)$$

where  $z = -2$  when  $\zeta \equiv 0 \pmod{2\eta}$  and  $\zeta \geq 4\eta$ ; otherwise,  $z = 0$ .

The representations of all vertices with respect to the second vertex of resolving set are as follows:

Case 1.  $1 \leq \zeta \leq 3\eta+1$ :

$$r_2(v_\zeta|\phi) = \begin{cases} \zeta - \xi, & \text{if } \zeta = \xi+1, \xi+2, \dots, \frac{2\xi+\eta-1}{2}, \\ \frac{\eta+1}{2}, & \text{if } \zeta = \frac{2\xi+\eta+1}{2}, \\ \xi - \zeta, & \text{if } \zeta = \frac{2\xi+\eta+1}{2}, \frac{2\xi+\eta+1}{2} + 1, \dots, \xi, \\ \zeta - \xi - \eta + 1, & \text{if } \zeta = \xi + \eta, \xi + \eta + 1, \xi + \eta + 2, \dots, \frac{2\xi+3\eta-1}{2}, \\ \frac{\eta+3}{2}, & \text{if } \zeta = \frac{2\xi+3\eta+1}{2}, \\ \frac{\eta-1}{2}, & \text{if } \zeta = 3\eta+1. \end{cases} \quad (27)$$

FIGURE 4:  $L_S(\eta, h)$ .

Case 2. If  $\zeta \equiv 2, 3, 4, \dots, ((\eta + 3)/2) \pmod{2\eta}$ ,

$$r_2(v_\zeta | \phi) = \left( \frac{\eta - 1}{2} + 3 \left( h - \frac{\zeta}{2\eta} - 1 \right) + 2 \left( h - 2 - \frac{\zeta}{2\eta} \right) + \zeta - \left( 2 + 2\eta \frac{\zeta}{2\eta} \right) \right). \quad (28)$$

Case 3. If  $\zeta \equiv ((\eta + 5)/2), ((\eta + 7)/2), \dots, \eta \pmod{2\eta}$ ,

$$r_2(v_\zeta | \phi) = \left( \frac{3\eta + 3}{2} + 3 \left( h - 1 - \frac{\zeta}{2\eta} \right) + 2 \left( h - 2 - \frac{\zeta}{2\eta} \right) - \zeta + \left( 2\eta \frac{\zeta}{2\eta} \right) \right). \quad (29)$$

Case 4. If  $\zeta \equiv 1 \pmod{2\eta}$ ,

$$r_2(v_\zeta | \phi) = \left( \frac{\eta - 1}{2} + 3 \left( h - \frac{\zeta}{2\eta} - 1 \right) + 2 \left( h - 2 - \frac{\zeta}{2\eta} \right) + \zeta - \left( 2\eta \frac{\zeta}{2\eta} \right) \right). \quad (30)$$

Case 5. If  $\zeta \equiv \eta + 2, \eta + 3, \dots, ((3\eta + 3)/2) \pmod{2\eta}$ ,

$$r_2(v_\zeta | \phi) = \left( \frac{\eta - 3}{2} + 3 \left( h - \frac{\zeta}{2\eta} - 1 \right) + 2 \left( h - 2 - \frac{\zeta}{2\eta} \right) + \zeta - \left( 2\eta \frac{\zeta}{2\eta} \right) - \eta + z \right), \quad (31)$$

where  $z = -2$  when  $\zeta \equiv 7 \pmod{2\eta}$  and, otherwise,  $z = 0$ .

Case 6. If  $\zeta \equiv 0, ((3\eta + 5)/2), ((3\eta + 7)/2), \dots, 2\eta - 1 \pmod{2\eta}$ ,

$$r_2(v_\zeta | \phi) = \left( \frac{5\eta + 5}{2} + 3 \left( h - \frac{\zeta}{2\eta} - 1 \right) + 2 \left( h - 2 - \frac{\zeta}{2\eta} \right) - \zeta + \left( 2\eta \frac{\zeta}{2\eta} \right) \right). \quad (32)$$

Case 7. If  $\zeta \equiv \eta + 1 \pmod{2\eta}$ ,



$$r_2(v_\zeta|\phi) = \left(\frac{3\eta+5}{2} + 3\left(h - \frac{\zeta}{2\eta} - 1\right)\right) + 2\left(h - 2 - \frac{\zeta}{2\eta}\right) - \zeta + \left(2\eta \frac{\zeta}{2\eta}\right). \quad (33)$$

Hence, it follows from the above discussion that  $\dim(L_S(\eta, h)) \leq 2$  because all the vertices of  $L_S(\eta, h)$  have unique representations with respect to resolving set  $\phi$ . For reverse inequality that  $\dim(L_S(\eta, h)) \geq 2$ , by contradiction, our assertion becomes  $\dim(L_S(\eta, h)) < 2$ , implying  $\dim(L_S(\eta, h)) = 1$ , and it is not possible because only the path graph exists having the metric dimension 1. All discussion concluding that when  $\eta \geq 5$  (odd) and  $h \geq 2$ ,

$$\dim(L_S(\eta, h)) = 2. \quad (34) \quad \square$$

### 3. Conclusion

We found the metric dimension of some chemical networks ortho-, meta-, and para-polyphenyl chains constructed with base graph  $C_\eta$  and sun graph  $S_\eta$ , and these networks have metric dimension  $\dim(O(\eta, h)) = \dim(M(\eta, h)) = h$  and  $\dim(L(\eta, h)) = 2$ .

### Data Availability

The data used to support the findings of this study are included within the article.

### Conflicts of Interest

The authors declare that there are no conflicts of interest.

### Authors' Contributions

All the authors contributed equally to prepare this article.

### Acknowledgments

The authors extend their appreciation to the Deanship of Scientific Research at King Saud University for funding this work through Research Group no. RG-1441-453.

### References

- [1] P. J. Slater, "Leaves of trees, proceeding of the 6th southeastern conference on combinatorics, graph theory, and computing," *Congressus Numerantium*, vol. 14, pp. 549–559, 1975.
- [2] F. Harary and R. A. Melter, "On the metric dimension of a graph," *Ars Combinatoria*, vol. 2, pp. 191–195, 1976.
- [3] P. J. Cameron and J. H. Van Lint, *Designs Graphs, Codes and Their Links*, Cambridge University Press, Cambridge, UK, 1991.
- [4] G. Chartrand, L. Eroh, M. A. O. Johnson, and R. Ortrud, "Resolvability in graphs and the metric dimension of a graph," *Discrete Applied Mathematics*, vol. 105, no. 1-3, pp. 99–113, 2000.
- [5] S. Khuller, B. Raghavachari, and A. Rosenfeld, "Landmarks in graphs," *Discrete Applied Mathematics*, vol. 70, no. 3, pp. 217–229, 1996.
- [6] A. Sebő and E. Tannier, "on metric generators of graphs," *Mathematics of Operations Research*, vol. 29, no. 2, pp. 383–393, 2004.
- [7] P. Erdős and P. R. Alfréd, "On two problems of information theory," *Magyar tudományos akademia matematikai kutató intézetének közleményei*, vol. 8, pp. 229–243, 1963.
- [8] B. Lindström, "On a combinatory detection problem I. I. Magyar Tud. Akad. Mat. Kutat & oaccute," *Int Kazi*, vol. 9, pp. 195–207, 1964.
- [9] S. Imran, M. K. Siddiqui, and M. Hussain, "Computing the upper bounds for the metric dimension of cellulose network," *Applied Mathematics E-Notes*, vol. 19, pp. 585–605, 2019.
- [10] M. K. Siddiqui and M. Imran, "Computing the metric and partition dimension of H-Naphtalenic and VC5C7 nanotubes," *Journal of Optoelectronics and Advanced Materials*, vol. 17, pp. 790–794, 2015.
- [11] F. Simonraj and A. George, "On the metric dimension of silicate stars," *ARPN Journal of Engineering and Applied Sciences*, vol. 10, no. 5, pp. 2187–2192, 2015.
- [12] Z. Hussain, M. Munir, M. Choudhary, and S. M. Kang, "Computing metric dimension and metric basis of 2 D lattice of alpha-boron nanotubes," *Symmetry*, vol. 10, no. 8, 2018.
- [13] P. Manuel, B. Rajan, I. Rajasingh, and C. Monica, "On minimum metric dimension of honeycomb networks," *Journal of Discrete Algorithms*, vol. 6, pp. 20–27, 2008.
- [14] A. Ahmad, M. Baca, and S. Sultan, "Computing the metric dimension of kayak paddles graph and cycles with chord," *Proyecciones (Antofagasta)*, vol. 39, no. 2, pp. 287–300, 2020.
- [15] M. Ali, G. Ali, M. Imran, A. Q. Baig, and M. K. Shafiq, "On the metric dimension of möbius ladders," *Ars Combinatoria*, vol. 105, pp. 403–410, 2012.
- [16] M. Ali, G. Ali, U. Ali, and M. T. Rahim, "On cycle related graphs with constant metric dimension," *Open Journal of Discrete Mathematics*, vol. 2, pp. 21–23, 2012.
- [17] S. Hayat, A. Khan, M. Y. H. Malik, M. Imran, and M. K. Siddiqui, "Fault-tolerant metric dimension of interconnection networks," *IEEE Access*, vol. 8, pp. 145435–145445, 2020.
- [18] M. Imran, A. Q. Baig, S. A. Bokhary, and I. Javaid, "On the metric dimension of circulant graphs," *Applied Mathematics Letters*, vol. 25, no. 3, pp. 320–325, 2012.
- [19] D. Kuziak, J. A. Rodríguez-Velázquez, and I. G. Yero, "On the strong metric dimension of product graphs," *Electronic Notes in Discrete Mathematics*, vol. 46, pp. 169–176, 2014.
- [20] J. B. Liu, M. F. Nadeem, H. M. A. Siddiqui, and W. Nazir, "computing metric dimension of certain families of toepfritz graphs," *IEEE Access*, vol. 7, pp. 126734–126741, 2019.
- [21] J. B. Liu, A. Zafari, and H. Zarei, "Metric dimension, minimal doubly resolving sets, and the strong metric dimension for jellyfish graph and cocktail party graph," *Complexity*, vol. 2020, Article ID 9407456, 7 pages, 2020.
- [22] M. F. Nadeem, M. Azeem, and A. Khalil, "The locating number of hexagonal möbius ladder network," *Journal of Applied Mathematics and Computing*, 2020.
- [23] H. Raza, J.-B. Liu, and S. Qu, "On mixed metric dimension of rotationally symmetric graphs," *IEEE Access*, vol. 8, pp. 11560–11569, 2019.
- [24] H. Raza and Y. Ji, "Computing mixed metric dimension in generalized Petersen graph  $P(n, 2)$ ," *Frontiers in Physics*, vol. 8, p. 211, 2020.

- [25] H. Raza, Y. Ji, and S. Qu, "On mixed metric dimension of some path related graphs," *IEEE Access*, vol. 8, pp. 188146–188153, 2020.
- [26] M. Somasundari and F. S. Raj, "Fault-tolerant resolvability of oxide interconnections," *International Journal of Innovative Technology and Exploring Engineering (IJITEE)*, vol. 8, pp. 2278–3075, 2019.
- [27] T. Vetrík and A. Ahmad, "Computing the metric dimension of the categorial product of some graphs," *International Journal of Computer Mathematics*, vol. 94, no. 2, pp. 363–371, 2017.
- [28] I. G. Yero, "Vertices, edges, distances and metric dimension in graphs," *Electronic Notes in Discrete Mathematics*, vol. 55, pp. 191–194, 2016.

## Research Article

# Degree-Based Topological Indices of Polysaccharides: Amylose and Blue Starch-Iodine Complex

Anam Rani<sup>1</sup> and Usman Ali <sup>2,3</sup>

<sup>1</sup>Department of Basic Sciences, Deanship of Preparatory Year, King Faisal University Al Ahsa, Al Hofuf, Saudi Arabia

<sup>2</sup>Institute de Mathematiques de Jussieu-Paris Rive Gauche-Paris, France (Universite de Paris/Sorbonne Universite), Paris, France

<sup>3</sup>CASPAM, Bahauddin Zakariya University, Multan 60000, Pakistan

Correspondence should be addressed to Usman Ali; [uali@bzu.edu.pk](mailto:uali@bzu.edu.pk)

Received 2 January 2021; Revised 15 March 2021; Accepted 19 March 2021; Published 2 April 2021

Academic Editor: Muhammad Faisal Nadeem

Copyright © 2021 Anam Rani and Usman Ali. This is an open access article distributed under the Creative Commons Attribution License, which permits unrestricted use, distribution, and reproduction in any medium, provided the original work is properly cited.

Starch is a polymer of glucose where alpha-linkages are associated with glucopyranose units. It comprises a mixture of amylose and amylopectin. Furthermore, amylose is a linear chain of hundreds of glucose molecules. Starches are not allowed to be dissolved in water. They can be digested by breaking down alpha bonds (glycosidic bonds). Its cyclic degradation products, called cyclodextrins, are the best role models for amylose. They can be considered simple turns of the amylose propeller that has imploded into a circular path. Both humans and animals have amylases, which allow them to digest starches. The important sources of starch include potatoes, rice, wheat, and maize for human consumption. The production of starches is how plants store glucose. The blue colour of starch produced by an iodine solution or iodine reaction is used for its identification. Polysaccharides with a reduced degree of polymerization, known as dextrans, are produced in the starch's partial acid hydrolysis. Complete hydrolysis leads to glucose. In this article, we compute the topological properties: Zagreb index  $M_1(\Gamma)$  and  $M_2(\Gamma)$ , Randić index  $R_\alpha(\Gamma)$  for  $\alpha = -(1/2), -1, (1/2), 1$ , atom-bond connectivity index  $ABC(\Gamma)$ , geometric-arithmetic index  $GA(\Gamma)$ , fourth atom-bond connectivity index  $ABC_4(\Gamma)$ , fifth geometric-arithmetic index  $GA_5(\Gamma)$ , and degree-based topological indices of a graph  $\Gamma$  representing polysaccharides, namely, amylose and blue starch-iodine complex. In the end, we compare these indices and depict their graphic behavior.

## 1. Introduction

Amylose has the most basic structure of all nutritional polysaccharides, composed purely of glucose polymers connected only by  $\alpha(1-4)$  bonds. Notice that starch is, in fact, a combination of amylose and amylopectin. Amylose is not allowed to be dissolved in water and is more difficult to digest compared to amylopectin. The complexing of amylopectin with amylose facilitates its water—another view of amylose solubility and digestibility. Amylose plays an important role in the storage of plant energy, and as plants do not require glucose to explode, its dense structure and slow breakdown features are under plant's growth. Another function of polysaccharides within cells refers to structural support. Besides, hemicelluloses are another group of polysaccharides located in plant cell walls.

In 1814, Colin and Claubry discovered the starch-iodine reaction, which is well renowned to any chemist from basic courses in qualitative and quantitative analysis.

The first topological index was derived in 1947 when Wiener worked on the boiling point of paraffin alkanes. It was known as the Wiener number. Later on, it is called a path number. The work [1] described the M-polynomial and degree-based topological indices of graphs. The authors in [2, 3] discussed the symmetric divisor deg index of graphs, first Zagreb after 30 years in changed form and topological indices of molecular structure. The authors in [4] also discussed the  $\pi$  electron energy of hydrocarbons. In recent years, Hasni et al. computed the degree-based topological indices of the line graph of benzene ring embedded in P-type surface in the 2D network [5]. In [6], the authors calculated the index numbers for the edge version of the geometric-

arithmetic index of nanocones. Much research has been done to explain the nature of chromophore absorption at 620 nm that yields starch-iodine complex, the distinctive dark blue colour. Still, there seem to have been many disputes that might be addressed to some extent in recent decades.

Let  $\Gamma$  be connected simple graph with  $V(\Gamma)$  a set of vertices and  $E(\Gamma)$  a set of edges. Let  $u \in V(\Gamma)$  and its degree is represented by  $\mathfrak{R}_u$ . The idea of degree-based topological indices began from Wiener index; in 1945, Wiener defined them while studying alkane's boiling point cf. [7]. The first degree-based topological index is Randić index given by Milan Randić in [8] and is described as

$$R_{-(1/2)} = \sum_{uv \in E(\Gamma)} \frac{1}{\sqrt{\mathfrak{R}_u \mathfrak{R}_v}} \quad (1)$$

Generalized Randić index (denoted as  $R_\alpha(\Gamma)$ ) is described as follows:

$$R_\alpha(\Gamma) = \sum_{uv \in E(\Gamma)} \left( \mathfrak{R}_u \mathfrak{R}_v \right)^\alpha, \quad \alpha = 1, \frac{1}{2}, -\frac{1}{2}, -1. \quad (2)$$

Inverse generalized Randić index (denoted as  $RR_\alpha(\Gamma)$ ) is described as

$$RR_\alpha(\Gamma) = \sum_{uv \in E(\Gamma)} \frac{1}{\left( \sqrt{\mathfrak{R}_u \mathfrak{R}_v} \right)^\alpha}. \quad (3)$$

In [4, 9, 10], Gutman and Trinajstić introduced and defined the first Zagreb index (denoted as  $M_1(\Gamma)$ ) and second Zagreb index (denoted as  $M_2(\Gamma)$ ) as

$$M_1(\Gamma) = \sum_{uv \in E(\Gamma)} (\mathfrak{R}_u + \mathfrak{R}_v), M_2(\Gamma) = \sum_{uv \in E(\Gamma)} (\mathfrak{R}_u \mathfrak{R}_v). \quad (4)$$

In [11], Estrada introduced and studied about the atom-bond connectivity index (denoted as  $ABC(\Gamma)$ ). It is defined as follows:

$$ABC(\Gamma) = \sum_{uv \in E(\Gamma)} \sqrt{\frac{\mathfrak{R}_u + \mathfrak{R}_v - 2}{\mathfrak{R}_u \mathfrak{R}_v}}. \quad (5)$$

Geometric-arithmetic index (denoted as  $GA(\Gamma)$ ) was given by Vukićević cf. [12] and is defined as follows:

$$GA(\Gamma) = \sum_{uv \in E(\Gamma)} 2 \frac{\sqrt{\mathfrak{R}_u \mathfrak{R}_v}}{\mathfrak{R}_u + \mathfrak{R}_v}. \quad (6)$$

The fourth version of the ABC index (denoted as  $ABC_4(\Gamma)$ ) was introduced by Ghorbani in [13] and is defined as

$$ABC_4(\Gamma) = \sum_{uv \in E(\Gamma)} \sqrt{\frac{S_u + S_v - 2}{S_u S_v}}, \quad (7)$$

where  $S_u = \sum_{v=N_\Gamma(u)} \mathfrak{R}_v$  and  $N_\Gamma(u) = \{v \in V(\Gamma) | uv \in E(\Gamma)\}$ .

The fifth version of the GA index (denoted as  $GA_5(\Gamma)$ ) was given by Graovac cf. [14] and is defined as

$$GA_5(\Gamma) = \sum_{uv \in E(\Gamma)} \frac{2\sqrt{S_u S_v}}{S_u + S_v}. \quad (8)$$

## 2. Result for Amylose

Starch is a polymer of glucose whose glucopyranose alpha bonds bind cells. It is a mixture of amylose and amylopectin. Amylose is a linear chain of hundreds of glucose molecules. Starches cannot be dissolved in water. They can be digested by breaking the alpha bonds (glycosidic bonds). Amylose is a polysaccharide composed of  $\alpha$ -D-glucose units, linked by  $\alpha(1-4)$  glycosidic bonds. It is one of the two starch components that make up about 20 to 30 percent. Due to its tight spiral structure, amylose seems to be more resilient to digestion than other starch molecules and is, thus, a significant form of resistant starch [15] (see Figure 1 for a molecular structure of amylose and Figure 2 for its unit graph and the graph model corresponding to amylose for  $n=4$ , where  $n$  is the number of units). In amylose, there are three types of vertices having degrees 1, 2, and 3. For  $n \geq 2$ , amylose has four types of edge partitions as

$$\begin{aligned} E_{1,2}(\Gamma) &= \{ \mathfrak{R}_u = 1, \mathfrak{R}_v = 2 \text{ and } u, v \in V(\Gamma) \}, \\ E_{1,3}(\Gamma) &= \{ \mathfrak{R}_u = 1, \mathfrak{R}_v = 3 \text{ and } u, v \in V(\Gamma) \}, \\ E_{2,3}(\Gamma) &= \{ \mathfrak{R}_u = 2, \mathfrak{R}_v = 3 \text{ and } u, v \in V(\Gamma) \}, \\ E_{3,3}(\Gamma) &= \{ \mathfrak{R}_u = 3, \mathfrak{R}_v = 3 \text{ and } u, v \in V(\Gamma) \}. \end{aligned} \quad (9)$$

**Theorem 1.** For all  $n \geq 2$ , let  $\Gamma$  be the graph of amylose, then we have the following:

$$\begin{aligned} R_1(\Gamma) &= 74n - 6, \\ R_{(1/2)}(\Gamma) &= 29.1258n - 1.4349, \\ R_{-(1/2)}(\Gamma) &= 5.2363n + 0.3382, \\ R_{-1}(\Gamma) &= 2.4444n + 0.3334. \end{aligned} \quad (10)$$

*Proof.* The general Randić connectivity index  $R_\alpha(\Gamma)$  for  $\alpha = 1$  is

$$R_1(\Gamma) = \sum_{uv \in E(\Gamma)} \mathfrak{R}_u \mathfrak{R}_v. \quad (11)$$

From Table 1 and equation (2), we get

$$\begin{aligned} R_1(\Gamma) &= n(1 \times 2) + (2n + 2)(1 \times 3) + (5n - 2)(2 \times 3) \\ &\quad + 4n(3 \times 3) = 74n - 6. \end{aligned} \quad (12)$$

Now, for  $\alpha = (1/2)$ , the general Randić connectivity index  $R_\alpha(\Gamma)$  is

$$R_{(1/2)}(\Gamma) = \sum_{uv \in E(\Gamma)} \sqrt{\mathfrak{R}_u \mathfrak{R}_v}. \quad (13)$$

Again, from Table 1 and equation (2), we have

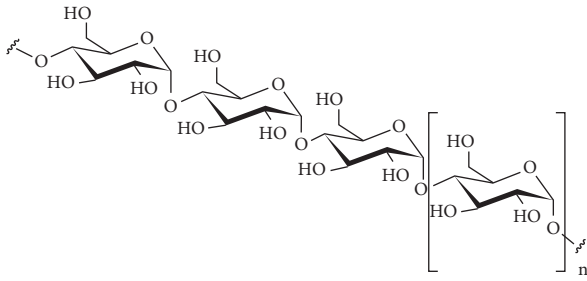


FIGURE 1: Molecular structure of amylose.

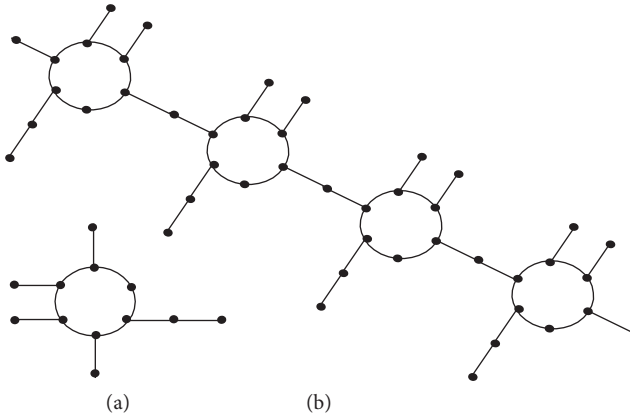
FIGURE 2: (a) Graph of amylose for  $n = 1$  and (b) graph of amylose for  $n = 4$ .

TABLE 1: Edge partition of edges based on the degree of vertices.

Types of edges	$E_{\{1,2\}}$	$E_{\{1,3\}}$	$E_{\{2,3\}}$	$E_{\{3,3\}}$
Edges	(1, 2)	(1, 3)	(2, 3)	(3, 3)
Frequency	$n$	$2n + 2$	$5n - 2$	$4n$

$$R_{(1/2)}(\Gamma) = n\sqrt{(1 \times 2)} + (2n + 2)\sqrt{(1 \times 3)} + (5n - 2)\sqrt{(2 \times 3)} + 4n\sqrt{(3 \times 3)} \quad (14)$$

$$= 29.1258n - 1.4349.$$

If  $\alpha = -(1/2)$ , then

$$R_{-(1/2)}(\Gamma) = \sum_{uv \in E(\Gamma)} \frac{1}{\sqrt{\mathfrak{R}_u \mathfrak{R}_v}} \quad (15)$$

From Table 1 and equation (2), it follows that

$$R_{-(1/2)}(\Gamma) = \frac{n}{\sqrt{(1 \times 2)}} + \frac{(2n + 2)}{\sqrt{(1 \times 3)}} + \frac{(5n - 2)}{\sqrt{(2 \times 3)}} + \frac{4n}{\sqrt{(3 \times 3)}} \quad (16)$$

$$= 5.2363n + 0.3382.$$

Now, for  $\alpha = -1$ , we have

$$R_{-1}(\Gamma) = \sum_{uv \in E(\Gamma)} \frac{1}{\mathfrak{R}_u \mathfrak{R}_v} \quad (17)$$

From Table 1 and equation (2), we get

$$R_{-1}(\Gamma) = \frac{n}{(1 \times 2)} + \frac{(2n + 2)}{(1 \times 3)} + \frac{(5n - 2)}{(2 \times 3)} + \frac{4n}{(3 \times 3)} \quad (18)$$

$$= 2.4444n + 0.3334. \quad \square$$

**Theorem 2.** For all  $n \geq 2$ , let  $\Gamma$  be the graph of amylose, then, we have the following:

$$M_1(\Gamma) = 60n - 2,$$

$$M_2(\Gamma) = 74n - 6,$$

$$ABC(\Gamma) = 8.5423n + 0.2188,$$

$$GA(\Gamma) = 11.5738n - 0.2276. \quad (19)$$

*Proof.* By using Table 1 and equation (4), we get

$$M_1(\Gamma) = \sum_{uv \in E(\Gamma)} (\mathfrak{R}_u + \mathfrak{R}_v)$$

$$= n(1 + 2) + (2n + 2)(1 + 3) + (5n - 2)(2 + 3) + 4n(3 + 3)$$

$$= 60n - 2,$$

$$M_2(\Gamma) = \sum_{uv \in E(\Gamma)} \mathfrak{R}_u \mathfrak{R}_v$$

$$= n(1 \times 2) + (2n + 2)(1 \times 3) + (5n - 2)(2 \times 3) + 4n(3 \times 3)$$

$$= 74n - 6.$$

$$M_2(\Gamma) = \sum_{uv \in E(\Gamma)} \widetilde{\mathfrak{R}_u} \widetilde{\mathfrak{R}_v}$$

$$= n(1 \times 2) + (2n + 2)(1 \times 3) + (5n - 2)(2 \times 3) + 4n(3 \times 3)$$

$$= 74n - 6. \quad (20)$$

By using Table 1 and equation (5), we get

$$ABC(\Gamma) = \sum_{uv \in E(\Gamma)} \sqrt{\frac{\mathfrak{R}_u + \mathfrak{R}_v - 2}{\mathfrak{R}_u \mathfrak{R}_v}}$$

$$= n\sqrt{\frac{1 + 2 - 2}{1 \times 2}} + (2n + 2)\sqrt{\frac{1 + 3 - 2}{1 \times 3}}$$

$$+ (5n - 2)\sqrt{\frac{2 + 3 - 2}{2 \times 3}} + 4n\sqrt{\frac{3 + 3 - 2}{3 \times 3}}$$

$$= 8.5423n + 0.2188. \quad (21)$$

By using Table 1 and equation (6), we get

$$\begin{aligned}
 GA(\Gamma) &= \sum_{uv \in E(\Gamma)} \frac{2\sqrt{\mathfrak{R}_u \mathfrak{R}_v}}{\mathfrak{R}_u + \mathfrak{R}_v} \\
 &= 2 \left( n \frac{\sqrt{1 \times 2}}{(1+2)} + (2n+2) \frac{\sqrt{1 \times 3}}{(1+3)} \right. \\
 &\quad \left. + (5n-2) \frac{\sqrt{2 \times 3}}{(2+3)} + 4n \frac{\sqrt{3 \times 3}}{(3+3)} \right) \\
 &= 11.5738n - 0.2276.
 \end{aligned} \tag{22}$$

In Table 2, we give the edge partition centered on degree sum of end vertices for each edge.  $\square$

**Theorem 3.** For all  $n \geq 2$ , let  $\Gamma$  be the graph of amylose, then we have

$$\begin{aligned}
 ABC_4(\Gamma) &= 6.4972n + 0.2874, \\
 GA_5(\Gamma) &= 11.7142n - 0.123.
 \end{aligned} \tag{23}$$

*Proof.* By using Table 2 and equation (7), we get

$$\begin{aligned}
 ABC_4(\Gamma) &= \sum_{uv \in E(\Gamma)} \sqrt{\frac{S_u + S_v - 2}{S_u S_v}} \\
 &= n \sqrt{\frac{2+4-2}{2 \times 4}} + \sqrt{\frac{3+6-2}{3 \times 6}} + (2n+1) \sqrt{\frac{3+7-2}{3 \times 7}} + n \sqrt{\frac{4+7-2}{4 \times 7}} + \sqrt{\frac{6+6-2}{6 \times 6}} \\
 &\quad + (3n-1) \sqrt{\frac{6+7-2}{6 \times 7}} + (n-1) \sqrt{\frac{6+8-2}{6 \times 8}} + (2n+1) \sqrt{\frac{7+7-2}{7 \times 7}} + (2n-2) \sqrt{\frac{7+8-2}{7 \times 8}} \\
 &= 6.4972n + 0.2874.
 \end{aligned} \tag{24}$$

By using Table 2 and equation (8), we get

$$\begin{aligned}
 GA_5(\Gamma) &= \sum_{uv \in E(\Gamma)} \frac{2\sqrt{S_u S_v}}{S_u + S_v} \\
 &= 2 \left( n \frac{\sqrt{2 \times 4}}{(2+4)} + \frac{\sqrt{3 \times 6}}{(3+6)} + (2n+1) \frac{\sqrt{3 \times 7}}{(3+7)} + n \frac{\sqrt{4 \times 7}}{(4+7)} + \frac{\sqrt{6 \times 6}}{(6+6)} + (3n-1) \frac{\sqrt{6 \times 7}}{(6+7)} \right. \\
 &\quad \left. + (n-1) \frac{\sqrt{6 \times 8}}{(6+8)} + (2n+1) \frac{\sqrt{7 \times 7}}{(7+7)} + (2n-2) \frac{\sqrt{7 \times 8}}{(7+8)} \right) \\
 &= 11.7142n - 0.123.
 \end{aligned} \tag{25}$$

$\square$

### 3. Numerical and Graphical Representation

The numeric representation of the results calculated above is illustrated in Tables 3 and 4, while the graphic representation is devoted to Figures 3 and 4.

### 4. Results for Blue Starch-Iodine Complex

The main structure of amylose are cyclic degradants known as cyclodextrins. They are obtained enzymatically and may be considered as single turns of the helix of amylose imploding into a circular path. In all of these complexes, cyclodextrin molecules are positioned in

front to form dimers and they are piled together to generate large cylinders that resemble the amylose helix in its global structure. The most interesting one is (trimesic acid  $H_2O$ )<sub>10</sub>HI<sub>5</sub> with linear polyiodide chain. This structural model was accepted, but, unfortunately, cannot shed light on the actual configuration of the polyiodide chain (see Figure 5 for the molecular structure of blue starch-iodine and Figure 6 for its unit graph and the graph model corresponding to blue starch-iodine for  $n=6$ , where  $n$  is the number of units). In starch-iodine, there are three types of vertices having degrees 1, 2, and 3. For  $n \geq 3$ , blue starch-iodine complex has five types of edge partitions as

TABLE 2: Edge partition based on the degree sum of end vertices of each edge.

Types of edges	$E_{\{2,4\}}$	$E_{\{3,6\}}$	$E_{\{3,7\}}$	$E_{\{4,7\}}$	$E_{\{6,6\}}$	$E_{\{6,7\}}$	$E_{\{6,8\}}$	$E_{\{7,7\}}$	$E_{\{7,8\}}$
Number of edges	(2, 4)	(3, 6)	(3, 7)	(4, 7)	(6, 6)	(6, 7)	(6, 8)	(7, 7)	(7, 8)
Frequency	$n$	1	$2n + 1$	$n$	1	$3n - 1$	$n - 1$	$2n + 1$	$2n - 2$

TABLE 3: Numerical comparison of  $M_1(\Gamma)$ ,  $M_2(\Gamma)$ ,  $ABC(\Gamma)$ ,  $GA(\Gamma)$ ,  $R_1(\Gamma)$ ,  $R_{-1}(\Gamma)$ ,  $R_{(1/2)}(\Gamma)$ , and  $R_{-(1/2)}(\Gamma)$ .

$n$	$M_1(\Gamma)$	$M_2(\Gamma)$	$ABC(\Gamma)$	$GA(\Gamma)$	$R_1(\Gamma)$	$R_{-1}(\Gamma)$	$R_{(1/2)}(\Gamma)$	$R_{-(1/2)}(\Gamma)$
1	58	68	8.7611	11.3462	68	2.7778	27.6909	5.5746
2	118	142	17.3034	22.92	142	5.2222	56.8166	10.8109
3	178	216	25.8457	34.4938	216	7.6667	85.9424	16.0474
4	238	290	34.388	46.0676	290	10.1111	115.0682	21.2837
5	298	364	42.9303	57.6414	364	12.5556	144.1939	26.5201
6	358	438	51.4726	69.2152	438	15	173.3197	31.7565
7	418	512	60.0149	80.789	512	17.4444	202.4455	36.9929
8	478	586	68.5572	92.3628	586	19.8889	231.5712	42.2293
9	538	660	77.0995	103.9366	660	22.3333	260.6969	47.4656
10	598	734	85.6418	115.5104	734	24.7778	289.8228	52.7020

TABLE 4: Numerical comparison of  $ABC_4(\Gamma)$  and  $GA_5(\Gamma)$ .

$n$	1	2	3	4	5	6	7	8	9	10
$ABC_4(\Gamma)$	6.785	13.282	19.779	26.276	32.773	39.271	45.768	52.265	58.762	65.259
$GA_5(\Gamma)$	11.591	23.305	35.019	46.734	58.448	70.162	81.876	93.5906	105.305	117.019

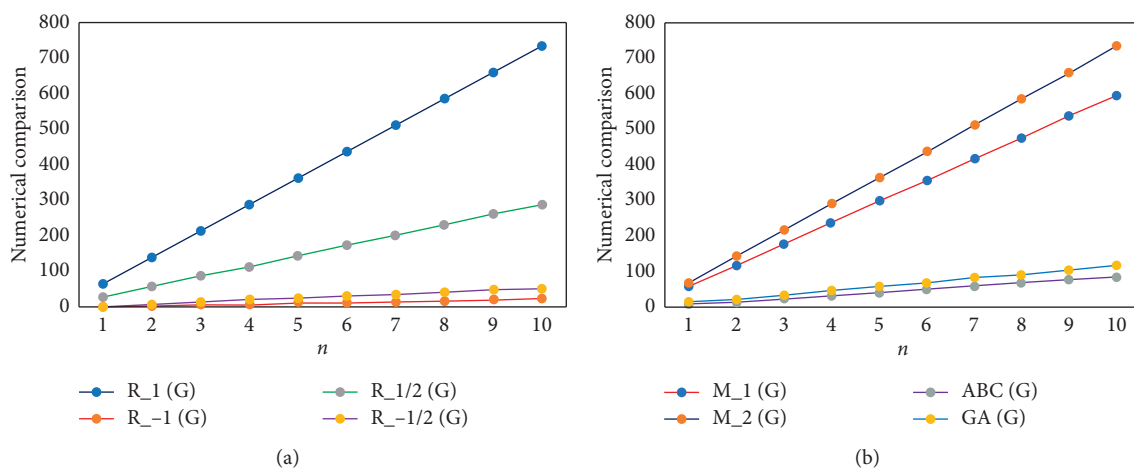
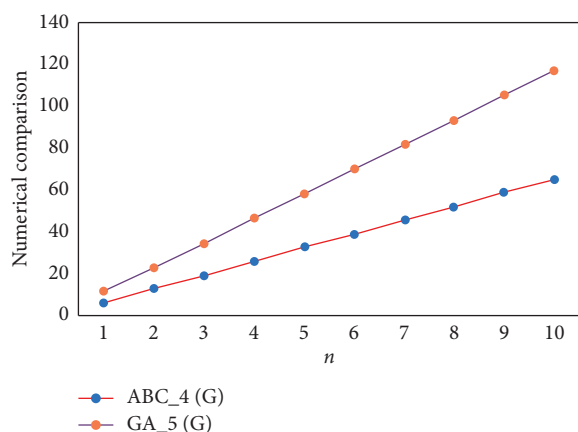
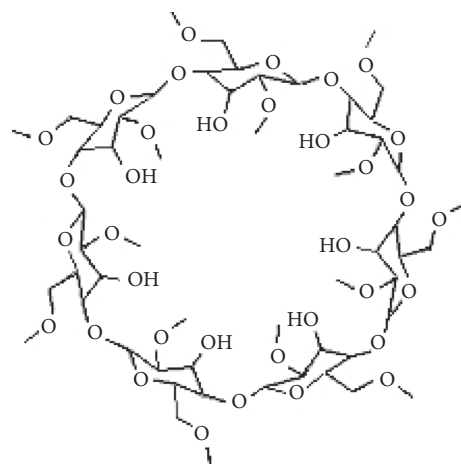
FIGURE 3: (a) Comparison of  $R_\alpha$  for  $\alpha = 1, -1, (1/2), -(1/2)$  and (b) comparison of  $M_1(\Gamma)$ ,  $M_2(\Gamma)$ ,  $ABC(\Gamma)$ , and  $GA(\Gamma)$ FIGURE 4: Comparison of  $ABC_4(\Gamma)$  and  $GA_5(\Gamma)$ 

FIGURE 5: Molecular structure of blue starch-iodine.

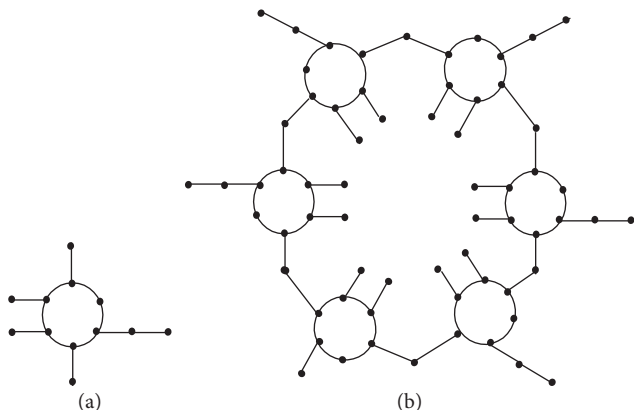


FIGURE 6: (a) Graph of blue starch-iodine for  $n = 1$  and (b) graph of blue starch-iodine for  $n = 6$ .

$$\begin{aligned}
 E_{1,2}(\Gamma) &= \{\widetilde{\mathfrak{R}}_u = 1, \widetilde{\mathfrak{R}}_v = 2 \text{ and } u, v \in V(\Gamma)\}, \\
 E_{1,3}(\Gamma) &= \{\widetilde{\mathfrak{R}}_u = 1, \widetilde{\mathfrak{R}}_v = 3 \text{ and } u, v \in V(\Gamma)\}, \\
 E_{2,2}(\Gamma) &= \{\widetilde{\mathfrak{R}}_u = 2, \widetilde{\mathfrak{R}}_v = 2 \text{ and } u, v \in V(\Gamma)\}, \\
 E_{2,3}(\Gamma) &= \{\widetilde{\mathfrak{R}}_u = 2, \widetilde{\mathfrak{R}}_v = 3 \text{ and } u, v \in V(\Gamma)\}, \\
 E_{3,3}(\Gamma) &= \{\widetilde{\mathfrak{R}}_u = 3, \widetilde{\mathfrak{R}}_v = 3 \text{ and } u, v \in V(\Gamma)\}.
 \end{aligned} \quad (26)$$

**Theorem 4.** For all  $n \geq 3$ , let  $\Gamma$  be the graph of blue starch-iodine complex, we have the following  $R_\alpha(\Gamma)$ ,  $\alpha \in R$ :

$$\begin{aligned}
 R_1(\Gamma) &= 39n^2 - n + 12, \\
 R_{(1/2)}(\Gamma) &= 16.429n^2 - 1.0354 + 2.8695, \\
 R_{-(1/2)}(\Gamma) &= 3.0272n^2 + .5585n - 0.6764, \\
 R_{-1}(\Gamma) &= 0.75n^2 + 0.6944n - 0.6667.
 \end{aligned} \quad (27)$$

*Proof.* For  $\alpha = 1$ , the general Randić connectivity index is

$$R_1(\Gamma) = \sum_{uv \in E(\Gamma)} \widetilde{\mathfrak{R}}_u \widetilde{\mathfrak{R}}_v. \quad (28)$$

From Table 5 (for edge partition) and equation (2), we get

$$\begin{aligned}
 R_1(\Gamma) &= 2n(1 \times 2) + \left[ \sum_{i=1}^{n-1} (n+2) - 2 \right] (1 \times 3) \\
 &\quad + n(2 \times 2) + \left[ \sum_{i=1}^{n-1} (6n-2) + 2 \right] (2 \times 3) + 4n(3 \times 3) \\
 &= 39n^2 - n + 12.
 \end{aligned} \quad (29)$$

Now, for  $\alpha = (1/2)$ , we have

$$R_{(1/2)}(\Gamma) = \sum_{uv \in E(\Gamma)} \sqrt{\widetilde{\mathfrak{R}}_u \widetilde{\mathfrak{R}}_v}. \quad (30)$$

By using Table 5 and equation (2), after simplification, we have

$$\begin{aligned}
 R_{(1/2)}(\Gamma) &= 2n\sqrt{(1 \times 2)} + \left[ \sum_{i=1}^{n-1} (n+2) - 2 \right] \sqrt{(1 \times 3)} \\
 &\quad + n\sqrt{(2 \times 2)} + \left[ \sum_{i=1}^{n-1} (6n-2) + 2 \right] \sqrt{(2 \times 3)} \\
 &\quad + 4n\sqrt{(3 \times 3)} \\
 &= 16.429n^2 - 1.0354 + 2.8695.
 \end{aligned} \quad (31)$$

For  $\alpha = -(1/2)$ , we have

$$R_{-(1/2)}(\Gamma) = \sum_{uv \in E(\Gamma)} \frac{1}{\sqrt{\widetilde{\mathfrak{R}}_u \widetilde{\mathfrak{R}}_v}} \quad (32)$$

From Table 5 and equation (2), it follows that

$$\begin{aligned}
 R_{-(1/2)}(\Gamma) &= \frac{2n}{\sqrt{(1 \times 2)}} + \frac{\left[ \sum_{i=1}^{n-1} (n+2) - 2 \right]}{\sqrt{(1 \times 3)}} \\
 &\quad + \frac{n}{\sqrt{(2 \times 2)}} + \frac{\left[ \sum_{i=1}^{n-1} (6n-2) + 2 \right]}{\sqrt{(2 \times 3)}} + \frac{4n}{\sqrt{(3 \times 3)}} \\
 &= 3.0272n^2 + .5585n - 0.6764.
 \end{aligned} \quad (33)$$

For  $\alpha = -1$ , we have

$$R_{-1}(\Gamma) = \sum_{uv \in E(\Gamma)} \frac{1}{\widetilde{\mathfrak{R}}_u \widetilde{\mathfrak{R}}_v}. \quad (34)$$

Again by using Table 5 and equation (2), we get

$$\begin{aligned}
 R_{-1}(\Gamma) &= \frac{2n}{(1 \times 2)} + \frac{\left[ \sum_{i=1}^{n-1} (n+2) - 2 \right]}{(1 \times 3)} + \frac{n}{(2 \times 2)} \\
 &\quad + \frac{\left[ \sum_{i=1}^{n-1} (6n-2) + 2 \right]}{(2 \times 3)} + \frac{4n}{(3 \times 3)} \\
 &= 0.75n^2 + 0.6944n - 0.6667.
 \end{aligned} \quad (35)$$

□

**Theorem 5.** For all  $n \geq 3$ , let  $\Gamma$  be the graph of blue starch-iodine complex, then we have the following:

$$\begin{aligned}
 M_1(\Gamma) &= 34n^2 - 2n + 4, \\
 M_2(\Gamma) &= 39n^2 - n + 12, \\
 ABC(\Gamma) &= 5.0591n^2 - 0.0523n - 0.4376, \\
 GA(\Gamma) &= 6.7448n^2 - 3.0868n + 0.4552.
 \end{aligned} \quad (36)$$

*Proof.* By using Table 5 and equation (4), we get



TABLE 5: Edge partition based on the degree of vertices.

Types of edges	$E_{\{1,2\}}$	$E_{\{1,3\}}$	$E_{\{2,2\}}$	$E_{\{2,3\}}$	$E_{\{3,3\}}$
Number of edges	(1, 2)	(1, 3)	(2, 2)	(2, 3)	(3, 3)
Frequency	$2n$	$\sum_{i=1}^{n-1} (n+2) - 2$	$n$	$\sum_{i=1}^{n-1} (6n-2) + 2$	$4n$

$$\begin{aligned}
M_1(\Gamma) &= \sum_{uv \in E(\Gamma)} (\overline{\mathfrak{R}}_u + \overline{\mathfrak{R}}_v) \\
&= 2n(1+2) + \left[ \sum_{i=1}^{n-1} (n+2) - 2 \right] (1+3) + n(2+2) \\
&\quad + \left[ \sum_{i=1}^{n-1} (6n-2) + 2 \right] (2+3) + 4n(3+3) \\
&= 34n^2 - 2n + 4, \\
M_2(\Gamma) &= \sum_{uv \in E(\Gamma)} \overline{\mathfrak{R}}_u \overline{\mathfrak{R}}_v \\
&= 2n(1 \times 2) + \left[ \sum_{i=1}^{n-1} (n+2) - 2 \right] (1 \times 3) + n(2 \times 2) \\
&\quad + \left[ \sum_{i=1}^{n-1} (6n-2) + 2 \right] (2 \times 3) + 4n(3 \times 3) \\
&= 39n^2 - n + 12.
\end{aligned} \tag{37}$$

TABLE 6: Edge partition based on the degree sum of end vertices of each edge.

Types of edges	No. of edges	Frequency
$E_{\{2,3\}}$	(2, 3)	$n$
$E_{\{2,4\}}$	(2, 4)	$n$
$E_{\{3,5\}}$	(3, 5)	$n$
$E_{\{3,6\}}$	(3, 6)	$\sum_{i=1}^{n-1} (1) - 1$
$E_{\{3,7\}}$	(3, 7)	$\sum_{i=1}^{n-1} (n) - 1$
$E_{\{4,8\}}$	(4, 8)	$n$
$E_{\{5,7\}}$	(5, 7)	$n$
$E_{\{6,6\}}$	(6, 6)	$\sum_{i=1}^{n-1} (1) - 1$
$E_{\{6,7\}}$	(6, 7)	$\sum_{i=1}^{n-1} (3n-2) + 2$
$E_{\{6,8\}}$	(6, 8)	$n$
$E_{\{7,7\}}$	(7, 7)	$\sum_{i=1}^{n-1} (2) - 2$
$E_{\{7,8\}}$	(7, 8)	$\sum_{i=1}^{n-1} (4n-3) + 3$

By using Table 5 and equation (5), we get

$$\begin{aligned}
ABC(\Gamma) &= \sum_{uv \in E(\Gamma)} \sqrt{\frac{\overline{\mathfrak{R}}_u + \overline{\mathfrak{R}}_v - 2}{\overline{\mathfrak{R}}_u \overline{\mathfrak{R}}_v}} \\
&= 2n \sqrt{\frac{1+2-2}{1 \times 2}} + \left[ \sum_{i=1}^{n-1} (n+2) - 2 \right] \sqrt{\frac{1+3-2}{1 \times 3}} + n \sqrt{\frac{2+2-2}{2 \times 2}} + \left[ \sum_{i=1}^{n-1} (6n-2) + 2 \right] \sqrt{\frac{2+3-2}{2 \times 3}} \\
&\quad + 4n \sqrt{\frac{3+3-2}{3 \times 3}} \\
&= 5.0591n^2 - 0.0523n - 0.4376.
\end{aligned} \tag{38}$$

By using Table 5 and equation (6), we get

$$\begin{aligned}
GA(\Gamma) &= \sum_{uv \in E(\Gamma)} \frac{2\sqrt{\overline{\mathfrak{R}}_u \overline{\mathfrak{R}}_v}}{(\overline{\mathfrak{R}}_u + \overline{\mathfrak{R}}_v)} \\
&= 2 \left( 2n \frac{\sqrt{1 \times 2}}{(1+2)} + \left[ \sum_{i=1}^{n-1} (n+2) - 2 \right] \frac{\sqrt{1 \times 3}}{(1+3)} + n \frac{\sqrt{2 \times 2}}{(2+2)} + \left[ \sum_{i=1}^{n-1} (6n-2) + 2 \right] \frac{\sqrt{2 \times 3}}{(2+3)} + 4n \frac{\sqrt{3 \times 3}}{(3+3)} \right) \\
&= 6.7448n^2 - 3.0868n + 0.4552.
\end{aligned} \tag{39}$$

□

TABLE 7: Numerical comparison of  $M_1(\Gamma)$ ,  $M_2(\Gamma)$ ,  $ABC(\Gamma)$ ,  $GA(\Gamma)$ ,  $R_1(\Gamma)$ ,  $R_{-1}(\Gamma)$ ,  $R_{(1/2)}(\Gamma)$ , and  $R_{-(1/2)}(\Gamma)$ .

$n$	$M_1(\Gamma)$	$M_2(\Gamma)$	$ABC(\Gamma)$	$GA(\Gamma)$	$R_1(\Gamma)$	$R_{-1}(\Gamma)$	$R_{(1/2)}(\Gamma)$	$R_{-(1/2)}(\Gamma)$
1	36	50	4.5692	4.1132	50	1.361	18.2633	2.9093
2	136	166	19.6942	21.2608	166	6.0553	66.5148	12.5488
3	304	360	44.9374	51.898	360	13.4162	147.6243	28.2419
4	540	632	80.2988	96.0248	632	23.4437	261.5918	49.9887
5	844	982	125.7784	153.6412	982	36.1378	408.4173	77.7891
6	1216	1410	181.3762	224.7472	1410	51.4985	588.1007	111.6433
7	1656	1916	247.0922	309.3428	1916	69.5258	800.6421	151.5512
8	2164	2500	322.9264	407.428	2500	90.2197	1046.0415	197.5126
9	2740	3162	408.8788	519.0028	3162	113.5802	1324.2989	249.5278
10	3384	3902	504.9494	644.0672	3902	139.6073	1635.4143	307.5967

TABLE 8: Numerical comparison of  $ABC_4(\Gamma)$  and  $GA_5(\Gamma)$ .

$n$	1	2	3	4	5	6	7	8	9	10
$ABC_4(\Gamma)$	3.35	14.82	34.45	62.24	98.19	142.30	194.57	255	323.59	400.34
$GA_5(\Gamma)$	5.94	26.49	62.86	115.02	182.97	266.72	366.27	481.62	612.76	759.70

**Theorem 6.** For all  $n \geq 3$ , let  $\Gamma$  be the graph of blue starch-iodine complex, we have

$$\begin{aligned} ABC_4(\Gamma) &= 4.0798n^2 - 0.7682n + 0.04, \\ GA_5(\Gamma) &= 7.8987n^2 - 3.1339n + 1.1727. \end{aligned} \quad (40)$$

*Proof.* By using Table 6 and equation (7), we get

$$\begin{aligned} ABC_4(\Gamma) &= \sum_{uv \in E(\Gamma)} \sqrt{\frac{S_u + S_v - 2}{S_u S_v}} \\ &= n\sqrt{\frac{2+3-2}{2 \times 3}} + n\sqrt{\frac{2+4-2}{2 \times 4}} + n\sqrt{\frac{3+5-2}{3 \times 5}} + (n-2)\sqrt{\frac{3+6-2}{3 \times 6}} + (n^2 - n - 1)\sqrt{\frac{3+7-2}{3 \times 7}} \\ &\quad + n\sqrt{\frac{4+8-2}{4 \times 8}} + n\sqrt{\frac{5+7-2}{5 \times 7}} + (n-2)\sqrt{\frac{6+6-2}{6 \times 6}} + (3n^2 - 5n + 4)\sqrt{\frac{6+7-2}{6 \times 7}} \\ &\quad + n\sqrt{\frac{6+8-2}{6 \times 8}} + (2n-4)\sqrt{\frac{7+7-2}{7 \times 7}} + (4n^2 - 7n + 6)\sqrt{\frac{7+8-2}{7 \times 8}} \\ &= 4.0798n^2 - 0.7682n + 0.04. \end{aligned} \quad (41)$$

By using Table 6 and equation (8), we get

$$\begin{aligned} GA_5(\Gamma) &= \sum_{uv \in E(\Gamma)} \frac{2\sqrt{S_u S_v}}{(S_u + S_v)} \\ &= 2\left( n\frac{\sqrt{2 \times 3}}{(2+3)} + n\frac{\sqrt{2 \times 4}}{(2+4)} + n\frac{\sqrt{3 \times 5}}{(3+5)} + (n-2)\frac{\sqrt{3 \times 6}}{(3+6)} + (n^2 - n - 1)\frac{\sqrt{3 \times 7}}{(3+7)} + n\frac{\sqrt{4 \times 8}}{(4+8)} + n\frac{\sqrt{5 \times 7}}{(5+7)} \right. \\ &\quad \left. + (n-2)\frac{\sqrt{6 \times 6}}{(6+6)} + (3n^2 - 5n + 4)\frac{\sqrt{6 \times 7}}{(6+7)} + n\frac{\sqrt{6 \times 8}}{(6+8)} + (2n-4)\frac{\sqrt{7 \times 7}}{(7+7)} + (4n^2 - 7n + 6)\frac{\sqrt{7 \times 8}}{(7+8)} \right) \\ &= 7.8987n^2 - 3.1339n + 1.1727. \end{aligned} \quad (42)$$

□

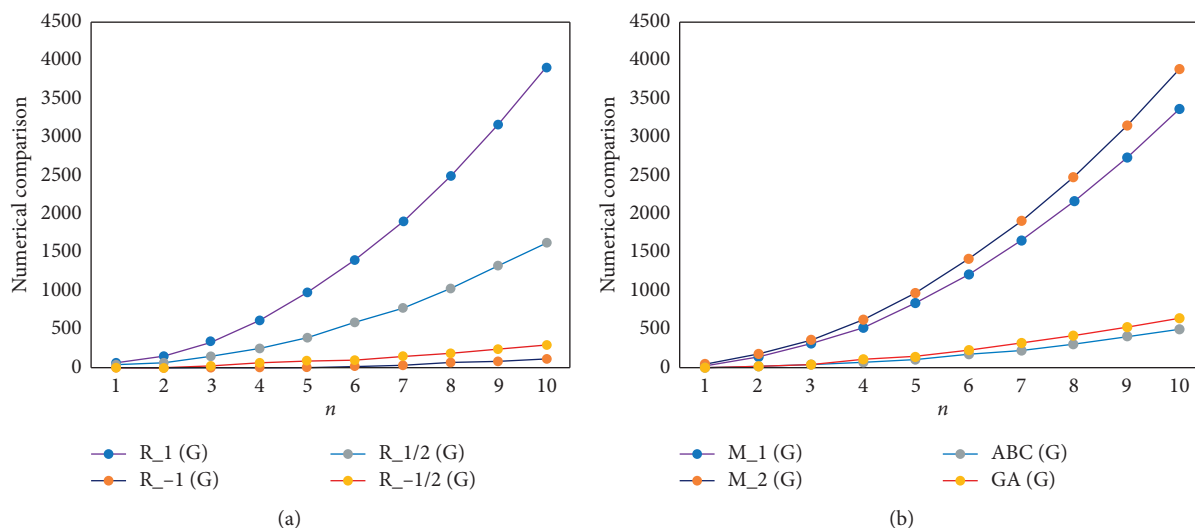


FIGURE 7: (a) Comparison of  $R_\alpha(\Gamma)$  for 1, -1, (1/2), -(1/2) and (b) comparison of  $M_1(\Gamma)$ ,  $M_2(\Gamma)$ ,  $ABC(\Gamma)$ , and  $GA(\Gamma)$ .

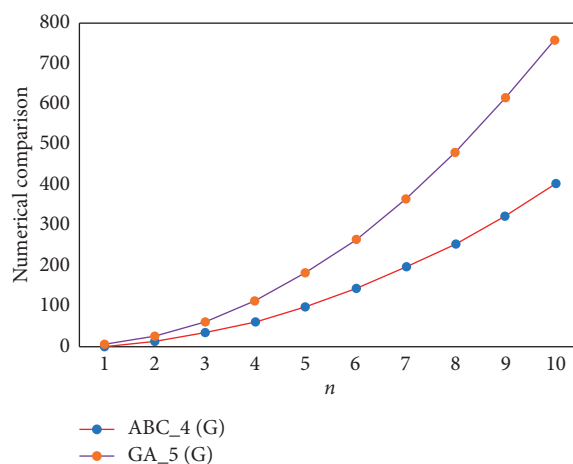


FIGURE 8: Comparison of  $ABC_4(\Gamma)$  and  $GA_5(\Gamma)$ .

## 5. Numerical and Graphical Representation

Here, we give numeric and graphic representation for the results calculated in the above section (see Tables 7 and 8).

## 6. Conclusion

Amylose has a significant function in the storage of plant energy. It is not easy to digest compared to amylopectin; however, it occupies less space than amylopectin due to its spiral structure. Consequently, for storage in plants, it is the preferred starch. A mixture of iodine and potassium iodide in water is light orange-brown. When added to a sample containing starch, such as the bread pictured above, the colour will change to a deep blue (see the comparison of different indices in Figures 7 and 8). In this study, we have calculated degree-dependent topological indices of amylose and blue starch-iodine. We observed that  $R_{(-1/2)}$  is closely related to geometric-arithmetic,  $R_{-1}$  is closely related to atom-bond connectivity and modified atom-bond

connectivity, the second Zagreb is the first Randic index, while  $R_{(1/2)}$  is approximately equal to the modified geometric-arithmetic of amylose. Similarly, other observations can take place from the graphical representations given in this paper.

## Data Availability

All kinds of data and materials, used to compute the results, are provided in Section 1.

## Conflicts of Interest

The authors declare that they have no conflicts of interest.

## Acknowledgments

This project was sponsored by the Deanship of Scientific Research under Nasher Proposal no. 206152, King Faisal University.

## References

- [1] E. Deutsch and S. Klavžar, "M-polynomial and degree-based topological indices," *Iranian Journal of Mathematical Chemistry*, vol. 6, no. 2, pp. 93–102, 2015.
- [2] C. Gupta, V. Lokesh, S. Shwetha, and P. Ranjini, "On the symmetric division deg index of graph," *Southeast Asian Bulletin of Mathematics*, vol. 40, no. 1, pp. 41–51, 2016.
- [3] I. Gutman and O. Polansky, *Topological Indices, Mathematical Concepts In Organic Chemistry*, Springer, Berlin, Germany, 1986.
- [4] I. Gutman and N. Trinajstić, "Graph theory and molecular orbitals. Total  $\phi$ -electron energy of alternant hydrocarbons," *Chemical Physics Letters*, vol. 17, no. 4, pp. 535–538, 1972.
- [5] A. Ahmad, K. Elahi, R. Hasni, and M. F. Nadeem, "Computing the degree based topological indices of line graph of benzene ring embedded in P-type-surface in 2D network," *Journal of Information and Optimization Sciences*, vol. 40, no. 7, pp. 1511–1528, 2019.
- [6] M. F. Nadeem, S. Zafar, and Z. Zahid, "On the edge version of geometric-arithmetic index of nanocones," *Studia Universitatis Babeş-Bolyai series Chemia*, vol. 61, no. 1, pp. 273–282, 2016.
- [7] H. Wiener, "Structural determination of paraffin boiling points," *Journal of the American Chemical Society*, vol. 69, no. 1, pp. 17–20, 1947.
- [8] M. Randić, "Characterization of molecular branching," *Journal of the American Chemical Society*, vol. 97, no. 23, pp. 6609–6615, 1975.
- [9] I. Gutman and K. Das, "The first zagreb index 30 years after," *MATCH Communications in Mathematical and in Computer Chemistry*, vol. 50, no. 1, pp. 83–92, 2004.
- [10] N. Trinajstić, S. Nikolić, A. Miličević, and I. Gutman, "About the zagreb indices," *Kemija U Industriji: Časopis Kemičara I Kemijskih Inženjera Hrvatske*, vol. 59, no. 12, pp. 577–589, 2010.
- [11] E. Estrada, L. Torres, L. Rodríguez, and I. Gutman, "An atom-bond connectivity index: modelling the enthalpy of formation of alkanes," *Indian Journal of Chemistry*, vol. 37A, pp. 849–855, 1998.
- [12] D. Vuckićević and B. Furtula, "Topological index based on the ratios of geometrical and arithmetical means of end-vertex degree of edges," *Journal of Mathematical Chemistry*, vol. 46, pp. 1369–1376, 2009.
- [13] M. Ghorbani and M. Hosseinzadeh, "Computing  $ABC_4$  index of nanostar dendrimers," *Optoelectronics and Advanced Materials, Rapid Communications*, vol. 4, pp. 1419–1422, 2010.
- [14] A. Graovac, M. Ghorbani, and M. Hosseinzadeh, "Computing fifth geometric-arithmetic index for nanostar dendrimers," *Journal of Mathematical Nanoscience*, vol. 1, pp. 33–42, 2011.
- [15] M. M. Green, G. Blankenhorn, and H. Hart, "Which starch fraction is water-soluble, Amylose or Amylopectin?" *Journal of Chemical Education*, vol. 52, no. 11, p. 729, 1975.

## Research Article

# Degree-Based Topological Indices of Boron B<sub>12</sub>

Nouman Saeed <sup>1</sup>, Kai Long <sup>1</sup>, Zeeshan Saleem Mufti <sup>2</sup>, Hafsa Sajid,<sup>2</sup>  
and Abdul Rehman <sup>2</sup>

<sup>1</sup>State Key Laboratory for Alternate Electrical Power System with Renewable Energy Sources,  
North China Electric Power University, Beijing 102206, China

<sup>2</sup>The University of Lahore, Lahore Campus, Lahore, Pakistan

Correspondence should be addressed to Kai Long; [longkai1978@163.com](mailto:longkai1978@163.com)

Received 11 February 2021; Revised 1 March 2021; Accepted 22 March 2021; Published 29 March 2021

Academic Editor: Kashif Ali

Copyright © 2021 Nouman Saeed et al. This is an open access article distributed under the Creative Commons Attribution License, which permits unrestricted use, distribution, and reproduction in any medium, provided the original work is properly cited.

Topological index sometimes called molecular descriptor is a numerical value which associates a chemical composition for correlating chemical structure with numerous physical properties, chemical reactivity, or biological activity. In this paper, we study some topological indices of boron and try to correlate the physicochemical properties such as freezing points, boiling points, melting points, infrared spectrum, electronic parameters, viscosity, and density of chemical graphs. We discuss these topological indices, and some of them are mentioned here such as Randić index, the first general Zagreb index, the general sum connectivity index, hyper-Zagreb index (HM), the atom-bond connectivity index (ABC), the geometric-arithmetic index (GA), the harmonic index (*H*), and the forgotten index (*F*).

## 1. Introduction and Applications

A chemical graph theory is an outlet of mathematical chemistry which applied graph theory to the molecular structure of chemical compounds. Topological index is a part of chemical graph theory which correlates the physicochemical properties such as freezing point, boiling point, melting point, infrared spectrum, electronic parameters, viscosity, and density of the underlying chemical graphs. The reader can find bulk of papers on topological indices which have been in print so far [1–5].

A graph can be recognized by a polynomial, a matrix, a sequence of numbers, or a numeric number which represents the whole graph, and these representations are designed to be uniquely defined for that graph. Topological indices are major tools for analyzing many physicochemical properties of molecules without performing any testing. Some most significant types of topological indices of graphs are distance-based topological indices, degree-based topological indices, and spectrum-based topological indices. One of the most investigated categories of topological indices used in mathematical chemistry is called degree-based

topological indices, which are defined in terms of the degrees of the vertices of a graph.

Topological index is a graph invariant which characterizes the topology of the molecular structure and converts the molecular graph into a real number that predicts some physicochemical properties such as freezing point, boiling point, and melting point. Nowadays, a biological testing of chemical compounds is too much expensive. It requires a very large laboratory and advanced equipment to test these compounds. This process is costly and time-consuming. Due to this factor, pharmaceutical companies are very eager to find such new ideas or methods by which cost could be reduced. One can reduce the cost in which no need of laboratories and no need of equipment, but just need to study the certain chemical structure using topological indices

Topological indices are of different types such as degree-based topological indices, distance-based topological indices, and spectrum-based topological indices. The notion of topological index was discovered in 1947 when Harold Wiener was working on the boiling point of paraffin. He named this index as path number. Later on, the path number

was renamed as the Wiener index, and then the theory of topological index started. The Wiener index is the first and the most studied topological index. Wiener index is defined as the sum of distances among all the sets of vertices in  $G$  [6]. Among all the types of topological indices, degree-based topological indices play an extensive role in chemical graph theory [7]. That motivated us to study the chemical structure of boron  $B_{12}$  under this phenomenon.

$B_{12}$  is a two-dimensional icosahedral network. A recent study of high-pressure solid boron affirmed that the icosahedral  $B_{12}$ -containing structures are quite universal [8]. On the other hand, previous experimental and theoretical studies of free-standing boron clusters have shown that the  $B_{12}$  structure is unstable in the gas phase [9, 10]. The  $(n, m)$  unit of boron  $B_{12}$  structure is given in the figure, where “ $n$ ” represents the number of rows and “ $m$ ” represents the number of columns of the boron  $B_{12}$  structure.

Let  $G$  be a simple graph with order  $p$  and size  $q$ . Let  $d_v$  represent the degree of the vertex  $v$  and is defined as the number of edges incident on  $v$ . Let  $S_v$  represent the sum of the degree of all the neighbors of  $v$  [11]. Graph theory is closely connected to the computer science, applied mathematics, optimization theory, web designing, operation research, biology, and chemistry.

The general Randić connectivity index of  $G$  is defined as

$$R_\alpha(G) = \sum_{rs \in E(G)} (d_r d_s)^\alpha, \quad (1)$$

where  $\alpha$  represents a real number. If  $\alpha$  is  $-1/2$ , then  $R_{-1/2}(G)$  is said to be the Randić connectivity index of  $G$ . Gutman and Trinajstić presented the first general Zagreb index in 1972 [12]:

$$M_\alpha(G) = \sum_{r \in V(G)} (d_r)^\alpha. \quad (2)$$

In 2010, the general sum connectivity index  $\chi_\alpha(G)$  has been invented:

$$\chi_\alpha(G) = \sum_{rs \in E(G)} (d_r + d_s)^\alpha. \quad (3)$$

The ABC index was presented by Estrada and Torres et al. in [13]. The ABC index of graph  $G$  is expressed as

$$ABC(G) = \sum_{rs \in E(G)} \sqrt{\frac{d_r + d_s - 2}{d_r d_s}}. \quad (4)$$

Das announced the geometric-arithmetic (GA) index in [14, 15]. The geometric-arithmetic index denoted by GA for graph  $G$  is presented by

$$GA(G) = \sum_{rs \in E(G)} \frac{2\sqrt{d_r d_s}}{d_r + d_s}. \quad (5)$$

In 2013, the hyper-Zagreb index has been introduced by Shirdel et al. as

$$HM(G) = \sum_{rs \in E(G)} (d_r + d_s)^2. \quad (6)$$

In 2012, Zhang introduced the harmonic index. It is defined as follows [16]:

$$H(G) = \sum_{rs \in E(G)} \frac{2}{(d_r + d_s)}. \quad (7)$$

After working on the Zagreb index, in 2015, Furtula and Gutman introduce the forgotten index  $F(G)$ :

$$F(G) = \sum_{rs \in E(G)} (d_r^2 + d_s^2). \quad (8)$$

Ghorbani and Azimi proposed two new types of Zagreb indices of a graph  $G$  in 2012.  $PM_1$  is the first multiple Zagreb index, and  $PM_2$  is the second multiple Zagreb index [6]:

$$PM_1(G) = \prod_{rs \in E(G)} (d_r + d_s), \quad (9)$$

$$PM_2(G) = \prod_{rs \in E(G)} (d_r \times d_s), \quad (10)$$

$M_1(G, p)$  and  $M_2(G, p)$ , the first Zagreb polynomial and the second Zagreb polynomial [12, 17], respectively, are defined as

$$M_1(G, p) = \sum_{rs \in E(G)} p^{(d_r + d_s)}, \quad (11)$$

$$M_2(G, p) = \sum_{rs \in E(G)} p^{(d_r \times d_s)}. \quad (12)$$

Recently, Furtula et al. proposed the second Zagreb index:

$$RM_2(G) = \sum_{rs \in E(G)} (d_r - 1)(d_s - 1). \quad (13)$$

After the success of the ABC index, Furtula et al. put forward its modified version in 2010 that they somewhat inadequately named “augmented Zagreb index.” It is defined as follows [18]:

$$AZI(G) = \sum_{rs \in E(G)} \left( \frac{d_r d_s}{d_r + d_s - 2} \right)^3. \quad (14)$$

The invariant RR seems to be first encountered in a paper by Favaron, Mah'eo. The reciprocal Randić index is defined as follows:

$$RR(G) = \sum_{rs \in E(G)} \sqrt{d_r d_s}. \quad (15)$$

In the same manner, the reduced second Zagreb index (equation (13)), is related to the ordinary second Zagreb index (equation (12)). The reduced reciprocal Randić index might be viewed as the reduced analogue of the reciprocal Randić index (equation (15)):

$$RRR(G) = \sum_{rs \in E(G)} \sqrt{(d_r - 1)(d_s - 1)}. \quad (16)$$

Vukicevic et al. introduce the symmetric division deg index in 2010 [19, 20] as

$$\text{SDD}(G) = \sum_{rs \in E(G)} \frac{d_r^2 + d_s^2}{d_r d_s}. \quad (17)$$

Vukicevic and Gašperov in [20] initiated the study on the inverse sum indeg index of a network. The inverse sum indeg index is defined as follows [21]:

$$\text{SDD}(G) = \sum_{rs \in E(G)} \frac{d_r d_s}{d_r + d_s}. \quad (18)$$

Another index which belongs to the 4th class of ABC index was invented by Ghorbani and Hosseinzadeh in 2010 [22] as

$$\text{ABC}(G) = \sum_{rs \in E(G)} \sqrt{\frac{S_r + S_s - 2}{S_r S_s}}. \quad (19)$$

The fifth class of geometric-arithmetic index, denoted by  $GA_5$ , was presented by Graovac et al. in 2011 [23] as

$$\text{GA}(G) = \sum_{rs \in E(G)} \frac{2\sqrt{S_r S_s}}{S_r + S_s}. \quad (20)$$

## 2. Main Results of Boron $B_{12}$ Graph

In this paper, we deal with the topological properties of boron  $B_{12}$ . Boron  $B_{12}$  is a two-dimensional icosahedral network. A recent study of high-pressure solid boron affirmed that the icosahedral  $B_{12}$ -containing structures are quite universal [8]. On the other hand, previous experimental and theoretical studies of freestanding boron clusters have shown that the  $B_{12}$  structure is unstable in the gas phase [9, 10].

The molecular graph of Boron  $B_{12}$  is shown in Figure 1. There are  $11mn + 11m + 11n + 9$  vertices and  $24mn + 22m + 22n + 18$  edges.

**Theorem 1.** Let  $G$  be the boron  $B_{12}$  network with  $m > 1$  and  $n > 1$ , then

$$\begin{aligned} M_\alpha &= 2(2m + 2n)2^\alpha + (3mn + m + 5)3^\alpha \\ &+ (3mn + 2m + 3n + 4)3^\alpha + (m + 2n + 1)4^\alpha \\ &+ (9mn + 7m + 6n + 5)4^\alpha + (9mn + 7m + 7n + 3)5^\alpha. \end{aligned} \quad (21)$$

*Proof.* In  $G$ , there are total  $11mn + 11m + 11n + 9$  vertices. There are  $2m + 2n$  vertices of degree 2,  $2mn + m + n + 3$  vertices of degree 3,  $3mn + 3m + 3n + 3$  vertices of degree 4, and  $36mn + 5m + 5n + 3$  vertices of degree 5. Since  $M_\alpha$  is expressed in equation (2),

$$M_\alpha(G) = \sum_{r \in V(G)} (d_r)^\alpha, \quad (22)$$

$$\begin{aligned} M_\alpha &= 2(2m + 2n)2^\alpha + (3mn + m + 5)3^\alpha \\ &+ (3mn + 2m + 3n + 4)3^\alpha \\ &+ (m + 2n + 1)4^\alpha + (9mn + 7m + 6n + 5)4^\alpha \\ &+ (9mn + 7m + 7n + 3)5^\alpha. \end{aligned} \quad (23)$$

In the following six theorems, we considered the Randic index, sum connectivity index, ABC index, GA index, harmonic index, reduced Randic index, forgotten index, symmetric division deg index, inverse sum indeg index,  $ABC_4$  index, and  $GA_5$  index. This is the edge partition of boron  $B_{12}$  on the basis of starting and ending vertices of each edge, and we proceed this edge division to compute the topological indices.

**Theorem 2.** Let  $G$  be the boron  $B_{12}$  network with  $m > 1$  and  $n > 1$ , then

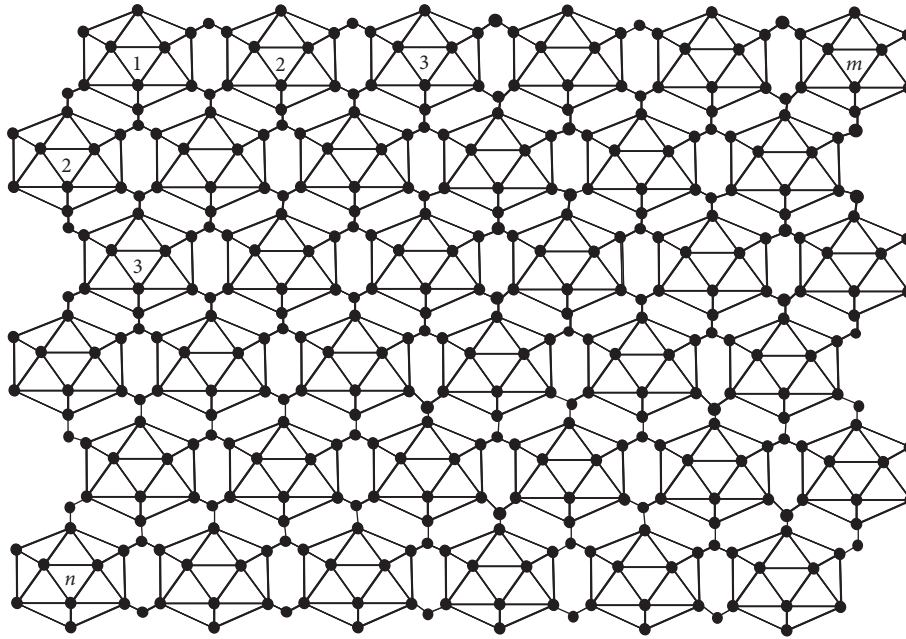
- (1)  $R_\alpha(G) = (2m + 2n)8^\alpha + (2m + 2n)10^\alpha + (3mn + m + 5)12^\alpha + (m + 2n + 1)16^\alpha + (3mn + 2m + 3n + 4)15^\alpha + (9mn + 7m)20^\alpha + (9mn + 7m + 7n + 3)25^\alpha + (6n + 5)20^\alpha$
- (2)  $\chi_\alpha(G) = (2m + 2n)6^\alpha + (2m + 2n)7^\alpha + (3mn + m + 5)7^\alpha + (m + 2n + 1)8^\alpha + (3mn + 2m + 3n + 4)8^\alpha + (9mn + 7m + 6n + 5)9^\alpha + (9mn + 7m + 7n + 3)10^\alpha$
- (3)  $\text{ABC}(G) = (2m + 2n)\sqrt{2} + (1/6)(3mn + m + 5)\sqrt{15} + (1/5)(3mn + 2m + 3n + 4)\sqrt{10} + (1/4)(m + 2n + 1)\sqrt{6} + (1/10)(9mn + 7m)\sqrt{35} + (1/10)(6n + 5)\sqrt{35} + (2/5)(9mn + 7m + 7n + 3)\sqrt{2}$
- (4)  $\text{GA}(G) = (2/3)(2m + 2n)\sqrt{2} + (2/7)(2m + 2n)\sqrt{10} + (4/7)(3mn + m + 5)\sqrt{3} + (1/4)(3mn + 2m + 3n + 4)\sqrt{15} + (4/9)(9mn + 7m + 6n + 5)\sqrt{5} + (9mn + 8m + 9n + 4)$

*Proof.* The network of boron  $B_{12}$  has  $24mn + 22m + 22n + 18$  number of edges. There are seven disjoint edge sets of edge set  $E(G)$  depending on the degrees of the end vertices, i.e.,  $E(G) = E_1(G) \cup E_2(G) \cup E_3(G) \cup E_4(G) \cup E_5(G) \cup E_6(G) \cup E_7(G)$ . The edge partition  $E_1(G)$  holds  $2m + 2n$  edges  $rs$ , where  $d_r = 2$  and  $d_s = 4$ , the edge partition  $E_2(G)$  holds  $2m + 2n$  edges  $rs$ , where  $d_r = 2$  and  $d_s = 5$ , the edge partition  $E_3(G)$  holds  $3mn + m + 5$  edges  $rs$ , where  $d_r = 3$  and  $d_s = 4$ , the edge partition  $E_4(G)$  holds  $3mn + 2m + 3n + 4$  edges  $rs$ , where  $d_r = 3$  and  $d_s = 5$ , the edge partition  $E_5(G)$  holds  $m + 2n + 1$  edges  $rs$ , where  $d_r = d_s = 4$ , the edge partition  $E_6(G)$  holds  $9mn + 7m + 6n + 5$  edges  $rs$ , where  $d_r = 4$  and  $d_s = 5$ , and the edge partition  $E_7(G)$  holds  $9mn + 7m + 7n + 3$  edges  $rs$ , where  $d_r = d_s = 5$ . From formulas (1) and (3)–(5), we get the desired results.

**Theorem 3.** Let  $G$  be the boron  $B_{12}$  network with  $m > 1$  and  $n > 1$ , then

- (1)  $HM(G) = 1678m + 1676n + 1968mn + 1270$
- (2)  $PM_1(G) = 6^{2m+2n} \times 7^{2m+2n} \times 7^{3mn+m+5} \times 8^{3mn+2m+3n+4} \times 8^{m+2n+1} \times 9^{9mn+7m+6n+5} \times 10^{9mn+7m+7n+3}$
- (3)  $PM_2(G) = 8^{2m+2n} \times 10^{2m+2n} \times 12^{3mn+m+5} \times 15^{3mn+2m+3n+4} \times 16^{m+2n+1} \times 20^{9mn+7m+6n+5} \times 25^{9mn+7m+7n+3}$

*Proof.* Let  $G$  be the network of boron  $B_{12}$ . The edge set  $E(G)$  is distributed in seven categories which depend on the degrees of the end vertices. The first disjoint edge set  $E_1(G)$

FIGURE 1:  $(n, m)$  unit of boron.

holds  $2m + 2n$  edges  $rs$ , where  $d_r = 2$  and  $d_s = 4$ , the second disjoint edge set  $E_2(G)$  holds  $2m + 2n$  edges  $rs$ , where  $d_r = 2$  and  $d_s = 5$ , the third disjoint edge set  $E_3(G)$  holds  $3mn + m + 5$  edges  $rs$ , where  $d_r = 3$  and  $d_s = 4$ , the fourth disjoint edge set  $E_4(G)$  holds  $3mn + 2m + 3n + 4$  edges  $rs$ , where  $d_r = 3$  and  $d_s = 5$ , the fifth disjoint edge set  $E_5(G)$  holds  $m + 2n + 1$  edges  $rs$ , where  $d_r = d_s = 4$ , the sixth disjoint edge set  $E_6(G)$  holds  $9mn + 7m + 6n + 5$  edges  $rs$ , where  $d_r = 4$  and  $d_s = 5$ , and the seventh disjoint edge set  $E_7(G)$  holds  $9mn + 7m + 7n + 3$  edges  $rs$ , where  $d_r = d_s = 5$ . Now,  $|E_1(G)| = e_{2,4}$ ,  $|E_2(G)| = e_{2,5}$ ,  $|E_3(G)| = e_{3,4}$ ,  $|E_4(G)| = e_{3,5}$ ,  $|E_5(G)| = e_{4,4}$ ,  $|E_6(G)| = e_{4,5}$ , and  $|E_7(G)| = e_{5,5}$ . We obtained results by using formulas (6), (9), and (10).

**Theorem 4.** Let  $G$  be the boron  $B_{12}$  network with  $m > 1$  and  $n > 1$ , then

- (1)  $M_1(G, p) = (2m + 2n)p^6 + (2m + 2n)p^7 + (3mn + m + 5)p^7 + (m + 2n + 1)p^8 + ((3mn + 2m)p^8 + (3n + 4))p^8 + (9mn + 7m + 6n + 5)p^9 + (9mn + 7m + 7n + 3)p^{10}$
- (2)  $M_1(G, p) = (2m + 2n)p^8 + (2m + 2n)p^{10} + (3mn + m + 5)p^{12} + ((3mn + 2m)p^{15} + (3n + 4))p^{15} + (m + 2n + 1)p^{16} + (9mn + 7m + 6n + 5)p^{20} + (9mn + 7m + 7n + 3)p^{25}$

*Proof.* Let  $G$  be the network of boron  $B_{12}$ . The edge set  $E(G)$  is distributed in seven categories which depend on the degree of end vertices of each edge. The disjoint set is represented by  $e_{r,s}$ . The first disjoint set is  $e_{2,4}$ , the second disjoint set is  $e_{2,5}$ , the third disjoint set is  $e_{3,4}$ , the fourth disjoint set is  $e_{3,5}$ , the fifth disjoint set is  $e_{4,4}$ , the sixth disjoint set is  $e_{4,5}$ , and the seventh disjoint set is  $e_{5,5}$ . By using formulas (11) and (12), we obtained the required results.

**Theorem 5.** Let  $G$  be the boron  $B_{12}$  network with  $m > 1$  and  $n > 1$ , then

- (1)  $RM_2(G) = 241m + 240n + 294mn + 179$
- (2)  $AZI(G) = (12576690219/21952000)mn + (40043532353/84672000)m + (2230300883/4741632)n + (42526959271/118540800)$

*Proof.* Let  $G$  be the network of boron  $B_{12}$ . The edge set  $E(G)$  is distributed in seven categories which depend on the degree of end vertices of each edge. The disjoint set is represented by  $e_{r,s}$ . The first disjoint set is  $e_{2,4}$ , the second disjoint set is  $e_{2,5}$ , the third disjoint set is  $e_{3,4}$ , the fourth disjoint set is  $e_{3,5}$ , the fifth disjoint set is  $e_{4,4}$ , the sixth disjoint set is  $e_{4,5}$ , and the seventh disjoint set is  $e_{5,5}$ . We get the results by using formulas (13) and (14).  $\square$

**Theorem 6.** Let  $G$  be the boron  $B_{12}$  network with  $m > 1$  and  $n > 1$ , then

- (1)  $H(G) = (6589/1260)m + (731/140)n + (757/140)mn + (5531/1260)$
- (2)  $RR(G) = 2(2m + 2n)\sqrt{2} + (2m + 2n)\sqrt{10} + 2(3mn + m + 5)\sqrt{3} + ((3mn + 2m)\sqrt{15} + (3n + 4))\sqrt{15} + 2(9mn + 7m + 6n + 5)\sqrt{5} + 45mn + 39m + 43n + 19$
- (3)  $RRR(G) = (2m + 2n)\sqrt{3} + 2(3mn + 2m)\sqrt{2} + 2(3n + 4)\sqrt{2} + 2(3mn + m + 5)\sqrt{6} + 2(9mn + 7m + 6n + 5)\sqrt{3} + 36mn + 35m + 38n + 15$

*Proof.* Let  $G$  be the network of boron  $B_{12}$ . The edge set  $E(G)$  is distributed in seven categories which depend on the degree of end vertices of each edge. The disjoint set is represented by  $e_{r,s}$ . The first disjoint set is  $e_{2,4}$ , the second disjoint set is  $e_{2,5}$ , the third disjoint set is  $e_{3,4}$ , the fourth



disjoint set is  $e_{3,5}$ , the fifth disjoint set is  $e_{4,4}$ , the sixth disjoint set is  $e_{4,5}$ , and the seventh disjoint set is  $e_{5,5}$ . By using formulas (7), (15), and (16), we get the desired results.

**Theorem 7.** Let  $G$  be the boron  $B_{12}$  network with  $m > 1$  and  $n > 1$ , then

- (1)  $F(G) = 860m + 860n + 996mn + 648$
- (2)  $SDD(G) = (1433/30)m + (479/10)n + (99/2)mn + (566/15)$
- (3)  $ISI(G) = (11603/252)m + (2575/25562)n + (2983/56)mn + (2311/63)$

*Proof.* Let  $G$  be the network of boron  $B_{12}$ . The edge set  $E(G)$  is distributed in seven categories which depend on the

degree of end vertices of each edge. The disjoint set is represented by  $e_{r,s}$ . The first disjoint set is  $e_{2,4}$ , the second disjoint set is  $e_{2,5}$ , the third disjoint set is  $e_{3,4}$ , the fourth disjoint set is  $e_{3,5}$ , the fifth disjoint set is  $e_{4,4}$ , the sixth disjoint set is  $e_{4,5}$ , and the seventh disjoint set is  $e_{5,5}$ . We obtained the required results by using formulas (8), (17), and (18).

In the following two theorems, we considered the fourth atom-bond connectivity index and the fifth geometric-arithmetic index. This is the edge partition of boron  $B_{12}$  on the basis of the degree sum of neighbors of end vertices of each edge. We proceed this edge division to compute  $ABC_4(G)$  and  $GA_5(G)$ .

**Theorem 8.** Let  $G$  be the boron  $B_{12}$  network with  $m > 1$  and  $n > 1$ , then

$$\begin{aligned}
 ABC_4(G) = & (1/2)\sqrt{2} + (4/221)\sqrt{1547} + (4/273)\sqrt{546} - (2/3) + (2/22)\sqrt{22} \\
 & + (1/22)\sqrt{42} + (1/10)(m-1)\sqrt{10} + (1/114)(m+2n+1)\sqrt{1330} + (1/68)(m-1)\sqrt{442} \\
 & + (1/391)(m+3)\sqrt{14858} + (1/374)(m+1)\sqrt{13838} + (1/34)(m-1)\sqrt{119} + (2/119)(m+1)\sqrt{357} \\
 & + (1/92)(m+2n+1)\sqrt{851} + (1/12)(m+2n+1)\sqrt{15} + (1/68)(m+3)\sqrt{527} + (2/115)(n-1)\sqrt{345} \\
 & + (4/285)(2n-2)\sqrt{570} + (1/238)(m+1)\sqrt{6902} + (1/266)(m+3)\sqrt{8246} + (1/154)(m+3)\sqrt{2618} \\
 & + (1/10)(m-1)\sqrt{14} + (1/8)(m+2n+1)\sqrt{11} + (1/68)(m-1)\sqrt{782} + (3/190)(m+2n+1)\sqrt{570} + (1/6)mn\sqrt{30} \\
 & + (1/35)mn\sqrt{1190} + (1/6)mn\sqrt{42} + (1/42)(3mn-2n-1)\sqrt{46} + (1/92)(m+4n-3)\sqrt{690} + (2/3)n\sqrt{11} + (1/6)(m+3)\sqrt{3} \\
 & + (1/506)(m+1)\sqrt{21758} + (1/84)(6mn-m-2n-1)\sqrt{602} + (1/23)(m+2n+3)\sqrt{46} + (1/20)(2m-2)\sqrt{35} \\
 & + (1/228)(m+2n+1)\sqrt{4674} + (2/437)(2n-2)\sqrt{4370} + (1/418)(m+3)\sqrt{16302} + (1/138)(2n-2)\sqrt{1794} \\
 & + (1/126)(6mn-2m-2n)\sqrt{1554} + (2/3)n.
 \end{aligned} \tag{24}$$

*Proof.* The network of boron  $B_{12}$  has  $24mn + 22m + 22n + 18$  number of edges. There are 41 disjoint degree sum of neighbors of end vertices of each edge, i.e.,  $e_{8,16}$ ,  $e_{8,17}$ ,  $e_{10,19}$ ,  $e_{10,20}$ ,  $e_{12,18}$ ,  $\dots$ ,  $e_{24,24}$ . By using formula (19), we get the desired result.

**Theorem 9.** Let  $G$  be the boron  $B_{12}$  network with  $m > 1$  and  $n > 1$ , then

$$\begin{aligned}
 GA_5(G) = & (1/20)(m+3)\sqrt{391} + (1/19)(m+1)\sqrt{357} + (1/39)(m+1)\sqrt{374} + (1/19)(n-1)\sqrt{345} \\
 & + (1/17)(2n-2)\sqrt{285} + (2/29)(m+2n+1)\sqrt{190} + (2/31)(m+1)\sqrt{238} + (2/33)(m+3)\sqrt{266} \\
 & + (2/41)(m+3)\sqrt{418} + (1/21)(2n-2)\sqrt{437} + (1/22)(m+2n+3)\sqrt{483} + (2/45)(m+1)\sqrt{506} \\
 & + (2/15)\sqrt{273} + (2/13)(6mn-2m-2n)\sqrt{42} + (6/37)(m+2n+1)\sqrt{38} + (6/19)(m-1)\sqrt{10} + (4/41)(m-1)\sqrt{102} \\
 & + (8/37)(m+2n+1)\sqrt{21} + (4/37)(m-1)\sqrt{85} + (8/39)(m+2n+1)\sqrt{23} + (8/33)(m+3)\sqrt{17} + (12/17)(2n-2)\sqrt{2} \\
 & + (2/3)(m-1)\sqrt{2} + (1/9)(m+3)\sqrt{77} + (2/3)(m+2n+1)\sqrt{2} + (4/25)(m-1)\sqrt{34} + (12/7)mn\sqrt{3} + (1/2)mn\sqrt{35} \\
 & + (6/5)mn\sqrt{6} + (6/41)(2n-2)\sqrt{46} + (2/11)(2m-2)\sqrt{30} + (4/43)(m+2n+1)\sqrt{114} + (4/15)(6mn-m-2n-1)\sqrt{14} \\
 & + (4/23)(m+3)\sqrt{33} + (4/47)(m+4n-3)\sqrt{138} + (8/15)\sqrt{14} + (8/19)\sqrt{22} - n + 3mn.
 \end{aligned} \tag{25}$$

*Proof.* The network of boron  $B_{12}$  has  $24mn + 22m + 22n + 18$  number of edges. There are 41 disjoint degree sum of neighbors of end vertices of each edge, i.e.,  $e_{8,16}$ ,  $e_{8,17}$ ,  $e_{10,19}$ ,  $e_{10,20}$ ,  $e_{12,18}$ ,  $\dots$ ,  $e_{24,24}$ . By using formula (20), we get the desired result.

### 3. Conclusion

We have computed the following topological indices such as Zagreb index, the Randic index, sum connectivity index, ABC index, GA index, hyper-Zagreb index, multiple Zagreb indices, Zagreb polynomials, reduced second Zagreb index, augmented Zagreb index, harmonic index, reduced Randic index, reduced reciprocal Randic index, forgotten index,  $ABC_4$  index, and  $GA_5$  index for boron  $B_{12}$  structure.

In cheminformatics, Randic index is used to study the organic compounds. It is correlated with physicochemical properties of alkane such as boiling points, surface area, and enthalpy of formation. ABC index is based on some physicochemical properties like the stability of cyclo-alkane as well as strain energy. GA index has more predictive power than Randic and ABC index. Multiple Zagreb indices and Zagreb polynomials are applied to predict the bioactivity of graphs. The forgotten index is correlated with some chemical properties relating to energies of molecular graphs. AZI index is a valuable predictive index which is used in the study of the heat of formation. RRR index is used to study the normal boiling points of the graphs.

We have discussed the graph theoretically not experimentally. The results obtained in this paper provide a significant contribution to graph theory and correlate the chemical structure of boron  $B_{12}$  with the large amount of information about physicochemical properties.

### Data Availability

No data were used to support this study.

### Conflicts of Interest

The authors declare that they have no conflicts of interest.

### Acknowledgments

The authors wish to acknowledge the financial support from the National Natural Science Foundation of Beijing (2182067) and the Fundamental Research Funds of the Central Universities (2018ZD09).

### References

- [1] H. M. A. Siddiqui, "Computation of Zagreb indices and Zagreb polynomials of Sierpinski graphs," *Hacetatepe Journal of Mathematics and Statistics*, vol. 49, no. 2, pp. 754–765, 2020.
- [2] H. M. A. Siddiqui, S. Baby, M. K. Shafiq, and M. Faisal Nadeem, "Bounds of some degree based indices of lexicographic product of some connected graphs," *Polycyclic Aromatic Compounds*, 2020.
- [3] J.-B. Liu, B. Ali, M. Aslam Malik, H. M. A. Siddiqui, and M. Imran, "Reformulated Zagreb indices of some derived graphs," *Mathematics*, vol. 7, p. 283, 2019.
- [4] B. L. Jia, M. Imran, S. Baby, H. M. A. Siddiqui, and M. K. Shafiq, "Graph indices for Cartesian product of F-sum of connected graphs," *Combinatorial Chemistry & High Throughput Screening*, 2021.
- [5] J. Xu, J.-B. Liu, A. Bilal et al., "Distance degree index of some derived graphs," *Mathematics*, vol. 7, no. 3, p. 283, 2019.
- [6] M. Ghorbani and N. Azimi, "Note on multiple Zagreb indices," *Iranian Journal of Mathematical Chemistry*, vol. 3, no. 2, pp. 137–143, 2012.
- [7] I. Gutman, "Degree-based topological indices," *Croatica Chemica Acta*, vol. 86, no. 4, pp. 351–361, 2013.
- [8] A. R. Oganov, J. Chen, C. Gatti et al., "Ionic high-pressure form of elemental boron," *Nature*, vol. 457, no. 7231, pp. 863–867, 2009.
- [9] I. Boustani, "Systematic ab initio investigation of bare boron clusters: mDetermination of the geometry and electronic structures of  $B_n$  ( $n = 2-14$ )," *Physical Review B*, vol. 55, no. 24, p. 16426, 1997.
- [10] H. Li, N. Shao, B. Shang, L.-F. Yuan, J. Yang, and X. C. Zeng, "Icosahedral  $B_{12}$ -containing core-shell structures of  $B_{80}$ ," *Chemical Communications*, vol. 46, no. 22, pp. 3878–3880, 2010.
- [11] L. W. Beineke and R. J. Wilson, *Applications of Graph Theory*, Academic Press, London, UK, 1979.
- [12] B. Horoldagva, L. Buyantogtokh, K. C. Das, and S. G. Lee, "On general reduced second Zagreb index of graphs," *Hacetatepe Journal of Mathematics and Statistics*, vol. 48, no. 4, pp. 1040–1056, 2019.
- [13] K. C. Das, I. Gutman, and B. Furtula, "On atom-bond connectivity index," *Chemical Physics Letters*, vol. 511, no. 4–6, pp. 452–454, 2011.
- [14] K. C. Das, "On geometric-arithmetic index of graphs," *MATCH Communications in Mathematical and in Computer Chemistry*, vol. 64, no. 3, pp. 619–630, 2010.
- [15] D. Vukievi and B. Furtula, "Topological index based on the ratios of geometrical and arithmetical means of end-vertex degrees of edges," *Journal of Mathematical Chemistry*, vol. 46, no. 4, pp. 1369–1376, 2009.
- [16] S. Fajtlowicz, "Harmonic index," *Congressus Numerantium*, vol. 60, pp. 187–197, 1987.
- [17] Z. Shao, M. Siddiqui, and M. Muhammad, "Computing Zagreb indices and Zagreb polynomials for symmetrical nanotubes," *Symmetry*, vol. 10, no. 7, p. 244, 2018.
- [18] A. Ali, Z. Raza, and A. A. Bhatti, "On the augmented Zagreb index," 2014, <http://arxiv.org/abs/1402.3078>.
- [19] D. Vukievi, "Bond additive modeling 2. mathematical properties of max-min Rodeg index," *Croatica Chemica Acta*, vol. 83, no. 3, pp. 261–273, 2010.
- [20] D. Vukievi and M. Gašperov, "Bond additive modeling 1. adriatic indices," *Croatica Chemica Acta*, vol. 83, no. 3, pp. 243–260, 2010.
- [21] J. Sedlar, D. Stevanović, and A. Vasilyev, "On the inverse sum indog index," *Discrete Applied Mathematics*, vol. 184, pp. 202–212, 2015.
- [22] M. Ghorbani and M. A. Hosseinzadeh, "Computing  $ABC_4$  index of nanostar dendrimers," *Optoelectronics and Advanced Materials-Rapid Communications*, vol. 4, no. 9, pp. 1419–1422, 2010.
- [23] A. Graovac, M. Ghorbani, and M. A. Hosseinzadeh, "Computing fifth geometric-arithmetic index for nanostar dendrimers," *Journal of Mathematical Nanoscience*, vol. 1, no. 1–2, pp. 33–42, 2011.

## Research Article

# COD Optimization Prediction Model Based on CAWOA-ELM in Water Ecological Environment

**Lili Jiang, Liu Yang , Yang Huang, Yi Wu, Huixian Li, XiYan Shen, Meng Bi, Lin Hong, Yiting Yang, Zuping Ding, and Wenjie Chen**

*Chongqing Key Laboratory of Spatial Data Mining and Big Data Integration for Ecology and Environment, Rongzhi College of Chongqing Technology and Business University, Chongqing 401320, China*

Correspondence should be addressed to Liu Yang; 23989060@qq.com

Received 28 December 2020; Revised 21 February 2021; Accepted 1 March 2021; Published 19 March 2021

Academic Editor: Muhammad Faisal Nadeem

Copyright © 2021 Lili Jiang et al. This is an open access article distributed under the Creative Commons Attribution License, which permits unrestricted use, distribution, and reproduction in any medium, provided the original work is properly cited.

The change of water quality can reflect the important indicators of ecological environment measurement. Sewage discharge is an important factor causing environmental pollution. Establishing an effective water ecological prediction model can detect changes in the ecological environment system quickly and effectively. In order to detect high error rate and poor convergence of the water ecological chemical oxygen demand (COD) prediction model, combining the limit learning machine (ELM) model and whale optimization algorithm, CAWOA is improved by the sin chaos search strategy, while the ELM optimizes the parameters of the algorithm to improve convergence speed, thus improving the generalization performance of the ELM. In the CAWOA, the global optimization results of the WOA are promoted by introducing a sin chaotic search strategy and adaptive inertia weights. On this basis, the COD prediction model of CAWOA-ELM is established and compared with similar algorithms by using the optimized ELM to predict the water ecological COD in a region. Finally, from the experimental results of the CAWOA-ELM algorithm, it has excellent prediction effect and practical application value.

## 1. Introduction

With the acceleration of economic development and industrialization, the situation of China's water pollution ecological environment is becoming more and more serious, and industrial and urban water discharge have become the main pollution source [1]. Therefore, the establishment of an effective water quality ecological prediction model can not only optimize urban water ecological detection but also is essential for reducing ecological water pollution. However, the formation of the water ecological environment is a complex physical and chemical process, which is influenced by many factors such as factory emissions, domestic water use, and human factors [2]. These variables are coupled with each other, making it difficult to describe these complex processes with mechanism models. The emergence of learning technology provides an effective way to establish a water ecological detection optimization model [3, 4].

A multiobjective problem proposed in the literature [5] is applied in the activated sludge process. Through the genetic algorithm, it is used to process under the conditions of 14 optimized parameters, and the wastewater COD concentration is reduced by 2.22 mg/L after optimization. The effect of multiobjective problem optimization is obvious, and the parameter optimization combination is the best. Dong et al. [6] proposed a system optimization plan to adjust sewage discharge and predicted COD concentration to adjust the sewage discharge model. The optimized model can improve the water quality of the river and optimize the drainage system more effectively. An et al. [7] proposed to optimize the low dissolved oxygen-oxygen-anoxia process, which can solve the problem of low-cost wastewater treatment, thereby providing a new method for low-cost treatment of COD. Nazrifar et al. [8] optimized the influence of COD, pH, H<sub>2</sub>O<sub>2</sub>, FeSO<sub>4</sub>, and 7H<sub>2</sub>O content on the overall target. When the value reaches 4, 8 ml/L, 2.33 g/L, the model is optimal, and the effect of COD is 83.51. In the CO<sub>2</sub>

emissions, Lim and Kim [9] proposed dynamic optimization to evaluate the production of concrete components. Reuse kinetics to optimize related parameters, and as a result, CO<sub>2</sub> emission costs can be saved. In the NO<sub>x</sub> and CO emission model, the dynamic optimization algorithm proposed in [10] greatly reduces the NO<sub>x</sub> and CO emissions. In terms of performance, the proposed dynamic optimization model can reduce emissions.

ELM is a new and effective machine learning technology based on the Moore–Penrose (MP) generalized inverse matrix theory [11]. Weights and thresholds in the neuron weights are given randomly, and then the output weights are calculated by the regularization principle. The ELM network can still approximate any continuous system. Compared with the ANN and SVM, ELM has an advantage of greatly improving learning speed relatively, which has attracted more and more scholars' attention [12, 13]. Therefore, the prediction model of boiler water ecological COD is adopted by the ELM.

However, ELM regression method is given at random. Without any prior experience, it is easy to cause problems such as the generalization ability and stability of the regression model. In practice, in order to achieve the desired error precision, the ELM usually needs to adjust the weight and threshold. Therefore, a sin chaos AWOA is proposed to accelerate the convergence of ELM parameters to improve the stability and the ELM prediction model and further propose a water ecological optimization prediction model of CAWOA-ELM. It is applied to the prediction of river surface water, domestic sewage, and industrial wastewater in a city. The results show that CAWOA-ELM can accurately predict COD, accurately predict water ecology, and provide an effective means for the promotion of relevant emission optimization.

## 2. Chaos Adaptive Whale Optimization Algorithm

**2.1. WOA.** WOA [14] is an optimization algorithm that simulates the natural world and was put forward in 2016 to simulate the predation behavior of whale populations. This algorithm is simple to set up and has few parameters. When optimizing the benchmark function, it has the advantages of the traditional imitation algorithm (such as particle swarm optimization algorithm (PSO) [15] and gravity search algorithm (GSA) [16]). However, compared with other swarm intelligence algorithms, traditional WOA also have problems of slow convergence, premature convergence, and global optimal value is not available. Based on this, in recent years, many scholars have implemented many effective improved WOA, such as Kaur and Arora [17] used the chaotic map to optimize the update probability  $p$  in WOA, proposed a CWOA, and verified the algorithm with higher convergence speed through the test of benchmark function; Mafarja and Mirjalili [18] combined the annealing algorithm and WOA for the optimization precision of the algorithm, improved the global search ability, and obtained good results in the experiment of publicly testing 18 datasets in the UCI library.

**2.1.1. Shrinkage Surrounding Mechanism.** In the WOA, assuming that the size of the whale population is expressed as  $N$  and  $d$  is to represent the dimensionality, the  $i$ -th position whale in the  $d$ -th dimension can be expressed as  $X_i = (x_i^1, \dots, x_i^d)$ ,  $i = 1, \dots, N$ . The position keeps changing as the problem is solved, and the most optimal solution is described by the optimal position. The whales are all surrounded by optimal solutions. The mathematical model is described as follows:

$$X_i = (x_i^1, \dots, x_i^d), \quad i = 1, \dots, N, \quad (1)$$

where  $t$  is the number of iterations.  $A$  and  $C$  are coefficient vectors, which are defined as follows:

$$A = 2a \times r_1 - a, \quad (2)$$

$$C = 2 \times r_2, \quad (3)$$

where  $r_1$  and  $r_2$  are the random numbers [0, 1] in the formula. The control parameters are defined as follows:

$$a = 2 - 2 \times \frac{t}{T_{\max}}, \quad (4)$$

where  $T_{\max}$  is the maximum iteration number. The contraction bounding mechanism is realized through the reduction of parameter  $\alpha$  by means of (1) and (4).

**2.1.2. Bubble Network Attack.** In the WOA, two methods are designed to describe the predation behavior of whales: shrinkage surrounding mechanism and spiral renewal position.

- (a) Shrinkage enveloping mechanism: it is achieved by reducing the convergence factor  $\alpha$  in equations (2) and (4).
- (b) Spiral update position: first, the distance between the whale individual and the current optimal position is calculated, and then the whale is simulated to capture food in a spiral manner. The mathematical model can be expressed as

$$X(t+1) = X_p(t) + \dot{D} \cdot e^{bl} \cdot \cos(2\pi l), \quad (5)$$

in which  $D' = |X_p(t) - X(t)|$  denotes the distance between whales and the prey,  $b$  is a constant that defines the shape of a logarithmic spiral, and  $L$  is a random number  $[-1, 1]$  in the middle.

The whale's contraction and envelopment mechanism and spiral updating position's mode are synchronized. The new mode of upd

ating  $P_i$  is usually chosen according to the probability value: if  $p < P_i$ ,  $X(t+1)$  is updated in formula (5); otherwise, formula (6) is used to update:

$$X(t+1) = \begin{cases} X(t) - A \cdot |CX_p(t) - X(t)|, & p < P_i, \\ X_p(t) + \dot{D} \cdot e^{bl} \cdot \cos(2\pi l), & p \geq P_i. \end{cases} \quad (6)$$

When  $|A| \geq 1$ , the whales are randomly selected to force them away from the reference whales to find a better prey in order to enhance the global exploration ability of the algorithm. The mathematical model is expressed as follows:

$$X(t+1) = X_r - A \cdot |C \cdot X_r - X(t)|, \quad (7)$$

in which  $X_r$  indicates the position vector of the whale randomly selected.

**2.2. CAWOA.** The shortcomings of the WOA algorithm in dealing with complex optimization problems are low convergence accuracy and easy to fall into local optimum. In view of the above deficiencies, the CAWOA is proposed to improve the global optimization capability of the algorithm. On the basis of WOA, logistic chaotic search strategy is introduced to enhance the ability of the algorithm to jump out of the local optimum. In addition, adaptive inertia weights are introduced into position updating to solve the problem of low convergence accuracy by balancing the development and exploration capabilities.

**2.2.1. Sin Chaotic Search Strategy.** Chaotic mapping is a stochastic motion state obtained by the deterministic equation, which has periodicity and inherent randomness in the phase space, realizing global optimization by optimizing the search ability. Yang and Jiaqiang [19] verified that sin chaos has more obvious chaotic characteristics than logistic chaos does. In order to overcome the shortcomings of the local optimum when WOA deals with complex function optimization problems, sin chaotic search is used to search the optimal individuals (elite individuals) of each generation of the WOA for  $M$  times of chaotic search. If better individuals are found, they are replaced. It can avoid the local optimum and effectively avoid the WOA falling into the local optimum. The sin chaotic mapping model is defined as follows:

$$Z_{n+1} = \sin\left(\frac{2}{Z_n}\right), \quad n = 0, 1, \dots, N, \quad (8)$$

$$-1 \leq Z_n \leq 1, \quad Z_n \neq 0,$$

in which  $Z^0 = [Z_1^0, Z_2^0, \dots, Z_D^0]$  is a randomly generated initial vector whose dimension cannot be zero, thus avoiding producing fixed points and zeros in  $[-1, 1]$ , and its dimension is the same as that of the optimization problem. The iteration counter of the chaotic map is represented by  $t$ , and the output of the system traverses the whole solution space by  $M$  chaotic iterations.

Assuming that the optimal individuals in the WOA population are  $X_i$ , the chaos optimization process in the feasible region is

$$V_i^{t+1} = X_i + \alpha Z^{t+1}, \quad V_i^{t+1} \in [V_{\min}, V_{\max}], \quad (9)$$

$$\alpha = \begin{cases} 1, & \gamma \geq 0.5, \\ -1, & \text{otherwise.} \end{cases}$$

Among them,  $V_i^t$  represents a new individual searched by the algorithm;  $\alpha$  is the adaptive parameter that controls the chaotic search direction;  $\gamma \in [0, 1]$ ; and  $[V_{\min}, V_{\max}]$  is the chaotic search space. Assuming that the elitist solution of the  $i$  generation of the WOA is  $X_i = (x_{i1}, x_{i2}, \dots, x_{iD})$ , the sin chaotic search steps are as follows:

Step 1: normalization of  $X_i$  by using the following formula:

$$x_{ij} = \frac{(x_{ij} - X_{\min}^j)}{(X_{\max}^j - X_{\min}^j)} \quad i = 1, 2, \dots, n; \quad j = 1, 2, \dots, D. \quad (10)$$

Step 2: generating chaotic sequences. Random generation vector  $Z^0 = [Z_1^0, Z_2^0, \dots, Z_D^0]$  based on formula (8) iterative generation of  $M$  chaotic sequences.

Step 3: generating  $M$  chaotic sequences by substituting formula (9), and generating  $M$  chaotic variable sequences  $V_i^k = [v_{i1}^k, v_{i2}^k, \dots, v_{iD}^k]$ ,  $k = 1, 2, \dots, M$ .

Step 4: using formula (10) to reverse the normalization of  $V_i^k$  and generate a new solution  $U_k$  in the field of the original solution space, where  $(k = 1, 2, \dots, M)$ :

$$u_{ij} = x_{ij} + \frac{X_{\max}^j - X_{\min}^j}{2} \times (2v_{ij} - 1). \quad (11)$$

The fitness value  $f(U_k)$  of  $U_k$  is calculated and compared with the fitness value  $f(X_i)$  of  $X_i$ , retaining the best solution.

**2.2.2. Adaptive Inertia Weight.** Inertia weight is an important parameter in WOA. The inertia weight of formulas (1) and (5) is larger than that of formula (1). Constant invariant inertia weight will reduce the efficiency of the algorithm, which is not conducive to the global optimization of the algorithm. Zhang et al. [20] pointed out that, as the inertia weight increases, the global optimal value is easier to obtain, while a smaller inertia weight can easily achieve local optimization [21, 22]. On this basis, an adaptive inertial weight algorithm based on the fitness value is proposed to ensure that Algorithm 1 has a large nonlinear weight at the beginning of the iteration, with different adaptive values, and a small nonlinear weight strategy at the end of the iteration.

The following adaptive inertia weights are introduced in formulas (1) and (6):

$$\omega = 0.2 + \frac{1}{0.4 + \exp(-f_{fit}(x)/u)^{iter}}. \quad (12)$$

In the formula,  $f_{fit}(x)$  represents the individual fitness value,  $u$  represents the best fitness value, and  $iter$  represents the iteration number.

The updated formula is as follows:

$$X(t+1) = \begin{cases} \omega X^*(t) - A \cdot D, & p < P_i, \\ \omega X^*(t) + D_p \cdot e^{bl} \cdot \cos(2\pi l), & p \geq P_i. \end{cases} \quad (13)$$

Using the dynamic nonlinear characteristics to improve the convergence accuracy and speed of the WOA, the flowchart of the CAWOA is as follows:  
 The maximum iteration is  $T_{\max}$ , the population number is  $N$ , and  $N$  initial whale populations  $\{X_i, i = 1, 2, \dots, N\}$  are generated. The fitness value  $\{f(X_i), i = 1, 2, \dots, N\}$  of each whale individual is calculated, and the best individuals are recorded.  
 While ( $t < T_{\max}$ ) do  
   for  $i = 1$  to  $N$  do  
     According to formula (10), the value of adaptive inertia weight  $W$  is calculated.  
     According to formula (4), the value of control parameter alpha is calculated.  
     Updating the values of other parameters  $A, C, l$ , and  $P$ .  
     If ( $p < 0.05$ ) do  
       According to formula (11), updating the current whale individual position;  
     Else if ( $p < 0.05$ ) do  
       According to formula (11), updating the current whale individual position;  
     End if  
   End for  
 Calculating the fitness values of individuals in groups  $\{f(X_i), i = 1, 2, \dots, N\}$ , and preserving and recording elite individuals.  
 Using sin chaotic search strategy to update elite individuals;  
 $T = t + 1$ ;  
 end while  $t = t + 1$ ;

ALGORITHM 1: CAWOA algorithm flow.

### 3. ELM Optimization Model

3.1. *Basic ELM.* ELM solves the problem of long time consumption of the BP neural network. However, because the common limit learning machine only contains one hidden layer, the characterization ability of the network is very limited. Compared with the BP neural network which uses the gradient descent method to update weights, ELM has two characteristics:

- (1) The weights are randomly set and do not need to be adjusted after setting
- (2) The weights are generated by solving the least squares without iterative updating

To solve the output weight of the hidden layer, a standard model can be expressed as follows.

The ELM model is defined as

$$\sum_{i=1}^M \beta_i g(\omega_i \cdot x_i + b_i) = o_j, \quad j = 1, 2, \dots, N, \quad (14)$$

where  $o$  is the actual model output, the training purpose of SLFNs is to minimize the output error, and the cost function  $E$  of the limit learning machine can be seen as follows:

$$E(S, \beta) = \sum_{j=1}^N \|o_j - y_j\|, \quad (15)$$

where  $y$  is the actual data tag, in the limit case, the output of the network is close to the zero error of the actual data tag, and  $\min(E(S, \beta))$  can be seen:

$$\min E = \min \|H(\omega, b, x)\beta - T\|, \quad (16)$$

where  $H, \beta$ , and  $T$  are, respectively, expressed by the following formula:

$$H(\omega, b, x) = \begin{bmatrix} g(\omega_1 x_1 + b_1) & \cdots & g(\omega_M x_1 + b_M) \\ \vdots & & \vdots \\ g(\omega_1 x_N + b_1) & \cdots & g(\omega_M x_N + b_M) \end{bmatrix}_{N \times M},$$

$$\beta = \begin{bmatrix} \beta_1^T \\ \vdots \\ \beta_M^T \end{bmatrix}_{M \times n}, \quad T = \begin{bmatrix} t_1^T \\ \vdots \\ t_N^T \end{bmatrix}_{N \times n}. \quad (17)$$

ELM uses this above model to obtain the output weight of the hidden layer. The above model can be expressed as follows:

$$Y = H\beta. \quad (18)$$

Then, the solution model of the hidden layer output weight can be expressed as

$$\min \|H\beta - Y\|^2. \quad (19)$$

The least squares solution is defined as

$$\beta = H^\dagger T, \quad (20)$$

where  $H^\dagger$  is the generalized inverse matrix of  $H$ , which can be obtained by singular value decomposition.

As can be seen from the above introduction, the learning process of the whole network of the limit learning machine only needs to be solved once. Relative to the BP network, the training time of the network is very short. At the same time, because the hidden layer input weights of the limit learning machine are randomly generated and do not need iterative updating, ELM solves the local minimum problem existing in the BP neural network.

3.2. *ELM Work Flow.* Because ELM has a good performance in function regression without prior knowledge, CAWOA is used in combination with the ELM model. The ELM model trains the input sample data, and CAWOA optimization is used to obtain the optimal parameter value.

Step 1: initialization of WOA:  $N$  is the population number, and the random input value of each individual is set to  $x_j = (\omega_{11}, \dots, \omega_{1M}, \omega_{21}, \omega_{22}, \dots, \omega_{m1}, \dots, \omega_{mM}, b_1, b_2, \dots, b_M)$ .

Step 2: variable selection and data acquisition: to verify good performance of the algorithm proposed, a variety of functions are applied for comparative analysis. Unimodal function and multimodal function are used.

Step 3: determining fitness function  $J$ :

$$J = \frac{1}{1 + \sqrt{\sum_{j=1}^N \|o_j - t_j\|_2^2 / nN}} \quad (21)$$

in which  $t_i = [t_{i1}, t_{i2}, \dots, t_{in}]^T$  is the output, and  $o_i = [o_{i1}, o_{i2}, \dots, o_{in}]^T$  represents the predicted output.

Step 4: model selection: generating the initial population  $(\omega_{11}, \dots, \omega_{1M}, \omega_{21}, \omega_{22}, \dots, \omega_{m1}, \dots, \omega_{mM}, b_1, b_2, \dots, b_M)$  by the random initialization method, randomly generating the sample data prediction model according to the initial population, optimizing parameters in this model until satisfactory results are obtained, and establishing the CAWOA-ELM model.

Step 5: model validation: verifying the performance of the CAWOA-ELM model using test data.

## 4. CAWOA-ELM Test Comparison

4.1. *Test Function Selection.* In order to test the CAWOA-ELM performance, a comprehensive and reasonable experiment is provided. Simulation experiments (including unimodal function and multimodal function) are carried out on 4 benchmark tests, and the corresponding functions are selected as follows:

$$f_1 = \sum_{i=1}^n |x_i| + \prod_{i=1}^n |x_i| \quad D = 30, \text{ lb} = -10, \text{ ub} = 10, f_{\min} = 0, \quad (22)$$

$$f_2 = \sum_{i=1}^{n-1} \left( 100(x_{i+1} - x_i^2)^2 + (x_i + 1)^2 \right) \quad D = 30, \text{ lb} = -30, \text{ ub} = 30, f_{\min} = 0, \quad (23)$$

$$f_3 = 20 \exp \left( -0.2 \sqrt{\frac{1}{n} \sum_{i=1}^n x_i^2} \right) - \exp \left( \frac{1}{n} \sum_{i=1}^n \cos(2\pi x_i) \right) + 20 + e \quad D = 30, \text{ lb} = -32, \text{ ub} = 32, f_{\min} = 0, \quad (24)$$

$$f_4 = \frac{1}{400} \sum_{i=1}^n x_i^2 - \prod_{i=1}^n \cos \left( \frac{x_i}{\sqrt{i}} \right) + 1 \quad D = 30, \text{ lb} = -600, \text{ ub} = 600, f_{\min} = 0, \quad (25)$$

where  $D$  is the dimension,  $ub$  and  $lb$  are the min and max bounds of decision variables, respectively, and  $f_{\min}$  represents the global optimal value.

Among the above four functions, formulas (22) and (23) are unimodal test functions, and formulas (25) and (26) are bimodal test functions.

4.2. *Algorithm Parameter Setting.* When simulating the algorithm, the population size  $N = 30$ , the dimension  $D = 30$ , and the maximum iteration  $t_{\max} = 1000$ . The running environment of the algorithm is "Windows 7 (64-bit)," "CPU E3-1230 with 32 GB," and "MATLAB 2016b." For the statistical analysis of the algorithm, each algorithm runs  $M = 20$  times independently for each benchmark test function and counts its results. All function experiment parameter settings are consistent, and the initial population of all algorithms is consistent.

In order to accurately analyze the CAWOA-ELM effect, the following five indexes are selected:

$$\text{Best} = \min\{\text{best}_1, \text{best}_2, \dots, \text{best}_n\},$$

$$\text{Worst} = \max\{\text{best}_1, \text{best}_2, \dots, \text{best}_n\},$$

$$\text{Mean} = \frac{1}{n} \sum_{i=1}^n \text{best}_i, \quad (26)$$

$$\text{STD} = \sqrt{\frac{1}{m} \sum_{i=1}^m (\text{best}_i - \text{Mean})^2},$$

$$\text{SR} = \frac{k}{m} * 100\%.$$

In the formula,  $k$  represents the number of successes in  $m$  repeated experiments (i.e., the results calculated by the algorithm in this experiment are better than the set standard).

**4.3. Algorithm Test Comparison.** In order to test the performance of CAWOA-ELM algorithm and the correlation test function to obtain the correlation output value when different input values are used, CAWOA-ELM is compared with whale optimization algorithm (WOA), particle swarm optimization (PSO), and biogeography-based optimization (BBO).

Table 1 displays the simulation value of 4 algorithms on 4 benchmark test functions. The best value (BV), worst value (WV), mean value (MV), standard deviation (SD), and success rate (SR) obtained by running all algorithms for 30 times are given. Table 1 shows that, under the condition of test level  $\alpha = 0.5$ , taking CAWOA-ELM algorithm as the benchmark, and comparing the other three algorithms, it is found that the proposed algorithm can have high experimental results.

The WOA, PSO algorithm, BBO algorithm, and CAWOA-ELM algorithm in Table 1 verify the good value and analyze the performance under the above four functions. When the variable dimension is 30, it can be seen from Table 1 that CAWOA-ELM algorithm obtains the optimal value in more aspects of sex.

After comparing the data obtained from 30 simulation experiments, the functions  $f_2$  and  $f_4$  can be optimized, all of which are 0. However, CAWOA-ELM is better than WOA, PSO, and BBO algorithms in the average and SD of functions. In CAWOA-ELM, the mean value and standard deviation of optimal values are obviously better than those of PSO algorithm. For test functions, GA, BBO algorithm, and CAWOA-ELM algorithm are obviously superior to the PSO algorithm in terms of MV and SD optimal values.

The convergence of CAWOA-ELM algorithm is further verified. By iterating through four algorithms, the convergence of the algorithm at different times is verified. The SD value decreases continuously with the increase of iteration times. The algorithm convergence analysis is shown in Figure 1.

The convergence analysis of the overall algorithm shows that CAWOA-ELM algorithm has better convergence than other algorithms in the overall performance. When the number of iterations is 500, the convergence of the CAWOA-ELM model tends to be stable, and the overall fitness value is better than that of other algorithms.

## 5. Water Ecological Environment COD Model Simulation Example

**5.1. Experimental Data.** The water environment quality prediction is the creation of a reliable prediction model through the stored water quality monitoring data. It is well known that water quality monitoring data are obtained through real-time monitoring of national or provincial water quality monitoring stations. pH, conductivity, turbidity, dissolved oxygen (DO), CODMnO<sub>4</sub>, ammonia nitrogen,

total nitrogen, and total phosphorus are proposed in the environmental protection industry standard "Automatic Analyzer Technology for Water Quality Index" (HJ-T100-2003) issued by the Ministry of Environmental Protection. The total organic carbon (TOC) 9 standards are environmental protection industry standards. The revised announcement includes routine monitoring projects such as pH, ammonia nitrogen, total nitrogen, and total phosphorus. At the same time, chemical oxygen demand (COD), biochemical oxygen demand (BOD), and some heavy metal ions are also the water quality parameters that people hope to monitor. Therefore, combined with the national announcement and actual needs, this paper selects five indicators that indicate water environmental quality provided by water quality monitoring stations, namely, COD, pH, dissolved oxygen, ammonia nitrogen, and total phosphorus. COD refers to the mass concentration of oxygen corresponding to an oxidant consumed by a strong oxidant in a chemical process to oxidize a reducing substance in water. COD is a key indicator for indicating the degree of pollutants in water and an important pollution parameter in the operation and management of wastewater treatment plants.

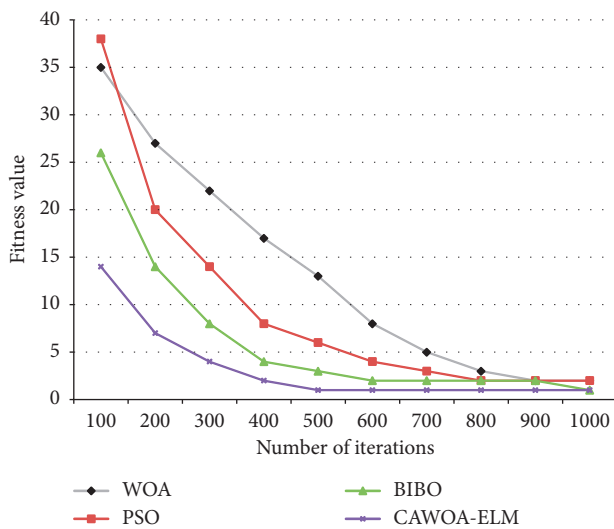
The monitoring data of a water plant monitoring station in a city are taken as the research object. The water plant monitoring station records the data of each parameter in the water body every 6 hours. Due to the reasonable interval between data collection, the recorded data can fully reflect the water quality of the water plant. The data of the water plant monitoring station from January 20 to June 18 are selected in the experiment, and the CAWOA model is trained using the data from January to May 2018. Subsequently, the water quality parameter data of June are input into other trained prediction models for testing, and the expected value is compared with the actual value and analyzed.

**5.2. CAWOA-ELM Simulation Experiment.** The CAWOA is combined with the ELM model to optimize the parameters of the water ecosystem to reduce the COD emission concentration of water pollution. Firstly, the CAWOA is applied to optimize the ELM model parameters, and then the test samples are used to verify the accuracy and generalization ability of the CAWOA-ELM model. Taking the ecological environment of a certain water area as the research object, the data of COD emissions are tested in multiple groups, and various operational parameters such as pH, DO, NH<sub>3</sub>-N, TP, and COD that affect the water quality characteristics are predicted and selected. 30 groups of data are compared experimentally, 20 groups of samples are selected for training optimization modeling, and the remaining 10 groups are used as test samples to verify the accuracy and generalization ability of the model. The selected 20 sets of training data and the other 10 sets of predicted data are subjected to regression prediction, and the predicted values are as shown in Figure 2. In order to verify the superiority of this algorithm in modeling, this algorithm is compared with four models of BBO-ELM, PSO-ELM, WOA-ELM, and

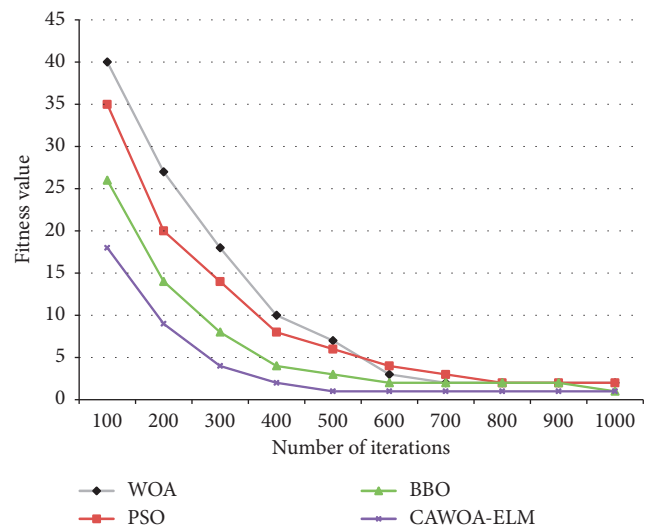


TABLE 1: Simulation results.

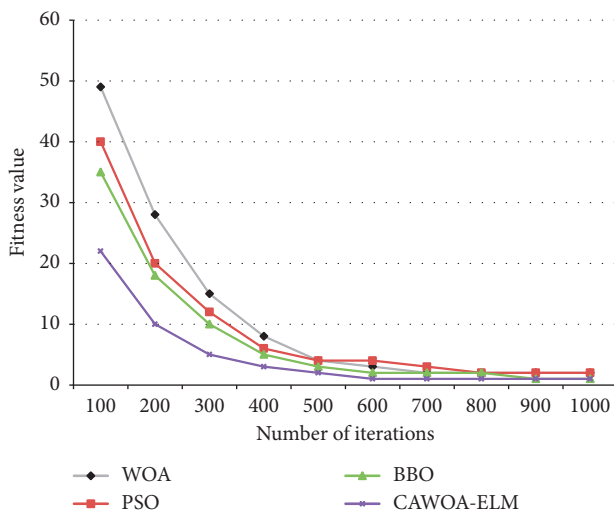
Function	Indicators	WOA	PSO	BBO	CAWOA-ELM
$f_1$	BV	$1.391E-65$	$5.352E-55$	$1.127 \times E-45$	$1.987E-167$
	WV	$4.117E-49$	$4.961E-39$	$5.238 \times E-34$	$2.343E-89$
	MV	$2.106E-55$	$9.871E-47$	$2.921 \times E-39$	$4.782 \times E-107$
	SD	$9.109E-57$	$6.431E-49$	$9.302 \times E-41$	$1.412 \times E-124$
	SR	10%	10%	16.67%	3.33%
$f_2$	BV	$3.345E-75$	$3.522E-65$	$3.342 \times E-42$	0
	WV	$5.727E-62$	$1.719E-51$	$7.231 \times E-31$	0
	MV	$8.234E-68$	$3.371E-58$	$8.823 \times E-35$	0
	SD	$6.349E-70$	$8.569E-62$	$7.467 \times E-36$	0
	SR	13.33%	10%	13.33%	0
$f_3$	BV	$8.881E-18$	$5.169E-37$	$1.122 \times E-31$	$7.387E-197$
	WV	$7.991E-16$	$5.387E-27$	$3.378 \times E-23$	$2.343E-78$
	MV	$5.442E-17$	$9.871E-30$	$2.278 \times E-28$	$4.78 \times E-116$
	SD	$2.833E-17$	$6.431E-32$	$9.976 \times E-29$	$1.42 \times E-135$
	SR	13.33%	13.33%	16.67%	3.33%
$f_4$	BV	$3.764E-23$	$7.654E-39$	$2.138 \times E-37$	0
	WV	$7.761E-17$	$8.659E-26$	$3.891 \times E-28$	0
	MV	$5.581E-20$	$9.871E-47$	$5.892 \times E-32$	0
	SD	$8.874E-21$	$6.431E-49$	$7.319 \times E-35$	0
	SR	13.33%	13.33%	10%	0



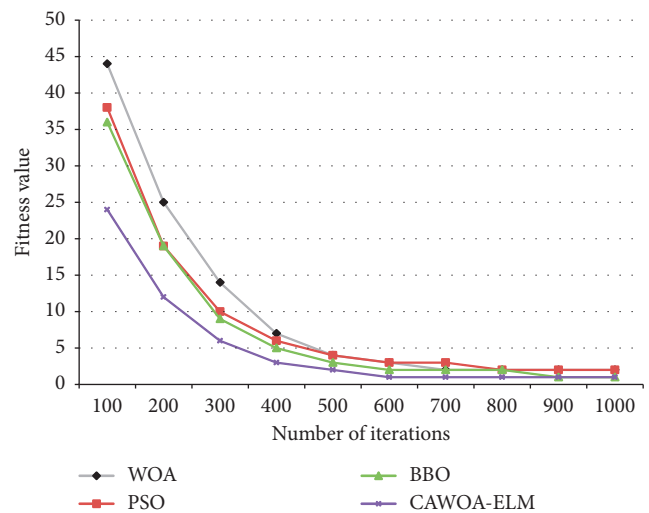
(a)



(b)



(c)



(d)

FIGURE 1: The algorithm convergence analysis (Dim = 30).

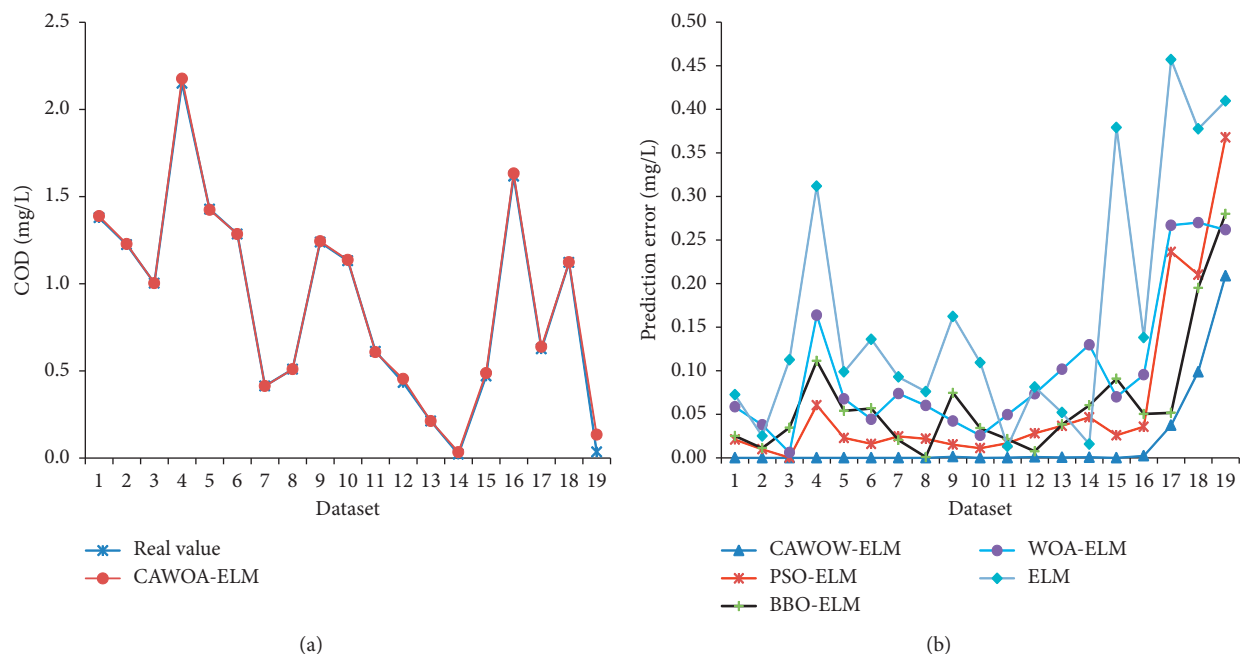


FIGURE 2: COD prediction model and comparison.

TABLE 2: Performance comparison of 4 algorithms.

Sample	True data	CAWOA-ELM			PSO-ELM			BBO-ELM			WOA-ELM		
		PV	ER	RE (%)	PV	ER	RE (%)	PV	ER	RE (%)	PV	ER	RE (%)
1	1.766	1.84	0.07	3.96	2.02	0.25	14.16	1.85	0.08	4.53	2.05	0.28	15.86
2	1.895	2.01	0.11	5.80	2.13	0.23	12.14	2.11	0.21	11.08	2.19	0.29	15.30
3	1.543	1.75	0.21	13.61	1.92	0.38	24.63	1.81	0.27	17.50	1.81	0.27	17.50

standard ELM. The absolute value of the prediction error of each method is shown in Figure 2.

As can be seen from Figure 2(a), the CAWOA-ELM model can better predict training and test samples, and there are some errors in predicting samples. As can be seen from Figure 2(b), the data in samples 17, 18, and 19 do not participate in the training of the model, and compared with other participating training samples, the error is relatively large, which is in line with the principle of system modeling. It can be further found that the predicted performance of BBO-ELM is comparable to that of PSO-ELM, while the predictive performance of WOA-ELM is poor, especially for the three future samples that are not involved in training. The performance of the ELWO model optimized by CAWOA has been greatly improved compared with the WOA-ELM model.

To further describe the superiority of the CAWOA-ELM, the predictive value (PV) and relative error (RE) of training samples 17, 18, and 19 are shown in Table 2. From Table 2, we can see that the predicted value of CAWOA-ELM works very well, and the error values are 0.07, 0.11, and 0.21, respectively. The error values of 0.07, 0.11, and 0.21 are the smallest of the five models, especially for WOA-ELM and standard ELM models. It shows that the CAWOA-ELM

model has good accuracy and generalization ability. The CAWOA-ELM prediction model provides an effective means for accurate prediction calculation of COD.

## 6. Conclusion

Water ecological environment discharge has multidimensional characteristics, many factors lead to the prediction effect, and the multidimensional characteristic relationship is relatively complex, which makes the prediction difficult. It can effectively predict the COD value of water ecological discharge. A combined prediction model based on the CAWOA-ELM algorithm is proposed. In order to test the advantages of the algorithm, CAWOA-ELM algorithm is compared with WOA, PSO, and BBO algorithms. The convergence proves that the CAWOA-ELM algorithm has faster convergence effect. A CAWOA-ELM model for predicting COD is set up, in which 30% of the samples are used as test samples and 70% as training sets. The model is used to train and test datasets. The COD values detected by the CAWOA-ELM model have good accuracy, and the differences between the other models can be used as an application model for predicting COD values.

## Data Availability

The raw data supporting the conclusions of this article will be made available from the corresponding author upon request, without undue reservation.

## Conflicts of Interest

The authors declare that they have no conflicts of interest regarding this work.

## Acknowledgments

This work was supported in part by the Science and Technology Research Program of Chongqing Municipal Education Commission (Grant no. KJQN201902102).

## References

- [1] Y. Li, S. Huang, and X. Qu, "Water pollution prediction in the three gorges reservoir area and countermeasures for sustainable development of the water environment," *International Journal of Environmental Research and Public Health*, vol. 14, no. 11, p. 1307, 2017.
- [2] Z.-P. Wang, L. Zhang, B. Wang et al., "Dissolved methane in groundwater of domestic wells and its potential emissions in arid and semi-arid regions of Inner Mongolia, China," *Science of the Total Environment*, vol. 626, pp. 1193–1199, 2018.
- [3] T. Cordier, P. Esling, F. Lejzerowicz et al., "Predicting the ecological quality status of marine environments from eDNA metabarcoding data using supervised machine learning," *Environmental Science & Technology*, vol. 51, no. 16, p. 9118, 2017.
- [4] C. K. Hatice, S. Feng, K. Liang et al., "Comparison of supervised machine learning algorithms for waterborne pathogen detection using mobile phone fluorescence microscopy," *Nanophotonics*, vol. 6, no. 4, pp. 731–741, 2017.
- [5] H. Dai, W. Chen, L. Peng, X. Wang, and X. Lu, "Modeling and performance improvement of an anaerobic-anoxic/nitrifying-induced crystallization process via the multi-objective optimization method," *Environmental Science and Pollution Research International*, vol. 26, no. 5, pp. 5083–5093, 2019.
- [6] Z. Dong, C. Kuang, J. Gu et al., "Total maximum allocated load of chemical oxygen demand near qinhuangdao in bohai sea: model and field observations," *Water*, vol. 12, no. 4, p. 1141, 2020.
- [7] Z. An, J. Yan, J. Sha, Y. Ma, and S. Mou, "Dynamic simulation for comprehensive water resources policies to improve water-use efficiency in coastal city," *Environmental Science and Pollution Research*, 2021.
- [8] M. Nazrifar, N. Bahramifar, and H. Younesi, "Optimization of fenton and photo-fenton-based advanced oxidation processes for COD reduction of petrochemical wastewater: application of response surface methodology," *Water Conservation Science and Engineering*, vol. 4, no. 2-3, pp. 89–112, 2019.
- [9] J. Lim and J. J. Kim, "Dynamic optimization model for estimating in-situ production quantity of PC members to minimize environmental loads," *Sustainability*, vol. 12, no. 19, p. 8202, 2020.
- [10] S. M. Safdarnejad, J. F. Tuttle, and K. M. Powell, "Dynamic modeling and optimization of a coal-fired utility boiler to forecast and minimize NO<sub>x</sub> and CO emissions simultaneously," *Computers & Chemical Engineering*, vol. 124, pp. 62–79, 2019.
- [11] G.-B. Huang, Q.-Y. Zhu, and C.-K. Siew, "Extreme learning machine: theory and applications," *Neurocomputing*, vol. 70, no. 1–3, pp. 489–501, 2006.
- [12] Y. Peng, W. Kong, and B. Yang, "Orthogonal extreme learning machine for image classification," *Neurocomputing*, vol. 266, pp. 458–464, 2017.
- [13] A. Bequé and S. Lessmann, "Extreme learning machines for credit scoring: an empirical evaluation," *Expert Systems with Applications*, vol. 86, pp. 42–53, 2017.
- [14] S. Mirjalili and A. Lewis, "The whale optimization algorithm," *Advances in Engineering Software*, vol. 95, pp. 51–67, 2016.
- [15] Y. Delice, E. Kızılkaya Aydoğan, U. Özcan, and M. S. İlkay, "A modified particle swarm optimization algorithm to mixed-model two-sided assembly line balancing," *Journal of Intelligent Manufacturing*, vol. 28, no. 1, pp. 23–36, 2017.
- [16] M. R. Penk and M. Dan, "Evaluating center-seeking and initialization bias: the case of particle swarm and gravitational search algorithms," *Information Sciences*, vol. 278, no. 10, pp. 802–821, 2014.
- [17] G. Kaur and S. Arora, "Chaotic whale optimization algorithm," *Journal of Computational Design and Engineering*, vol. 5, no. 3, pp. 275–284, 2018.
- [18] M. M. Mafarja and S. Mirjalili, "Hybrid whale optimization algorithm with simulated annealing for feature selection," *Neurocomputing*, vol. 260, pp. 302–312, 2017.
- [19] H. Yang and E. Jiaqiang, "An adaptive chaos immune optimization algorithm with mutative scale and its application," *Control Theory & Applications*, vol. 26, no. 10, pp. 1069–1074, 2009.
- [20] L. Zhang, Y. Tang, C. Hua, and X. Guan, "A new particle swarm optimization algorithm with adaptive inertia weight based on Bayesian techniques," *Applied Soft Computing*, vol. 28, no. C, pp. 138–149, 2015.
- [21] J. B. Liu, J. Zhao, and Z. X. Zhu, "On the number of spanning trees and normalized Laplacian of linear octagonal-quadrilateral networks," *International Journal of Quantum Chemistry*, vol. 119, no. 17, pp. 1–21, 2019.
- [22] J. B. Liu, J. Zhao, and Z. Cai, "On the generalized adjacency, Laplacian and signless Laplacian spectra of the weighted edge corona networks," *Physica A*, vol. 540, pp. 1–11, 2020.

## Research Article

# Computing Bounds of Fractional Metric Dimension of Metal Organic Graphs

Mohsin Raza,<sup>1</sup> Dalal Awadh Alrowaili,<sup>2</sup> Muhammad Javaid ,<sup>1</sup> and Khurram Shabbir<sup>3</sup>

<sup>1</sup>Department of Mathematics, School of Science, University of Management and Technology, Lahore 54770, Pakistan

<sup>2</sup>Department of Mathematics, College of Science, Jouf University, Sakaka 2014, Saudi Arabia

<sup>3</sup>Department of Mathematics, GC University, Lahore 54000, Pakistan

Correspondence should be addressed to Muhammad Javaid; javaidmath@gmail.com

Received 14 January 2021; Revised 10 February 2021; Accepted 27 February 2021; Published 12 March 2021

Academic Editor: Kashif Ali

Copyright © 2021 Mohsin Raza et al. This is an open access article distributed under the Creative Commons Attribution License, which permits unrestricted use, distribution, and reproduction in any medium, provided the original work is properly cited.

Metal organic graphs are hollow structures of metal atoms that are connected by ligands, where metal atoms are represented by the vertices and ligands are referred as edges. A vertex  $x$  resolves the vertices  $u$  and  $v$  of a graph  $G$  if  $d(u, x) \neq d(v, x)$ . For a pair  $(u, v)$  of vertices of  $G$ ,  $R(u, v) = \{x \in V(G) : d(x, u) \neq d(x, v)\}$  is called its resolving neighbourhood set. For each pair of vertices  $u$  and  $v$  in  $V(G)$ , if  $f(R(u, v)) \geq 1$ , then  $f$  from  $V(G)$  to the interval  $[0, 1]$  is called resolving function. Moreover, for two functions  $f$  and  $g$ ,  $f$  is called minimal if  $f \leq g$  and  $f(v) \neq g(v)$  for at least one  $v \in V(G)$ . The fractional metric dimension (FMD) of  $G$  is denoted by  $\dim_f(G)$  and defined as  $\dim_f(G) = \min\{|g| : g \text{ is a minimal resolving function of } G\}$ , where  $|g| = \sum_{v \in V(G)} g(v)$ . If we take a pair of vertices  $(u, v)$  of  $G$  as an edge  $e = uv$  of  $G$ , then it becomes local fractional metric dimension (LFMD) ( $\dim_{lf}(G)$ ). In this paper, local fractional and fractional metric dimensions of MOG( $n$ ) are computed for  $n \equiv 1 \pmod{2}$  in the terms of upper bounds. Moreover, it is obtained that metal organic is one of the graphs that has the same local and fractional metric dimension.

## 1. Introduction

For a connected graph  $G$ , a vertex  $x \in V(G)$  is said to resolve a pair  $(u, v)$  of vertices of  $G$  if  $d(x, u) \neq d(x, v)$ . A set  $S \subseteq V(G)$  is called a resolving set of  $G$  if each pair of vertices of  $G$  is resolved by some vertex in  $S$ . The metric dimension of  $G$  is denoted by  $\dim(G)$  and is defined as

$$\dim(G) = \min\{|S| : S \text{ is a resolving set of } G\}. \quad (1)$$

For a pair  $(u, v)$  of vertices of  $G$ , the resolving neighborhood  $R(u, v)$  is defined as  $R(u, v) = \{w \in V(G) : d(w, u) \neq d(w, v)\}$ . A resolving function is a real-valued function  $g : V(G) \rightarrow [0, 1]$  such that  $g(R(u, v)) \geq 1$  for each distinct pair of vertices of  $G$ , where  $g(R(u, v)) = \sum_{x \in R(u, v)} g(x)$ . A resolving function  $g$  is called minimal if any function  $f : V(G) \rightarrow [0, 1]$  such that  $f \leq g$  and  $f(v) \neq g(v)$  for at least one  $v \in V$  is not a resolving function of  $G$ . The fractional metric dimension (FMD) of  $G$  is denoted by  $\dim_f(G)$  and defined as

$$\dim_f(G) = \min\{|g| : g \text{ is a minimal resolving function of } G\}, \quad (2)$$

where  $|g| = \sum_{v \in V(G)} g(v)$ . Now, if we take a pair of vertices  $(u, v)$  of  $G$  as an edge  $e = uv$  of  $G$ , then the aforesaid defined resolving neighborhood  $R(u, v)$ , minimal resolving function  $g$ , and FMD  $\dim_f(G)$  become local resolving neighborhood (LR( $uv$ )), local minimal resolving function, and local fractional metric dimension ( $\dim_{lf}(G)$ ), respectively.

First of all, Harary and Melter [1] defined the concept of metric dimension to study the substructures of chemical compounds having similar properties which are used in pharmaceutical industries for the drug discoveries. Later on, Chartrand et al. [2] and Currie & Oellermann [3, 4] improved the solution of IPP with the help of the procedure of metric dimension. Moreover, it is used in navigation system, image processing, and robotic problems [5]. For various results of metric dimension on different graphs, refer to [6–9].

Fehr et al. [10] introduced the concept of fractional metric dimension (FMD), and they obtained the optimal solution of a certain linear programming relaxation problem with the help of FMD. Arumugam and Mathew [11] present various properties of FMD. The FMD of metal organic framework (MOF) is computed in [12], where MOF is obtained from the cycle of odd order. Moreover, different classes of graphs such as product-based graphs and Hamming, Johnson, and permutation graphs are studied with the help of FMD [13–17]. Liu et al. [18] computed the FMD of generalized Jahangir graph. Recently, Aisyah et al. defined the concept of local fractional metric dimension (LFMD) and computed it for the corona product of graphs [19]. Liu et al. [20] computed the LFMD of rotationally symmetric networks. Javaid et al. [21] calculated the sharp bounds of LFMD of connected networks.

Metal organic graph (MOG) consists of metal atoms, where atoms are linked with the help of organic ligands which act like a linker. Therefore, MOG has led to a new world of remarkable applications and it has a large surface area that allows these chemical compounds to absorb huge quantity of several gases such as carbon dioxide hydrogen and methane acting as a gas storage chemical compound. It is also utilized for environmental protection and cleaning energy with the help of capturing carbon dioxide. Being small density, high surface structure flexibility, and tuneable pore functionality, metal organic frameworks also play an important role in liquid-phase separation that is industrial step with critical roles in petrochemical, chemical, nuclear, and pharmaceutical industries. These frameworks are also used in heterogeneous catalyst, drugs delivery, and sensing conductivity [22–25].

In this paper, upper bounds for LFMD and FMD of the metal organic graphs are calculated, where MOGs are obtained with the help of the cycles of even order. Moreover, the unboundedness of the obtained results is also discussed. Rest of the paper is organized as follows: Section 1 includes the introduction. Construction of MOG is discussed in Section 2. LFMD of metal organic graphs is added in Section 3. FMD of MOG is calculated in Section 4. Conclusion is presented in Section 5.

## 2. Construction of Metal Organic Graphs

In this section, we describe the construction of metal organic graphs. Let  $MOG(n)$  for  $n \geq 3$  be a metal organic graph with vertex set  $V(MOG(n)) = \{u_i: 1 \leq i \leq n\} \cup \{v_j: 1 \leq j \leq 2n\}$  and edge set  $E(MOG(n)) = \{u_i u_{i+1}: 1 \leq i \leq n-1\} \cup \{v_j v_{j+1}: 1 \leq j \leq 2n-1\} \cup \{u_n u_1, v_{2n} v_1\} \cup \{u_i v_j, u_i v_{j+1}: 1 \leq i \leq n, 1 \leq j \leq 2n\}$ , where  $|V(MOG(n))| = |E(MOG(n))| = 3n$ . Figure 1 shows  $MOG(n)$  for  $n \in \{5, 7, 9\}$ .

## 3. LFMD of Metal Organic Graphs

In this section, local resolving neighbourhood sets of metal organic graphs are discussed in Lemmas 1 and 2 and local fractional metric dimension is calculated in Theorem 1.

**Lemma 1.** Let  $MOG(n)$  for  $n \equiv 1 \pmod{2}$  and  $n \geq 5$  be metal organic graph, then  $|LR(e_t)| = |LR(e_t = v_i v_j)| = 8$ . For  $1 \leq k \leq n$ ,  $j = i + 1$ ,  $i \in [2k - 1]$ ,  $1 \leq t \leq n$ . Moreover,  $\cup LR(e_t) = \{v_m: 1 \leq m \leq 2n\}$  and  $|\cup LR(e_t)| = \alpha = 2n$ .

*Proof.* The local resolving neighborhood of metal organic graphs, for  $1 \leq k \leq n$ ,  $j = i + 1$ ,  $i \in [2k - 1]$ ,  $1 \leq t \leq n$ .  $LR(v_i v_j) = \{v_l: 2k - 1 \leq l \leq k - 3, 2k - 4 \leq l \leq 2k - 2\}$  with  $|LR(e_t)| = 8$  and  $\cup_{t=1}^n LR(e_t) = \{v_s: 1 \leq s \leq 2n\}$ , and we have  $|\cup_{t=1}^n LR(e_t)| = 2n$ .  $\square$

**Lemma 2.** Let  $MOG(n)$  for  $n \equiv 1 \pmod{2}$  and  $n \geq 9$  be a metal organic graph with  $1 \leq t \leq n$ . Then, the following holds:

- For  $1 \leq k \leq n$ ,  $j = i + 1$ ,  $i \in [2k]$ ,  $|LR(e_t)| < |LR(v_i v_j)|$  and  $|LR(v_i v_j) \cap (\cup_{t=1}^n LR(e_t))| \geq |LR(e_t)|$ .
- For  $1 \leq i \leq n - 1$ ,  $j = i + 1$ ,  $|LR(e_t)| < |LR(u_i u_j)|$  and  $|LR(u_i u_j) \cap (\cup_{t=1}^n LR(e_t))| \geq |LR(e_t)|$ .
- For  $1 \leq i \leq n$ ,  $j = 2i - 1$ ,  $2i$ ,  $|LR(e_t)| < |LR(u_i u_j)|$  and  $|LR(u_i u_j) \cap (\cup_{t=1}^n LR(e_t))| \geq |LR(e_t)|$ .
- For  $1 \leq i \leq n$ ,  $j = 2i$ ,  $|LR(e_t)| < |LR(u_i u_j)|$  and  $|LR(u_i u_j) \cap (\cup_{t=1}^n LR(e_t))| \geq |LR(e_t)|$ .

*Proof.* (a) The local resolving neighborhood for  $1 \leq k \leq n$ ,  $j = i + 1$ ,  $i \in [2k]$ ,  $1 \leq t \leq n$ ,

$$LR(v_i v_j) = \begin{cases} u_p: & 1 \leq p \leq n, \text{ where } p \neq \frac{n+1}{2} + k = m, \\ v_q: & 1 \leq q \leq 2n, \text{ where } q \neq 2m, 2m - 1, \end{cases} \quad (3)$$

with  $|LR(v_i v_j)| = 3n - 3 > 8 = |LR(e_t)|$ ,  $LR(v_i v_j) \cap (\cup_{t=1}^n LR(e_t)) = \{v_q: 1 \leq q \leq 2n, q \neq 2m, 2m - 1\}$ .

Therefore,

$$|LR(v_i v_j) \cap (\cup_{t=1}^n LR(e_t))| = 2n - 2 > |LR(e_t)|.$$

(b) The local resolving neighborhood for  $1 \leq i \leq n - 1$ ,  $j = i + 1$ ,  $1 \leq t \leq n$ ,

$$LR(u_i u_j) = \begin{cases} u_p: & 1 \leq p \leq n, \text{ where } p \neq \frac{n+i+j}{2} + k = m, \\ v_q: & 1 \leq q \leq 2n, \text{ where } q \neq 2m, 2m - 1, \end{cases} \quad (4)$$

with  $|LR(u_i u_j)| = 3n - 3 > 8 = |LR(e_t)|$  and  $LR(u_i u_j) \cap (\cup_{t=1}^n LR(e_t)) = \{v_q: 1 \leq q \leq 2n, q \neq 2m, 2m - 1\}$ . Therefore, we have  $|LR(u_i u_j) \cap (\cup_{t=1}^n LR(e_t))| = 2n - 2 > |LR(e_t)|$ .

(c) The local resolving neighborhood for  $1 \leq i \leq n$ ,  $j = 2i - 1$ ,  $1 \leq t \leq n$ ,

$$LR(u_i v_j) = \begin{cases} u_p: & 1 \leq p \leq n; \\ v_q: & 1 \leq q \leq 2n \text{ where } q \neq j + 1, 2, -2, -3, \end{cases} \quad (5)$$

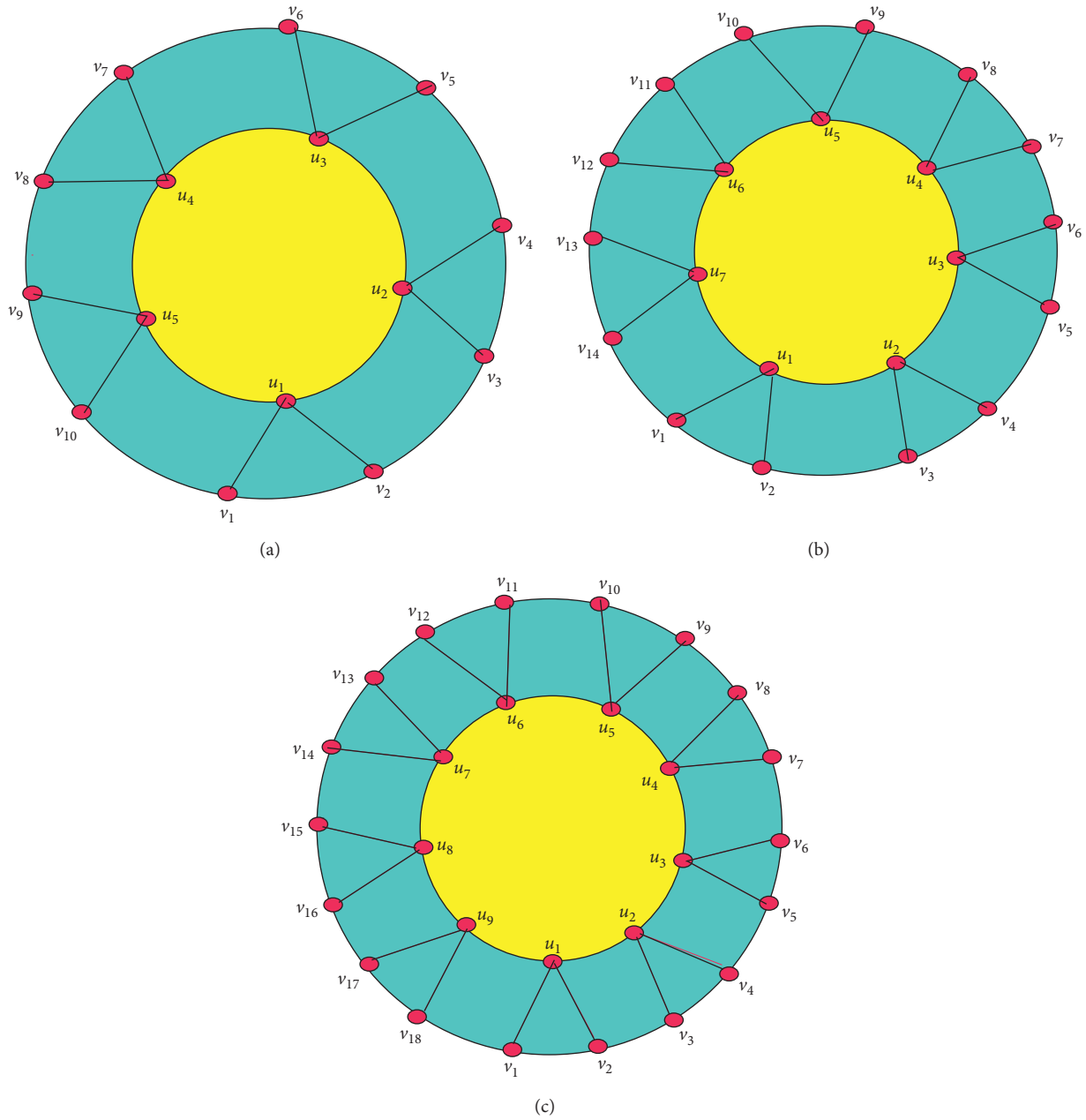


FIGURE 1:  $MOG(n)$  for  $n = 5$  (a),  $n = 7$  (b), and  $n = 9$  (c).

with  $|LR(u_i u_j)| = 3n - 4 > 8 = |LR(e_t)|$  and  $LR(u_i u_j) \cap (\cup_{t=1}^n LRe_t) = \{v_q : q \neq j + 1, 2, -2, -3\}$ . Therefore, we have  $|LR(u_i u_j) \cap (\cup_{t=1}^n LRe_t)| = 2n - 4 > |LR(e_t)|$ .

(d) The local resolving neighborhood for  $1 \leq i \leq n$ ,  $j = 2i - 1$ ,  $1 \leq t \leq n$ ,

$$LR(u_i v_j) = \begin{cases} u_p & 1 \leq p \leq n; \\ v_q & 1 \leq q \leq 2n, \text{ where } q \neq j + 2, 3, -1, -2, \end{cases} \quad (6)$$

with  $|LR(u_i u_j)| = 3n - 4 > 8 = |LR(e_t)|$  and  $LR(u_i u_j) \cap (\cup_{t=1}^n LRe_t) = \{v_q : q \neq j + 2, 3, -1, -2\}$ .

Therefore, we have  $|LR(u_i u_j) \cap (\cup_{t=1}^n LRe_t)| = 2n - 4 > |LR(e_t)|$ .  $\square$

**Theorem 1.** Let  $MOG(n)$  for  $n \equiv 1 \pmod{2}$  and  $n \geq 5$  be the metal organic graphs, then  $dim_{lf}(MOG(n)) \leq n/4$ .

*Proof.* In view of Lemmas 1 and 2 for for  $1 \leq k \leq n$ ,  $j = i + 1$ ,  $i \in [2k - 1]$ ,  $1 \leq t \leq n$ ,  $|LR(e_t)| = |LR(v_i v_j)| = 8$  and  $|X| = |\cup_{t=1}^n LRe_t| = 2n$ .

We have  $|R(xy)| \leq |R(e_t)|$  for all  $xy \in E(MOG(n))$ . Moreover, the local resolving neighbourhood of minimum cardinality is not disjoint. Therefore, local fractional metric of  $MOG(n)$  is given as follows:

$$\dim_{lf}(\text{MOG}(n)) \leq \sum_{t=1}^{|X|} \frac{1}{|\text{LR}(e_t)|}. \quad (7)$$

For  $|X| = 2n$  and  $|\text{LR}(e_t)| = 8$ , we have

$$\dim_{lf}(\text{MOG}(n)) \leq \sum_{t=1}^{2n} \frac{1}{8}. \quad (8)$$

Hence,  $\dim_{lf}(\text{MOG}(n)) \leq n/4$ .  $\square$

#### 4. FMD of Metal Organic Graphs

In this section, the resolving neighbourhood sets of metal organic graphs are calculated in Lemmas 3–8. Bounds of FMD are computed in Theorems 2 and 3.

**Lemma 3.** Let  $\text{MOG}(n)$  for  $n \equiv 1 \pmod{2}$  and  $n \geq 9$  be metal organic graph, then  $|\text{R}(e_t)| = |\text{R}(e_t = v_i, v_j)| = 8$ . For  $1 \leq k \leq n$ ,  $j = i + 1$ ,  $i \in [2k - 1]$ ,  $1 \leq t \leq n$ . Moreover,  $\cup_{t=1}^n \text{R}(e_t) = \{v_m: 1 \leq m \leq 2n\}$  and  $|\cup_{t=1}^n \text{R}(e_t)| = \alpha = 2n$ .

*Proof.* The resolving neighborhood sets of metal organic graph for  $1 \leq k \leq n$ ,  $j = i + 1$ ,  $i \in [2k - 1]$ ,  $1 \leq t \leq n$ ,  $\text{R}(v_i, v_j) = \{v_l: 2k - 1 \leq l \leq k - 3, 2k - 4 \leq l \leq 2k - 2\}$  with  $|\text{R}(e_t)| = 8$  and  $\cup_{t=1}^n \text{R}(e_t) = \{v_s: 1 \leq s \leq 2n\}$ , and we have  $|\cup_{t=1}^n \text{R}(e_t)| = 2n$ .  $\square$

**Lemma 4.** Let  $\text{MOG}(n)$  for  $n \equiv 1 \pmod{2}$  and  $n \geq 9$  be metal organic graphs, then for  $1 \leq k \leq n$ ,  $i \in [2k - 1]$ ,  $1 \leq t \leq n$ ,  $|\text{R}(e_t)| < |\text{R}(v_i, v_j)|$  and  $|\text{R}(v_i, v_j) \cap (\cup_{t=1}^n \text{R}(e_t))| \geq |\text{R}(e_t)|$ :

- $j \in \{i + 1\}$ .
- $j \in \{i + 2, i + 6\}$ .
- $j \in \{i + 3, i + 7\}$ .
- $j \in \{i + 4, i + 8\}$ .
- $j \in \{i + 5\}$ .

*Proof.* (a) The resolving neighborhood for  $1 \leq k \leq n$ ,  $i \in [2k - 1]$   $j = i + 1$ ,  $1 \leq t \leq n$ ,

$$\text{R}(v_i, v_j) = \begin{cases} u_p: & 1 \leq p \leq n, \text{ where } p \neq \frac{n+1}{2} + k = m, \\ v_q: & 1 \leq q \leq 2n, \text{ where } q \neq 2m, 2m - 1, \end{cases} \quad (9)$$

with  $|\text{R}(v_i, v_j)| = 3n - 3 > 8 = |\text{R}(e_t)|$  and  $\text{R}(v_i, v_j) \cap (\cup_{t=1}^n \text{R}(e_t)) = \{v_q: 1 \leq q \leq 2n: q \neq 2m, 2m - 1\}$ . Therefore, we have  $|\text{R}(v_i, v_j) \cap (\cup_{t=1}^n \text{R}(e_t))| = 2n - 2 > |\text{R}(e_t)|$ .

(b) The resolving neighborhood for  $1 \leq k \leq n$ ,  $i \in [2k - 1]$   $j = i + 2, i + 6$ ,  $1 \leq t \leq n$ .

When  $j \in \{i + 2\}$ ,

$$\text{R}(v_i, v_j) = \begin{cases} u_p: & 1 \leq p \leq n, \text{ where } p \neq \frac{n+2i+1}{2} = m, \\ v_q: & 1 \leq q \leq 2n, \text{ where } q \neq 2m, 2m - 1, i + 1. \end{cases} \quad (10)$$

When  $j \in \{i + 6\}$ ,

$$\text{R}(v_i, v_j) = \begin{cases} u_p: & 1 \leq p \leq n, \text{ where } p \neq \frac{n+2i+3}{2} = m, \\ v_q: & 1 \leq q \leq 2n, \text{ where } q \neq 2m, 2m - 1, i + 3, \end{cases} \quad (11)$$

with  $|\text{R}(v_i, v_j)| = 3n - 4 > 8 = |\text{R}(e_t)|$ ,  $\text{R}(v_i, v_j) \cap (\cup_{t=1}^n \text{R}(e_t)) = \{v_q: 1 \leq q \leq 2n: q \neq 2m, 2m - 1, i + 1\}$ , and  $j \in \{i + 2\}$ .  $|\text{R}(v_i, v_j) \cap (\cup_{t=1}^n \text{R}(e_t))| = \{v_q: 1 \leq q \leq 2n: q \neq 2m, 2m - 1, i + 3\}$  and  $j \in \{i + 6\}$ . Therefore, we have  $|\text{R}(v_i, v_j) \cap (\cup_{t=1}^n \text{R}(e_t))| = 2n - 3 > |\text{R}(e_t)|$ .

(c) The resolving neighborhood for  $1 \leq k \leq n$ ,  $i \in [2k - 1]$   $j = i + 3, i + 7$ ,  $1 \leq t \leq n$ .

When  $j \in \{i + 3\}$ ,

$$\text{R}(v_i, v_j) = \begin{cases} u_p: & 1 \leq p \leq n, \text{ where } p \neq \frac{n+2i+1}{2} = m, \\ v_q: & 1 \leq q \leq 2n, \text{ where } q \neq 2m, 2m - 1. \end{cases} \quad (12)$$

When  $j \in \{i + 7\}$ ,

$$\text{R}(v_i, v_j) = \begin{cases} u_p: & 1 \leq p \leq n, \text{ where } p \neq \frac{n+2i+3}{2} = m, \\ v_q: & 1 \leq q \leq 2n, \text{ where } q \neq 2m, 2m - 1, \end{cases} \quad (13)$$

with  $|\text{R}(v_i, v_j)| = 3n - 3 > 8 = |\text{R}(e_t)|$ ,  $\text{R}(v_i, v_j) \cap (\cup_{t=1}^n \text{R}(e_t)) = \{v_q: 1 \leq q \leq 2n: q \neq 2m, 2m - 1\}$ , and  $j \in \{i + 3\}$ .  $\text{R}(v_i, v_j) \cap (\cup_{t=1}^n \text{R}(e_t)) = \{v_q: 1 \leq q \leq 2n: q \neq 2m, 2m - 1\}$  and  $j \in \{i + 7\}$ . Therefore, we have  $|\text{R}(v_i, v_j) \cap (\cup_{t=1}^n \text{R}(e_t))| = 2n - 2 > |\text{R}(e_t)|$ .

(d) The resolving neighborhood for  $1 \leq k \leq n$ ,  $i \in [2k - 1]$   $j = i + 4, i + 8$ ,  $1 \leq t \leq n$ .

When  $j \in \{i + 4\}$ ,

$$\text{R}(v_i, v_j) = \begin{cases} u_p: & 1 \leq p \leq n, \text{ where } p \neq \frac{j-1}{2}, \\ v_q: & 1 \leq q \leq 2n, \text{ where } q \neq \frac{i+j}{2}. \end{cases} \quad (14)$$

When  $j \in \{i + 8\}$ ,

$$R(v_i, v_j) = \begin{cases} u_p: & 1 \leq p \leq n, \text{ where } p \neq \frac{j-3}{2}, \\ v_q: & 1 \leq q \leq 2n, \text{ where } q \neq \frac{i+j}{2}, \end{cases} \quad (15)$$

with  $|R(v_i, v_j)| = 3n - 2 > 8 = |R(e_t)|$  and  $R(v_i, v_j) \cap (\cup_{t=1}^n Re_t) = \{v_q: 1 \leq q \leq 2n: q \neq i + j/2\}$ . Therefore, we have  $|R(v_i, v_j) \cap (\cup_{t=1}^n Re_t)| = 2n - 1 > |R(e_t)|$ .

- (e) The resolving neighborhood for  $1 \leq k \leq n$ ,  $i \in [2k - 1] j \in i + 5, 1 \leq t \leq n$ .

$$R(v_i, v_j) = \begin{cases} u_p: & 1 \leq p \leq n, \text{ where } p \neq \frac{j-2}{2}, \\ v_q: & 1 \leq q \leq 2n, \end{cases} \quad (16)$$

with  $|R(v_i, v_j)| = 3n - 1 > 8 = |R(e_t)|$  and  $R(v_i, v_j) \cap (\cup_{t=1}^n Re_t) = \{v_q: 1 \leq q \leq 2n\}$ . Therefore, we have  $|R(v_i, v_j) \cap (\cup_{t=1}^n Re_t)| = 2n > |R(e_t)|$ .  $\square$

**Lemma 5.** Let  $MOG(n)$  for  $n \equiv 1 \pmod{2}$  and  $n \geq 9$  be metal organic graph. Then, for  $1 \leq k \leq n$ ,  $i \in [2k]$ ,  $1 \leq t \leq n$ ,  $|R(e_t)| < |R(v_i, v_j)|$  and  $|R(v_i, v_j) \cap (\cup_{t=1}^n Re_t)| \geq |R(e_t)|$ :

- (a)  $j \in \{i + 2, i + 6\}$ .  
 (b)  $j \in \{i + 3, i + 7\}$ .  
 (c)  $j \in \{i + 4, i + 8\}$ .  
 (d)  $j \in \{i + 5\}$ .

*Proof.* (a) The resolving neighborhood for  $1 \leq k \leq n$ ,  $i \in [2k] j \in i + 2, i + 6, 1 \leq t \leq n$ .

When  $j \in \{i + 2\}$ ,

$$R(v_i, v_j) = \begin{cases} u_p: & 1 \leq p \leq n, \text{ where } p \neq \frac{n+i+1}{2} = m, \\ v_q: & 1 \leq q \leq 2n, \text{ where } q \neq 2m, 2m - 1, i + 1. \end{cases} \quad (17)$$

When  $j \in \{i + 6\}$ ,

$$R(v_i, v_j) = \begin{cases} u_p: & 1 \leq p \leq n, \text{ where } p \neq \frac{n+i+3}{2} = m, \\ v_q: & 1 \leq q \leq 2n, \text{ where } q \neq 2m, 2m - 1, i + 3, \end{cases} \quad (18)$$

with  $|R(v_i, v_j)| = 3n - 4 > 8 = |R(e_t)|$ ,  $R(v_i, v_j) \cap (\cup_{t=1}^n Re_t) = \{v_q: 1 \leq q \leq 2n: q \neq 2m, 2m - 1, i + 1\}$ , and  $j \in i + 2$ .  $R(v_i, v_j) \cap (\cup_{t=1}^n Re_t) = \{v_q: 1 \leq q \leq 2n: q \neq 2m, 2m - 1, i + 3\}$  and  $j \in i + 6$ . Therefore, we have  $|R(v_i, v_j) \cap (\cup_{t=1}^n Re_t)| = 2n - 3 > |R(e_t)|$ .

- (b) The resolving neighborhood for  $1 \leq k \leq n$ ,  $i \in [2k] j \in i + 3, i + 7, 1 \leq t \leq n$ .

$$R(v_i, v_j) = \begin{cases} u_p: & 1 \leq p \leq n, \text{ where } p \neq \frac{j+i+1}{4}, \\ v_q: & 1 \leq q \leq 2n, \end{cases} \quad (19)$$

with  $|R(v_i, v_j)| = 3n - 1 > 8 = |R(e_t)|$  and  $R(v_i, v_j) \cap (\cup_{t=1}^n Re_t) = \{v_q: 1 \leq q \leq 2n\}$ . Therefore, we have  $|R(v_i, v_j) \cap (\cup_{t=1}^n Re_t)| = 2n > |R(e_t)|$ .

- (c) The resolving neighborhood for  $1 \leq k \leq n$ ,  $i \in [2k] j \in i + 4, i + 8, 1 \leq t \leq n$ ,

$$R(v_i, v_j) = \begin{cases} u_p: & 1 \leq p \leq n, \text{ where } p \neq \frac{i+j}{4}, \\ v_q: & 1 \leq q \leq 2n: q \neq \frac{i+j}{2}, \end{cases} \quad (20)$$

with  $|R(v_i, v_j)| = 3n - 2 > 8 = |R(e_t)|$  and  $R(v_i, v_j) \cap (\cup_{t=1}^n Re_t) = \{v_q: 1 \leq q \leq 2n: q \neq i + j/2\}$ . Therefore, we have  $|R(v_i, v_j) \cap (\cup_{t=1}^n Re_t)| = 2n - 1 > |R(e_t)|$ .

- (d) The resolving neighborhood for  $1 \leq k \leq n$ ,  $i \in [2k] j \in \{i + 5\}, 1 \leq t \leq n$ .

$$R(v_i, v_j) = \begin{cases} u_p: & 1 \leq p \leq n, \text{ where } p \neq \frac{n+i+3}{2} = m, \\ v_q: & 1 \leq q \leq 2n, \text{ where } q \neq 2m, 2m - 1, \end{cases} \quad (21)$$

with  $|R(v_i, v_j)| = 3n - 3 > 8 = |R(e_t)|$  and  $R(v_i, v_j) \cap (\cup_{t=1}^n Re_t) = \{v_q: 1 \leq q \leq 2n: q \neq 2m, 2m - 1\}$ . Therefore, we have  $|R(v_i, v_j) \cap (\cup_{t=1}^n Re_t)| = 2n - 2 > |R(e_t)|$ .  $\square$

**Lemma 6.** Let  $MOG(n)$  for  $n \equiv 1 \pmod{2}$  and  $n \geq 9$  be metal organic graph. Then, the following holds.

- (a) For  $1 \leq k \leq n$ ,  $j = i + 1$ ,  $i \in [2k]$ ,  $1 \leq t \leq n$ ,  $|R(e_t)| < |R(v_i, v_j)|$  and  $|R(v_i, v_j) \cap (\cup_{t=1}^n Re_t)| \geq |R(e_t)|$ .

*Proof.* The resolving neighborhood for  $1 \leq i \leq n$ ,  $j \in \{9 + i + k: 1 \leq k \leq 2n - 18\}$ .

When  $k = 4t - 3, 4t - 2$ , for  $1 \leq t \leq n - 9/2$ ,

$$R(v_i, v_j) = \begin{cases} u_p: & 1 \leq p \leq n, \text{ where } p \neq \frac{n+i+6}{2} = m, \\ v_q: & 1 \leq q \leq 2n, \text{ where } q \neq 2m, 2m - 1. \end{cases} \quad (22)$$

When  $k = 4t - 1, 4t$ , for  $1 \leq t \leq n - 9/2$ ,

$$R(v_i, v_j) = \begin{cases} u_p: & 1 \leq p \leq n, \text{ where } p \neq \frac{i+7}{2} = m, \\ v_q: & 1 \leq q \leq 2n, \text{ where } q \neq 2m, 2m - 1, \end{cases} \quad (23)$$



with  $|R(v_i, v_j)| = 3n - 3 > 8 = |R(e_t)|$  and  $R(v_i, v_j) \cap (\cup_{t=1}^n Re_t) = \{v_q: 1 \leq q \leq 2n: q \neq 2m, 2m - 1\}$ . Therefore, we have  $|R(v_i, v_j) \cap (\cup_{t=1}^n Re_t)| = 2n - 2 > |R(e_t)|$ .  $\square$

**Corollary 1.**

- (i) For  $1 \leq k \leq n$ ,  $i \in [2k - 1]$ ,  $|R(v_i, v_j)| = |R(v_i, v_m)|$ , where  $j \in \{i + s: 2 \leq s \leq 8\}$  and  $m \in \{i - s: 2 \leq s \leq 8\}$ .
- (ii) For  $1 \leq k \leq n$ ,  $i \in [2k]$ ,  $|R(v_i, v_j)| = |R(v_i, v_j)|$ , where  $j \in \{i + s, i - s: 2 \leq s \leq 7\}$ .

**Lemma 7.** Let  $MOG(n)$  for  $n \equiv 1 \pmod{2}$  and  $n \geq 9$  be metal organic graph. Then, for  $1 \leq i \leq n$ ,  $1 \leq k \leq n - 1$ ,  $j = i + k$ ,  $1 \leq t \leq n$ ,  $|R(e_t)| < |R(u_i, u_j)|$  and  $|R(u_i, u_j) \cap (\cup_{t=1}^n Re_t)| = \geq |R(e_t)|$ .

*Proof.* The resolving neighborhood for  $1 \leq i \leq n$ ,  $1 \leq k \leq n - 1$ ,  $j = i + k$ .

When  $k \equiv 1 \pmod{2}$ ,

$$R(u_i, u_j) = \begin{cases} u_p: & 1 \leq p \leq n, \text{ where } p \neq \frac{n+i+j}{2} = m, \\ v_q: & 1 \leq q \leq 2n, \text{ where } q \neq 2m, 2m - 1. \end{cases} \quad (24)$$

When  $k \equiv 0 \pmod{2}$ ,

$$R(u_i, u_j) = \begin{cases} u_p: & 1 \leq p \leq n, \text{ where } p \neq \frac{i+j}{2} = m, \\ v_q: & 1 \leq q \leq 2n, \text{ where } q \neq 2m, 2m - 1, \end{cases} \quad (25)$$

$$R(u_i, v_j) = \begin{cases} u_p: & 1 \leq p \leq n, \\ v_q: & 1 \leq q \leq 2n, \text{ where } q \neq j + 2, j + 3, j - 1, j - 1, \end{cases} \quad (27)$$

with  $|R(u_i, v_j)| = 3n - 4 > 8 = |R(e_t)|$  and  $R(u_i, v_j) \cap (\cup_{t=1}^n Re_t) = \{v_q: 1 \leq q \leq 2n: q \neq j + 1, j + 2, j - 2, j - 3\}$ , when  $j \in \{2i - 1\}$ .  $R(u_i, v_j) \cap (\cup_{t=1}^n Re_t) = \{v_q: 1 \leq q \leq 2n: q \neq j + 2, j + 3, j - 1,$

with  $|R(u_i, u_j)| = 3n - 3 > 8 = |R(e_t)|$  and  $R(u_i, u_j) \cap (\cup_{t=1}^n Re_t) = \{v_q: 1 \leq q \leq 2n, q \neq 2m, 2m - 1\}$ . Therefore, we have  $|R(u_i, u_j) \cap (\cup_{t=1}^n Re_t)| = 2n - 2 > |R(e_t)|$ .  $\square$

**Lemma 8.** Let  $MOG(n)$  for  $n \equiv 1 \pmod{2}$  and  $n \geq 9$  be metal organic graph. Then, for  $1 \leq i \leq n$ ,  $|R(e_t)| < |R(u_i, v_j)|$  and  $|R(u_i, u_j) \cap (\cup_{t=1}^n Re_t)| \geq |R(e_t)|$ .

- (a)  $j \in \{2i - 1, 2i\}$ .  
 (b)  $j \in \{2i + 1\}$ .  
 (c)  $j \in \{2i + 2\}$ .  
 (d)  $j \in \{2i + 3, 2i + 4\}$ .  
 (e)  $j \in \{2i + 5\}$ .  
 (f)  $j \in \{2i + 6\}$ .  
 (g)  $j \in \{2i + 7\}$ .  
 (h)  $j \in \{2i + 8\}$ .  
 (i)  $j \in \{2i + 9\}$ .  
 (j)  $j \in \{2i + 10\}$ .  
 (k)  $j \in \{2i + 10 + k: 1 \leq k \leq 2n - 22\}$ .

*Proof:*

- (a) The resolving neighborhood for  $1 \leq i \leq n$ .

When  $j \in \{2i - 1\}$ ,

$$R(u_i, v_j) = \begin{cases} u_p: & 1 \leq p \leq n, \\ v_q: & 1 \leq q \leq 2n: q \neq j + 1, j + 2, j - 2, j - 3. \end{cases} \quad (26)$$

When  $j \in \{2i\}$ ,

$j - 1$ , when  $j \in \{2i\}$ . Therefore, we have  $|R(u_i, v_j) \cap (\cup_{t=1}^n Re_t)| = 2n - 4 > |R(e_t)|$ .

- (b) The resolving neighborhood for  $1 \leq i \leq n$ ,  $j \in \{2i + 1\}$ :

$$R(u_i, v_j) = \begin{cases} u_p: & 1 \leq p \leq n, \text{ where } p \neq m \text{ and } j - i \leq m \leq \frac{n+1}{2}, \\ v_q: & 1 \leq q \leq 2n, \text{ where } q \neq j - 1, s \text{ where } j + 3 \leq s \leq n + j - 2, \end{cases} \quad (28)$$

with  $|R(u_i, v_j)| = 3n - 16 > 8 = |R(e_t)|$  and  $R(u_i, v_j) \cap (\cup_{t=1}^n Re_t) = \{v_q: 1 \leq q \leq 2n: q \neq j - 1, s, \text{ where } j + 3 \leq s \leq n + j - 2\}$ . Therefore, we have  $|R(u_i, v_j) \cap (\cup_{t=1}^n Re_t)| = 2n - 7 > |R(e_t)|$ .

- (c) The resolving neighborhood for  $1 \leq i \leq n$ ,  $j \in \{2i + 2\}$ .

When  $j \in i + 3$ ,

$$R(u_i, v_j) = \begin{cases} u_p: & 1 \leq p \leq n, \text{ where } p \neq m, \text{ and } j - i - 1 \leq m - \frac{n+1}{2}, \\ v_q: & 1 \leq q \leq 2n, \text{ where } q \neq s \text{ and } 2(j - i - 1) \leq s \leq n + j - 4, \end{cases} \quad (29)$$

with  $|R(u_i, v_j)| = 3n - 13 > 8 = |R(e_t)|$  and  $R(u_i, v_j) \cap (\cup_{t=1}^n Re_t) = \{v_q: 1 \leq q \leq 2n: q \neq s, 2(j - i - 1) \leq s \leq n + j - 4\}$ . Therefore, we have  $|R(u_i, v_j) \cap (\cup_{t=1}^n Re_t)| = 2n - 8 > |R(e_t)|$ .

(d) The resolving neighborhood for  $1 \leq i \leq n$ ,  $j \in \{2i + 3, 2i + 4\}$ :

$$R(u_i, v_j) = \begin{cases} u_p: & 1 \leq p \leq n, \text{ where } p \neq \frac{n+1}{2} = s, \\ v_q: & 1 \leq q \leq 2n, \text{ where } q \neq j - 2, q \neq 2s, 2s - 1, \end{cases} \quad (30)$$

with  $|R(u_i, v_j)| = 3n - 4 > 8 = |R(e_t)|$  and  $R(u_i, v_j) \cap (\cup_{t=1}^n Re_t) = \{v_q: 1 \leq q \leq 2n: q \neq j - 2, q \neq 2s, 2s - 1\}$ . Therefore, we have  $|R(u_i, v_j) \cap (\cup_{t=1}^n Re_t)| = 2n - 3 > |R(e_t)|$ .

(e) The resolving neighborhood for  $1 \leq i \leq n$ ,  $j \in \{2i + 5\}$ :

$$R(u_i, v_j) = \begin{cases} u_p: & 1 \leq p \leq n, \text{ where } p \neq \frac{j-1}{2}, \\ v_q: & 1 \leq q \leq 2n, \end{cases} \quad (31)$$

with  $|R(u_i, v_j)| = 3n - 1 > 8 = |R(e_t)|$  and  $R(u_i, v_j) \cap (\cup_{t=1}^n Re_t) = \{v_q: 1 \leq q \leq 2n\}$ . Therefore, we have  $|R(u_i, v_j) \cap (\cup_{t=1}^n Re_t)| = 2n > |R(e_t)|$ .

(f) The resolving neighborhood for  $1 \leq i \leq n$ ,  $j \in \{2i + 6\}$ :

$$R(u_i, v_j) = \begin{cases} u_p: & 1 \leq p \leq n, \text{ where } p \neq \frac{j-1}{2}, \\ v_q: & 1 \leq q \leq 2n, \text{ where } q \neq j - 3, \end{cases} \quad (32)$$

with  $|R(u_i, v_j)| = 3n - 2 > 8 = |R(e_t)|$  and  $R(u_i, v_j) \cap (\cup_{t=1}^n Re_t) = \{v_q: 1 \leq q \leq 2n: q \neq j - 3\}$ . Therefore, we have  $|R(u_i, v_j) \cap (\cup_{t=1}^n Re_t)| = 2n - 1 > |R(e_t)|$ .

(g) The resolving neighborhood for  $1 \leq i \leq n$ ,  $j \in \{2i + 3, 2i + 4\}$ :

$$R(u_i, v_j) = \begin{cases} u_p: & 1 \leq p \leq n, \text{ where } p \neq \frac{n+2i+3}{2} = s, \\ v_q: & 1 \leq q \leq 2n, \text{ where } q \neq j - 3, q \neq 2s, 2s - 1, \end{cases} \quad (33)$$

with  $|R(u_i, v_j)| = 3n - 4 > 8 = |R(e_t)|$  and  $R(u_i, v_j) \cap (\cup_{t=1}^n Re_t) = \{v_q: 1 \leq q \leq 2n: q \neq j - 3, q \neq 2s, 2s - 1\}$ . Therefore, we have  $|R(u_i, v_j) \cap (\cup_{t=1}^n Re_t)| = 2n - 3 > |R(e_t)|$ .

(h) The resolving neighborhood for  $1 \leq i \leq n$ ,  $j \in \{2i + 8\}$ :

$$R(u_i, v_j) = \begin{cases} u_p: & 1 \leq p \leq n, \text{ where } p \neq \frac{n+2i+3}{2} = s, \\ v_q: & 1 \leq q \leq 2n, \text{ where } q \neq 2s, 2s - 1, \end{cases} \quad (34)$$

with  $|R(u_i, v_j)| = 3n - 3 > 8 = |R(e_t)|$  and  $R(u_i, v_j) \cap (\cup_{t=1}^n Re_t) = \{v_q: 1 \leq q \leq 2n: q \neq 2s, 2s - 1\}$ . Therefore, we have  $|R(u_i, v_j) \cap (\cup_{t=1}^n Re_t)| = 2n - 2 > |R(e_t)|$ .

(i) The resolving neighborhood for  $1 \leq i \leq n$ ,  $j \in \{2i + 9\}$ ,

$$R(u_i, v_j) = \begin{cases} u_p, & 1 \leq p \leq n, \text{ where } p \neq \frac{j-3}{2} = s, \\ v_q, & 1 \leq q \leq 2n, \text{ where } q \neq j - 4, \end{cases} \quad (35)$$

with  $|R(u_i, v_j)| = 3n - 2 > 8 = |R(e_t)|$  and  $R(u_i, v_j) \cap (\cup_{t=1}^n Re_t) = \{v_q: 1 \leq q \leq 2n: q \neq j - 4\}$ . Therefore, we have  $|R(u_i, v_j) \cap (\cup_{t=1}^n Re_t)| = 2n - 1 > |R(e_t)|$ .

(j) The resolving neighborhood for  $1 \leq i \leq n$ ,  $j \in \{2i + 9\}$ :

$$R(u_i, v_j) = \begin{cases} u_p: & 1 \leq p \leq n, \text{ where } p \neq \frac{j-4}{2} = s, \\ v_q: & 1 \leq q \leq 2n, \text{ where } q \neq 2s, 2s - 1, \end{cases} \quad (36)$$

with  $|R(u_i, v_j)| = 3n - 3 > 8 = |R(e_t)|$  and  $R(u_i, v_j) \cap (\cup_{t=1}^n Re_t) = \{v_q: 1 \leq q \leq 2n: q \neq 2s, 2s - 1\}$ . Therefore, we have  $|R(u_i, v_j) \cap (\cup_{t=1}^n Re_t)| = 2n - 2 > |R(e_t)|$ .

(k) The resolving neighborhood for  $1 \leq i \leq n$ ,  $j \in \{10 + 2i + k: 1 \leq k \leq 2n - 22\}$ .

When  $k \equiv 1 \pmod{4}, 2 \pmod{4}$ ,

$$R(u_i, v_j) = \begin{cases} u_p: & 1 \leq p \leq n, \text{ where } p \neq \frac{n+7}{2} = m, \\ v_q: & 1 \leq q \leq 2n, \text{ where } q \neq 2m, 2m - 1. \end{cases} \quad (37)$$

When  $k \equiv 0 \pmod{4}, 3 \pmod{4}$ ,

$$R(u_i, v_j) = \begin{cases} u_p: & 1 \leq p \leq n, \text{ where } p \neq \frac{i+4}{2} = s, \\ v_q: & 1 \leq q \leq 2n, \text{ where } q \neq 2s, 2s - 1, \end{cases} \quad (38)$$

TABLE 1: FMD of metal organic graphs.

Resolving sets ( $n = 3$ )	Elements
$R(e_1) = R(u_1, u_2)$	$V(\text{MOG}(3) - \{u_3, v_5, v_6\})$
$R(e_2) = R(u_1, u_3)$	$V(\text{MOG}(3) - \{u_2, v_3, v_4\})$
$R(e_3) = R(u_1, v_1)$	$V(\text{MOG}(3) - \{v_2, v_3, v_5\})$
$R(e_4) = R(u_1, v_2)$	$V(\text{MOG}(3) - \{v_1, v_4, v_6\})$
$R(e_5) = R(u_1, v_3)$	$V(\text{MOG}(3) - \{u_2, v_2, v_5\})$
$R(e_6) = R(u_1, v_6)$	$V(\text{MOG}(3) - \{u_3, v_1, v_4\})$
$R(e_7) = R(u_2, u_3)$	$V(\text{MOG}(3) - \{u_1, v_1, v_2\})$
$R(e_8) = R(u_2, v_2)$	$V(\text{MOG}(3) - \{u_1, v_3, v_6\})$
$R(e_9) = R(u_2, v_3)$	$V(\text{MOG}(3) - \{v_1, v_4, v_5\})$
$R(e_{10}) = R(u_2, v_4)$	$V(\text{MOG}(3) - \{v_2, v_3, v_6\})$
$R(e_{11}) = R(u_2, v_5)$	$V(\text{MOG}(3) - \{u_3, v_1, v_4\})$
$R(e_{12}) = R(u_3, v_1)$	$V(\text{MOG}(3) - \{u_1, v_3, v_6\})$
$R(e_{13}) = R(u_3, v_4)$	$V(\text{MOG}(3) - \{u_2, v_2, v_5\})$
$R(e_{14}) = R(u_3, v_5)$	$V(\text{MOG}(3) - \{v_1, v_3, v_6\})$
$R(e_{15}) = R(u_3, v_6)$	$V(\text{MOG}(3) - \{v_2, v_4, v_5\})$
$R(e_{16}) = R(v_1, v_2)$	$V(\text{MOG}(3) - \{u_1, u_2, u_3\})$
$R(e_{17}) = R(v_1, v_3)$	$V(\text{MOG}(3) - \{u_3, v_2, v_5\})$
$R(e_{18}) = R(v_1, v_5)$	$V(\text{MOG}(3) - \{u_2, v_3, v_6\})$
$R(e_{19}) = R(v_2, v_4)$	$V(\text{MOG}(3) - \{u_3, v_3, v_6\})$
$R(e_{20}) = R(v_2, v_6)$	$V(\text{MOG}(3) - \{u_2, v_1, v_4\})$
$R(e_{21}) = R(v_3, v_4)$	$V(\text{MOG}(3) - \{u_1, u_2, u_3\})$
$R(e_{22}) = R(v_3, v_5)$	$V(\text{MOG}(3) - \{u_1, v_1, v_4\})$
$R(e_{23}) = R(v_4, v_6)$	$V(\text{MOG}(3) - \{u_1, v_4, v_5\})$
$R(e_{24}) = R(v_5, v_6)$	$V(\text{MOG}(3) - \{u_1, u_2, u_3\})$

TABLE 2: FMD of metal organic graphs.

Resolving sets ( $n = 3$ )	Elements
$R_1 = R(u_1, v_4)$	$V(\text{MOG}(3) - \{u_2, v_6\})$
$R_2 = R(u_1, v_5)$	$V(\text{MOG}(3) - \{u_3, v_3\})$
$R_3 = R(u_2, v_1)$	$V(\text{MOG}(3) - \{u_1, v_5\})$
$R_4 = R(u_2, v_6)$	$V(\text{MOG}(3) - \{u_3, v_2\})$
$R_5 = R(u_3, v_2)$	$V(\text{MOG}(3) - \{u_1, v_4\})$
$R_6 = R(u_3, v_3)$	$V(\text{MOG}(3) - \{u_2, v_1\})$
$R_7 = R(v_1, v_4)$	$V(\text{MOG}(3) - \{u_3\})$
$R_8 = R(v_1, v_6)$	$V(\text{MOG}(3) - \{u_5\})$
$R_9 = R(v_2, v_3)$	$V(\text{MOG}(3) - \{u_3\})$
$R_{11} = R(v_3, v_6)$	$V(\text{MOG}(3) - \{u_1\})$
$R_{12} = R(v_4, v_5)$	$V(\text{MOG}(3) - \{u_1\})$

TABLE 3: FMD of metal organic graphs.

Resolving sets ( $n = 5$ )	Elements
$R(e_1) = R(v_1, v_2)$	$V(\text{MOG}(5) - \{u_1, u_2, u_3, u_4, u_5, v_6, v_7\})$
$R(e_1) = R(v_3, v_4)$	$V(\text{MOG}(5) - \{u_1, u_2, u_3, u_4, u_5, v_8, v_9\})$
$R(e_1) = R(v_5, v_6)$	$V(\text{MOG}(5) - \{u_1, u_2, u_3, u_4, u_5, v_1, v_{10}\})$
$R(e_1) = R(v_7, v_8)$	$V(\text{MOG}(5) - \{u_1, u_2, u_3, u_4, u_5, v_2, v_3\})$
$R(e_1) = R(v_9, v_{10})$	$V(\text{MOG}(5) - \{u_1, u_2, u_3, u_4, u_5, v_4, v_5\})$

with  $|R(v_i, v_j)| = 3n - 3 > 8 = |R(e_t)|$  and  $R(u_i, v_j) \cap (\cup_{t=1}^n Re_t) = \{v_q : 1 \leq q \leq 2n, q \neq 2m, 2m - 1\}$ , when  $k \equiv 1 \pmod{4}$ ,  $2 \pmod{4}$  and  $R(u_i, v_j) \cap (\cup_{t=1}^n Re_t) = \{v_q : 1 \leq q \leq 2n, q \neq 2s, 2s - 1\}$ , when  $k \equiv 1 \pmod{4}$ ,  $2 \pmod{4}$ . Therefore, we have  $|R(u_i, v_j) \cap (\cup_{t=1}^n Re_t)| = 2n - 2 > |R(e_t)|$ .

**Corollary 2.** For  $1 \leq i \leq n$ ,  $|R(u_i, v_j)| = |R(u_i, v_m)|$ , where  $j \in \{2i + s : -1 \leq s \leq 10\}$  and  $m \in \{2i + s : -2 \leq s \leq -9\}$ .

TABLE 4: FMD of metal organic graphs.

Resolving sets ( $n = 5$ )	Elements
$R_1 = R(u_1, u_2)$	$V(\text{MOG}(5) - \{u_4, v_7, v_8\})$
$R_2 = R(u_1, u_3)$	$V(\text{MOG}(5) - \{u_2, v_3, v_4\})$
$R_3 = R(u_1, u_4)$	$V(\text{MOG}(5) - \{u_5, v_9, v_{10}\})$
$R_4 = R(u_1, u_5)$	$V(\text{MOG}(5) - \{u_3, v_5, v_{06}\})$
$R_5 = R(u_1, v_1)$	$V(\text{MOG}(5) - \{v_2, v_3, v_8, v_{09}\})$
$R_6 = R(u_1, v_2)$	$V(\text{MOG}(5) - \{v_1, v_4, v_5, v_{10}\})$
$R_7 = R(u_1, v_3)$	$V(\text{MOG}(5) - \{u_2, u_3, v_2, v_6\})$
$R_8 = R(u_1, v_4)$	$V(\text{MOG}(5) - \{u_2, u_3, v_7\})$
$R_9 = R(u_1, v_5)$	$V(\text{MOG}(5) - \{u_4, v_3, v_8\})$
$R_{10} = R(u_1, v_6)$	$V(\text{MOG}(5) - \{u_4, v_4\})$
$R_{11} = R(u_1, v_7)$	$V(\text{MOG}(5) - \{u_3, v_9\})$
$R_{12} = R(u_1, v_8)$	$V(\text{MOG}(5) - \{u_3, v_5, v_{10}\})$
$R_{13} = R(u_1, v_9)$	$V(\text{MOG}(5) - \{u_4, u_5, v_6\})$
$R_{14} = R(u_1, v_{10})$	$V(\text{MOG}(5) - \{u_4, u_5, v_1, v_7\})$
$R_{15} = R(u_2, u_3)$	$V(\text{MOG}(5) - \{u_5, v_9, v_{10}\})$
$R_{16} = R(u_2, u_4)$	$V(\text{MOG}(5) - \{u_3, v_5, v_6\})$
$R_{17} = R(u_2, u_5)$	$V(\text{MOG}(5) - \{u_1, v_1, v_2\})$
$R_{18} = R(u_2, v_1)$	$V(\text{MOG}(5) - \{u_1, u_5, v_8\})$
$R_{19} = R(u_2, v_2)$	$V(\text{MOG}(5) - \{u_1, u_5, v_9\})$
$R_{20} = R(u_2, v_3)$	$V(\text{MOG}(5) - \{v_1, v_4, v_5, v_{10}\})$
$R_{21} = R(u_2, v_4)$	$V(\text{MOG}(5) - \{v_2, v_3, v_6, v_7\})$
$R_{22} = R(u_2, v_5)$	$V(\text{MOG}(5) - \{u_3, u_4, v_4, v_8\})$
$R_{23} = R(u_2, v_6)$	$V(\text{MOG}(5) - \{u_3, u_4, v_9\})$
$R_{24} = R(u_2, v_7)$	$V(\text{MOG}(5) - \{u_5, v_5, v_{10}\})$
$R_{25} = R(u_2, v_8)$	$V(\text{MOG}(5) - \{u_5, v_6\})$
$R_{26} = R(u_2, v_9)$	$V(\text{MOG}(5) - \{u_4, v_1\})$
$R_{27} = R(u_2, v_{10})$	$V(\text{MOG}(5) - \{u_4, v_2, v_7\})$
$R_{28} = R(u_3, u_4)$	$V(\text{MOG}(5) - \{u_1, v_1, v_2\})$
$R_{29} = R(u_3, u_5)$	$V(\text{MOG}(5) - \{u_4, v_7, v_8\})$
$R_{30} = R(u_3, v_1)$	$V(\text{MOG}(5) - \{u_5, v_3\})$
$R_{31} = R(u_3, v_2)$	$V(\text{MOG}(5) - \{u_5, v_4, v_9\})$
$R_{32} = R(u_3, v_3)$	$V(\text{MOG}(5) - \{u_1, u_2, v_{10}\})$
$R_{33} = R(u_3, v_4)$	$V(\text{MOG}(5) - \{u_1, u_2, v_1, v_5\})$
$R_{34} = R(u_3, v_5)$	$V(\text{MOG}(5) - \{v_2, v_3, v_6, v_7\})$
$R_{35} = R(u_3, v_6)$	$V(\text{MOG}(5) - \{v_4, v_5, v_8, v_9\})$
$R_{36} = R(u_3, v_7)$	$V(\text{MOG}(5) - \{u_4, u_5, v_6, v_{10}\})$
$R_{37} = R(u_3, v_8)$	$V(\text{MOG}(5) - \{u_4, u_5, v_1\})$
$R_{38} = R(u_3, v_9)$	$V(\text{MOG}(5) - \{u_1, v_2, v_7\})$
$R_{39} = R(u_3, v_{10})$	$V(\text{MOG}(5) - \{u_1, v_8\})$
$R_{40} = R(u_4, u_5)$	$V(\text{MOG}(5) - \{u_2, v_3, v_4\})$
$R_{41} = R(u_4, v_1)$	$V(\text{MOG}(5) - \{u_2, v_4, v_9\})$
$R_{42} = R(u_4, v_2)$	$V(\text{MOG}(5) - \{u_2, v_{10}\})$
$R_{43} = R(u_4, v_3)$	$V(\text{MOG}(5) - \{u_1, v_5\})$
$R_{44} = R(u_4, v_4)$	$V(\text{MOG}(5) - \{u_1, v_1, v_6\})$
$R_{45} = R(u_4, v_5)$	$V(\text{MOG}(5) - \{u_2, u_3, v_2\})$
$R_{46} = R(u_4, v_6)$	$V(\text{MOG}(5) - \{u_2, u_3, v_2, v_7\})$
$R_{47} = R(u_4, v_7)$	$V(\text{MOG}(5) - \{v_4, v_5, v_8, v_9\})$
$R_{48} = R(u_4, v_8)$	$V(\text{MOG}(5) - \{v_1, v_6, v_7, v_{10}\})$
$R_{49} = R(u_4, v_9)$	$V(\text{MOG}(5) - \{u_1, u_5, v_2, v_8\})$
$R_{50} = R(u_4, v_{10})$	$V(\text{MOG}(5) - \{u_1, u_5, v_3\})$
$R_{51} = R(u_5, v_1)$	$V(\text{MOG}(5) - \{u_1, u_2, v_4, v_{10}\})$
$R_{52} = R(u_5, v_2)$	$V(\text{MOG}(5) - \{u_1, u_2, v_5\})$
$R_{53} = R(u_5, v_3)$	$V(\text{MOG}(5) - \{u_3, v_1, v_6\})$
$R_{54} = R(u_5, v_4)$	$V(\text{MOG}(5) - \{u_3, v_2\})$
$R_{55} = R(u_5, v_5)$	$V(\text{MOG}(5) - \{u_2, v_7\})$
$R_{56} = R(u_5, v_6)$	$V(\text{MOG}(5) - \{u_2, v_3, v_8\})$
$R_{57} = R(u_5, v_7)$	$V(\text{MOG}(5) - \{u_3, u_4, v_4\})$
$R_{58} = R(u_5, v_8)$	$V(\text{MOG}(5) - \{u_3, u_4, v_5, v_9\})$
$R_{59} = R(u_5, v_9)$	$V(\text{MOG}(5) - \{v_1, v_6, v_7, v_9\})$
$R_{60} = R(u_5, v_{10})$	$V(\text{MOG}(5) - \{v_2, v_3, v_8, v_9\})$

TABLE 4: Continued.

Resolving sets ( $n = 5$ )	Elements
$R_{61} = R(v_{01}, v_{03})$	$V(\text{MOG}(5) - \{u_4, v_2, v_7\})$
$R_{62} = R(v_{01}, v_{04})$	$V(\text{MOG}(5) - \{u_4\})$
$R_{63} = R(v_{01}, v_{05})$	$V(\text{MOG}(5) - \{u_2, v_3, v_8\})$
$R_{64} = R(v_{01}, v_{06})$	$V(\text{MOG}(5) - \{u_2\})$
$R_{65} = R(v_{01}, v_{07})$	$V(\text{MOG}(5) - \{u_5, v_4, v_9\})$
$R_{66} = R(v_{01}, v_{08})$	$V(\text{MOG}(5) - \{u_5\})$
$R_{67} = R(v_{01}, v_{09})$	$V(\text{MOG}(5) - \{u_3, v_5\})$
$R_{68} = R(v_{01}, v_{10})$	$V(\text{MOG}(5) - \{u_3, v_5, v_6\})$
$R_{69} = R(v_{02}, v_{03})$	$V(\text{MOG}(5) - \{u_4, v_7, v_8\})$
$R_{70} = R(v_{02}, v_{04})$	$V(\text{MOG}(5) - \{u_4, v_3, v_8\})$
$R_{71} = R(v_{02}, v_{05})$	$V(\text{MOG}(5) - \{u_2\})$
$R_{72} = R(v_{02}, v_{06})$	$V(\text{MOG}(5) - \{u_2, v_4, v_9\})$
$R_{73} = R(v_{02}, v_{07})$	$V(\text{MOG}(5) - \{u_5\})$
$R_{74} = R(v_{02}, v_{08})$	$V(\text{MOG}(5) - \{u_5, v_5, v_{10}\})$
$R_{75} = R(v_{02}, v_{09})$	$V(\text{MOG}(5) - \{u_6\})$
$R_{76} = R(v_{02}, v_{10})$	$V(\text{MOG}(5) - \{u_3, v_1, v_6\})$
$R_{77} = R(v_{03}, v_{05})$	$V(\text{MOG}(5) - \{u_5, v_4, v_9\})$
$R_{78} = R(v_{03}, v_{06})$	$V(\text{MOG}(5) - \{u_5\})$
$R_{79} = R(v_{03}, v_{07})$	$V(\text{MOG}(5) - \{u_3, v_5, v_{10}\})$
$R_{80} = R(v_{03}, v_{08})$	$V(\text{MOG}(5) - \{u_3\})$
$R_{81} = R(v_{03}, v_{09})$	$V(\text{MOG}(5) - \{u_1, v_1, v_6\})$
$R_{82} = R(v_{03}, v_{10})$	$V(\text{MOG}(5) - \{u_1\})$
$R_{83} = R(v_{04}, v_{05})$	$V(\text{MOG}(5) - \{u_5, v_9, v_{10}\})$
$R_{84} = R(v_{04}, v_{06})$	$V(\text{MOG}(5) - \{u_5, v_5, v_{10}\})$
$R_{85} = R(v_{04}, v_{07})$	$V(\text{MOG}(5) - \{u_3\})$
$R_{86} = R(v_{04}, v_{08})$	$V(\text{MOG}(5) - \{u_3, v_1, v_6\})$
$R_{87} = R(v_{04}, v_{09})$	$V(\text{MOG}(5) - \{u_1\})$
$R_{88} = R(v_{04}, v_{10})$	$V(\text{MOG}(5) - \{u_1, v_2, v_7\})$
$R_{89} = R(v_{05}, v_{07})$	$V(\text{MOG}(5) - \{u_1, v_1, v_6\})$
$R_{90} = R(v_{05}, v_{08})$	$V(\text{MOG}(5) - \{u_1\})$
$R_{91} = R(v_{05}, v_{09})$	$V(\text{MOG}(5) - \{u_4, v_4, v_7\})$
$R_{92} = R(v_{05}, v_{10})$	$V(\text{MOG}(5) - \{u_4\})$
$R_{93} = R(v_{06}, v_{07})$	$V(\text{MOG}(5) - \{u_1, v_1, v_2\})$
$R_{94} = R(v_{06}, v_{08})$	$V(\text{MOG}(5) - \{u_1, v_2, v_7\})$
$R_{95} = R(v_{06}, v_{09})$	$V(\text{MOG}(5) - \{u_4\})$
$R_{96} = R(v_{06}, v_{10})$	$V(\text{MOG}(5) - \{u_4, v_3, v_8\})$
$R_{97} = R(v_{07}, v_{09})$	$V(\text{MOG}(5) - \{u_2, v_3, v_8\})$
$R_{98} = R(v_{07}, v_{10})$	$V(\text{MOG}(5) - \{u_2\})$
$R_{99} = R(v_{08}, v_{09})$	$V(\text{MOG}(5) - \{u_2, v_3, v_4\})$
$R_{100} = R(v_{08}, v_{10})$	$V(\text{MOG}(5) - \{u_2, v_4, v_9\})$

**Theorem 2.** The FMD of metal organic graph  $\text{MOG}(n)$  for  $3 \leq n \leq 7, n \equiv 1 \pmod{2}$  is

$$\dim_f \text{MOG}(n) = \begin{cases} \frac{3}{2} & \text{if } n = 3, \\ \frac{5}{4} & \text{if } n = 5, \\ \frac{7}{4} & \text{if } n = 7. \end{cases} \quad (39)$$

*Proof.* Case 1: when  $n = 3$ , then the RNs are as follows.

Since, for  $1 \leq t \leq 24$ , the cardinality of each RN  $R(e_t)$  is 6, as given in Table 1, which is less than the cardinalities of all other RNs  $R_m$  of  $\text{MOG}(3)$ , as given in Table 2, where  $1 \leq m \leq 12$ . Moreover,  $\cup_{t=1}^{24} R(e_t) = V(\text{MOG}(3))$ ;

TABLE 5: FMD of metal organic graphs.

Resolving sets ( $n = 5$ )	Elements
$R(e_1) = R(v_1, v_2)$	$\{v_1, v_2, v_3, v_4, v_5, v_{12}, v_{13}, v_{14}\}$
$R(e_2) = R(v_3, v_4)$	$\{v_1, v_2, v_3, v_4, v_5, v_6, v_7, v_{14}\}$
$R(e_3) = R(v_5, v_6)$	$\{v_2, v_3, v_4, v_5, v_6, v_7, v_8, v_9\}$
$R(e_4)R(v_7, v_8)$	$\{v_4, v_5, v_6, v_7, v_8, v_9, v_{10}, v_{11}\}$
$R(e_5) = R(v_9, v_{10})$	$\{v_6, v_7, v_8, v_9, v_{10}, v_{11}, v_{12}, v_{13}\}$
$R(e_6) = R(v_{11}, v_{12})$	$\{v_1, v_8, v_9, v_{10}, v_{11}, v_{12}, v_{13}, v_{14}\}$
$R(e_7) = R(v_{13}, v_{14})$	$\{v_1, v_2, v_3, v_{10}, v_{11}, v_{12}, v_{13}, v_{14}\}$

this implies that  $\cup_{t=1}^{24} R(e_t) = 9$  and  $|R_m \cap \cup_{t=1}^{24} R(e_t)| > |R(e_t)| = 6$ .

Consequently,  $\dim_f(\text{MOG}(3)) = \sum_{t=1}^9 1/6 \leq 3/2$ .

Case 2: when  $n = 5$ , as shown in Figure 1, the RNs are as follows.

Since, for  $1 \leq t \leq 5$ , the cardinality of each RN  $R(e_t)$  is 8, as given in Table 3, which is less than the cardinalities of all other RNs  $R_m$  of  $(\text{MOG}(5))$ , as given in Table 4, where  $1 \leq m \leq 100$ . Moreover,  $\cup_{t=1}^5 R(e_t) = V((\text{MOG}(5))$ ; this implies that  $|\cup_{t=1}^5 R(e_t)| = 10$  and  $R_m \cap |\cup_{t=1}^5 R(e_t)| > |R(e_t)| = 8$ .

Consequently,  $\dim_f((\text{MOG}(5))) \leq \sum_{t=1}^{10} 1/8 = 5/4$ .

Case 3: when  $n = 7$ , as shown in Figure 1, then the RNs are as follows.

Since, for  $1 \leq t \leq 7$ , the cardinality of each RN  $R(e_t)$  is 8, as given in Table 5, which is less than the cardinalities of all other RNs  $R_m$  of  $(\text{MOG}(5))$ , as given in Table 6, where  $1 \leq m \leq 203$ . Moreover,  $\cup_{t=1}^7 R(e_t) = V(\text{MOG}(7))$ ; this implies that  $|\cup_{t=1}^7 R(e_t)| = 14$  and  $|R_m \cap \cup_{t=1}^7 R(e_t)| > |R(e_t)| = 8$ .

Consequently,  $\dim_f(\text{MOG}(5)) \leq \sum_{t=1}^{14} 1/8 \leq 7/4$ .  $\square$

**Theorem 3.** Let  $\text{MOG}(n)$  for  $n \geq 9$  and  $n \equiv 1 \pmod{2}$  be the metal organic graph. Then,  $\dim_f \text{MOG}(n) \leq n/4$ .

*Proof.* In view of Lemmas 3–8 for  $1 \leq k \leq n, j = i + 1, i \in [2k - 1], 1 \leq t \leq n, |R(e_t)| = |R(v_i v_j)| = 8$  and  $|X| = |\cup_{t=1}^n R(e_t)| = 2n$ . Also, we have  $|R(xy)| \leq |R(e_t)|$  for all  $xy \in E(\text{MOG}(n))$ . Moreover, the local resolving neighbourhood of minimum cardinality is not disjoint. Therefore, the fractional metric of  $\text{MOG}(n)$  is given as follows:

$$\dim_f \text{MOG}(n) \leq \sum_{t=1}^{|X|} \frac{1}{|R(e_t)|}. \quad (40)$$

For  $|X| = 2n$  and  $|R(e_t)| = 8$ , we have

$$\dim_f \text{MOG}(n) \leq \sum_{t=1}^{2n} \frac{1}{8}. \quad (41)$$

Hence,  $\dim_f \text{MOG}(n) \leq n/4$ .  $\square$

TABLE 6: FMD of MOG(7).

Resolving sets ( $n = 7$ )	Elements
$R_1 = R(u_1, u_2)$	$V(\text{MOG}(7) - \{u_5, v_9, v_{10}\})$
$R_2 = R(u_1, u_3)$	$V(\text{MOG}(7) - \{u_2, v_3, v_4\})$
$R_3 = R(u_1, u_4)$	$V(\text{MOG}(7) - \{u_6, v_{11}, v_{12}\})$
$R_4 = R(u_1, u_5)$	$V(\text{MOG}(7) - \{u_3, v_5, v_{06}\})$
$R_5 = R(u_1, u_6)$	$V(\text{MOG}(7) - \{u_7, v_{13}, v_{14}\})$
$R_6 = R(u_1, u_7)$	$V(\text{MOG}(7) - \{u_4, v_7, v_{08}\})$
$R_7 = R(u_1, v_1)$	$V(\text{MOG}(7) - \{v_2, v_3, v_{12}, v_{13}\})$
$R_8 = R(u_1, v_2)$	$V(\text{MOG}(7) - \{v_1, v_4, v_5, v_{14}\})$
$R_9 = R(u_1, v_3)$	$V(\text{MOG}(7) - \{u_2, u_3, u_4, v_2, v_6, v_7, v_8\})$
$R_{10} = R(u_1, v_4)$	$V(\text{MOG}(7) - \{u_2, u_3, u_4, v_8\})$
$R_{11} = R(u_1, v_5)$	$V(\text{MOG}(7) - \{u_5, v_3, v_9, v_{10}\})$
$R_{12} = R(u_1, v_6)$	$V(\text{MOG}(7) - \{u_5, v_4, v_{10}\})$
$R_{13} = R(u_1, v_7)$	$V(\text{MOG}(7) - \{u_3\})$
$R_{14} = R(u_1, v_8)$	$V(\text{MOG}(7) - \{u_3, v_5, v_{11}\})$
$R_{15} = R(u_1, v_9)$	$V(\text{MOG}(7) - \{u_6, v_6, v_{12}\})$
$R_{16} = R(u_1, v_{10})$	$V(\text{MOG}(7) - \{u_4, v_7\})$
$R_{17} = R(u_1, v_{11})$	$V(\text{MOG}(7) - \{u_4, v_7\})$
$R_{18} = R(u_1, v_{12})$	$V(\text{MOG}(7) - \{u_4, v_7, v_8, v_{14}\})$
$R_{19} = R(u_1, v_{13})$	$V(\text{MOG}(7) - \{u_5, u_6, u_7, v_9\})$
$R_{20} = R(u_1, v_{14})$	$V(\text{MOG}(7) - \{u_5, u_6, u_7, v_1, v_9\})$
$R_{21} = R(u_2, u_3)$	$V(\text{MOG}(7) - \{u_6, v_{11}, v_{12}\})$
$R_{22} = R(u_2, u_4)$	$V(\text{MOG}(7) - \{u_3, v_5, v_6\})$
$R_{23} = R(u_2, u_5)$	$V(\text{MOG}(7) - \{u_7, v_{13}, v_{14}\})$
$R_{24} = R(u_2, u_6)$	$V(\text{MOG}(7) - \{u_4, v_7, v_8\})$
$R_{25} = R(u_2, u_7)$	$V(\text{MOG}(7) - \{u_1, v_1, v_2\})$
$R_{26} = R(u_2, v_1)$	$V(\text{MOG}(7) - \{u_1, u_6, u_7, v_{11}\})$
$R_{27} = R(u_2, v_2)$	$V(\text{MOG}(7) - \{u_1, u_6, u_7, v_3, u_{11}, v_{12}, v_{13}\})$
$R_{28} = R(u_2, v_3)$	$V(\text{MOG}(7) - \{v_1, v_4, v_5, v_{14}\})$
$R_{29} = R(u_2, v_4)$	$V(\text{MOG}(7) - \{v_2, v_3, v_6, v_7\})$
$R_{30} = R(u_2, v_5)$	$V(\text{MOG}(7) - \{u_3, u_4, u_5, v_4, v_8, v_9, v_{10}\})$
$R_{31} = R(u_2, v_6)$	$V(\text{MOG}(7) - \{u_3, u_4, u_5, v_{10}\})$
$R_{32} = R(u_2, v_7)$	$V(\text{MOG}(7) - \{u_6, v_5, v_{11}, v_{12}\})$
$R_{33} = R(u_2, v_8)$	$V(\text{MOG}(7) - \{u_6, v_6, v_{12}\})$
$R_{34} = R(u_2, v_9)$	$V(\text{MOG}(7) - \{u_4\})$
$R_{35} = R(u_2, v_{10})$	$V(\text{MOG}(7) - \{u_4, v_7, v_{13}\})$
$R_{36} = R(u_2, v_{11})$	$V(\text{MOG}(7) - \{v_8, v_{14}\})$
$R_{37} = R(u_2, v_{12})$	$V(\text{MOG}(7) - \{u_7\})$
$R_{38} = R(u_2, v_{13})$	$V(\text{MOG}(7) - \{u_5, v_1, v_9\})$
$R_{39} = R(u_2, v_{14})$	$V(\text{MOG}(7) - \{u_5, v_2, v_9, v_{10}\})$
$R_{40} = R(u_3, u_4)$	$V(\text{MOG}(7) - \{u_7, v_{13}, v_{14}\})$
$R_{41} = R(u_3, u_5)$	$V(\text{MOG}(7) - \{u_4, v_7, v_8\})$
$R_{42} = R(u_3, u_6)$	$V(\text{MOG}(7) - \{u_1, v_1, v_2\})$
$R_{43} = R(u_3, u_7)$	$V(\text{MOG}(7) - \{u_5, v_9, v_{10}\})$
$R_{44} = R(u_3, v_1)$	$V(\text{MOG}(7) - \{u_6, v_3, v_{11}\})$
$R_{45} = R(u_3, v_2)$	$V(\text{MOG}(7) - \{u_6, v_4, v_{11}, v_{12}\})$
$R_{46} = R(u_3, v_3)$	$V(\text{MOG}(7) - \{u_1, u_2, u_7, v_{13}, v_{14}\})$
$R_{47} = R(u_3, v_4)$	$V(\text{MOG}(7) - \{u_1, u_2, u_7, v_1, v_5, v_{13}, v_{14}\})$
$R_{48} = R(u_3, v_5)$	$V(\text{MOG}(7) - \{v_2, v_3, v_6, v_7\})$
$R_{49} = R(u_3, v_6)$	$V(\text{MOG}(7) - \{v_4, v_5, v_8, v_9\})$
$R_{50} = R(u_3, v_7)$	$V(\text{MOG}(7) - \{u_4, u_5, u_6, v_6, v_{10}, v_{11}, v_{12}\})$
$R_{51} = R(u_3, v_8)$	$V(\text{MOG}(7) - \{u_4, u_5, u_6, v_{12}\})$
$R_{52} = R(u_3, v_9)$	$V(\text{MOG}(7) - \{u_7, v_7, v_{13}\})$
$R_{53} = R(u_3, v_{10})$	$V(\text{MOG}(7) - \{u_7, v_8, v_{14}\})$
$R_{54} = R(u_3, v_{11})$	$V(\text{MOG}(7) - \{u_5\})$
$R_{55} = R(u_3, v_{12})$	$V(\text{MOG}(7) - \{u_5, v_1\})$
$R_{56} = R(u_3, v_{13})$	$V(\text{MOG}(7) - \{u_1, u_2, v_{10}\})$
$R_{57} = R(u_3, v_{14})$	$V(\text{MOG}(7) - \{u_1, v_{10}\})$
$R_{58} = R(u_4, u_5)$	$V(\text{MOG}(7) - \{u_1, v_1, v_2\})$
$R_{59} = R(u_4, u_6)$	$V(\text{MOG}(7) - \{u_5, v_9, v_{10}\})$
$R_{60} = R(u_4, u_7)$	$V(\text{MOG}(7) - \{u_2, v_3, v_4\})$

TABLE 6: Continued.

Resolving sets ( $n = 7$ )	Elements
$R_{61} = R(u_4, v_1)$	$V(\text{MOG}(7) - \{u_2, u_7, v_4, v_{12}\})$
$R_{62} = R(u_4, v_2)$	$V(\text{MOG}(7) - \{u_2, u_7\})$
$R_{63} = R(u_4, v_3)$	$V(\text{MOG}(7) - \{u_7, v_5, v_{13}\})$
$R_{64} = R(u_4, v_4)$	$V(\text{MOG}(7) - \{u_7, u_6, v_{13}, v_{14}\})$
$R_{65} = R(u_4, v_5)$	$V(\text{MOG}(7) - \{u_2, u_3, v_1\})$
$R_{66} = R(u_4, v_6)$	$V(\text{MOG}(7) - \{u_2, u_3, u_7, v_1, v_2, v_3, v_7\})$
$R_{67} = R(u_4, v_7)$	$V(\text{MOG}(7) - \{v_4, v_5, v_8, v_9\})$
$R_{68} = R(u_4, v_8)$	$V(\text{MOG}(7) - \{v_6, v_7, v_{10}, v_{11}\})$
$R_{69} = R(u_4, v_9)$	$V(\text{MOG}(7) - \{u_5, u_6, v_7, v_8, v_{12}, v_{13}\})$
$R_{70} = R(u_4, v_{10})$	$V(\text{MOG}(7) - \{u_5, u_6, u_7, v_{14}\})$
$R_{71} = R(u_4, v_{11})$	$V(\text{MOG}(7) - \{u_1, v_1, v_2, v_9\})$
$R_{72} = R(u_4, v_{12})$	$V(\text{MOG}(7) - \{u_1, v_1, v_2, v_{10}\})$
$R_{73} = R(u_4, v_{13})$	$V(\text{MOG}(7) - \{u_6, v_{11}\})$
$R_{74} = R(u_4, v_{14})$	$V(\text{MOG}(7) - \{u_6, v_3, v_{11}\})$
$R_{75} = R(u_5, u_6)$	$V(\text{MOG}(7) - \{u_2, v_3, v_4\})$
$R_{76} = R(u_5, u_7)$	$V(\text{MOG}(7) - \{u_6, v_{11}, v_{12}\})$
$R_{77} = R(u_5, v_1)$	$V(\text{MOG}(7) - \{u_7\})$
$R_{78} = R(u_5, v_2)$	$V(\text{MOG}(7) - \{u_7, u_5, v_{13}\})$
$R_{79} = R(u_5, v_3)$	$V(\text{MOG}(7) - \{u_3, v_6, v_{14}\})$
$R_{80} = R(u_5, v_4)$	$V(\text{MOG}(7) - \{u_3\})$
$R_{81} = R(u_5, v_5)$	$V(\text{MOG}(7) - \{u_1, v_1, v_7\})$
$R_{82} = R(u_5, v_6)$	$V(\text{MOG}(7) - \{u_1, v_1, v_2, v_8\})$
$R_{83} = R(u_5, v_7)$	$V(\text{MOG}(7) - \{u_2, u_3, u_4, v_3\})$
$R_{84} = R(u_5, v_8)$	$V(\text{MOG}(7) - \{u_2, u_3, u_4, v_3, v_4, v_5, v_9\})$
$R_{85} = R(u_5, v_9)$	$V(\text{MOG}(7) - \{v_6, v_7, v_{10}, v_{11}\})$
$R_{86} = R(u_5, v_{10})$	$V(\text{MOG}(7) - \{v_8, v_9, v_{12}, v_{13}\})$
$R_{87} = R(u_5, v_{11})$	$V(\text{MOG}(7) - \{u_1, u_6, u_7, v_1, v_2, v_{10}, v_{14}\})$
$R_{88} = R(u_5, v_{12})$	$V(\text{MOG}(7) - \{u_1, u_6, u_7, v_2\})$
$R_{89} = R(u_5, v_{13})$	$V(\text{MOG}(7) - \{u_2, v_3, v_4, v_{11}\})$
$R_{90} = R(u_5, v_{14})$	$V(\text{MOG}(7) - \{u_2, v_4, v_{12}\})$
$R_{91} = R(u_6, u_7)$	$V(\text{MOG}(7) - \{u_3, v_5, v_6\})$
$R_{92} = R(u_6, v_1)$	$V(\text{MOG}(7) - \{u_3, v_5, v_6, v_{13}\})$
$R_{93} = R(u_6, v_2)$	$V(\text{MOG}(7) - \{u_1, v_6\})$
$R_{94} = R(u_6, v_3)$	$V(\text{MOG}(7) - \{u_1\})$
$R_{95} = R(u_6, v_4)$	$V(\text{MOG}(7) - \{u_1, v_1\})$
$R_{96} = R(u_6, v_5)$	$V(\text{MOG}(7) - \{u_1, u_4, v_2, v_8\})$
$R_{97} = R(u_6, v_6)$	$V(\text{MOG}(7) - \{u_1, u_4\})$
$R_{98} = R(u_6, v_7)$	$V(\text{MOG}(7) - \{u_2, v_3, v_9\})$
$R_{99} = R(u_6, v_8)$	$V(\text{MOG}(7) - \{u_2, v_3, v_4, v_{10}\})$
$R_{100} = R(u_6, v_9)$	$V(\text{MOG}(7) - \{u_3, u_4, u_5, v_5\})$
$R_{101} = R(u_6, v_{10})$	$V(\text{MOG}(7) - \{u_3, u_4, u_5, v_5, v_6, v_7\})$
$R_{102} = R(u_6, v_{11})$	$V(\text{MOG}(7) - \{v_8, v_9, v_{12}, v_{13}\})$
$R_{103} = R(u_6, v_{12})$	$V(\text{MOG}(7) - \{v_1, v_{10}, v_{11}, v_{14}\})$
$R_{104} = R(u_6, v_{13})$	$V(\text{MOG}(7) - \{u_1, u_2, u_7, v_2, v_3, v_4\})$
$R_{105} = R(u_6, v_{14})$	$V(\text{MOG}(7) - \{u_1, u_2, u_7, v_4\})$
$R_{106} = R(u_7, v_1)$	$V(\text{MOG}(7) - \{u_1, u_2, u_3, v_6, v_{14}\})$
$R_{107} = R(u_7, v_2)$	$V(\text{MOG}(7) - \{u_1, u_2, u_3, v_6\})$
$R_{108} = R(u_7, v_3)$	$V(\text{MOG}(7) - \{u_4, v_1, v_7, v_8\})$
$R_{109} = R(u_7, v_4)$	$V(\text{MOG}(7) - \{u_4, v_2, v_8\})$
$R_{110} = R(u_7, v_5)$	$V(\text{MOG}(7) - \{u_2\})$
$R_{111} = R(u_7, v_6)$	$V(\text{MOG}(7) - \{u_2, v_3, v_9\})$
$R_{112} = R(u_7, v_7)$	$V(\text{MOG}(7) - \{u_5, v_4, v_{10}\})$
$R_{113} = R(u_7, v_8)$	$V(\text{MOG}(7) - \{u_5, v_4\})$
$R_{114} = R(u_7, v_9)$	$V(\text{MOG}(7) - \{u_3, v_5, v_{11}\})$
$R_{115} = R(u_7, v_{10})$	$V(\text{MOG}(7) - \{u_3, v_5, v_6, v_{12}\})$
$R_{116} = R(u_7, v_{11})$	$V(\text{MOG}(7) - \{u_4, u_5, u_6, v_7\})$
$R_{117} = R(u_7, v_{12})$	$V(\text{MOG}(7) - \{u_4, u_5, u_6, v_7, v_8, v_9, v_{13}\})$
$R_{118} = R(u_7, v_{13})$	$V(\text{MOG}(7) - \{v_1, v_{10}, v_{11}, v_{14}\})$
$R_{119} = R(u_7, v_{14})$	$V(\text{MOG}(7) - \{v_2, v_3, v_{12}, v_{13}\})$
$R_{120} = R(v_1, v_3)$	$V(\text{MOG}(7) - \{u_5, v_2, v_9, v_{10}\})$

TABLE 6: Continued.

Resolving sets ( $n = 7$ )	Elements
$R_{121} = R(v_1, v_4)$	$V(\text{MOG}(7) - \{u_5, v_9, v_{10}\})$
$R_{122} = R(v_1, v_5)$	$V(\text{MOG}(7) - \{u_2, v_3\})$
$R_{123} = R(v_1, v_6)$	$V(\text{MOG}(7) - \{u_2\})$
$R_{124} = R(v_1, v_7)$	$V(\text{MOG}(7) - \{u_6, v_4, v_{11}\})$
$R_{125} = R(v_1, v_8)$	$V(\text{MOG}(7) - \{u_6\})$
$R_{126} = R(v_1, v_9)$	$V(\text{MOG}(7) - \{u_3, v_5, v_{12}\})$
$R_{127} = R(v_1, v_{10})$	$V(\text{MOG}(7) - \{u_3, v_5, v_6\})$
$R_{128} = R(v_1, v_{11})$	$V(\text{MOG}(7) - \{u_7, v_{13}\})$
$R_{129} = R(v_1, v_{12})$	$V(\text{MOG}(7) - \{u_7\})$
$R_{130} = R(v_1, v_{13})$	$V(\text{MOG}(7) - \{u_4, v_7, v_8, v_{14}\})$
$R_{131} = R(v_1, v_{14})$	$V(\text{MOG}(7) - \{u_4, v_7, v_8\})$
$R_{132} = R(v_2, v_3)$	$V(\text{MOG}(7) - \{u_5, v_9, v_{10}\})$
$R_{133} = R(v_2, v_4)$	$V(\text{MOG}(7) - \{u_5, v_3, v_9, v_{10}\})$
$R_{134} = R(v_2, v_5)$	$V(\text{MOG}(7) - \{u_2\})$
$R_{135} = R(v_2, v_6)$	$V(\text{MOG}(7) - \{u_6, u_{11}, v_{12}\})$
$R_{136} = R(v_2, v_7)$	$V(\text{MOG}(7) - \{u_6, u_{11}, v_{12}\})$
$R_{137} = R(v_2, v_8)$	$V(\text{MOG}(7) - \{u_6, v_5, v_{12}\})$
$R_{138} = R(v_2, v_9)$	$V(\text{MOG}(7) - \{u_3\})$
$R_{139} = R(v_2, v_{10})$	$V(\text{MOG}(7) - \{u_3, v_6, v_{13}\})$
$R_{140} = R(v_2, v_{11})$	$V(\text{MOG}(7) - \{u_7\})$
$R_{141} = R(v_2, v_{12})$	$V(\text{MOG}(7) - \{u_7, v_{14}\})$
$R_{142} = R(v_2, v_{13})$	$V(\text{MOG}(7) - \{u_4, v_7, v_8\})$
$R_{143} = R(v_2, v_{14})$	$V(\text{MOG}(7) - \{u_4, v_1, v_7, v_8\})$
$R_{144} = R(v_3, v_5)$	$V(\text{MOG}(7) - \{u_6, v_4, v_{11}, v_{12}\})$
$R_{145} = R(v_3, v_6)$	$V(\text{MOG}(7) - \{u_6, v_{11}, v_{12}\})$
$R_{146} = R(v_3, v_7)$	$V(\text{MOG}(7) - \{u_3, v_5\})$
$R_{147} = R(v_3, v_8)$	$V(\text{MOG}(7) - \{u_3\})$
$R_{148} = R(v_3, v_9)$	$V(\text{MOG}(7) - \{u_7, v_6, v_{13}\})$
$R_{149} = R(v_3, v_{10})$	$V(\text{MOG}(7) - \{u_7\})$
$R_{150} = R(v_3, v_{11})$	$V(\text{MOG}(7) - \{u_4, v_7, v_{14}\})$
$R_{151} = R(v_3, v_{12})$	$V(\text{MOG}(7) - \{u_4, v_7, v_8\})$
$R_{152} = R(v_3, v_{13})$	$V(\text{MOG}(7) - \{u_1, v_1\})$
$R_{153} = R(v_3, v_{14})$	$V(\text{MOG}(7) - \{u_1\})$
$R_{154} = R(v_4, v_5)$	$V(\text{MOG}(7) - \{u_6, v_{11}, v_{12}\})$
$R_{155} = R(v_4, v_6)$	$V(\text{MOG}(7) - \{u_6, v_5, v_{11}, v_{12}\})$
$R_{156} = R(v_4, v_7)$	$V(\text{MOG}(7) - \{u_3\})$
$R_{157} = R(v_4, v_8)$	$V(\text{MOG}(7) - \{u_3, v_6\})$
$R_{158} = R(v_4, v_9)$	$V(\text{MOG}(7) - \{u_7, v_{13}, v_{14}\})$
$R_{159} = R(v_4, v_{10})$	$V(\text{MOG}(7) - \{u_7, v_7, v_{14}\})$
$R_{160} = R(v_4, v_{11})$	$V(\text{MOG}(7) - \{u_4\})$
$R_{161} = R(v_4, v_{12})$	$V(\text{MOG}(7) - \{u_4, v_1, v_8\})$
$R_{162} = R(v_4, v_{13})$	$V(\text{MOG}(7) - \{u_1\})$
$R_{163} = R(v_4, v_{14})$	$V(\text{MOG}(7) - \{u_1, v_2\})$
$R_{164} = R(v_5, v_7)$	$V(\text{MOG}(7) - \{u_7, v_6\})$
$R_{165} = R(v_5, v_8)$	$V(\text{MOG}(7) - \{u_7, u_{12}, v_{14}\})$
$R_{166} = R(v_5, v_9)$	$V(\text{MOG}(7) - \{u_4, v_7\})$
$R_{167} = R(v_5, v_{10})$	$V(\text{MOG}(7) - \{u_4\})$
$R_{168} = R(v_5, v_{11})$	$V(\text{MOG}(7) - \{u_1, v_1, v_8\})$
$R_{169} = R(v_5, v_{12})$	$V(\text{MOG}(7) - \{u_1\})$
$R_{170} = R(v_5, v_{13})$	$V(\text{MOG}(7) - \{u_5, v_2, v_9\})$
$R_{171} = R(v_5, v_{14})$	$V(\text{MOG}(7) - \{u_5, v_9, v_{10}\})$
$R_{172} = R(v_6, v_7)$	$V(\text{MOG}(7) - \{u_7, v_{13}, v_{14}\})$
$R_{173} = R(v_6, v_8)$	$V(\text{MOG}(7) - \{u_7, v_7, v_{13}, v_{14}\})$
$R_{174} = R(v_6, v_9)$	$V(\text{MOG}(7) - \{u_4\})$
$R_{175} = R(v_6, v_{10})$	$V(\text{MOG}(7) - \{u_4, v_8\})$
$R_{176} = R(v_6, v_{11})$	$V(\text{MOG}(7) - \{u_1, v_1, v_2\})$
$R_{177} = R(v_6, v_{12})$	$V(\text{MOG}(7) - \{u_1, v_2, v_9\})$
$R_{178} = R(v_6, v_{13})$	$V(\text{MOG}(7) - \{u_5\})$
$R_{179} = R(v_6, v_{14})$	$V(\text{MOG}(7) - \{u_5, v_3, v_{10}\})$
$R_{180} = R(v_7, v_9)$	$V(\text{MOG}(7) - \{u_1, v_1, v_2, v_8\})$

TABLE 6: Continued.

Resolving sets ( $n = 7$ )	Elements
$R_{181} = R(v_7, v_{10})$	$V(\text{MOG}(7) - \{u_1, v_1, v_2\})$
$R_{182} = R(v_7, v_{11})$	$V(\text{MOG}(7) - \{u_5, v_9\})$
$R_{183} = R(v_7, v_{12})$	$V(\text{MOG}(7) - \{u_5\})$
$R_{184} = R(v_7, v_{13})$	$V(\text{MOG}(7) - \{u_3, v_3, v_{10}\})$
$R_{185} = R(v_7, v_{14})$	$V(\text{MOG}(7) - \{u_2\})$
$R_{186} = R(v_8, v_9)$	$V(\text{MOG}(7) - \{u_1, v_1, v_2\})$
$R_{187} = R(v_8, v_{10})$	$V(\text{MOG}(7) - \{u_1, v_1, v_2, v_9\})$
$R_{188} = R(v_8, v_{11})$	$V(\text{MOG}(7) - \{u_5\})$
$R_{189} = R(v_8, v_{12})$	$V(\text{MOG}(7) - \{u_5, v_{10}\})$
$R_{190} = R(v_8, v_{13})$	$V(\text{MOG}(7) - \{u_2, v_3, v_4\})$
$R_{191} = R(v_8, v_{14})$	$V(\text{MOG}(7) - \{u_2, v_4, v_{11}\})$
$R_{192} = R(v_9, v_{11})$	$V(\text{MOG}(7) - \{u_2, v_3, v_4, v_{10}\})$
$R_{193} = R(v_9, v_{12})$	$V(\text{MOG}(7) - \{u_2, v_3, v_4\})$
$R_{194} = R(v_9, v_{13})$	$V(\text{MOG}(7) - \{u_6, v_{11}\})$
$R_{195} = R(v_9, v_{14})$	$V(\text{MOG}(7) - \{u_6\})$
$R_{196} = R(v_{10}, v_{11})$	$V(\text{MOG}(7) - \{u_2, v_3, v_4\})$
$R_{197} = R(v_{10}, v_{12})$	$V(\text{MOG}(7) - \{u_2, v_3, v_4, v_{11}\})$
$R_{198} = R(v_{10}, v_{13})$	$V(\text{MOG}(7) - \{u_6\})$
$R_{199} = R(v_{10}, v_{14})$	$V(\text{MOG}(7) - \{u_6, v_{12}\})$
$R_{200} = R(v_{11}, v_{13})$	$V(\text{MOG}(7) - \{u_3, v_5, v_6, v_{12}\})$
$R_{201} = R(v_{11}, v_{14})$	$V(\text{MOG}(7) - \{u_3, v_5, v_6\})$
$R_{202} = R(v_{12}, v_{13})$	$V(\text{MOG}(7) - \{u_3, v_5, v_6\})$
$R_{203} = R(v_{12}, v_{14})$	$V(\text{MOG}(7) - \{u_3, v_5, v_6, v_{13}\})$

TABLE 7: FMD of metal organic graphs.

MOG( $n$ ) and $n \equiv 1 \pmod{2}$	Upper bounds of FMD
MOG(3)	3/2
MOG(5)	5/4
MOG(7)	7/4
MOG( $n$ ) if $n \geq 9$	$n/4$

## 5. Conclusion

In this section, we conclude the obtained results as follows:

- (i) The FMD of MOG( $n$ ) for  $n \equiv 1 \pmod{2}$  is obtained as given in Table 7.
- (ii) We note that as we increase  $n$  in MOG( $n$ ) for  $n \equiv 1 \pmod{2}$ , the FMD also increases.
- (iii) This is one of the important graphs that has same FMD and LFMD having unique resolving and local resolving neighbourhood sets.
- (iv) The problem is still open to characterize the graphs with same FMD and LFMD.

## Data Availability

The data used to support the finding of this study are included within the article. Additional data can be obtained from the corresponding author upon request.

## Disclosure

There is no funding source.

## Conflicts of Interest

The authors declare that there are no conflicts of interest.

## References

- [1] F. Harary and R. A. Melter, "The metric dimension of a graph," *Ars Combinatorica*, vol. 2, pp. 191–195, 1976.
- [2] G. Chartrand, L. Eroh, M. A. Johnson, and O. R. Oellermann, "Resolvability in graphs and the metric dimension of a graph," *Discrete Applied Mathematics*, vol. 105, no. 1–3, pp. 99–113, 2000.
- [3] J. Currie and O. R. Oellermann, "The metric dimension and metric independence of a graph," *Journal of Combinatorial Mathematics and Combinatorial Computing*, vol. 39, pp. 157–167, 2001.
- [4] Z. Beerliova, F. Eberhard, T. Erlebach et al., "Network discovery and verification," *IEEE Journal on Selected Areas in Communications*, vol. 24, no. 12, pp. 2168–2181, 2006.
- [5] S. Khuller, B. Raghavachari, and A. Rosenfeld, Localization in graphs, CCR-93-07462 DACA76-92-C-0009, 1994.
- [6] Y.-M. Chu, M. F. Nadeem, M. Azeem, and M. K. Siddiqui, "On sharp bounds on partition dimension of convex polytopes," *IEEE Access*, vol. 8, pp. 224781–224790, 2020.
- [7] J. Liu and M. F. Nadeem, "Bounds on the partition dimension of convex polytopes," *Combinatorial Chemistry and High Throughput Screening*, vol. 23, 2020.
- [8] M. F. Nadeem, M. Azeem, and A. Khalil, "The locating number of hexagonal Möbius ladder network," *Journal of Applied Mathematics and Computing*, 2020.
- [9] Z. S. Mufti, M. F. Nadeem, A. Ahmad, and Z. Ahmad, "Computation of edge metric dimension of barycentric subdivision of cayley graphs," *Italian Journal of Pure and Applied Mathematics*, vol. 44, pp. 714–722, 2020.
- [10] M. Fehr, S. Gosselin, and O. R. Oellermann, "The metric dimension of Cayley digraphs," *Discrete Mathematics*, vol. 306, no. 1, pp. 31–41, 2006.
- [11] S. Arumugam and V. Mathew, "The fractional metric dimension of graphs," *Discrete Mathematics*, vol. 312, no. 9, pp. 1584–1590, 2012.
- [12] M. Raza, M. Javaid, and N. Saleem, Fractional metric dimension of metal organic frameworks, main group metal chemistry in press, 2021.
- [13] S. Arumugam and V. Mathew, "The fractional metric dimension of graphs," *Discrete Mathematics*, vol. 5, pp. 1–8, 2013.
- [14] M. Feng and K. Wang, "On the metric dimension and fractional metric dimension for hierarchical product of graphs," *Applicable Analysis and Discrete Mathematics*, vol. 7, no. 2, pp. 302–313, 2013.
- [15] M. Feng and Q. Kong, "On the fractional metric dimension of corona product graphs and lexicographic product graphs," *Ars Combinatorica*, vol. 138, pp. 249–260, 2018.
- [16] S. W. Saputro, A. S. Fenovcikova, M. Baca, and M. Lascsakova, "On fractional metric dimension of comb product graphs," *Statistics, Optimization and Information Computing*, vol. 6, pp. 150–158, 2018.
- [17] E. Yi, "The fractional metric dimension of permutation graphs," *Acta Mathematica Sinica, English Series*, vol. 31, no. 3, pp. 367–382, 2015.
- [18] J. Liu, A. Kashif, T. Rashid, and M. Javaid, "Fractional metric dimension of generalized Jahangir graph," *Mathematics*, vol. 7, pp. 1–10, 2019.
- [19] S. Aisyah, U. M. Imam, and L. Susilowati, "Local fractional metric dimension of cornea product of graphs," *IOP Conference Series: Earth and Environmental Science*, vol. 243, 2019.
- [20] J.-B. Liu, M. K. Aslam, and M. Javaid, "Local fractional metric dimensions of rotationally symmetric and planar networks," *IEEE Access*, vol. 8, pp. 82404–82420, 2020.
- [21] M. Javaid, M. Raza, P. Kumam, and J.-B. Liu, "Sharp bounds of local fractional metric dimensions of connected networks," *IEEE Access*, vol. 8, pp. 172329–172342, 2020.
- [22] J. Liu, J. Y. Ruseow, W. Scotskinner, and Z. U. Wang, "Metal organic frameworks: structures and functional applications," *Materials Today*, vol. 27, pp. 43–68, 2019.
- [23] C. Pettinari, F. Marchetti, N. Mosca, G. Tosi, and A. Drozdov, "Application of metal – organic frameworks," *Polymer International*, vol. 66, no. 6, pp. 731–744, 2017.
- [24] J. Liu, L. Chen, H. Cui, J. Zhang, L. Zhang, and C.-Y. Su, "Applications of metal-organic frameworks in heterogeneous supramolecular catalysis," *Chemical Society Reviews*, vol. 43, no. 16, pp. 6011–6061, 2014.
- [25] Z. Hasan and S. H. Jhung, "Removal of hazardous organics from water using metal-organic frameworks (MOFs): plausible mechanisms for selective adsorptions," *Journal of Hazardous Materials*, vol. 283, pp. 329–339, 2015.

## Research Article

# An Approach to the Extremal Inverse Degree Index for Families of Graphs with Transformation Effect

Muhammad Asif <sup>1</sup>, Muhammad Hussain <sup>1</sup>, Hamad Almohamedh <sup>2</sup>,  
Khalid M. Alhamed <sup>3</sup> and Sultan Almotairi <sup>4</sup>

<sup>1</sup>Department of Mathematics, COMSATS University Islamabad, Lahore Campus, Lahore 54000, Pakistan

<sup>2</sup>Faculty of King Abdulaziz City for Science and Technology (KACST) Riyadh, Riyadh, Saudi Arabia

<sup>3</sup>IT Programs Center, Faculty of IT Department, Institute of Public Administration, Riyadh 11141, Saudi Arabia

<sup>4</sup>Department of Natural and Applied Sciences, Faculty of Community College, Majmaah University, Majmaah 11952, Saudi Arabia

Correspondence should be addressed to Hamad Almohamedh; [halmohamedh@kacst.edu.sa](mailto:halmohamedh@kacst.edu.sa) and Sultan Almotairi; [almotairi@mu.edu.sa](mailto:almotairi@mu.edu.sa)

Received 11 December 2020; Revised 10 January 2021; Accepted 17 February 2021; Published 28 February 2021

Academic Editor: Teodorico C. Ramalho

Copyright © 2021 Muhammad Asif et al. This is an open access article distributed under the Creative Commons Attribution License, which permits unrestricted use, distribution, and reproduction in any medium, provided the original work is properly cited.

The inverse degree index is a topological index first appeared as a conjuncture made by computer program Graffiti in 1988. In this work, we use transformations over graphs and characterize the inverse degree index for these transformed families of graphs. We established bonds for different families of  $n$ -vertex connected graph with pendent paths of fixed length attached with fully connected vertices under the effect of transformations applied on these paths. Moreover, we computed exact values of the inverse degree index for regular graph specifically unicyclic graph.

## 1. Introduction and Preliminary Results

Graph theory has many applications in chemistry, physics, computer sciences, and other applied sciences. Topological indices are graph invariants used to study the topology of graphs. Along with the computer networks, graph theory considers as a powerful tool in other areas of research, such as in coding theory, database management system, circuit design, secret sharing schemes, and theoretical chemistry [1]. Cheminformatics is the combination of technology, graph theory, and chemistry. It develops a relationship between structure of organic substances and their physicochemical properties through some useful graph invariants with the help of their associated molecular graph. The molecular graph is the combination of vertices and edges which are representatives of atoms and bonds between atoms of corresponding substance, respectively. Theoretical study of underlying chemical structure by some useful graph invariants is an attractive area of research in mathematical

chemistry due to its effective applications in the QSAR/QSPR investigation [2, 3]. Topological indices among these invariants have special place and used to estimate the physicochemical properties of chemical compound. A topological index can be considered as a function which maps a graph to a real number.

Throughout this work, we used standard notations,  $G = G(V, E)$  for graph,  $V(G)$  set of vertices,  $E(G)$  the set of edges,  $d_v$  degree of vertex  $v_i$  (the number of edges incident to  $v_i$ ),  $\Delta$  and  $\delta$  be the maximum and minimum degrees of fully connected vertices, vertices with degree one are pendent vertices, and path attached with fully connected vertices taken as a pendent paths.

In the last five decades, after the Wiener index, many topological indices had been introduced. Probably, the Randić connectivity index [4]

$$R(G) = \sum_{uv \in E(G)} \frac{1}{\sqrt{d_u d_v}}, \quad (1)$$



is one of the best predictive invariants among these topological indices. The accuracy in predictability of indices is the main interest of researchers which leads them to propose a new topological index.

The zeroth-order general Randić index  ${}^0R_\alpha(G) = \sum_{u \in V(G)} d_u^\alpha$  was conceived by Li and Zheng in their work [5].  ${}^0R_{1/2}(G) = \sum_{u \in V(G)} 1/\sqrt{d_u}$  equivalent to  ${}^0R_\alpha(G)$  for  $\alpha = -1/2$ . Hu et al. in [6] and others [7–10] characterize  ${}^0R_\alpha$  for different values of  $\alpha$ . For  $\alpha = -1$ ,  ${}^0R_{-1} = \text{ID}$  is modified total adjacency index or inverse degree, first appears in the conjecture over computer program Graffiti [11]. The

$$\text{ID}(G) = \sum_{v \in V(G)} \frac{1}{d_v} = \sum_{uv \in E(G)} \frac{d_u + d_v}{d_u^2 d_v^2}, \quad (2)$$

for graphs without isolated vertices are well discussed in [12, 13]. Extremal characterization and bounds of  $\text{ID}(G)$  also discussed at some extent in [14–18]. For more detail, one can review survey [19].

In this work, we investigated the effect of transformations over families of graphs for ID and established inequalities for these transformed graphs. Graph transformations are very important in chemistry, computer designing, and animations. Moreover, we determined the exact value of ID for some major families of graphs under the effect of transformations over pendent paths.

## 2. Results and Discussion

In this section, we present some transformations over pendent paths. These have solid effect over increase and decrease of  $\text{ID}(G)$ . Through out this work, we considered

$n_0$ -vertex connected graph  $G_0$ .  $G_k^l$  be the graph  $G_0$  with  $k$  pendent paths of length  $l \geq 1$  having order  $n = n_0 + kl$  with degree sequence  $d_1 = \delta \leq d_2 \leq d_3 \leq \dots \leq \Delta + 1$ .

**2.1. Graph Transformations.** Let  $E'(G) \subset E(G)$ , the  $G_1 = G - E'(G)$  be subgraph obtained by removing edges of  $E'(G)$ , and  $G'_1 = G - V'(G)$  be the subgraph obtained by deleting vertices set  $V'(G) \subset V(G)$  along with their incident edges. We give following transformations using these techniques which have solid effect on  $\text{ID}(G)$ .

**2.1.1. Transformation A.** Let  $w_j \in V(G_0)$ ,  $d_{w_j} \geq 3$ ,  $j = 1, 2, 3, \dots, k \leq n$  and  $\{w_j u_j^1, u_j^1 u_j^2, u_j^2 u_j^3, \dots, u_j^{l-1} u_j^l\}$  be the pendent paths attached with fully connected vertex  $w_j$  of  $G_0$  forms  $G_k^l$ . Then,

$$A(G_k^l) = G_1 = G_0 - \sum_{j=1}^k \{u_j^2 u_j^3, u_j^3 u_j^4, \dots, u_j^{l-1} u_j^l\} + \sum_{j=1}^k \{w_j u_j^2, u_j^2 u_j^3, \dots, u_j^{l-1} u_j^l\}. \quad (3)$$

Figure 1 depicts successive application of transformation A as  $A_i$ ,  $i = 1, 2, 3, \dots, l-1$ .

**2.1.2. Transformation B.** Let  $w_j \in V(G_0)$ ,  $d_{w_j} \geq 3$ ,  $j = 1, 2, 3, \dots, k \leq n$  and  $\{w_j u_j^1, w_j u_j^2, w_j u_j^3, \dots, w_j u_j^{l-1}\}$  be the leaves attached with fully connected vertex  $w_j$  of  $G$ . Then, for fixed vertex  $w_1$ ,

$$G'_j = G - \{u_j^1, u_j^2, u_j^3, \dots, u_j^{l-1}\} \cup \{u_j^{l-(q-1)}, u_j^{l-(q-2)}, u_j^{l-(q-2)}, u_j^{l-(q-3)}, \dots, u_j^{l-1} u_j^l\} + \{w_1 u_j^1, w_1 u_j^2, w_1 u_j^3, \dots, w_1 u_j^{l-1}\} \cup \{w_1 u_j^{l-(q-1)}, u_j^{l-(q-1)}, u_j^{l-(q-2)}, u_j^{l-(q-2)}, u_j^{l-(q-3)}, \dots, u_j^{l-1} u_j^l\}. \quad (4)$$

**Theorem 1.** Let  $G_0$  be the graph of order  $n_1$  with maximum degrees  $\Delta$  and minimum  $\delta$ . Then,

$$\begin{aligned} \text{ID}(G_k^l) &\leq \text{ID}(A(G_k^l)), \\ \text{ID}(G_k^l) &\leq \text{ID}(B(G_k^l)). \end{aligned} \quad (5)$$

*Proof.* Let  $G_k^l$  be the graph of order  $n = n_1 + kl$ , minimum degree  $\delta$ , and maximum degree  $\Delta + 1$ .  $G_k^l$  is the composition of  $G_0$  and  $k$  pendent paths of length  $l$ . In  $G_k^l$ , there are at least  $k$  vertices of degree 1 and  $k(l-1)$  having 2 and  $n_1$  vertices with degree  $d_{v_s} + 1, \delta \leq d_{v_s} + 1 \leq \Delta + 1$ :

$$\text{ID}(G_k^l) = \sum_{s=1}^{n-k(l+1)} \frac{1}{d_{v_s}} + \sum_{s=1}^k \frac{1}{d_{v_s} + 1} + k + \frac{k(l-1)}{2}. \quad (6)$$

The transformation A transforms  $k$  vertices from degree 2 to 1 and another  $k$  vertices from  $d_s + 1$  to  $d_s + 2$  which have an effect in ID as

$$\text{ID}(A(G_k^l)) = \sum_{s=1}^{n-k(l+1)} \frac{1}{d_{v_s}} + \sum_{s=1}^k \frac{1}{d_{v_s} + 2} + 2k + \frac{k(l-2)}{2}. \quad (7)$$

So, from equations (6) and (7), we have

$$\begin{aligned} \text{ID}(G_k^l) - \text{ID}(A(G_k^l)) &= \sum_{s=1}^k \left( \frac{1}{d_{v_s} + 1} - \frac{1}{d_{v_s} + 2} \right) - k + \frac{k}{2} \\ &= \sum_{s=1}^k \frac{1}{(d_{v_s} + 1)(d_{v_s} + 2)} - \frac{k}{2}. \end{aligned} \quad (8)$$

Replace  $d_{v_s}$  with minimum degree  $\delta$ . It maximizes the term  $\sum_{s=1}^k 1/((d_{v_s} + 1)(d_{v_s} + 2))$ , which implies

$$\begin{aligned} &= \sum_{s=1}^k \frac{1}{(\delta + 1)(\delta + 2)} - \frac{k}{2} = \frac{k}{(\delta + 1)(\delta + 2)} - \frac{k}{2} \\ &= \frac{k(2 - (\delta + 1)(\delta + 2))}{(\delta + 1)(\delta + 2)} = \frac{k(-\delta^2 - 3\delta)}{(\delta + 1)(\delta + 2)}. \end{aligned} \quad (9)$$

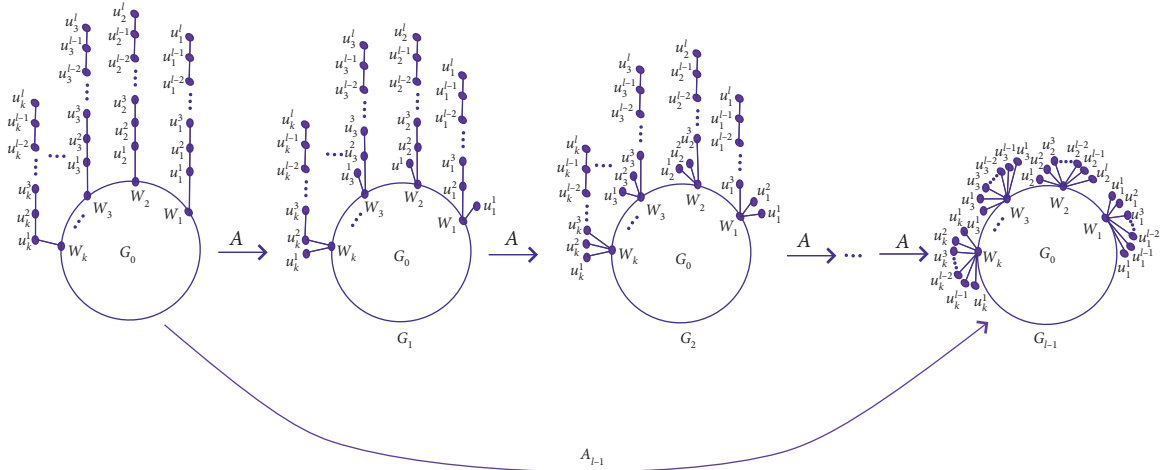


FIGURE 1: Transformation A.

It is clear from (9) that  $ID(G_k^l) - ID(A(G_k^l)) \leq 0$ . Hence,

$$ID(G_k^l) \leq ID(A(G_k^l)). \quad (10)$$

The transformation B shown in Figure 2 decreases the degree of one vertex and makes the same increase into the degree of fixed selected vertex:

$$ID(B(G_k^l)) = \sum_{s=1}^{n-k(l+1)} \frac{1}{d_{v_s}} + \sum_{s=1}^{k-2} \frac{1}{d_{v_s} + 1} + \frac{1}{d_{v_k}} + \frac{1}{d_{v_{(k-1)}} + 2} + \frac{k(l-2)}{2} + k. \quad (11)$$

So, from equations (6) and (11), we get

$$ID(G_k^l) - ID(B(G_k^l)) = \sum_{s=1}^k \frac{1}{d_{v_s} + 1} - \sum_{s=1}^{k-2} \frac{1}{d_{v_s} + 1} - \frac{1}{d_{v_k}} - \frac{1}{d_{v_{(k-1)}} + 2}, \quad (12)$$

to maximize the fraction involved in above expression replace  $d_{v_s}$ ,  $0 \leq s \leq k$  with  $\delta$ , and we get

$$ID(G_k^l) - ID(B(G_k^l)) = \frac{2}{\delta + 1} - \frac{1}{\delta} - \frac{1}{\delta + 2} = \frac{-2\delta - 2\delta^2 - 2}{(\delta)(\delta + 1)(\delta + 2)} \leq 0. \quad (13)$$

The equation (13) implies

$$ID(G_k^l) \leq ID(B(G_k^l)). \quad (14) \quad \square$$

2.1.3. Transformation  $A_i^j$ . The transformation  $A_i^j$  is composition of  $A_i$ ,  $0 \leq i \leq l-1$  and  $B_j$ ,  $0 \leq j \leq k-1$  which is

shown in Figure 3. Here,  $A_i$ ,  $0 \leq i \leq l-1$  be the repetition of transformation A and  $B_j$ ,  $0 \leq j \leq k-1$  be the repetition of transformation B.

For main results related to the transformation  $A_i^j$  shown in Figure 3, we need to prove Propositions 1 and 2.

**Proposition 1.** Let  $g: N \times W \rightarrow Q$  defined as  $g(\eta, \zeta) = 1/(\eta + \zeta)$ . Then,

- (1)  $g(\eta, \zeta) + 1 \geq g(\eta, \zeta - 1) + (1/2)$  for  $\zeta \geq 1$
- (2) For  $\alpha, \beta \geq 0$ ,  $g[\eta, (\alpha + 1)(\beta + 1)] + g(\eta, 0) \geq [g[\eta, \alpha(\beta + 1)] + g(\eta, \beta + 1)]$

*Proof.* (1) If transformation A applied on pendent path attached with vertex  $w_j$  of G having degree  $\eta + \zeta$ . The degree of vertex  $w_j$  increased by one with change of vertex having degree 2 to leaf attached to  $w_j$ . This change has effect on ID in the following way.

Let  $g(\eta, \zeta) = 1/(\eta + \zeta)$ . Then,

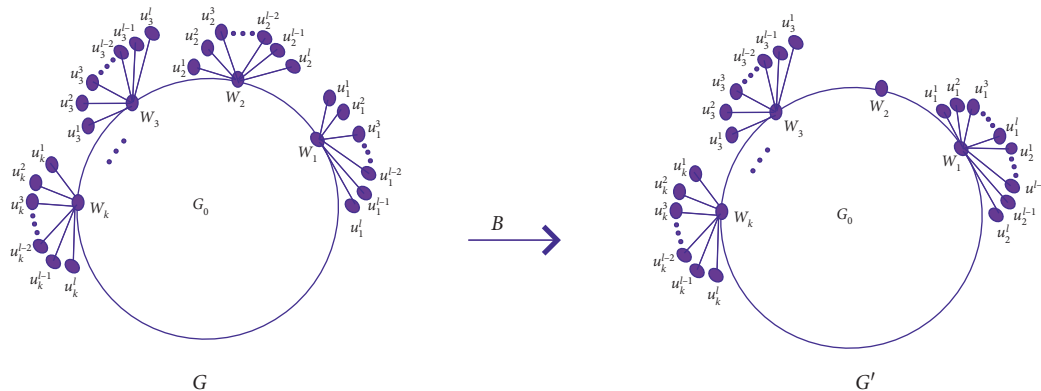
$$g(\eta, \zeta) + 1 - \left[ g(\eta, \zeta - 1) + \frac{1}{2} \right] = \frac{1}{\eta + \zeta} + 1 - \frac{1}{\eta + \zeta - 1} - \frac{1}{2} = \frac{1}{2} - \frac{1}{(\eta + \zeta)(\eta + \zeta - 1)}. \quad (15)$$

It is clear from basic calculus that  $(1/\alpha) \geq (1/(\alpha + \beta))$ ;  $\beta \geq 0$ . So,

$$= \frac{1}{2} - \frac{1}{(\eta + \zeta)(\eta + \zeta - 1)} \geq 0, \quad (16)$$

implies  $g(\eta, \zeta) + \zeta \geq g(\eta, \zeta - 1)$ .

(2) The 2nd part of this proposition is related to the effect of transformation  $A_i^j$  shown in Figure 3:

FIGURE 2: Transformation  $B$  for  $q = 1$ .

$$\begin{aligned}
 & g[\eta, (\alpha + 1)(\beta + 1)] + g(\eta, 0) - g[\eta, \alpha(\beta + 1)] + g(\eta, \beta + 1) \\
 &= \frac{1}{(\alpha + 1)\beta + \eta} + \frac{1}{\eta} - \frac{1}{\alpha * \beta + \eta} - \frac{1}{\beta + \eta + 1} \\
 &= \frac{\alpha^2 \beta^3 + 3\alpha^2 \beta^2 + 3\alpha^2 \beta + \alpha^2 + \alpha \beta^3 + 2\alpha \beta^2 \eta + 3\alpha \beta^2 + 4\alpha \beta \eta + 3\alpha \beta + 2\alpha \eta + \alpha}{\eta(\beta + \eta + 1)(\alpha(\beta + 1) + \eta)(\eta + \beta + 1)} \geq 0.
 \end{aligned} \tag{17}$$

Thus,  $g[\eta, (\alpha + 1)(\beta + 1)] + g(\eta, 0) \geq g[\eta, \alpha(\beta + 1)] + g(\eta, \beta + 1)$ .  $\square$

**Proposition 2.** Let  $f(\eta) = (1/\eta) + (3/2)$  and  $g(\eta) = (1/(\eta + 1)) + 2$ , then for  $\eta \geq 1$ ,  $g(\eta) \geq f(\eta)$ .

*Proof*

$$\begin{aligned}
 g(\eta) - f(\eta) &= \frac{1}{\eta + 1} + 2 - \left( \frac{1}{\eta} + \frac{3}{2} \right) = \frac{1}{\eta + 1} - \frac{1}{\eta} + \frac{1}{2} \\
 &= \frac{2\eta - 2(\eta + 1) + \eta(\eta + 1)}{2\eta(\eta + 1)} \\
 &= \frac{(\eta - 1) + (\eta^2 - 1)}{2\eta(\eta + 1)} \geq 0.
 \end{aligned} \tag{18}$$

This fraction is nonnegative for all  $\eta \geq 1$  which implies that  $g(\eta) \geq f(\eta)$ .  $\square$

**Theorem 2.** Let  $G$  be the graph of order  $n$  having  $p$  pendent vertices.  $G_k^l$  is the graph having  $k$  pendent paths attached to the fully connected vertices with maximum degree of a vertex  $\Delta + 1$ . Then, for  $0 \leq i \leq l - 1$  and  $\alpha \leq \beta$ ,

$$\text{ID}(A_i^\alpha(G_k^l)) \leq \text{ID}(A_i^\beta(G_k^l)). \tag{19}$$

*Proof.* Let  $G_k^l$  be the graph with order  $n = n + kl$ , minimum degree  $\delta$ , and maximum degree  $\Delta + 1$ . Using the fact of  $A_i^j$  over  $G_k^l$ , we get

$$\begin{aligned}
 \text{ID}(A_i^j(G_k^l)) &= k(i + 1) + \frac{k[l - (i + 1)]}{2} + \sum_{r=1}^{k-(j+1)} \frac{1}{d_{v_r} + (i + 1)} \\
 &+ \sum_{s=1}^{n-p-k+j} \frac{1}{d_{v_s}} + \frac{1}{d_{v_r} + (j + 1)(i + 1)} + p,
 \end{aligned} \tag{20}$$

for  $1 \leq d_r, d_s \leq \Delta \leq n - 1$  and  $0 \leq i \leq l - 1, 0 \leq j \leq k - 1$ . Then, for  $\alpha \leq \beta$ ,

$$\begin{aligned}
 & \text{ID}(A_i^\alpha(G_k^l)) - \text{ID}(A_i^\beta(G_k^l)) \\
 &= \sum_{r=1}^{k-(\alpha+1)} \frac{1}{d_{v_r} + i + 1} + \sum_{s=1}^{n-p-k+\alpha} \frac{1}{d_{v_s}} + \frac{1}{d_{v_r} + (\alpha + 1)(i + 1)} \\
 &- \left[ \sum_{r=1}^{k-(\beta+1)} \frac{1}{d_{v_r} + i + 1} + \sum_{s=1}^{n-p-k+\beta} \frac{1}{d_{v_s}} + \frac{1}{d_{v_r} + (\beta + 1)(i + 1)} \right] \\
 &= \sum_{r=k-\beta}^{k-\alpha-1} \frac{1}{d_{v_r} + i + 1} - \sum_{s=n-p-k+\alpha+1}^{n-p-k+\beta} \frac{1}{d_{v_s}} \\
 &+ \frac{(i + 1)(\beta - \alpha)}{(d_{v_r} + (i + 1)(\alpha + 1))(d_{v_r} + (i + 1)(\beta + 1))}.
 \end{aligned} \tag{21}$$

So, by using Proposition 1 and replacing  $\Delta$  with  $d_{v_r}$  and  $\delta$  with  $d_{v_s}$ , it is clear that  $\Delta$  minimizes the positive terms and  $\delta$  maximizes the negative term. After simplification, we get

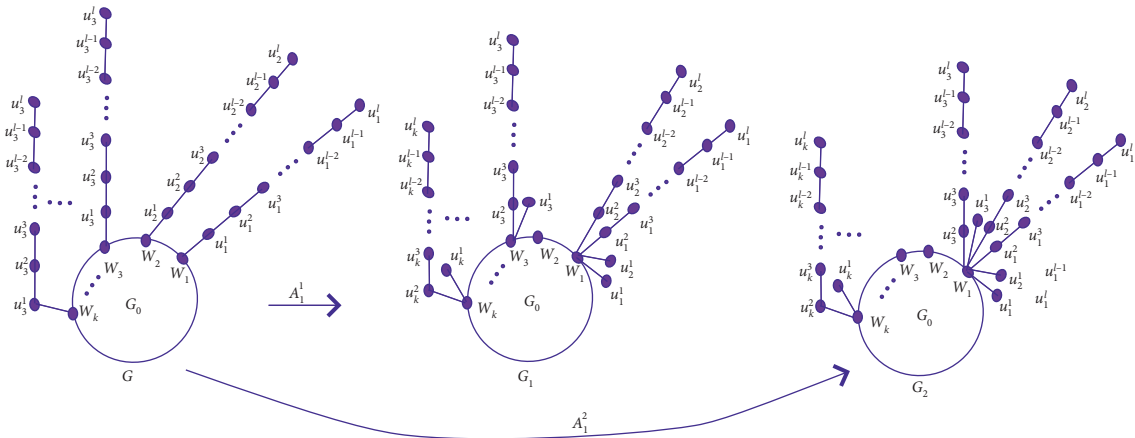


FIGURE 3: Transformation  $A_i^j$ .

$$= \frac{(\beta - \alpha)(\delta - \Delta)(\Delta + (i + 1)(\beta + 1))(\Delta + (i + 1)(\alpha + 1)) + (\delta - \Delta)(\Delta + i + 1)(i + 1) - (i + 1)^2(\alpha\Delta + (\Delta + (i + 1)(\alpha + 1))(\beta + 1))}{(\Delta + l(\alpha + 1))(\Delta + l(\beta + 1))\delta(\Delta + 1)} \quad (22)$$

It is clear that for  $\alpha \leq \beta$ , the nominator is a negative number and denominator is positive which implies that

$$ID(A_i^\alpha(G_k^l)) - ID(A_i^\beta(G_k^l)) \leq 0. \quad (23)$$

Thus, for  $\beta \geq \alpha$ ,

$$ID(A_i^\alpha(G_k^l)) \leq ID(A_i^\beta(G_k^l)). \quad (24)$$

In the following theorem, we determined bonds of ID for graph  $G_k^l$  under the effect of transformation  $A_i^j$  by using Propositions 1 and 2.

**Theorem 3.** Let  $G$  be the graph of order  $n$  having  $p$  pendent vertices.  $G_k^l$  is the graph with maximum degree  $\Delta + 1$  having order  $n + kl$  with  $k \leq n - p$  of pendent paths of length  $l$ . Then, for  $ID(A_i^j(G_k^l))$ ;  $0 \leq i \leq l - 1$ ,  $0 \leq j \leq k - 1$ ,

$$\frac{(\Delta + 1)[\Delta(l + 1) + 2(p\Delta + n - p - 1)] + 2\Delta}{2\Delta(\Delta + 1)} \leq ID(A_i^j(G_k^l)). \quad (25)$$

Equality holds for  $r$ -regular graph with  $i = 0$ ,  $j = 0$ , and  $k = 1$ . And

$$ID(A_i^j(G_k^l)) \leq \frac{(\delta + (n - p)l)[\delta l(n - p) + n - 1 + p\delta] + \delta}{((n - p)l + \delta)\delta}, \quad (26)$$

equality holds if under consideration graph is  $r$ -regular with  $k = n - p$  pendent paths of length  $l$  and  $i = l - 1$ ,  $j = k - 1$ .

*Proof.* Let  $G$  be the graph having order  $n \geq 3$  with  $0 \leq p \leq n - 1$  pendent vertices with minimum degree  $\delta$  and maximum degree  $\Delta$ .  $G_k^l$  is the graph with maximum degree  $\Delta + 1$  and

maximum number of pendent paths  $k = n - p$  of length  $l$ . Then, by using equation (20),

$$ID(A_i^j(G_k^l)) = k(i + 1) + \frac{k[l - (i + 1)]}{2} + \sum_{r=1}^{k-(j+1)} \frac{1}{d_{v_r} + (i + 1)} + \sum_{s=1}^{n-p-k+j} \frac{1}{d_{v_s}} + \frac{1}{d_{v_r} + (j + 1)(i + 1)} + p, \quad (27)$$

where  $1 \leq d_r, d_s \leq \Delta \leq n - 1$ , and  $0 \leq i \leq l - 1$ ,  $0 \leq j \leq k - 1$ .

The order of  $G_k^l$  is fixed. So, the increase in pendent paths causes to decrease their lengths  $l$ . This fact increases the number of pendent paths and decreases the vertices of degree two. So, Proposition 2 clears that  $ID(A_i^j(G_k^l))$  increases with the increase in  $k$ . It is clear from Theorems 1 and 2 and Propositions 1 and 2 that the least value of  $ID(A_i^j(G_k^l))$  was obtained by setting  $i, j = 0$ ,  $d_r = d_s = \Delta$ , and  $k = 1$ :

$$ID(A_0^0(G_1^l)) \geq 1 + \frac{1[l - 1]}{2} + \frac{1 - 1}{\Delta + 1} + \frac{n - p - 1}{\Delta} + \frac{1}{\Delta + 1} + p. \quad (28)$$

After simplification, we get

$$\frac{(\Delta + 1)[\Delta(l + 1) + 2(p\Delta + n - p - 1)] + 2\Delta}{2\Delta(\Delta + 1)} \leq ID(A_i^j(G_k^l)), \quad (29)$$

and equality holds in (28) for  $r$ -regular graph with the  $k = 1$  pendent path of length  $l$  and  $i = 0$ ,  $j = 0$ .

Now again from (20), setting  $i = l - 1$ ,  $j = k - 1$ ,  $d_r = d_s = \delta$ ,  $k = n - p$  and using Proposition 1 and Theorems 1, 2, we get maximal value of  $ID(A_i^j(G_k^l))$  as

$$\begin{aligned} \text{ID}(A_{l-1}^{k-1}(G_k^l)) &\leq (n-p)(l-1+1) + \frac{(n-p)[l-(l-1+1)]}{2} + \sum_{s=1}^{n-(n-p)+(n-p)-1} \frac{1}{\delta} \\ &+ \sum_{r=1}^{(n-p)-((n-p)-1+1)} \frac{1}{\delta+(l-1+1)} + \frac{1}{[\delta+((n-p)-1+1)(l-1+1)]} + p. \end{aligned} \quad (30)$$

After simplification, we get maximal value of  $\text{ID}(A_i^j(G_k^l))$  as

$$\text{ID}(A_i^j(G_k^l)) \leq \frac{(\delta+(n-p)l)[\delta l(n-p)+n-1+p\delta]+\delta}{((n-p)l+\delta)\delta}, \quad (31)$$

in which equality holds for  $r$ -regular graph with  $k=n-p$  pendent paths of length  $l$  and  $i=l-1, j=k-1$ .

Inequalities (29) and (31) complete the proof.  $\square$

**Theorem 4.** Let  $G$  be the graph without pendent vertices and  $G_k^l$  for  $k > 1$  be the graph with maximum degree  $\Delta + 1$ . Then, for  $0 \leq i \leq l-1, 0 \leq j \leq k-1$ , the lower bond of  $\text{ID}(A_i^j(G_k^l))$  is

$$\text{ID}(A_i^j(G_k^l)) \geq \frac{(\Delta+1)[\Delta k(l+1)+2(n-k)]+2k\Delta}{2\Delta(\Delta+1)}. \quad (32)$$

Equality holds for  $r$ -regular graph with  $k$  pendent paths of length  $l$  and  $i=0, j=0$ .

*Proof.* Let  $G$  be the graph of order  $n$  without pendent vertices having minimum degree  $\delta$  and maximum degree  $\Delta$ .  $G_k^l$  be the graph with maximum degree  $\Delta + 1$  and  $k \geq 1$  be the count of pendent paths of length  $l$ . Then, by using (20),

$$\text{ID}(A_i^j(G_k^l)) = \frac{[\Delta+(i+1)j](\Delta+i+1)[2(n-k+j)+k(i+l+1)][2\Delta(\Delta+(i+1)j)](k-j)+\Delta(k-j-1)+\Delta(\Delta+l)}{2\Delta(\Delta+i+1)(\Delta+j(i+1))}. \quad (36)$$

*Proof.* Let  $G$  be the  $\Delta$ -regular graph and  $k$  be the count of pendent paths of length  $l$ . Then,  $G_k^l$  is the graph with maximum degree  $\Delta + 1$ . Then, for  $0 \leq i \leq l-1, 0 \leq j \leq k-1$ , equation (20) takes the form

$$\begin{aligned} \text{ID}(A_i^j(G_k^l)) &= k(i+1) + \frac{k[l-(i+1)]}{2} + \sum_{r=1}^{k-(j+1)} \frac{1}{\Delta+(i+1)} \\ &+ \sum_{s=1}^{n-k+j} \frac{1}{\Delta} + \frac{1}{[\Delta+(j+1)(i+1)]}. \end{aligned} \quad (37)$$

$$\text{ID}(A_i^j(G_k^l)) = \frac{[\Delta+(i+1)j](\Delta+i+1)[2(n-k+j)+k(i+l+1)][2\Delta(\Delta+(i+1)j)](k-j)+\Delta(k-j-1)+\Delta(\Delta+l)}{2\Delta(\Delta+i+1)(\Delta+j(i+1))}. \quad (38) \quad \square$$

$$\begin{aligned} \text{ID}(A_i^j(G_k^l)) &= k(i+1) + \frac{k[l-(i+1)]}{2} + \sum_{r=1}^{k-(j+1)} \frac{1}{d_{v_r}+(i+1)} \\ &+ \sum_{s=1}^{n-k+j} \frac{1}{d_{v_s}} + \frac{1}{d_{v_r}+(j+1)(i+1)}, \end{aligned} \quad (33)$$

where  $1 \leq d_r, d_s \leq \Delta \leq n-1$ , and  $0 \leq i \leq l-1, 0 \leq j \leq k-1$ . Using Propositions 1 and 2 and setting  $i, j=0, d_r=d_s=\Delta$ , we get least value of  $\text{ID}(A_i^j(G_k^l))$  as  $\text{ID}(A_0^0(G_k^l))$ :

$$\text{ID}(A_0^0(G_k^l)) = k + \frac{k[l-1]}{2} + \frac{k-1}{\Delta+1} + \frac{n-k}{\Delta} + \frac{1}{\Delta+1}. \quad (34)$$

After simplification, we get minimal value as

$$\frac{(\Delta+1)[\Delta k(l+1)+2(n-k)]+2k\Delta}{2\Delta(\Delta+1)} \leq \text{ID}(A_i^j(G_k^l)). \quad (35)$$

Equality for equation (3) holds for  $r$ -regular graph with  $k$  pendent paths of length  $l$  and  $i=0, j=0$ .  $\square$

**Theorem 5.** Let  $G$  be the  $\Delta$ -regular graph.  $\text{ID}(A_i^j(G_k^l))$  be the graph with  $k$  pendent paths of length  $l$ . Then, for  $0 \leq i \leq l-1, 0 \leq j \leq k-1$ :

After simplification, we get required result:

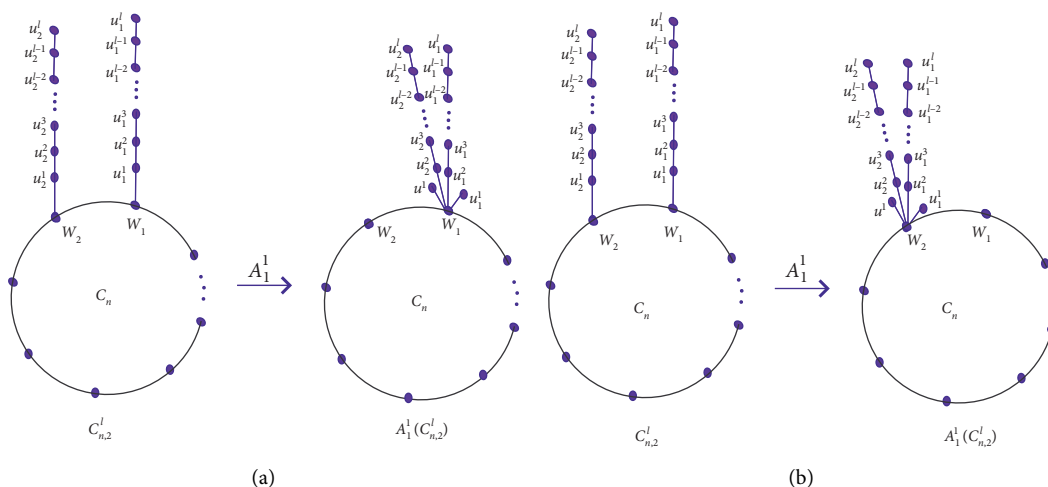


FIGURE 4: Transformation  $A_i^j$  effect over  $G_k^l = C_{n,2}^l$ : (a) transformed graph  $A_1^1(C_{n,2}^l)$  with fixed vertex  $w_1$ ; (b) transformed graph  $A_1^1(C_{n,2}^l)$  with fixed vertex  $w_2$ .

In Corollary 1, we determined exact values of ID for unicyclic graphs with  $k$  pendent paths of length  $l$  under transformation  $A_i^j$ . Figure 4(a) depicts transformed graph  $A_i^j(C_{n,k}^l)$  for  $i = j = 1$ ,  $k = 2$  with fixed vertex  $w_1$  and Figure 4(b) with fixed vertex  $w_2$ .

**Corollary 1.** Let  $C_n$  be the unicyclic graph of order  $n$ .  $C_{n,k}^l$  is the graph with  $k$  pendent paths of length  $l$ . Then, for  $0 \leq i \leq l - 1$ ,  $0 \leq j \leq k - 1$ ,

$$\text{ID}(A^j(G_k^l)) = \frac{(2 + (i + 1)j)(3 + i)[2(n - k + j) + k(i + l + 1)]4(2 + (i + 1)j)(k - j) + 2(k - j - 1) + 2(2 + l)}{4(3 + i)(2 + j(i + 1))}. \quad (39)$$

*Proof.*  $C_n$  is the unicyclic graph of order  $n$ .  $C_n$  is 2-regular graph. Then, we get required result by replacing  $\Delta$  by 2 in Theorem 5:

$$\text{ID}(A^j(G_k^l)) = \frac{(2 + (i + 1)j)(3 + i)[2(n - k + j) + k(i + l + 1)]4(2 + (i + 1)j)(k - j) + 2(k - j - 1) + 2(2 + l)}{4(3 + i)(2 + j(i + 1))}. \quad (40)$$

### 3. Conclusions

Topological indices and graph transformations play a significant role in modern chemistry and computer networks. It is an interesting problem to determine the bonds of the topological index for different families of graphs [5, 6, 9, 16]. In this work, we give graph transformations,  $A$ ,  $B$ , and  $A_i^j$  for variable values of  $i$  and  $j$  over pendent paths attached with the fully connected vertices of graphs and characterized ID for these transformed graphs. At first, we determined the effect of transformations  $A$  and  $B$  over increase and decrease of ID individually. Then, we established result for  $A_i^j$  for arbitrary values of  $i$  and  $j$  which provides moving graphs such as animation. We also determined the exact result for  $\Delta$ -regular graph under transformation effect. Moreover, we computed the exact formula for the family of unicyclic graphs with pendent paths under the action of transformation as an application of proved results.

### Data Availability

No data were used to support this study.

### Disclosure

The paper has not been published elsewhere, and it will not be submitted anywhere else for publication.

### Conflicts of Interest

The authors declare that they have no conflicts of interest.

### Authors' Contributions

All the authors have equal contribution.

## Acknowledgments

The authors extend their appreciation to the Deanship of Scientific Research at Majmaah University for funding this work under project number no. RGP-2019-29.

## References

- [1] J. A. Bondy and U. S. R. Murty, *Graph Theory with Applications*, Macmillan, London, UK, 1976.
- [2] A. A. Dobrynin, R. Entringer, and I. Gutman, "Wiener index of trees: theory and applications," *Acta Applicandae Mathematicae*, vol. 66, no. 3, pp. 211–249, 2001.
- [3] G. Rücker and C. Rücker, "On topological indices, boiling points, and cycloalkanes," *Journal of Chemical Information and Computer Sciences*, vol. 39, no. 5, pp. 788–802, 1999.
- [4] M. Randić, "Characterization of molecular branching," *Journal of the American Chemical Society*, vol. 97, no. 23, pp. 6609–6615, 1975.
- [5] X. Li and J. Zheng, "A unified approach to the extremal trees for different indices," *MATCH Communications in Mathematical and in Computer Chemistry*, vol. 54, pp. 195–208, 2005.
- [6] Y. Hu, X. Li, Y. Shi, and T. Xu, "Connected  $(n, m)$ -graphs with minimum and maximum zeroth-order general Randić index," *Discrete Applied Mathematics*, vol. 155, pp. 1044–1054, 2007.
- [7] H. Ahmed, A. A. Bhatti, and A. Ali, "Zeroth-order general Randić index of cactus graphs," *AKCE International Journal of Graphs and Combinatorics*, vol. 16, no. 2, pp. 182–189, 2019.
- [8] A. Ali, A. A. Bhatti, and Z. Raza, "A note on the zeroth-order general Randić index of cacti and polyomino chains," *Iranian Journal of Mathematical Chemistry*, vol. 5, pp. 143–152, 2014.
- [9] H. Hua and H. Deng, "On unicycle graphs with maximum and minimum zeroth-order general Randić index," *Journal of Mathematical Chemistry*, vol. 41, no. 2, pp. 173–181, 2007.
- [10] G. Su, J. Tu, and K. C. Das, "Graphs with fixed number of pendent vertices and minimal Zeroth-order general Randić index," *Applied Mathematics and Computation*, vol. 270, pp. 705–710, 2015.
- [11] S. Fajtlowicz, "On conjectures of Graffiti-II," *Congressus Numerantium*, vol. 60, pp. 187–197, 1987.
- [12] S. Mukwembi, "On diameter and inverse degree of a graph," *Discrete Mathematics*, vol. 310, no. 4, pp. 940–946, 2010.
- [13] B. Yao, X.-e. Chen, M. Yao, J. Zhang, and J. Guo, "Leaves and inverse degree of a graph," in *Proceedings of the 2010 3rd International Conference on Biomedical Engineering and Informatics*, Yantai, China, October 2010.
- [14] K. Das, S. Balachandran, and I. Gutman, "Inverse degree, Randić index and harmonic index of graphs," *Applicable Analysis and Discrete Mathematics*, vol. 11, no. 2, pp. 304–313, 2017.
- [15] K. Das, K. Xu, and J. Wang, "On inverse degree and topological indices of graphs," *Filomat*, vol. 30, no. 8, pp. 2111–2120, 2016.
- [16] J. M. Rodríguez, J. L. Sánchez, and J. M. Sigarreta, "Inequalities on the inverse degree index," *Journal of Mathematical Chemistry*, vol. 57, no. 5, pp. 1524–1542, 2019.
- [17] R. Xing, B. Zhou, and F. Dong, "On atom-bond connectivity index of connected graphs," *Discrete Applied Mathematics*, vol. 159, no. 15, pp. 1617–1630, 2011.
- [18] K. Xu and K. C. Das, "Some extremal graphs with respect to inverse degree," *Discrete Applied Mathematics*, vol. 203, pp. 171–183, 2016.
- [19] A. Ali, I. Gutman, E. Milovanovic, and I. Milovanovic, "Sum of powers of the degrees of graphs: extremal results and bounds," *MATCH Communications in Mathematical and in Computer Chemistry*, vol. 80, pp. 5–84, 2018.

## Research Article

# M-Polynomials and Degree-Based Topological Indices of the Molecule Copper(I) Oxide

Faryal Chaudhry,<sup>1</sup> Iqra Shoukat,<sup>1</sup> Deeba Afzal ,<sup>1</sup> Choonkil Park ,<sup>2</sup> Murat Cancan ,<sup>3</sup> and Mohammad Reza Farahani <sup>4</sup>

<sup>1</sup>Department of Mathematics and Statistics, University of Lahore, Lahore 54000, Pakistan

<sup>2</sup>Research Institute for Natural Sciences, Hanyang University, Seoul 04763, Republic of Korea

<sup>3</sup>Faculty of Education, Van Yüzüncü Yıl University, Van 65080, Turkey

<sup>4</sup>Department of Applied Mathematics, Iran University of Science and Technology (IUST), Narmak, Tehran 16844, Iran

Correspondence should be addressed to Choonkil Park; [baak@hanyang.ac.kr](mailto:baak@hanyang.ac.kr) and Mohammad Reza Farahani; [mrfarahani88@gmail.com](mailto:mrfarahani88@gmail.com)

Received 4 December 2020; Revised 20 December 2020; Accepted 28 January 2021; Published 24 February 2021

Academic Editor: Teodorico C. Ramalho

Copyright © 2021 Faryal Chaudhry et al. This is an open access article distributed under the Creative Commons Attribution License, which permits unrestricted use, distribution, and reproduction in any medium, provided the original work is properly cited.

Topological indices are numerical parameters used to study the physical and chemical residences of compounds. Degree-based topological indices have been studied extensively and can be correlated with many properties of the understudy compounds. In the factors of degree-based topological indices, M-polynomial played an important role. In this paper, we derived closed formulas for some well-known degree-based topological indices like first and second Zagreb indices, the modified Zagreb index, the symmetric division index, the harmonic index, the Randić index and inverse Randić index, and the augmented Zagreb index using calculus.

## 1. Introduction

*1.1. Application Background.* A graph that represents the construction of a molecule and also their connectivity is known as a molecular graph, and such a representation is generally known as topological representations of molecule. Molecular graphs are normally characterized by means of exclusive topological basis for parallel of chemicals shape of a molecule with organic, chemical, or bodily homes. Study of graph has some programs of various topological indices in quantitative structure-activity relationship (QSAR) and quantitative structure-property relationship (QSPR), digital screenings, and computational drug designing citations as shown in [1, 2]. Thus far, several exclusive topological indices have been established, and maximum of them are most effective graph descriptors in [3, 4]; apart, some indices have proven their parallel with organic, chemical, or physical residences of secure molecules in [5–17].

In the field of mathematics, any graph has vertices and edges that are represented by the atoms and chemical bonds.

Graph that represents the construction of molecules and their connectivity is known as a molecular graph, and such representation is usually referred as topological representation of molecules. There are some significant topological indices like distance-based topological indices, degree-based topological indices, and primarily based topological indices. Among these works, distance primarily based topological indices unit works out a crucial task in a chemical graph started, specifically in chemistry [18,19]. Many fields have many features that can be solved with the help of graphs. In the physiochemical compounds or network systems, we have a tendency to abstractly outline exclusive ideas in modeling of mathematics. We have a tendency to refer to as the distinctive names, such as Randić index and national capital index.

A topological index is a numerical parameter of a graph and describes its topology. It describes the molecular shape numerically and is applied within the advancement of qualitative structure-activity relationships (QSARs). The following are the 3 types of topological indices:



- (1) Degree-based.
- (2) Distance-based.
- (3) Spectral-based.

Degree-based topological indices were studied extensively and may be correlated with many residences of the understudy molecular compounds. There is a strong relationship among distance-based and degree-based topological indices in [20]. Most commonly known invariants of such kinds are degree-based topological indices. These are actually the numerical values that correlate the structure with various physical properties, chemical reactivities, and biological activities. Topological indices are sincerely the numerical values that relate the shape to one of a kind of physical residences, artificial reactivity, and natural biological activities [21,22].

Loads of research has been executed inside the course of M-polynomial, as in the case of Munir et al., processed M-polynomial and related lists of triangular boron nanotubes in [6], polyhex nanotubes in [23], nanostar dendrimers in [4], and titania nanotubes in [5]. M-Polynomials and topological lists of V-phenylenic nanotubes and nanotori. In this paper, the objective is to process the M-polynomial of the crystallographic realistic structure of the atom copper(I) oxide ( $\text{Cu}_2\text{O}$ ) [8,24].

**1.2. Crystallographic Structure of  $\text{Cu}_2\text{O}(m; n)$ .** Copper oxide is a p-type semiconductor and inorganic compound. Copper oxide is a chemical element with formula  $\text{Cu}_2\text{O}(m; n)$ .  $\text{Cu}_2\text{O}(m; n)$  is a certainly happening reddish coral that is particularly used in chemical sensors and solar orientated cells in [8, 24]. It has many advantages such as photochemical effects, stability, pigment, a fungicide, nontoxicity, and low cost. It has potential applications in new energy, sensing, sterilization, and other fields. It has narrow band gap and is easily excited by visible light.

$\text{Cu}_2\text{O}(m; n)$  is additionally responsible for the pink shading in Benedict's test and is the essential cause to select  $\text{Cu}_2\text{O}$  (see Figures 1 and 2). The promising projects of  $\text{Cu}_2\text{O}(m; n)$  are mainly on chemical sensors, sunlight-based cells, photocatalysis, lithium particle batteries, and catalysis. Here, we have taken into consideration a monolayer of  $\text{Cu}_2\text{O}(m; n)$  for satisfaction. To ultimate the basis for  $\text{Cu}_2\text{O}(m; n)$ , we pick out the setting of this graph as  $\text{Cu}_2\text{O}(m; n)$  be the chemical graph of copper(I) oxide with  $(m; n)$  unit cells within the aircraft.

## 2. Definitions and Literature Review

**2.1. M-Polynomial.** M-Polynomial is defined by S. Klavžar or E. Deutsch in 2015 [3, 8]. Within the factors of degree-based topological indices, we compete necessary role of M-polynomial. Readers can refer to [9–17, 27–35]. It is the foremost general progressive polynomial and an additionally closed formula alongside 10 distance-based topological indices is given by M-polynomial. It is explained as

$$M(G, a, b) = \sum_{\delta \leq i \leq j \leq \Delta} m_{ij}(G) a^i b^j, \quad (1)$$

and we have  $\delta = \text{Min}\{d_r \mid r \in V(G)\}$  and  $\Delta = \text{Max}\{d_r \mid r \in V(G)\}$ , where  $m_{ij}(G)$  is the edge  $E(G)$ , where  $i \leq j$ .

**2.2. Degree-Based Topological Indices.** Any purpose on a graph which does not build upon numbering of its vertices is molecular descriptor. This is also called as topological index. Topological indices are most useful in the field of isomeric discrimination, chemical validation, QSAR, QSPR, and a pharmaceutical drug form. Topological indices are accessed from the system of molecule.

There are some important degree-based topological indices defined, and the first Zagreb index was introduced by Gutman and Trinajstić as follows:

$$M_1(G) = \sum_{r,s \in E(G)} (d_r + d_s). \quad (2)$$

Gutman and Trinajstić proposed the second Zagreb index in 1972, which is stated as

$$M_2(G) = \sum_{r,s \in E(G)} (d_r \times d_s). \quad (3)$$

The second modified Zagreb index is defined as

$${}^m M_2(G) = \sum_{r,s \in E(G)} \frac{1}{d(r)d(s)}. \quad (4)$$

General 1<sup>st</sup> and 2<sup>nd</sup> multiplicative Zagreb indices are introduced by Kulli, Stone, Wang, and Wei and are stated as

$$\begin{aligned} MZ_1^a II(G) &= \prod_{r,s \in E(G)} (d_r + d_s)^a, \\ MZ_2^a II(G) &= \prod_{r,s \in E(G)} (d_r d_s)^a. \end{aligned} \quad (5)$$

The general 1<sup>st</sup> and 2<sup>nd</sup> Zagreb indices proposed by Kulli, Stone, Wang, and Wei are stated as

$$\begin{aligned} Z_1^a(G) &= \sum_{r,s \in E(G)} (d_r + d_s)^a, \\ Z_2^a(G) &= \sum_{r,s \in E(G)} (d_r d_s)^a. \end{aligned} \quad (6)$$

In 1987, Fajtlowicz in [36] proposed the harmonic index and stated

$$H(G) = \sum_{r,s \in E(G)} \frac{2}{d_r + d_s}. \quad (7)$$

The inverse sum index is defined:

$$I(G) = \sum_{r,s \in E(G)} \frac{d_r d_s}{d_r + d_s}. \quad (8)$$

Symmetric division index is described as

$$SS D(G) = \sum_{r,s \in E(G)} \frac{\min(d_r, d_s)}{\max(d_r, d_s)} + \frac{\max(d_r, d_s)}{\min(d_r, d_s)}. \quad (9)$$

SU and XU recognized general Randić index or general multiplicative Randić index stated as follows (Table 1):

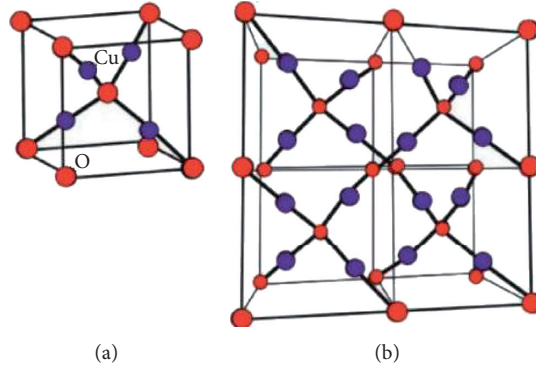


FIGURE 1: (a) Cu<sub>2</sub>O [1, 1] [25]; (b) Cu<sub>2</sub>O [2, 2] [1].

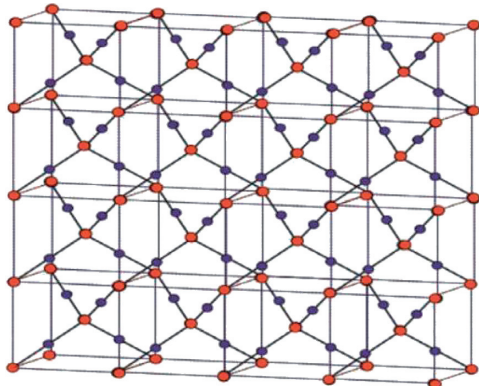


FIGURE 2: Copper(I) oxide [4, 4] [26].

$$R_\alpha(G) = \sum_{r,s \in E(G)} d_r + d_s^\alpha, \quad (10)$$

$$R_\alpha II(G) = \prod_{r,s \in E(G)} d_r + d_s^\alpha.$$

**Theorem 1.** Crystallographic structure of the graph of copper(I) oxide  $G \approx Cu_2O[m; n]$ , where  $n; m \geq 1$ . We have

$$M(G; a; b) = f(a; b) = (4m + 4n - 4)ab^2 + (4mn - 4n - 4m + 4)a^2b^2 + 4mna^2b^4. \quad (11)$$

*Proof.* suppose  $G$  be the crystallographic structure of  $Cu_2O[l; m; n]$ . The edge set of  $Cu_2O[l; m; n]$  has the following three partitions by Figures 1 and 2:

$$E_1 = E_{\{1;2\}} = \{e = rs \in E(G) | d_r = 1; d_s = 2\},$$

$$E_2 = E_{\{2;2\}} = \{e = rs \in E(G) | d_r = 2; d_s = 2\}, \quad (12)$$

$$E_3 = E_{\{2;4\}} = \{e = rs \in E(G) | d_r = 2; d_s = 4\},$$

such that

$$|E_1(G)| = 4mm + 4n - 4,$$

$$|E_2(G)| = 4mn - 4m - 4n + 4, \quad (13)$$

$$|E_3(G)| = 4mn.$$

Thus, the M-polynomial of  $Cu_2O[l; m; n]$  is

$$M(G, a, b) = \sum_{i \leq j} m_{ij}(G) a^i b^j,$$

$$M(G, a, b) = \sum_{1 \leq 2} m_{12}(G) ab^2 + \sum_{2 \leq 2} m_{22}(G) a^2 b^2 + \sum_{2 \leq 4} m_{24}(G) a^2 b^4,$$

$$M(G, a, b) = \sum_{rs \in E_1} m_{12}(G) ab^2 + \sum_{uv \in E_2} m_{22}(G) a^2 b^2 + \sum_{uv \in E_3} m_{24}(G) a^2 b^4, \quad (14)$$

$$M(G; a; b) = |E_1(G)| ab^2 + |E_2(G)| a^2 b^2 + |E_3(G)| a^2 b^4,$$

$$M(G; a; b) = (4m + 4n - 4)ab^2 + (4mn - 4n - 4m + 4)a^2b^2 + 4mna^2b^4.$$

**Theorem 2.** Crystallographic structure of the graph of copper(I) oxide  $G \approx Cu_2O[m; n]$ , where  $n; m \geq 1$ . We have  $M_1(G) = 40mn - 4m - 4n + 4$ .

*Proof.* suppose

$$M(G; a; b) = f(a; b) = (4m + 4n - 4) \times ab^2 + (4mn - 4n - 4m + 4) \times a^2b^2 + 4mn \times a^2b^4. \quad (15)$$

We have to find

TABLE 1: Formulas of degree-based topological indices from M-polynomial.

Topological Indices	$f(t, s)$	$M(G; t, s)$
First Zagreb index	$t + s$	$M_1(G; t, s) = (D_t + D_s)M(G; t, s) _{t=s=1}$
Second Zagreb index	$Ts$	$M_2(G; t, s) = (D_t D_s)M(G; t, s) _{t=s=1}$
Second modified Zagreb index	$1/ts$	${}^m M_2(G; t, s) = (\delta_t \delta_s)M(G; t, s) _{t=s=1}$
General Randić index, $\alpha \neq 0$	$(ts)^\alpha$	$R_\alpha(G) = (D_t^\alpha D_s^\alpha)M(G; t, s) _{t=s=1}$
Inverse general Randić index, $\alpha \neq 0$	$1/(ts)^\alpha$	$RR_\alpha(G) = (\delta_t^\alpha \delta_s^\alpha)M(G; t, s) _{t=s=1}$
Symmetric division index	$(t^2 + s^2)/ts$	$SSD(G) =  D_t \delta_s = \delta_s D_t _{t=s=1}$
Harmonic index	$2/(t + s)$	$H(G) = 2\delta_t J M(G; t, s) _{t=1}$
Inverse sum index	$ts/(t + s)$	$I(G) = \delta_t J D_t D_s M(G; t, s) _{t=1}$

$$D_s = s(\partial/\partial s)M(G; t, s)|_{t=s=1}, D_t = t(\partial/\partial t)M(G; t, s)|_{t=s=1}, \delta_t = \int_0^t (M(G; y, s))/y dy, \delta_s = \int_0^s (M(G; t, y))/y ds, J = M(G; t, t), Q_\alpha = x^\alpha M(G; t, s), \alpha \neq 0.$$

$$D_a = \frac{\partial f}{\partial a} a,$$

$$\frac{\partial f}{\partial a} = (4n + 4m - 4)b^2 + 2(4mn - 4n - 4m + 4)ab^2 + 8mnab^4. \quad (16)$$

Multiply  $a$  on both sides:

$$D_a = a \frac{\partial f}{\partial a} = (4m + 4n - 4)ab^2 + 2(4mn - 4m - 4n + 4)a^2b^2 + 8mna^2b^4. \quad (17)$$

Similarly,

$$D_b f(a, b) = b \frac{\partial f}{\partial b} = 2(4n + 4m - 4)ab^2 + 2(4mn - 4n - 4m + 4)a^2b^2 + 16mnab^4, \\ M_1(G) = (D_a + D_b)f(a, b)|_{a=b=1}. \quad (18)$$

Now, the first Zagreb index is

$$M_1(G) = (D_a + D_b)f(a, b)|_{a=b=1}, \\ M_1(G) = [(4m + 4n - 4) + 2(4mn - 4m - 4n + 4) + 8mn] + [2(4n + 4m - 4) + 2(4mn - 4m - 4n + 4) + 16mn], \\ M_1(G) = [4m + 4n - 4 + 8mn - 8m - 8n + 8 + 8mn + 8n + 8m - 8 + 8mn - 8m - 8n + 8 + 16mn]. \quad (19)$$

After solving, the result is

$$M(G) = 40mn - 4m - 4n + 4. \quad (20)$$

The 3D plot of first Zagreb index is given in Figure 3 ( $f$  or  $u=1$  left,  $v=1$  middle, and  $w=1$  right), and we see the dependent variables of the first Zagreb index on the involved parameters.  $\square$

**Theorem 3.** Crystallographic structure of the graph of copper(I) oxide  $G \approx Cu_2O[m; n]$ , where  $n; m \geq 1$ . We have  $M_2(G) = 48mn - 8m - 8n + 8$ .

*Proof.* suppose

$$M(G; a; b) = (4m + 4n - 4) \times ab^2 + (4mn - 4n - 4m + 4) \times a^2b^2 + 4mn \times a^2b^4. \quad (21)$$

We have to find  $D_b D_a$ ; first, we take  $D_a$ :

$$D_a = (4m + 4n - 4) \times ab^2 + (4mn - 4m - 4n + 4)^2 a \times a \times b^2 + 4mn^2 a \times a \times b^4, \\ D_a = (4m + 4n - 4) \times ab^2 + 2(4mn - 4m - 4n + 4) \times a^2b^2 + 8mn \times a^2b^4. \quad (22)$$

Now, take  $D_b$ :

$$D_b D_a f(a; b) = 2(4m + 4n - 4)ab + 2(4mn - 4m - 4n + 4)a^2 \times 2b: b + 8mna^2 \times 4b^3 \times b, \\ D_b D_a f(a; b) = 2(4m + 4n - 4) \times ab^2 + 4(4mn - 4m - 4n + 4) \times a^2b^2 + 32mn \times a^2b^4. \quad (23)$$

The second Zagreb index is

$$M_2(G) = D_b D_a (f(a, b))|_{a=b=1}, \\ M_2(G) = 2(4m + 4n - 4) + 4(4mn - 4m - 4n + 4) + 32mn, \\ M_2(G) = 8mn + 8m - 8 + 16mn - 16m - 16n + 16 + 32mn. \quad (24)$$

After solving, the result is

$$M_2(G) = 48mn - 8m - 8n + 8. \quad (25)$$

The 3D plot of second Zagreb index is given in Figure 4 ( $f$  or  $u=1$  left,  $v=1$  middle, and  $w=1$  right), and we see the dependent variables of the second Zagreb index on the involved parameters.  $\square$

**Theorem 4.** Crystallographic structure of the graph of copper(I) oxide  $G \approx Cu_2O[m; n]$ , where  $n; m \geq 1$ , and we have

$${}^m M^2(G) = \frac{3}{2}mn + m + n - 1.3. \quad (26)$$

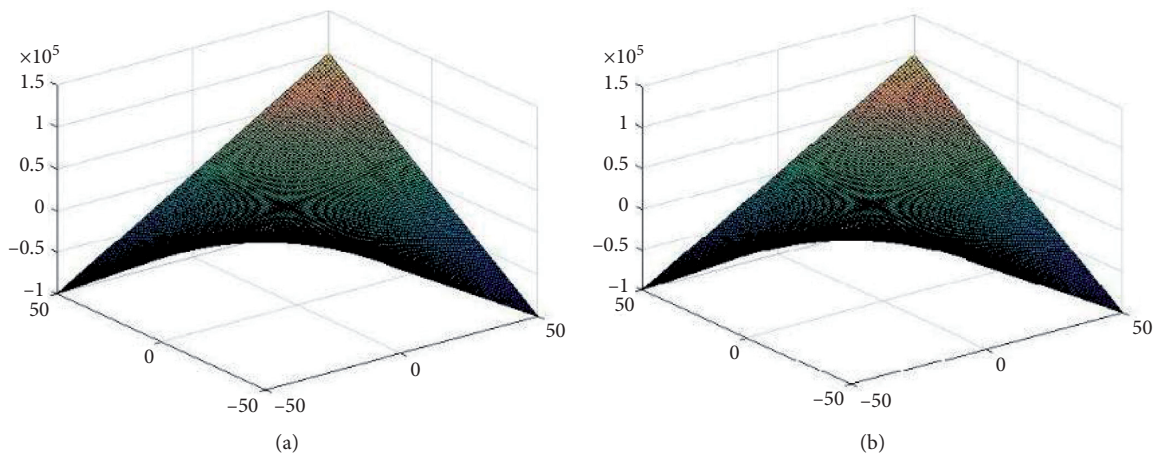


FIGURE 3: First Zagreb index plotted in 3D.

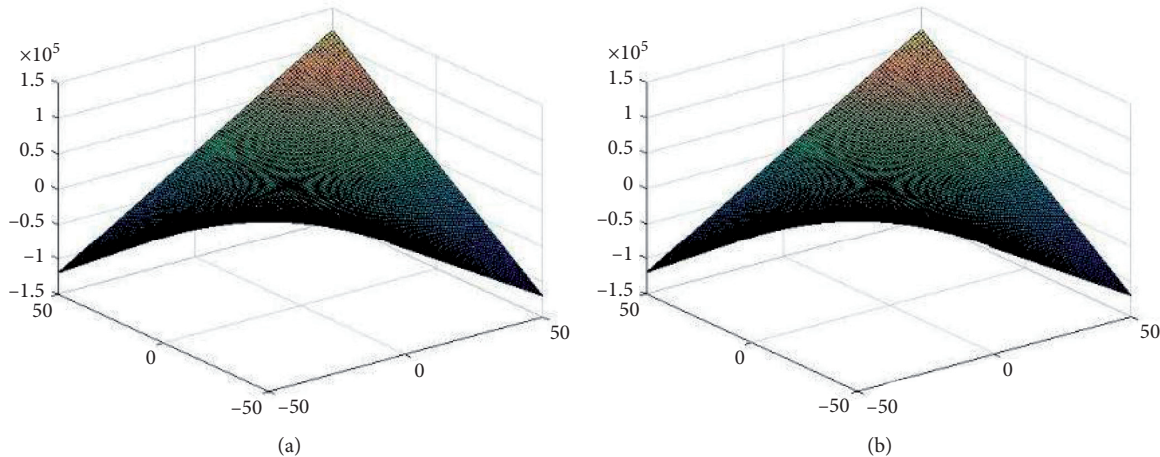


FIGURE 4: Second Zagreb index plotted in 3D.

*Proof.* suppose

$$M(G; a; b) = (4m + 4n - 4)ab^2 + (4mn - 4m - 4n + 4)a^2b^2 + 4mna^2b^4. \tag{27}$$

Now, we have to find  $S_a S_b$ ; first, we find  $S_a$ :

$$S_a = \int_0^a \frac{f(x, b)}{x} dx,$$

$$f(x, b) = (4n + 4m - 4)xb^2 + (4mn - 4m - 4n + 4)x^2b^2 + 4mnx^2b^4,$$

$$\frac{f(x, b)}{x} = (4m + 4n - 4)b^2 + (4mn - 4n - 4m + 4)xb^2 + 4mnxb^4. \tag{28}$$

Taking integration on both sides,

$$\begin{aligned} \int_0^a \frac{f(x, b)}{x} dx &= \int_0^a (4m + 4n - 4)b^2 dx \\ &+ \int_0^a (4mn - 4m - 4n + 4)xb^2 dx \\ &+ 4mn \int_0^a x dx b^4, \\ S_a &= (4m + 4n - 4)ab^2 \\ &+ \frac{1}{2} (4mn - 4n - 4m + 4)a^2b^2 + 2mna^2b^4. \end{aligned} \tag{29}$$

Now, take  $S_b$  and then

$$\begin{aligned}
S_a S_b f(a, b) &= (4m + 4n - 4)ax^2 \\
&+ \frac{1}{2} (4mn - 4m - 4n + 4)a^2x^2 + 2mna^2x^4, \\
S_a S_b f(a, b) &= \frac{1}{2} (4m + 4n - 4)ab^2 \\
&+ \frac{1}{4} (4mn - 4m - 4n + 4)a^2b^2 + \frac{1}{2} mna^2b^4.
\end{aligned}
\tag{30}$$

Now, the second modified Zagreb index is

$$\begin{aligned}
{}^m M_2(G) &= S_a S_b f(a, b)|_{a=b=1} = \frac{1}{2} (4m + 4n - 4) + \frac{1}{4} (4mn - 4m - 4n + 4) + \frac{1}{2} mn \\
&= (2m + 2n - 2) + (mn - m - n + 1) + \frac{1}{2} mn \\
&= 2m - m + 2n - n - 2 + 1 + mn \left(1 + \frac{1}{2}\right).
\end{aligned}
\tag{31}$$

After solving, the result is

$${}^m M_2(G) = \frac{3}{2} mn + m + n - 1. \tag{32}$$

The 3D plot of modified second Zagreb index is given in Figure 5 ( $f$  or  $u = 1$  left,  $v = 1$  middle, and  $w = 1$  right), and we see the dependent variables of the modified second Zagreb index on the involved parameters.  $\square$

**Theorem 5.** Crystallographic structure of the graph of copper(I) oxide  $G \approx Cu_2O[m; n]$ , where  $n; m \geq 1$ , and we have

$$R_\alpha(G) = (2^{\alpha+2} - 2^{2\alpha+2})(m + n - 1) + (2^{2\alpha+2} + 2^{3\alpha+2})mn. \tag{33}$$

*Proof.* suppose

$$\begin{aligned}
M(G; a, b) &= (4m + 4n - 4) \times ab^2 + (4mn - 4m - 4n + 4) \\
&\times a^2b^2 + (4mn) \times a^2b^4.
\end{aligned}
\tag{34}$$

We have to find  $D_a D_b$  first, and we find  $D_a$ :

$$\begin{aligned}
D_a &= (4m + 4n - 4) \times ab^2 + 2(4mn - 4m - 4n + 4) \\
&\times a^2b^2 + 8mn \times a^2b^4.
\end{aligned}
\tag{35}$$

Now, take  $D_b$ :

$$\begin{aligned}
D_a D_b &= (4m + 4n - 4)a \times 2b \times b + 2(4mn - 4m - 4n + 4)a^2 \\
&\times 2b \times b + 2(4mn)a^2 \times 4b^3 \times b.
\end{aligned}
\tag{36}$$

Take  $\alpha$  on the above equation:

$$\begin{aligned}
D_a^\alpha D_b^\alpha &= 2^\alpha (4m + 4n - 4)ab^2 + 4^\alpha (4mn - 4m - 4n + 4)a^2b^2 \\
&+ 8^\alpha (4mn)a^2b^4, \\
D_a^\alpha D_b^\alpha &= 2^{\alpha+2}m + n - 1ab^2 + 2^{2\alpha+2}(mn - m - n + 1)a^2b^2 \\
&+ 2^{3\alpha+2}mna^2b^4.
\end{aligned}
\tag{37}$$

Now, the general Randić index is

$$\begin{aligned}
R_\alpha(G) &= D_a^\alpha D_b^\alpha (f(a, b))|_{a=b=1}, \\
R_\alpha(G) &= 2^{\alpha+2}(m + n - 1) + 2^{2\alpha+2}(mn - m - n + 1) + 2^{3\alpha+2}mn, \\
R_\alpha(G) &= 2^{\alpha+2}m + 2^{\alpha+2}n - 2^{\alpha+2} + 2^{2\alpha+2}mn - 2^{2\alpha+2}m \\
&- 2^{2\alpha+2}n + 2^{2\alpha+2} + 2^{3\alpha+2}mn.
\end{aligned}
\tag{38}$$

The result is

$$R_\alpha(G) = (2^{\alpha+2} - 2^{2\alpha+2})(m + n - 1) + (2^{2\alpha+2} + 2^{3\alpha+2})mn. \tag{39}$$

The 3D plot of Randić index is given in Figure 6 ( $f$  or  $u = 1$  left,  $v = 1$  middle, and  $w = 1$  right), and we see the dependent variables of the Randić index on the involved parameters.  $\square$

**Theorem 6.** Crystallographic structure of the graph of copper(I) oxide  $G \approx Cu_2O[m; n]$ , where  $n; m \geq 1$ , and we have

$$\begin{aligned}
RR_\alpha(G) &= \left[ \frac{1}{2^{\alpha-2}} - \frac{1}{2^{2\alpha-2}} \right] (m + n) + \left[ \frac{1}{2^{2\alpha-2}} + \frac{2}{2^{3\alpha-2}} \right] (mn) \\
&+ \left[ \frac{1}{2^{\alpha-2}} + \frac{1}{2^{2\alpha-2}} \right].
\end{aligned}
\tag{40}$$

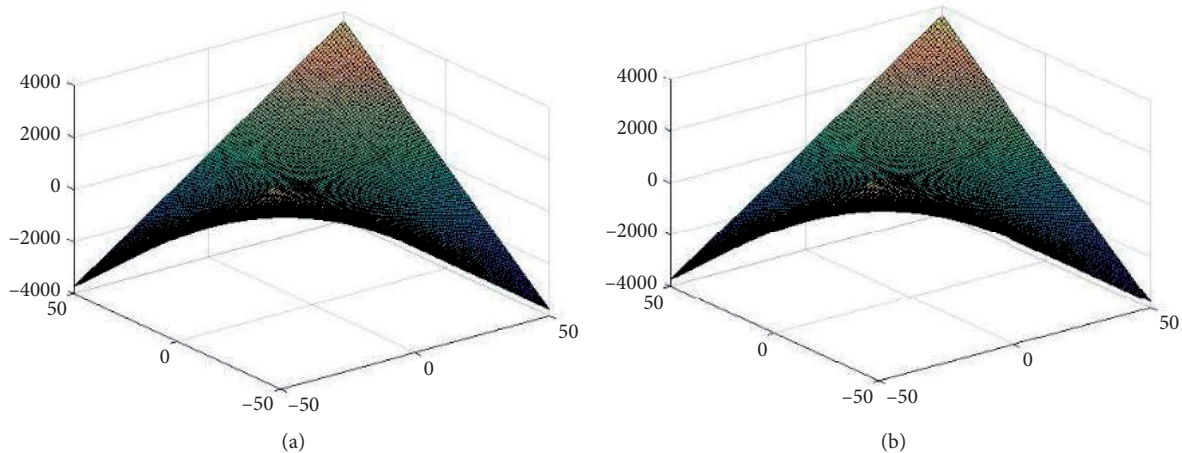


FIGURE 5: Modified the second Zagreb index plotted in 3D.

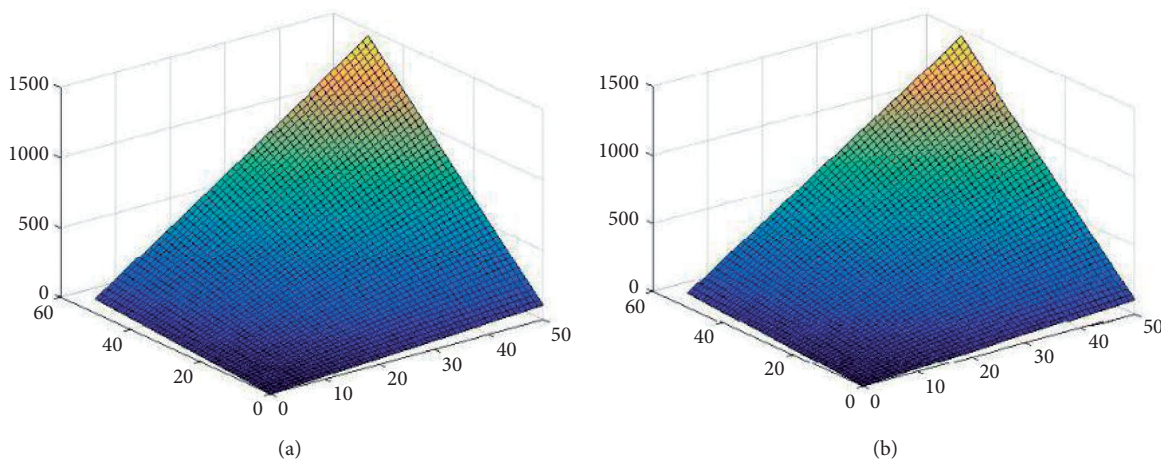


FIGURE 6: Randić index plotted in 3D.

*Proof.* suppose

$$M(G; a; b) = (4m + 4n - 4) \times ab^2 + (4mn - 4m - 4n + 4) \times a^2b^2 + (4mn) \times a^2b^4. \tag{41}$$

Now, we have to find  $S_a S_b$ , and first, we find  $S_a$ :

$$S_a = (4m + 4n - 4) \int_0^a dx.b^2 + (4mn - 4m - 4n + 4) \cdot \int_0^a xdx.b^2 + 8mn \int_0^a xdx.b^4$$

$$S_a = (4m + 4n - 4)ab^2 + 2(mn - m - n + 1)a^2b^2 + 4mna^2b^4. \tag{42}$$

Similarly, take  $S_b$ :

$$S_a S_b = 4(m + n - 1)a \cdot \int_0^b xdx + 2(mn - n - m + 1)a^2 \cdot \int_0^b xdx + 4mna^2 \int_0^b x^3 dx,$$

$$S_a S_b = 2(m + n - 1)ab^2 + (mn - m - n + 1)a^2b^2 + mna^2b^4. \tag{43}$$

Take  $\alpha$  on the above equation:

$$S_a^\alpha S_b^\alpha = \frac{1}{2^{\alpha-2}} (m + n - 1)ab^2 + \frac{1}{2^{2\alpha-2}} (mn - m - n + 1)a^2b^2 + \frac{1}{2^{3\alpha-2}} mna^2b^4. \tag{44}$$

The inverse Randić is

$$\begin{aligned}
RR_{\alpha}(G) &= (f(a, b))|_{a=b=1} = \frac{1}{2^{\alpha-2}}(m+n-1) \\
&+ \frac{1}{2^{2\alpha-2}}(mn-m-n+1) \\
&+ \frac{2}{2^{3\alpha-2}}mn = \left[ \frac{1}{2^{\alpha-2}} - \frac{1}{2^{2\alpha-2}} \right](m+n) \\
&+ \left[ \frac{1}{2^{2\alpha-2}} + \frac{2}{2^{3\alpha-2}} \right](mn) + \left[ \frac{1}{2^{\alpha-2}} + \frac{1}{2^{2\alpha-2}} \right].
\end{aligned} \tag{45}$$

The 3D plot of inverse Randić index is represented in Figure 7 ( $f$  or  $u = 1$  left,  $v = 1$  middle, and  $w = 1$  right), and we see the dependent variables of the inverse Randić index on the involved parameters.  $\square$

**Theorem 7.** Crystallographic structure of the graph of copper(I) oxide  $G \approx Cu_2O[m; n]$ , where  $n; m \geq 1$ , and we have  $SS D(G) = 18mn + 2m + 2n - 2$ .

*Proof.* suppose

$$\begin{aligned}
M(G; a; b) &= (4m + 4n - 4) \times ab^2 + (4mn - 4m - 4n + 4) \\
&\times a^2b^2 + (4mn) \times a^2b^4.
\end{aligned} \tag{46}$$

First, we have to find  $S_b$ :

$$\begin{aligned}
SS D(G) &= \left[ \frac{1}{2}(4m + 4n - 4) + (4mn - 4m - 4n + 4) + 2mn \right] + [2(4m + 4n - 4) + (4mn - 4m - 4n + 4) + 8mn], \\
SS D(G) &= (2m + 2n - 2) + (4mn - 4m - 4n + 4) + (2mn + 8m + 8n - 8) + (4mn - 4m - 4n + 4) + 8mn, \\
SS D(G) &= (2m - 4m + 8m - 4m) + (2n - 4n + 8n - 4n) - (2 - 4 + 8 - 8) + (4mn + 2mn + 4mn + 8mn).
\end{aligned} \tag{52}$$

After the calculation, the result is

$$SS D(G) = 18mn + 2m + 2n - 2. \tag{53}$$

The 3D plot of symmetric division index is given in Figure 8 ( $f$  or  $u = 1$  left,  $v = 1$  middle, and  $w = 1$  right), and we see the dependent variables of the symmetric division index on the involved parameters.  $\square$

**Theorem 8.** Crystallographic structure of the graph of copper(I) oxide  $G \approx Cu_2O[m; n]$ , where  $n; m \geq 1$ , and we have

$$H(G) = \frac{5}{3}(m+n-1) + \frac{7}{3}mn. \tag{54}$$

$$\begin{aligned}
S_b &= (4n + 4m - 4)a \int_0^b x dx + (4mn - 4m - 4n + 4)a^2 \\
&\cdot \int_0^b x dx + 4mna^2 \int_0^b x^3 dx, \\
S_b &= \frac{1}{2}(4n + 4m - 4)ab^2 + \frac{1}{2}(4mn - 4m - 4n + 4)a^2b^2 \\
&+ mna^2b^4.
\end{aligned} \tag{47}$$

Now, take  $D_a$ :

$$S_b D_a = \frac{1}{2}(4m + 4n - 4)ab^2 + (4mn - 4m - 4n + 4)a^2b^2 + 2mna^2b^4. \tag{48}$$

Similarly,

$$S_a = (4m + 4n - 4)ab^2 + \frac{1}{2}(4mn - 4n - 4m + 4)a^2b^2 + 2mna^2b^4. \tag{49}$$

Take  $D_b$ :

$$\begin{aligned}
S_a D_b (f(a, b)) &= 2(4m + 4n - 4)ab^2 \\
&+ (4mn - 4m - 4n + 4)a^2b^2 + 8mna^2b^4.
\end{aligned} \tag{50}$$

Now, the symmetric division index is

$$SS D(G) = (S_b D_a + S_a D_b)(f(a, b))|_{a=b=1}. \tag{51}$$

Put the values

*Proof.* suppose

$$\begin{aligned}
M(G; a; b) &= (4m + 4n - 4) \times ab^2 + (4mn - 4m - 4n + 4) \\
&\times a^2b^2 + (4mn) \times a^2b^4.
\end{aligned} \tag{55}$$

First, we have to find  $J_f(a; b)$ :

$$\begin{aligned}
Jf(a, b) &= Jf(a, a) = 4(m+n-1)a^3 \\
&+ 4(mn-m-n+1)a^4 + 8mna^6.
\end{aligned} \tag{56}$$

Take  $S_a$ :

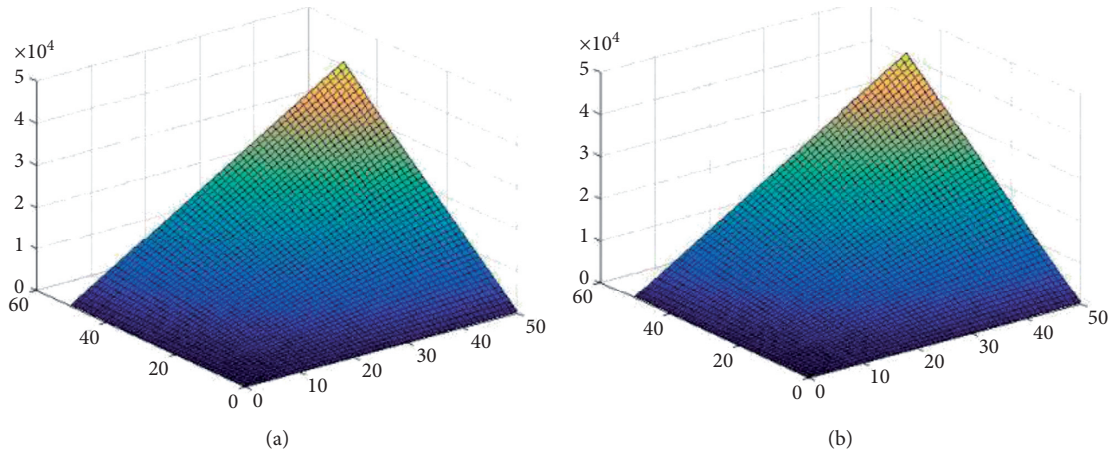


FIGURE 7: Inverse Randić index plotted in 3D.

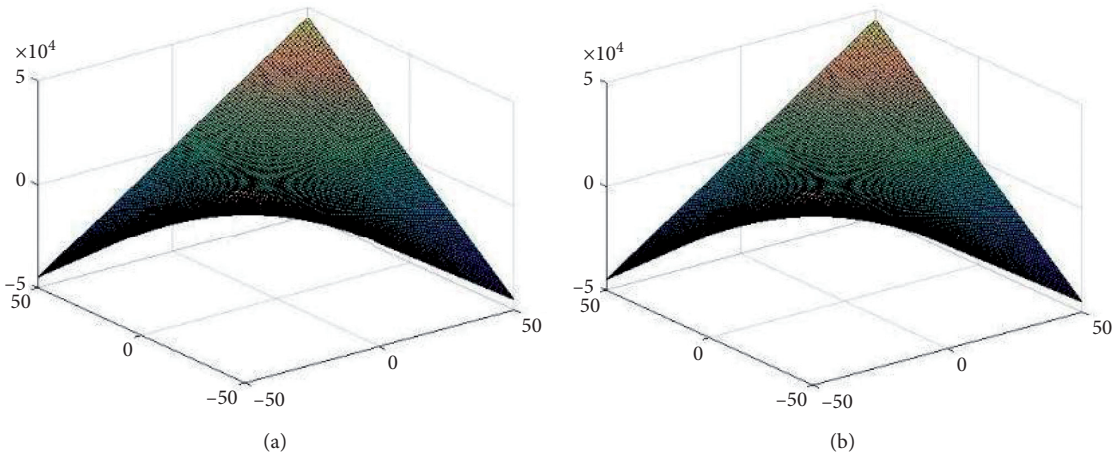


FIGURE 8: Symmetric division index plotted in 3D.

$$\begin{aligned}
 S_a J f(x, b) &= 4(m+n-1) \int_0^a x^2 dx + 4(mn-m-n+1) \\
 &\quad \cdot \int_0^a x^3 dt + 8mn \int_0^a x^5 dx, \\
 S_a J f(a, b) &= \frac{4}{3}(m+n-1)a^3 + \frac{1}{2}(mn-m-n+1)a^4 \\
 &\quad + \frac{2}{3}mna^6.
 \end{aligned}
 \tag{57}$$

The harmonic index is

$$\begin{aligned}
 H(G) &= 2S_a J f(a, b)|_{a=1} \\
 &= 2\left[\frac{4}{3}(m+n-1) + \frac{1}{2}(mn-m-n+1) + \frac{2}{3}mn\right], \\
 H(G) &= 2\left[\left(\frac{4}{3}-\frac{1}{2}\right)m + \left(\frac{4}{3}-\frac{1}{2}\right)n + \left(\frac{1}{2}-\frac{4}{3}\right) + \left(\frac{4}{3}+\frac{1}{2}\right)\right]mn, \\
 H(G) &= 2\left[\frac{5}{6}m + \frac{5}{6}n + \frac{7}{6}mn - \frac{5}{6}\right].
 \end{aligned}
 \tag{58}$$

Now, the result is

$$H(G) = \frac{5}{3}(m+n-1) + \frac{7}{3}mn. \tag{59}$$

The 3D plot of harmonic index is given in Figure 9 ( $f$  or  $u=1$  left,  $v=1$  middle, and  $w=1$  right), and we see the dependent variables of the harmonic index on the involved parameters.  $\square$

**Theorem 9.** Crystallographic structure of the graph of copper(I) oxide  $G \approx Cu_{20}[m; n]$ , where  $n; m \geq 1$ , and we have

$$S_a J D_a D_b(f(a, b)) = \frac{44}{3}mn - \frac{4}{3}(m+n-1). \tag{60}$$

*Proof.* suppose

$$\begin{aligned}
 M(G; a; b) &= (4m+4n-4) \times ab^2 + (4mn-4m-4n+4) \\
 &\quad \times a^2b^2 + (4mn) \times a^2b^4.
 \end{aligned}
 \tag{61}$$

First, we have to find  $D_b$ :



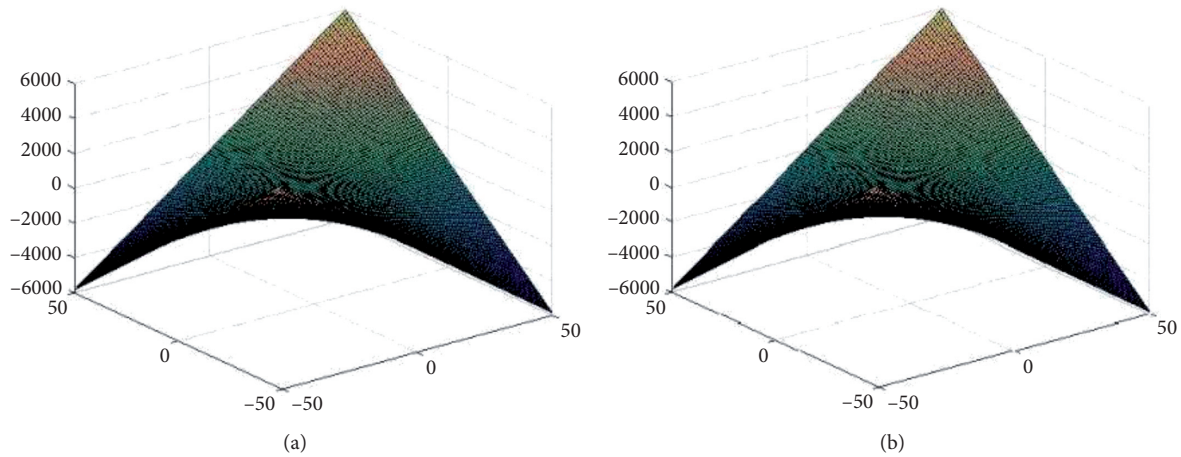


FIGURE 9: Harmonic index plotted in 3D.

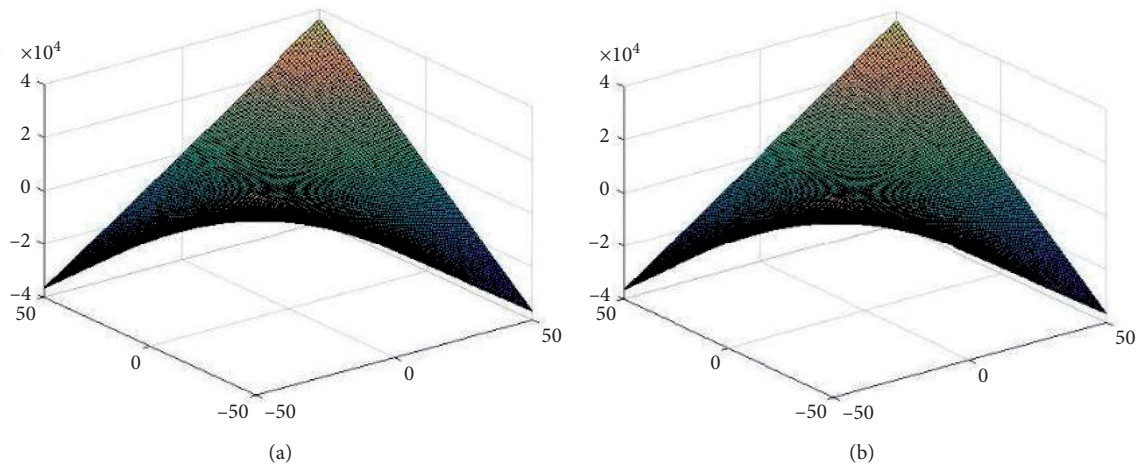


FIGURE 10: Inverse sum index plotted in 3D.

$$D_b f(a, b) = 8(m + n - 1)ab^2 + 8(mn + m + n - 1)a^2b^2 + 32mna^2b^4. \tag{62}$$

Take  $D_a$ :

$$D_a D_b f(a, b) = 8(m + n - 1)ab^2 + 16(mn - n - m + 1)a^2b^2 + 64mna^2b^4. \tag{63}$$

Take  $J_f(a; b)$ :

$$JD_a D_b f(a, b) = 8(m + n - 1)x^3 + 16(mn - m - n + 1)x^4 + 64mnx^6. \tag{64}$$

Take  $S(a)$ :

$$S_a JD_a D_b f(a, b) = \frac{8}{3}(m + n - 1)a^3 + 4(mn - n - m + 1)a^4 + \frac{32}{3}mna^6. \tag{65}$$

The inverse sum index is

$$S_a JD_a D_b (f(a, b))|_{a=1} = \frac{8}{3}(m + n - 1) + 4(mn - m - n + 1) + \frac{32}{3}mn = \left(\frac{8}{3} - 4\right)m + \left(\frac{8}{3} - 4\right)n + \left(\frac{32}{3} + 4\right)mn + \left(4 - \frac{8}{3}\right). \tag{66}$$

After the calculation, the result is

$$S_a J D_a D_b (f(a, b)) = \frac{44}{3} mn - \frac{4}{3} (m + n - 1). \quad (67)$$

The 3D plot of inverse sum index is given in Figure 10 ( $f$  or  $u=1$  left,  $v=1$  middle, and  $w=1$  right), and we see the dependent variables of the inverse sum index on the involved parameters.  $\square$

## Data Availability

No data were used in this study.

## Disclosure

All authors have not any fund, grant, and sponsor for supporting publication charges.

## Conflicts of Interest

The authors declare that there are no conflicts of interest regarding the publication of this paper.

## References

- [1] A. Q. Baig, M. Naeem, M. Naeem, W. Gao, and J.-B. Liu, "General fifth M-Zagreb indices and fifth M-Zagreb polynomials of carbon graphite," *Eurasian Chemical Communications*, vol. 2, no. 3, pp. 634–640, 2020.
- [2] F. A. Cotton, G. Wilkinson, C. A. Murillo, and M. Bochmann, *Advanced Inorganic Chemistry*, John Wiley & Sons, Hoboken, NJ, USA, 6th edition, 1999.
- [3] H. Deng, J. Yang, and F. Xia, "A general modeling of some vertex-degree based topological indices in benzenoid systems and phenylenes," *Computers & Mathematics with Applications*, vol. 61, no. 10, pp. 3017–3023, 2011.
- [4] W. Gao, Y. Wang, B. Basavanagoud, and M. K. Jamil, "Characteristics studies of molecular structures in drugs," *Saudi Pharmaceutical Journal*, vol. 25, no. 4, pp. 580–586, 2017.
- [5] G. Gayathri, U. Priyanka, and U. Priyanka, "Degree based topological indices of zig zag chain," *Journal of Mathematics and Informatics*, vol. 11, pp. 83–93, 2017.
- [6] I. Gutman, "Some properties of the Wiener polynomial," *Graph Theory Notes N. Y.* vol. 125, pp. 13–18, 1993.
- [7] L. B. Kier and L. H. Hall, *Molecular Connectivity in Structure Activity Analysis*, Wiley, New York, NY, USA, 1986.
- [8] X. Li and Y. Shi, "A survey on the Randic index," *MATCH Communications in Mathematical and in Computer Chemistry*, vol. 59, pp. 127–156, 2008.
- [9] M. Alaeiyan, C. Natarajan, C. Natarajan, G. Sathiamoorthy, and M. R. Farahani, "The eccentric connectivity index of polycyclic aromatic hydrocarbons (PAHs)," *Eurasian Chemical Communications*, vol. 2, no. 6, pp. 646–651, 2020.
- [10] M. Cancan, S. Ediz, H. Mutee-Ur-Rehman, and D. Afzal, "M-polynomial and topological indices Poly (EThyleneAmido-Amine) dendrimers," *Journal of Information and Optimization Sciences*, vol. 41, no. 4, pp. 1117–1131, 2020.
- [11] M. Cancan, S. Ediz, S. Ediz, and M. R. Farahani, "On ve-degree atom-bond connectivity, sum-connectivity, geometric-arithmetic and harmonic indices of copper oxide," *Eurasian Chemical Communications*, vol. 2, no. 5, pp. 641–645, 2020.
- [12] M. Imran, S. A. Bokhary, S. A. U. h. Bokhary, S. Manzoor, and M. K. Siddiqui, "On molecular topological descriptors of certain families of nanostar dendrimers," *Eurasian Chemical Communications*, vol. 2, no. 6, pp. 680–687, 2020.
- [13] M. R. Farahani, "Some connectivity indices and Zagreb index of polyhex nanotubes," *Acta Chimica Slovenica*, vol. 59, pp. 779–783, 2012.
- [14] M. Randic, "Characterization of molecular branching," *Journal of the American Chemical Society*, vol. 97, no. 23, pp. 6609–6615, 1975.
- [15] B. Zhou and I. Gutman, "Relations between wiener, hyper-wiener and Zagreb indices," *Chemical Physics Letters*, vol. 394, no. 1–3, pp. 93–95, 2004.
- [16] Z. Ahmad, M. Naseem, M. Naseem, M. K. Jamil, M. F. Nadeem, and S. Wang, "Eccentric connectivity indices of titania nanotubes  $TiO_2[m; n]$ ," *Eurasian Chemical Communications*, vol. 2, no. 6, pp. 712–721, 2020.
- [17] Z. Ahmad, M. Naseem, M. Naseem, M. Kamran Jamil, M. Kamran Siddiqui, and M. Faisal Nadeem, "New results on eccentric connectivity indices of V-Phenylenic nanotube," *Eurasian Chemical Communications*, vol. 2, no. 6, pp. 663–671, 2020.
- [18] J. B. Babujee and S. Ramakrishnan, "Topological indices and new graph structures," *Applied Mathematical Sciences*, vol. 6, no. 108, pp. 5383–5401, 2012.
- [19] E. Deutsch and S. Klavžar, "M-polynomial and degree-based topological indices," *Iranian Journal of Mathematical Chemistry*, vol. 6, p. 93102, 2015.
- [20] A. A. Dobrynin, R. Entringer, and I. Gutman, "Wiener index of trees: theory and applications," *Acta Applicandae Mathematicae*, vol. 66, no. 3, pp. 211–249, 2001.
- [21] D. Dimitrov, "On structural properties of trees with minimal atom-bond connectivity index IV: solving a conjecture about the pendent paths of length three," *Applied Mathematics and Computation*, vol. 313, pp. 418–430, 2017.
- [22] F. Afzal, M. A. Razaq, M. Abdul Razaq, D. Afzal, and S. Hameed, "Weighted entropy of penta chains graph," *Eurasian Chemical Communications*, vol. 2, no. 6, pp. 652–662, 2020.
- [23] I. Gutman and B. Furtula, *Recent Results in the Theory of Randić Index*, University of Kragujevac, Kragujevac, Serbia, 2008.
- [24] L. B. Kier and L. H. Hall, *Molecular Connectivity in Chemistry and Drug Research*, Academic Press, New York, NY, USA, 1976.
- [25] M. S. Ahmad, W. Nazeer, S. M. Kang, M. Imran, and W. Gao, "Calculating degree-based topological indices of dominating David derived networks," *Open Physics*, vol. 15, no. 1, pp. 1015–1021, 2017.
- [26] A. Q. Baig, M. Imran, W. Khalid, and M. Naeem, "Molecular description of carbon graphite and crystal cubic carbon structures," *Canadian Journal of Chemistry*, vol. 95, no. 6, p. 674, 2017.
- [27] F. M. Brückler, T. Došlić, A. Graovac, and I. Gutman, "On a class of distance-based molecular structure descriptors," *Chemical Physics Letters*, vol. 503, no. 4–6, pp. 336–338, 2011.
- [28] E. A. Ekimov, V. A. Sidorov, E. D. Bauer, N. N. Melnik, N. J. Curro, and J. D. Thompson, "Superconductivity in diamond," *Nature*, vol. 428, p. 5425, 2004.
- [29] F. Afzal, S. Hussain, D. Afzal, and S. Razaq, "Some new degree based topological indices via M-polynomial," *Journal of Information and Optimization Sciences*, vol. 41, no. 4, pp. 1061–1076, 2020.

- [30] W. Gao, Z. Iqbal, M. Ishaq, R. Sarfraz, M. Aamir, and A. Aslam, "On eccentricity-based topological indices study of a class of porphyrin-cored dendrimers," *Biomolecules*, vol. 8, no. 3, p. 71, 2018.
- [31] W. Gao, H. Wu, M. K. Siddiqui, and A. Q. Baig, "Study of biological networks using graph theory," *Saudi Journal of Biological Sciences*, vol. 25, no. 6, pp. 1212–1219, 2018.
- [32] Y. Hu, X. Li, Y. Shi, T. Xu, and I. Gutman, "On molecular graphs with smallest and greatest zeroth-order general Randić index," *MATCH Communications in Mathematical and in Computer Chemistry*, vol. 54, p. 425, 2005.
- [33] H. Yang and X. Zhang, "The independent domination numbers of strong product of two cycles," *Journal of Discrete Mathematical Sciences and Cryptography*, vol. 21, no. 7-8, pp. 1495–1507, 2018.
- [34] O. Ivanciuc, "Chemical graphs, molecular matrices and topological indices in chemoinformatics and quantitative structure-activity relationships," *Current Computer Aided-Drug Design*, vol. 9, no. 2, pp. 153–163, 2013.
- [35] S. M. Kang, M. A. Zahid, A. u. R. Virk, W. Nazeer, and W. Gao, "Calculating the degree-based topological indices of dendrimers," *Open Chemistry*, vol. 16, no. 1, pp. 681–688, 2018.
- [36] G. Caporossi, I. Gutman, P. Hansen, and L. Pavlović, "Graphs with maximum connectivity index," *Computational Biology and Chemistry*, vol. 27, no. 1, pp. 85–90, 2003.

## Research Article

# Topological Indices of Derived Networks of Benzene Ring Embedded in $P$ -Type Surface on $2D$

Feng Yin,<sup>1</sup> Muhammad Numan,<sup>2</sup> Saad Ihsan Butt ,<sup>3</sup> Adnan Aslam ,<sup>4</sup> and Andleeb Kausar<sup>2</sup>

<sup>1</sup>Suzhou Vocational Technical College, Suzhou, China

<sup>2</sup>Department of Mathematics, COMSATS University Islamabad, Attock Campus, Attock, Pakistan

<sup>3</sup>Department of Mathematics, COMSATS University Islamabad, Lahore Campus, Lahore, Pakistan

<sup>4</sup>Department of Natural Sciences, University of Engineering and Technology, Lahore, Pakistan

Correspondence should be addressed to Adnan Aslam; [adnanaslam15@yahoo.com](mailto:adnanaslam15@yahoo.com)

Received 20 December 2020; Accepted 27 January 2021; Published 9 February 2021

Academic Editor: Teodorico C. Ramalho

Copyright © 2021 Feng Yin et al. This is an open access article distributed under the Creative Commons Attribution License, which permits unrestricted use, distribution, and reproduction in any medium, provided the original work is properly cited.

Topological index (TI) is a numerical number assigned to the molecular structure that is used for correlation analysis in pharmacology, toxicology, and theoretical and environmental chemistry. Benzene ring embedded in the  $P$ -type surface on  $2D$  network has stability similar to  $C_{60}$  and can be defined as  $3D$  linkage of  $C_8$  rings. This structure is the simplest possible tiling of the periodic minimal surface  $P$  which contains one type of carbon atom. In this paper, we compute general Randić, general Zagreb, general sum-connectivity, first Zagreb, second Zagreb, and  $ABC$  and  $GA$  indices of two operations (simple medial and stellation) of  $2D$  network of benzene ring. Also, the exact expressions of  $ABC_4$  and  $GA_5$  indices of these structures are computed.

## 1. Introduction and Preliminaries

All the graphs in this work are finite and connected. Let  $\mathcal{H}$  be a graph with vertex set and edge set denoted by  $V(\mathcal{H})$  and  $E(\mathcal{H})$ , respectively. We denote the degree of a vertex  $\mathbf{u} \in V(G)$  by  $d_{\mathbf{u}}$  and it is the number of edges incident to  $\mathbf{u}$ . The neighbor of a vertex  $\mathbf{v}$  is a vertex  $\mathbf{u}$  such that  $\mathbf{u}\mathbf{v} \in E(G)$ . The neighborhood of a vertex  $\mathbf{u}$  is the set of all its neighbors and is denoted by  $\mathcal{N}(\mathbf{u})$ . Let  $S_{\mathbf{u}}$  be the sum of degrees of all the vertices that are adjacent to  $\mathbf{u}$ . In other words,

$$S(\mathbf{u}) = \sum_{\mathbf{v} \in \mathcal{N}(\mathbf{u})} d_{\mathbf{v}}, \quad \text{where } \mathcal{N}(\mathbf{u}) = \{\mathbf{v} \in V(\mathcal{H}) : \mathbf{u}\mathbf{v} \in E(\mathcal{H})\}. \quad (1)$$

For more insight on basic definitions and terminologies of graph theory, see [1].

In this paper, we consider two operations, stellation and simple medial of  $2D$  network of benzene ring. The medial of a graph  $\mathcal{H}$ , denoted by  $M(\mathcal{H})$ , is defined as follows: we put a new vertex in the middle of every old edge of  $\mathcal{H}$  and the new vertices have an edge if they lie on the consecutive edges.

Note that the medial of a graph  $\mathcal{H}$  is a 4-regular planar graph and not necessarily simple. Sjostrand [2] introduced the idea of transforming the graph with multiple edges and loops in to a simple graph by finite sequence of double edge swaps. If  $M(\mathcal{H})$  is not simple, we transform the graph into simple graph and call it the simple medial of  $\mathcal{H}$ , denoted by  $SM(\mathcal{H})$ . Stellation of a graph planar  $\mathcal{H}$ , denoted as  $St(\mathcal{H})$ , is obtained by putting a vertex in every face of  $\mathcal{H}$  and then we join this vertex to each vertex of respective face.

In the last couple of decades, topological and graph theoretical models have shown applications in many scientific research areas such as theoretical physics, chemistry, pharmaceutical chemistry, and toxicology. The interaction of graph theory with chemistry has enriched both the field. Topological index/descriptor is a numerical number attached to a molecular graph which is expected to predict certain physical or chemical properties of the underlying molecular structure. The simplest topological descriptors one can attach to a graph  $\mathcal{H}$  is its order and size. The importance of the topological indices is because of their use in quantitative structure activity relationship (QSAR)/

quantitative structure property relationship (QSPR). The first topological index was introduced by Wiener in 1947, who showed that the index is well correlated with boiling point of alkanes. In 1975, the first degree based topological index was proposed by Milan Randić [3]. After that many degree-based topological indices were defined which were found to be useful in modeling the properties of organic molecules. Few of the important degree-based topological indices are presented in Table 1.

The Randić index was first named as branching index and is found appropriate for calculating the extent of branching of the carbon atom skeleton of saturated hydrocarbons. The first and second Zagreb indices were first introduced by Gutman and Transjistic in [8] and applied to branching problem. The Zagreb indices and their different variants are used to study chirality [16], molecular complexity [17, 18], ZE isomerism [19], and heterosystems [20]. The overall Zagreb indices are used to derive multilinear regression models. The importance of ABC index is due to its correlation with the thermodynamic properties of alkanes, see [21, 22]. Details on the computation of topological indices of graphs can be seen in [23–25].

## 2. Topological Indices of Simple Medial of $P[m, n]$

The preparation [26] of  $C_{60}$  leads to assumption about the stability of other crystalline forms of three coordinated carbons. In particular, Mackay and Terrones [27] raised the interesting prospect of creating possible tricoordinated solid carbon forms by lining the infinite periodic minimal surfaces known as  $P$  and  $D$ . These surfaces divide the space into two unconnected labyrinths. O’Keeffe et al. [28] reported the results of initial calculations of molecular dynamic relaxation in the simplest treatment, which contains only one type of carbon atom. These structures contain six- and eight-membered rings in ratio of 2 : 3 and their primitive single cells have only 24 atoms. The stability of this structure is similar to  $C_{60}$  and it can be defined as a three-dimensional connection of  $C_8$  rings. This structure is the simplest possible treatment of the periodic minimum surface  $P$ , which has only one type of carbon atom. From now onward, we denote the molecular structure of 2D network of benzene ring embedded in  $P$ -type surface by  $P[m, n]$ . Figure 1 depicts the molecular graph of  $P[m, n]$ .

Note that  $P[m, n]$  contains  $24mn$  vertices and  $32mn - 2m - 2n$  edges. The medial of  $P[m, n]$  is obtained as follows:

we put a new vertex in the middle of every old edge of  $P[m, n]$  and the new vertices have an edge if they lie on the consecutive edges. The graph of medial of  $P[m, n]$  is depicted in Figure 2. Observe that the graph of medial of  $P[m, n]$  contains multiple edges. It can be made simple by using the double edge swaps defined by Sjostrand [2]. Figure 3 depicts the graph of simple medial of  $P[m, n]$  and we denote it by  $SM(P[m, n])$ . By a simple calculation, we can compute that  $SM(P[m, n])$  contains  $32mn - 2m - 2n$  vertices and  $64mn - 20m - 20n + 12$  edges. Suppose  $V_i = \{\mathbf{u} \in V(SM(P[m, n])) : d_{\mathbf{u}} = i\}$  and  $E_{i,j} = \{\mathbf{u}\mathbf{v} \in E(SM(P[m, n])) : d_{\mathbf{u}} = i, d_{\mathbf{v}} = j\}$ . Let  $n_i$  and  $e_{i,j}$  be the cardinalities of  $V_i$  and  $E_{i,j}$ , respectively.

**Theorem 1.** Let  $\mathcal{K}$  be the graph of  $SM(P[m, n])$  and  $\alpha$  is a real number, then we have

- (1)  $M_{\alpha}(\mathcal{K}) = (16m + 16n - 12)2^{\alpha} + (32mn - 18m - 18n + 12)4^{\alpha}$ ,
- (2)  $R_{\alpha}(\mathcal{K}) = (4m + 4n)2^{2\alpha} + (24m + 24n - 24)2^{3\alpha} + (64mn - 48m - 48n + 36)2^{4\alpha}$ ,
- (3)  $\chi_{\alpha}(\mathcal{K}) = (4m + 4n)2^{2\alpha} + (24m + 24n - 24)6^{\alpha} + (64mn - 48m - 48n + 36)2^{3\alpha}$ ,
- (4)  $ABC(\mathcal{K}) = (1/\sqrt{2})(28m + 28n - 24) + (1/2)\sqrt{(3/2)}(64mn - 48m - 48n + 36)$ ,
- (5)  $GA(\mathcal{K}) = (4m + 4n) + (\sqrt{2}/3)(24m + 24n - 24) + (64mn - 48m - 48n + 36)$ ,
- (6)  $PM_1(\mathcal{K}) = 2^{192mn - 136m - 136n + 108} \times 6^{24m + 24n - 24}$ , and
- (7)  $PM_2(\mathcal{K}) = 2^{256mn - 112m - 112n + 72}$ .

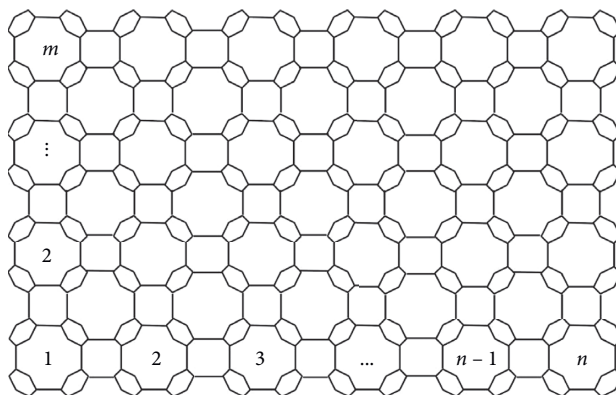
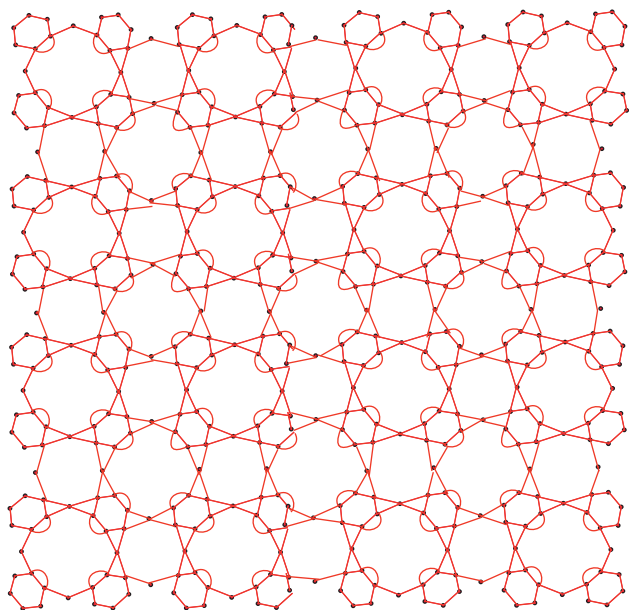
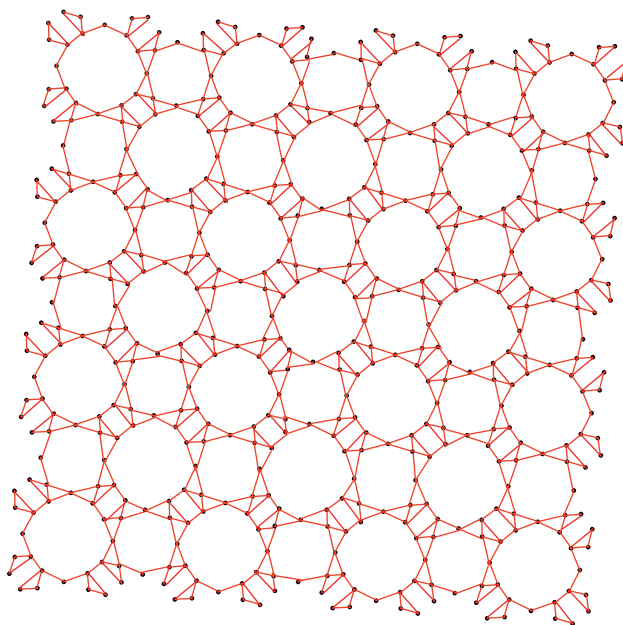
*Proof.* We can partition  $V(\mathcal{K})$  into three sets based on vertex degrees. Table 2 shows this partition. By using the values presented in Table 2, the general Zagreb index of  $\mathcal{K}$  can be computed as follows:

$$\begin{aligned} M_{\alpha}(\mathcal{K}) &= \sum_{\mathbf{u} \in V(\mathcal{K})} (d_{\mathbf{u}})^{\alpha} \\ &= (16m + 16n - 12)2^{\alpha} + (32mn - 18m - 18n + 12)4^{\alpha}. \end{aligned} \quad (2)$$

Similarly, we can partition  $E(\mathcal{K})$  into three sets based on the degree of end vertices of each edge. Table 3 shows this partition. By using the values presented in Table 3, the values of  $R_{\alpha}, \chi_{\alpha}, ABC, GA, PM_1$ , and  $PM_2$  indices of  $\mathcal{K}$  can be computed as

TABLE 1: Degree-based topological descriptors.

Topological descriptors	Mathematical forms
General Randić index [4,5]	$R_\alpha(\mathcal{H}) = \sum_{uv \in E(\mathcal{H})} (d_u d_v)^\alpha$
General sum-connectivity index [6]	$\chi_\alpha(\mathcal{H}) = \sum_{uv \in E(\mathcal{H})} (d_u + d_v)^\alpha$
First general Zagreb index [7]	$M_\alpha(\mathcal{H}) = \sum_{u \in V(\mathcal{H})} (d_u)^\alpha$
Randić index [3]	$R_{(-1/2)}(\mathcal{H}) = \sum_{uv \in E(\mathcal{H})} (1/\sqrt{d_u d_v})$
First Zagreb index [8]	$M_1(\mathcal{H}) = \sum_{uv \in E(\mathcal{H})} (d_u + d_v)$
Second Zagreb index [8]	$M_2(\mathcal{H}) = \sum_{uv \in E(\mathcal{H})} (d_u \times d_v)$
First multiplicative Zagreb index [9]	$PM_1(\mathcal{H}) = \prod_{uv \in E(\mathcal{H})} (d_u + d_v)$
Second multiplicative Zagreb index [10]	$PM_2(\mathcal{H}) = \prod_{uv \in E(\mathcal{H})} (d_u d_v)$
Hyper-Zagreb index [11]	$HM(\mathcal{H}) = \sum_{uv \in E(\mathcal{H})} (d_u + d_v)^2$
Atom-bond connectivity index [12]	$ABC(\mathcal{H}) = \sum_{uv \in E(\mathcal{H})} \sqrt{(d_u + d_v - 2)/(d_u d_v)}$
Geometric arithmetic index [13]	$GA(\mathcal{H}) = \sum_{uv \in E(\mathcal{H})} ((2\sqrt{d_u d_v})/(d_u + d_v))$
Fourth version of atom-bond connectivity index [14]	$ABC_4(\mathcal{H}) = \sum_{uv \in E(\mathcal{H})} \sqrt{((S(\mathbf{u}) + S(\mathbf{v}) - 2)/(S(\mathbf{u})S(\mathbf{v})))}$
Fifth version of geometric arithmetic index [15]	$GA_5(\mathcal{H}) = \sum_{uv \in E(\mathcal{H})} ((2\sqrt{S(\mathbf{u})S(\mathbf{v})})/(S(\mathbf{u}) + S(\mathbf{v})))$

FIGURE 1: Graph of  $P[m, n]$ .FIGURE 2: Molecular graph of medial of  $P[m, n]$ .FIGURE 3: Molecular graph  $SM(P[m, n])$  of simple medial of  $P[m, n]$ .

$$\begin{aligned}
R_\alpha(\mathcal{K}) &= \sum_{\mathbf{uv} \in E(\mathcal{K})} (d_u d_v)^\alpha \\
&= (4m + 4n)(2 \times 2)^\alpha + (24m + 24n - 24)(2 \times 4)^\alpha + (64mn - 48m - 48n + 32)(4 \times 4)^\alpha \\
&= (4m + 4n)2^{2\alpha} + (24m + 24n - 24)2^{3\alpha} + (64mn - 48m - 48n + 32)2^{4\alpha}, \\
\chi_\alpha(\mathcal{K}) &= \sum_{\mathbf{uv} \in E(\mathcal{K})} (d_u + d_v)^\alpha \\
&= (4m + 4n)(2 + 2)^\alpha + (24m + 24n - 24)(2 + 4)^\alpha + (64mn - 48m - 48n + 32)(4 + 4)^\alpha \\
&= (4m + 4n)2^{2\alpha} + (24m + 24n - 24)6^\alpha + (64mn - 48m - 48n + 32)2^{3\alpha}, \\
ABC(\mathcal{K}) &= \sum_{\mathbf{uv} \in E(\mathcal{K})} \sqrt{\frac{d_u + d_v - 2}{d_u d_v}} \\
&= (4m + 4n)\sqrt{\frac{2 + 2 - 2}{2 \times 2}} + (24m + 24n - 24)\sqrt{\frac{2 + 4 - 2}{2 \times 4}} \\
&\quad + (64mn - 48m - 48n + 32)\sqrt{\frac{4 + 4 - 2}{4 \times 4}} \\
&= \frac{1}{\sqrt{2}}(28m + 28n - 24) + \frac{1}{2}\sqrt{\frac{3}{2}}(64mn - 48m - 48n + 36), \\
GA(\mathcal{K}) &= \sum_{\mathbf{uv} \in E(\mathcal{K})} \frac{2\sqrt{d_u d_v}}{d_u + d_v} \\
&= (4m + 4n)\frac{2\sqrt{2 \times 2}}{2 + 2} + (24m + 24n - 24)\frac{2\sqrt{2 \times 4}}{2 + 4} \\
&\quad + (64mn - 48m - 48n + 32)\frac{2\sqrt{4 \times 4}}{4 + 4} \\
&= (4m + 4n) + \frac{\sqrt{2}}{3}(24m + 24n - 24) + (64mn - 48m - 48n + 36), \\
PM_1(\mathcal{K}) &= \prod_{\mathbf{uv} \in E(\mathcal{K})} (d_u + d_v) \\
&= (2 + 2)^{4m+4n} \times (2 + 4)^{24m+24n-24} \times (4 + 4)^{64mn-48m-48n+32} \\
&= 2^{192mn-136m-136n+108} \times 6^{24m+24n-24}, \\
PM_2(\mathcal{K}) &= \prod_{\mathbf{uv} \in E(\mathcal{K})} (d_u d_v) \\
&= (2 \times 2)^{4m+4n} \times (2 \times 4)^{24m+24n-24} \times (4 \times 4)^{64mn-48m-48n+32} \\
&= 2^{(256mn-112m-112n+72)}.
\end{aligned}
\tag{3}$$

□

TABLE 2: Vertex partition of  $\mathcal{K}$ .

$V_i$	2	4
$n_i$	$16m + 16n - 12$	$32mn - 18m - 18n + 12$

TABLE 3: Edge partition  $E_{i,j}$  of  $\mathcal{K}$ .

$E_{i,j}$	$E_{2,2}$	$E_{2,4}$	$E_{4,4}$
$e_{i,j}$	$4m + 4n$	$24m + 24n - 24$	$64mn - 48m - 48n + 36$

From Theorem 1, we can compute the values of Randić, first Zagreb, second Zagreb, and hyper-Zagreb index of  $\mathcal{K}$ .

**Corollary 1.** Let  $\mathcal{K}$  be the graph of simple medial of  $P[m, n]$ , then we have

$$\begin{aligned}
 (1) \ ABC_4(\mathcal{K}) &= \frac{1}{3} \sqrt{\frac{5}{2}}(4m + 4n) + \sqrt{\frac{7}{30}}(8m + 8n) + \sqrt{\frac{1}{5}}(4m + 4n) + \frac{1}{2} \sqrt{\frac{5}{7}}(4m + 4n - 8) \\
 &\quad + \frac{12}{5} \sqrt{\frac{1}{2}} + \sqrt{\frac{1}{7}}(4m + 4n - 8) + \frac{1}{2} \sqrt{\frac{13}{21}}(4m + 4n - 8) + \frac{1}{2} \sqrt{\frac{1}{2}}(4m + 4n - 8) \\
 &\quad + \sqrt{\frac{11}{70}}(4m + 4n - 8) + \frac{1}{8} \sqrt{\frac{15}{2}}(64mn - 60m - 60n + 56), \\
 (2) \ GA_5(\mathcal{K}) &= (4m + 4n) + \frac{1}{4} \sqrt{15}(8m + 8n) + \frac{4}{9} \sqrt{5}(4m + 4n) + \frac{4}{11} \sqrt{7}(4m + 4n - 8) + (4) \\
 &\quad + \frac{1}{3} \sqrt{35}(4m + 4n - 8) + \frac{2}{13} \sqrt{42}(4m + 4n - 8) + \frac{4}{7} \sqrt{3}(4m + 4n - 8) \\
 &\quad + \frac{4}{15} \sqrt{14}(4m + 4n - 8) + 64mn - 60m - 60n + 56.
 \end{aligned} \tag{4}$$

*Proof.* The edge partition of  $\mathcal{K}$  depending on the sum of degree of end vertices is presented in Table 4. The result follows by using the values from Table 4 in the definition of  $ABC_4(\mathcal{K})$  and  $GA_5(\mathcal{K})$ .  $\square$

### 3. Topological Indices of Stellation of $P[m, n]$

Let  $\mathcal{L}$  be the molecular graph of stellation of  $P[m, n]$ . It is obtained adding a vertex in each face of  $P[m, n]$  and then joining this vertex to each vertex of the respective face. The graph of  $\mathcal{L}$  is shown in Figure 4. In  $\mathcal{L}$ , there are  $32mn - 2n + 1$  vertices and  $96mn - 22m - 22n + 12$  edges. Suppose  $V_i = \{\mathbf{u} \in V(\mathcal{L}): d_{\mathbf{u}} = i\}$  and  $E_{i,j} = \{\mathbf{u}\mathbf{v} \in E(\mathcal{L}): d_{\mathbf{u}} = i, d_{\mathbf{v}} = j\}$ . Let  $n_i$  and  $e_{i,j}$  be the cardinalities of the vertex set  $V_i$  and edge set  $E_{i,j}$ , respectively.

**Theorem 3.** Let  $\mathcal{L}$  be the graph of stellation of  $P[m, n]$  and  $\alpha$  is a real number, then we have

$$\begin{aligned}
 (1) \ M_\alpha(\mathcal{L}) &= (8m + 8n - 4)3^\alpha + (8mn - 4m - 4n + 4)4^\alpha + (8m + 8n - 8)5^\alpha + (20mn - 12m - 12n + 8)6^\alpha \\
 &\quad + (2mn - 6m - 6n)8^\alpha + (2mn - m - n + 1)12^\alpha, \\
 (2) \ R_\alpha(\mathcal{L}) &= (4m + 4n)3^{2\alpha} + (8m + 8n - 8)15^\alpha + (8m + 8n - 4)18^\alpha + (4m + 4n)20^\alpha + (24mn - 16m - 16n + 12)24^\alpha + (24mn - 16m - 16n + 12)48^\alpha + (4m + 4n -
 \end{aligned}$$

$$\begin{aligned}
 (1) \ R_{(-1/2)}(\mathcal{K}) &= ((4m + 4n)/2) + ((24m + 24n - 24)/(2\sqrt{2})) + (((64mn - 48m - 48n + 36))/4), \\
 (2) \ M_1(\mathcal{K}) &= 512mn - 224(m + n) + 144, \\
 (3) \ M_2(\mathcal{K}) &= 1024mn - 560(m + n) + 384, \text{ and} \\
 (4) \ HM(\mathcal{K}) &= 4096mn - 2144(m + n) + 1440.
 \end{aligned}$$

Next, we will compute the  $ABC_4$  and  $GA_5$  indices of  $\mathcal{K}$ . For this, we need to find the edge partition  $S_{i,j}$  of the graph  $\mathcal{K}$ , where  $S_{i,j} = \{\mathbf{u}\mathbf{v} \in E(\mathcal{K}): S_{\mathbf{u}} = i, S_{\mathbf{v}} = j\}$ . Let  $m_{i,j}$  denote the cardinality of the set  $S_{i,j}$ . The edge partition  $S_{i,j}$  of  $\mathcal{K}$  is given in Table 4.

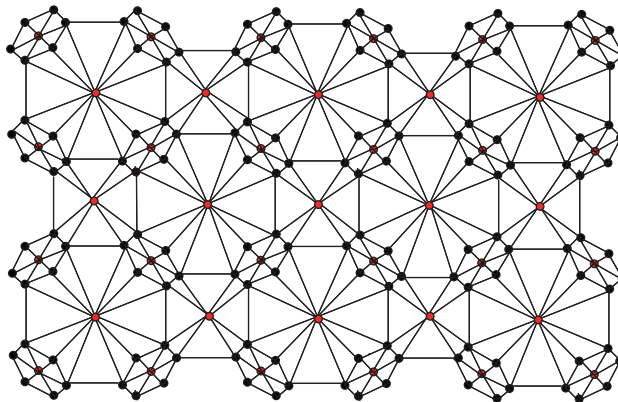
**Theorem 2.** Let  $\mathcal{K}$  be the graph of simple medial of  $P[m, n]$ , then we have

$$\begin{aligned}
 &4)5^{2\alpha} + (12m + 12n - 16)30^\alpha + (4m + 4n - 8)40^\alpha + (4m + 4n)60^\alpha + (32mn - 26m - 26n + 20)6^{2\alpha} + (16mn - 12m - 12n + 8)72^\alpha, \\
 (3) \ \chi_\alpha(\mathcal{L}) &= (4m + 4n)6^\alpha + (8m + 8n - 8)8^\alpha + (12m + 12n - 4)3^{2\alpha} + (24mn - 16m - 16n + 12)10^\alpha + (8mn - 4m - 4n + 4)16^\alpha + (4m + 4n - 4)10^\alpha + (12m + 12n - 16)11^\alpha + (4m + 4n - 8)13^\alpha + (4m + 4n)17^\alpha + (32mn - 26m - 26n + 20)12^\alpha + (16mn - 12m - 12n + 8)14^\alpha + (16mn - 12m - 12n + 8)18^\alpha, \\
 (4) \ ABC(\mathcal{L}) &= (((24\sqrt{3} + 2\sqrt{42} + 16\sqrt{10} + 16\sqrt{2})/3) + 8)mn + (((4\sqrt{14} - 16\sqrt{3} - \sqrt{42} - 13\sqrt{10} - 4)/3) + ((8\sqrt{10} + 2\sqrt{35} + 6\sqrt{30} + \sqrt{110} - 12\sqrt{2})/5))(m + n) + (((-2\sqrt{14} + 12\sqrt{3} + 10\sqrt{10} + \sqrt{42} + 8\sqrt{2})/3) + ((-8\sqrt{2} - 8\sqrt{30} - 2\sqrt{110} - 8\sqrt{10})/5) + 4), \\
 (5) \ GA(\mathcal{L}) &= (32 + ((48\sqrt{6})/5) + ((32\sqrt{2})/3) + ((92\sqrt{3})/7))mn + (((16\sqrt{5})/9) - ((32\sqrt{6})/5) + ((24\sqrt{30})/11) + ((16\sqrt{10})/13) - ((8\sqrt{2})/3) + ((50\sqrt{15})/17) - ((62\sqrt{3})/7))(m + n) + (((24\sqrt{6})/5) - ((32\sqrt{30})/11) - (32\sqrt{10}/13) + ((8\sqrt{2})/3) + ((46\sqrt{3})/7) - 2\sqrt{15}), \\
 (6) \ PM_1(\mathcal{L}) &= 2^{(152mn - 76m - 76n + 56)} \times 3^{(64mn - 22m - 22n + 28)} \times 5^{(24mn - 12m - 12n + 8)} \times 7^{(16mn - 12m - 12n + 8)} \times 11^{(12m + 12n - 16)} \times 13^{(4m + 4n - 8)} \times 17^{(4m + 4n)}, \text{ and}
 \end{aligned}$$



TABLE 4: Edge partition  $S_{i,j}$  of  $\mathcal{X}$ .

$S_{i,j}$	$S_{6,6}$	$S_{6,10}$	$S_{8,10}$	$S_{8,12}$	$S_{8,14}$	$S_{10,10}$
$m_{i,j}$	$4m + 4n$	$8m + 8n$	$4m + 4n$	$4m + 4n - 8$	$4m + 4n - 8$	4
$S_{i,j}$	$S_{10,14}$	$S_{12,14}$	$S_{12,16}$	$S_{14,16}$	$S_{16,16}$	
$m_{i,j}$	$4m + 4n - 8$	$4m + 4n - 8$	$4m + 4n - 8$	$4m + 4n - 8$	$64mn - 60m - 60n + 56$	

FIGURE 4: Molecular graph of  $st(P[m, n])$ .

$$(7) PM_2(\mathcal{L}) = 2^{(216mn-100m-100n+64)} \times 3^{(144mn-60m-60n+48)} \times 5^{(40m+40n-40)}.$$

*Proof.* We can partition  $V(\mathcal{L})$  into six sets based on vertex degrees. Table 5 shows this partition. By using the values presented in Table 5, the general Zagreb index of  $\mathcal{L}$  can be computed as

$$\begin{aligned}
 M_\alpha(\mathcal{L}) &= \sum_{u \in V(\mathcal{L})} (d_u)^\alpha \\
 &= (8m + 8n - 4)3^\alpha + (8mn - 4m - 4n + 4)4^\alpha + (8m + 8n - 4)5^\alpha \\
 &\quad + (20mn - 12m - 12n + 8)6^\alpha + (2mn - m - n)8^\alpha + (2mn - m - n + 1)12^\alpha.
 \end{aligned} \tag{5}$$

Similarly, we can partition  $E(\mathcal{L})$  into three sets based on the degree of end vertices of each edge. Table 6 shows this partition.

By using the values presented in Table 6, the values of  $R_\alpha$ ,  $\chi_\alpha$ ,  $ABC$ ,  $GA$ ,  $PM_1$ , and  $PM_2$  indices of  $\mathcal{L}$  can be computed as

$$\begin{aligned}
 R_\alpha(\mathcal{L}) &= \sum_{uv \in E(\mathcal{L})} (d_u d_v)^\alpha \\
 &= (4m + 4n)(3 \times 3)^\alpha + (24mn - 16m - 16n + 12)(3 \times 5)^\alpha + (8m + 8n - 8)(3 \times 6)^\alpha \\
 &\quad + (4m + 4n)(4 \times 5)^\alpha + (8m + 8n - 8)(4 \times 6)^\alpha + (8mn - 4m - 4n + 4)(4 \times 12)^\alpha \\
 &\quad + (4m + 4n - 4)(5 \times 5)^\alpha + (12m + 12n - 16)(5 \times 6)^\alpha + (4m + 4n - 8)(5 \times 8)^\alpha \\
 &\quad + (4m + 4n)(5 \times 12)^\alpha + (32mn - 26m - 26n + 20)(6 \times 6)^\alpha \\
 &\quad + (16mn - 12m - 12n + 8)(6 \times 8)^\alpha + (16mn - 12m - 12n + 8)(6 \times 12)^\alpha \\
 &= (4m + 4n)3^{2\alpha} + (8m + 8n - 8)15^\alpha + (8m + 8n - 4)18^\alpha + (4m + 4n)20^\alpha \\
 &\quad + (24mn - 16m - 16n + 12)24^\alpha + (24mn - 16m - 16n + 12)48^\alpha + (4m + 4n - 4)5^{2\alpha} \\
 &\quad + (12m + 12n - 16)30^\alpha + (4m + 4n - 8)40^\alpha + (4m + 4n)60^\alpha \\
 &\quad + (32mn - 26m - 26n + 20)6^{2\alpha} + (16mn - 12m - 12n + 8)72^\alpha.
 \end{aligned}$$

$$\begin{aligned}
\chi_\alpha(\mathcal{L}) &= \sum_{uv \in E(\mathcal{L})} (d_u + d_v)^\alpha \\
&= (4m + 4n)(3 + 3)^\alpha (24mn - 16m - 16n + 12)(3 + 5)^\alpha + (8m + 8n - 8)(3 + 6)^\alpha \\
&\quad + (4m + 4n)(4 + 5)^\alpha + (8m + 8n - 8)(4 + 6)^\alpha + (8mn - 4m - 4n + 4)(4 + 12)^\alpha \\
&\quad + (4m + 4n - 4)(5 + 5)^\alpha + (12m + 12n - 16)(5 + 6)^\alpha + (4m + 4n - 8)(5 + 8)^\alpha \\
&\quad + (4m + 4n)(5 + 12)^\alpha + (32mn - 26m - 26n + 20)(6 + 6)^\alpha \\
&\quad + (16mn - 12m - 12n + 8)(6 + 8)^\alpha + (16mn - 12m - 12n + 8)(6 + 12)^\alpha \\
&= (4m + 4n)6^\alpha + (8m + 8n - 8)8^\alpha + (12m + 12n - 4)3^{2\alpha} \\
&\quad + (24mn - 16m - 16n + 12)10^\alpha + (8mn - 4m - 4n + 4)16^\alpha + (4m + 4n - 4)10^\alpha \\
&\quad + (12m + 12n - 16)11^\alpha + (4m + 4n - 8)13^\alpha + (4m + 4n)17^\alpha \\
&\quad + (32mn - 26m - 26n + 20)12^\alpha + (16mn - 12m - 12n + 8)14^\alpha \\
&\quad + (16mn - 12m - 12n + 8)18^\alpha. \\
ABC(\mathcal{L}) &= \sum_{uv \in E(\mathcal{L})} \sqrt{\frac{d_u + d_v - 2}{d_u d_v}} \\
&= (4m + 4n)\sqrt{\frac{3 + 3 - 2}{3 \times 3}} + (24mn - 16m - 16n + 12)\sqrt{\frac{3 + 5 - 2}{3 \times 5}} \\
&\quad + (8m + 8n - 8)\sqrt{\frac{3 + 6 - 2}{3 \times 6}} + (4m + 4n)\sqrt{\frac{4 + 5 - 2}{4 \times 5}} \\
&\quad + (8m + 8n - 8)\sqrt{\frac{4 + 6 - 2}{4 \times 6}} + (8mn - 4m - 4n + 4)\sqrt{\frac{4 + 12 - 2}{4 \times 12}} \\
&\quad + (4m + 4n - 4)\sqrt{\frac{5 + 5 - 2}{5 \times 5}} + (12m + 12n - 16)\sqrt{\frac{5 + 6 - 2}{5 \times 6}} \\
&\quad + (4m + 4n - 8)\sqrt{\frac{5 + 8 - 2}{5 \times 8}} + (4m + 4n)\sqrt{\frac{5 + 12 - 2}{5 \times 12}} \\
&\quad + (32mn - 26m - 26n + 20)\sqrt{\frac{6 + 6 - 2}{6 \times 6}} + (16mn - 12m - 12n + 8)\sqrt{\frac{6 + 8 - 2}{6 \times 8}} \\
&\quad + (16mn - 12m - 12n + 8)\sqrt{\frac{6 + 12 - 2}{6 \times 12}} \\
&= \left( \frac{24\sqrt{3} + 2\sqrt{42} + 16\sqrt{10} + 16\sqrt{2}}{3} + 8 \right) mn \\
&\quad + \left( \frac{4\sqrt{14} - 16\sqrt{3} - \sqrt{42} - 13\sqrt{10} - 4}{3} + \frac{8\sqrt{10} + 2\sqrt{35} + 6\sqrt{30} + \sqrt{110} - 12\sqrt{2}}{5} \right) (m + n) \\
&\quad + \left( \frac{-2\sqrt{14} + 12\sqrt{3} + 10\sqrt{10} + \sqrt{42} + 8\sqrt{2}}{3} + \frac{-8\sqrt{2} - 8\sqrt{30} - 2\sqrt{110} - 8\sqrt{10}}{5} + 4 \right) \\
GA(\mathcal{L}) &= \sum_{uv \in E(\mathcal{L})} \frac{2\sqrt{d_u d_v}}{d_u + d_v} \\
&= (4m + 4n)\frac{2\sqrt{3 \times 3}}{3 + 3} + (24mn - 16m - 16n + 12)\frac{2\sqrt{3 \times 5}}{3 + 5} \\
&\quad + (8m + 8n - 8)\frac{2\sqrt{3 \times 6}}{3 + 6} + (4m + 4n)\frac{2\sqrt{4 \times 5}}{4 + 5} \\
&\quad + (8m + 8n - 8)\frac{2\sqrt{4 \times 6}}{4 + 6} + (8mn - 4m - 4n + 4)\frac{2\sqrt{4 \times 12}}{4 + 12} \\
&\quad + (4m + 4n - 4)\frac{2\sqrt{5 \times 5}}{5 + 5} + (12m + 12n - 16)\frac{2\sqrt{5 \times 6}}{5 + 6} \\
&\quad + (4m + 4n - 8)\frac{2\sqrt{5 \times 8}}{5 + 8} + (4m + 4n)\frac{2\sqrt{5 \times 12}}{5 + 12} \\
&\quad + (32mn - 26m - 26n + 20)\frac{2\sqrt{6 \times 6}}{6 + 6} + (16mn - 12m - 12n + 8)\frac{2\sqrt{6 \times 8}}{6 + 8} \\
&\quad + (16mn - 12m - 12n + 8)\frac{2\sqrt{6 \times 12}}{6 + 12} \\
&= \left( 32 + \frac{48\sqrt{6}}{5} + \frac{32\sqrt{2}}{3} + \frac{92\sqrt{3}}{7} \right) mn \\
&\quad + \left( \frac{16\sqrt{5}}{9} - \frac{32\sqrt{6}}{5} + \frac{24\sqrt{30}}{11} + \frac{16\sqrt{10}}{13} - \frac{8\sqrt{2}}{3} + \frac{50\sqrt{15}}{17} - \frac{62\sqrt{3}}{7} \right) (m + n) \\
&\quad + \left( \frac{24\sqrt{6}}{5} - \frac{32\sqrt{30}}{11} - \frac{32\sqrt{10}}{13} + \frac{8\sqrt{2}}{3} + \frac{46\sqrt{3}}{7} - 2\sqrt{15} \right),
\end{aligned}$$

TABLE 5: Vertex partition of  $\mathcal{L}$ .

$V_i$	3	4	5
$n_i$	$8m + 8n - 4$	$8mn - 4m - 4n + 4$	$8m + 8n - 8$
$V_i$	6	8	12
$n_i$	$20mn - 12m - 12n + 8$	$2mn - m - n$	$2mn - m - n + 1$

TABLE 6: Edge partition of  $E_{i,j}$  of  $\mathcal{L}$ .

$E_{i,j}$	$E_{3,3}$	$E_{3,5}$	$E_{3,6}$
$e_{i,j}$	$4m + 4n$	$8m + 8n - 8$	$8m + 8n - 4$
$E_{i,j}$	$E_{4,5}$	$E_{4,6}$	$E_{4,12}$
$e_{i,j}$	$4m + 4n$	$24mn - 16m - 16n + 12$	$8mn - 4m - 4n + 4$
$E_{i,j}$	$E_{5,5}$	$E_{5,6}$	$E_{5,8}$
$e_{i,j}$	$4m + 4n - 4$	$12m + 12n - 16$	$4m + 4n - 8$
$E_{i,j}$	$E_{5,12}$	$E_{6,6}$	$E_{6,8}$
$e_{i,j}$	$4m + 4n$	$32mn - 26m - 26n + 20$	$16mn - 12m - 12n + 8$
$E_{i,j}$	$E_{6,12}$		
$e_{i,j}$	$16mn - 12m - 12n + 8$		

$$\begin{aligned}
PM_1(\mathcal{L}) &= \prod_{\mathbf{uv} \in E(\mathcal{L})} (d_{\mathbf{u}} + d_{\mathbf{v}}) \\
&= (3 + 3)^{4m+4n} \times (3 + 5)^{24mn-16m-16n+12} \times (3 + 6)^{(8m+8n-8)} \\
&\quad \times (4 + 5)^{4m+4n} \times (4 + 6)^{8m+8n-8} \times (4 + 12)^{8mn-4m-4n+4} \\
&\quad \times (5 + 5)^{4m+4n-4} \times (5 + 6)^{12m+12n-16} \times (5 + 8)^{4m+4n-8} \\
&\quad \times (5 + 12)^{4m+4n} \times (6 + 6)^{32mn-26m-26n+20} \times (6 + 8)^{16mn-12m-12n+8} \\
&\quad \times (6 + 12)^{16mn-12m-12n+8} \\
&= 2^{(152mn-76m-76n+56)} \times 3^{(64mn-22m-22n+28)} \times 5^{(24mn-12m-12n+8)} \times 7^{(16mn-12m-12n+8)} \\
&\quad \times 11^{(12m+12n-16)} \times 13^{(4m+4n-8)} \times 17^{(4m+4n)}, \\
PM_2(\mathcal{L}) &= \prod_{\mathbf{uv} \in E(\mathcal{L})} (d_{\mathbf{u}} d_{\mathbf{v}}) \\
&= (3 \times 3)^{4m+4n} \times (3 \times 5)^{24mn-16m-16n+12} \times (3 \times 6)^{(8m+8n-8)} \\
&\quad \times (4 \times 5)^{4m+4n} \times (4 \times 6)^{8m+8n-8} \times (4 \times 12)^{8mn-4m-4n+4} \\
&\quad \times (5 \times 5)^{4m+4n-4} \times (5 \times 6)^{12m+12n-16} \times (5 \times 8)^{4m+4n-8} \\
&\quad \times (5 \times 12)^{4m+4n} \times (6 \times 6)^{32mn-26m-26n+20} \times (6 \times 8)^{16mn-12m-12n+8} \\
&\quad \times (6 \times 12)^{16mn-12m-12n+8} \\
&= 2^{(216mn-100m-100n+64)} \times 3^{(144mn-60m-60n+48)} \times 5^{(40m+40n-40)}. \tag{6}
\end{aligned}$$

□

From Theorem 3, we can compute the values of Randić, first Zagreb, second Zagreb, and hyper-Zagreb index of  $\mathcal{L}$ .

**Corollary 2.** Let  $\mathcal{L}$  be the graph of stellation of  $P[m, n]$ , then we have

$$\begin{aligned}
(1) R_{\alpha}(\mathcal{L}) &= (\sqrt{24} + (24/\sqrt{48}) + (16/\sqrt{72}) + (16/3)) \\
&\quad mn + ((8/\sqrt{15}) - (8/\sqrt{18}) + (4/\sqrt{20}) - (16/\sqrt{24}) \\
&\quad - (16/\sqrt{48}) + (12/\sqrt{30}) + (4/\sqrt{40}) - (4/\sqrt{60}) - \\
&\quad (12/\sqrt{72}) - (11/5))(m+n) - (8/\sqrt{15}) - (4/\sqrt{18}) -
\end{aligned}$$

$$(12/\sqrt{24}) + (12/\sqrt{48}) - (16/\sqrt{30}) - (8/\sqrt{40}) + (8/\sqrt{72}) + (12/5),$$

$$(2) M_1(\mathcal{L}) = 1372mn - 432(m+n) + 260,$$

$$(3) M_2(\mathcal{L}) = 4032mn - 1712(m+n) + 1068, \text{ and}$$

$$(4) HM(\mathcal{L}) = 17376mn - 7296(m+n) + 4740.$$

Next, we will compute the  $ABC_4$  and  $GA_5$  indices of  $\mathcal{L}$ . For this, we need to find the edge partition  $S_{i,j}$  of the graph  $\mathcal{L}$ , where  $S_{i,j} = \{\mathbf{uv} \in E(\mathcal{L}) : S_{\mathbf{u}} = i, S_{\mathbf{v}} = j\}$ . Let  $m_{i,j}$  denote

the cardinality of the set  $S_{i,j}$ . The edge partition  $S_{i,j}$  of  $\mathcal{L}$  is given in Table 7.

**Theorem 4.** Let  $\mathcal{L}$  be the graph of stellation of  $P[m, n]$ , then we have

$$\begin{aligned}
 (1) \text{ABC}_4(\mathcal{L}) &= \left( \frac{8\sqrt{82}}{21} + \frac{8\sqrt{2}}{3} + \frac{4\sqrt{42}}{7} + \frac{4\sqrt{273}}{21} + \frac{\sqrt{690}}{15} + \frac{8\sqrt{77}}{21} + 2 \right) mn + \left( \frac{2\sqrt{10}}{5} + \frac{\sqrt{58}}{15} + \frac{3\sqrt{6}}{14} + \right. \\
 &\quad \frac{4\sqrt{3458}}{91} + \frac{2\sqrt{41538}}{249} + \frac{4\sqrt{5}}{7} + \frac{2\sqrt{26}}{7} + \frac{2\sqrt{14}}{7} + \frac{2\sqrt{39962}}{377} + \frac{2\sqrt{5510}}{145} + \frac{4\sqrt{80852}}{1189} + \frac{2\sqrt{19229}}{287} + \frac{6\sqrt{130}}{65} + \\
 &\quad \frac{2\sqrt{410}}{41} + \frac{2\sqrt{160310}}{943} + \frac{12\sqrt{161}}{161} + \frac{6\sqrt{1722}}{287} - \frac{3\sqrt{82}}{7} - \frac{8\sqrt{2}}{3} - \frac{4\sqrt{42}}{7} - \frac{2\sqrt{273}}{7} - \frac{\sqrt{690}}{10} - \frac{4\sqrt{77}}{7} + \frac{2\sqrt{160022}}{899} + \\
 &\quad \left. \frac{2\sqrt{256742}}{1271} + \frac{4\sqrt{186}}{31} + \frac{4\sqrt{7378}}{217} - 2 \right) (m+n) + \left( -\frac{3\sqrt{6}}{7} - \frac{8\sqrt{3458}}{91} - \frac{8\sqrt{41538}}{483} - \frac{8\sqrt{5}}{7} - \frac{4\sqrt{26}}{7} \right. \\
 &\quad \frac{4\sqrt{14}}{7} - \frac{4\sqrt{39962}}{377} - \frac{4\sqrt{5510}}{145} - \frac{8\sqrt{80852}}{1189} - \frac{4\sqrt{19229}}{287} - \frac{12\sqrt{130}}{65} - \frac{4\sqrt{410}}{41} - \frac{4\sqrt{160310}}{943} - \frac{24\sqrt{161}}{161} \\
 &\quad \frac{12\sqrt{1722}}{287} + \frac{10\sqrt{82}}{21} + \frac{8\sqrt{2}}{3} + \frac{4\sqrt{42}}{7} + \frac{10\sqrt{273}}{21} + \frac{\sqrt{690}}{6} + \frac{16\sqrt{77}}{21} - \frac{8\sqrt{160022}}{899} - \frac{8\sqrt{256742}}{1271} - \frac{16\sqrt{186}}{31} \\
 &\quad \left. \frac{16\sqrt{7378}}{217} + \frac{8\sqrt{7}}{7} + \frac{4\sqrt{230}}{23} + \frac{8\sqrt{15}}{15} + \frac{4\sqrt{5}}{5} + \frac{4\sqrt{6765}}{205} + \frac{4\sqrt{70}}{21} + \frac{2\sqrt{253}}{23} + \frac{2\sqrt{161}}{23} + \frac{\sqrt{9030}}{105} + \frac{20\sqrt{11}}{15} + 2 \right), \\
 (2) \text{GA}_5(\mathcal{L}) &= \left( 8\frac{\sqrt{35}}{3} + \frac{128\sqrt{21}}{37} + \frac{64\sqrt{15}}{31} + \frac{128\sqrt{42}}{53} + \frac{64\sqrt{30}}{47} + \frac{64\sqrt{14}}{15} + 16 \right) mn + \left( \frac{4\sqrt{105}}{11} + \frac{4\sqrt{91}}{5} + \right. \\
 &\quad \frac{4\sqrt{483}}{11} + \frac{8\sqrt{2}}{3} + \frac{8\sqrt{182}}{27} + \frac{8\sqrt{754}}{55} + \frac{8\sqrt{870}}{59} + \frac{4\sqrt{1189}}{35} + \frac{16\sqrt{287}}{69} + \frac{2\sqrt{195}}{7} + \frac{8\sqrt{1066}}{67} + \frac{8\sqrt{1886}}{87} + \\
 &\quad \frac{8\sqrt{322}}{37} + \frac{8\sqrt{1722}}{83} - \frac{8\sqrt{35}}{3} - \frac{128\sqrt{21}}{37} - \frac{64\sqrt{15}}{31} - \frac{192\sqrt{42}}{53} - \frac{96\sqrt{30}}{47} - \frac{96\sqrt{14}}{15} + \frac{8\sqrt{1798}}{91} + \frac{8\sqrt{2542}}{103} + \\
 &\quad \left. \frac{8\sqrt{465}}{23} + \frac{8\sqrt{651}}{26} - 10 \right) (m+n) + \left( -\frac{8\sqrt{91}}{5} - \frac{8\sqrt{483}}{11} - \frac{16\sqrt{182}}{27} - \frac{16\sqrt{754}}{55} - \frac{16\sqrt{870}}{59} - \frac{8\sqrt{1189}}{35} \right. \\
 &\quad \frac{32\sqrt{287}}{69} - \frac{4\sqrt{195}}{7} - \frac{16\sqrt{1066}}{67} - \frac{16\sqrt{1886}}{87} - \frac{16\sqrt{322}}{37} - \frac{16\sqrt{1722}}{83} + \frac{8\sqrt{35}}{3} + \frac{128\sqrt{21}}{37} + \frac{64\sqrt{15}}{31} + \frac{320\sqrt{42}}{53} + \\
 &\quad \frac{160\sqrt{30}}{47} + \frac{128\sqrt{14}}{15} - \frac{32\sqrt{1798}}{91} - \frac{32\sqrt{2542}}{103} - \frac{32\sqrt{465}}{23} - \frac{16\sqrt{651}}{13} + \frac{16\sqrt{42}}{13} + \frac{16\sqrt{322}}{37} + \frac{16\sqrt{690}}{53} + \\
 &\quad \left. \frac{16\sqrt{210}}{29} + \frac{32\sqrt{435}}{89} + \frac{32\sqrt{615}}{101} + \frac{16\sqrt{70}}{17} + \frac{16\sqrt{69}}{35} + \frac{61\sqrt{161}}{51} + \frac{4\sqrt{105}}{11} + 8\sqrt{2} + 16 \right). \\
 &\quad \frac{4\sqrt{3458}}{91} + \frac{2\sqrt{41538}}{249} + \frac{4\sqrt{5}}{7} + \frac{2\sqrt{26}}{7} + \frac{2\sqrt{14}}{7} + \frac{2\sqrt{39962}}{377} + \frac{2\sqrt{5510}}{145} + \frac{4\sqrt{80852}}{1189} + \frac{2\sqrt{19229}}{287} + \frac{6\sqrt{130}}{65} + \\
 &\quad \frac{2\sqrt{410}}{41} + \frac{2\sqrt{160310}}{943} + \frac{12\sqrt{161}}{161} + \frac{6\sqrt{1722}}{287} - \frac{3\sqrt{82}}{7} - \frac{8\sqrt{2}}{3} - \frac{4\sqrt{42}}{7} - \frac{2\sqrt{273}}{7} - \frac{\sqrt{690}}{10} - \frac{4\sqrt{77}}{7} + \frac{2\sqrt{160022}}{899} + \\
 &\quad \frac{2\sqrt{256742}}{1271} + \frac{4\sqrt{186}}{31} + \frac{4\sqrt{7378}}{217} - 2) (m+n) + \left( -\frac{3\sqrt{6}}{7} - \frac{8\sqrt{3458}}{91} - \frac{8\sqrt{41538}}{483} - \frac{8\sqrt{5}}{7} - \frac{4\sqrt{26}}{7} \right. \\
 &\quad \frac{4\sqrt{14}}{7} - \frac{4\sqrt{39962}}{377} - \frac{4\sqrt{5510}}{145} - \frac{8\sqrt{80852}}{1189} - \frac{4\sqrt{19229}}{287} - \frac{12\sqrt{130}}{65} - \frac{4\sqrt{410}}{41} - \frac{4\sqrt{160310}}{943} - \frac{24\sqrt{161}}{161} \\
 &\quad \frac{12\sqrt{1722}}{287} + \frac{10\sqrt{82}}{21} + \frac{8\sqrt{2}}{3} + \frac{4\sqrt{42}}{7} + \frac{10\sqrt{273}}{21} + \frac{\sqrt{690}}{6} + \frac{16\sqrt{77}}{21} - \frac{8\sqrt{160022}}{899} - \frac{8\sqrt{256742}}{1271} - \frac{16\sqrt{186}}{31} \\
 &\quad \left. \frac{16\sqrt{7378}}{217} + \frac{8\sqrt{7}}{7} + \frac{4\sqrt{230}}{23} + \frac{8\sqrt{15}}{15} + \frac{4\sqrt{5}}{5} + \frac{4\sqrt{6765}}{205} + \frac{4\sqrt{70}}{21} + \frac{2\sqrt{253}}{23} + \frac{2\sqrt{161}}{23} + \frac{\sqrt{9030}}{105} + \frac{20\sqrt{11}}{15} + 2 \right).
 \end{aligned}$$

TABLE 7: Edge partition  $S_{i,j}$  of  $\mathcal{L}$ .

$S_{i,j}$	$S_{12,14}$	$S_{12,23}$	$S_{14,14}$	$S_{14,23}$	$S_{14,26}$
$m_{i,j}$	8	4	$4m + 4n - 8$	8	$8m + 8n - 16$
$S_{i,j}$	$S_{14,28}$	$S_{14,30}$	$S_{23,28}$	$S_{23,30}$	$S_{26,28}$
$m_{i,j}$	$4m + 4n - 8$	$4m + 4n$	4	8	$4m + 4n - 8$
$S_{i,j}$	$S_{26,29}$	$S_{26,30}$	$S_{26,41}$	$S_{28,28}$	$S_{28,30}$
$m_{i,j}$	$2m + 2n - 4$	$4m + 4n - 8$	$4m + 4n - 8$	$2m + 2n - 4$	8
$S_{i,j}$	$S_{28,41}$	$S_{28,46}$	$S_{28,60}$	$S_{29,30}$	$S_{29,41}$
$m_{i,j}$	$4m + 4n - 8$	$4m + 4n - 8$	4	$4m + 4n - 8$	$4m + 4n - 8$
$S_{i,j}$	$S_{29,60}$	$S_{29,62}$	$S_{30,30}$	$S_{30,32}$	$S_{30,42}$
$m_{i,j}$	8	$4m + 4n - 16$	$2m + 2n$	$8mn - 8m - 8n + 8$	$16mn - 16m - 16n + 16$
$S_{i,j}$	$S_{30,60}$	$S_{30,62}$	$S_{30,64}$	$S_{32,42}$	$S_{41,42}$
$m_{i,j}$	20	$8m + 8n - 32$	$8mn - 12m - 12n + 20$	$16mn - 16m - 16n + 16$	$4m + 4n - 8$
$S_{i,j}$	$S_{41,46}$	$S_{41,60}$	$S_{41,62}$	$S_{42,42}$	$S_{42,46}$
$m_{i,j}$	$4m + 4n - 8$	8	$4m + 4n - 16$	$16mn - 18m - 18n + 20$	$8m + 8n - 16$
$S_{i,j}$	$S_{42,48}$	$S_{42,60}$	$S_{42,62}$	$S_{42,64}$	
$m_{i,j}$	$16mn - 24m - 24n + 32$	8	$4m + 4n - 16$	$16mn - 24m - 24n + 40$	

*Proof.* The edge partition of  $\mathcal{L}$  depending on the sum of degree of end vertices is presented in Table 7. The result follows by using the values from Table 7 in the definition of  $ABC_4(\mathcal{L})$  and  $GA_5(\mathcal{L})$ .  $\square$

#### 4. Conclusion

In this work, we have considered two transformations (medial and stellation) on benzene ring embedded in  $P$ -type surface on 2  $D$  network. We have computed general Randić, general Zagreb, general sum-connectivity, first Zagreb, second Zagreb, first multiple Zagreb, second multiple Zagreb,  $ABC$ ,  $GA$ ,  $ABC_4$ , and  $GA_5$  indices of these transformation graphs.

#### Data Availability

No data were used in this study.

#### Conflicts of Interest

The authors declare that they have no conflicts of interest.

#### References

- [1] K. H. Rosen and K. Krithivasan, *Discrete Mathematics and its Applications: With Combinatorics and Graph Theory*, Tata McGraw-Hill Education, New York, NY, USA, 2012.
- [2] J. Sjostrand, "Making multigraphs simple by a sequence of double edge swaps," 2019, <http://arxiv.org/abs/1904.06999>.
- [3] M. Randić, "Characterization of molecular branching," *Journal of the American Chemical Society*, vol. 97, no. 23, pp. 6609–6615, 1975.
- [4] B. Bollobas and P. Erdos, "Graphs of extremal weights," *Ars Combinatoria*, vol. 50, pp. 225–233, 1998.
- [5] D. Amic, D. Beslo, B. Lucic, S. Nilolic, and N. Trinajstić, "The vertex-connectivity index revisited," *Journal of Chemical Information and Modeling*, vol. 38, pp. 819–822, 1998.
- [6] B. Zhou and N. Trinajstić, "On general sum-connectivity index," *Journal of Mathematical Chemistry*, vol. 47, no. 1, pp. 210–218, 2010.
- [7] X. Li and H. Zhao, "Trees with the first three smallest and largest generalized topological indices," *MATCH Communications in Mathematical and in Computer Chemistry*, vol. 50, pp. 57–62, 2004.
- [8] I. Gutman and N. Trinajstić, "Graph theory and molecular orbitals: total  $\phi$ -electron energy of alternant hydrocarbons," *Chemical Physics Letters*, vol. 17, no. 4, pp. 535–538, 1972.
- [9] I. Gutman, "Multiplicative Zagreb indices of trees," *Bulletin of the Veterinary Institute in Pulawy*, vol. 1, pp. 13–19, 2011.
- [10] M. Ghorbani and N. Azimi, "Note on multiple Zagreb indices," *Iranian Journal of Mathematical Chemistry*, vol. 3, pp. 137–143, 2012.
- [11] G. H. Shirdel, H. RezaPour, and A. M. Sayadi, "The hyper-Zagreb index of graph operations," *Iranian Journal of Mathematical Chemistry*, vol. 4, pp. 213–220, 2013.
- [12] E. Estrada, L. Torres, L. Rodriguez, and I. Gutman, *An Atom-Bond Connectivity Index: Modelling the Enthalpy of Formation of Alkanes*, NISCAIR-CSIR, India, 1998.
- [13] D. Vukicevic and B. Furtula, "Topological index based on the ratios of geometrical and arithmetical means of end-vertex degrees of edges," *Journal of Mathematical Chemistry*, vol. 46, no. 4, pp. 1369–1376, 2009.
- [14] M. Ghorbani and M. Hosseinzadeh, "Computing  $abc_4$  index of nanostar dendrimers," *Optoelectronics and Advanced Materials, Rapid Communications*, vol. 4, pp. 1419–1422, 2010.
- [15] Z. Du, B. Zhou, and N. Trinajstić, "On geometric-arithmetic indices of (molecular) trees, unicyclic graphs and bicyclic graphs," *MATCH Communications in Mathematical and in Computer Chemistry*, vol. 66, pp. 681–697, 2011.
- [16] M. Ghorbani and M. A. Hosseinzadeh, *Optoelectronics and Advanced Materials, Rapid Communications*, vol. 4, pp. 1419–1422, 2010.
- [17] S. H. Bertz and W. F. Wright, "The graph theory approach to synthetic analysis: Definition and application of molecular complexity and synthetic complexity," *Graph Theory Notes of New York*, vol. 35, pp. 32–48, 1998.
- [18] S. Nikoli, I. M. Toli, and N. Trinajstić, *MATCH Communications in Mathematical and in Computer Chemistry*, vol. 40, pp. 187–201, 1999.
- [19] A. Golbraikh, D. Bonchev, and A. Tropsha, "Novel ZE-isomerism descriptors derived from molecular topology and their application to QSAR analysis," *Journal of Chemical Information and Computer Sciences*, vol. 42, no. 4, pp. 769–787, 2002.

- [20] A. Miličević and S. Nikolić, "On variable zagreb indices," *Croatica Chemica Acta*, vol. 77, no. 1-2, pp. 97–101, 2004.
- [21] E. Estrada, "Atom-bond connectivity and the energetic of branched alkanes," *Chemical Physics Letters*, vol. 463, no. 4, pp. 422–425, 2008.
- [22] I. Gutman, J. Tosovic, S. Radenkovic, and S. Markovic, "On atom-bond connectivity index and its chemical applicability," *Indian Journal of Chemistry*, vol. 51A, pp. 690–694, 2012.
- [23] A. Aslam, Y. Bashir, S. Ahmad, and W. Gao, "On topological indices of certain dendrimer structures," *Zeitschrift für Naturforschung A*, vol. 72, no. 6, pp. 559–566, 2017.
- [24] A. Aslam, S. Ahmad, and W. Gao, "On certain topological indices of boron triangular nanotubes," *Zeitschrift für Naturforschung A*, vol. 72, no. 8, pp. 711–716, 2017.
- [25] A. Aslam, M. K. Jamil, W. Gao, and W. Nazeer, "Topological aspects of some dendrimer structures," *Nanotechnology Reviews*, vol. 7, no. 2, pp. 123–129, 2018.
- [26] W. Krätschmer, L. D. Lamb, K. Fostiropoulos, and D. R. Huffman, "Solid C60: a new form of carbon," *Nature*, vol. 347, no. 6291, p. 354, 1990.
- [27] A. L. Mackay and H. Terrones, "Diamond from graphite," *Nature*, vol. 352, no. 6338, p. 762, 1991.
- [28] M. O'Keeffe, G. B. Adams, and O. F. Sankey, "Predicted new low energy forms of carbon," *Physical Review Letters*, vol. 68, no. 15, pp. 23–25, 1992.

## Research Article

# Computing Analysis of Zagreb Indices for Generalized Sum Graphs under Strong Product

Muhammad Javaid <sup>1</sup>, Saira Javed <sup>1</sup>, Abdulaziz Mohammed Alanazi,<sup>2</sup>  
and Majdah R. Alotaibi<sup>3</sup>

<sup>1</sup>Department of Mathematics, School of Science, University of Management and Technology, Lahore 54770, Pakistan

<sup>2</sup>Department of Mathematics, University of Tabuk, Tabuk 71412, Saudi Arabia

<sup>3</sup>Department of Chemistry, University of Tabuk, Tabuk 71412, Saudi Arabia

Correspondence should be addressed to Muhammad Javaid; [javidmath@gmail.com](mailto:javidmath@gmail.com)

Received 29 November 2020; Revised 13 December 2020; Accepted 20 December 2020; Published 9 January 2021

Academic Editor: Muhammad Faisal Nadeem

Copyright © 2021 Muhammad Javaid et al. This is an open access article distributed under the Creative Commons Attribution License, which permits unrestricted use, distribution, and reproduction in any medium, provided the original work is properly cited.

Numerous studies based on mathematical models and tools indicate that there is a strong inherent relationship between the chemical properties of the chemical compounds and drugs with their molecular structures. In the last two decades, the graph-theoretic techniques are frequently used to analyse the various physicochemical and structural properties of the molecular graphs which play a vital role in chemical engineering and pharmaceutical industry. In this paper, we compute Zagreb indices of the generalized sum graphs in the form of the different indices of their factor graphs, where generalized sum graphs are obtained under the operations of subdivision and strong product of graphs. Moreover, the obtained results are illustrated with the help of particular classes of graphs and analysed to find the efficient subclass with dominant indices.

## 1. Introduction

In many fields (chemistry, physics, computer science, and electrical networks) various physicochemical and structural properties such as melting point, boiling point, chemical bonds, bond energy, solubility, surface tension, critical temperature, connectivity, stability, density, and polarizability are studied with the help of various TIs (degree-based, distance-based, and polynomial-based). Moreover, degree-based TIs have been used as a powerful approach to discover many new drugs, such as aneoplastics, anticonvulsants, antiallergics, antimalarials, and silico generation (see [1]). Therefore, this practice has proven that the TIs and the quantitative structure-activity (or structure-property) relationships (QSAR or QSPR) have presented a foundation stone in chemical engineering and pharmaceutical industry for the process of the drug design and discovery (see [2, 3]).

Let  $\Omega$  be a collection of (molecular) graphs in which each graph is considered as a simple graph without multiedges and loops. A topological index (TI) is a function

$Top: \Omega \rightarrow \mathbb{R}$  that assigns a real number to each element (graph) of  $\Omega$ , where  $\mathbb{R}$  is a set of real numbers. Moreover, for two graphs  $G_1$  and  $G_2$ ,  $Top(G_1) = Top(G_2)$  if and only if  $G_1$  is isomorphic to  $G_2$ . Mostly, TIs are computed for the hydrogen-suppressed molecular graphs in which the atoms are represented by nodes and bonds between them by edges. In 1947, Wiener index (path number), first distance-based TI, is utilized in the study of paraffin's boiling point [4]. Gutman and Trinajstić [5] calculated total  $\pi$ -electrons energy of the molecules through a degree-based TI called as the first Zagreb index (FZI). They also studied the various properties of the second Zagreb index (SZI) in the same paper. In chemical graph theory, many more TIs are introduced in [6], but degree-based TIs are prominent than others. For more details, we refer to [7, 8].

On the other hand, operations on graphs (addition, complement, deletion, switching, subdivision, union, intersection, and product) also play a very important role in the construction of new graphs and structures. Yan et al. [9] introduced the four operations  $S_1, R_1, Q_1$ , and  $T_1$  on the

subdivision of a graph and obtained the Wiener index of these resultant graphs  $(S_1(G), R_1(G), Q_1(G), T_1(G))$ . For  $\Phi_1 \in \{S_1, R_1, Q_1, T_1\}$ , Taeri and Eliasi [10] defined the  $\Phi_1$ -sum graphs  $(G_{1+\Phi_1} G_2)$  using the Cartesian product on graphs  $\Phi_1(G_1)$  and  $G_2$ , where  $G_1$  and  $G_2$  are connected graphs. They also studied the Wiener index of these  $\Phi_1$ -sum graphs. Liu et al. [11] constructed  $\Phi$ -sum graphs with the help of the Cartesian product on the graphs  $\Phi(G_1)$  and  $G_2$  and calculated the first general Zagreb index for these graphs, i.e.,  $M_1^\alpha((G_{1+\Phi_1} G_2))$ . Liu et al. [12] introduced the generalized  $\Phi$ -sum ( $\Phi_k$ -sum) graphs with the help of the Cartesian product on the graphs  $\Phi_k(G_1)$  and  $G_2$ , where  $k$  represents some integral value. Moreover, they calculated the mathematical expressions of the Zagreb indices for these graphs, i.e.,  $M_1((G_{1+\Phi_1} G_2))$  and  $M_2((G_{1+\Phi_1} G_2))$ . Furthermore, Awais et al. [13, 14] computed the forgotten topological and hyper-Zagreb indices of generalized  $F$ -sum graphs based on Cartesian product in terms of its factor graphs. Recently, Awais et al. [15] computed the first general Zagreb index of  $F_k$ -sum graphs in terms of TIs of their factor graphs.

In the current study, we study the generalized  $\Phi$ -sum graphs which are obtained under the operation of strong product on the graphs  $\Phi_k(G_1)$  and  $G_2$ , where  $\Phi_k \in \{S_k, R_k, Q_k, T_k\}$  and  $k$  is some counting number. Mainly, we compute the Zagreb indices of these generalized  $\Phi$ -sum graphs based on strong product such as  $M_1((G_{1\otimes\Phi_k} G_2))$  and  $M_2((G_{1\otimes\Phi_k} G_2))$ . Moreover, a comparison is also organized of the generalized  $\Phi$ -sum graphs  $(G_{1\otimes S_k} G_2)$ ,  $(G_{1\otimes R_k} G_2)$ ,  $(G_{1\otimes Q_k} G_2)$ , and  $(G_{1\otimes T_k} G_2)$  with respect to both the Zagreb indices ( $M_1$  and  $M_2$ ). The rest of the paper is settled as follows: Section 2 covers basic notions, Section 3 predicated on main results, and conclusively Section 4 included the application and conclusion."

## 2. Preliminaries

A graph  $G_1$  is a structure consisting of two finite sets of vertices  $V(G)$  and edges  $E(G)$  in which pairs of vertices are connected by edges. In particular, a graph will refer to a simple undirected graph if each edge connects two distinct vertices and there are no parallel edges. Throughout the paper, the order of  $G_1$  is  $|V(G_1)| = n_{G_1}$ , and the size of a  $G_1$  is  $|E(G_1)| = e_{G_1}$ . Given two vertices  $p$  and  $z$ , if  $pz \in G_1$ , then  $p$  and  $z$  are said to be adjacent. The strength of edges which are incident on any node  $p \in V(G_1)$  is known as its degree  $d_{G_1}(p)$  [16]. Here, we defined few topological indices.

**Definition 1.** Let  $G_1$  be a simple undirected graph. The first Zagreb index ( $M_1(G_1)$ ) and second Zagreb index ( $M_2(G_1)$ ) are:

$$M_1(G_1) = \sum_{p \in V(G_1)} [d_{G_1}(p)]^2 = \sum_{p, z \in E(G_1)} [d_{G_1}(p) + d_{G_1}(z)],$$

$$M_2(G_1) = \sum_{p, z \in E(G_1)} [d_{G_1}(p) \times d_{G_1}(z)].$$
(1)

In 1972, Trinajsti and Gutman [5] introduced these two TIs which are used in study of structure-based properties of (molecular) graphs (see [17–19]). In 1960, Sabidussi [6] introduced the strong product  $(G_1 \boxtimes G_2)$  for two graphs  $G_1$  and  $G_2$  with vertex set as Cartesian product  $V(G_1 \boxtimes G_2) = V(G_1) \times V(G_2)$  such that  $(p_1, p_2)$  and  $(z_1, z_2)$  will be adjacent in  $G_1 \boxtimes G_2$  iff  $p_1 = z_1$  and  $p_2$  is adjacent to  $z_2$  or  $p_2 = z_2$  and  $p_1$  is adjacent to  $z_1$  or  $p_1$  is adjacent to  $z_1$  and  $p_2$  is adjacent to  $z_2$ . Strong product is union of tensor product and Cartesian product.

**Definition 2.** The four generalized operations related to the subdivision of graphs defined in [15] are given as follows:

- (i)  $k$ -subdivision operation  $S_k = S_k(G_1)$  can be made by adding  $k$  new node in each  $uv \in E(G_1)$  of  $G_1$ , where  $k \geq 1$  is an integral value
- (ii)  $k$ -semitotal-point graph  $R_k = R_k(G_1)$  with node set  $V(R_k) = V(G_1) \cup kE(G_1)$  and link set  $E(R_k) = E(S_k) \cup E(G_1)$
- (iii)  $k$ -semitotal line graph  $Q_k = Q_k(G_1)$  with node set  $V(Q_k) = V(G_1) \cup kE(G_1)$  and link set  $E(Q_k) = E(S_k) \cup E(L_k)$ .
- (iv)  $k$ -total point graph  $T_k = T_k(G_1)$  with node set  $V(T_k) = V(G_1) \cup kE(G_1)$  and link set  $E(T_k) = E(S_k) \cup E(L_k) \cup E(G_1)$  (for more details, see Figure 1).

**Definition 3.** Let  $G_1$  and  $G_2$  be two graphs,  $\Phi_k \in \{S_k, R_k, Q_k, T_k\}$  is an operation, and  $\Phi_k(H_1)$  is obtained after applying  $\Phi_k$  on  $G_1$  having edge-set  $E(\Phi_k(G_1))$  and node set  $V(\Phi_k(G_1))$ . The generalized  $\Phi$ -sum graph  $(G_{1\otimes\Phi_k} G_2)$  is a graph having node set:

$$V(G_{1\otimes\Phi_k} G_2) = V(\Phi_k(G_1)) \times V(G_2) \\ = (V(G_1) \cup kE(G_1)) \times V(G_2),$$
(2)

such that two nodes  $(p_1, z_1) \& (p_2, z_2)$  of  $V(G_{1\otimes\Phi_k} G_2)$  are adjacent iff  $p_1 = p_2 \in V(G_1)$  and  $(z_1, z_2) \in E(G_2)$  or  $z_1 = z_2 \in V(G_2)$  and  $(p_1, p_2) \in E(\Phi_k(G_1))$  or  $[(z_1, z_2) \in E(G_2)$  and  $(p_1, p_2) \in E(\Phi_k(G_1))]$ , where  $k \geq 1$  is a positive number. We noticed that the generalized  $\Phi$ -sum graphs  $(G_{1\otimes\Phi_k} G_2)$  contain  $|V(G_2)|$  copies of graphs  $\Phi_k(G_1)$  that are labeled with the nodes of  $G_2$ . For more details, see Figures 2 and 3.

## 3. Main Results

Now, we will prove the key results of  $M_1(G_{1\otimes\Phi_k} G_2)$  and  $M_2(G_{1\otimes\Phi_k} G_2)$  in terms of its factor graphs  $G_1$  and  $G_2$ . We assume that  $G_1$  and  $G_2$  be two simple, undirected, and connected graphs with order and size,  $|V(G_1)| = n_{G_1}$  &  $|E(G_1)| = e_{G_1}$  and  $|V(G_2)| = n_{G_2}$  &  $|E(G_2)| = e_{G_2}$  respectively.

**Theorem 1.** Let  $G_1$  and  $G_2$  be two connected graphs such that  $|V(G_1)| \geq 3$ ,  $|V(G_2)| \geq 2$ . For  $k \geq 1$ ,



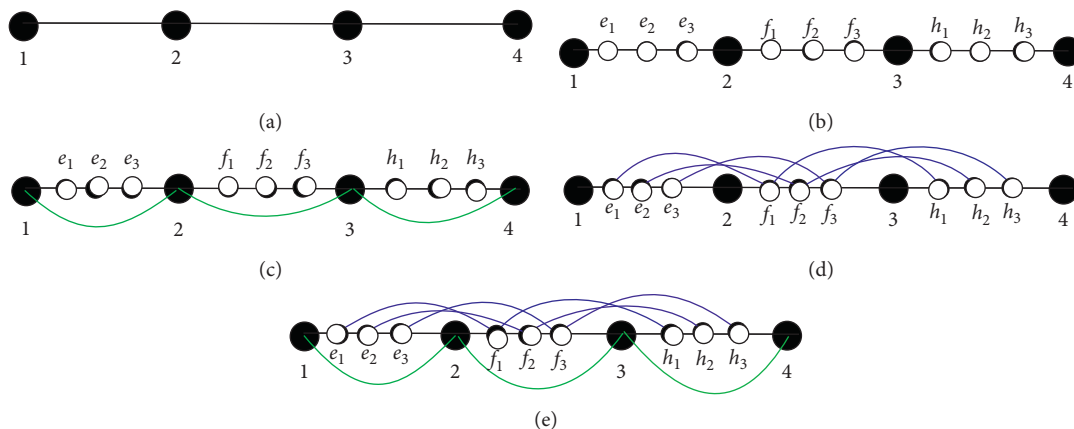


FIGURE 1: (a)  $G_1 \cong P_4$ . (b)  $S_3(G_1)$ . (c)  $R_3(GP1)$ . (d)  $Q_3(G_1)$ . (e)  $T_3(G_1)$ .

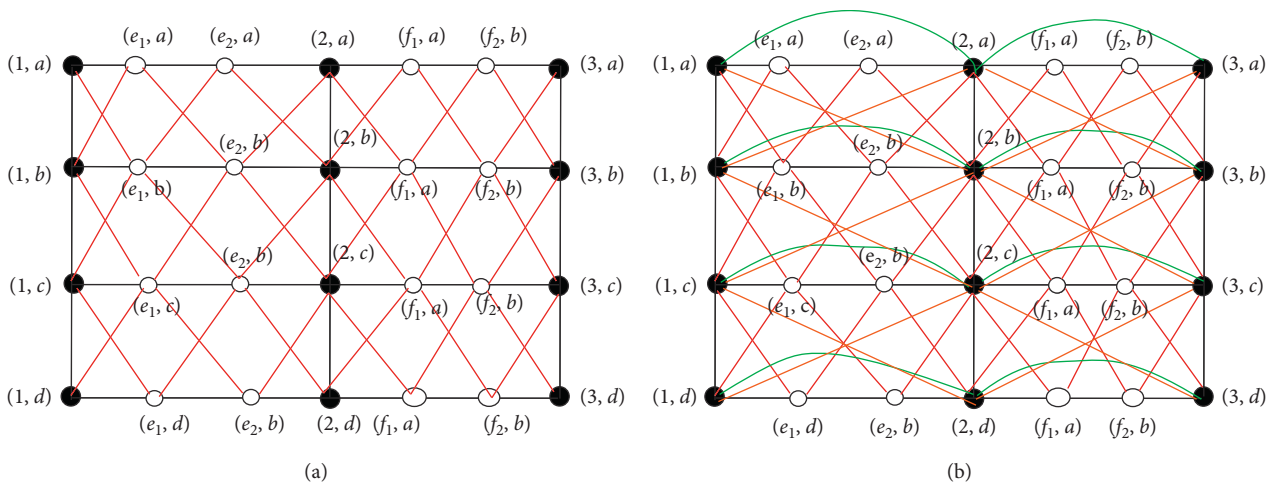


FIGURE 2: Right:  $= P_{3\otimes S_2} P_4$ . Left:  $= P_{3\otimes R_2} P_4$ .

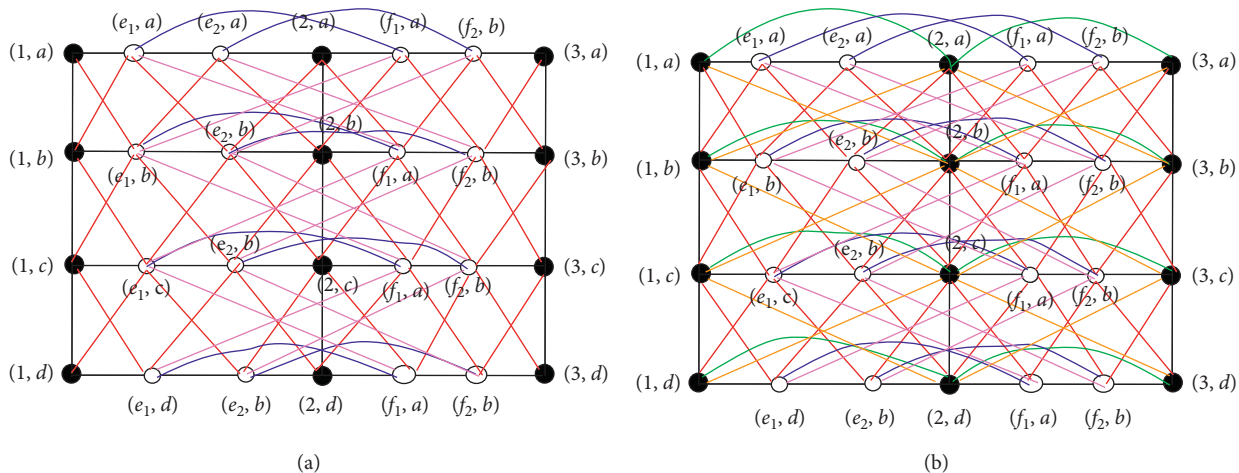


FIGURE 3: Right:  $= P_{3\otimes Q_2} P_4$ . Left:  $= P_{3\otimes T_2} P_4$ .

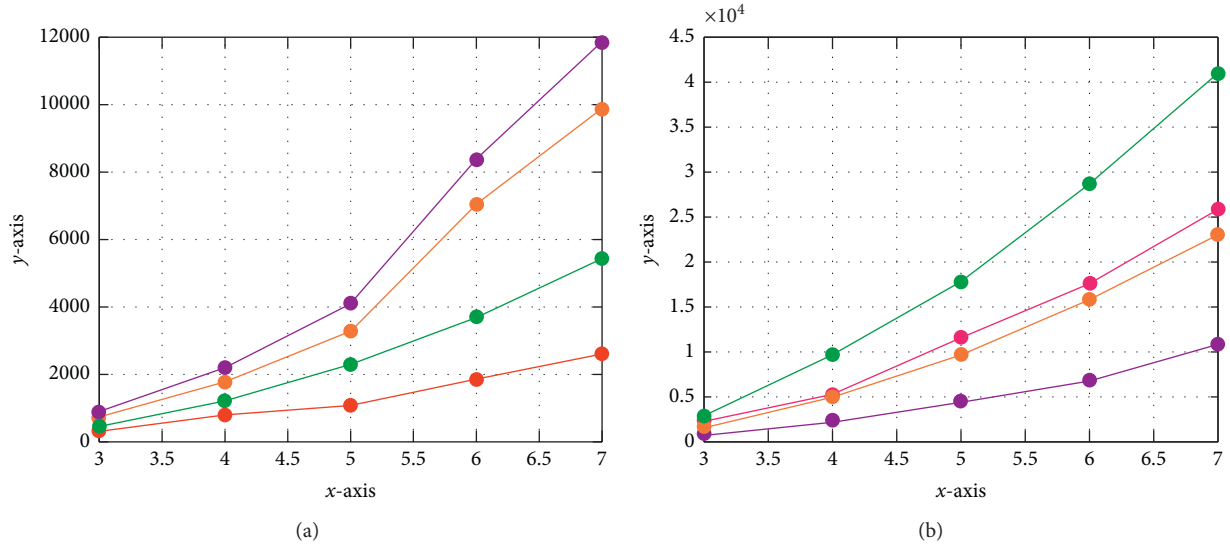


FIGURE 4: (a) Graphical representation of  $M_1(P_{n_{S_1}} \boxtimes P_m)$ ,  $M_1(P_{n_{Q_1}} \boxtimes P_m)$ ,  $M_1(P_{n_{R_1}} \boxtimes P_m)$ , and  $M_1(P_{n_{T_1}} \boxtimes P_m)$  by red, green, orange, and purple colour, respectively. (b)  $M_2(P_{n_{S_1}} \boxtimes P_m)$ ,  $M_2(P_{n_{Q_1}} \boxtimes P_m)$ ,  $M_2(P_{n_{R_1}} \boxtimes P_m)$ , and  $M_2(P_{n_{T_1}} \boxtimes P_m)$  by purple, orange, pink, and green colour, respectively.

$$\begin{aligned}
 \text{(a)} \quad M_1(G_1 \boxtimes_{S_k} G_2) &= M_1(S_1 G_1) [n_{G_2} + 2e_{G_2}] + 8(2k-1)e_{G_1}e_{G_2} + [M_1(G_1) + 4e_{G_1}] [M_1(G_2) + 2e_{G_2}] \\
 &\quad + M_1(G_2) [4e_{G_1} + n_{G_1}] + 4(k-1)e_{G_1} [n_2 + M_1(G_2)], \\
 \text{(b)} \quad M_2(G_1 \boxtimes_{S_k} G_2) &= [M_2(G_1) + 4e_{G_1}] [5e_{G_2} + 3M_1(G_2) + 2M_2(G_2) + n_{G_2}] + M_1(G_1) [e_{G_2} + M_1(G_2) + M_2(G_2)] \\
 &\quad + 4(k-1)e_{G_1} [6e_{G_2} + 3M_1(G_2) + M_2(G_2) + n_{G_2}] + M_2(G_2) [12e_{G_1} + n_{G_1}] \\
 &\quad + 8e_{G_1}e_{G_2} + M_1(G_2) [14e_{G_1}].
 \end{aligned} \tag{3}$$

*Proof.* Let  $d(p, z) = d_{G_1 \boxtimes_{S_k} G_2}(p, z)$  be the degree of a vertex  $(p, z)$  in the graph  $G_1 \boxtimes_{S_k} G_2$ .

$$\begin{aligned}
 M_1(G_1 \boxtimes_{S_k} G_2) &= \sum_{(p,z) \in V(G_1 \boxtimes_{S_k} G_2)} d^2(p, z) = \sum_{(p_1, z_1), (p_2, z_2) \in E(G_1 \boxtimes_{S_k} G_2)} [d(p_1, z_1) + d(p_2, z_2)] \\
 &= \sum_{p \in V(G_1)} \sum_{z_1, p_2 \in E(G_2)} [d(p, z_1) + d(p, z_2)] + \sum_{z \in V(G_2)} \sum_{p_1, p_2 \in E(S_k(G_1))} [d(p_1, z) + d(p_2, z)] \\
 &\quad + \sum_{p_1, p_2 \in E(S_k(G_1))} \sum_{z_1, z_2 \in V(G_2)} [d(p_1, z_1) + d(p_2, z_2)] = \sum 1 + \sum 2 + \sum 3.
 \end{aligned} \tag{4}$$

Consider

$$\begin{aligned}
 \sum 1 &= \sum_{p \in V(G_1)} \sum_{z_1, z_2 \in E(G_2)} [d(p, z_1) + d(p, z_2)] = \sum_{p \in V(G)} \sum_{z_1, z_2 \in E(H)} [2d(p) + d(z_1) + d(z_2) + d(p)(d(z_1) + d(z_2))] \\
 &= 4e_{G_1}e_{G_2} + M_1(G_2)n_{G_1} + 2M_1(G_2)e_{G_1}. \\
 \sum 2 &= \sum_{z \in V(G_2)} \sum_{p_1, p_2 \in E(S_k(G_1))} [d(p_1, z) + d(p_2, z)] = \sum_{z \in V(G_2)} \sum_{p_1 \in V(G_1), p_2 \in V(S_k(G_1)-G_1)} [d(p_1, z) + d(p_2, z)] \\
 &+ \sum_{z \in V(G_2)} \sum_{p_1, p_2 \in V(S_k(G_1)-G_1)} [d(p_1, z) + d(p_2, z)] = \sum 2' + \sum 2'', \\
 \sum 2' &= \sum_{z \in V(G_2)} \sum_{p_1, p_2 \in E(S_k(G_1))} \sum_{p_1 \in V(G_1), p_2 \in V(S_k(G_1)-V(G_1))} [d(p_1, z) + d(p_2, z)] \\
 &= \sum_{z \in V(G_2)} \sum_{p_1, p_2 \in E(S_k(G_1))} \sum_{p_1 \in V(G_1), p_2 \in V(S_k(G_1)-V(G_1))} [(d(p_1) + d(p_2)) + d(z) + (d(p_1) + d(p_2))d(z)].
 \end{aligned} \tag{5}$$

Since in this case  $|E(S_1(G))| = 2|E(G)|$ , we have

$$\begin{aligned}
 &= M_1(S_1(G_1))n_{G_2} + 4e_{G_1}e_{G_2} + 2M_1(S_1(G_1))e_{G_2}, \\
 \sum 2'' &= \sum_{z \in V(G_2)} \sum_{p_1, p_2 \in E(S_k(G_1))} \sum_{p_1, p_2 \in V(S_k(G_1)-V(G_1))} [d(p_1, z) + d(p_2, z)] \\
 &= \sum_{z \in V(G_2)} \sum_{p_1, p_2 \in E(S_k(G_1))} \sum_{p_1, p_2 \in V(S_k(G_1)-V(G_1))} [d(p_1) + d(p_1)d(z) + d(p_2) + d(p_2)d(z)].
 \end{aligned} \tag{6}$$

Since in this case  $|E(S_k(G_1))| = (k-1)|E(G_1)|$ , we have

$$\begin{aligned}
 &= \sum_{z \in V(G_2)} (4(k-1)e_{G_1} + 4d(z)(k-1)e_{G_1}) = 4(k-1)e_{G_1}n_{G_2} + 8e_{G_1}(k-1)e_{G_2}, \\
 \sum 3 &= \sum_{p_1, p_2 \in E(S_k(G_1))} \sum_{z_1, z_2 \in V(G_2)} [d(p_1, z_1) + d(p_2, z_2)] \\
 &= \sum_{z_1, z_2 \in V(G_2)} \sum_{p_1, p_2 \in E(S_k(G_1))} \sum_{p_1 \in V(G_1), p_2 \in V(S_k(G_1)-V(G_1))} [d(p_1, z_1) + d(p_2, z_2)] \\
 &+ \sum_{z_1, z_2 \in V(G_2)} \sum_{p_1, p_2 \in E(S_k(G_1))} \sum_{p_1, p_2 \in V(S_k(G_1)-V(G_1))} [d(p_1, z_1) + d(p_2, z_2)] = \sum 3' + \sum 3'', \\
 \sum 3' &= \sum_{z_1, z_2 \in V(G_2)} \sum_{p_1, p_2 \in E(S_k(G_1))} \sum_{p_1 \in V(G_1), p_2 \in V(S_k(G_1)-V(G_1))} [d(p_1, z_1) + d(p_2, z_2)] \\
 &= \sum_{z_1, z_2 \in V(G_2)} \sum_{p_1 \in V(G_1), p_2 \in V(S_k(G_1)-V(G_1))} [(d(p_1) + d(p_2)) + d(z_1) + d(p_1)d(z_1) + d(p_2)d(z_2)] \\
 &= 2e_{G_2}[M_1(G_1) + 4e_{G_1}] + 2e_{G_1}M_1(G_2) + M_1(G_2)[M_1(G_1) + 4e_{G_1}], \\
 \sum 3'' &= \sum_{z_1, z_2 \in V(G_2)} \sum_{p_1, p_2 \in E(S_k(G_1))} \sum_{p_1, p_2 \in V(S_k(G_1)-V(G_1))} [d(p_1, z_1) + d(p_2, z_2)] \\
 &= \sum_{z_1, z_2 \in V(G_2)} \sum_{p_1, p_2 \in E(S_k(G_1))} \sum_{p_1, p_2 \in V(S_k(G_1)-V(G_1))} [4 + 2(d(z_1) + d(z_2))] = 8(k-1)e_{G_1}e_{G_2} + 4(k-1)e_{G_1}M_1(G_2).
 \end{aligned} \tag{7}$$

Consequently, we get

$$\begin{aligned}
 M_1(G_1 \boxtimes_{S_k} G_2) &= M_1(S_1 G_1) [n_{G_2} + 2e_{G_2}] + 8(2k-1)e_{G_1} e_{G_2} + [M_1(G_1) + 4e_{G_1}] [M_1(G_2) + 2e_{G_2}] \\
 &\quad + M_1(G_2) [4e_{G_1} + n_{G_1}] + 4(k-1)e_{G_1} [n_2 + M_1(G_2)], \\
 \text{(b)} M_2(G_1 \boxtimes_{S_k} G_2) &= \sum_{(p,z) \in V(G_1 \boxtimes_{S_k} G_2)} d^2(p, z) = \sum_{(p_1, z_1) \in V(G_1 \boxtimes_{S_k} G_2)} [d(p_1, z_1) d(p_2, z_2)] \\
 &= \sum_{p \in V(G_1)} \sum_{z_1, z_2 \in E(G_2)} [d(p, z_1) d(p, z_2)] + \sum_{z \in V(G_2)} \sum_{p_1, p_2 \in E(S_k(G_1))} [d(p_1, z) d(p_2, z)] \\
 &\quad + \sum_{p_1, p_2 \in E(S_k(G_1))} \sum_{z_1, z_2 \in V(G_2)} [d(p_1, z_1) d(p_2, z_2)] = \sum 1 + \sum 2 + \sum 3.
 \end{aligned} \tag{8}$$

Consider

$$\begin{aligned}
 \sum 1 &= \sum_{p \in V(G_1)} \sum_{z_1, z_2 \in E(G_2)} [d(p, z_1) d(p, z_2)] = \sum_{p \in V(G_1)} \sum_{z_1, z_2 \in E(G_2)} [d(p) + d(z_1)] [d(p) + d(z_2)] \\
 &= \sum_{p \in V(G_1)} \sum_{z_1, z_2 \in E(G_2)} [d^2(p) + d^2(p) (d(z_1) + d(z_2)) + d(p) (d(z_1) + d(z_2)) + 2d(z_1) d(z_2) + d(z_1) d(z_2)] \\
 &= M_1(G_1) e_{G_2} + M_1(G_1) [M_1(G_2) + M_2(G_2)] + 2e_{G_1} [M_1(G_2) + 2M_2(G_2)] + M_2(G_2) n_{G_1}, \\
 \sum 2 &= \sum_{z \in V(G_2)} \sum_{p_1, p_2 \in E(S_k(G_1))} [d(p_1, z) d(p_2, z)] \\
 &\quad + \sum_{z \in V(G_2)} \sum_{p_1, p_2 \in E(S_k(G_1))} [d(p_1, z) d(p_2, z)] \\
 &= \sum 2' + \sum 2'', \\
 \sum 2' &= \sum_{z \in V(G_2)} \sum_{p_1, p_2 \in E(S_k(G_1))} [d(p_1, z) d(p_2, z)] \\
 &= \sum_{z \in V(G_2)} \sum_{p_1, p_2 \in E(S_k(G_1))} [(d(p_1) + d(z) + d(p_1) d(z)) (d(p_2) + d(p_2) d(z))] \\
 &= \sum_{z \in V(G_2)} \sum_{p_1, p_2 \in E(S_k(G_1))} [d(p_1) d(p_2) + 2d(p_1) d(p_2) d(z) + d(p_2) d(y) + d(p_2) d^2(z) \\
 &\quad + d(p_1) d(p_2) d^2(z)] \\
 &= [M_2(G_1) + 4e_{G_1}] [n_{G_2} + 4e_{G_2} + M_1(G_2)] + 8e_{G_1} e_{G_2} + 4e_{G_1} M_1(G_2), \\
 \sum 2'' &= \sum_{z \in V(G_2)} \sum_{p_1, p_2 \in E(S_k(G_1))} [d(p_1, z) d(p_2, z)] \\
 &= \sum_{z \in V(G_2)} \sum_{p_1, p_2 \in E(S_k(G_1))} [(d(p_1) + d(p_1) d(z)) (d(p_2) + d(p_2) d(z))] \\
 &= \sum_{z \in V(G_2)} \sum_{p_1, p_2 \in E(S_k(G_1))} [4 + 8d(z) + 4d^2(z)] = 4(k-1)e_{G_1} [n_{G_2} + 4e_{G_2} + M_1(G_2)], \\
 \sum 3 &= \sum_{z_1, z_2 \in V(G_2)} \sum_{p_1, p_2 \in E(S_k(G_1))} [d(p_1, z_1) d(p_2, z_2)] \\
 &\quad + \sum_{z_1, z_2 \in V(G_2)} \sum_{p_1, p_2 \in E(S_k(G_1))} [d(p_1, z_1) d(p_2, z_2)] = \sum 3' + \sum 3'',
 \end{aligned}$$

$$\begin{aligned}
\sum 3' &= \sum_{z_1 z_2 \in V(G_2)} \sum_{p_1 p_2 \in E(S_k(G_1))} \sum_{p_1 \in V(G_1), p_2 \in V(S_k(G_1)) - V(G_1)} [d(p_1, z_1) d(p_2, z_2)] \\
&= \sum_{z_1 z_2 \in V(G_2)} \sum_{p_1 p_2 \in E(S_k(G_1))} \sum_{p_1 \in V(G_1), p_2 \in V(S_k(G_1)) - V(G_1)} (d(p_1) + d(z_1) + d(p_1) d(z_1))(d(p_2) + d(p_2) d(z_2)) \\
&= \sum_{z \in V(G_2)} \sum_{p_1 p_2 \in E(S_k(G_1))} \sum_{p_1 \in V(G_1), p_2 \in V(S_k(G_1)) - V(G_1)} \\
&\quad \cdot [d(p_1) d(p_2) + d(p_1) d(p_2) d(z_2) + d(p_2) d(z_1) + d(p_1) d(z_1) d(z_2) + d(p_1) d(p_2) d(z_1) + d(p_1) d(p_2) d(z_1) d(z_2)] \\
&= [M_2(G_1) + 4e_{G_1}] [e_{G_2} + 2M_1(G_2) + 2M_2(G_2)] + 8e_{G_1} M_1(G_2) + 8e_{G_1} M_2(G_2), \\
\sum 3'' &= \sum_{z \in V(G_2)} \sum_{p_1 p_2 \in E(S_k(G_1))} \sum_{z_1, p_2 \in V(S_k(G_1)) - V(G_1)} [d(p_1, z_1) d(p_2, z_2)] \\
&= \sum_{z \in V(G_2)} \sum_{p_1 p_2 \in E(S_k(G_1))} \sum_{p_1, p_2 \in V(S_k(G_1)) - V(G_1)} [(d(p_1) + d(p_1) d(z_1))(d(p_2) + d(p_2) d(z_2))] \\
&= \sum_{z \in V(G_2)} \sum_{p_1 \in V(G_1), p_2 \in V(S_k(G_1)) - V(G_1)} [4 + 4(d(z_2) + d(z_1)) + 4d(z_1) d(z_2)] = 8(k-1)e_{G_1} [e_{G_2} + M_1(G_2) + M_2(G_2)].
\end{aligned} \tag{9}$$

Therefore,

$$\begin{aligned}
M_2(G_1 \boxtimes_{S_k} G_2) &= [M_2(G_1) + 4e_{G_1}] [5e_{G_2} + 3M_1(G_2) + 2M_2(G_2) + n_{G_2}] + M_1(G_1) [e_{G_2} + M_1(G_2) + M_2(G_2)] \\
&\quad + 4(k-1)e_{G_1} [6e_{G_2} + 3M_1(G_2) + M_2(G_2) + n_{G_2}] + M_2(G_2) [12e_{G_1} + n_{G_1}] \\
&\quad + 8e_{G_1} e_{G_2} + M_1(G_2) [14e_{G_1}].
\end{aligned} \tag{10}$$

**Theorem 2.** Let  $G_1$  and  $G_2$  be two connected graphs such that  $|V(G_1)|, |V(G_2)| \geq 4$ . For  $k \geq 1$ ,

$$\begin{aligned}
\text{(a)} \quad M_1(G_1 \boxtimes_{R_k} G_2) &= M_1(G_2) [n_{G_1} + 12e_{G_1} + 4M_1(G_1)] + M_1(G_1) [12e_{G_2} + 2n_{G_2}] + 24e_{G_1} e_{G_2} \\
&\quad + [M_1(R_1(G_1)) - 2M_1(G_1)] [n_{G_2} + 2e_{G_2}] + 4(k-1)e_{G_1} [n_{G_2} + 4e_{G_2} + M_1(G_2)], \\
\text{(b)} \quad M_2(G_1 \boxtimes_{R_k} G_2) &= M_1(G_1) [8e_{G_2} + 12M_1(G_2) + 4M_2(G_2)] + 4M_2(G_1) [n_{G_2} + 6e_{G_2} + 3M_1(G_2)] \\
&\quad + [M_2(R_1(G_1)) - 4M_2(G_1) + 4(k-1)e_{G_1}] [6e_{G_2} + 3M_1(G_2) + 2M_2(G_2) + n_{G_2}] \\
&\quad + M_2(G_2) [n_{G_1} + 2e_{G_1}] + 4e_{G_1} [3M_1(G_2) + 3M_2(G_2) + 4e_{G_2}] + e_{G_1} M_1(G_2).
\end{aligned} \tag{11}$$

*Proof.* Let  $d(p, z) = d_{G_1 \boxtimes_{R_k} G_2}(p, z)$  be the degree of a vertex  $(p, z)$  in the graph  $G_1 \boxtimes_{R_k} G_2$ .

$$\begin{aligned}
 M_1(G_1 \boxtimes_{R_k} G_2) &= \sum_{(p,z) \in V(G_1 \boxtimes_{R_k} G_2)} d^2(x, z) = \sum_{(p_1, z_1) (p_2, z_2) \in E(G_1 \boxtimes_{R_k} G_2)} [d(p_1, z_1) + d(p_2, z_2)] \\
 &= \sum_{p \in V(G_1)} \sum_{z_1, z_2 \in E(G_2)} [d(p, z_1) + d(p, z_2)] + \sum_{z \in V(G_2)} \sum_{p_1, p_2 \in E(R_k(G_1))} [d(p_1, z) + d(p_2, z)] \\
 &\quad + \sum_{p_1, p_2 \in E(R_k(G_1))} \sum_{z_1, z_2 \in V(G_2)} [d(p_1, z_1) + d(p_2, z_2)] = \sum 1 + \sum 2 + \sum 3, \\
 \sum 1 &= \sum_{p \in V(G_1)} \sum_{z_1, z_2 \in E(G_2)} [d(p, y_1) + d(p, y_2)] \\
 &= \sum_{p \in V(G_1)} \sum_{z_1, z_2 \in E(G_2)} [2d(p) + d(z_1) + 2d(p)d(z_1) + 2d(p) + d(z_2) + 2d(p)d(z_2)] \\
 &= \sum_{p \in V(G_1)} \sum_{z_1, z_2 \in E(G_2)} [4d(p) + d(z_1) + d(z_2) + 2d(p)(d(z_1) + d(z_2))] \\
 &= 8e_{G_1}e_{G_2} + M_1(G_2)n_{G_1} + 4M_1(G_2)e_{G_1}, \\
 \sum 2 &= \sum_{z \in V(G_2)} \sum_{p_1, p_2 \in E(R_k(G_1))} [d(p_1, z) + d(p_2, z)] = \sum_{z \in V(G_2)} \sum_{p_1, p_2 \in E(R_k(G_1))} \sum_{p_1, p_2 \in V(G_1)} [d(p_1, z) + d(p_2, z)] \\
 &\quad + \sum_{z \in V(G_2)} \sum_{p_1, p_2 \in E(R_k(G_1))} \sum_{p_1 \in V(G_1), p_2 \in V(R_k(G_1) - G_1)} [d(p_1, y) + d(p_2, z)] + \sum_{z \in V(G_2)} \sum_{p_1, p_2 \in E(R_k(G_1))} \sum_{p_1, p_2 \in V(R_k(G_1) - G_1)} \\
 &\quad \cdot [d(p_1, z) + d(p_2, y)] \\
 &= \sum 2' + \sum 2'' + \sum 2''', \\
 \sum 2' &= \sum_{z \in V(G_2)} \sum_{p_1, p_2 \in E(R_k(G_1))} \sum_{p_1, p_2 \in V(G_1)} [d(p_1, z) + d(p_2, z)] \\
 &= \sum_{z \in V(G_2)} \sum_{p_1, p_2 \in E(R_k(G_1))} \sum_{p_1, p_2 \in V(G_1)} [d(p_1) + d(z) + d(p_1)d(z) + d(p_2) + d(z) + d(p_2)d(z)] \\
 &= \sum_{z \in V(G_2)} \sum_{p_1, p_2 \in E(R_k(G_1))} \sum_{p_1, p_2 \in V(G_1)} [d(p_1) + d(p_2) + 2d(z) + d(y)(d(p_1) + d(p_2))] \\
 &= 2n_{G_2}M_1(G_1) + 4e_{G_1}e_{G_2} + 4e_{G_2}M_1(G_1), \\
 \sum 2'' &= \sum_{z \in V(G_2)} \sum_{p_1, p_2 \in E(R_k(G_1))} \sum_{p_1 \in V(G_1), p_2 \in V(S_k(G_1) - V(G_1))} [d(p_1, z) + d(p_2, y)] \\
 &= \sum_{z \in V(G_2)} \sum_{p_1, p_2 \in E(R_k(G_1))} \sum_{p_1 \in V(G_1), p_2 \in V(S_k(G_1) - V(G_1))} [d(p_1) + d(p_2) + d(z) + (d(p_1) + d(p_2))d(z)] \\
 &= [M_1(R_1(G_1)) - 2M_1(G_1)][n_{G_2} + 2e_{G_2}] + 4e_{G_1}e_{G_2}, \\
 \sum 2''' &= \sum_{z \in V(G_2)} \sum_{p_1, p_2 \in E(R_k(G_1))} \sum_{p_1, p_2 \in V(R_k(G_1) - V(G_1))} [d(p_1, z) + d(p_2, z)] \\
 &= \sum_{z \in V(G_2)} \sum_{p_1, p_2 \in E(R_k(G_1))} \sum_{p_1, p_2 \in V(R_k(G_1) - V(G_1))} [d(p_1) + d(p_2) + (d(p_1) + d(p_2))d(z)] \\
 &= 4(k-1)e_{G_1}n_{G_2} + 8(k-1)e_{G_1}e_{G_2}, \\
 \sum 3 &= \sum_{p_1, p_2 \in E(R_k(G_1))} \sum_{z_1, z_2 \in V(G_2)} [d(p_1, z_1) + d(p_2, z_2)] = \sum_{z_1, z_2 \in V(G_2)} \sum_{p_1, p_2 \in E(R_k(G_1))} \sum_{p_1, p_2 \in V(G_1)} [d(p_1, z_1) + d(p_2, z_2)] \\
 &\quad + \sum_{z_1, z_2 \in V(G_2)} \sum_{p_1, p_2 \in E(R_k(G_1))} \sum_{p_1 \in V(G_1), p_2 \in V(R_k(G_1) - V(G_1))} [d(p_1, z_1) + d(p_2, z_2)] \\
 &\quad + \sum_{z_1, z_2 \in V(G_2)} \sum_{p_1, p_2 \in E(R_k(G_1))} \sum_{p_1, p_2 \in V(R_k(G_1) - V(G_1))} [d(p_1, z_1) + d(p_2, z_2)] = \sum 3' + \sum 3'' + \sum 3''',
 \end{aligned}$$

$$\begin{aligned}
\sum 3' &= \sum_{z_1 z_2 \in V(G_2)} \sum_{p_1 p_2 \in E(R_k(G_1))} [d(p_1, z_1) + d(p_2, z_2)] \\
&= \sum_{z_1 z_2 \in V(G_2)} \sum_{p_1 p_2 \in E(R_k(G_1))} [d(p_1) + d(z_1) + d(p_1)d(z_1) + d(p_2) + d(z_2) + d(p_2)d(z_2)] \\
&= \sum_{z_1 z_2 \in V(G_2)} \sum_{p_1 p_2 \in E(R_k(G_1))} [d(p_1) + d(p_2) + d(z_1) + d(z_2) + d(p_1)d(z_1) + d(p_2)d(z_2)] \\
&= 4e_{G_2} M_1(G_1) + 2M_1(G_2)e_{G_1} + 2M_1(G_2)M_1(G_1), \\
\sum 3'' &= \sum_{z_1 z_2 \in V(G_2)} \sum_{p_1 p_2 \in E(R_k(G_1))} [d(p_1, z_1) + d(p_2, z_2)] \\
&= \sum_{z_1 z_2 \in V(G_2)} \sum_{p_1 \in V(G_1), p_2 \in V(R_k(G_1))^{-V(G_1)}} [d(p_1) + d(z_1) + d(p_1)d(z_1) + d(p_2) + d(p_2 z_2)] \\
&= 4e_{G_2} M_1(G_1) + 2M_1(G_2)e_{G_1} + 2M_1(G_2)M_1(G_1) + 8e_{G_1}e_{G_2} + 4e_{G_1}M_1(G_2), \\
\sum 3''' &= \sum_{z_1 z_2 \in V(G_2)} \sum_{p_1 p_2 \in E(R_k(G_1))} [d(p_1, z_1) + d(p_2, z_2)] \\
&= \sum_{z_1 z_2 \in V(G_2)} \sum_{p_1 p_2 \in E(R_k(G_1))} [d(p_1) + d(p_2) + d(p_1)d(z_1) + d(p_2)d(z_2)] \\
&= 8(k-1)e_{G_1}e_{G_2} + 4(k-1)e_{G_1}M_1(G_2). \tag{12}
\end{aligned}$$

Hence,

$$\begin{aligned}
M_1(G_1 \boxtimes_{R_k} G_2) &= M_1(G_2)[n_{G_1} + 12e_{G_1} + 4M_1(G_1)] + M_1(G_1)[12e_{G_2} + 2n_{G_2}] + 24e_{G_1}e_{G_2} \\
&\quad + [M_1(R_1(G_1)) - 2M_1G_1][n_{G_2} + 2e_{G_2}] + 4(k-1)e_{G_1}[n_{G_2} + 4e_{G_2} + M_1(G_2)], \\
\text{(b)} M_2(G_1 \boxtimes_{R_k} G_2) &= \sum_{(x,z) \in V(G_1 \boxtimes_{R_k} G_2)} d^2(p, z) = \sum_{(p_1, z_1)(p_2, z_2) \in E(G_1 \boxtimes_{R_k} G_2)} [d(p_1, z_1)d(p_2, z_2)] \\
&= \sum_{p \in V(G_1)} \sum_{z_1 z_2 \in E(G_2)} [d(p, z_1)d(p, z_2)] + \sum_{z \in V(G_2)} \sum_{p_1 p_2 \in E(R_k(G_1))} [d(p_1, z)d(p_2, z)] \\
&\quad + \sum_{p_1 p_2 \in E(R_k(G_1))} \sum_{z_1 z_2 \in V(G_2)} [d(p_1, z_1)d(p_2, z_2)] = \sum 1 + \sum 2 + \sum 3. \tag{13}
\end{aligned}$$

Consider

$$\begin{aligned}
 \sum 1 &= \sum_{p \in V(G_1)} \sum_{z_1, z_2 \in E(G_2)} [d(p, z_1)d(p, z_2)] = \sum_{p \in V(G_1)} \sum_{z_1, z_2 \in E(G_2)} [d(p) + d(z_1)][d(p) + d(z_2)] \\
 &= \sum_{p \in V(G_1)} \sum_{z_1, z_2 \in E(G_2)} [d^2(p) + d^2(p)(d(z_1) + d(z_2)) + d^2(p)(d(z_1) + d(z_2)) + 2d(p)d(z_1)d(z_2) + d(z_1)d(z_2)] \\
 &= \sum_{z_1, z_2 \in E(G_2)} [4M_1(G_1) + 4M_1(G_1)][d(z_1) + d(z_2) + d(z_1)d(z_2)] + 4e_{G_1}[d(z_1) + d(z_2) + 2d(z_1)d(z_2)] \\
 &\quad + d(z_1)d(z_2)(n_{G_1}) = 4M_1(G_1)[e_{G_2} + M_1(G_2) + M_2(G_2)] + 4e_{G_1}[M_1(G_2) + 2M_2(G_2)] + M_2(G_2)n_{G_1}, \\
 \sum 2 &= \sum_{z \in V(G_2)} \sum_{p_1, p_2 \in E(R_k(G_1))} [d(p_1, z)d(p_2, z)] \\
 &= \sum_{z \in V(G_2)} \sum_{p_1, p_2 \in E(R_k(G_1))} [d(p_1, z)d(p_2, z)] + \sum_{z \in V(G_2)} \sum_{p_1, p_2 \in E(R_k(G_1))} \sum_{p_1 \in V(G_1), p_2 \in V(R_k(G_1) - G_1)} [d(p_1, z)d(p_2, z)] \\
 &\quad + \sum_{z \in V(G_2)} \sum_{p_1, p_2 \in E(R_k(G_1))} [d(p_1, z)d(p_2, z)] = \sum 2' + \sum 2'' + \sum 2''', \\
 \sum 2' &= \sum_{z \in V(G_2)} \sum_{p_1, p_2 \in E(R_k(G_1))} [d(p_1, z)d(p_2, z)] \\
 &= \sum_{z \in V(G_2)} \sum_{p_1, p_2 \in E(R_k(G_1))} [d(p_1) + d(z) + d(p_1)d(z)][d(p_2) + d(z) + d(p_2)d(z)] \\
 &= \sum_{z \in V(G_2)} \sum_{p_1, p_2 \in E(R_k(G_1))} [4d(p_1)d(p_2) + 2d(p_1)d(z) + 4d(p_1)d(p_2)d(z) + 2d(p_2)d(z) \\
 &\quad + d^2(z) + 2d(p_2)d^2(z) + 4d(p_1)d(p_2)d(z) + 4d(p_1)d(p_2)d^2(z)] \\
 &= 4M_2(G_1)[n_{G_2} + 4e_{G_2} + M_1(G_2) + 2M_1(G_1)[M_1(G_2) + 2e_{G_2} + e_{G_1}M_1(G_2)], \\
 \sum 2'' &= \sum_{z \in V(G_2)} \sum_{p_1, p_2 \in E(R_k(G_1))} \sum_{p_1 \in V(G_1), p_2 \in V(R_k(G_1) - V(G_1))} [d(p_1, z)d(p_2, z)] \\
 &= \sum_{z \in V(G_2)} \sum_{p_1, p_2 \in E(R_k(G_1))} \sum_{p_1 \in V(G_1), p_2 \in V(R_k(G_1) - V(G_1))} [(d(p_1) + d(z) + d(p_1)d(z))(d(p_2) + d(p_2)d(z))] \\
 &= \sum_{z \in V(G_2)} \sum_{p_1, p_2 \in E(R_k(G_1))} \sum_{p_1 \in V(G_1), p_2 \in V(R_k(G_1) - V(G_1))} [2d(p_1)[1 + d(z) + d(y) + d^2(z) + 2d(z) + 2d^2(y)] \\
 &= [M_2(R_1(G_1)) - 4M_2(G_1)][n_{G_2} + 4e_{G_2} + M_1(G_2) + 8e_{G_1}e_{G_2} + 4e_{G_1}M_1(G_2)], \\
 \sum 2''' &= \sum_{z \in V(G_2)} \sum_{p_1, p_2 \in E(R_k(G_1))} \sum_{p_1, p_2 \in V(R_k(G_1) - V(G_1))} [d(p_1, z)d(p_2, z)] \\
 &= \sum_{z \in V(G_2)} \sum_{p_1, p_2 \in E(R_k(G_1))} \sum_{p_1, p_2 \in V(R_k(G_1) - V(G_1))} [(d(p_1) + d(p_1)d(z))(d(p_2) + d(p_2)d(z))] \\
 &= \sum_{z \in V(G_2)} \sum_{p_1 \in V(G_1), p_2 \in V(R_k(G_1) - V(G_1))} [4 + 8d(y) + 4d^2(z)] = 4(k-1)e_{G_1}[n_{G_2} + 4e_{G_2} + M_1(G_2)],
 \end{aligned}$$



$$\begin{aligned}
\sum 3 &= \sum_{z_1 z_2 \in V(G_2)} \sum_{p_1 p_2 \in E(R_k(G_1))} [d(p_1, z_1) d(p_2, z_2)] \\
&+ \sum_{z_1 z_2 \in V(G_2)} \sum_{p_1 p_2 \in E(R_k(G_1))} [d(p_1, z_1) d(p_2, z_2)] \\
&+ \sum_{z_1 z_2 \in V(G_2)} \sum_{p_1 p_2 \in E(R_k(G_1))} [d(p_1, z_1) d(p_2, z_2)] = \sum 3' + \sum 3'' + \sum 3''', \\
\sum 3' &= \sum_{z_1 z_2 \in V(G_2)} \sum_{p_1 p_2 \in E(R_k(G_1))} [d(p_1, z_1) d(p_2, z_2)] \\
&= \sum_{z_1 z_2 \in V(G_2)} \sum_{p_1 p_2 \in E(R_k(G_1))} [4d(p_1) d(p_2) + 2[d(p_1) d(z_2) + d(p_2) d(z_1)] + d(z_1) d(z_2)] \\
&+ 4d(p_1) d(p_2) d(z_1) d(z_2) + 4d(p_1) d(p_2) [d(z_1) + d(z_2)] + 2[d(p_1) + d(p_2)] d(z_1) d(z_2)] \\
&= 8M_2(G_1) e_{G_2} + 2M_1(G_1) M_1(G_2) + 2M_2(G_2) e_{G_1} + 8M_2(G_1) [M_2(G_2) + M_1(G_2)] + 4M_1(G_1) M_2(G_2), \\
\sum 3'' &= \sum_{z_1 z_2 \in V(G_2)} \sum_{p_1 p_2 \in E(R_k(G_1))} [d(p_1, z_1) d(p_2, z_2)] \\
&= \sum_{z_1 z_2 \in V(G_2)} \sum_{p_1 p_2 \in E(R_k(G_1))} [(d(p_1) + d(z_1) + d(p_1) d(z_1)) (d(p_2) + d(p_2) d(z_2))] \\
&= \sum_{z_1 z_2 \in V(G_2)} \sum_{p_1 p_2 \in E(R_k(G_1))} [4d(p_1) [1 + d(z_2) + d(z_1)] \\
&+ d(z_1) d(z_2)] + 2[d(z_1) + d(z_1) d(z_2)]] \\
&= [M_2(R_1(G_1)) - 4M_2(G_1)] [2e_{G_2} + 2M_1(G_2) + 2M_2(G_2)] + 4e_{G_1} [M_1(G_2) + M_2(G_2)], \\
\sum_3''' &= \sum_{z_1 z_2 \in V(G_2)} \sum_{p_1 p_2 \in E(R_k(G_1))} [d(p_1, z_1) d(p_2, z_2)] \\
&= \sum_{z_1 z_2 \in V(G_2)} \sum_{p_1 p_2 \in E(R_k(G_1))} [(d(p_1) + d(p_1) d(z_1)) (d(p_2) + d(p_2) d(z_2))] \\
&= \sum_{z_1 z_2 \in V(G_2)} \sum_{p_1 p_2 \in E(R_k(G_1))} [d(p_1) d(p_2) [1 + (d(z_2) + d(z_1)) + d(z_1) d(z_2)]] \\
&= 8(k-1) e_{G_1} [e_{G_2} + M_1(G_2) + M_2(G_2)]. \tag{14}
\end{aligned}$$

Consequently, we have

$$\begin{aligned}
M_2(G_1 \boxtimes_{R_k} G_2) &= M_1(G_1) [8e_{G_2} + 12M_1(G_2) + 4M_2(G_2)] + 4M_2(G_1) [n_{G_2} + 6e_{G_2} + 3M_1(G_2)] \\
&+ [M_2(R_1(G_1)) - 4M_2(G_1) + 4(k-1)e_{G_1}] [6e_{G_2} + 3M_1(G_2) + 2M_2(G_2) + n_{G_2}] \\
&+ M_2(G_2) [n_{G_1} + 2e_{G_1}] + 4e_{G_1} [3M_1(G_2) + 3M_2(G_2) + 4e_{G_2}] + e_{G_1} M_1(G_2). \tag{15}
\end{aligned}$$

□

**Theorem 3.** Let  $G_1$  and  $G_2$  be two connected graphs such that  $|V(G_1)|, |V(G_2)| \geq 4$ . For  $k \geq 1$ ,

$$\begin{aligned}
 \text{(a)} \quad M_1(G_1 \boxtimes_{Q_k} G_2) &= k[M_3(G_1) + 2M_2(G_1) - 2M_1(G_1)][n_{G_2} + 4e_{G_2} + M_1(G_2)] + 8e_{G_1}e_{G_2} \\
 &\quad + M_1(G_1)[2(k-1) + 3][n_{G_2} + 4e_{G_2} + M_1(G_2)] + M_1(G_2)[n_{G_1} + 4e_{G_1}], \\
 \text{(b)} \quad M_2(G_1 \boxtimes_{Q_k} G_2) &= k[n_{G_2} + 6e_{G_2} + 3M_1(G_2) + 2M_2(G_2)] \left[ \frac{1}{2} \sum_{v \in V(G_1)} (d_{G_1}^4(v) - d_{G_1}^3(v)) \right] \\
 &\quad + \left[ \sum_{uv \in E(G_1)} rd_{G_1}(u)d_{G_1}(v) + \sum_{v \in V(G_1)} d_{G_1}^2(v) \sum_{u \in V(G_1)} d_{G_1}(u) - 2M_2(G_1) \right. \\
 &\quad \left. + M_2(G_2)[4e_{G_1} + n_{G_1}] + 2e_{G_1}M_1(G_2) + M_1(G_1)[5e_2 + 5M_1(G_2) + 5M_2(G_2)] \right. \\
 &\quad \left. + k[M_3(G_1) + 2M_2(G_1)][6e_{G_2} + 3M_1(G_2) + 2M_2(G_2) + n_{G_2}] \right]. \tag{16}
 \end{aligned}$$

*Proof.* Let  $d(p, z) = d_{G_1 \boxtimes_{Q_k} G_2}(p, z)$  be the degree of a vertex  $(p, z)$  in the graph  $G_1 \boxtimes_{Q_k} G_2$ .

$$\begin{aligned}
 M_1(G_1 \boxtimes_{Q_k} G_2) &= \sum_{(p,z) \in V(G_1 \boxtimes_{Q_k} G_2)} d^2(p, z) = \sum_{(p_1, z_1)(p_2, z_2) \in E(G_1 \boxtimes_{Q_k} G_2)} [d(p_1, z_1) + d(p_2, z_2)] \\
 &= \sum_{p \in V(G_1)} \sum_{z_1, z_2 \in E(G_2)} [d(p, z_1) + d(p, z_2)] + \sum_{z \in V(G_2)} \sum_{p_1, p_2 \in E(Q_k(G_1))} [d(p_1, z) + d(p_2, z)] \\
 &\quad + \sum_{p_1, p_2 \in E(Q_k(G_1))} \sum_{z_1, z_2 \in V(G_2)} [d(p_1, z_1) + d(p_2, z_2)] = \sum 1 + \sum 2 + \sum 3, \\
 \sum 1 &= \sum_{p \in V(G_1)} \sum_{z_1, z_2 \in E(G_2)} [d(p, z_1) + d(p, z_2)] \\
 &= \sum_{p \in V(G_1)} \sum_{z_1, z_2 \in E(G_2)} [d(p) + d(z_1) + d(p)d(z_1) + d(p) + d(z_2) + d(p)d(z_2)] \\
 &= \sum_{p \in V(G_1)} \sum_{z_1, z_2 \in E(G_2)} [2d(p) + d(z_1) + d(z_2) + d(p)[d(z_1) + d(z_2)]] \\
 &= 4e_{G_1}e_{G_2} + M_1(G_2)n_{G_1} + 2M_1(G_2)e_{G_1}, \\
 \sum 2 &= \sum_{z \in V(G_2)} \sum_{p_1, p_2 \in E(Q_k(G_1))} [d(p_1, z) + d(p_2, z)] \\
 &= \sum_{z \in V(G_2)} \sum_{p_1, p_2 \in E(Q_k(G_1))} \sum_{p_1 \in V(G_1), p_2 \in V(Q_k(G_1) - G_1)} [d(p_1, z) + d(p_2, z)] \\
 &\quad + \sum_{z \in V(G_2)} \sum_{p_1, p_2 \in E(Q_k(G_1))} \sum_{p_1, p_2 \in V(Q_k(G_1) - G_1)} [d(p_1, y) + d(p_2, z)] = \sum 2' + \sum 2'',
 \end{aligned}$$

$$\begin{aligned}
\sum 2' &= \sum_{z \in V(G_2)} \sum_{p_1 p_2 \in E(Q_k(G_1))} \sum_{p_1 \in V(G_1), p_2 \in V(Q_k(G_1)) - V(G_1)} [d(p_1, z) + d(p_2, z)] \\
&= \sum_{z \in V(G_2)} \sum_{p_1 p_2 \in E(Q_k(G_1))} \sum_{p_1 \in V(G_1), p_2 \in V(Q_k(G_1)) - V(G_1)} [d(p_1) + d(z) + d(p_1)d(z) + d(p_2) + d(p_2)d(z)] \\
&= M_1(G_1)n_{G_2} + 4e_{G_1}e_{G_2} + 6M_1(G_1)e_{G_2} + 2n_{G_2}M_1(G_1), \\
\sum 2'' &= \sum_{z \in V(G_2)} \sum_{p_1 p_2 \in E(Q_k(G_1))} \sum_{p_1 p_2 \in V(Q_k(G_1)) - V(G_1)} [d(p_1, z)d(p_2, z)]. \tag{17}
\end{aligned}$$

Now, we split this sum into two parts for the vertices,  $p_1$  and  $p_2$ , where  $p_1 p_2 \in V(Q_k(G_1)) - V(G_1)$ . Assume that  $\sum 2'' = \sum 2''a + \sum 2''b$ , where  $\sum 2''a$  cover the edges of

$Q_k(G_1)$  which are in the same edges of  $G_1$  and  $\sum 2''b$  of  $Q_k(G_1)$  in two different adjacent edges of  $G_1$ .

$$\begin{aligned}
\sum 2''a &= \sum_{z \in V(G_2)} \sum_{p_1 p_2 \in E(Q_k(G_1))} \sum_{p_1, p_2 \in V(Q_k(G_1)) - V(G_1)} [d(p_1, z) + d(p_2, z)] \\
&= \sum_{z \in V(G_2)} \sum_{p_1 p_2 \in E(Q_k(G_1))} \sum_{p_1, p_2 \in V(Q_k(G_1)) - V(G_1)} [d(p_1) + d(p_1)d(z) + d(p_2) + d(p_2)d(z)] \\
&= 2(k-1)n_{G_2}M_1(G_1) + 4(k-1)e_{G_2}M_1(G_1), \\
\sum 2''b &= \sum_{z \in V(G_2)} \sum_{p_1 p_2 \in E(Q_k(G_1))} \sum_{p_1, p_2 \in V(Q_k(G_1)) - V(G_1)} [d(p_1, y) + d(p_2, z)] \\
&= \sum_{z \in V(G_2)} \sum_{p_1 p_2 \in E(Q_k(G_1))} \sum_{p_1, p_2 \in V(Q_k(G_1)) - V(G_1)} [d(p_1) + d(p_1)d(z) + d(p_2) + d(p_2)d(z)] \\
&= \sum_{z \in V(G_2)} \sum_{u, v, w \in V(G_1)} \sum_{uv, vw \in E(G_1)} [d(u) + d(v) + d(v) + d(w) + [d(u) + d(v) + d(v) + d(w)]d(z)] \\
&= k[M_3(G_1) + 2M_2(G_1) - 2M_1(G_1)][n_{G_2} + 2e_{G_2}], \\
\sum 3 &= \sum_{p_1 p_2 \in E(Q_k(G_1))} \sum_{z_1 z_2 \in V(G_2)} [d(p_1, z_1) + d(p_2, z_2)] \\
&= \sum_{z_1 z_2 \in V(G_2)} \sum_{p_1 p_2 \in E(Q_k(G_1))} \sum_{p_1 \in V(G_1), p_2 \in V(Q_k(G_1)) - V(G_1)} [d(p_1, z_1) + d(p_2, z_2)] \\
&\quad + \sum_{z_1 z_2 \in V(G_2)} \sum_{p_1 p_2 \in E(Q_k(G_1))} \sum_{p_1, p_2 \in V(Q_k(G_1)) - V(G_1)} [d(p_1, z_1) + d(p_2, z_2)] \\
&= \sum 3' + \sum 3'', \\
\sum 3' &= \sum_{z_1 z_2 \in V(G_2)} \sum_{p_1 p_2 \in E(Q_k(G_1))} \sum_{p_1, p_2 \in V(G_1)} [d(p_1, z_1) + d(p_2, z_2)] \\
&= \sum_{z_1 z_2 \in V(G_2)} \sum_{p_1 p_2 \in E(Q_k(G_1))} \sum_{p_1, p_2 \in V(G_1)} [d(p_1) + d(z_1) + d(p_1)d(z_1) + d(p_2) + d(z_2) + d(p_2z_2)] \\
&= 6e_{G_2}M_1(G_1) + 2M_1(G_2)e_{G_1} + 3M_1(G_2)M_1(G_1). \tag{18}
\end{aligned}$$

Now, we split this sum into two parts for the vertices,  $p_1$  and  $p_2$ , where  $p_1, p_2 \in V(Q_k(\Gamma_1)) - V(\Gamma_1)$ . Assume that  $\sum 3'' = \sum 3''a + \sum 3''b$ , where  $\sum 3''a$  cover the edges of  $Q_k(G_1)$  which are in the same edges of  $G_1$  and  $\sum 3''b$  of  $Q_k(G_1)$  in two different adjacent edges of  $G_1$ .

$$\begin{aligned}
 \sum 3''a &= \sum_{z_1, z_2 \in V(G_2)} \sum_{p_1, p_2 \in E(Q_k(G_1))} \sum_{p_1 \in V(G_1), p_2 \in V(Q_k(G_1)) - V(G_1)} [d(p_1, z_1) + d(p_2, z_2)] \\
 &= \sum_{z_1, z_2 \in V(G_2)} \sum_{p_1, p_2 \in E(Q_k(G_1))} \sum_{p_1 \in V(G_1), p_2 \in V(Q_k(G_1)) - V(G_1)} [d(p_1) + d(p_1)d(z_1) + d(p_2) + d(p_2)d(z_2)] \\
 &= 4(k-1)e_{G_2}M_1(G_1) + 2(k-1)M_1(G_2)M_1(G_1), \\
 \sum 3''b &= \sum_{z_1, z_2 \in V(G_2)} \sum_{p_1, p_2 \in E(Q_k(G_1))} \sum_{p_1, p_2 \in V(Q_k(G_1)) - V(G_1)} [d(p_1, z_1) + d(p_2, z_2)] \\
 &= \sum_{z_1, z_2 \in V(G_2)} \sum_{p_1, p_2 \in E(Q_k(G_1))} \sum_{p_1, p_2 \in V(Q_k(G_1)) - V(G_1)} [d(p_1) + d(p_2) + d(p_1)d(z_1) + d(p_2)d(z_2)] \\
 &= k[M_3(G_1) + 2M_2(G_1) - 2M_1(G_1)][2e_{G_2} + M_1(G_2)].
 \end{aligned} \tag{19}$$

Consequently, we have

$$\begin{aligned}
 M_1(G_1 \boxtimes_{Q_k} G_2) &= k[M_3(G_1) + 2M_2(G_1) - 2M_1(G_1)][n_{G_2} + 4e_{G_2} + M_1(G_2)] + 8e_{G_1}e_{G_2} \\
 &\quad + M_1(G_1)[2(k-1) + 3][n_{G_2} + 4e_{G_2} + M_1(G_2)] + M_1(G_2)[n_{G_1} + 4e_{G_1}].
 \end{aligned} \tag{20}$$

Next,

$$\begin{aligned}
 (b) M_2(G_1 \boxtimes_{Q_k} G_2) &= \sum_{(p,z) \in V(G_1 \boxtimes_{Q_k} G_2)} d^2(p, z) = \sum_{(p_1, z_1), (p_2, z_2) \in E(G_1 \boxtimes_{Q_k} G_2)} [d(p_1, z_1)d(p_2, z_2)] \\
 &= \sum_{p \in V(G_1)} \sum_{z_1, z_2 \in E(G_2)} [d(p, z_1)d(p, z_2)] + \sum_{z \in V(G_2)} \sum_{p_1, p_2 \in E(Q_k(G_1))} [d(p_1, z)d(p_2, z)] \\
 &\quad + \sum_{p_1, p_2 \in E(Q_k(G_1))} \sum_{z_1, z_2 \in V(G_2)} [d(p_1, z_1)d(p_2, z_2)] = \sum 1 + \sum 2 + \sum 3.
 \end{aligned} \tag{21}$$

Consider

$$\begin{aligned}
 \sum 1 &= \sum_{p \in V(G_1)} \sum_{z_1 z_2 \in E(G_2)} [d(p, z_1)d(p, z_2)] = \sum_{p \in V(G_1)} \sum_{z_1 z_2 \in E(G_2)} [d(p) + d(z_1)][d(p) + d(z_2)] \\
 &= M_1(G_1)e_{G_2} + M_1(G_1)[M_1(G_2) + M_2(G_2)] + 2e_{G_1}[M_1(G_2) + 2M_2(G_2)] + M_2(G_2)n_{G_1}, \\
 \sum 2 &= \sum_{z \in V(G_2)} \sum_{p_1 p_2 \in E(Q_k(G_1))} [d(p_1, z)d(p_2, z)] = \sum_{z \in V(G_2)} \sum_{\substack{p_1 p_2 \in E(Q_k(G_1)) \\ p_1 \in V(G_1) p_2 \in V(Q_k(G_1)) - V(G_2)}} [d(p_1, z)d(p_2, z)] \\
 &+ \sum_{z \in V(G_2)} \sum_{\substack{p_1 p_2 \in E(Q_k(G_1)) \\ p_1 p_2 \in V(Q_k(G_1)) - V(G_1)}} [d(p_1, z)d(p_2, z)] = ' \sum 2 + '' \sum 2, \\
 ' \sum 2 &= \sum_{z \in V(G_2)} \sum_{\substack{p_1 p_2 \in E(Q_k(G_1)) \\ p_1 \in V(G_1) p_2 \in V(Q_k(G_1)) - V(G_1)}} [d(p_1, z)d(p_2, z)] \\
 &= \sum_{z \in V(G_2)} \sum_{\substack{p_1 p_2 \in E(Q_k(G_1)) \\ p_1 \in V(G_1) p_2 \in V(Q_k(G_1)) - V(G_1)}} [d(p_1) + d(z) + d(p_1)d(z)][d(p_2) + d(z) + d(p_2)d(z)] \\
 &= \sum_{z \in V(G_2)} \sum_{p_1 p_2 \in E(Q_k(G_1))} [d(p_1)d(p_2)(1 + 2d(z) + d^2(z)) + d(p_2)(d(z) + d^2(z))] \\
 &= [M_3(G_1) + 2M_2(G_1)][n_{G_2} + 4e_{G_2} + M_1(G_2)] + 2M_1(G_1)[2e_{G_2} + M_1(G_2)], \\
 \sum 2'' &= \sum_{z \in V(G_2)} \sum_{\substack{p_1 p_2 \in E(Q_k(G_1)) \\ p_1 p_2 \in V(Q_k(G_1)) - V(G_1)}} [d(p_1, z)d(p_2, z)].
 \end{aligned} \tag{22}$$

Now, we split this sum into two parts for the vertices,  $p_1$  and  $p_2$ , where  $p_1 p_2 \in V(Q_k(G_1)) - V(G_1)$ . Assume that

$\sum 2'' a$  which are in the same edges of  $G_1$  and  $\sum 2'' b$  of  $Q_k(G_1)$  in two different adjacent edges of  $G_1$ .

$$\begin{aligned}
 \sum 2'' a &= \sum_{z \in V(G_2)} \sum_{\substack{p_1 p_2 \in E(Q_k(G_1)) \\ p_1 p_2 \in V(Q_k(G_1)) - V(G_1)}} [(d(p_1) + d(p_1)d(z))(d(p_2) + d(p_2)d(z))] \\
 &= \sum_{z \in V(G_2)} \sum_{\substack{p_1 p_2 \in E(Q_k(G_1)) \\ p_1 p_2 \in V(Q_k(G_1)) - V(G_1)}} [d(p_1)d(p_2) + 2d(p_1)d(p_2)d(z) + d(p_1)d(p_2)d^2(z)] \\
 &= \sum_{z \in V(G_2)} \sum_{\substack{p_1 p_2 \in E(Q_k(G_1)) \\ p_1 p_2 \in V(Q_k(G_1)) - V(G_1)}} [d(p_1)d(p_2)][1 + 2d(z) + d^2(z)] \\
 &= (k-1)[M_3(G_1) + 2M_2(G_1)][n_{G_2} + 4e_{G_2} + M_1(G_2)], \\
 \sum 2'' b &= \sum_{z \in V(G_2)} \sum_{\substack{p_1 p_2 \in E(Q_k(G_1)) \\ p_1 p_2 \in V(Q_k(G_1)) - V(G_1)}} [(d(p_1) + d(p_1)d(z))(d(p_2) + d(p_2)d(z))] \\
 &= k \sum_{z \in V(G_2)} [1 + 2d(z) + d^2(z)] \sum_{\substack{p_1 p_2 \in E(Q_k(G_1)) \\ p_1 p_2 \in V(Q_k(G_1)) - V(G_1)}} [d(p_1)d(p_2)] \\
 &= k[n_{G_2} + 4e_{G_2} + M_1(G_2)] \sum_{\substack{uv \in E(G_1) \\ vw \in E(G_2)}} [d_{G_1}(u) + d_{G_1}(v)][d_{G_1}(v) + d_{G_1}(w)],
 \end{aligned} \tag{23}$$

where  $p_1$  is the added vertex in the edge  $uv$  and  $p_2$  is added vertex in the edges  $vw$  of  $G_1$ :

$$\begin{aligned}
 &= (k) \left[ n_{G_2} + 4e_{G_2} + M_1(G_2) \right] \left[ \frac{1}{2} \sum_{v \in V(G_1)} (d_{G_1}^4(v) - d_{G_1}^3(v)) + \sum_{uv \in E(G_1)} r d_{G_1}(u) d_{G_1}(v) \right] \\
 &+ \left[ \sum_{v \in V(G_1)} d_{G_1}^2(v) \sum_{\substack{ue \in V(G_1) \\ uv \in E(G_1)}} d_{G_1}(u) - 2M_2(G_1) \right], \tag{24}
 \end{aligned}$$

where  $r$  is the number of neighbors which are common vertices of  $u$  and  $v$  in  $(G_1)$ .

$$\begin{aligned}
 \sum 3 &= \sum_{z_1 z_2 \in V(G_2)} \sum_{p_1 p_2 \in E(Q_k(G_1))} \sum_{p_1 \in V(G_1), p_2 \in V(Q_k(G_1)) - V(G_1)} [d(p_1, z_1) d(p_2, z_2)] \\
 &+ \sum_{y_1 z_2 \in V(G_2)} \sum_{p_1 p_2 \in E(Q_k(G_1))} \sum_{p_1, p_2 \in V(Q_k(G_1)) - V(G_1)} [d(p_1, z_1) d(p_2, z_2)] = \sum 3' + \sum 3'', \\
 \sum 3' &= \sum_{z_1 z_2 \in V(G_2)} \sum_{p_1 p_2 \in E(Q_k(G_1))} \sum_{p_1 \in V(G_1), p_2 \in V(Q_k(G_1)) - V(G_1)} [d(p_1, z_1) d(p_2, z_2)] \\
 &= \sum_{z_1 z_2 \in V(G_2)} \sum_{p_1 p_2 \in E(Q_k(G_1))} \sum_{p_1 \in V(G_1), p_2 \in V(Q_k(G_1)) - V(G_1)} [(d(p_1) + d(z_1) + d(p_1) d(z_1)) (d(p_2) + d(p_2) d(z_2))] \tag{25} \\
 &= [M_3(G_1) + 2M_2(G_1)] [2e_{G_2} + 2M_1(G_2) + 2M_2(G_2)] + 2M_1(G_1) [2M_2(G_2) + M_1(G_2)], \\
 \sum 3'' &= \sum_{z_1 z_2 \in V(G_2)} \sum_{p_1 p_2 \in E(Q_k(G_1))} \sum_{p_1 p_2 \in V(Q_k(G_1)) - V(G_1)} [d(p_1, z) d(p_2, z)].
 \end{aligned}$$

Now, we split this sum into two parts for the vertices,  $p_1$  and  $p_2$ , where  $p_1 p_2 \in V(Q_k(G_1)) - V(G_1)$ . Assume that

$\sum 3'' a$  which are in the same edges of  $G_1$  and  $\sum 3'' b$  of  $Q_k(G_1)$  in two different adjacent edges of  $G_1$ .

$$\begin{aligned}
\sum 3'' a &= \sum_{z_1 z_2 \in V(G_2)} \sum_{p_1 p_2 \in E(Q_k(G_1))} [d(p_1, z_1) d(p_2, z_2)] \\
&= \sum_{z_1 z_2 \in V(G_2)} \sum_{p_1 p_2 \in E(Q_k(G_1))} [(d(p_1) + d(p_1) d(z_1)) (d(p_2) + d(p_2) d(z_2))] \\
&= \sum_{z_1 z_2 \in V(G_2)} [1 + d(z_2) + d(z_1) + d(z_1) d(z_2)] \sum_{p_1 p_2 \in E(Q_k(G_1))} [d(p_1) d(p_2)] \\
&= (k-1) [2e_{G_2} + 2M_1(G_2) + 2M_2(G_2)] [M_3(G_1) + 2M_2(G_1)], \\
\sum 3'' b &= \sum_{z_1 z_2 \in V(G_2)} \sum_{p_1 p_2 \in E(Q_k(G_1))} [d(p_1, z_1) d(p_2, z_2)] \\
&= \sum_{z_1 z_2 \in V(G_2)} \sum_{p_1 p_2 \in E(Q_k(G_1))} [(d(p_1) + d(p_1) d(z_1)) (d(p_2) + d(p_2) d(z_2))] \\
&= \sum_{z_1 z_2 \in V(G_2)} [1 + d(z_2) + d(z_1) + d(z_1) d(z_2)] \sum_{p_1 p_2 \in E(Q_k(G_1))} [d(p_1) d(p_2)] \\
&= k [2e_{G_2} + 2M_1(G_2) + 2M_2(G_2)] \sum_{\substack{uv \in E(G_1) \\ vw \in E(G_2)}} [d_{G_1}(u) + d_{G_1}(v)] [d_{G_1}(v) + d_{G_1}(w)],
\end{aligned} \tag{26}$$

where  $p_1$  is the added vertex in the edge  $uv$  and  $p_2$  is added vertex in the edges  $vw$  of  $G_1$ :

$$\begin{aligned}
&= (k) [2e_{G_2} + 2M_1(G_2) + 2M_2(G_2)] \left[ \frac{1}{2} \sum_{v \in V(G_1)} (d_{G_1}^4(v) - d_{G_1}^3(v)) + \sum_{uv \in V(G_1)} r d_{G_1}(u) d_{G_1}(v) \right. \\
&\quad \left. + \sum_{v \in V(G_1)} d_{G_1}^2(v) \sum_{\substack{u \in V(G_1) \\ uv \in E(G_1)}} d_{G_1}(u) - 2M_2(G_1) \right],
\end{aligned} \tag{27}$$

where  $r$  is the number of neighbors which are common vertices of  $u$  and  $v$  in  $(G_1)$ .

Consequently, we have

$$\begin{aligned}
M_2(G_1 \boxtimes_{Q_k} G_2) &= k [n_{G_2} + 6e_{G_2} + 3M_1(G_2) + 2M_2(G_2)] \left[ \frac{1}{2} \sum_{v \in V(G_1)} (d_{G_1}^4(v) - d_{G_1}^3(v)) \right. \\
&\quad \left. + \sum_{uv \in V(G_1)} r d_{G_1}(u) d_{G_1}(v) + \sum_{v \in V(G_1)} d_{G_1}^2(v) \sum_{\substack{u \in V(G_1) \\ uv \in E(G_1)}} d_{G_1}(u) - 2M_2(G_1) \right] \\
&\quad + M_2(G_2) [4e_{G_1} + n_{G_1}] + 2e_{G_1} M_1(G_2) + M_1(G_1) [5e_2 + 5M_1(G_2) + 5M_2(G_2)] \\
&\quad + k [M_3(G_1) + 2M_2(G_1)] [6e_{G_2} + 3M_1(G_2) + 2M_2(G_2) + n_{G_2}].
\end{aligned} \tag{28}$$

□

**Theorem 4.** Let  $G_1$  and  $G_2$  be two connected graphs such that  $|V(G_1)|, |V(G_2)| \geq 4$ . For  $k \geq 1$ ,

$$\begin{aligned}
 (a) M_1(G_1 \boxtimes_{T_k} G_2) &= M_1(G_2)[8e_{G_1} + n_{G_1} + 6M_1(G_1)] + 2(k-1)M_1(G_1)[2e_{G_2} + M_1(G_2)] \\
 &\quad + k[M_3(G_1) + 2M_2(G_1) - 2M_1(G_1)][4e_{G_2} + n_{G_2} + M_1(G_2)] + 16e_{G_1}e_{G_2} \\
 &\quad + M_1(G_1)[2(11+k)e_{G_2} + 2(k+2)n_{G_2}], \\
 (b) M_2(G_1 \boxtimes_{T_k} G_2) &= k[n_{G_2} + 6e_{G_2} + 3M_1(G_2) + 2M_2(G_2)] \left[ \frac{1}{2} \sum_{v \in V(G_1)} (d_{G_1}^4(v) - d_{G_1}^3(v)) + \sum_{uv \in V(G_1)} rd_{G_1}(u)d_{G_1}(v) \right. \\
 &\quad \left. + \sum_{v \in V(G_1)} d_{G_1}^2(v) \sum_{\substack{ue \in V(G_1) \\ uv \in E(G_1)}} d_{G_1}(u) - 2M_2(G_1) \right] + M_2(G_1)[4n_{G_2} + 24e_{G_2} + 8M_2(G_2) + 12M_1(G_2)] \\
 &\quad + k[M_3(G_1) + 2M_2(G_1)][6e_{G_2} + n_{G_2} + 3M_1(G_2) + 2M_2(G_2)] + 5M_1(G_2)e_{G_1} \\
 &\quad + M_2(G_2)[10e_{G_1} + n_{G_1}] + M_1(G_1)[10e_{G_2} + 11M_1(G_2) + 10M_2(G_2)].
 \end{aligned} \tag{29}$$

#### 4. Applications and Conclusion

In this section, we have computed the first and second Zagreb indices of generalized  $\Phi$ -sum graphs based on strong product as application of Theorem 1 to Theorem 4 for  $k = 1$

given as follows. We also find the subclass with better Zagreb indices as presented in Tables 1 and 2 and Figure 4

(i)  $S_1$ -sum:

$$\begin{aligned}
 (a) M_1(G_1 \boxtimes_{S_1} G_2) &= M_1(S_1 G_1)[n_{G_2} + 2e_{G_2}] + 8e_{G_1}e_{G_2} + [M_1(G_1) + 4e_{G_1}][M_1(G_2) + 2e_{G_2}] \\
 &\quad + M_1(G_2)[4e_{G_1} + n_{G_1}], \\
 (b) M_2(G_1 \boxtimes_{S_1} G_2) &= [M_2(G_1) + 4e_{G_1}][5e_{G_2} + 3M_1(G_2) + 2M_2(G_2) + n_{G_2}] + 14e_{G_1}M_1(G_2) \\
 &\quad + M_2(G_2)[12e_{G_1} + n_{G_1}] + M_1(G_1)[e_{G_2} + M_1(G_2) + M_2(G_2)] + 8e_{G_1}e_{G_2}.
 \end{aligned} \tag{30}$$

(ii)  $R_1$ -sum:

$$\begin{aligned}
 (a) M_1(G_1 \boxtimes_{R_1} G_2) &= 24e_{G_1}e_{G_2} + M_1(G_2)[n_{G_1} + 12e_{G_1} + M_1(G_1)][12e_{G_2} + 2n_{G_2}] \\
 &\quad + [M_1(R_1(G_1)) - 2M_1 G_1][n_{G_2} + 2e_{G_2}], \\
 (b) M_2(G_1 \boxtimes_{R_1} G_2) &= 2M_1(G_1)[4e_{G_2} + 6M_1(G_2) + 2M_2(G_2)] + 4e_{G_1}[3M_1(G_2) + 3M_2(G_2) + 4e_{G_2}] \\
 &\quad + [M_2(R_1(G_1)) - 4M_2 G_1][6e_{G_2} + 3M_1(G_2) + 2M_2(G_2) + n_{G_2}] + e_{G_1}M_1(G_2) \\
 &\quad + 4M_2(G_1)[n_{G_2} + 6e_{G_2} + 3M_1(G_2)] + M_2(G_2)[n_{G_1} + 2e_{G_1}].
 \end{aligned} \tag{31}$$



TABLE 1:  $M_1(P_n \boxtimes_{\Phi_1} P_m)$  for path graph.

$[m, n]$	$M_1(P_n \boxtimes_{S_1} P_m)$	$M_1(P_n \boxtimes_{R_1} P_m)$	$M_1(P_n \boxtimes_{Q_1} P_m)$	$M_1(P_n \boxtimes_{T_1} P_m)$
(3, 3)	336	722	472	892
(4, 4)	804	1776	1220	2204
(5, 5)	1086	3294	2296	4108
(6, 6)	1854	7040	3700	8368
(7, 7)	2606	9878	5432	11848

TABLE 2:  $M_2(P_n \boxtimes_{\Phi_1} P_m)$  for path graph.

$[m, n]$	$M_2(P_n \boxtimes_{S_1} P_m)$	$M_2(P_n \boxtimes_{R_1} P_m)$	$M_2(P_n \boxtimes_{Q_1} P_m)$	$M_2(P_n \boxtimes_{T_1} P_m)$
(3, 3)	824	2384	1535	2899
(4, 4)	2262	5230	5002	9700
(5, 5)	4404	11636	9674	17818
(6, 6)	6738	17546	15818	28696
(7, 7)	10740	25816	23026	40942

(iii)  $Q_1$ -sum:

$$\begin{aligned}
 \text{(a)} \quad M_1(G_1 \boxtimes_{Q_1} G_2) &= [M_3(G_1) + 2M_2(G_1) - 2M_1(G_1)] [n_{G_2} + 4e_{G_2} + M_1(G_2)] + 8e_{G_1}e_{G_2} \\
 &\quad + 3M_1(G_1)[n_{G_2} + 4e_{G_2} + M_1(G_2)] + M_1(G_2)[n_{G_1} + 4e_{G_1}], \\
 \text{(b)} \quad M_2(G_1 \boxtimes_{Q_1} G_2) &= [n_{G_2} + 6e_{G_2} + 3M_1(G_2) + 2M_2(G_2)] \left[ \frac{1}{2} \sum_{v \in V(G_1)} (d_{G_1}^4(v) - d_{G_1}^3(v)) \right. \\
 &\quad \left. + \sum_{uv \in E(G_1)} rd_{G_1}(u)d_{G_1}(v) + \sum_{v \in V(G_1)} d_{G_1}^2(v) \sum_{\substack{u \in V(G_1) \\ uv \in E(G_1)}} d_{G_1}(u) - 2M_2(G_1) \right] \\
 &\quad + M_2(G_2)[4e_{G_1} + n_{G_1}] + 2e_{G_1}M_1(G_2) + M_1(G_1)[5e_2 + 5M_1(G_2) + 5M_2(G_2)] \\
 &\quad + [M_3(G_1) + 2M_2(G_1)][6e_{G_2} + 3M_1(G_2) + 2M_2(G_2) + n_{G_2}],
 \end{aligned} \tag{32}$$

(iv)  $T_1$ -sum:

$$\begin{aligned}
 \text{(a)} \quad M_1(G_1 \boxtimes_{T_1} G_2) &= M_1(G_2)[8e_{G_1} + n_{G_1} + 6M_1(G_1)] + M_1(G_1)[24e_{G_2} + 6n_{G_2}] \\
 &\quad + [M_3(G_1) + 2M_2(G_1) - 2M_1(G_1)][4e_{G_2} + n_{G_2} + M_1(G_2)] + 16e_{G_1}e_{G_2}, \\
 \text{(b)} \quad M_2(G_1 \boxtimes_{T_1} G_2) &= [n_{G_2} + 6e_{G_2} + 3M_1(G_2) + 2M_2(G_2)] \left[ \frac{1}{2} \sum_{v \in V(G_1)} (d_{G_1}^4(v) - d_{G_1}^3(v)) \right. \\
 &\quad \left. + \sum_{uv \in E(G_1)} rd_{G_1}(u)d_{G_1}(v) + \sum_{v \in V(G_1)} d_{G_1}^2(v) \sum_{\substack{u \in V(G_1) \\ uv \in E(G_1)}} d_{G_1}(u) - 2M_2(G_1) \right] \\
 &\quad + [M_3(G_1) + 2M_2(G_1)][6e_{G_2} + n_{G_2} + 3M_1(G_2) + 2M_2(G_2)] + 5M_1(G_2)e_{G_1} \\
 &\quad + M_2(G_2)[10e_{G_1} + n_{G_1}] + M_1(G_1)[10e_{G_2} + 11M_1(G_2) + 10M_2(G_2)] \\
 &\quad + M_2(G_1)[4n_{G_2} + 24e_{G_2} + 8M_2(G_2) + 12M_1(G_2)].
 \end{aligned} \tag{33}$$

Now, we close our discussion with the conclusion that both the Zagreb indices of the generalized T-sum graph are dominant among the Zagreb indices of all the generalized sum graphs as shown in Figure 4. We also conclude that, in the generalized T-sum graph, the number of vertices (atoms) and edges (bonds) between them are more than the other graphs of this family for each integral values of  $k$ . Thus, the role of Zagreb indices for generalized T-sum graph remains dominant for each integral values of  $k$ . However, the problem is still open to find different degree- and distance-based TIs for the generalized sum graphs obtained under the various operations of product of graphs.

### Data Availability

The data used to support the findings of this study are included within the article. Additional data can be obtained from the corresponding author upon request.

### Conflicts of Interest

The authors declare no conflicts of interest.

### Acknowledgments

This work was supported by University of Tabuk, Tabuk, Saudi Arabia.

### References

- [1] I. Gutman, B. Ruscic, N. Trinajstic, and C. F. Wilcox, "Graph theory and molecular orbitals. XII. Acyclic polyenes," *The Journal of Chemical Physics*, vol. 62, no. 9, pp. 3399–3405, 1975.
- [2] L. B. Kier and L. H. Hall, "Structure-activity studies on hallucinogenic amphetamines using molecular connectivity," *Journal of Medicinal Chemistry*, vol. 20, no. 12, pp. 1631–1636, 1977.
- [3] O. M. Minailiuc and M. V. Diudea, "TI-MTD model. applications in molecular design," *QSPR=QSAR Studies by Molecular Descriptors*, pp. 363–388, 2001.
- [4] H. Wiener, "Structural determination of paraffin boiling points," *Journal of the American Chemical Society*, vol. 69, no. 1, pp. 17–20, 1947.
- [5] I. Gutman and N. Trinajstic, "Graph theory and molecular orbitals. Total  $\phi$ -electron energy of alternant hydrocarbons," *Chemical Physics Letters*, vol. 17, no. 4, pp. 535–538, 1972.
- [6] I. Gutman and N. Trinajstic, *Graph Theory and Molecular Orbitals*, vol. 2, pp. 49–93, In New Concept, Berlin, Heidelberg, 1973.
- [7] Y.-M. Chu, S. Javed, M. Javaid, and M. Kamran Siddiqui, "On bounds for topological descriptors of  $\phi$ -sum graphs," *Journal of Taibah University for Science*, vol. 14, no. 1, pp. 1288–1301, 2020.
- [8] G. Hong, Z. Gu, M. Javaid, H. M. Awais, and M. K. Siddiqui, "Degree-based topological invariants of metal-organic networks," *IEEE Access*, vol. 8, pp. 68288–68300, 2020.
- [9] W. Yan, B.-Y. Yang, and Y.-N. Yeh, "The behavior of Wiener indices and polynomials of graphs under five graph decorations," *Applied Mathematics Letters*, vol. 20, no. 3, pp. 290–295, 2007.
- [10] M. Eliasi and B. Taeri, "Four new sums of graphs and their Wiener indices," *Discrete Applied Mathematics*, vol. 157, no. 4, pp. 794–803, 2009.
- [11] J.-B. Liu, S. Javed, M. Javaid, and K. Shabbir, "Computing first general Zagreb index of operations on graphs," *IEEE Access*, vol. 7, pp. 47494–47502, 2019.
- [12] J. B. Liu, M. Javaid, and H. M. Awais, "Computing Zagreb indices of the subdivision-related generalized operations of graphs," *IEEE Access*, vol. 7, pp. 105479–105488, 2019.
- [13] H. M. Awais, M. Javaid, and M. Jamal, "Forgotten index of generalized F-sum graphs," *Journal of Prime Research in Mathematics*, vol. 15, pp. 115–128, 2019.
- [14] H. M. Awais, M. Javaid, and A. Raheem, "Hyper-Zagreb index of graphs based on generalized subdivision related operations," *Punjab University Journal of Mathematics*, vol. 52, no. 5, pp. 89–103, 2019.
- [15] H. M. Awais, M. Javaid, and A. Akbar, "First general zagreb index of generalized F-sum graphs," *Discrete Dynamics in Nature and Society*, vol. 2020, Article ID 2954975, 16 pages, 2020.
- [16] A. Ali, "Tetracyclic graphs with maximum second Zagreb index: a simple approach," *Asian-European Journal of Mathematics*, vol. 11, no. 05, p. 1850064, 2018.
- [17] H. M. Awais, M. Jamal, and M. Javaid, "Topological properties of metal-organic frameworks," *Main Group Metal Chemistry*, vol. 43, no. 1, pp. 67–76, 2020.
- [18] X. Zhang, H. M. Awais, M. Javaid, and M. K. Siddiqui, "Multiplicative zagreb indices of molecular graphs," *Journal of Chemistry*, pp. 1–19, 2019.
- [19] H. Deng, D. Sarala, S. K. Ayyaswamy, and S. Balachandran, "The Zagreb indices of four operations on graphs," *Applied Mathematics and Computation*, vol. 275, pp. 422–431, 2016.